CORA Cork Open Research Archive
Cartlann Taighde Oscailte Chorcaí

Title	Physical properties of feeds for novel bioactives - encapsulating bead formation
Authors	Hansen, Mackenzie M.
Publication date	2021-10
Original Citation	Hansen, M. M. 2021. Physical properties of feeds for novel bioactives - encapsulating bead formation. PhD Thesis, University College Cork.
Type of publication	Doctoral thesis
Rights	© 2021, Mackenzie May Hansen. - https://creativecommons.org/licenses/by-nc-nd/4.0/
Download date	2026-10-30 19:01:44
Item downloaded from	https://hdl.handle.net/10468/12407



UCC
University College Cork, Ireland
Coláiste na hOllscoile Corcaigh

Ollscoil na hÉireann, Corcaigh

National University of Ireland, Cork



Physical Properties of Feeds for Novel Bioactives-Encapsulating Bead Formation

Thesis presented by

Mackenzie May Hansen

B.Sc. Food Science, University of Wisconsin-Madison

ORCID iD: 0000-0001-6237-4655

for the degree of

Doctor of Philosophy

in

Food Science and Technology

University College Cork

School of Food and Nutritional Sciences

Head of School: Mairead Kiely

Supervisor: Professor Yrjö H. Roos

October 2021

Declaration

The thesis submitted is, unless stated, entirely my own original work. It has not been submitted to this or any other academic institution for any other degree.

Signature: _____Date:_____

Mackenzie M. Hansen

Dedication

To all the women in my family,

and their mothers before them,

whose steadfast dedication to their loved ones

encouraged and gave me the tools me to pursue my goals.

This is for you.

Acknowledgements

I would first like to thank Professor Roos for affording me the opportunity to pursue my PhD under one of the greatest minds in the field. Thank you for facilitating my development as an independent and resourceful researcher and scientist, while providing latitude to write my own script. I appreciate the support I received from many others during my time at University College Cork, especially Mr. Jim McNamara, Mr. Dave Waldron, Ms. Anne Fenton, and Dr. Karen McCarthy. I am grateful for the financial support from the Lauritzson Foundation to pursue my academic endeavors, as well as serving as the catalyst for my friendship with Meg Ross. Meg, it has been such a comfort to go through this PhD process together. Many thanks to my viva examiners, Drs. Tom O'Connor and Yael Vodovotz, for their thoughtful reading of and recommendations to strengthen my thesis.

I am very thankful to have had the opportunity to complete some of my research abroad at my alma mater, the Food Science Department at the University of Wisconsin-Madison. It has been such a privilege to return to the Hartel Laboratory for inclusion into the group, to collaborate with Professor Brad Bolling and Dr. Audrey Girard, and to work closely with Tami and Karen. I want to express my deepest gratitude to Professor Rich Hartel, for his continued guidance, support, and mentorship throughout my academic career. Thank you for never teaching me what to think, but *how* to think.

I want to sincerely thank everyone who made Cork feel like home for 2 years. Aine, Megan, Tiffany, and everyone at Inniscarrig Terrace, thank you for your friendship. Lisa- I could not have hoped for a greater resource to look to during this process, and I am so grateful for the friendship we developed. Joe, Harry, and Chris- you truly became my family in Ireland. Thank

you for being constant sources of comfort and laughter, and for reminding me that I was doing a great job whenever I needed to hear it. My life is so much richer for having known and loved these people.

My greatest and final thank you is for everyone that welcomed me back home, where my story began. ‘Thank you’ is hardly enough to say to my parents, after moving heaven and earth to support me and see me succeed. Their endless sacrifices and encouragement to follow my dreams, even when those were over 3,500 miles away, never went unnoticed. Thank you to my sisters, a reliable source of levity and reminders to not take myself too seriously. Thanks to Kristie and Chris for being strong advocates and providing great advice and encouragement, my grandparents for always making the effort to celebrate my achievements. I am so grateful for my friends, Lauren, Leo, and Katherine, who welcomed me back to Madison with open arms. Olivia, thank for being a valued friend and support system, regardless of what letters come after my name.

In the words of Dr. Suess, “The more that you read, the more things you will know. The more that you learn, the more places you’ll go.” Pursuing a PhD and living as an expat have truly been the most enriching and transformative experiences of my life. None of this growth would have been possible without the support of so many, and I am so grateful.

Table of Contents

Declaration 2

Dedication 3

Acknowledgements 4

Table of contents 6

List of Publications 7

List of Conference Presentations 8

Abstract 9

List of Figures 12

List of Tables 20

Introduction 21

Chapter 1- Literature Review 23

Chapter 2- Thermal gelation and hardening of whey protein beads for subsequent dehydration and encapsulation using vitrifying sugars 51

Chapter 3- Encapsulant-bioactives interactions impact on physico-chemical properties of concentrated dispersions 86

Chapter 4- Effects of Aronia polyphenols on the physico-chemical properties of whey, soy, and pea protein isolate dispersions 121

Chapter 5- Bioactives and extract effects on the physico-chemical properties of concentrated whey protein isolate dispersions 154

Chapter 6- Formation of dry beads for bioactives encapsulation by freeze granulation 185

Chapter 7- General Discussion 220

References 234

Appendix 1- Additional Figures for Chapter 2 273

Appendix 2- Published manuscripts 274

Publications

Hansen, M.M., Maidannyk, V.A., Roos, Y.H. Thermal gelation and hardening of whey protein beads for subsequent dehydration and encapsulation using vitrifying sugars. *Journal of Food Engineering* 279 (2020), 10.1016/j.jfoodeng.2020.109966

Hansen, M.M., Hartel, R.W., Roos, Y.H. Encapsulant-bioactives interactions impact on physico-chemical properties of concentrated dispersions. *Journal of Food Engineering,* 302 (2021), 11.0586/j.jfoodeng.2021.110586

Hansen, M. M., Hartel, R. W., & Roos, Y. H. Formation of dry beads for bioactives encapsulation by freeze granulation. *Journal of Food Engineering,* 317 (2022), 10.1016/j.jfoodeng.2021.110847

Hansen, M.M., Hartel, R.W. & Roos, Y.H. Effects of Aronia polyphenols on the physico-chemical properties of whey, soy, and pea protein isolate dispersions. *Food Production, Processing and Nutrition,* 3, 29 (2021), 10.1186/s43014-021-00074-w

Manuscripts under review

Hansen, M. M., Hartel, R. W., & Roos, Y. H. (2021). Bioactives and extract effects on the physico-chemical properties of concentrated whey protein isolate dispersions. *Food Production, Processing and Nutrition*, "Natural Products and Bioactive Compounds in Food" Special Issue. Status: Reviewers assigned.

Conference Oral Presentations

Hansen, M.M. “Drop formation and hardening process for concentrated protein solutions.” *Conference of Food Engineering,* Minneapolis, MN. September 2018.

Hansen, M.M. “Development of a Continuous Encapsulation Process using Protein Matrices.” *47th Annual Food Science and Technology Conference*, Cork, Ireland. December 2018.

Hansen, M.M. “Continuous bioactives encapsulation and food structuring using protein-carbohydrate matrices.” *International Symposium on the Properties of Water 14*, Dijon, France. August 2019.

Hansen, M.M. “Continuous process using protein-carbohydrate matrices for structuring and encapsulation.” *13th International Congress on Engineering and Food*, Melbourne, Australia. September 2019.

Abstract

Encapsulation involves the entrapment of sensitive bioactive compounds with structure-forming food components to enhance protection and delivery. Blends of proteins and glass-forming carbohydrates are often used as encapsulation matrices and for structure formation. When bioactives intended for encapsulation are mixed with structuring proteins under acidic and neutral pH conditions and ambient temperatures, weak, non-covalent protein-bioactive interactions have been reported to occur. Complex formation may influence the physical properties of dispersions as well as dried products formed by feed mixtures. We hypothesized that: (i) Processes forming concentrated protein-carbohydrate feed dispersions into dry, solid beads could be developed, and (ii) formulation composition changes such as varied total solids, protein-carbohydrate ratios, protein isolates with different purities and structures, carbohydrate types, bioactives contents, and bioactives sources with diverse structures and sizes of predominant compounds would result in changes to the physico-chemical properties and drop formation abilities of dispersions, as well as the physical characteristics of dry beads formed. Key objectives of the present study were: (i) the development of two different simple, continuous processes forming feed dispersions into dried, novel bead structures, and (ii) characterization of the effects of changes in formulation compositions on the physical properties of liquid feeds and resulting dry beads.

A full process design for simple solidification of concentrated liquid dispersions and a structure-forming formulation used for subsequent vitrification are reported, producing solid bead structures suitable for inclusion of bioactives in protein-carbohydrate matrices. Increasing total solids contents generally resulted in enhanced dispersion viscosities, altering surface tensions as well. Altering protein:carbohydrate ratios in dispersions generally did not strongly

affect surface tension or particle sizes, increasing ratios often resulted in slightly increased viscosities. In comparing the effects of protein isolate types on the physical properties of dispersions with WPI, SPI, and PPI, WPI feeds had the highest surface tensions, lowest viscosities, and smallest particle sizes, while PPI had the lowest surface tensions, highest viscosities, and largest particle sizes. Upon altering the carbohydrate type used in dispersions between sucrose, maltitol, and trehalose, the physical properties of dispersions were not notably affected. Addition of bioactives to protein-carbohydrate dispersions resulted in slightly reduced pH values and increasing bioactives concentrations resulted in slightly increased surface tensions of dispersions under some conditions. Viscosities of dispersions with varying bioactives concentrations were generally not strongly affected, except for decreases in viscosities of PPI dispersions and increases in SPI dispersion viscosities with increasing polyphenols concentrations under few conditions. Particle sizes of remaining unhydrated/insoluble protein particles and aggregates in WPI dispersions were slightly reduced, SPI dispersions slightly increased, and PPI dispersions generally decreased with increasing Aronia polyphenols concentrations. Particle sizes of WPI-sucrose dispersions increased when cranberry extract and gallotannin polyphenols concentrations increased. Dispersions with cranberry extract had significantly higher surface tensions than those with Aronia and beet extracts, but not gallotannin. Beet extract affected particle sizes of dispersions the least, and cranberry extract resulted in the largest particle sizes detected. Dispersions with cranberry extract also had the highest viscosities. Dried beads containing sucrose were found to have lower hardness upon texture analysis (smaller compression forces required to compress beads 3 mm) than those with only WPI but did not undergo shrinkage upon drying. Beads formed by freeze granulation had water contents in the same range as those from the drop formation method involving gelation in

hot oil and subsequent drying but lower water activities, potentially due to the lack of a gel network structure within beads entrapping water available for reactions after drying. Formulating with trehalose resulted in beads with the highest T_g and maltitol the lowest T_g. 1% Aronia PP did not strongly impact T_g of beads. Beads formed without WPI were harder than those formed with proteins. A strong, continuous glassy phase formed in the absence of proteins, but the glassy phase of beads containing WPI was interrupted by proteins dispersed throughout, weakening the continuous glassy structure. Aronia extract did not strongly affect the hardness of beads, and those formulated with maltitol tended to be softest, while those with trehalose were hardest. A modified method for bead formation by freeze granulation was also presented, forming structures under different conditions than the heated oil drop formation method.

Results of this study provide insight into physical behaviors of high solids-concentrated protein-carbohydrate dispersions and effects of bioactives and protein-bioactives interactions in the aqueous blends and in dried materials formed from mixtures. These findings advance formulating high protein products with bioactives to obtain desired textural attributes and natural color preservation. Two processes for making foods with high physical stabilities and potential for the entrapment of flavors, emulsion droplets, colors, or bioactives are presented, which may serve as novel alternatives to drying or extrusion.

Figures

Figure 1. Schematic drawings of common encapsulation structures: reservoir (Left), matrix (Center), and coated matrix systems (Right), adapted from Lakkis et al. (2016).

Figure 2. Primary interactions (hydrophobic interactions and hydrogen bonding) driving non-covalent complexation between proteins and polyphenols in mixtures, adapted from Quan et al. (2019) and Li et al. (2021).

Figure 3. Schematic drawings depicting the non-covalent binding of polyphenols to proteins in solution, the formation and growth of aggregates, and ultimate precipitation of large, insoluble protein-polyphenol complexes, adapted from Charlton et al. (2002).

Figure 2.1. A- Effect of protein concentration (%) in feeds containing 0, 10, and 20% sucrose on the apparent viscosity at 100 s^{-1}; n = 3. Lines are for guiding purposes only. **B-** Effect of sucrose concentration (%) in feeds containing 30, 35, and 40% WPI on apparent viscosity at 100 s^{-1}; n = 3. Lines are for guiding purposes only. Inset: Effect of 10% w/w sucrose on viscosity. **C-** Effect of pH in feeds containing 35% WPI with 10%, 15%, and 20% sucrose on apparent viscosity at 100 s^{-1}; n = 3. Lines are for guiding purposes only. Data points connected by the same letter are not significantly different ($p > 0.05$) from other points connected by the same line.

Figure2.2. A. Effect of WPI concentration (%) in feeds containing 0 and 10% sucrose on calculated surface tension in N/m; n = 3. Lines are for guiding purposes only. **B.** Effect of sucrose concentration (%) in feeds containing 30, 35, and 40% WPI on calculated surface tension; n = 3. Lines are for guiding purposes only. Data points connected by the same letter are not significantly different ($p > 0.05$) from other points connected by the same line.

Figure 2.3. A- Effect of oil temperature (°C) on dehydration shown by a_w of fresh drops comprised of 40% WPI with 10% sucrose for 2 min; n = 3. Lines are for guiding purposes only. **B-** Effect of heating time (min) at 100°C on dehydration shown by a_w of fresh drops comprised of 40% WPI with 10% sucrose; n = 3. Lines are for guiding purposes only. Data points connected by the same letter are not significantly different ($p > 0.05$) from other points connected by the same line.

Figure 2.4. Effect of dehydration shown by heating time (min) at 100°C on the volume (mm^3) of drops comprised of 40% WPI with 10% sucrose; n = 3. Lines are for guiding purposes only. Data points connected by the same letter are not significantly different ($p > 0.05$) from other points connected by the same line.

Figure 2.5. Effect of dehydration shown by heating time (min) at 100°C on the hardness (N) of drops comprised of 40% WPI with 10% sucrose; n = 3. Data points connected by the same letter are not significantly different ($p > 0.05$) from other points connected by the same line.

Figure 2.6. A- Scanning electron micrograph image at 500x magnification, depicting the microstructure of a dried, 40% WPI bead. **B-** Left: Scanning electron micrograph image at 1000x magnification, depicting the microstructure of a dried, 40% WPI bead. Center: Scanning electron micrograph image at 5000x magnification, depicting the microstructure of a dried, 40% WPI bead. Right: Confocal laser scanning micrograph image depicting the microstructure of a dried, 40% WPI bead, with oil droplets dispersed throughout image. The left arrow points towards the appearance of the protein network in the left and center images, and the right arrow highlights the oil droplets protruding throughout the structure in the center and right images.

Figure 2.7. A- Left: Optical light microscope image at 4x magnification, depicting the microstructure of a dried, 40% WPI with 10% sucrose bead. Right: Optical light microscope image at 10x magnification, depicting the microstructure of a dried, 40% WPI with 10% sucrose bead. **B-** Left: Scanning electron micrograph image at 500x magnification, depicting the microstructure of a dried, 40% WPI with 10% sucrose bead. Center: Scanning electron micrograph image at 1000x magnification, depicting the microstructure of a dried, 40% WPI with 10% sucrose bead. Right: Scanning electron micrograph image at 2000x magnification, depicting the microstructure of a dried, 40% WPI with 10% sucrose bead.

Figure 2.8 A-D. Confocal laser scanning micrograph images depicting the microstructure of a dried, 40% WPI with 10% sucrose bead, with oil droplets dispersed throughout image. A and C: Highlight protein in bright red and other components as darker colors. B and D: Highlight fat in bright green and other components as darker colors.

Figure 2.9. Confocal laser scanning micrograph image depicting the microstructure of a dried, 40% WPI with 10% sucrose bead, with oil droplets dispersed throughout image; highlighting proteins in bright red, fat in bright green, and other components (mainly sucrose) as darker colors. The darker colored sucrose is thought to form the translucent, glassy fragments shown throughout the image.

Figure 3.1. Effect of total solids content (%) [**A**], WPI:sucrose ratio [**B**], and PP content (%) [**C**] on the calculated surface tension (N/m) of dispersions at 25˚C; (n = 6). Lines are for guiding purposes only.

Figure 3.2. The relationship between the surface tensions (N/m) of feed dispersions containing WPI:sucrose ratios of 0.75, 1.0, and 1.25, polyphenols contents of 0, 0.5, and 1%, and total solids contents of 25, 35, and 45% at 25˚C and calculated diameters (mm) of drops.

Figure 3.3. Effect of total solids content (%) [**A**], WPI:sucrose ratio [**B**], and PP content (%) [**C**] on the complex viscosity (Pa*s) of dispersions at 25˚C; (n = 6). Lines are for guiding purposes only.

Figure 3.4. Effect of total solids content (%) [**A**] and PP content (%) [**B**] on the average particle size (μm) of dispersions at 25˚C; (n = 6). Lines are for guiding purposes only.

Figure 3.5. Optical light microscope images at 40x (left) and 200x magnification (right), depicting the microstructures of diluted feed dispersions with a 1.25 WPI:sucrose ratio and 1% PP at 25% (**A**), 35% (**B**), and 45% total solids contents (**C**).

Figure 3.6. Optical light microscope images at 40x (left) and 200x magnification (right), depicting the microstructures of diluted feed dispersions with a 1.0 WPI:sucrose ratio at 25% TS with 0% PP (**A**), 0.5% PP (**B**), and 1% PP (**C**).

Figure 3.7. Image depicting the precipitated fractions (highlighted in boxes) of centrifuged 10x-diluted dispersions with 1.25 WPI:sucrose ratios and 45% total solids contents with 0% PP (Left), 0.5% PP (Center), and 1% PP (Right).

Figure 3.8. Effect of total solids content (%) [**A**], WPI:sucrose ratio [**B**], and PP content (%) [**C**] on the on the diameters (mm) of frozen drops formed from dispersions; (n = 6). Lines are for guiding purposes only.

Figure 4.1. Effect of protein:sucrose ratio [**A**] and PP content (%) [**B**] on the calculated surface tension (N/m) of dispersions at 25˚C; (averaged data plotted, n = 9). Legend entries marked * contain data reported in previous work (Hansen et al., 2021a; averaged data plotted, n = 6). Lines are for guiding purposes only.

Figure 4.2. The relationship between the average surface tensions (N/m) of feed dispersions containing protein:sucrose ratios of 0.75, 1.0, and 1.25, PP contents of 0, 0.5, 1, and 1.5%, and protein isolates including WPI, SPI, and PPI at 25˚C and average calculated diameters (mm) of drops.

Figure 4.3. Effect of protein:sucrose ratio [**A**] and PP content (%) [**B**] on the average complex viscosity (Pa*s) of dispersions at 25˚C; (averaged data plotted, n = 9). Legend entries marked * contain data points reported in previous work (Hansen et al., 2021a; averaged data plotted, n = 6). Lines are for guiding purposes only.

Figure 4.4. Effect of protein:sucrose ratio [**A**] and PP content (%) [**B**] on the average particle size (μm) of dispersions at 25˚C; (averaged data plotted, n = 9). Legend entries marked * contain data points reported in previous work (Hansen et al., 2021a; averaged data plotted, n = 6). Lines are for guiding purposes only.

Figure 4.5. Particle size distributions of dispersions with 1.25 protein:sucrose ratios and 1.5% PP contents comprised of WPI, SPI, and PPI at 25˚C; (averaged data plotted, n = 9).

Figure 4.6. Optical light microscope images at 200x magnification depicting the microstructures of diluted feed dispersions with a 1.25 protein:sucrose ratio and 1.5% PP formulated with WPI (**A**), SPI (**B**), and PPI (**C**).

Figure 4.7. Optical light microscope images at 200x magnification depicting the microstructures of diluted feed dispersions with 1.0 SPI:sucrose with 0% (**A**), 0.5% (**B**), 1% (**C**), and 1.5% PP addition (**D**).

Figure 4.8. Optical light microscope images at 40x magnification depicting the microstructures of diluted feed dispersions with 1.0 PPI:sucrose with 0% (**A**), 0.5% (**B**), 1% (**C**), and 1.5% PP addition (**D**).

Figure 4.9. Image depicting the precipitated fractions (highlighted in boxes) of centrifuged 5x-diluted dispersions with 1.25 protein:sucrose and 1.5% PP with WPI (Left), SPI (Center), and PPI (Right).

Figure 4.10. Images depicting the precipitated fractions (highlighted in boxes) of centrifuged 5x-diluted dispersions with 1.25 SPI:sucrose (**A**) and 5:4 PPI:sucrose (**B**) and 0% (Left), 0.5% (Center, left), 1% (Center, right), and 1.5% PP addition (Right).

Figure 4.11. Effect of protein:sucrose ratio [**A**], protein isolate type [**B**], and PP content (%) [**C**] on the on the diameters (mm) of frozen drops formed from dispersions; (averaged data plotted, n = 9). Legend entries marked * contain data points reported in previous work (Hansen et al., 2021a; averaged data plotted, n = 3). Lines are for guiding purposes only [**A, B**]. Values connected by the same letter are not significantly different ($p > 0.05$).

Figure 5.1. Effect of bioactives content (%) [**A**] on the surface tensions (N/m) of dispersions at 25˚C (n=9); the effect of bioactives source [**B**] on the average surface tensions of all dispersions formulated with pure gallotannin, Aronia berry, beet, and cranberry extracts, respectively, at 25˚C; (n = 12 for gallotannin, Aronia, and beet dispersions, n = 9 for cranberry dispersions). Lines are for guiding purposes only [**A**]. Values connected by the same letter are not significantly different ($p > 0.05$).

Figure 5.2. The relationship between the surface tensions (N/m) of feed dispersions containing WPI:sucrose ratios of 1:0 and 1:1, bioactives contents of 0, 0.5, and 1%, and bioactives sources including pure gallotannin and Aronia berry, beet, and cranberry extracts at 25˚C, and calculated diameters (mm) of drops.

Figure 5.3. Effect of bioactives content (%) [**A**] on the average particle sizes (μm) of dispersions at 25˚C; the effect of bioactives source [**B**] on the average particle sizes (μm) of all dispersions comprised of pure gallotannin, Aronia berry, beet, and cranberry extracts, respectively, at 25˚C; (n = 9). Lines are for guiding purposes only [**A**]. Values connected by the same letter are not significantly different ($p > 0.05$).

Figure 5.4. Particle size distributions of feed dispersions comprised of 1:0 WPI:sucrose ratios with 0% bioactives and 1% bioactives from pure gallotannin, Aronia berry, beet, and cranberry extracts at 25˚C; (n = 9).

Figure 5.5. Optical light microscope images at 200x magnification depicting the microstructures of diluted feed dispersions with 1:0 WPI:sucrose with 0% bioactives (**A**), 0.5% bioactives (**B**), and 1% bioactives from cranberry extract (**C**).

Figure 5.6. Optical light microscope images at 200x magnification depicting the microstructures of diluted feed dispersions with 1:0 WPI:sucrose with 1% bioactives from pure gallotannin (**A**), Aronia berry extract (**B**), beet extract (**C**), and cranberry extract (**D**).

Figure 5.7. Effect of bioactives content (%) [**A**] on the complex viscosities (Pa*s) of dispersions at 25˚C; the effect of bioactives source [**B**] on the averaged complex viscosities of dispersions comprised of 1:0 and 1:1 WPI:sucrose with pure gallotannin, Aronia berry, beet, and cranberry extracts at 0.5 and 1% at 25˚C; (n = 9). Lines are for guiding purposes only [**A**]. Values connected by the same letter are not significantly different ($p > 0.05$).

Figure 5.8. Image depicting the precipitated fractions (highlighted in boxes) of 7 times diluted, centrifuged dispersions with 1:0 WPI:sucrose and 0% (Left), 0.5% (Center), and 1% bioactives (Right) from pure gallotannin [A], Aronia berry extract [B], beet extract [C], and cranberry extract [D].

Figure 5.9. Image depicting the precipitated fractions (highlighted in boxes) of 7 times diluted, centrifuged dispersions with 1:0 WPI:sucrose and 0% bioactives (Left) and 1% bioactives from pure gallotannin (Center, Left), Aronia berry extract (Center), beet extract (Center, Right), and cranberry extract (Left).

Figure 6.1. Modified freeze granulation process adapted to produce dry beads from concentrated liquid feed dispersions with varied WPI:sugar ratios, sugar types, polyphenols concentrations, and pH.

Figure 6.2. Schematic drawing of the cross-sectional structure of dry beads containing WPI, sugars, and Aronia extract after freeze drying; Inset: the proposed structure of the continuous glassy phase (not to scale).

Figure 6.3. Effect of WPI:sugar ratio [**A**] on the surface tensions (N/m) of dispersions at 25˚C; the effect of sugar type [**B**] on the average surface tensions of all dispersions comprised of maltitol, sucrose, and trehalose, respectively, at 25˚C; (n = 9). Open markers with dotted lines- 0% PP, filled markers with solid lines- 1% PP [**A**]; lines are for guiding purposes only [**A**]. Values connected by the same letter are not significantly different ($p > 0.05$).

Figure 6.4. The relationship between the surface tensions (N/m) of feed dispersions containing WPI:sugar ratios of 0, 0.75, 1.0, and 1.25, sugars including maltitol, sucrose, and trehalose, and polyphenols contents of 0 and 1%, at 25˚C and calculated diameters (mm) of drops.

Figure 6.5. Effect of WPI:sugar ratio [**A**] on the complex viscosities (Pa*s) of dispersions at 25˚C; the effect of sugar type [**B**] on the average complex viscosities of all dispersions comprised of maltitol, sucrose, and trehalose, respectively, at 25˚C; (n = 9). Open markers with dotted lines- 0% PP, filled markers with solid lines- 1% PP [**A**]; lines are for guiding purposes only [**A**]. Values connected by the same letter are not significantly different ($p > 0.05$).

Figure 6.6. Particle size distributions of feed dispersions comprised of 1.0 WPI:sucrose ratios with 0% and 1% PP, and 0.75 and 1.25 WPI:sucrose ratios with 1% PP at 25˚C; (n = 9).

Figure 6.7. Effect of WPI:sugar ratio [**A**] on the average particle sizes (μm) of dispersions at 25˚C; effect of sugar type [**B**] on the average particle sizes (μm) of all dispersions comprised of maltitol, sucrose, and trehalose, respectively, averaged together at 25˚C; (n = 9). Open markers with dotted lines- 0% PP, filled markers with solid lines- 1% PP [**A**]; lines are for guiding purposes only [**A**]. Values connected by the same letter are not significantly different ($p > 0.05$).

Figure 6.8. Optical light microscope images at 200x magnification depicting the microstructures of diluted feed dispersions with 1.0 WPI:sucrose with 0% PP (**A**) and 1% PP (**B**).

Figure 6.9. Image depicting the precipitated fractions (highlighted in boxes) of centrifuged dispersions with 1.0 WPI:sucrose with 0% PP (Left) and 1% PP (Right).

Figure 6.10. Effect of WPI:sugar ratio [**A**] on the glass transition onset temperatures (˚C) of beads; the effect of sugar type [**B**] on the average glass transition onset temperatures (˚C) of all dried beads comprised of maltitol, sucrose, and trehalose, respectively, at 25˚C; (n = 9). Values connected by the same letter are not significantly different ($p > 0.05$).

Figure 6.11. Effect of WPI:sugar ratio [**A**] on the hardness (N) of dried beads at 25˚C; the effect of sugar type [**B**] on the average hardness values of all dried beads comprised of maltitol, sucrose, and trehalose, respectively, at 25˚C; (n = 9). Open markers with dotted lines- 0% PP, filled markers with solid lines- 1% PP [**A**]; lines are for guiding purposes only [**A**]. Values connected by the same letter are not significantly different ($p > 0.05$).

Figure 7. Schematic state diagram of sucrose overlaid with the modified bead formation method presented in Chapter 6.

Tables

Table 2.1. Feed formulations with WPI and sucrose concentrations (% w/w) as well as pH.

Table 2.2. Composition of liquid feeds chosen for bead formation.

Table 2.3. Water activity (a_w) of intermediate, fresh beads prior to drying.

Table 2.4. Composition and a_w of final, dried beads.

Table 2.5. Total solids, viscosity, and surface tension data for feed dispersions that formed beads; n = 3.

Table 2.6. Total volumes (cm^3) and true densities (g/cm^3) of dried drops comprised of 40% WPI with 10% sucrose (40/10) obtained at various heating times (min) at 100°C; values were used to calculate average total volumes and average solids volumes (cm^3), respectively, in order to calculate porosity (%).

Table 3.1. Estimated drop diameters calculated from flow tests data and measured diameters (mm) of frozen drops formed from feed dispersions with varied WPI:sucrose, total solids contents, polyphenols concentrations, and pH.

Table 4.1. Density and estimated drop diameters measured and calculated from flow tests data and measured diameters (mm) of frozen drops (averaged data reported, n = 9) formed from feed dispersions with varied protein:sucrose, protein isolates, polyphenols (PP) concentrations, and pH.

Table 4.2. Water hydration capacity of WPI, SPI (hydrolyzed), and PPI powders, reported as grams of water absorbed per gram of protein isolate powder.

Table 5.1. Density and estimated drop diameters from flow tests data and measured diameters (mm) of frozen drops formed from feed dispersions with varied WPI:sucrose, bioactives sources and concentrations, and pH.

Table 6.1. Formulations, pH, and estimated drop diameters (mm) calculated from flow tests data for liquid dispersions with varied WPI:sugar ratios, sugar types, and polyphenols concentrations, as well as water activity (a_w), water content (%), T_g midpoint, and measured diameters of dried drops formed from dispersions.

Introduction

Consumer demand for ‘foods for health’ has driven the development of functional foods, sources of high nutritional value and delivery vehicles for bioactive compounds linked to health benefits. Proteins and carbohydrates are popular food macromolecules used to form structures with diverse functional properties and encapsulation abilities, and interactions formed upon blending provide synergistic stabilizing effects. Mixing structure forming proteins with bioactive compounds intended for encapsulation, such as plant polyphenols, is known to result in the formation of weak, non-covalent complexation interactions under ambient temperatures and neutral or acidic pH conditions. The formation of complexes in mixtures has been reported to affect the physico-chemical properties of mixtures, although more extensive research has been conducted to examine the effects of covalent conjugation on mixtures (Schneider, 2016; Cao and Xiong, 2017; Ma and Zhao, 2019; Xue et al., 2020).

A key objective of this study was the development and presentation of continuous processes for forming concentrated protein-carbohydrate feed dispersions into solid, stable bead structures with the potential for bioactives encapsulation, as we hypothesized that such novel processes could be developed. Even small compositional shifts can alter the physical properties of dispersions including surface tension, particle size, and viscosity, all of which determine the ability of a feed to form drops. We hypothesized that changes in formulation compositions would result in alterations of the physical properties of feed dispersions and resulting dry beads. As such, another key theme explored in this thesis was the effects of compositional changes including varied total solids, protein:carbohydrate ratios, bioactives contents, protein isolates with different purities and structures, carbohydrate types, and bioactives sources with diverse

structures and sizes of predominant compounds on the physico-chemical properties of feed dispersions. Additionally, we aimed to study the effects of formulation composition on the physical properties of solid beads formed from feed dispersions.

The present thesis presents two processes for the formation of dry beads with high protein contents and good physical stabilities, with potential for the entrapment of flavors, emulsion droplets, bioactives, and colors. In addition to providing information on the physico-chemical properties of concentrated dispersions in general, this work also presents data describing the effects of mixing proteins with bioactive compounds on the physical properties of dispersions. Effects observed contribute to the exploration of the physico-chemical effects of non-covalent complexation interactions between proteins and bioactives under certain conditions. Findings reported in this thesis may be relevant for the formulation of high protein functional foods containing bioactives, such as nutritional bars, sports beverages, smoothies, yogurts, and frozen desserts.

Chapter 1

Literature review

Mackenzie M. Hansen

Table of contents

1. **Introduction** 25

2. **Encapsulation in food applications** 26

2.1. *Forming structures with proteins and carbohydrates* 27

2.1.1. *Proteins as functional materials* 27

2.1.1.1. *Whey proteins: structure and functionality* 27

2.1.2. *Carbohydrate functionality: formation of glassy matrices for entrapment* 29

2.1.2.1. *Stability of glassy carbohydrate matrices* 29

2.1.2.2. *Water content effects on T_g* 31

2.1.3. *Stabilization in mixed protein-carbohydrate glassy matrices* 31

3. **Formulating with polyphenols** 34

3.1. *Polyphenols as health-promoting compounds* 34

3.2. *Instability of polyphenols* 35

3.3. *Encapsulation for protection of polyphenols* 36

4. **Non-covalent interactions between polyphenols and proteins** 38

4.1. Formation of non-covalent interactions 38

4.2. Factors affecting non-covalent protein-polyphenol interactions 40

4.3. Effects of non-covalent protein-polyphenol interactions 42

4.3.1. Structural effects 42

4.3.2. Effects on the physico-chemical properties of mixtures 43

4.3.2.1. Effects on particle size distribution of dispersions 43

4.3.2.2. Effects on viscosities of dispersions 45

4.4. *Effects on the physical properties of food products* 46

5. **Conclusions** 49

1. Introduction

Functional foods possess high nutritional value and serve as delivery vehicles for active ingredients associated with positive health outcomes. Demand for the development of such products has grown in recent years as consumer interest in foods for health has increased (Kapsak et al., 2011). Proteins and carbohydrates are two of the most common macromolecules found in foods, and have demonstrated their versatility and functionality in a wide variety of food products (Kulmyrzaev et al., 2000; Livney, 2010; Zhou and Roos, 2012). They are popular choices when selecting wall materials for encapsulation of sensitive bioactive compounds, and their interactions formed upon blending have been reported to impart synergistic stabilization on structures formed (López-Díez and Bone, 2000; Chang and Pikal, 2009; Wang et al., 2009b; Ohtake et al., 2011; Mensink et al., 2017). Combining bioactive compounds, such as polyphenols from fruits and vegetables, with proteins in mixtures can result in the formation of weak, non-covalent complexation interactions between constituents under certain conditions (Hagerman and Butler, 1981; Foegeding et al., 2017). Protein-polyphenol complex formation in mixtures is reported to impact a number of physical properties including viscosities and particle sizes (Harbourne et al., 2011; Thongkaew et al., 2014; Schneider, 2016). Comprehensive knowledge of component properties and awareness of their propensities for interactions with other constituents in mixtures are critical for thoughtful product formulation. Thoughtful formulation, coupled with careful selection of processing parameters, can be utilized for the strategic development of food structures designed to have specific functional properties. This literature review will introduce the concept of encapsulation in foods and explain the strengths of proteins and carbohydrates as stabilizing materials, particularly in the context of encapsulating plant polyphenols. Non-covalent protein-polyphenol complexation interactions occurring naturally in

mixed systems will also be covered, detailing the factors affecting interactions as well as the impact of complexation on the physico-chemical properties of mixtures.

2. Encapsulation in food applications

Encapsulation aims at entrapment of an active inner material within a protective outer material, and includes forming particles with diameters ranging from a few nm to a few mm (Zuidam and Nedovic, 2010). Encapsulation technologies should be simple, continuous, and preserving to be successful. Benefits of encapsulation relevant to the food industry include the stabilization of sensitive materials, flavor masking and dilution of core materials, separation of reactive compounds, and controlled release of sensitive core materials (Desai and Park, 2005; Bleiel et al., 2017). Multiple types of encapsulation structures exist, including reservoir, matrix, and coated matrix (**Figure 1**). Reservoirs have a capsule layer of wall material surrounding the inner substance. Matrix types have the active substance dispersed across the wall matrix, with active sometimes being found at the surface of particles. The coated matrix type is a combination of the other two encapsulates, where there is an additional capsule wall layer around the matrix 'core' (Lakkis, 2016). Methods of encapsulation currently utilized in food production include drying methods such as (but not limited to) spray drying, freeze-drying, extrusion, and fluidized bed drying, formation of wet systems such as gels or emulsions through methods such as injection, and novel techniques like liposomes, crystallization, and coacervation. Wall matrices are often formed by varying combinations of food materials including proteins, fats, polysaccharides such as maltodextrins, sugars and other sweeteners, and other hydrocolloids and low molecular weight surfactants (Bleiel et al., 2017).

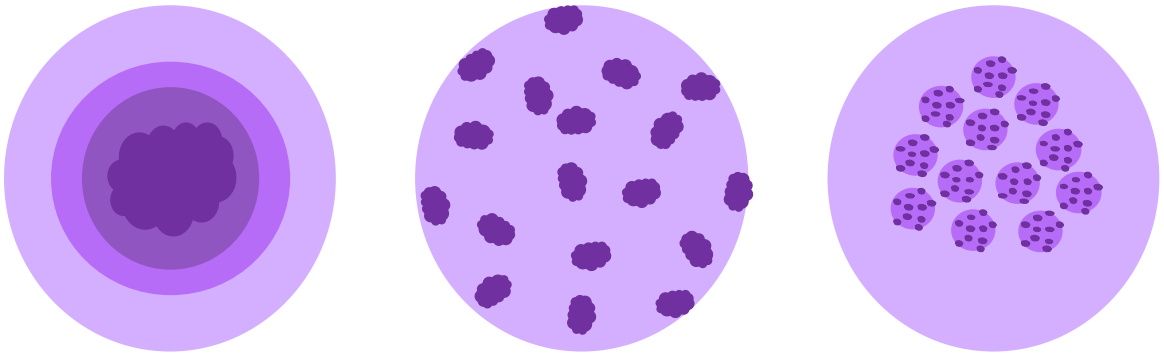


Figure 1. Schematic drawings of common encapsulation structures: reservoir (Left), matrix (Center), and coated matrix systems (Right), adapted from Lakkis et al. (2016).

2.1. Forming structures with proteins and carbohydrates

2.1.1. Proteins as functional materials

Proteins are some of the most widely-utilized molecules to manipulate and engineer structural properties of food products by cross-linking and aggregation due to their nutritional and technical functionality (Gerrard, 2002; Purwanti et al., 2010). As polymers of amino acids, functional properties of proteins are determined by the molecular characteristics of the amino acid monomers that make up the chain (McClements, 2002; McClements et al., 2009). The conformation of native proteins, then, is determined by a balance of the interactions within the molecule including hydrophobic interactions, electrostatic interactions, hydrogen bonding, van der Waals forces, and configurational entropy (McClements, 2002; McClements et al., 2009; Semenova and Dickinson, 2010).

2.1.1.1 Whey proteins: structure and functionality

Bovine whey proteins are a popular choice when aiming to develop new textures, structures, functions, and products in food (Kulmyrzaev et al., 2000), and serve as natural carriers for bioactives (Livney, 2010). While there are numerous minor constituent proteins that

are classified as whey proteins, the bulk of whey protein functionality is driven by the properties of ß-lactoglobulin and α-lactalbumin proteins. These two proteins constitute about 80% of total whey proteins in milk, with ~55% attributed to ß-lactoglobulin alone (Fennema, 2017). These proteins possess typical, native globular protein structures: compact and relatively spherical in shape, with a physically and chemically heterogeneous external surface and a dense, well-defined secondary and ternary structure (McClements, 2002; Nicolai and Durand, 2013). Both protein structures tend to have a uniform distribution of hydrophobic, polar, and charged residues across their chains, causing them to take up an intermolecularly-folded structure to bury the hydrophobic residues to avoid self-association with other protein molecules (Fennema, 2017). It is most thermodynamically favorable for the proteins to adopt a compact conformation with hydrophobic groups located within the interior of the structure to avoid contact with water, while the hydrophilic groups are located on the exterior of the structure to better engage and complex with the water (McClements, 2002).

Derived from milk and often a by-product of cheese manufacture, whey proteins are often utilized for their nutritional contribution as well as wide range of functional properties including (but not limited to) solubility, foaming, emulsifying, viscosity enhancement, and gelation (Verheul and Roefs, 1998). Of particular interest is their ability to form gels under a number of environmental conditions including pH adjustment, addition of ions, and thermal treatment (Kulmyrzaev et al., 2000). All gelation processes require is at least partial unfolding of proteins from their native state in order to denature and form aggregates- the beginning of a 3-D network of proteins interacting with both themselves and each other on a molecular level. For all of these reasons, whey proteins are considered to be effective and versatile wall materials for encapsulation of both hydrophobic and hydrophilic bioactives, and are able to be used in

combination with other food ingredients or alone for microencapsulation in foods (Livney, 2010; Augustin and Oliver, 2014; Quan et al., 2019).

2.1.2 Carbohydrate functionality: formation of glassy matrices for entrapment

Sugars and other carbohydrates can be found as crystalline or amorphous (glassy) solids in foods, depending on product formulation, processing, and storage conditions. Amorphous sugar glasses are not strictly defined or ordered like that of the crystalline state. This structural disorder allows glasses formed to accommodate 'impurities' in the matrices including other molecules, volatiles, and bioactives, demonstrating the entrapment abilities of glassy carbohydrates and their ability to serve as encapsulant materials for stabilization (Zhou and Roos, 2012). Such compounds can be dispersed throughout the glassy matrix and released continuously upon consumption, but would be kicked out of crystalline structures due to limited free volume, with the majority of 'impurities' collecting at the surface of crystals or in small gaps between individual crystals (Williams et al., 1955; To and Flink, 1978b; Hartel et al., 2018).

2.1.2.1 Stability of glassy carbohydrate matrices

Sugar and other carbohydrate glasses are metastable materials that may retain desirable properties and entrapped compounds over extended time periods, as long as they are stored under proper conditions (Hartel et al., 2018). Glass stability is related to its glass transition temperature (T_g) range, where a glassy phase transitions to a rubbery or syrupy state, and is affected by product composition and water content (Ergun et al., 2010). Different carbohydrates possess a diverse array of properties and glass transition temperatures (T_g). Generally, sugar glasses have higher stabilities when their T_g are greater than ambient temperature (White and Cakebread, 1966; Kawai and Suzuki, 2007; Roos and Drusch, 2015; Hartel et al., 2018). Under these conditions, degradation mechanisms including flavor loss, stickiness, sugar crystallization, and

cold flow may be regulated, and rates of diffusion-based deterioration mechanisms may be diminished more successfully (Ergun et al., 2010; Roos, 2020). Imamura et al. (2002, 2003) explained that glass transition of an amorphous solid results from breaks in intermolecular interactions holding the matrix due to thermal vibrations, and thus T_g is determined by the strength of interactions forming the glassy matrix. Understanding how sensitive carbohydrate glasses are to changes in water and temperature, proper storage conditions are critical to maintaining the integrity of the glassy state and the texture imparted on the product against environmentally-driven phase transitions (Islesias and Chirife, 1978).

When exposed to high temperatures above T_g and/or high relative humidity conditions, freeze-dried carbohydrate matrices can undergo structural transitions, collapse, and plasticization of amorphous structures, as well as crystallization of sugars, associated with increased molecular mobility, reduced viscosity, and increased reaction rates (To and Flink, 1978b; Roos and Karel, 1991d; te Booy et al., 1992; Souillac et al., 2002a). Changes controlled by glass transition, including collapse and recrystallization, have resulted in the reduced stability of active compounds and lower entrapment abilities in the dry state (To and Flink, 1978c). Foods formulated with different carbohydrates would be expected to exhibit a variety of physico-chemical characteristics unique to their respective carbohydrate compositions; glasses formed from carbohydrates with higher T_g would be more likely to maintain stability as encapsulants under ambient conditions compared to those made from carbohydrates with lower T_g (Roos, 2010).

2.1.2.2 Water content effects on T_g

It has been observed that sugar glasses tend to be very unstable in the presence of water, with T_g decreasing even with small increases in water content to below room temperature due to plasticization by water and the resulting increase in free volume, where resulting instability can lead to various defects in amorphous products such as caking and stickiness (White and Cakebread, 1966; Roos, 1987; Roos and Karel, 1991c, d; te Booy et al., 1992; Imamura et al., 2002; Lu et al., 2007; Pikal et al., 2007; Ergun et al., 2010; Yu and Li, 2012; Hartel et al., 2018). In theory, T_g of the pure amorphous sugar decreases towards the theoretical T_g of pure water as water content increases due to environmental uptake. The hygroscopicity of sugar glasses can lead to enhanced water pick up, resulting in decreased viscosities and the liquefication or crystallization of sugars present; Roos and Karel (1991b) reported that viscosity at the endpoint of T_g and associated onset of stickiness would be close to 10^7 Pa*s. Ergun et al. (2010) explained that the end of shelf life for a product is often due to problems with water loss or uptake, followed by subsequent changes in textural and other properties, so control of these processes during storage is critical for preserving desired product properties.

2.1.3 Stabilization in mixed protein-carbohydrate glassy matrices

Synergistic stabilizing effects are known to occur between proteins and carbohydrates in dried mixtures during storage (López-Díez and Bone, 2000; Chang and Pikal, 2009; Wang et al., 2009b; Ohtake et al., 2011; Mensink et al., 2017). In addition to bioactive compounds and flavors, amorphous sugar matrices also embed proteins due to their high structural flexibility, where proteins may then form hydrogen bonds with surrounding sugar molecules and impart higher orders of structure and stabilization during processing as well as long-term storage (Meister and Gieseler, 2009; Povey et al., 2009). When high molecular mass carbohydrates,

gums, starches, proteins, and other substances are mixed with sucrose and other small molecular mass carbohydrates to form glassy matrices in biomedical, food, pharmaceutical applications, the resulting T_g of glassy mixtures are notably higher than those of pure sugar glasses (Imamura et al., 1998; Yoshioka et al., 2011). In binary systems of sugars and higher molecular mass substances, three types of intermolecular interactions are possible: hydrogen bonds between sugar molecules, between sugars and other constituents, and between constituent molecules. At low quantities of other substances, sugar-sugar and sugar-non-sugar hydrogen bonds are dominant; when other components content increases, non-sugar-non-sugar interactions become more significant while sugar-sugar hydrogen bonds decrease notably until largely disappearing (Imamura et al., 2010). Weak sugar-sugar interactions present in carbohydrates with low T_g are easily broken and replaced by protein-sugar interactions (Soltanizadeh et al., 2014).

Mixtures with higher sugar contents were found to have more sugar-sugar interactions, resulting in phase separation of the mixtures due to preferential exclusion and reduced total protein-sucrose contacts for interaction and protein protection upon drying (Tzannis and Prestrelski, 1999). Imamura et al. (2002) reported that when dextran contents increased above a certain level in amorphous sugar-dextran mixtures, the number of dextran-dextran interactions increased and became predominant in the matrices rather than sucrose-dextran interactions, causing a remarkable increase in T_g due to the higher strength interactions compared to sucrose-sucrose interactions. They also reported that dried sucrose-dextran mixtures adsorbed less water than the individual dry components, suggesting that fewer sites were available for water interactions on dextran molecules due to sucrose interactions occupying some hydration sites (Imamura et al., 2002). Later, they noted that preservation effects of sugar on protein secondary structures embedded within generally increased with increasing amounts of sugar up to a certain

level, but excess addition resulted in lowering of protein stability, likely due to the dominance of sugar-sugar interactions over protective protein-sugar interactions and leading to collapse in samples (Imamura et al., 2003).

In mixed amorphous matrices, the lower molecular mass components present (sugars) largely contribute to the stabilization of proteins during the freeze-drying process as well as during storage, and the high molecular weight components (proteins) improve the overall physical stability of the amorphous matrix during storage (Souillac et al., 2002b; Imamura et al., 2003; Chang et al., 2005; Nilsson and Larsson, 2007; Wang et al., 2009a, b). When lactate dehydrogenase was formulated with disaccharides, enzymatic activity was almost fully maintained in storage, independent of stabilizer type and water content, and it has been reported that protein preservation in freeze-thawed formulations was enhanced as protein concentration increased due to the self-protection activity of proteins (Kawai and Suzuki, 2007). Regarding potential mechanisms of mixture stabilization, Meister and Gieseler (2009) suggested that, considering the differences in molecular size between the proteins and sugars used in their experiments, it may be possible that at low sugar and high protein concentrations, small sugar molecules act as ‘gap fillers’ between and interact with protein molecules. Similarly, Wang et al. (2009a, b) reported that sucrose molecules may act to decrease the fractional free volume of freeze-dried protein-sugar systems by filling voids left between larger protein molecules, ultimately improving protein stability by reducing mobility. It is critical that the stabilizing sugars remain glassy during freeze-drying and subsequent storage to be effective cryoprotectants and further stabilize proteins upon storage, as crystallization or phase separation would impair the sugar’s stabilizing effects on the proteins (Jena et al., 2017).

Additionally, the process of crystallization tends to be delayed compared to pure sucrose and other sugars when high molecular mass compounds such as proteins are blended into the matrices, which may be attributed to interactions between the components and increased medium viscosity slowing molecular mobility (Islesias and Chirife, 1978; To and Flink, 1978b; te Booy et al., 1992; Souillac et al., 2002a; Liao et al., 2005; Roe and Labuza, 2005). Increasing protein contents in dried protein-sugar mixtures (exceeding ~30-50% of matrix composition) have been reported to increase mixture T_g values and stabilities, and significantly delay or inhibit crystallization, even when stored under high relative humidity; in contrast, higher sugar contents resulted in reduced mixture T_g values and facilitated water-induced crystallization (Sarciaux and Hageman, 1997; Tzannis and Prestrelski, 1999). Heljo et al. (2011) reported that even very small amounts of protein, such as a 40:1 mass ratio of sucrose to β-galactosidase, inhibited sucrose crystallization in freeze-dried mixtures upon storage at 45˚C for 90 days.

3. Formulating with polyphenols

3.1. Polyphenols as health-promoting compounds

Many studies have been published reporting health-supportive benefits of plant polyphenols (PP). While low levels of PP can be delivered into our diets via fruit, juice, and tea consumption, concentrated extracts provide a way to enhance delivery in foods at higher levels (Schneider, 2016). This awareness motivates developers to create foods with these compounds, in the hopes of delivering enhanced health benefits for consumers in addition to nutritional value (Ćujić et al., 2018). Aronia berries and their juices are reported to have high antioxidant capacities compared to other berries and fruits (Kulling and Rawel, 2008), and are an abundant source of PP including anthocyanins, flavonoids, and proanthocyanidins (Taheri et al., 2013; Xie et al., 2016, 2017). This knowledge makes Aronia a source of interest for incorporation of PP

into food products to maximize potential health impacts. Anthocyanins have been reported to exhibit strong anti-oxidant and anti-inflammatory activities, which aid in the prevention and mitigation of symptoms of numerous disorders and diseases (Yousuf et al., 2016; Khoo et al., 2017; Li et al., 2017). Work by Simeonov et al. (2002) indicated that Aronia anthocyanins and other PP may aid in Type II diabetes control. Additionally, berries and extracts have been reported to exhibit protective and anti-proliferative effects against colon cancer in numerous studies (Malik et al., 2003; Zhao et al., 2004; Bermudez-Soto et al., 2007). Experiments involving rats and humans demonstrated that Aronia juice aided to reduce and maintain healthy levels of serum cholesterol (Valcheva-Kuzmanova et al., 2007a; b; c). Additional research has indicated that Aronia juice decreases oxidative stress and may be useful in obesity disorder treatments (Zielińska-Przyjemska et al., 2007). Anthocyanins and other PP from Aronia scavenge free radicals and have demonstrated hepatoprotective effects as well (Kulling and Rawel, 2008).

3.2. Instability of polyphenols

Polyphenolic compounds are highly unstable and degrade easily during storage, illustrating the need for protective measures in order to successfully deliver the compounds into human diets and impart health benefits (Mazza and Brouillard, 1987; Francis and Markakis, 1989; Volf et al., 2014). PP stability is affected by environmental conditions including exposure to light, temperature, and oxygen, compositional factors such as solvent, pH, water activity, ionic strength, the presence of metals, acids, sugars, or enzymes in mixtures, and interactions occurring between constituents in formulations, as well as their own concentrations and molecular structures (Mazza and Brouillard, 1990; Rodriguez-Saona et al., 1999; Friedman and Jürgens, 2000; Bąkowska et al., 2003; Castañeda-Ovando et al., 2009). Anthocyanins are

reported to be highly unstable in food matrices, and while beyond the scope of this review, the dissertation "*Copigmentation reactions and color stability of berry anthocyanins*" submitted by Maarit Rein (2005) thoroughly describes the mechanisms for destabilizing effects on anthocyanins. Polyphenolic stability under a variety of conditions remains a critical consideration to ensure that bioactivities, structural properties, and concentrations are maintained throughout formulation and processing and delivered to consumers via the final product (Castañeda-Ovando et al., 2009; Volf et al., 2014).

3.3 Encapsulation for protection of polyphenols

Due to the instability of isolated PP, protective measures such as encapsulation must be taken to ensure improved stability in formulated products (Fang and Bhandari, 2010; Ozdal et al., 2013; Schneider, 2016). Cai and Corke (2000) reported that freeze-drying is the best way to dry sensitive PP, but spray drying may be a less costly alternative for powder formation. Many studies have demonstrated retention of PP derived from numerous sources when spray dried with a variety of wall materials (Ersus and Yurdagel, 2007; Obón et al., 2009; Robert et al., 2010; Tonon et al., 2010; Fang and Bhandari, 2011; Bakowska-Barczak and Kolodziejczyk, 2011; Pang et al., 2014). When a mixture of grape and peach juices was combined with milk and spray dried to form a powder, a glassy product was formed with a T_g higher than that of a commercial milk powder control, experiencing less structural collapse and enhanced stability of proteins against denaturation during storage, indicating the ability of milk proteins to act as carriers (Afifi et al., 2009). Fang and Bhandari (2012) investigated the efficiency of WPI versus maltodextrin (MD) on spray drying bayberry juice, reporting that less WPI was required for good powder recovery. They attributed the drying efficiency of WPI to its surface-active properties and migration to the air/water interface to form films at droplet surfaces upon drying. Further

analysis indicated that ~60% of particle surfaces were covered with WPI proteins (T_g of ~150˚C), and as such powders were not sticky because particle surfaces could maintain the glassy state despite low bulk T_g measurements (~14-15.5˚C at 22% RH) reflecting the T_g of bayberry solids (Fang and Bhandari, 2012). Du et al. (2014), when attempting to spray dry persimmon pulp, observed that low levels of whey proteins were more effective wall materials than larger quantities of MD and other carriers because of their ability to modify particle surfaces to avoid stickiness. Moser et al. (2017) found that spray drying grape juice with higher concentrations of blended carriers including whey and soy proteins with MD resulted in higher yields, better powder properties, and increased anthocyanin retention, and later reported that powders encapsulated in a blended matrix of SPI and MD maintained higher stability than whey protein-MD matrices (Moser et al., 2018).

Using encapsulation technologies to form complexes between PP and protectant macromolecules such as proteins has also gained popularity (Chen et al., 2006; Livney, 2010; Chung et al., 2015; Schneider, 2016; Cao and Xiong, 2017; Quan et al., 2019). Laine et al. (2008) formed complexes between cloudberry PP and a variety of maltodextrins and subsequently freeze-dried them into powders. Roopchand et al. (2013) complexed Concord grape pomace PP with soy protein isolate (SPI) in liquid mixtures, dried by mixing then tray drying, and formed a product that could be milled into powder. Correia et al. (2017) produced powders comprised of wild blueberry PP-protein complexes with multiple drying methods: spray drying, freeze-drying, and vacuum oven drying, ultimately determining spray drying to be the best option. In many cases, positive outcomes have been reported for the stability of proteins and/or PP in complexed formulations, imparting greater protection and sometimes PP color retention

(Viljanen et al., 2005; von Staszewski et al., 2011; Schneider, 2016; Cao and Xiong, 2017; Ma and Zhao, 2019; Quan et al., 2019; Zhao et al., 2020; Baba et al., 2021).

4. Non-covalent interactions between polyphenols and proteins

4.1. Formation of non-covalent interactions

Proteins and polyphenols are reported to possess an inherent, mutual attraction that may substantiate in the formation of protein-PP complexes and can grow into insoluble aggregates, as long as threshold levels of PP are present for protein precipitation (Hagerman and Butler, 1978; von Staszewski et al., 2011; Foegeding et al., 2017). While covalent conjugation interactions are also known to occur between proteins and PP under certain conditions in food matrices and may occur simultaneously, non-covalent interactions occurring under neutral and acidic pH conditions are of particular interest in this review, as they commonly occur in processed food products (Rawel et al., 2005). Generally weak interactions- primarily hydrogen bonding and hydrophobic interactions- as well as van der Waal's forces can result in non-covalent complex formation due to interactions between different groups on the protein and PP structures, as demonstrated in **Figure 2** (Rawel et al., 2005; Gad and El-Salam, 2010; Kanakis et al., 2011; Bohin et al., 2012; Le Bourvellec and Renard, 2012; Chung et al., 2015; Schneider, 2016; Oancea et al., 2017; Girard and Awika, 2020; Zhao et al., 2020). Hydrogen bonds often form when groups on PP structures act as hydrogen donors for carboxyl groups on proteins (Buitimea-Cantúa et al., 2018; Quan et al., 2019), as well as between PP hydroxyl groups and hydroxyl and/or amino groups on protein structures (Yildirim-Elikoglu and Erdem, 2018; Quan et al., 2019). Non-covalent complexation is also known to occur via hydrophobic interactions between

nonpolar aromatic rings on PP and hydrophobic amino acid groups on protein structures (Kanakis et al., 2011; Ozdal et al., 2013; Quan et al., 2019).

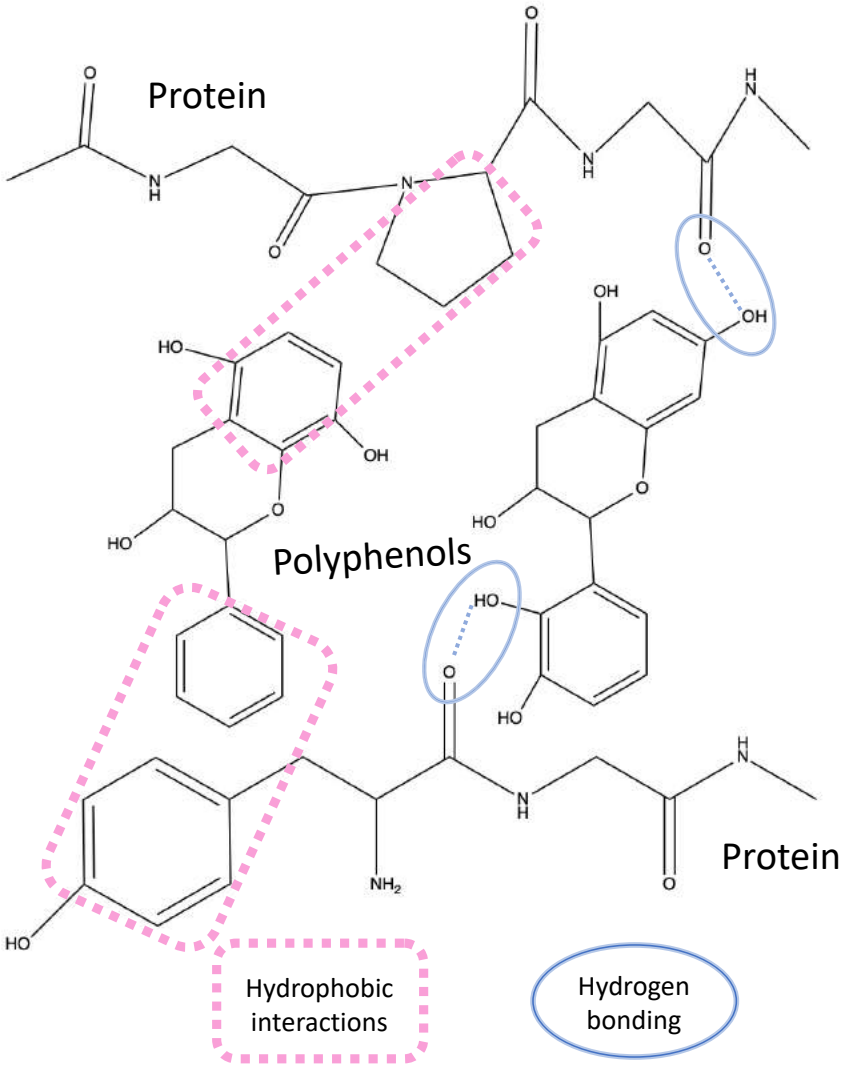


Figure 2. Primary interactions (hydrophobic interactions and hydrogen bonding) driving non-covalent complexation between proteins and polyphenols in mixtures, adapted from Quan et al. (2019) and Li et al. (2021).

At low concentrations, polyphenols (relatively small molecules compared to protein structures) have been reported to interact non-covalently with proteins at multiple sites and bind to form small, soluble complexes (Spencer et al., 1988; Charlton et al., 2002; Rawel et al., 2005;

Ozdal et al., 2013). Complexation interactions continue to form with increasing [PP] until PP act as bridges for protein cross-linking to form larger, hydrophobic aggregates, as demonstrated in **Figure 3** (Spencer et al., 1988; Charlton et al., 2002; Rawel et al., 2005; Ozdal et al., 2013).

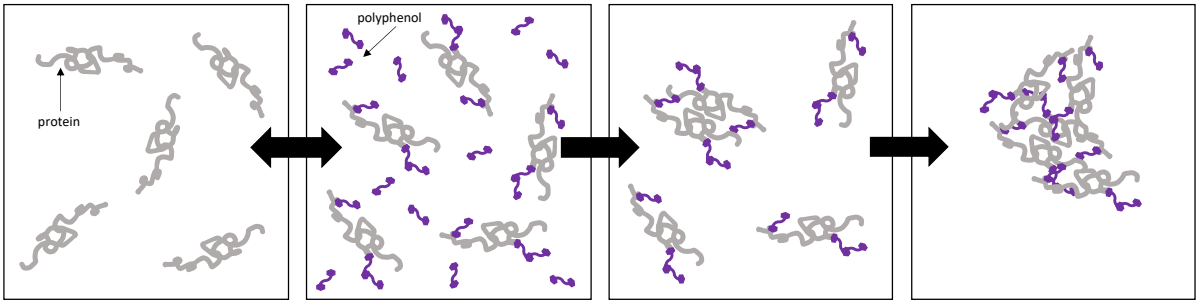


Figure 3. Schematic drawings depicting the non-covalent binding of polyphenols to proteins in solution, the formation and growth of aggregates, and ultimate precipitation of large, insoluble protein-polyphenol complexes, adapted from Charlton et al. (2002).

4.2 Factors affecting non-covalent protein-polyphenol interactions

Three critical properties of polyphenols were listed by Spencer et al. (1988) as essential for successful complexation with proteins: (i) molecular size, (ii) conformational flexibility, and (iii) water solubility. Highly polymerized PP (having larger molecular sizes) with high conformational flexibility generally form greater numbers of strong protein-PP interactions when more hydroxyl groups and hydrophobic regions are present and available for hydrogen bonding and hydrophobic interactions with proteins (Hagerman, 1989; Harbertson et al., 2014; Ropiak et al., 2017; Quan et al., 2019; Girard and Awika, 2020). Findings reported by Uekusa et al. (2008) were generally in agreement, indicating that the amount of phenol incorporated into hydrophobic liposomes was dependent on polyphenolic chemical structure and affinity for lipophilic membranes. Studies by Girard et al. (2018) showed similar observations: higher molecular mass PP had greater binding affinities for wheat gluten proteins, perhaps due to enhanced

opportunities for cross-linking provided by an increased presence of hydroxyl groups and hydrophobic regions in close proximity in larger PP, with potential for complexation with carbonyl groups and hydrophobic amino acids of proteins. Studies by Bayraktar et al. (2019) reported that thermally denatured whey proteins may increase the binding capacity in protein-PP systems, as protein conformations may expose side groups available for more interactions. Proteins from different sources have diverse surface characteristics, determined by their amino acid compositions, isoelectric points, and hydrophobicities of their folded structures; these properties impact the extent of protein-PP interactions that may occur in a system (Ozdal et al., 2013; Quan et al., 2019). Environmental pH, temperature, protein and PP varieties and concentrations, and reaction times are also reported to affect interactions (Thongkaew et al., 2014; Schneider, 2016; Quan et al., 2019).

Polyphenols are most likely to interact with proteins at optimum pH values near a protein's isoelectric point (pI), where net charges of complexes are minimal, suggesting the significance of hydrophobic interactions in binding (Spencer et al., 1988; Harbourne et al., 2011). Reduced binding affinities at other pH values are likely due to pH-dependent changes in protein structures, causing reduced numbers of binding sites for phenols, and leading to more insoluble complex precipitates (Rawel et al., 2005; Harbourne et al., 2011; von Staszewski et al., 2011). Fuhrmann et al. (2019) also attributed the induction of protein-PP complexes to the attractive, non-covalent π–π stacking of aromatic rings, in addition to the other interactions mentioned. von Staszweski et al. (2011) reported that precipitation and particle size of precipitates are pH-dependent, with low system stabilities at lower pH values explained by low zeta potentials. This is in agreement with later findings by Thongkaew et al. (2014) reporting that protein precipitation capacity via polyphenolic addition depends on pH. Quan et al. (2019) add

that since pH impacts protein conformation as well as PP structure, it also determines the covalent/non-covalent nature of complexation interactions occurring.

4.3 Effects of non-covalent protein-polyphenol interactions

4.3.1 Structural effects

Non-covalent complexation interactions between proteins and PP have been reported to alter secondary and ternary structures of proteins in dispersions as well as their hydrodynamic volumes (Rawel et al., 2005; Song, 2009; Bandyopadhyay et al., 2012; Cao and Xiong, 2017; Girard et al., 2018; Ma and Zhao, 2019; Martínez et al., 2019; Sęczyk et al., 2019; Zhao et al., 2020). These changes lead to rearrangements in conformations and folding of proteins, determining their surface properties depending on the amino acid residues exposed (Schneider, 2016; Quan et al., 2019).

While investigating complex formation between tea PP and milk β-lactoglobulin, Kanakis et al. (2011) reported that weak binding observed in solution stabilized protein secondary structures by increasing β-sheets and α-helices. Bohin et al. (2012) explained the weak binding phenomenon observed in earlier studies, stating that amino acid residues in folded globular proteins may have limited accessibility for binding with PP, resulting in lower volumes of interactions. Work by Cao and Xiong (2017) reported that both gallic acid and epigallocatechin gallate PP compounds also caused significant structural changes to WPI at ambient temperatures and neutral pH due to complexation interactions. Significant alterations in soy protein secondary structures were observed upon mixing with anthocyanins, with increases in α-helices and decreases in β-sheets (Sui et al., 2018; Zhang et al., 2018). Authors suggested that anthocyanins bind to the same sites that connect proteins to their own structures and break upon denaturation (hydrogen bonds) to form new bonds with other proteins and sugars, so the nature of

anthocyanin-protein bonds are likely similar to those formed between proteins and sugars or other proteins. Anthocyanins led to reduced thiol groups within SPI, with continued reductions as anthocyanin content increased; the decrease in thiol groups was attributed to protein interactions with the numerous hydroxyl groups on anthocyanin structures, and decreased fluorescence intensity in complexes suggested strong interactions between SPI and anthocyanins (Sui et al., 2018). Ma and Zhao (2019) reported that non-covalent complex formation between commercial WPI and galangin and genistein PP at neutral pH also resulted in changes to the secondary structures of whey proteins, driven mainly by hydrophobic interactions. Similarly, combining SPI with (-)-epigallocatechin gallate PP resulted in changes to the secondary structure of SPI with the formation of non-covalent and covalent protein-PP complexes (Zhou et al., 2020).

4.3.2 Effects on the physico-chemical properties of mixtures

4.3.2.1 Effects on particle size distribution of dispersions

Non-covalent protein-PP interactions have been reported to affect particle size distributions of dispersions differently, as different conditions within the systems will result in varying extents of aggregation and precipitation of complexed particles (Song, 2009; Coupland, 2014). Early studies by Siebert et al. (1996) emphasized the critical role of optimal protein-PP ratios in haze development and particle sizes in protein solutions, reporting decreasing haze formation and thus reduced average particle sizes when either protein or PP concentrations became too abundant in model systems. They explained that saturation of potential interaction sites on proteins likely occurred, resulting in repulsive interactions preventing large aggregate formation if either component was in excess in solution.

Many studies have reported that the formation of non-covalent protein-PP interactions in dispersions have resulted in increased average particle sizes. Charlton et al. (2002) observed almost immediate aggregate formation upon mixing proteins with PP in solution. They reported increased protein-PP complex sizes with increasing [PP], indicating that secondary aggregation occurred between complexes when more PP were present. Studies by von Staszewski et al. (2011) reported that increasing [PP] from 0.25 to 0.5% w/v resulted in minor increases in whey protein-green tea PP complex sizes in dispersions at pH 6 (away from the protein pI), likely due to the high net charges resulting in greater repulsion between particles, but when higher levels of PP (1%) were in the system, larger aggregates precipitated, indicating that other factors besides net charge on particles/ pH of the system were affecting sedimentation. Similarly, particle sizes of beverages were found to increase with increasing [PP] in whey protein-juice mixtures, indicating that the larger particles (> 100 μm) may have been secondary aggregates that formed with greater PP concentration when pH was approaching pI (Schneider, 2016).

Interestingly, Thongkaew et al. (2014) observed only minor changes in the particle sizes of WPI solutions as PP were used when pH was below or near pI, but major changes in particle sizes occurred at pH 6.1. Their results reported for the effects of PP on particle sizes were mixed: If catechin or grape seed extract were with WPI, particle sizes generally were larger, in agreement with the findings of Charlton et al. (2002) and Schneider (2016). In contrast, when tannic acid or hibiscus extract were with WPI, particle sizes generally showed decreasing trends, indicating that differences in PP chemical structures resulted in different protein interactions (Thongkaew et al., 2014). When cyanidin-3-galactoside PP were used with SPI in mixtures, average particle sizes were found to decrease (Xue et al., 2020). The authors explained that SPI had larger particle sizes due to the presence of large aggregates, but that PP and subsequent non-

covalent protein-PP complexation interactions induced aggregate break down by interrupting SPI hydrogen bonds and reducing hydrophobic interactions (Xue et al., 2020). This resulted in electrostatic repulsions dominating the system and preventing aggregate growth, ultimately resulting in smaller particle sizes and increased solubility of complexes (Xue et al., 2020).

In contrast to studies reporting increasing or decreasing particle sizes in protein dispersions with PP, Han et al. (2019) reported negligible changes in aggregate sizes, indicative of minimal protein-PP interactions, when studying interactions between milk proteins and pure, single phenolic compounds as well as green tea, grape, and cranberry extracts. In agreement, Zhou et al. (2020) reported that PP with SPI and subsequent non-covalent binding had little-to-no effect on particle size distributions of dispersions. The lack of changes observed in these studies may have been affected by the pH of systems, the ratios and types of proteins and PP in mixtures, as well as other intrinsic and extrinsic factors affecting interactions.

4.3.2.2 Effects on viscosities of dispersions

At high solids concentrations, particle aggregation can strongly affect rheology in many applications, both food and non-food, by increasing effective solids volumes and resulting viscosities of suspensions (Barthelmes et al., 2003). This would suggest that changes in the particle size distributions of dispersions as a result of non-covalent protein-PP complexation would influence dispersion viscosities, although the body of literature documenting such changes is limited at this time. Harbourne et al. (2011) reported that the use of small amounts of tannic and gallic acid PP resulted faster acid milk gel formation and stronger gels, likely resulting from the increased incidence of hydrophobic interactions and hydrogen bonds in the system. Fast gelation would increase the viscosity of the system significantly, transitioning quickly from more liquid-like to more solid-like behavior, indicating that protein-PP complexation contributed to

these shifts by inducing gelation. Aggregates and complexed particles are also known to increase the continuous phase viscosities of foams, and it can be inferred that a similar effect would occur in dispersions (Schneider, 2016). Beverage viscosities increased with increasing cranberry juice concentrations in mixtures with whey proteins, especially at lower pH conditions nearer to protein pI, indicating changes in colloidal structures of dispersions due to aggregate formation via non-covalent protein-PP complexation interactions (Schneider, 2016).

4.4 Effects on the physical properties of food products

Changes in protein functionality due to non-covalent protein-PP interactions have also been reported to affect the physico-chemical, functional, and nutritional properties of food products to varying extents, depending on the properties desired (Saluja and Kalonia, 2005; Le Bourvellec and Renard, 2012; Girard et al., 2016; Schneider, 2016; Ma and Zhao, 2019; Xue et al., 2020; Zhou et al., 2020; Li et al., 2021; Sharma et al., 2021). Protein-PP complexation interactions have been reported to improve physical properties of formulated products, with milk protein-PP conjugates showing good potential as bioactives delivery vehicles (Harbourne et al., 2011; Quan et al., 2019). Chung et al. (2015) reported that heat-denatured whey proteins enhanced the stability of anthocyanins in beverages significantly, postulating that protein-PP complexation via hydrogen bond formation and hydrophobic interactions conferred protection upon anthocyanins from degradation in storage.

Depending on the conditions within a system, complexation interactions may enhance or reduce protein solubility, which is known to impact other functional properties of proteins in foods (Quan et al., 2019). Solubility was reduced when non-covalent protein-PP complexes formed between alpha lactalbumin, lysozyme, and BSA proteins and procyanidin PP (Prigent et

al., 2009). In contrast, Jiang et al. (2018) reported that the formation of non-covalent complexes between chlorogenic acid and milk proteins improved solubility.

Non-covalent protein-PP complexation has also been reported to increase thermal stability in a number of studies, presenting a potential protein stabilization method for products requiring thermal processing (Quan et al., 2019). Thermal stability was improved by complexation between ß-lactoglobulin and tea PP (Kanakis et al., 2011), as well as between BSA proteins and ferulic acid (Ojha et al., 2012). Similarly, SPI-cyanidin-3-galactoside complexes had higher thermal stabilities in solution as well as dry powder form than SPI alone (Xue et al., 2020). Along with improved thermal stabilities, non-covalent complexation between protein and PP has been reported to affect the formation and properties of gels. von Staszewski et al. (2011) reported that when higher levels of green tea PP (1%) were added to whey protein solutions at pH 6, larger aggregates precipitated and negatively impacted textures of gels formed. In contrast, Harbourne et al. (2011) reported reduced acid milk gelation rates and stronger resulting gels with tannic and gallic acids.

Non-covalent protein-PP complexes have also been reported to affect the stability of foams (Quan et al., 2019). When combining procyanidins of varied degrees of polymerization with α-lactalbumin, lysozyme, and BSA proteins, foam stability was found to improve (Prigent et al., 2009). Further investigations into the functional effects of non-covalent protein-PP complexes on foam stability indicated that cranberry PP-whey protein complexes aided in enhancing both foam stability and rigidity under all pH conditions studied (Schneider, 2016). Foaming capacity was also reported to improve when non-covalent complex formation occurred between WPI and chlorogenic acid (Jiang et al., 2018).

Unfrozen dairy dessert mixes containing berry powders as sources of PP were found to have higher viscosities than plain mixes, and while the formation of protein-PP complexes may have had a minor effect on viscosity, the rheological changes observed were mainly attributed the increased fiber and total solids contents in mixes (Bilbao-Sainz et al., 2019a). In later experiments, the functionality of frozen dairy desserts containing strawberry powder and frozen desserts containing strawberry extract of equal PP content were compared to distinguish between the effects of fiber and effects of PP (Bilbao-Sainz et al., 2019b). Strawberry extract enhanced mix viscosities compared to plain mixes, likely as a result of increased total solids contents as well as some extent of network formation via protein-PP interactions. These effects, however, were much weaker than the thickening effects of strawberry powder with extra fiber and pectin in mixes (Bilbao-Sainz et al., 2019b). Similarly, only small increases in particle sizes and viscosities of beverages were observed when Giloy juice was included with goat's milk as a source of PP, and while non-covalent protein-PP complex formation was confirmed with microscopy, the effects on beverage viscosity were minor (Sharma et al., 2021).

Larger polyphenols with higher degrees of polymerization were found to better strengthen gluten proteins upon mixing, and consequently enhanced the elasticity of bread doughs (Girard et al., 2016). Similarly, highly polymerized PP altered properties of gluten proteins more extensively than smaller PP in multiple applications: large PP improved the tensile strength and aqueous stability of gluten films compared to small PP (Girard et al., 2019). Additionally, when smaller sized, monomeric PP were introduced into pastry flour batters containing proteins, changes in viscosity were negligible, indicating minimal non-covalent protein-PP interactions; when larger, polymerized PP were added, however, batter viscosities were increased as a result of enhanced protein-PP complexation (Girard et al., 2019).

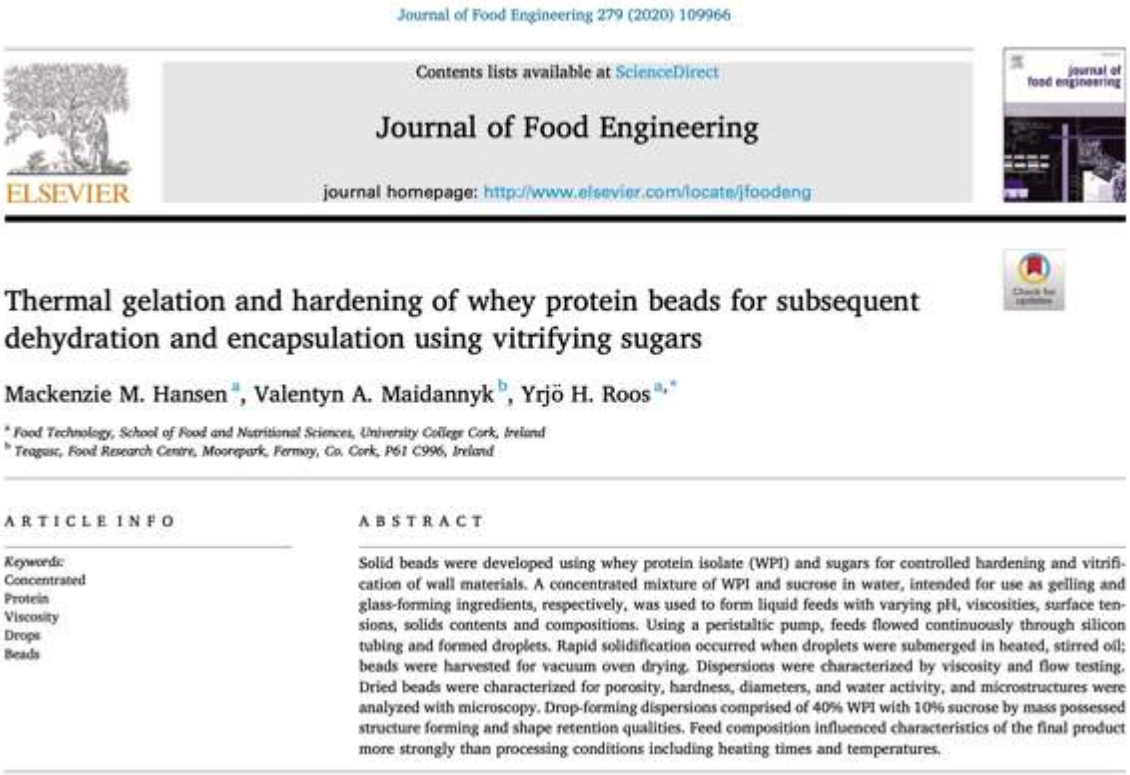
Nutritional bars formulated with non-covalently complexed whey protein-cranberry PP particles experienced less hardening over their shelf lives than protein bars without protein-PP complexes. Texture retention was explained by the presence of the large, insoluble particles dispersed throughout the bars, preventing proteins from engaging in large volumes of protein-protein interactions or network formation that would lead to hardening (Schneider, 2016).

5. Conclusions

Increased consumer interest in foods for health has driven food scientists to develop convenient, functional products that provide high nutritional value while also serving as delivery vehicles for additional health-promoting compounds like polyphenols and other bioactive compounds. Proteins present a versatile array of functional properties that are useful for the development of novel health foods, and are commonly utilized in combination with carbohydrates for encapsulation technologies intended for protection of sensitive compounds. Based on the body of literature reviewed, we hypothesized that careful formulation and proper processing of proteins mixed with carbohydrates in concentrated aqueous dispersions may result in the formation of novel products with glassy structures, desirable textures, the potential for bioactives entrapment and protection, and good predicted storage stability. It has been well-documented that proteins and polyphenols in mixtures under neutral and acidic pH conditions naturally interact non-covalently to form complexes mainly via hydrogen bonding and hydrophobic interactions, which may result in improved protein and bioactives stability (Livney, 2010; Foegeding et al., 2017; Sharma et al., 2021). The extent of protein-polyphenol interactions and complex formation in a system are strongly influenced by several intrinsic and extrinsic factors and have been reported to affect the physico-chemical properties of proteins, dispersions, and resulting foods. Changes to the physical properties of individual proteins in solution as a

result of non-covalent interactions with isolated polyphenols have been well-studied in model systems, while fewer investigations have studied these effects in more complex food systems involving several proteins and plant extracts as sources of polyphenols (Schneider, 2016). Further investigations of the effects of varied proteins, carbohydrates, and bioactives compositions on the physical properties of concentrated dispersions, as well as characteristics of products formed from dispersions would be useful for designing functional foods.

Chapter 2



Journal of Food Engineering 279 (2020) 109966

Contents lists available at ScienceDirect

Journal of Food Engineering

journal homepage: http://www.elsevier.com/locate/jfoodeng

Thermal gelation and hardening of whey protein beads for subsequent dehydration and encapsulation using vitrifying sugars

Mackenzie M. Hansen [a], Valentyn A. Maidannyk [b], Yrjö H. Roos [a,*]

[a] Food Technology, School of Food and Nutritional Sciences, University College Cork, Ireland
[b] Teagasc, Food Research Centre, Moorepark, Fermoy, Co. Cork, P61 C996, Ireland

ARTICLE INFO

Keywords:
Concentrated
Protein
Viscosity
Drops
Beads

ABSTRACT

Solid beads were developed using whey protein isolate (WPI) and sugars for controlled hardening and vitrification of wall materials. A concentrated mixture of WPI and sucrose in water, intended for use as gelling and glass-forming ingredients, respectively, was used to form liquid feeds with varying pH, viscosities, surface tensions, solids contents and compositions. Using a peristaltic pump, feeds flowed continuously through silicon tubing and formed droplets. Rapid solidification occurred when droplets were submerged in heated, stirred oil; beads were harvested for vacuum oven drying. Dispersions were characterized by viscosity and flow testing. Dried beads were characterized for porosity, hardness, diameters, and water activity, and microstructures were analyzed with microscopy. Drop-forming dispersions comprised of 40% WPI with 10% sucrose by mass possessed structure forming and shape retention qualities. Feed composition influenced characteristics of the final product more strongly than processing conditions including heating times and temperatures.

Thermal gelation and hardening of whey protein beads for subsequent dehydration and encapsulation using vitrifying sugars

Mackenzie M. Hansen[a], Valentyn A. Maidannyk[b], Yrjö H. Roos[a*]

[a]Food Technology, School of Food and Nutritional Sciences, University College Cork, Ireland

[b]Teagasc, Food Research Centre, Moorepark, Fermoy, Co. Cork, P61 C996

Published as: Hansen, M. M., Maidannyk, V. A., and Roos, Y. H. (2020). Thermal gelation and hardening of whey protein beads for subsequent dehydration and encapsulation using vitrifying sugars. *Journal of Food Engineering*, *279*, 109966.

Declaration: Microscope imaging was performed by Valentyn Maidannyk. All other experimental work was performed by the first author.

Abstract

Solid beads were developed using whey protein isolate (WPI) and sugars for controlled hardening and vitrification of wall materials. A concentrated mixture of WPI and sucrose in water, intended for use as gelling and glass-forming ingredients, respectively, was used to form liquid feeds with varying pH, viscosities, surface tensions, solids contents and compositions. Using a peristaltic pump, feeds flowed continuously through silicon tubing and formed droplets. Rapid solidification occurred when droplets were submerged in heated, stirred oil; beads were harvested for vacuum oven drying. Dispersions were characterized by viscosity and flow testing. Dried beads were characterized for porosity, hardness, diameters, and water activity, and microstructures were analyzed with microscopy. Drop-forming dispersions comprised of 40% WPI with 10% sucrose by mass possessed structure forming and shape retention qualities. Feed composition influenced characteristics of the final product more strongly than processing conditions including heating times and temperatures.

2.1 Introduction

Bovine whey proteins are a popular choice when aiming to develop new textures, structures, functions, and products in food (Kulmyrzaev et al., 2000). Whey proteins are often utilized for their nutritional contribution as well as wide range of functional properties including foaming, emulsifying, and gelation. Thermal treatment of whey proteins in solution may result in the formation of a gel network, driving the formation of desired food structures. The first step in gel formation from globular proteins is denaturation. Applying heat causes protein conformations to shift and structures unravel, exposing formerly internally oriented hydrophobic groups. In β-lactoglobulin, a free thiol group from Cys_{121} is exposed, promoting its availability to adopt new intramolecular and intermolecular linkages (Sawyer, 2003; Nicolai et al., 2011). At high protein concentrations, intermolecular protein-protein interactions between denatured molecules will lead to aggregation, the second step in gel formation (Fennema, 2017). Segments of different protein molecules interacting via hydrophobic interactions, electrostatic interactions, hydrogen bond formation, and disulfide bond formation leads to formation of aggregates. The final step is the formation of the gel network by successive addition of intermolecular bonds (particularly hydrogen-bonds and hydrophobic interactions) between subunits to make up the 3D structure (Kamerzell et al., 2011).

When sugar was included in protein solutions, Lee and Timasheff (1981) reported an unfavorable change in free energy, resulting in sugar molecules being preferentially excluded from the region immediately surrounding proteins. Exclusion occurred due to the higher cohesive force of the sucrose-water system and effect of sucrose to increase surface tension of water (Lee and Timasheff, 1981), as well as a combination of excluded volume effects (sugar molecules are larger than water molecules) and differential interaction effects including protein-

dependent interactions comprising of the sum of numerous types of interactions at varied locations on protein surfaces, and protein-independent interactions involving cosolvent molecules at interfaces, depending on cosolvent molecular properties (Baier & McClements, 2001; McClements, 2001, 2002; Semenova et al., 2002). Preferential hydration of proteins results in differences in the composition of the solvent surrounding proteins and that of the bulk solution, thus forming a concentration gradient and applied osmotic stress to protein molecules, where proteins have tendencies to alter their conformations and fold to limit exposure to sugars; some studies suggest that sucrose may be near to fully excluded from protein domains (Lee and Timasheff, 1981; McClements, 2002).

In the liquid state, proteins are both protected against unfolding and encouraged to form aggregates after denaturation due to the presence of sucrose in the system. There are two major hypotheses to explain the impact of sugars on proteins in the solid state resulting from dehydration: the glass dynamics/ vitrification theory and the water replacement theory (Allison et al., 1999; Chang and Pikal, 2009; Mensink et al., 2017). Both theories require sugar to be in the same amorphous phase as protein in order to impart their effects (Wang et al., 2009), and emphasize the significance of reducing the molecular mobility of proteins (Ohtake et al., 2011). It can be presumed, then, that glass formation occurs in the preferentially excluded sucrose fraction of protein-sucrose dispersions.

Most previous studies have been performed under low concentration conditions; our interest is in highly concentrated systems. Schmidt et al. (1984) found that more aggregated, opaque gels would be expected to form at higher protein concentrations and under more severe heating (above 90°C). Additionally, it has been reported that preferential exclusion of sugars increases at higher protein concentrations when sugars and proteins have been combined (He et

al., 2011). Regarding relatively dilute protein-solvent-cosolvent systems, McClements (2002) conceded that in practice, it was not possible to completely determine all molecular characteristics of a system due to a large number of differing chemical groups and interactions occurring simultaneously, the highly dynamic nature of the system itself, and limitations of analytical techniques. The challenge to understand the entire body of molecular characteristics of a highly concentrated protein-water-sucrose dispersion is likely even more improbable.

The design and formation of desired food ingredient-based structures, such as biopolymer hydrogel beads from proteins, can be accomplished when the material and functional properties of the components are understood. The injection method of drop formation involves filling syringes or tubing with solution, which is then extruded/ injected into a different solution that promotes gelation at selected conditions (Burey et al., 2008; Matalanis et al., 2011; McClements, 2017). The solution drop detachment mechanism is inter-influenced by the physical properties of solution, tip diameter, and solution flow rates (Lee and Chan, 2013), which aid in determining the physiochemical and structural properties of drops such as size, shape, porosity, and hardness (Joye and McClements, 2014; Zhang et al., 2016a, b).

The hypothesis for this study was that a continuous process forming concentrated, liquid feeds into dry, stable particles could be developed. A blend of ice powder and whey protein isolate powder were used for rapid protein hydration during microwave thawing. Rehydrated WPI provided gelation properties of whey proteins to harden beads from a continuous liquid feed with subsequent glass formation of sucrose intended for encapsulation and protection of functional feed components. Our objective was to investigate effects of feed composition and pH on viscosity, surface tension, and bead formation as well as to analyze physicochemical

properties of dehydrated beads. Results of this study provide insight into physical behaviors of high solids-concentrated protein dispersions.

2.2 Materials and Methods

2.2.1 Materials

Whey Protein Isolate, WPI (Isolac®), used in the present study was supplied by Carbery Food Ingredients (Ballineen, Cork, Ireland). Sunflower oil (Musgrave Excellence™, Musgrave Wholesale Partners, Dublin, Ireland) was purchased from local suppliers. Sucrose (≥ 99.5 GC) of analytical grade was purchased from Sigma-Aldrich, Co. (St. Louis, MO, USA). Citric acid was purchased from KB Scientific Ltd. (Cork, Ireland). Ice was utilized as the source of water in experiments.

2.2.2 Dispersion preparation

A dry blend of sucrose and WPI powder was prepared and stored in a -40°C chest freezer. To prepare liquid feeds, ice at -20°C was weighed and blended in a Duronic BL 1200 stainless steel kitchen blender (4 blades, 1200 W, Duronic, United Kingdom) into a powder with 'ice crush' mode inside a walk-in freezer at -20°C, to prevent melting. The blend of dry ingredients with the powdered ice was mixed together for 15 s prior to thawing in a microwave oven (White manual microwave oven, frequency 2450 MHz, power output 650-700 W, Argos, Ireland) first for 5 min on low settings (120 W, 17% microwave output). The dispersions were mixed by hand to break up any clumps and then heated an additional 1-9 min with the same settings, depending on solids content. Once all ice was melted, dispersions were mixed with a Tefal Infinityforce Ultimate hand blender (ActivFlow Technology with 4 blades, 1000 W, Tefal, Ireland) on 'turbo' mode at a speed setting of '15' for 60 s to break up any larger agglomerates

prior to analysis. The pH was measured with the SevenEasy™ probe by Mettler Toledo (Scientific Laboratory Supplies, Nottingham, UK) and adjusted to desired levels with aqueous, 2M citric acid.

2.2.3 Feed characterization

2.2.3.1 Viscosity

Viscosity of liquid feed was measured with a Haake RotoVisco 1 (Thermo Scientific, MA, USA). Samples (~13 g) were weighed into a DG43 cup, and a Z41 standard rotor was employed. The water bath surrounding the sample cup was temperature-controlled and held at 20°C. Samples were sheared in a ramp from 0-100 s^{-1} over 3 min, held at 100 s^{-1} for 3 min, then ramped back down to 0 s^{-1} within 3 min. A total of 100 measurements were taken over each 3-minute period. Haake RheoWin Job Manager software was used to view and analyze data.

2.2.3.2 Flow testing

Flow properties of liquid feed at room temperature were measured by pumping through a benchtop, manual control, variable speed, peristaltic pump (120 S/DV; Watson Marlow, Falmouth, England) with silicon tubing of 85 cm length, 2 mm bore, and 1 mm wall thickness (BÜCHI Labortechnik AG, Flawil, Switzerland) at a pump speed of 10 rpm. The time required to deposit 10 mL of liquid feed was measured. Additionally, the number of drops deposited per 1 min was recorded. Mass of 10mL of liquid feed was taken, as well as the average mass of a drop (triplicate measurement). These measured and recorded values allowed for mass flow rates, volume flow rates, liquid feed densities, drop surface tensions, drop diameters, and drop volumes to be calculated.

Density of liquid feed (kg/m^3) was calculated by:

$$\frac{mass\ (g)\ of\ 10\ mL\ feed}{10\ mL} \tag{1}$$

Average drop volume (mL) was calculated by:

$$\frac{10\ mL\ feed}{time\ (s)\ to\ deposit\ 10\ mL} * \frac{60s\ \ per\ min}{\#\ drops\ per\ min} \tag{2}$$

Mass flow rate (kg/s) was calculated by:

$$\frac{mass\ (g)\ of\ 10\ mL\ feed}{time\ (s)\ to\ deposit\ 10\ mL} \tag{3}$$

Volume flow rate (m^3/s) was calculated by:

$$\frac{mass\ flow\ rate\ (\frac{kg}{s})}{feed\ density\ (\frac{kg}{m^3})} \tag{4}$$

Drop surface tension was calculated with Tate's Law (Worley, 1992):

$$\frac{(Average\ drop\ mass\ (g) * gravitational\ constant\ \left[9.8\ kg\ \frac{m}{s^2}\right])}{2\pi * (external\ radius\ of\ tubing\ tip\ [mm] * correction\ factor\ \left[\frac{capillary\ radius}{(drop\ volume)^{\frac{1}{3}}}\right])} \tag{5}$$

The correction factor in this calculation is in place because the total drop formed at the tip of the outlet tubing does not release, and residual liquid is left on the end of the tube.

Drop diameter was calculated by:

$$\left[\frac{(3 * average\ drop\ volume\ [mL])}{4 * \pi}\right]^{\frac{1}{3}} * 2 \tag{6}$$

This equation is built off the assumption that drops form a perfectly spherical shape, and thus is derived from the equation for the volume of a sphere:

$$V = \frac{4}{3}\pi r^3 \quad (7)$$

and the fact that $diameter = 2 * radius.$ (8)

2.2.4 Drop preparation

Liquid feeds at room temperature were pumped through a peristaltic pump (120 S/DV; Watson Marlow, Falmouth, England) with silicon tubing of 85 cm length, 2 mm bore, and 1 mm wall thickness (BÜCHI Labortechnik AG, Flawil, Switzerland). Pump speed settings of 150-200 RPM were used to fill the tube, then pump speed was set to 10 RPM, forming drops of liquid feed. The outlet tubing was placed between a clamp on a retort stand. For bead formation, a 500 mL glass beaker with a magnetic stir bar was set on a Stuart hotplate and magnetic mixer (Cole-Parmer, Staffordshire, UK), filled with 450 mL of heated sunflower oil. The retort stand was arranged so that the end of the outlet tubing was situated above the surface of the hot oil. Liquid feed was pumped through the tubing and dispensed dropwise into the hot oil, being gently stirred with low magnetic agitation by the magnetic stir bar. Drops were allowed to harden in the oil and harvested to dry on absorbent paper before being transferred to Anumbra® glass petri dishes (80 x 15 mm, Scientific Glass Laboratories Ltd., Staffs, UK) for drying. To determine the optimal heating time and temperature conditions to produce beads, drops of the same composition were formed under a range of temperatures and times: at 100°C for 1, 2, 5, and 10 min, and for 2 min at 80, 100, 110, and 120°C.

Glass dishes with beads were placed into a WTB Binder vacuum oven (Binder GmbH, Tuttingen, Germany) at 70°C for 3 h. After drying a_w and diameters were measured prior to

packaging in heat-sealed, 12/40 Camplex® Metallized Polyester Laminate packaging (Solventless adhesive laminate of: 12 µm printable polyester film, Camplus® metallized on one side, 40 µm polyethylene film; Camvac Limited, UK). After processing for a total of ~5 h, packages containing beads were weighed and placed into an incubator (Cooling Incubator, KBP 6151, Series 6000, Termaks, Bergen, Norway) set at 25°C until testing. Packages were reweighed when removed from the incubator for testing, prior to opening (data not reported.)

A range of formulations of varied solids concentrations and compositions, pH, and viscosities were developed and assessed for their ability to form spherical, solid drops that retained their shape and did not stick to one another (see **Table 2.1**). Liquid feed dispersions of 35% WPI with 10% sucrose at pH 3.5 and 35% WPI with 15% sucrose at pH 4.0 were not pumpable and thus flow testing was not performed.

Table 2.1.

[WPI]	[Sucrose]	pH
%		-
10	0	6.6
15	10	6.6
20	0	6.6
20	20	6.6
25	10	6.6
30	0	6.6
30	10	6.6
30	20	6.6
35	10	3.5, 4.0, 4.1, 4.2, 4.5, 5.0, 6.7
35	15	4.0, 4.5, 5.0, 6.6
35	20	4.5, 5.4, 6.6
40	0	6.6
40	5	6.6
40	10	4.5, 6.5

Feed formulations with WPI and sucrose concentrations (% w/w) as well as pH.

2.2.5 Bead characterization

2.2.5.1 Water activity, a_w

Bead a_w was measured with a water activity meter (4TE, AquaLab, Decagon Devices, Inc., WA, USA) at 20°C before and after drying. Approximately 0.5 g of sample was placed in glass Steriplan dishes (6 mm internal height x 35 mm internal diameter) used as sample cups.

2.2.5.2 Water content

Fresh bead water content was measured gravimetrically by placing approximately 0.5 g of beads into pre-weighed, glass dishes and recording the mass before placing into a vacuum oven for drying at 70°C for 24 h. Masses were recorded again after drying to obtain the difference in mass due to water loss as well as the sum of total solids plus oil remaining in dry beads.

2.2.5.3 Drop diameters

Diameters of beads were measured 5 times per sample before and after drying with digital Vernier calipers (0-150 mm; Mitutoyo, Japan), and an average value was reported. Accuracy was not a concern as products measured were not particularly viscoelastic or soft, but had semi-solid structures and held their shape (Lee and Chan, 2013). To compare with calculated values for bead diameters, 3 of the 5 measurements were used.

2.2.5.4 Hardness

Sample preparation - Beads were removed from storage at 25°C and weighed. Drops were placed in a single layer, covering the bottom area (1520 mm^2) of a transparent, polypropylene sample cup with a yellow screw cap (70 mL, 55 x 44 mm, Starstedt, Australia),

samples weights were recorded, and lids were placed on the samples until testing. All samples were prepared for texture analysis in triplicate.

Texture analysis - Beads were tested for hardness with TA-XT2i Texture Analyser (Stable Micro Systems, Surrey, UK). A 35 mm platen was utilized to compress drops 3 mm once contact was made with samples. Compression force was measured, and Texture Expert Exceed software was employed to analyze data.

2.2.5.5 Density

A Micromeritics AccuPyc II 1340 Gas Pycnometer (Micromeritics Instrument Corporation, GA, USA) was utilized to measure average apparent volume and true density of beads by using Helium gas to 4.5 standard (99.995% purity; Irish Oxygen Company Ltd, Cork, Ireland) as the displacement medium, pumped at a steady rate of 145-172 kPa. A sample cup with 10 cm^3 capacity was partially filled, and each sample was measured 10 times during a single test. AccuPyc II 1340 for Windows software was utilized to run tests and view data reports. A Micromeritics GeoPyc™ 1360 (Micromeritics Instrument Corporation, GA, USA) envelope density analyzer was utilized to measure the average envelope density and volume of samples by combining Micromeritics DryFlo™ displacement material and sample (filling roughly ¼ of the chamber) in a 38.1 mm I.D. chamber and measuring 7 times during a single test. The volumes given from the two tests were utilized to calculate sample porosities. All density testing was completed in duplicate.

Porosity was calculated by: $\frac{Total\ volume - Volume\ of\ solids}{Total\ volume} * 100$ or $\frac{GeoPyc\ volume - AccuPyc\ volume}{GeoPyc\ volume}$

2.2.5.6 Optical light microscopy

Microscopy observation of dried beads was done using an Olympus BX51 (Olympus Corporation, Tokyo, Japan) light microscope with 20x dry objective lens with polarized light. Digital images (TIFF, 8-bit) were taken and captured using Jenoptik C14 Imagic camera. Beads were crushed to produce fragments of smaller sizes that could be imaged.

2.2.5.7 Confocal laser scanning microscopy

Leica TCS SP5 confocal laser scanning microscope (CLSM; Leica Microsystems CMS GmbH, Wetzlar, Germany) was used for dried beads visualization. Fragments of broken beads were placed onto a glass slide and labeled using a mixture of Fast Green and Nile Red (Auty et al., 2001; Maher et al., 2015). The dye mixture containing Fast Green (aq. 0.01 g/0.1 L) and Nile Red were dissolved in polyethylene glycol 400 g/mol (0.1 g/0.1 L) mixed in a ratio 1:40 of Fast Green to Nile Red, which allowed diffusion of the dye molecules into the particles whilst not influencing the particle morphology and preventing solubilization (Maher et al., 2015). Dual excitation at 488 nm/633 nm was used. The confocal images of drop fragments were taken using 20x oil immersion objective with numerical aperture 0.7 z. Stacks were obtained in order to generate a three-dimensional structure of the particle and to identify surface lipid staining (Maher et al., 2015). Red and Green pseudo-colored pictures (8-bit), 512 x 512 pixels in size, were acquired using a zoom factor of 1-3.

2.2.5.8 Scanning electron microscopy

Fragments from broken dried beads were attached to double-sided adhesive carbon tabs mounted on scanning electron microscope stubs, and then coated with chromium (K550X, Emitech, Ashford, UK). Scanning electron microscopy images were collected using a Zeiss Supra

40P field emission SEM (Carl Zeiss SMT Ltd., Cambridge, UK) at 2.00 kV. Representative micrographs were taken at 200×, 500×, 1000×, 5000×, and 10000× magnification.

2.2.6 Statistical analysis

All analyses were carried out in triplicate with the exception of envelope and true densities, done in duplicate. The obtained data were analyzed by calculating mean values and standard deviations. Additionally, t-test and analysis of variance (ANOVA; Tukey's HSD test) were performed using R i386 version 3.5.1 (R Foundation for Statistical Computing, Vienna, Austria) on mean values for different samples. The level of significance was determined at $p < 0.05$.

2.3 Results and Discussion

2.3.1 Feed characterization:

2.3.1.1 Viscosity

Feed viscosity plays a significant role in drop formation, requiring sufficiently high viscosities to form and retain spherical shapes upon hardening, as competing forces exist between the viscous, surface tension forces of the droplet that must exceed the impact, drag forces from the bath attempting to disrupt shape (Chan et al., 2009). Increasing the concentration of biopolymers in the dispersion is known to increase feed viscosity exponentially (Chan et al., 2009; Matalanis et al., 2011; Lee and Chan, 2013). Highly concentrated WPI dispersions exhibited pseudoplastic flow behavior (data not shown), also observed by Pradipasena and Rha (1977) for β-lactoglobulin above 5% w/w. The apparent viscosity of liquid feeds sheared at 100 s^{-1} increases non-linearly with WPI concentration, with an extreme, significant jump occurring above 30% WPI w/w (**Fig. 2.1A**), potentially highlighting a critical packing point where particle volume fractions and interactions become sufficiently high to arrest feed dynamics. Above this

critical concentration, feed dispersions undergo a transition from fluid-like to more solid-like behavior due to the crowding or jamming of the mobility of particles and aggregates, resulting in the formation of a stress-bearing, interconnected network (Trappe et al., 2001; Coupland, 2014). Our results are in agreement with those reported by Alizadehfard and Wiley (1995) and Patocka et al. (2006), who found that WPI dispersions sheared at a fixed rate of 6.45 s^{-1} showed marginally increasing viscosity up to 30% WPI concentration followed by sharp increases. He et al. (2011) reported similar findings, with increases being minimal at lower protein concentrations and the slope of viscosity change significantly increasing at higher protein concentrations when two types of monoclonal antibody proteins were studied. Small shifts in solution conditions, including altered concentration of solutes, can result in the partial unfolding of protein molecules and the exposure of hydrophobic groups. This increases the tendency of protein particles to cluster and form aggregates, as exposed hydrophobic groups are attracted, ultimately increasing the viscosity of the aqueous phase (Song, 2009). Matalanis et al. (2011) explained that increased concentrations of biopolymers increase viscosity until the packing of molecules becomes so tight that a critical packing parameter is reached, above which systems behave more like solids. When protein molecules exceed a critical concentration in a sol, increased entangling and overlap results in increased system viscosity (Coupland, 2014). Crowding results in increased viscosities due to steric repulsion between molecules causing jamming of protein particle movement and ultimately adopting solid-like behavior (Hong et al., 2018a). We observed the solid-like behavior of dispersions as feeds that were unable to flow through tubing to form drops.

Sugars increase biopolymer dispersion viscosities (McClements, 2002; Semenova et al., 2002). He et al. (2011) demonstrated that seven different sugars significantly increased viscosity of highly-concentrated protein dispersions. Disaccharides showed stronger effects than

monosaccharides when dispersions contained equal amounts of monosaccharide units. Our study showed that feeds of equal protein concentrations exhibited increasing viscosities with increased sucrose concentrations, potentially due to the increase in total system solids as well (**Fig. 2.1B)**. Dispersions containing 35% w/w WPI alone were not assessed, as priority was given to feeds formulated with blends of both WPI and sucrose.

Proteins are particles that may exhibit more hydrophilic or hydrophobic behavior, depending on which constituent groups are exposed to the bulk solvent. Globular proteins in their native, folded state are often fairly soluble in water due to their 3D structures having mainly hydrophilic surface groups exposed to water in solution, while the majority of hydrophobic residues are buried within the internal core of the molecule and shielded from interacting with water (Coupland, 2014). The hydrophilic residues exposed to the bulk solvent may contribute to hydrogen bond formation with water molecules. At pH values away from the protein isoelectric point (pI), charged protein molecules repel one another strongly and hydrophobic groups are not exposed. These conditions are unfavorable for the formation of intermolecular interactions and allow protein molecules to exist as separated, suspended particles in water with low solution viscosities (Song, 2009; Coupland, 2014). At pH values near the protein pI, net charges on protein molecules are neutralized and electrostatic interactions are weak. Under these conditions, protein molecules have a stronger tendency to aggregate due to attractive electrostatic forces, reducing solubility. Therefore, altering pH conditions may change the viscosity of biopolymer dispersions, as the volume of electrostatic repulsions and attractive forces between molecules in solution can change with pH (Hong et al., 2018).

Effects of pH of feeds on viscosity are shown in **Figure 2.1C**. Dispersions comprised of 35% WPI with 10% sucrose showed high viscosities below and up to pH 4, followed by a rapid

decrease in viscosity between pH 4 and 4.5, and finally an increasing viscosity with increasing pH above 4.5. Higher pH ranging over 4 to 6.8 showed no significant differences ($p > 0.05$). Our findings were in line with those of Hermansson (1975), who found that increased pH slightly increased viscosities of aqueous whey protein concentrates above the isoelectric point range (pH 4-5). Dissanayake et al. (2013) also reported that whey protein dispersions at pH 4 had higher initial viscosities than at pH 5 and 6. Hong et al. (2018b) reported that bovine serum albumin (BSA) has a pI of 5.1 and a U-shaped curve for viscosity as a function of pH. BSA solutions with acidic and basic pH were more viscous than BSA solutions at the pI, indicating that monopole-monopole electrostatic repulsions were the dominant factor in solution viscosity and were most reduced at neutral pH.

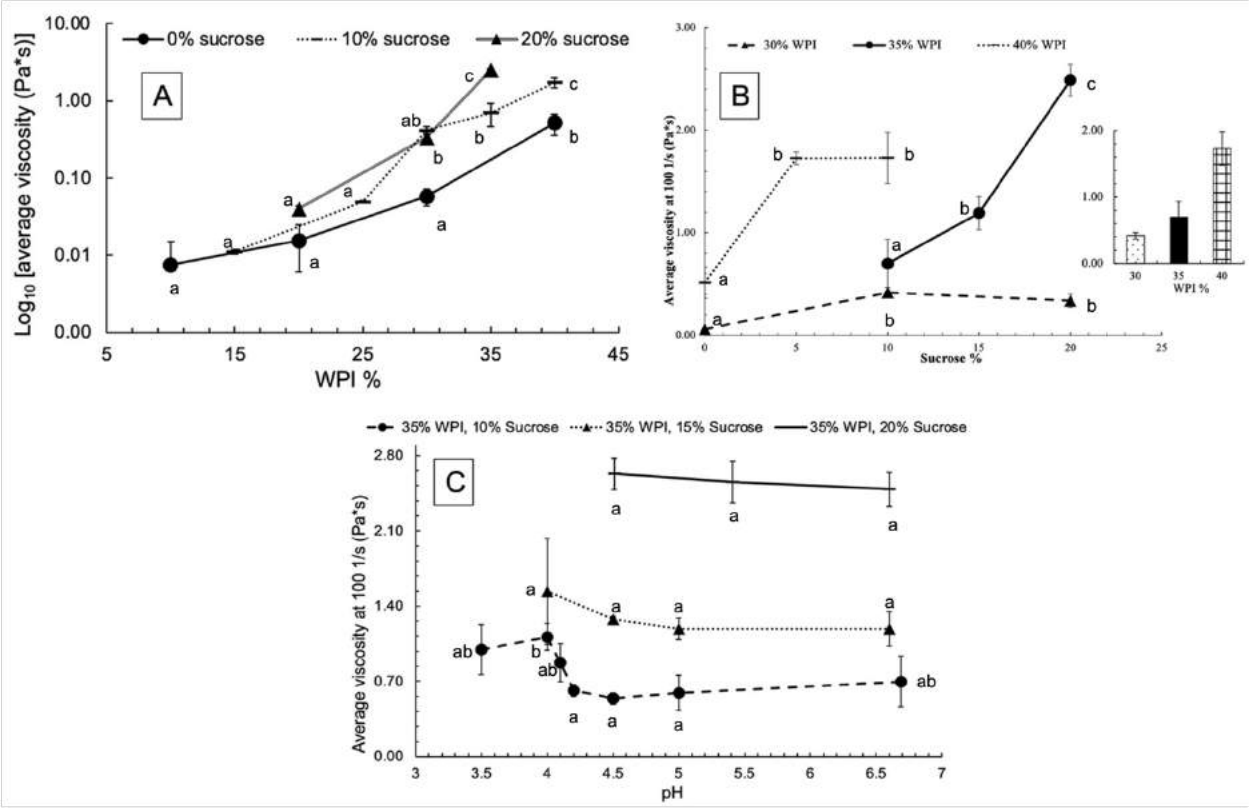


Figure 2.1.

A- Effect of protein concentration (%) in feeds containing 0, 10, and 20% sucrose on the apparent viscosity at 100 s^{-1}; n = 3. Lines are for guiding purposes only. Data points connected by the same letter are not significantly different ($p > 0.05$) from other points connected by the same line.

B- Effect of sucrose concentration (%) in feeds containing 30, 35, and 40% WPI on apparent viscosity at 100 s^{-1}; n = 3. Lines are for guiding purposes only. Inset: Effect of 10% w/w sucrose on viscosity. Data points connected by the same letter are not significantly different ($p > 0.05$) from other points connected by the same line.

C- Effect of pH in feeds containing 35% WPI with 10%, 15%, and 20% sucrose on apparent viscosity at 100 s^{-1}; n = 3. Lines are for guiding purposes only. Data points connected by the same letter are not significantly different ($p > 0.05$) from other points connected by the same line.

2.3.1.2 Flow

The surface tension of feed dispersions strongly determines the mass and size of detached drops, as drops only detach once the gravitational forces pulling down exceed the surface tension forces acting around the circumference of the dripping tip; diameters of drops formed tend to decrease with the surface tension of feeds (Lee and Chan, 2013). Previous studies indicated that surface tension decreased as viscosity and biopolymer concentrations were increased (Chan et al., 2009; Lee and Chan, 2013). Our findings demonstrated that surface tension increased marginally with WPI concentration until there was a significant increase ($p < 0.05$) above 30% w/w WPI (**Fig. 2.2A**). Sucrose concentrations did not appear to affect surface tension to the same extent observed with WPI (**Fig. 2.2B**). Proteins are generally more surface-active molecules than sugars, as they contain both hydrophilic and hydrophobic groups and amino acid residues, and can participate in self-assembly as factors such as charges, temperature, or pH are adjusted (Nicolai, 2016). Adjusting the pH of formulations containing 35% WPI with 10 and 15% sucrose showed very similar effects on surface tension as on viscosity, indicating that pH adjustment was not effective for improving drop formation and retention of spherical shapes (data not shown).

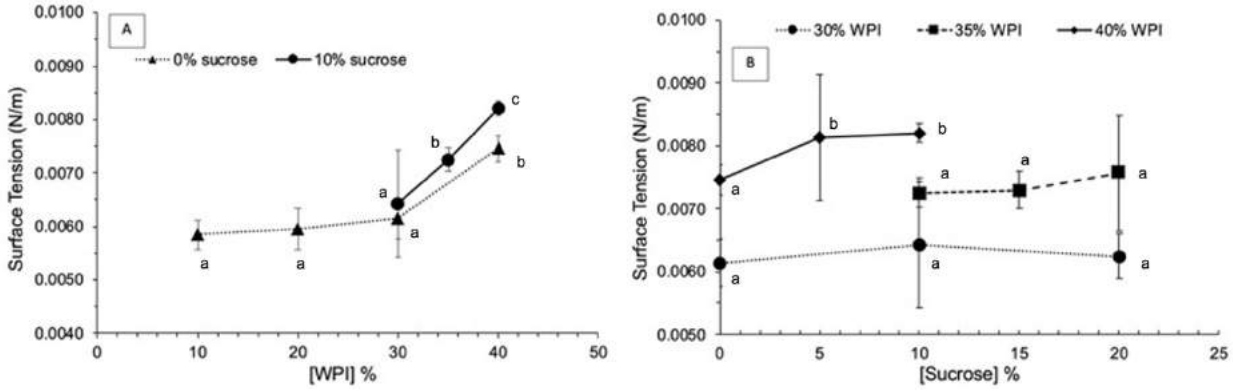


Figure 2.2.

A. Effect of WPI concentration (%) in feeds containing 0 and 10% sucrose on calculated surface tension in N/m; n = 3. Lines are for guiding purposes only. Data points connected by the same letter are not significantly different ($p > 0.05$) from other points connected by the same line.

B. Effect of sucrose concentration (%) in feeds containing 30, 35, and 40% WPI on calculated surface tension; n = 3. Lines are for guiding purposes only. Data points connected by the same letter are not significantly different ($p > 0.05$) from other points connected by the same line.

While the overall effect of sucrose and protein concentration on surface tension was unexpected (Chan et al., 2009; Lee and Chan, 2013), drop diameters and surface tension had high correlation. Higher solids concentrations result in increased intermolecular interactions and may increase the viscosity of fluid systems, resulting in complex fluid behaviors (He et al., 2011; Tro et al., 2014). Additionally, there may have been variations in protein hydration levels in different feed dispersions. A corresponding effect applies to surface tension; liquids containing molecules with stronger and larger numbers of attractive intermolecular forces tend to have higher surface tension values (Tro et al., 2014). WPI dispersions were highly concentrated and as such, it may be inferred that feeds had high levels of intermolecular interactions and thus displayed highly viscous behavior and high surface tensions as well. Another example of

increasing viscosities and corresponding increases in surface tension is in water as temperature decreases (Tro et al., 2014).

2.3.2 Bead characterization

2.3.2.1 Drop formation and composition

Formulations in **Table 2.1** include 4 formulations that showed potential for solid beads formation (30% WPI with 20% sucrose, 35% WPI with 15% sucrose at pH 4.5, 40% WPI, and 40% WPI with 10% sucrose). Compositional and water activity data collected from the liquid feeds, fresh beads, and dry beads are provided in **Tables 2.2**, **2.3**, and **2.4**. Feed dispersions that formed solid beads were comprised of similar total system solids (40-50%) but exhibited a wide range of apparent viscosities (**Table 2.5**), indicating that viscosity may not be the strongest parameter determining drop forming abilities in this process. Interestingly, all 4 dispersions fell within a narrow range of surface tension values from 0.006 to 0.008 N/m, indicating that surface tension was a more significant factor in determining the ability of feeds to form solid beads with our process. Two formulations (40% WPI and 40% WPI with 10% sucrose) produced uniform, spherical beads chosen for further characterization.

Table 2.2

Liquid Feed Formulation	Water %	Total solids %	Protein (WPI) %	Sucrose %
30% WPI with 20% sucrose	50	50	30	20
35% WPI with 15% sucrose, pH 4.5	50	50	35	15
40% WPI	60	40	40	n/a
40% WPI with 10% sucrose	50	50	40	10

Composition of liquid feeds chosen for bead formation.

Table 2.3.

Fresh Bead Formulation	a_w
30% WPI with 20% sucrose	0.91 ± 0.01
35% WPI with 15% sucrose, pH 4.5	0.91 ± 0.01
40% WPI	0.95 ± 0.01
40% WPI with 10% sucrose	0.90 ± 0.02

Water activity (a_w) of intermediate, fresh beads prior to drying.

Table 2.4.

Dry Bead Formulation	a_w	Water %	[Solids + Oil] %
30% WPI with 20% sucrose	0.22 ± 0.05	2 ± 1	98 ± 1
35% WPI with 15% sucrose, pH 4.5	0.19 ± 0.03	1 ± 1	99 ± 1
40% WPI	0.20 ± 0.01	3 ± 1	97 ± 1
40% WPI with 10% sucrose	0.14 ± 0.02	1 ± 1	99 ± 1

Composition and a_w of final, dried beads.

Table 2.5.

Feed	Total Solids (%)	Viscosity (Pa-s)	Surface tension (N/m)
40% WPI	40	0.51 ± 0.15	0.007± 0.001
40% WPI, 10% sucrose	50	1.73 ± 0.25	0.008 ± 0.001
30% WPI, 20% sucrose	50	0.34 ± 0.07	0.006 ± 0.001
35% WPI, 15% sucrose- pH 4.5	50	1.28 ± 0.03	0.008 ± 0.001

Total feed solids, viscosity, and surface tension data for feed dispersions that formed beads; n = 3

Studies by Kulmyrzaev et al. (2000) and Fitzsimons et al. (2007) showed differential scanning calorimetry (DSC) heating of native WPI gave a broad, endothermic transition between 60 and 90°C with 2 peaks, the more significant around 70-71°C corresponding to β-lactoglobulin denaturation, and the minor peak shoulder at around 60°C representing α-lactalbumin (Ruffin et al., 2014). Knowledge of these temperatures for thermal denaturation allowed the presumption that when liquid drops enter the oil at 100°C they solidify as the whey proteins aggregate and

form a gel network. Additionally, drops of the hydrophilic feeds are likely driven to assume compact, spherical conformations within the oil bath to reduce the surface area in contact with the hydrophobic oil. Simultaneous, rapid vaporization of water expands the protein gel, followed by diffusion and dehydration. Heating and evaporation of the water in liquid drops results in droplet expansion, occurring concomitantly with dehydration and gel formation. Expansion can occur due elasticity of the gel network structure, while removal of water from the structure results in pore formation (as seen in **Figs. 2.7A**, **B** and **2.8A**, **D**) and decreased drop densities. Hardening decreases shrinkage and the final volume is dependent on the extent of viscous flow during dehydration. Further dehydration in the vacuum oven transforms the sucrose to form a glass with fragile sucrose membranes on the dry protein. Such conclusion was based on the glass formation properties of sugars in mixes with proteins when glass transition of sucrose occurs above normal ambient temperature at $a_w < 0.2$ (Roos & Drusch, 2015).

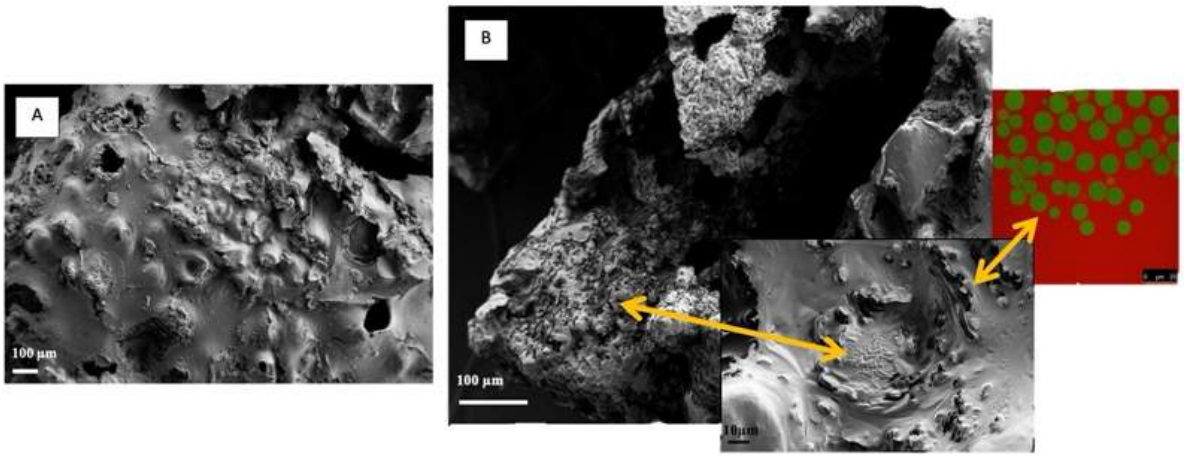


Figure 2.6.

A- Scanning electron micrograph image at 500x magnification, depicting the microstructure of a dried, 40% WPI bead.

B- Left: Scanning electron micrograph image at 1000x magnification, depicting the microstructure of a dried, 40% WPI bead. Center: Scanning electron micrograph image at 5000x magnification, depicting the microstructure of a dried, 40% WPI bead. Right: Confocal laser scanning micrograph image depicting the microstructure of a dried, 40% WPI bead, with oil droplets dispersed throughout image. The left arrow points towards the appearance of the protein network in the left and center images, and the right arrow highlights the oil droplets protruding throughout the structure in the center and right images.

Figure 2.6A depicts the appearance of a 40% WPI, dried product with dispersed oil droplets and the dehydrated protein network spanning the structure. **Fig. 2.6B**, left shows the structure with the mixture of protein network and oil droplets. **Fig. 2.6B**, center shows a more magnified view of the mixed protein and oil droplet structures, indicated by the arrows. The left arrow points towards the appearance of the protein network, and the right arrow highlights the oil droplets protruding throughout the structure. **Fig. 2.6B**, right (confocal) shows a number of the tiny oil droplets found in the structure and confirms their identity, as their sizes are of the same magnitude as those in the SEM images. Thermal gelation of whey proteins involves the self-aggregation of protein molecules into the 3D network which entraps water by capillary forces (Chen et al., 2006); as water diffuses out of the structures in this process, it is possible that the

same capillary forces responsible for water entrapment may drive oil uptake into the structure of the bead during gelation and hardening (oil droplets dispersion in the structure may be seen in **Figs. 2.7B**, **2.8B** and **D**, **and 2.9**). The forces driving this oil uptake appear to be strong enough to force the bulk liquid into tiny droplets that fit throughout the structure and could potentially be enhanced by the gentle magnetic stirring of the oil bath (Kornev & Neimark, 2001). Further investigation would be required to determine the mechanism of such oil droplet formation.

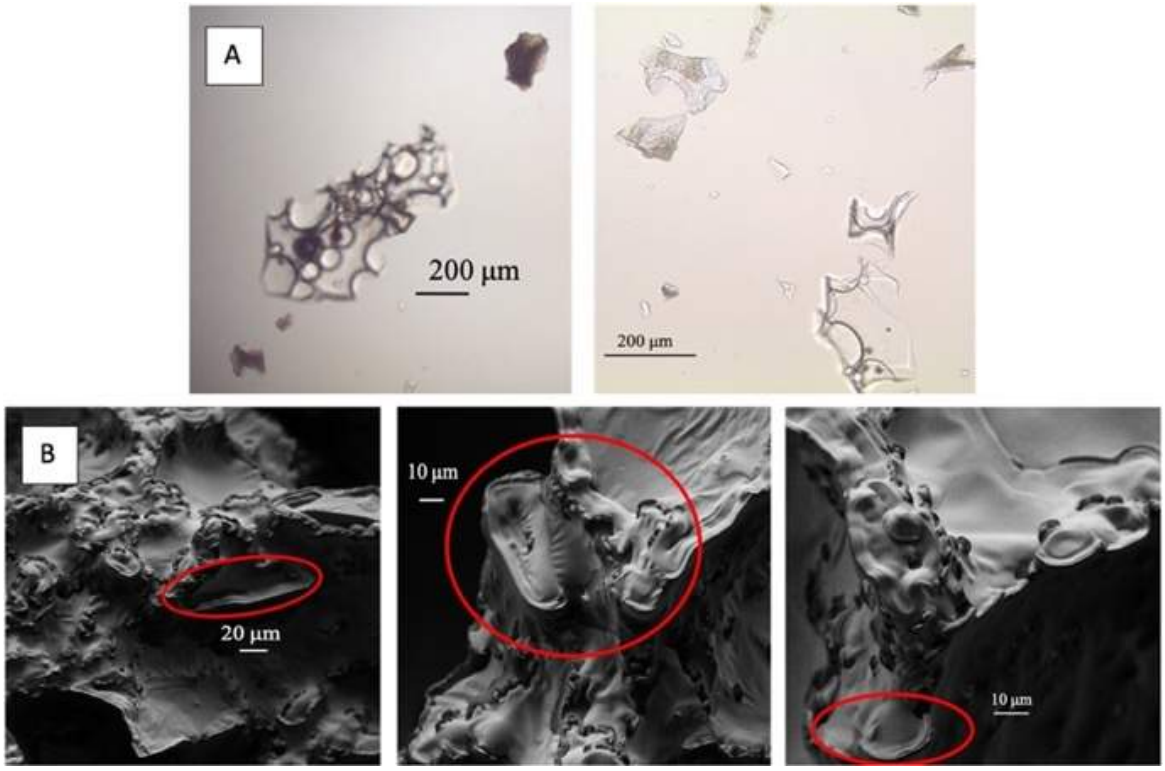


Figure 2.7.

A- Left: Optical light microscope image at 4x magnification, depicting the microstructure of a dried, 40% WPI with 10% sucrose bead. Right: Optical light microscope image at 10x magnification, depicting the microstructure of a dried, 40% WPI with 10% sucrose bead.

B- Left: Scanning electron micrograph image at 500x magnification, depicting the microstructure of a dried, 40% WPI with 10% sucrose bead. Center: Scanning electron micrograph image at 1000x magnification, depicting the microstructure of a dried, 40% WPI with 10% sucrose bead. Right: Scanning electron micrograph image at 2000x magnification, depicting the microstructure of a dried, 40% WPI with 10% sucrose bead.

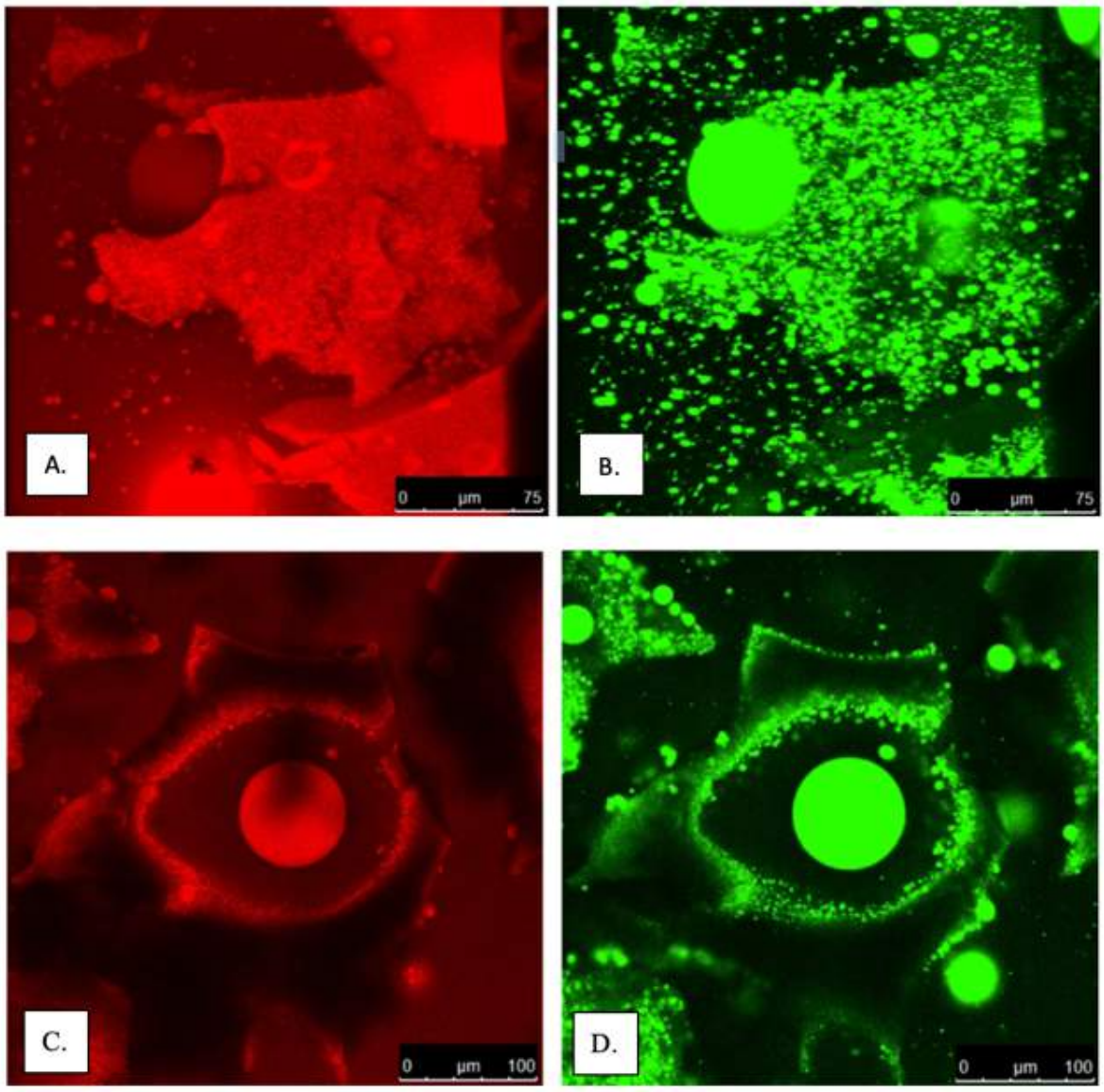


Figure 2.8 A-D. Confocal laser scanning micrograph images depicting the microstructure of a dried, 40% WPI with 10% sucrose bead, with oil droplets dispersed throughout image. A and C: Highlight protein in bright red and other components as darker colors. B and D: Highlight fat in bright green and other components as darker colors.

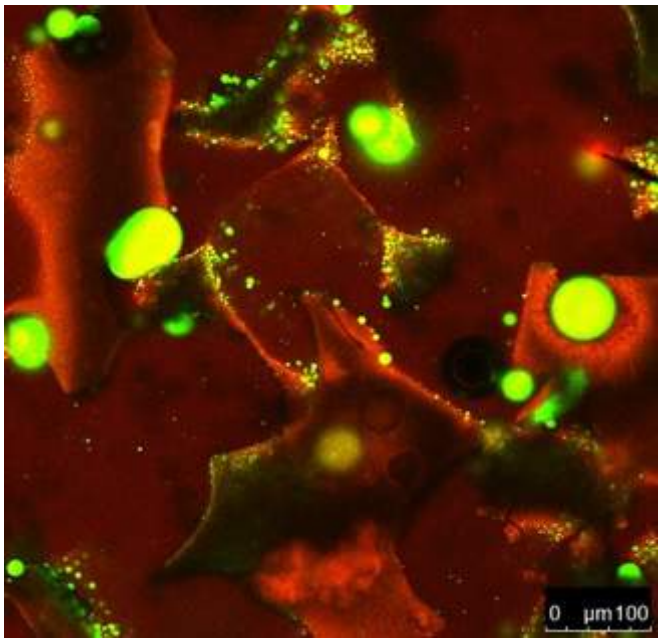


Figure 2.9. Confocal laser scanning micrograph image depicting the microstructure of a dried, 40% WPI with 10% sucrose bead, with oil droplets dispersed throughout image; highlighting proteins in bright red, fat in bright green, and other components (mainly sucrose) as darker colors. The darker colored sucrose is thought to form the translucent, glassy fragments shown throughout the image.

2.3.2.2 Water activity, a_w

The process of drying fresh beads at 70°C for 3 h in the vacuum oven resulted in the reduction of a_w (from ~0.9 (**Table 2.3**) to ~0.2 (**Table 2.4**)), resulting in increased microbial stability. In the comparison of thermal treatments of drops, it was found that increased oil temperatures and heating times resulted in reduced a_w values of fresh beads (**Fig. 2.3A**, **B**). Results show a decreasing trend in a_w as oil temperature is increased, with a significant reduction ($p < 0.05$) in a_w occurring between 100 and 110°C (from 0.90 to 0.77 a_w, respectively). A similar, decreasing trend in a_w is observed with increased heating times, with a significant reduction ($p < 0.05$) in a_w occurring between 2 and 5 min of heating (from 0.90 to 0.84 a_w,

respectively). Apparently heating time and oil temperature determine the extent of drying, as shown by reduced water contents and water activities.

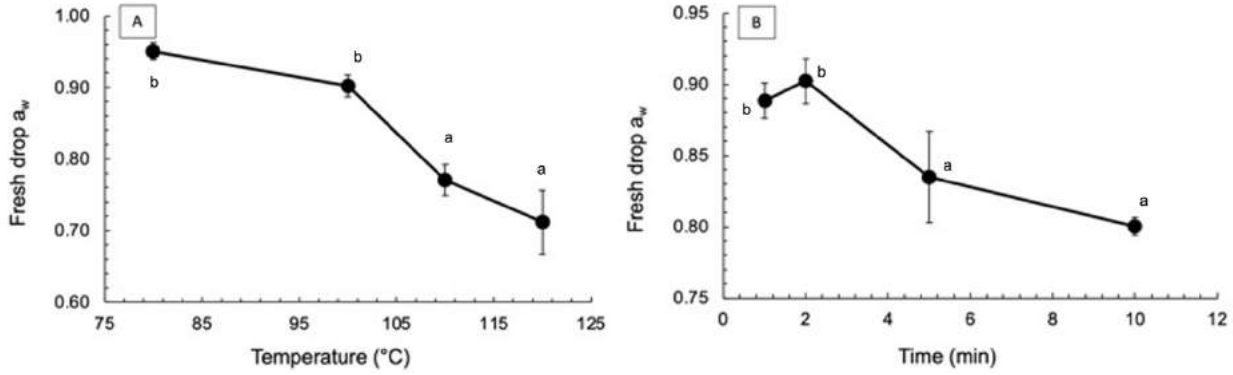


Figure 2.3.

A- Effect of oil temperature (°C) on dehydration shown by a_w of fresh drops comprised of 40% WPI with 10% sucrose for 2 min; n = 3. Lines are for guiding purposes only. Data points connected by the same letter are not significantly different ($p > 0.05$) from other points connected by the same line.

B- Effect of heating time (min) at 100°C on dehydration shown by a_w of fresh drops comprised of 40% WPI with 10% sucrose; n = 3. Lines are for guiding purposes only. Data points connected by the same letter are not significantly different ($p > 0.05$) from other points connected by the same line.

2.3.2.3 Drop diameter

Diameters were measured for beads made from 40% WPI, 40% WPI with 10% sucrose, and 30% WPI with 20% sucrose. Beads obtained from 35% WPI with 15% sucrose at pH 4.5 were not spherical in shape (data not reported). Our results indicated that upon drying, significant shrinkage (as obtained from bead diameters; $p < 0.05$) occurred in the beads made from 40% WPI (from 5.06 fresh to 4.50 mm dried), while beads containing sucrose did not experience shrinkage. This was likely due to the formation of sucrose glass upon drying, preventing further shrinking by stabilizing the protein network structure.

Chan et al. (2009) reported that drops formed from calcium-alginate by dripping sometimes have smaller size than predicted, possibly due to shrinkage experienced in gelling solutions. Our beads produced with 40% WPI had larger fresh diameters than predicted with Equation 6, with the 40% WPI products having significantly larger ($p < 0.05$) diameters than predicted (5.06 and 4.79 mm, respectively). While all beads were observed to show expansion behaviors of the gel networks within the heated oil, it would appear that beads without sucrose underwent more extensive expansion. Feeds containing 40% WPI with 10% sucrose had significantly higher ($p < 0.05$) viscosity compared to those with 40% WPI (1.73 and 0.51 Pa*s, respectively) (**Fig. 2.1b**); as a result of its higher viscosity, 40% WPI with 10% sucrose beads may have undergone expansion to a lesser extent upon heating. Additionally, feeds with 40% WPI and 10% sucrose contained less water than 40% WPI feeds and thus underwent less drying. Corresponding results would be expected for the beads comprised of 30% WPI with 20% sucrose, but the data showed a significant reduction ($p < 0.05$) in drop diameters compared to predicted values (only 2.19 mm fresh compared to predicted 4.39 mm; data not reported). That may be due to the reduced protein content causing weakness in the typically strong forces of self-assembly imparted by high (40% w/w) concentrations of protein within the feed drops, which were overcome by the drag forces upon impact with the oil as well as the magnetic stir bar, thus causing the observed breaking of drop structures within the oil bath. The diameters of 40% WPI with 10% sucrose drops were only slightly larger than predicted and not statistically significant, indicating that calculations used to predict drop diameters were accurate.

Drop diameters were also measured to compare thermal treatments of beads and used to calculate bead volumes (**Fig. 2.4)**. Results show a relationship between decreasing bead volumes and increasing heating times, with a significant reduction ($p < 0.05$) in bead volume occurring

between 5 and 10 min of heating (from 83 to 53 mm^3). Decreasing volumes of beads with increasing heating times could be a result of more extensive dehydration occurring within the drops, as confirmed by a_w data, causing further shrinking as more water was lost and structure hardening occurred. Products formed at increasing temperatures were more irregular in morphology and structures were broken, therefore diameters could not be measured.

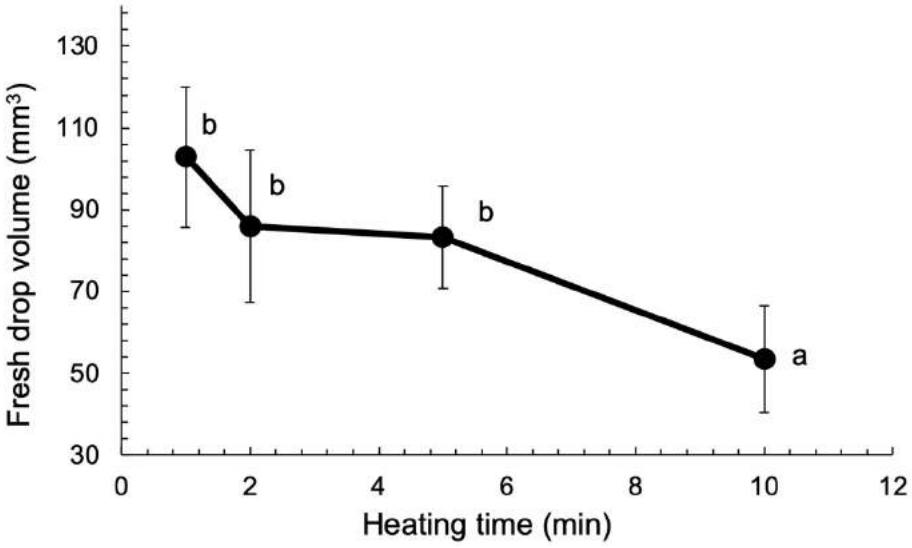


Figure 2.4. Effect of dehydration shown by heating time (min) at 100°C on the volume (mm^3) of drops comprised of 40% WPI with 10% sucrose; n = 3. Lines are for guiding purposes only. Data points connected by the same letter are not significantly different ($p > 0.05$) from other points connected by the same line.

2.3.2.4 Hardness

The hardness of dried beads formed by 40% WPI and 40% WPI with 10% sucrose were compared. Hardness was shown to be less with 10% w/w sucrose (from 232 to 155 N), likely due to the formation of a sucrose glass upon drying; **Fig. 2.7B** shows that the gel structure is largely not visible in dried beads, and it is assumed that much of the gel network may have the smooth, amorphous sucrose glass form around it. When injection methods have been employed to extrude biopolymer solutions containing multiple components, it is possible to form particles with

heterogeneous, dispersion-type internal structures where one component may be dispersed within the other (Matalanis et al., 2011). This describes what our data suggests is happening within bead structures, as it appears that the protein phase is independent and forms a gel that is surrounded by the protective, smooth, glassy matrix after dehydration. The presence of glass may cause the product to be more fragile by breaking up regions of dense protein-protein interactions with brittle glass, potentially weakening the otherwise dense protein gel network that would form if no sucrose were present. **Figures 2.7A**, **2.8A, B,** and **C**, and **2.9** all depict the glass that forms upon drying, and the clouded appearance of some pieces may be due to the dried, aggregated protein network dispersed throughout or located at the glassy interface. A study by Al-Marhoobi and Kasapis (2005) of concentrated dispersions of gelatin with sugar as a co-solvent indicated that sugars were preferentially excluded from the protein region, with TEM analysis confirming the presence of separate sugar- and protein-rich phases in the product rather than homogeneous mixtures. They reported that the presence of sugars promoted protein association in their system, giving high network strength retention.

In the comparison of thermal treatments of beads, it was found that the hardness of fresh beads increased linearly with heating time (**Fig. 2.5**). The irregular morphologies and broken nature of beads formed with varied oil temperatures prevented the samples from being measured for hardness, as uniform beads were critical for accuracy of comparisons. Overall, large variations in hardness were recorded, potentially due to the nature of the products as well as the test involving multiple beads per single measurement. Testing of multiple products at once was determined important in describing the products overall, with inherent variability better accounted for.

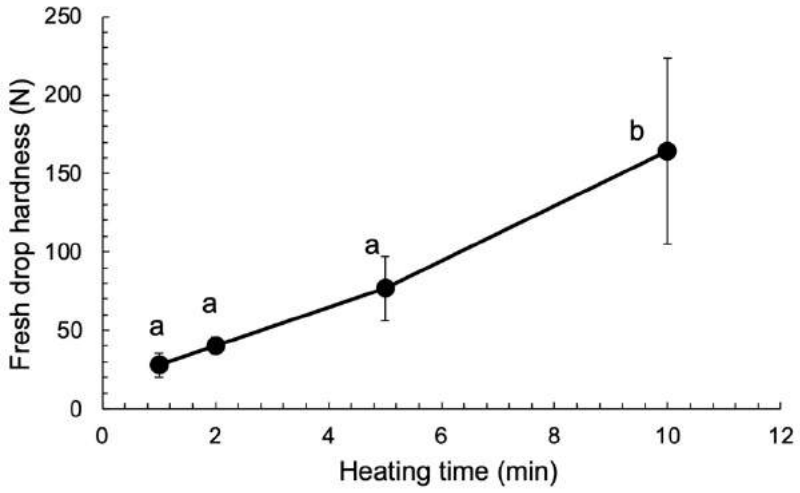


Figure 2.5. Effect of dehydration shown by heating time (min) at 100°C on the hardness (N) of drops comprised of 40% WPI with 10% sucrose; n = 3. Data points connected by the same letter are not significantly different ($p > 0.05$) from other points connected by the same line.

2.3.2.5 Densities and porosity

The total volume and true densities of dried beads formed by 40% WPI and 40% WPI with 10% sucrose were measured and used to calculate average total volume and average solids volume in order to calculate porosity. Porosity was not significantly ($p > 0.05$) different for beads prepared from feeds containing 40% WPI and 40% WPI with 10% sucrose. Water dehydrates out of structures containing only WPI and leaves pores in the structure, as can be seen in **Figures 2.7A**, and **2.8 A, C,** and **D** with rounded cavities throughout the fragments. Structures containing sucrose experience some dehydration and loss of water, but likely remain more fluid and may experience slightly more collapse as the protein network may be diluted by sugars present. These concentrated sucrose solutions form a glassy structure when oven dried, slightly reducing total unoccupied space in the structure as sucrose molecules are sterically larger than water. This is visualized in **Figure 2.7B**, where smooth, fractured edges highlighted in the

images tend to have relatively rounded edges, indicating that sucrose glass formed within the pores left behind from water drying from the product.

In the comparison of thermal treatments of beads composed of 40% WPI with 10% sucrose, it was found that there was no significant variation in porosity of beads with increased heating (**Table 2.6**). This may indicate that feed composition may more strongly determine drop porosity than processing conditions.

Table 2.6

Sample	Heating time at 100°C (min)	Total volume (cm^3)		Calculated average total volume (cm^3)	True density (g/cm^3)		Calculated average solids volume (cm^3)	Calculated Porosity (%)
		Rep 1	Rep 2		Rep 1	Rep 2		
40/10	1	3.90 ± 0.01	5.16 ± 0.02	4.53	1.11 ± 0.01	1.10 ± 0.01	2.61	42 ± 3[a]
40/10	2	3.86 ± 0.01	3.75 ± 0.01	3.80	1.07 ± 0.01	1.08 ± 0.01	2.27	41 ± 2[a]
40/10	5	4.09 ± 0.01	2.30 ± 0.02	3.19	0.99 ± 0.01	1.07 ± 0.01	2.09	34 ± 4[a]
40/10	10	2.65 ± 0.01	3.88 ± 0.01	3.26	1.07 ± 0.01	1.09± 0.01	2.02	38 ± 1[a]

Superscript letters in the same column indicate statistically significant ($p < 0.05$) difference

Total volumes (cm^3) and true densities (g/cm^3) of dried drops comprised of 40% WPI with 10% sucrose (40/10) obtained at various heating times (min) at 100˚C; values were used to calculate average total volumes and average solids volumes (cm^3), respectively, in order to calculate porosity (%).

2.3.2.6 Microscopy

Combinations of optical light-, confocal laser scanning-, and scanning electron microscope images of fractured beads aided in demonstrating the porous, oil-embedded, aggregated protein network structures produced by feeds containing 40% WPI and indicated the presence of a glassy structure in samples containing sucrose.

Fig. 2.8 A-D are confocal images for 40% WPI with 10% sucrose, and aid in discerning the ‘layers’ of the structure of the fractured material. Image ‘A’ highlights proteins in bright red, while other components have darker color. The broken, glassy, translucent structure appears in

the image, either embedded with red protein particles or populated with proteins at the glassy surface, and having a round cavity carved into its side, indicative of a broken porous structure. Image 'B' highlights oil in bright green, with other components having a darker color. It is apparent that the glassy structure is covered with oil droplets, as oil is known to be dispersed throughout the 3D structure based on videos comprised of 'stacked' confocal images taken at different depths. Images 'C' and 'D' also aid in demonstrating the porous structure of the beads as well as the presence of a glassy matrix, protein network, and oil droplets in the structure. Image 'C' highlights proteins in bright red and other components with darker hues. A glassy, fractured piece of the structure is at the center of the image in the shape of a cavity, indicative of the presence of a pore in the 3D structure, and an oil droplet (confirmed by image 'D,' highlighting oil in bright green) directly at its center. The dark areas of the glassy structures may be sucrose, while the bright red parts lining the pore shows the presence of the protein network. Image 'D' shows a dispersion of small oil droplets along the glassy pore. The dark background of the glassy portion indicates the presence of sucrose.

Fig. 2.9 is a confocal image of the 40% WPI with 10% sucrose beads and a good example of the protein- and oil-highlighted images being layered to give an idea of overall structure composition. Fat appears as bright green, proteins are bright red, and other components (mainly sucrose in this case) are darker. Translucent, glassy fragments are present in the image, with protein scattered throughout, as well as oil droplets dispersed throughout the structure.

2.4 Conclusions

We report a full process design for simple solidification of liquid dispersions (in an oil bath at 100°C for 2 min) and a structure-forming formulation (40% WPI with 10% sucrose) used further to vitrify; apparent bulk oil inclusion and its emulsification into small drops throughout

the structure is demonstrated. This study presents a potential process to make foods with entrapped flavors or actives, including emulsion droplets. The process may be a novel alternative to drying or extrusion that is simple, economic, and effective.

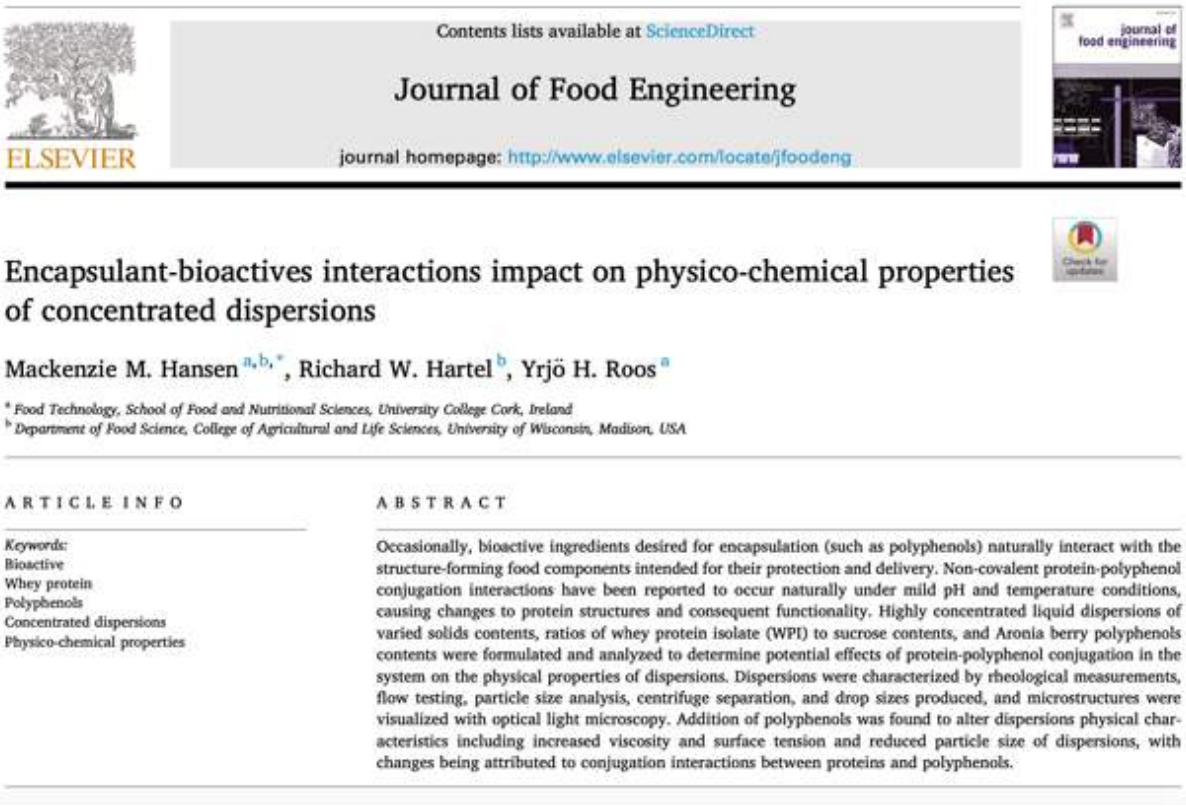
Future work is necessary to expand our understanding of the physical properties of feed dispersions including thermal properties and physical states of final beads, to adapt the process to form beads containing active ingredients, and to determine the protectant abilities of wall components and the location of active ingredients in the matrix. A major challenge when aiming to encapsulate bioactive ingredients is the retention of the active throughout the process in order to obtain final materials in which the actives are still accessible. Similar to spray drying, the process presented forms beads capable of containing bioactives that are not expected to suffer exposure to high temperatures; evaporation of water from the structures keeps beads at low temperatures, and the oil temperature is primarily a measure of energy input.

Acknowledgements

This research was supported by funding provided by the Lauritzson Foundation in the form of the Lauritzson Research Scholarship, through the College of Science, Engineering and Food Science (SEFS) at University College Cork. The authors would like to thank the anonymous reviewers and Journal Editor for thorough reading of the manuscript and helpful comments for revision.

Chapter 3

Journal of Food Engineering 302 (2021) 110586



Contents lists available at ScienceDirect

Journal of Food Engineering

journal homepage: http://www.elsevier.com/locate/jfoodeng

Encapsulant-bioactives interactions impact on physico-chemical properties of concentrated dispersions

Mackenzie M. Hansen [a,b,*], Richard W. Hartel [b], Yrjö H. Roos [a]

[a] Food Technology, School of Food and Nutritional Sciences, University College Cork, Ireland
[b] Department of Food Science, College of Agricultural and Life Sciences, University of Wisconsin, Madison, USA

ARTICLE INFO

Keywords:
Bioactive
Whey protein
Polyphenols
Concentrated dispersions
Physico-chemical properties

ABSTRACT

Occasionally, bioactive ingredients desired for encapsulation (such as polyphenols) naturally interact with the structure-forming food components intended for their protection and delivery. Non-covalent protein-polyphenol conjugation interactions have been reported to occur naturally under mild pH and temperature conditions, causing changes to protein structures and consequent functionality. Highly concentrated liquid dispersions of varied solids contents, ratios of whey protein isolate (WPI) to sucrose contents, and Aronia berry polyphenols contents were formulated and analyzed to determine potential effects of protein-polyphenol conjugation in the system on the physical properties of dispersions. Dispersions were characterized by rheological measurements, flow testing, particle size analysis, centrifuge separation, and drop sizes produced, and microstructures were visualized with optical light microscopy. Addition of polyphenols was found to alter dispersions physical characteristics including increased viscosity and surface tension and reduced particle size of dispersions, with changes being attributed to conjugation interactions between proteins and polyphenols.

Encapsulant-bioactives interactions impact on physico-chemical properties of concentrated dispersions

Mackenzie M. Hansen[a,b*], Richard W. Hartel[b], Yrjö H. Roos[a]

[a] Food Technology, School of Food and Nutritional Sciences, University College Cork, Ireland

[b] Department of Food Science, College of Agricultural and Life Sciences, University of Wisconsin-Madison

Published as: Hansen, M. M., Hartel, R. W., & Roos, Y. H. (2021). Encapsulant-bioactives interactions impact on physico-chemical properties of concentrated dispersions. *Journal of Food Engineering*, *302*, 110586.

Abstract

Occasionally, bioactive ingredients desired for encapsulation (such as polyphenols) naturally interact with the structure-forming food components intended for their protection and delivery. Non-covalent protein-polyphenol complexation interactions have been reported to occur naturally under mild pH and temperature conditions, causing changes to protein structures and consequent functionality. Highly concentrated liquid dispersions of varied solids contents, ratios of whey protein isolate (WPI) to sucrose contents, and Aronia berry polyphenols contents were formulated and analyzed to determine potential effects of protein-polyphenol complexation in the system on the physical properties of dispersions. Dispersions were characterized by rheological measurements, flow testing, particle size analysis, centrifuge separation, and drop sizes produced, and microstructures were visualized with optical light microscopy. Addition of polyphenols was found to alter physical characteristics including increased viscosity and surface tension and reduced particle size of dispersions, with changes being attributed to complexation interactions between proteins and polyphenols.

3.1 Introduction

When aiming to develop novel food products with high nutritional value, satisfactory processing properties, and unique structures and functional properties, Bovine whey proteins continue to be a popular choice (Kulmyrzaev et al., 2000). Whey protein isolate (WPI) is often selected in particular for development due to its solubility, wide range of functionality, and broad food applications (Cao and Xiong, 2017). Foods with enhanced protein contents and fruit components are in high demand due to increased consumer interest in health foods containing bioactives. Bioactives are natural compounds found in foods that may affect human health, and polyphenols from fruits are one type of bioactive compound known to have many benefits (Biesalski et al., 2009; Schneider, 2016; Fang and Bhandari, 2017).

Polyphenols (PP) are a group of compounds found naturally in plants, including tea, coffee, fruits, and vegetables regularly consumed in the human diet. The compounds strong antioxidant and anti-inflammatory activities have been shown to aid in preventing the development of diseases and disorders including colon cancer (Malik et al., 2003; Zhao et al., 2004; Bermudez-Soto et al., 2007), cardiovascular disease (Mink et al., 2007), neurodegenerative diseases encountered upon aging (Moskovitz et al., 2002; Li et al., 2017), diabetes (Simeonov et al., 2002), and obesity (Zielińska-Przyjemska et al., 2007; D. Li et al., 2017). Polyphenols antioxidant and anti-inflammatory properties are associated with mitigation of heart attack risk (Cassidy et al., 2013) and atherosclerosis (Yousuf et al., 2016; Khoo et al., 2017; Li et al., 2017), as well as promoting healthy serum cholesterol levels (Valcheva-Kuzmanova et al., 2007a; b; c). These findings have driven developers to formulate food products with polyphenols in an attempt to impart additional nutritional benefits (Cao and Xiong, 2017; Ćujić et al., 2018).

Polyphenols are known to be chemically unstable in storage and highly susceptible to degradation (Mazza and Brouillard, 1987; Francis and Markakis, 1989; Volf et al., 2014). Stability can be affected by polyphenolic molecular structure, concentration, environmental conditions including solvent, water activity, pH, temperature, light, oxygen, ionic strength, the presence of other compounds including ascorbic acid, metals, sugars and their degradation products, enzymes, and reactions including copigmentation, self-association, and condensation (Mazza and Brouillard, 1990; Rodriguez-Saona et al., 1999; Friedman & Jürgens, 2000; Bąkowska et al., 2003; Castañeda-Ovando et al., 2009). Fresh polyphenol sources tend to have short shelf lives, and much care must be taken to maintain polyphenols through formulation and processing of food products with longer shelf lives. Recently, complexation of polyphenols with other molecules has been utilized as a method of active stabilization, with milk protein-polyphenol complexes being widely popular to study for potential bioactive delivery and health benefits (Chung et al., 2015; Cao and Xiong, 2017; Quan et al., 2019).

Decades of research focused on the addition of phenolic compounds to protein-containing food matrices have reported a common finding: a natural affinity exists between polyphenols and proteins to complex and form conjugates (Hagerman and Butler, 1978; Foegeding et al., 2017). Polyphenols (relatively small molecules, ~180-700 Da) are able to bind to sites on proteins (comparatively large molecules; average MW of WPI ~17,000 Da (Ma and Zhao, 2019)) forming small, soluble complexes of varied nature at low concentrations. While Spencer et al. (1988) postulated that protein-polyphenol complexation was likely pH-dependent, Schneider (2016) found that large complexed particles formed from mixtures of proteins and juices containing polyphenols were not formed in corresponding ‘imitation juices’ with identical pH but without polyphenols, confirming that changes to physicochemical properties of dispersions were not

simply due to a pH effect. Complexation interactions between polyphenols and proteins in food systems are mainly divided into non-covalent and covalent interactions. The extent and type of interactions are dependent on pH, protein and polyphenol types present, concentration ratios, and reaction times (Schneider, 2016; Quan et al., 2019). Non-covalent interactions are common in processed foods, occur under neutral and acidic environmental pH conditions, and consist mainly of weak binding interactions including van der Waal's forces, hydrogen bonding, and hydrophobic interactions (Kanakis et al., 2011; Bohin et al., 2012; Le Bourvellec and Renard, 2012; Chung et al., 2015; Schneider, 2016; Oancea et al., 2017). Non-covalent complexes formed between proteins and polyphenols, driven mainly by hydrophobic interactions, have been reported to significantly change the structures of the proteins at room temperature (Rawel et al., 2005; Cao and Xiong, 2017; Ma and Zhao, 2019; Quan et al., 2019).

In previous work, we presented a continuous process for forming concentrated, liquid dispersions comprised of WPI and sucrose into dry, stable beads with high protein contents that could serve to encapsulate active ingredients (Hansen et al., 2020). We identified the "next step" to be completed in subsequent experiments was the addition of an active ingredient to the protein-sucrose matrix. Aronia berries are reported to be a rich source of dietary polyphenols including anthocyanins, flavonoids, chlorogenic acid, proanthocyanidins, and hydroxycinnamic acids (Taheri et al., 2013; Xie et al., 2016, 2017). Thus, Aronia is of interest for formulation. Though acknowledged to occur, the functional effects of non-covalent interactions under neutral and acidic pH conditions at mild temperatures have not been investigated as thoroughly as their covalent counterparts, despite developers opting for gentle processing conditions to better protect actives in nutritional products (Cao and Xiong, 2017; Ma and Zhao, 2019; Xue et al., 2020).

The aim of this study is to investigate and characterize the physical, functional, and practical processing consequences of non-covalent complexation interactions on the physical properties of liquid feed dispersions. We hypothesize that the addition of polyphenols (via Aronia extract) will give rise to changes in the physical properties of feeds including viscosity, flow behavior, and particle size distribution due to protein-polyphenol complexation, compared to properties of dispersions without Aronia. This work would contribute to the limited body of research describing non-covalent interactions between proteins and polyphenols under mild conditions, characterizing their effects on the physical properties of mixtures. In addition, we hope to provide practical knowledge for further applications such as encapsulation, protection, and delivery with concentrated protein-polyphenol mixtures.

3.2 Materials and Methods

3.2.1 Materials

Whey Protein Isolate, WPI (IsoChill 9000), was supplied by Agropur, Inc. (Luxemburg, Wisconsin, USA). Sucrose (pure cane, extra fine, granulated sugar) was supplied by Domino Foods, Inc. (Yonkers, New York, USA). Standardized Aronia berry (Chokeberry) Powder, containing a minimum level of 15% anthocyanins and 55.6% total polyphenols, was supplied by Artemis International (Fort Wayne, Indiana, USA) and stored in a freezer at -18°C in the absence of light. Deionized (D.I.) water was utilized in all experiments.

3.2.2 Dispersion preparation

A dry blend of sucrose and WPI powder was prepared at room temperature. To prepare liquid feeds, D.I. water was weighed and the WPI-sucrose blend was mixed into the water with a Fisher Scientific PowerGen 125 Homogenizer (125 W, 115 V, 50/60 Hz; maximum volume 100

mL; speed 8,000-30,000 RPM; Hampton, New Hampshire, USA) at a speed setting of '6' for ~45 s. The WPI-sucrose solution was subsequently combined with an aliquot of 50% Aronia extract solution (Aronia powder containing 55.6% total polyphenols mixed into D.I. water) to obtain desired WPI, sucrose, polyphenols (PP), and water proportions (~30 s additional mixing). More extract solution was required to reach the desired polyphenol content of mixtures due to the presence of other compounds besides PP in the Aronia extract. pH was measured with an Accumet Basic AB15 meter (Fisher Scientific, Hampton, New Hampshire, USA) after calibrating the electrode at pH four and seven.

Duplicates of twenty-seven formulations of varied solids contents and compositions were prepared for subsequent triplicate analysis in a 3x3x3 factorial design, with experiments conducted in a random order (**Table 3.1**). Ratios of WPI to sucrose and total solids contents were selected based on findings from our previous work (Hansen et al., 2020); all formulations were prepared within a range of total solids (%) projected to pump successfully under the selected conditions. Levels of Aronia extract/ PP were selected to compare formulations without the active (0%) to formulations with 2 different levels of addition. Studies have indicated that complexation may occur at PP addition levels from 0.1% to 1%, rendering the selection of 0.5 and 1% PP reasonable (Harbourne et al., 2011; von Staszewski et al., 2011; Thongkaew et al., 2014; Bayraktar et al., 2019). All dispersions were left to defoam for at least one hour before analysis.

Table 3.1.

WPI:sucrose	Total solids	[PP]	pH	Diameter (calculated)	Diameter (frozen)
-	%		-	mm	mm
0.75	25	0	6.03	4.59 ± 0.02	4.45 ± 0.09
1	25	0	6.08	4.60 ± 0.02	4.58 ± 0.10
1.25	25	0	6.01	4.54 ± 0.03	4.48 ± 0.05
0.75	25	0.5	5.73	4.67 ± 0.03	4.63 ± 0.03
1	25	0.5	5.94	4.67 ± 0.04	4.63 ± 0.09
1.25	25	0.5	5.95	4.65 ± 0.06	4.55 ± 0.14
0.75	25	1	5.57	4.65 ± 0.08*	4.39 ± 0.08*
1	25	1	5.72	4.70 ± 0.03	4.50 ± 0.12
1.25	25	1	5.84	4.67 ± 0.05	4.65 ± 0.02
0.75	35	0	6.00	4.37 ± 0.14	4.22 ± 0.10
1	35	0	6.19	4.55 ± 0.05	4.50 ± 0.03
1.25	35	0	6.09	4.57 ± 0.03*	4.41 ± 0.03*
0.75	35	0.5	5.79	4.55 ± 0.02	4.51 ± 0.03
1	35	0.5	5.98	4.51 ± 0.10	4.35 ± 0.06
1.25	35	0.5	5.92	4.52 ± 0.03	4.44 ± 0.08
0.75	35	1	5.79	4.63 ± 0.04*	4.46 ± 0.04*
1	35	1	5.81	4.63 ± 0.03	4.52 ± 0.11
1.25	35	1	5.82	4.63 ± 0.03	4.59 ± 0.07
0.75	45	0	6.16	4.51 ± 0.03*	4.24 ± 0.10*
1	45	0	6.10	4.50 ± 0.02	4.37 ± 0.11
1.25	45	0	6.06	4.50 ± 0.02	4.39 ± 0.16
0.75	45	0.5	5.89	4.53 ± 0.04	4.41 ± 0.10
1	45	0.5	5.82	4.23 ± 0.02	4.31 ± 0.09
1.25	45	0.5	6.03	4.55 ± 0.06	4.49 ± 0.05
0.75	45	1	5.78	4.51 ± 0.05	4.35 ± 0.12
1	45	1	5.88	4.57 ± 0.06	4.45 ± 0.12
1.25	45	1	5.79	4.52 ± 0.05	4.48 ± 0.06

* indicates significant differences between calculated and measured diameters

Estimated drop diameters calculated from flow tests data and measured diameters (mm) of frozen drops formed from feed dispersions with varied WPI:sucrose, total solids contents, polyphenols concentrations, and pH.

3.2.3 Feed characterization:

3.2.3.1 Flow testing

Flow properties of feed dispersions at room temperature were measured as reported in our previous work (Hansen et al., 2020). Briefly, dispersions were pumped through a benchtop, manual control, variable speed, peristaltic pump (120 S/DV; Watson Marlow, Falmouth, England) with silicon tubing 85 cm length, 2 mm bore, and 1 mm wall thickness (BÜCHI Labortechnik AG, Flawil, Switzerland) at a constant speed (13 RPM). The time required to deposit 10 mL of feed, the number of drops deposited per 1 min, mass of 10 mL of feed, and average masses of individual drops were measured in triplicate and recorded, allowing for mass flow rates, volume flow rates, feed densities, drop surface tensions, drop diameters, and drop volumes to be calculated.

Density of liquid feed (kg/m^3) was calculated by:

$$\frac{mass\ (g)\ of\ 10\ mL\ feed}{10\ mL} \tag{1}$$

Average drop volume (mL) was calculated by:

$$\frac{10\ mL\ feed}{time\ (s)\ to\ deposit\ 10\ mL} * \frac{60s\ \ per\ min}{\#\ drops\ per\ min} \tag{2}$$

Mass flow rate (kg/s) was calculated by:

$$\frac{mass\ (g)\ of\ 10\ mL\ feed}{time\ (s)\ to\ deposit\ 10\ mL} \tag{3}$$

Volume flow rate (m^3/s) was calculated by:

$$\frac{mass\ flow\ rate\ (\frac{kg}{s})}{feed\ density\ (\frac{kg}{m^3})} \tag{4}$$

Drop surface tension was calculated with Tate's Law (Worley, 1992):

$$\frac{(Average\ drop\ mass\ (g) * gravitational\ constant\ \left[9.8\ kg\ \frac{m}{s^2}\right])}{2\pi * (external\ radius\ of\ tubing\ tip\ [mm] * correction\ factor\ \left[\frac{capillary\ radius}{(drop\ volume)^{\frac{1}{3}}}\right])} \tag{5}$$

The correction factor in this calculation is in place because the total drop formed at the tip of the outlet tubing does not release, and residual liquid is left on the end of the tube.

Drop diameter was calculated by:

$$\left[\frac{(3 * average\ drop\ volume\ [mL])}{4 * \pi}\right]^{\frac{1}{3}} * 2 \tag{6}$$

This equation is built off the assumption that drops form a perfectly spherical shape, and thus is derived from the equation for the volume of a sphere:

$$V = \frac{4}{3}\pi r^3 \tag{7}$$

3.2.3.2 Rheology

A DHR-2 rheometer (TA Instruments, Delaware, USA) was used to measure the rheological properties of feed dispersions in triplicate, modifying the methods used by Harbourne et al. (2011) and Wang and Hartel (2020). Small-strain oscillatory measurements were conducted with a concentric cylinder attachment set, with a bob (28 mm diameter, 42 mm length) and cup

(30 mm diameter). Dispersions (20 mL samples) were poured into the cup and the bob was inserted into the sample until it reached the geometry gap (5917.1 μm). After the system was conditioned at 25°C for 60s, the samples were oscillated within their linear viscoelastic region (LVR; not shown) for 180s under 1% strain and 1 Hz frequency. *G*', *G*", complex viscosity, and other parameters were recorded.

To confirm that the strain selected for oscillatory measurements (1%) was within the LVR, a strain sweep test from 0.1 to 10% at a frequency of 1 Hz was performed along with oscillatory measurements for each formulation.

3.2.3.3 Particle size distribution

Particle size distribution of feed dispersions was measured in triplicate using a Malvern Mastersizer 2000 (Malvern Instruments Ltd., Worcestershire, U.K.) with Hydro 2000S liquid sampler. The laser light diffraction and light scattering techniques described by Warren and Hartel (2014) were modified to measure the sizes of insoluble WPI particles and potential WPI-polyphenol complexes in the dispersions. Dispersions were injected dropwise into the liquid sampling unit to obtain distributions. D.I. water was used as the dispersant, with a refractive index of 1.33. The WPI refractive index was set at 1.545 with absorbance set at 0.001. Measurements were taken at obscurations between 11% and 15% as described by Alawode (2014).

3.2.3.4 Optical light microscopy

The sizes of WPI particles and potential WPI-polyphenol complexes in dispersions were observed by optical light microscopy. The preparation method described by Warren and Hartel (2014) was utilized; 2 drops of feed dispersion were diluted with ~2 mL of D.I. water. Samples

were lightly mixed to obtain a homogeneous mixture with the water. One drop of diluted sample was placed on a glass slide and covered with a cover slip. Samples were imaged at 40x and 200x magnification via Nikon Eclipse FN1 optical microscope (Nikon Instruments Inc., Melville, NY, USA) with a Nikon Digital Sight DS-U3 camera control unit attached (ver. 1). Sample observation, photo capturing, and error-bars placement were performed in NIS-Elements D Imaging Software (ver. 4).

3.2.3.5 Centrifuge separation

Aliquots (1.25 g) of not diluted and 10 times diluted feed dispersions containing 45% total solids, as well as 1% Aronia polyphenols solution, were pipetted into microcentrifuge tubes in duplicate (1.5mL graduated tubes with flat caps, Fisherbrand ®, Fisher Scientific, Hampton, New Hampshire, USA) to observe separation after centrifugation at 12,000 rpm (~13,523 x g) and 20˚C for 20 min in a microcentrifuge (Centrifuge 5424 R with FA-45-24-11 rotor, Eppendorf, Hamburg, Germany). Sample tubes were visually assessed and photographed to identify the location of the colored polyphenolic compounds after centrifugation, as a colored precipitate after separation could confirm the formation of protein-polyphenol complexes. Supernatant was carefully removed from one of the sample tubes and placed in an empty tube so that supernatant and precipitate could be observed separately as well.

3.2.4 Frozen drop preparation

For solid bead formation, an aluminum pan was filled with liquid nitrogen (LN_2) (100% purity; Airgas, Madison, WI, USA) and placed on a Styrofoam layer to insulate between the pan and the worktop. A retort stand was arranged so that the end of the outlet tubing was situated above the surface of the LN_2. Liquid feed was pumped through the tubing and dispensed

dropwise into the LN_2, with irregular, gentle hand-stirring via metal spatula to discourage drop coalescence prior to solidification. Drops were left to freeze/harden in the LN_2 for ~5 min before removal and immediate triplicate diameter measurements.

3.2.4.1 Frozen drop diameters

Diameters of frozen beads were measured 3 times per formulation after hardening in LN_2 with digital Vernier calipers (0-150 mm; Stainless Hard), and an average value was reported. Accuracy was not a concern as beads were measured immediately upon removal from LN_2 to prevent any shrinkage due to melting, maintaining solid structures and shapes for measurements (Lee and Chan, 2013). Measured bead diameters were compared with calculated estimate values.

3.2.5 Statistical analysis

Repeated experiments were analyzed in triplicate. The obtained data were analyzed by calculating mean values and standard deviations. Analysis of variance (3-way ANOVA; Tukey's HSD test) and independent measures t-tests (equal variance not assumed) were performed to compare mean values when appropriate using JMP® Pro version 15.0.0 (SAS Institute Inc., Cary, North Carolina, USA). The level of significance was determined at $p < 0.05$.

3.3 Results and Discussion

3.3.1 Feed characterization:

3.3.1.1 pH

pH of dispersions were observed to decrease slightly with increasing PP addition (**Table 3.1**). pH effects have potential to influence intermolecular interactions and functional properties

including viscosity and particle size (Spencer et al., 1988; Saluja & Kalonia, 2005; Cao & Xiong, 2017; Hong et al., 2018b). When solution pH is away from the protein isoelectric point (pI) intermolecular interactions are unfavorable, allowing proteins to remain suspended with a relatively low viscosity; when pH approaches pI proteins are more likely to aggregate (Song, 2009; Coupland, 2014). pH may also influence which protein side groups are exposed in the system and thus determine the number of binding sites available for protein-polyphenol interactions to occur, which may affect the size of complexes formed (Rawel et al., 2005). Assuming an average pI for WPI between pH 4.2 and 5.3, it is unlikely that the slight downward shift in pH resulting from the addition of small proportions of Aronia extract was cause for measurable changes to dispersions physical properties or protein functionality, as pH was still substantially higher than the pI values reported in the literature for constituent β-lactoglobulin (pI ~ 5.2-5.3) and α-lactalbumin (~ 4.2-4.8) (Kilara & Harwalkar, 1996; Demetriades & McClements, 1998; Jean et al., 2006). Work by Schneider (2016) also verified that particle size changes in protein- juice dispersions were not due to changes in pH alone.

3.3.1.2 Interfacial tension

Individual drops will form out of feeds when the gravitational forces acting on the drop overcome the surface tension forces acting around the circumference of the tip of tubing, rendering surface tension properties critical in determination of drop sizes produced. Feeds containing 1% PP had slightly higher surface tensions than corresponding feed formulations with lower PP, though generally no large changes in surface tension were observed with increasing % TS (**Figure 3.1a**). According to the ANOVA, % TS significantly impacted the surface tension of feeds. Tukey's HSD tests further clarified that feeds with lower solids contents (25% TS) had

significantly higher ($p < 0.05$) surface tension values than those with higher solids concentrations (35 and 45% TS); this finding is best demonstrated by feeds containing 0.5% PP in **Figure 3.1A**. Previous studies have found that increased biopolymer concentrations and viscosities in dispersions have resulted in decreased surface tensions as well (Chan et al., 2009; Lee & Chan, 2013).

Changing the ratio of WPI to sucrose in feeds was not found to meaningfully impact the surface tension of feeds studied (**Figure 3.1B**) according to the ANOVA, though feeds containing 1% PP had slightly higher surface tensions than corresponding formulations with lower levels of PP. WPI to sucrose ratios of 1.25 and 1.0 were found to be significantly different from one another ($p < 0.05$) when Tukey's HSD tests were applied, but neither ratio was significantly different from the 0.75 WPI to sucrose ratio. Sucrose alone is not thought to affect surface tension notably, as sugars are not particularly surface-active molecules. The differences in whey proteins, which are known to behave as surfactants, were not sufficient to affect surface tension in these systems.

According to the ANOVA, changing the PP concentration in feeds had a significant overall effect on surface tension ($p < 0.05$). Tukey's HSD tests expanded on this, indicating that increasing PP content from 0 or 0.5% to 1% resulted in significantly increased surface tension values ($p < 0.05$). This trend was only observed under a few conditions, while many conditions showed no meaningful trends (**Figure 3.1C**); the variations in trends may be attributed to air entrapped in feeds giving altered surface tension calculations. Feeds comprised of 25% TS were observed to have the highest surface tensions of the formulations. Interactions between polyphenols and proteins are known to form complexes that can grow to the point of forming

larger aggregates, if environmental conditions, polyphenol and protein concentrations, ratios, and types are optimal (Schneider, 2016; Quan et al., 2019). As polyphenol concentrations increase (in this case, > 0.5%), so does complexation until sufficient coating promotes protein cross-linking via polyphenols serving as cooperative bridges, ultimately leading to precipitation of larger aggregates formed from smaller complexes when the 'critical coating level' is exceeded (Spencer et al., 1988; Charlton et al., 2002; Rawel et al., 2005; Ozdal et al., 2013). The increased presence of larger protein-polyphenol complexes and aggregates in dispersions would likely result in increased total intermolecular interactions in the system; liquids containing larger numbers of strong attractive intermolecular forces often have higher surface tensions (He et al., 2011; Tro et al., 2014), which may explain increased surface tensions observed with increasing PP for some formulations.

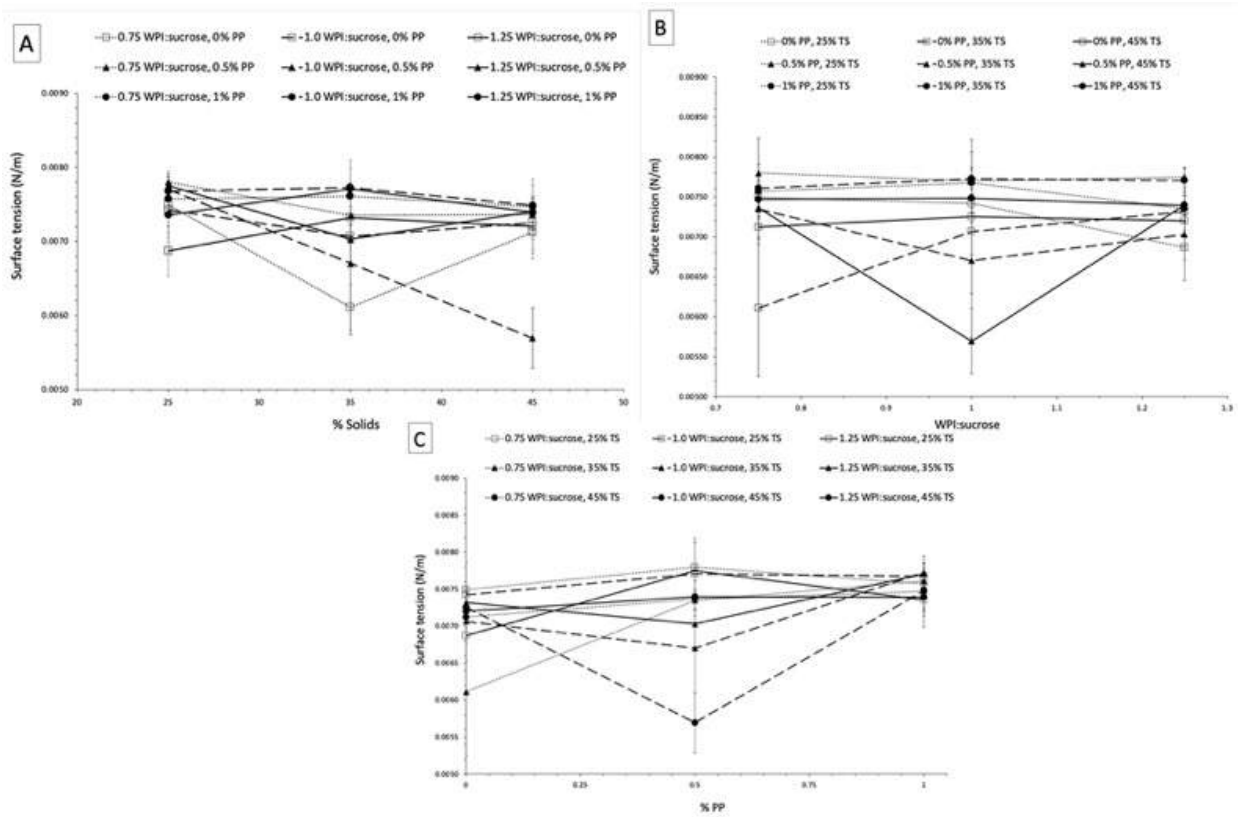


Figure 3.1. Effect of total solids content (%) [**A**], WPI:sucrose ratio [**B**], and PP content (%) [**C**] on the calculated surface tension (N/m) of dispersions at 25˚C; (n = 6). Lines are for guiding purposes only.

It has been reported that drop diameters and surface tension are directly related; as surface tension decreases, so does the diameter of the resulting drop, indicating that the pendant drop is sufficiently dense or packed with solids to detach at lower volumes and its surface tension was more easily overcome by gravitational forces. Upon plotting the calculated diameters of drops against the calculated surface tension of feed formulations the best fit line applied to our data showed a positive slope value (**Figure 3.2**) illustrating a positive, direct correlation, as described by Lee and Chan (2013). The scatter in the correlation is likely due to drop diameter and surface tension calculations built from calculated drop volumes and densities

measured, which may change with inclusion of unavoidable air in the dispersions, as well as the inherent variation within food ingredients.

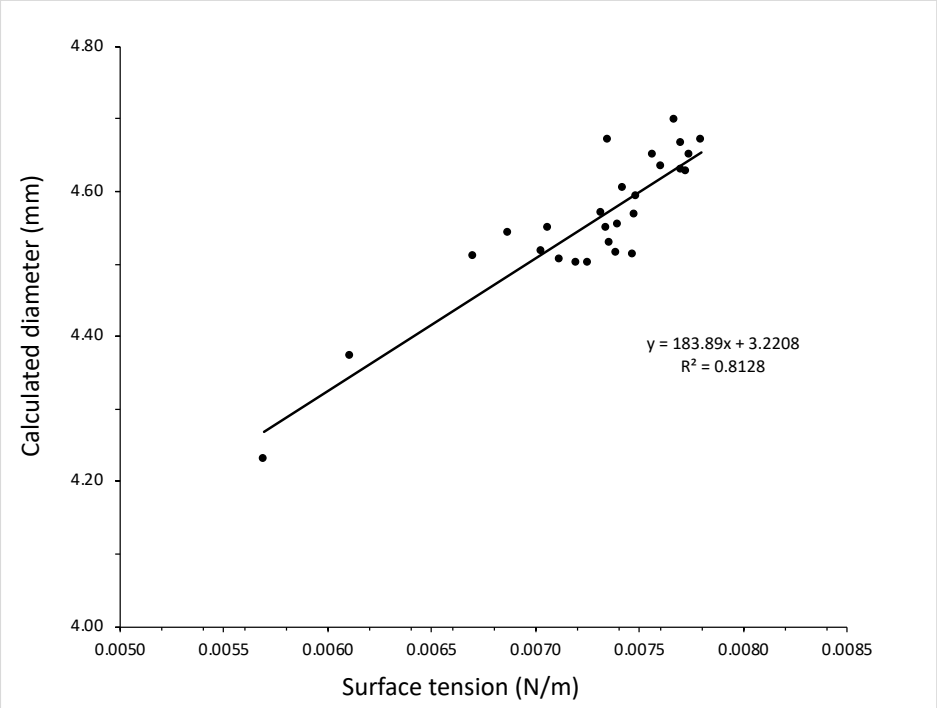


Figure 3.2. The relationship between the surface tensions (N/m) of feed dispersions containing WPI:sucrose ratios of 0.75, 1.0, and 1.25, polyphenols contents of 0, 0.5, and 1%, and total solids contents of 25, 35, and 45% at 25˚C and calculated diameters (mm) of drops.

Worley (1992) found that Tate's law could be used to determine unknown surface tensions within reasonable accuracy despite the simplicity of the drop weight method used. Other more traditional, commonly used methods including Wilhelmy plates, du Nuoy rings, capillary rise, maximum bubble pressure, and pendant drop measurements may provide more accuracy, but were not as compatible with the feed dispersions of interest due to their viscosity, stickiness, turbidity, remaining air bubbles present, and dark coloration when Aronia is present. All of these characteristics would make it harder to measure surface tension with conventional methods.

3.3.1.3 Viscosity

Viscosity is another important physical property of dispersions related to fluid flow properties, and often informs processing and manufacturing operations for a given product (Johnson et al., 1975; Hartel et al., 2018). Even slight alterations to composition and other dispersion conditions can cause increased crowding and entangling of particles, as well as promote conformational changes to protein structures that may enhance aggregation depending on side groups exposed, both of which increase viscosity (Song, 2009; Coupland, 2014). In addition to averaged complex viscosity data obtained from oscillatory time sweeps, information about the internal friction of feed materials was also obtained by measuring the viscous/ loss modulus- G", the storage modulus describing elasticity- G', and their ratio- tan δ (data not shown). G' was always greater than G" (tan δ was always < 1) for all formulations, indicating that feed dispersions demonstrated more elastic behaviors than viscous. Feeds comprised of 25% TS, 35% TS, and 45% TS had tan δ values < 0.1, < 0.2, and < 0.9 on average, respectively.

In previous work with dispersions containing only WPI and sucrose, we observed that viscosity increased with WPI concentration, in agreement with the findings from numerous earlier studies reporting direct, positive relationships between biopolymer concentrations and viscosity (Alizadehfard & Wiley, 1995; Patocka et al., 2006; Chan et al., 2009; He et al., 2011; Matalanis et al., 2011; Lee & Chan, 2013; Coupland, 2014; Hong et al., 2018b). Specifically, we observed minimally increasing viscosities with increasing concentrations at lower levels until a significant increase was observed at what was thought to be a 'critical packing point' concentration, where particle volume fractions and interactions became so abundant and crowded that viscosity was significantly increased due to steric repulsion between molecules causing

jamming and arrested feed dynamics (Hansen et al., 2020). This experiment yields complementary findings: although the ANOVA reported that % TS significantly ($p < 0.05$) impacted viscosity, when % TS increased from 25 to 35%, no appreciable change in viscosity was observed with Tukey's HSD tests for any feed formulations, indicating no significant differences between the conditions. Further increase to 45% TS resulted in significantly increased viscosities for all formulations ($p < 0.05$), with feeds comprised of 1.25 and 1.0 WPI:sucrose ratios generally having higher viscosities at 45% TS than those with 0.75 WPI:sucrose ratios (**Figure 3.3A**). It is likely that the threshold for 'critical packing concentration' was reached between 35 and 45% TS, as increased solids contents led to increased intermolecular interactions in the system, resulting in the significant increase in viscosity (Tro et al., 2014). Correspondingly, the ANOVA indicated that as the ratio of WPI to sucrose (and as a result, total protein content) increased in feed dispersions, complex viscosity was also found to significantly increase ($p < 0.05$). The increasing trend described by the ANOVA is only clearly demonstrated by feeds containing 45% TS in **Figure 3.3B**, which may be a result of the strong effect of 45% solids content on viscosity. The effect of increasing the WPI:sucrose ratio may be relatively weak compared to that of % TS, and thus may not demonstrate strong, clear trends consistently unless more extreme (in this case, 45% TS) conditions are present. These results build upon those from our previous work, providing further evidence that specifically increasing WPI content results in increased viscosity, even as % total solids in the system remains constant. **Figure 3.3B** also shows that among all feeds containing

45% TS, those containing 1% PP had consistently higher viscosities than corresponding feeds with lower PP.

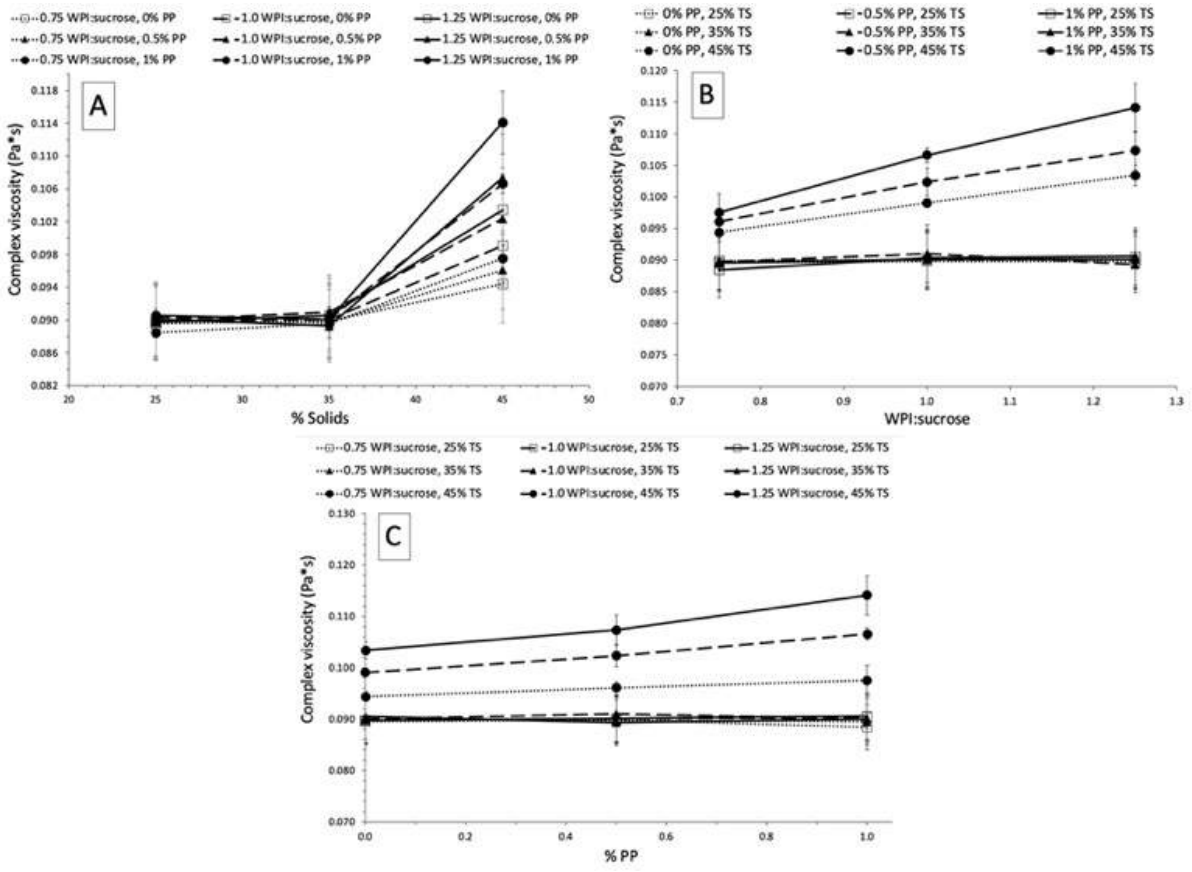


Figure 3.3. Effect of total solids content (%) [**A**], WPI:sucrose ratio [**B**], and PPO content (%) [**C**] on the complex viscosity (Pa*s) of dispersions at 25˚C; (n = 6). Lines are for guiding purposes only.

According to the ANOVA, with all other parameters (% TS and WPI:sucrose ratios) being held constant, viscosity was significantly ($p < 0.05$) influenced by PP content; Tukey's HSD tests expanded on this, reporting significantly increased ($p < 0.05$) viscosities with increasing addition of Aronia PP to feed dispersions. This increasing trend described by the ANOVA is only clearly demonstrated by feeds containing 45% TS in **Figure 3.3C**, which may also be attributed to the strong effect of 45% TS on viscosity discussed earlier. Additionally,

feeds containing 45% TS were observed to have higher viscosities at higher WPI:sucrose ratios in **Figure 3.3C**. The effect of increased PP may be weak relative to that of % TS (similar to the WPI:sucrose effect), and thus may not demonstrate strong trends consistently unless more extreme conditions (high % TS) are also present that may make slight shifts more noticeable. It is known that polyphenols and proteins interact under weak acidic pH conditions and form non-covalent complexes where polyphenols may act as bridges to polymerize protein molecules. The extent and type of interactions formed depend on factors including system pH, protein and polyphenol types, concentration ratios, etc., but when concentrations of both components are optimal, proteins have been shown to form relatively large network structures non-covalently (Siebert et al., 1996; Schneider, 2016; Zhou et al., 2020). Protein-polyphenol interactions have been found to induce significant changes to protein structures, which can consequently alter their functional and nutritional properties (Schneider, 2016; Ma & Zhao, 2019; Xue et al., 2020; Zhou et al., 2020). The addition of polyphenols to WPI-sucrose feeds increases intermolecular interactions within the fluid system with the formation of protein-polyphenol complexes and may result in increases in viscosity and behavioral complexity.

3.3.1.4 Power requirements for pumping

Viscosity, density, and flow rate data collected for dispersions were used to determinate representative values for use in calculations of the estimated power requirements for the benchtop peristaltic pump to pump feed dispersions at a constant rate of 13 RPM. Power requirements for the pump (Φ; Watts) were calculated by multiplying an average mass flow rate representative of feeds studied ($\dot{m}$ = 5 x 10^{-5} kg/s) by the work done per unit mass by the pump on the feeds (E_p; J/kg). E_p was calculated from derivations of Bernoulli's equation, based on

assumptions including constant density of feeds (Singh & Heldman, 2013). No major changes in pressure, elevation, or feed velocities were thought to occur with the process studied, so E_p was calculated based on the energy losses due to friction (both major and minor). Expansions and contractions were accounted for as minor frictional losses resulting from the rotary peristaltic pumping action. With known dimensions for the tubing and containers used for uptake and depositing feeds, and representative values selected for feed density (ρ = 1000 kg/m^3), mean velocity ($\bar{u}$ = 0.016 m/s), mass flow rate ($\dot{m}$), and feed viscosity (μ = 0.09 Pa*s) based on experimental data, E_p was calculated to be approximately 9.67 J/kg, and Φ = 0.00048 Watts.

3.3.1.5 Particle size distribution

Numerous studies have reported structural changes to proteins imparted by interactions with polyphenols, since protein-polyphenol complexation can alter dispersion conditions that influence protein conformation and electrostatic repulsion in solution (Rawel et al., 2005; Song, 2009; Bandyopadhyay et al., 2012; Coupland, 2014; Cao & Xiong, 2017; Girard et al., 2018; Ma & Zhao, 2019; Quan et al., 2019). These changes have the potential to amplify the formation of protein-protein aggregates as well as the growth of protein-polyphenol complexes (Hong et al., 2018b). It may be expected, then, that dispersion particle sizes may undergo measurable changes due to these interaction effects as well. Particle size analysis could be considered a useful tool in assessing protein-polyphenol interactions, as particle size may influence numerous functional properties (Le Bourvellec & Renard, 2012; Schneider, 2016).

According to the ANOVA, % TS had a significant ($p < 0.05$) effect on the average particle size (volume-weighted mean, $d_{4,3}$) of dispersions. Tukey's HSD tests clarified that increasing % TS resulted in significantly increased average particle sizes ($p < 0.05$) in feeds.

This increasing trend was most clearly demonstrated by feeds containing 0.5 and 1% PP in **Figure 3.4A**; feeds with 0% PP showed virtually no change in particle size with increasing % TS. Increases in average particle sizes with increasing % TS in feeds containing PP are indicative of complexation interactions between proteins and PP aiding in the formation of larger particles, as more proteins are present for interactions with other proteins as well as PP. Similarly, the largest particles detected in the dispersions also shifted towards larger sizes with increasing total solids, with all feeds displaying approximately normal distributions. Increased solids concentrations, and thus more total protein in feeds, resulted in more extensive and larger aggregate formation due to more frequent overlapping and entangling interactions (Coupland, 2014).

According to the ANOVA report, altered ratios of WPI to sucrose in dispersions did not significantly ($p > 0.05$) affect particle size distributions (data not shown). No significant differences in particle size were observed between dispersions prepared at three different WPI-sucrose ratios ($p > 0.05$), as indicated by the Tukey's HSD tests, with all feeds displaying approximately normal distributions. This suggests that varying levels of sucrose in the highly concentrated systems do not strongly affect the occurrence of protein-protein interactions in solution that result in aggregate formation. This may be due in part to the hygroscopic nature of the sugar and its strong affinity for water and easy dissolution into the bulk solvent at room temperature at the concentrations used. In this case, more protein present in feeds did not result in increased aggregate sizes as was observed when total system solids increased.

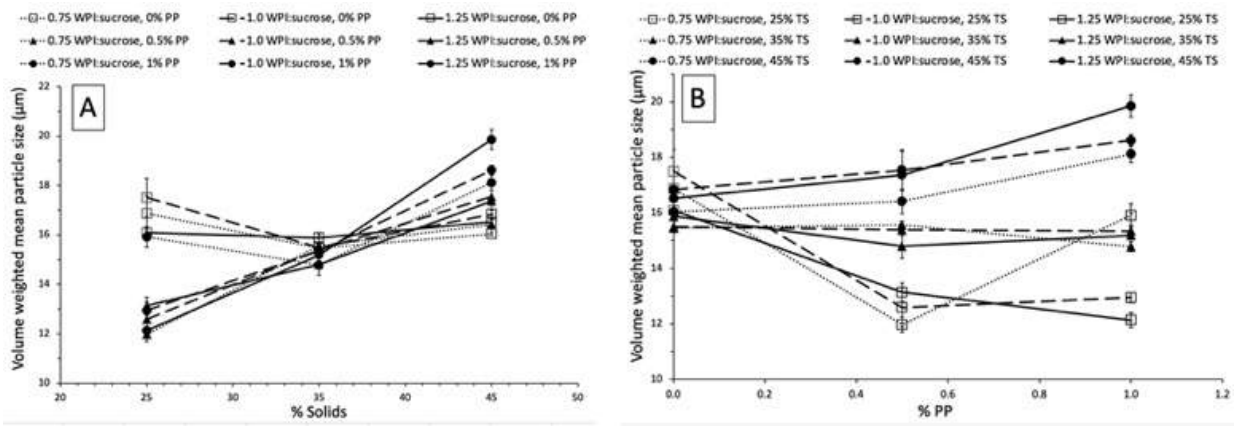


Figure 3.4. Effect of total solids content (%) [**A**] and PP content (%) [**B**] on the average particle size (µm) of dispersions at 25˚C; (n = 6). Lines are for guiding purposes only.

According to the ANOVA, average particle sizes of dispersions were significantly affected by PP content ($p < 0.05$); Tukey's HSD tests expanded on this, reporting that feeds formulated with 0% PP had significantly larger average particle sizes ($p < 0.05$) than those formulated with 0.5 and 1% PP. Although these effects were attributed to PP addition, they were dependent on feed % TS as well. Feeds containing 25% TS most clearly demonstrated the decreasing trend described by the ANOVA (**Figure 3.4B**) and generally had the smallest particle sizes compared to feeds with higher % TS; those containing 35% TS showed only slight reductions in particle size with increasing PP. Interestingly, feeds containing 45% TS showed increased particle sizes with increasing PP, which may be attributed to the strong effect of % TS interfering with the visibility of comparatively weaker PP effects on average particle sizes of dispersions. Siebert et al. (1996) also detected small particle sizes with light scattering techniques, and attributed the smaller particle sizes observed at higher polyphenol concentrations to the saturation of possible binding sites on proteins with polyphenols, causing repulsive interactions to dominate the system and prevent formation of larger aggregates. Thongkaew et al.

(2014) observed reduced particle sizes even at low levels of polyphenol addition to dispersions with WPI and WPI-pectin complexes. Similar trends were observed by Xue et al. (2020) when studying complexation between soy protein isolate (SPI) and cyanidin-3-galactoside; complexation was found to break down aggregates and lead to reduced particle sizes by disrupting SPI hydrogen bonds, increasing electrostatic repulsion, and decreasing hydrophobic interactions between protein molecules, thus reducing protein-protein interactions.

3.3.1.6 Optical light microscopy

Particle size distributions and average particle size measurements of feed dispersions generated by Mastersizer light scattering were supported by optical light microscopy. Microscope images illustrate the findings from Mastersizer data visually, depicting the increases in average and largest aggregate sizes in the dispersions as total solids content increased in the system, promoting more extensive aggregation (**Figure 3.5A, B, C**). Microscopy also mirrored the Mastersizer findings indicating that increasing the ratio of WPI to sucrose in dispersions resulted in no changes in average particle size (images not shown). Mastersizer data reporting reduced particle size with the addition of polyphenols to dispersions were reinforced with optical light microscopy as well (images not shown). Microscope images were useful for visual demonstration of the increased incidence of small particles in feeds formulated with Aronia extract (**Figure 3.6A, B, C**), also shown in Mastersizer particle size distributions (not shown). Comparing particle size distributions and frequencies at which certain sizes occur between laser light scattering techniques and microscope imaging may be difficult due to inherent differences between methods (Schneider, 2016); nevertheless, optical microscopy generally confirmed the Mastersizer results.

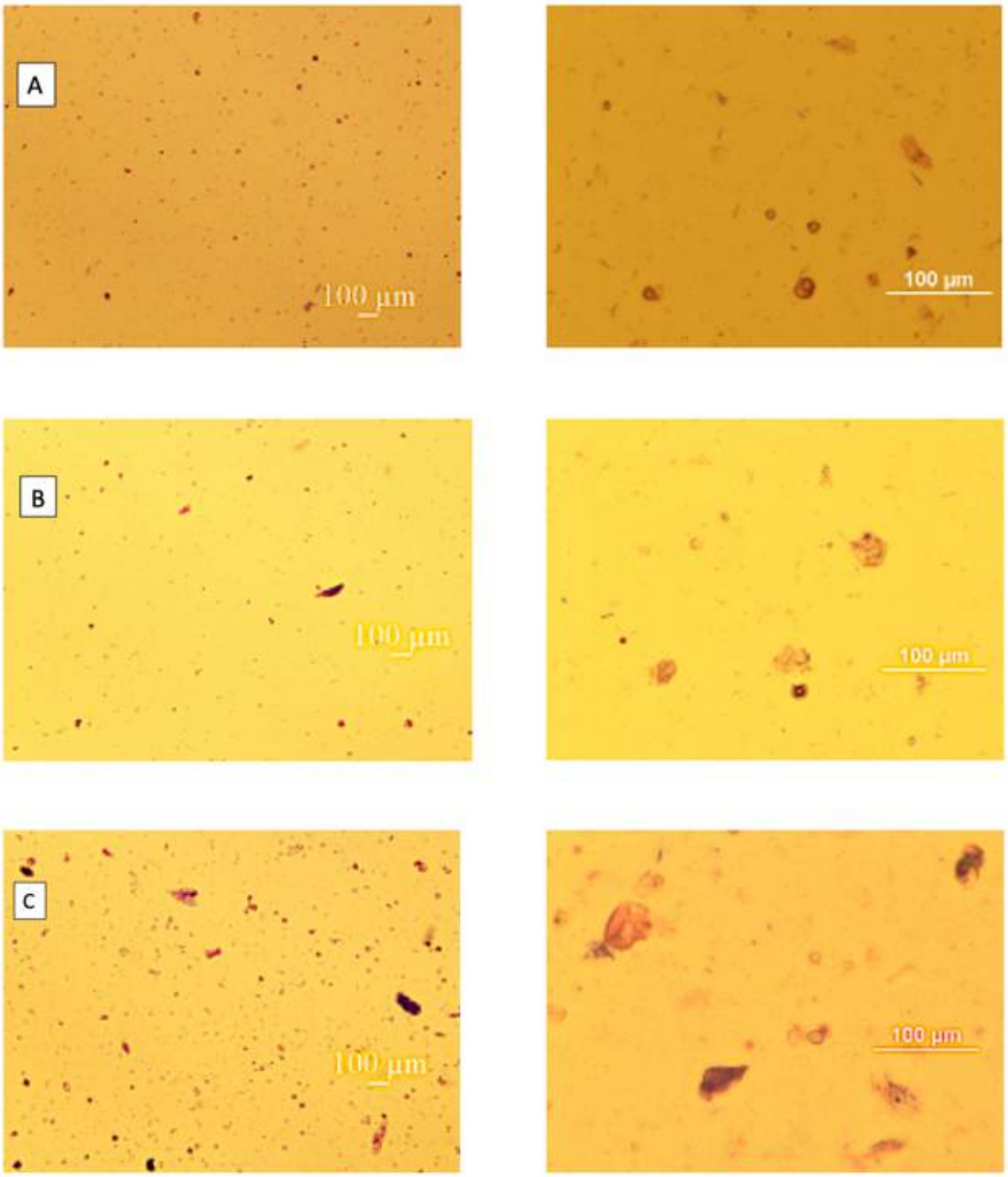


Figure 3.5. Optical light microscope images at 40x (left) and 200x magnification (right), depicting the microstructures of diluted feed dispersions with a 1.25 WPI:sucrose ratio and 1% PP at 25% (**A**), 35% (**B**), and 45% total solids contents (**C**).

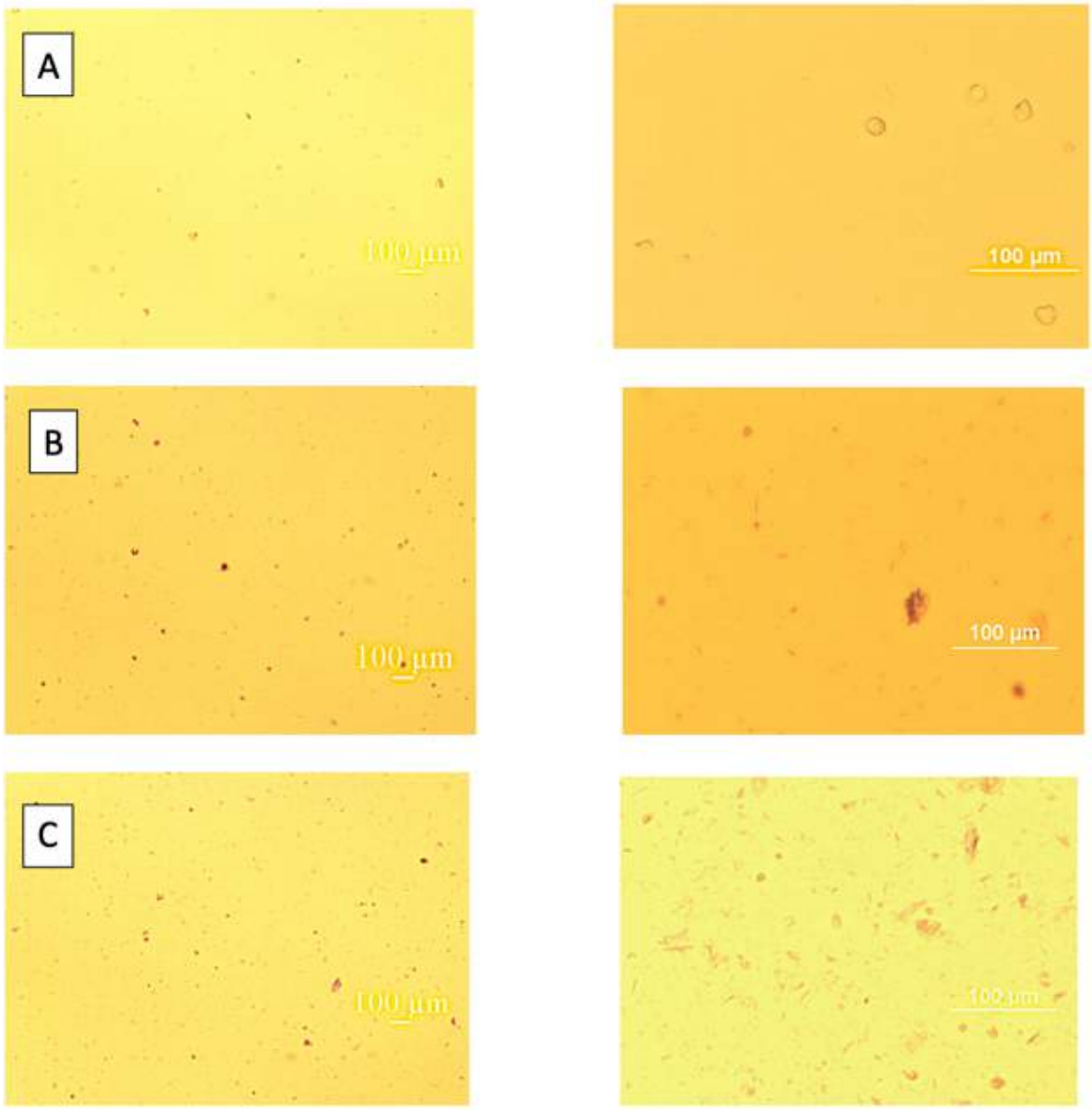


Figure 3.6. Optical light microscope images at 40x (left) and 200x magnification (right), depicting the microstructures of diluted feed dispersions with a 1.0 WPI:sucrose ratio at 25% TS with 0% PP (**A**), 0.5% PP (**B**), and 1% PP (**C**).

3.3.1.7 Centrifuge separation

Centrifuge treatments resulted in the formation of precipitated pellets from feed dispersions and their dilutions, indicating that the 'gels' were weak in nature and underwent

separation relatively easily. Dispersions were visually assessed to identify the location of the colored polyphenolic compounds after centrifugation, as sedimentation of a colored precipitate has been used as a crude method to confirm the formation of protein-polyphenol complexes (Van Teeling et al., 1971). An Aronia berry powder similar to the extract used in this study was found to be most abundant in cyanidin-3-galactoside, cyanidin-3-glucoside, and chlorogenic acid polyphenols (Xie et al., 2016, 2017), with cyanidin-3-galactoside and cyanidin-3-glucoside both being anthocyanins. The powder used in this study was standardized to contain a minimum of 15% anthocyanins and 10% proanthocyanidins. Both compounds are known to contribute pigmentation to Aronia and make up the majority of polyphenolic compounds in the extract (a minimum 25g of the 40g total PP in 100g of extract). Dispersions formulated without polyphenols had white-colored pellets after centrifugation; inclusion of Aronia PP resulted in dark purple pellet formation (**Figure 3.7**). Thus, formation of colored precipitates was an indicator for protein-polyphenol complexation. After being diluted 10x, PP-containing dispersions had dark purple precipitated pellets and transparent supernatant fractions that maintained slight purple-pink coloration. The pigmentation may be due in part to the saturation of potential complexation sites (as influenced by factors including system pH, temperature, protein and polyphenol types involved, and relative concentration ratios), resulting in uncomplexed polyphenols remaining in solution and imparting pigmentation (Schneider, 2016; Quan et al., 2019). Alternatively, supernatant pigmentation may be due to the presence of smaller sized protein-polyphenol complexes that remain dispersed in solution as they had not become heavy or insoluble enough to precipitate out (Spencer et al., 1988; Charlton et al., 2002; Rawel et al., 2005; Ozdal et al., 2013).

No changes in appearance were observed for the relative amount of precipitate formed as the ratio of WPI to sucrose was increased. Precipitated pellet size appeared to increase slightly upon addition of polyphenols to feed dispersions and their dilutions, as compared to those containing 0% polyphenols (**Figure 3.7**). Dilution of a 1% Aronia polyphenol solution by a factor of 10x and the extremely small precipitate formed upon centrifugation (image not shown) helped to confirm that the apparent increase in precipitate formed with addition of PP cannot be attributed only to an increase in Aronia extract carbohydrates, fiber, and protein solids, but likely a result of the formation of larger, aggregated complexes that fell out of solution.

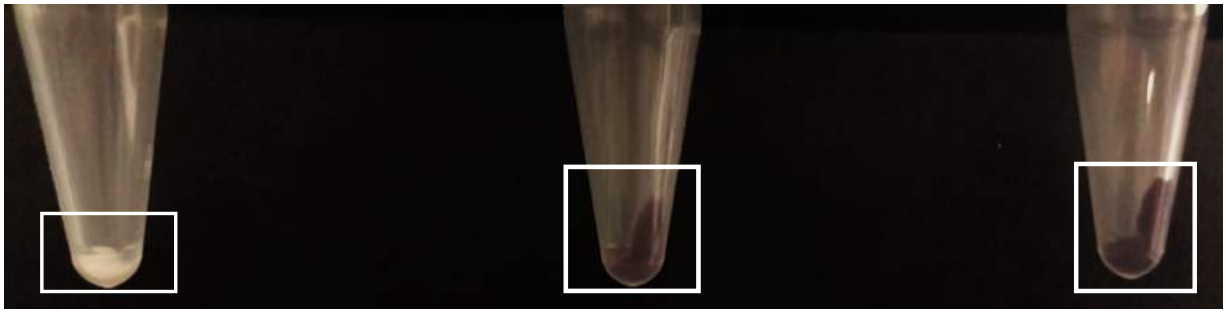


Figure 3.7. Image depicting the precipitated fractions (highlighted in boxes) of centrifuged 10x-diluted dispersions with 1.25 WPI:sucrose ratios and 45% total solids contents with 0% PP (Left), 0.5% PP (Center), and 1% PP (Right).

3.3.2 Frozen drop characterization:

3.3.2.1 Comparison of diameters

The surface tension of feed dispersions strongly determines the size of drops formed, as detachment of pendant drops only occurs when gravitational forces pulling down exceed the surface tension forces acting around the circumference of the tubing tip. Surface tension has been reported to decrease with increased viscosity and biopolymer concentrations, and drop diameters

tend to decrease with decreasing surface tension of feeds (Chan et al., 2009; Lee and Chan, 2013).

Diameters of frozen drops were measured to observe the effects of composition on drop sizes. According to the ANOVA, drop diameters were significantly ($p < 0.05$) affected by % TS; diameters were generally found to decrease with increasing % TS in dispersions (**Figure 3.8A**). Tukey's HSD tests reported significant decreases in diameters when % TS increased from 25 to 35% ($p < 0.05$), but the decrease in size between 35 and 45% TS was not found to be statistically significant. The reduction in diameters of drops formed by feeds containing higher total solids contents may be a result of increasing density, ultimately resulting in pendant drops becoming heavier and overcoming reduced surface tension forces more quickly and thus detaching at smaller volumes. Any variations observed in the generally decreasing trends may be attributed to larger drops forming in order to release from the tubing tip due to entrapped air reducing feed density.

According to the ANOVA, diameters were significantly ($p < 0.05$) impacted by the WPI to sucrose ratio in feeds; diameters were generally observed to increase with increasing ratios of WPI to sucrose in dispersions, best visualized by feeds containing 1% PP in **Figure 3.8B**. Tukey's HSD tests clarified, reporting a significant ($p < 0.05$) increase in diameters with increased WPI to sucrose ratios from 0.75 to 1.0, though the change in size between 1.0 and 1.25 WPI:sucrose ratios was not found to be statistically significant. These trends are best demonstrated in feeds containing 0 and 1% PP, as feeds containing 0.5% PP showed more variation from the trends described by the ANOVA (**Figure 3.8B**). Despite the larger molecular mass of proteins and space occupied, dispersions containing more protein have higher foaming

ability and may entrap more air that cannot be removed entirely from feeds as they are left to defoam prior to analysis. In this case, it is possible that pendant drops comprised of more WPI had to grow to larger sizes and heavier in order to overcome surface tension forces and detach, as feed density was lower than would be expected due to air bubbles being entrapped during dispersion preparation. Variation with 0.5% PP feeds may be due to minor inhibition of protein-protein interactions with the presence of protein-PP interactions.

The ANOVA indicated that PP content had a significant ($p < 0.05$) impact on drop diameters; Tukey's HSD tests reported significant increases in diameters ($p < 0.05$) when PP content increased from 0 to 0.5%. The minor increase in diameters from 0.5% to 1% PP was not found to be statistically significant. With the addition of Aronia PP to feeds, drop diameters were generally observed to increase, although with significant scatter; this trend is most clearly demonstrated for feeds comprised of 1.25 WPI:sucrose in **Figure 3.8C**. The increasing trend described by the statistical analysis and observed in **Figure 3.8C** may be influenced by the effects of the high WPI:sucrose ratio enhancing diameters as well. Additionally, feeds containing 25% TS generally had larger average drop diameters than those containing 35-45% TS. Although comprised mainly of small molecular weight polyphenolic compounds, the Aronia extract also contributed small quantities of fiber and protein (1.3 and 2.3% of extract composition, respectively) to dispersions. These additional compounds may have enabled dispersions to entrap more air bubbles upon preparation of feeds, resulting in increased drop diameters as drops needed to grow larger and heavier to detach.

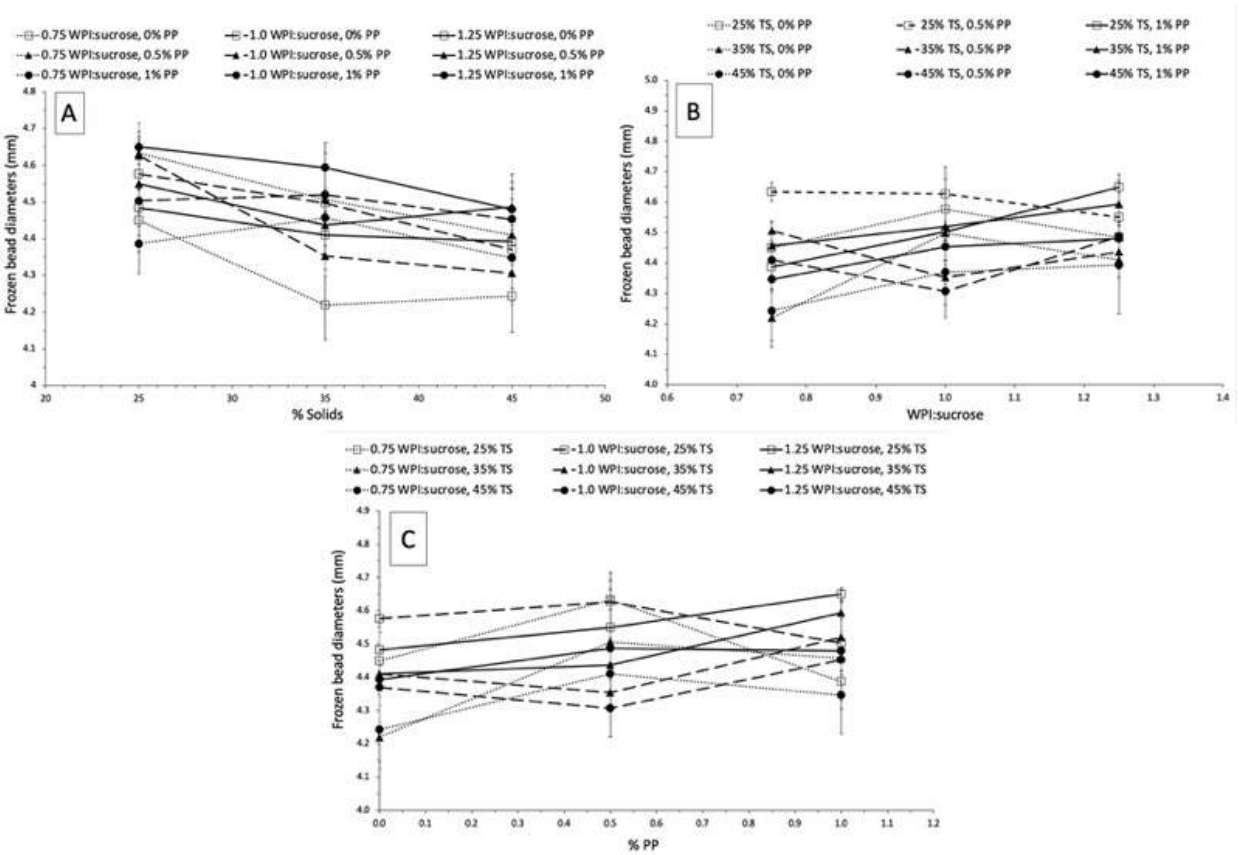


Figure 3.8. Effect of total solids content (%) [**A**], WPI:sucrose ratio [**B**], and PP content (%) [**C**] on the on the diameters (mm) of frozen drops formed from dispersions; (n = 6). Lines are for guiding purposes only.

Diameters of frozen drops were compared with calculated estimate values from data produced by flow testing of dispersions (Equation 6) (**Table 3.1**). No significant differences ($p < 0.05$) were found between the estimated diameters calculated from flow data and the actual measured diameters for 23 of the 27 feed dispersions studied. One possible reason that the calculations did not always accurately predict diameters could be that the calculated values were built from measured density data. Density measurements may not always be perfectly representative of feeds, as they cannot account for the air that is inevitably part of the viscous dispersions and is unable to be fully removed by allowing feeds to settle before testing, depending on composition of feeds and their ability to entrap air bubbles. Thus, inaccurate

density measurements may carry through the calculations to give less accurate drop diameter estimates as a result of the air present. Nevertheless, estimated drop size calculations accurately estimated drop diameters the majority of the time, indicating that the method was generally successful, similar to findings from earlier experiments (Hansen et al., 2020).

3.4 Conclusions

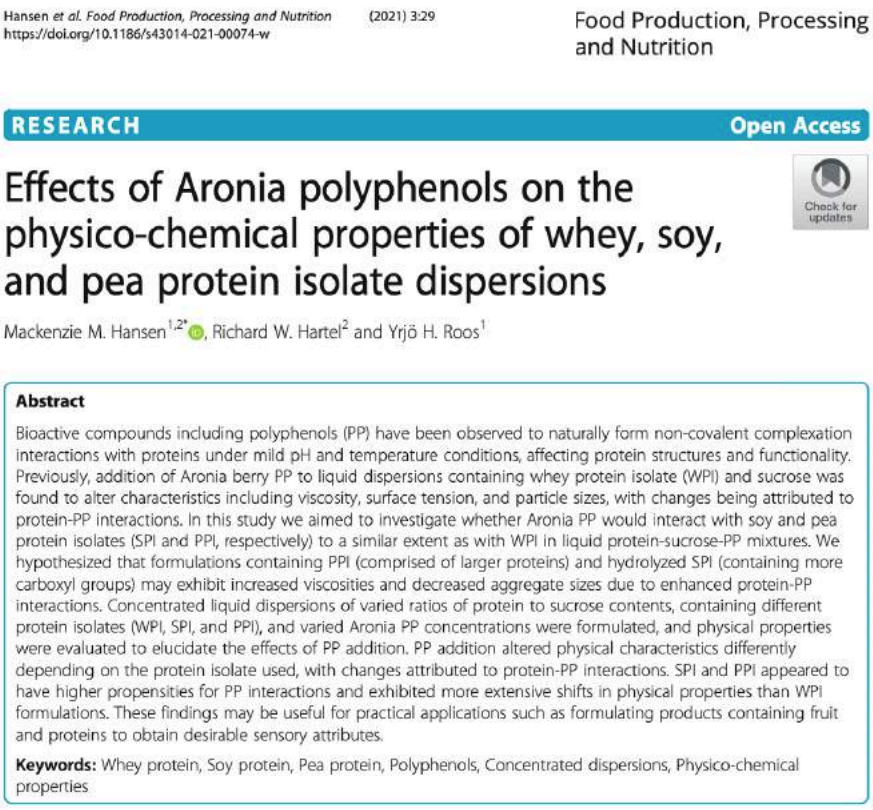
In an effort to expand on previous work in which a continuous process for forming concentrated, liquid dispersions of WPI-sucrose combinations into structures with potential to encapsulate active ingredients was presented, this work aimed to study the effects of formulation with Aronia extract polyphenols as the active ingredient. Naturally occurring, non-covalent WPI-polyphenol interactions were found to have functional, physical, and practical processing consequences including increased viscosities and surface tensions and reduced particle sizes of feeds, though the effect of total solids content appeared to most strongly influence dispersion properties. These findings contribute to the body of research describing the physical effects of non-covalent interactions between proteins and polyphenols under mild pH and temperature conditions, as well as provide practical knowledge for further applications such as encapsulation, protection, and delivery with concentrated protein-polyphenol mixtures.

Acknowledgements

This research was supported by funding provided by the Lauritzson Foundation in the form of the Lauritzson Research Scholarship, through the College of Science, Engineering and Food Science (SEFS) at University College Cork. The authors would like to thank the

anonymous reviewers and Journal Editor for thorough reading of the manuscript and helpful comments for revision.

Chapter 4



Hansen *et al. Food Production, Processing and Nutrition* (2021) 3:29
https://doi.org/10.1186/s43014-021-00074-w

Food Production, Processing and Nutrition

RESEARCH Open Access

Effects of Aronia polyphenols on the physico-chemical properties of whey, soy, and pea protein isolate dispersions

Mackenzie M. Hansen[1,2*], Richard W. Hartel[2] and Yrjö H. Roos[1]

Abstract

Bioactive compounds including polyphenols (PP) have been observed to naturally form non-covalent complexation interactions with proteins under mild pH and temperature conditions, affecting protein structures and functionality. Previously, addition of Aronia berry PP to liquid dispersions containing whey protein isolate (WPI) and sucrose was found to alter characteristics including viscosity, surface tension, and particle sizes, with changes being attributed to protein-PP interactions. In this study we aimed to investigate whether Aronia PP would interact with soy and pea protein isolates (SPI and PPI, respectively) to a similar extent as with WPI in liquid protein-sucrose-PP mixtures. We hypothesized that formulations containing PPI (comprised of larger proteins) and hydrolyzed SPI (containing more carboxyl groups) may exhibit increased viscosities and decreased aggregate sizes due to enhanced protein-PP interactions. Concentrated liquid dispersions of varied ratios of protein to sucrose contents, containing different protein isolates (WPI, SPI, and PPI), and varied Aronia PP concentrations were formulated, and physical properties were evaluated to elucidate the effects of PP addition. PP addition altered physical characteristics differently depending on the protein isolate used, with changes attributed to protein-PP interactions. SPI and PPI appeared to have higher propensities for PP interactions and exhibited more extensive shifts in physical properties than WPI formulations. These findings may be useful for practical applications such as formulating products containing fruit and proteins to obtain desirable sensory attributes.

Keywords: Whey protein, Soy protein, Pea protein, Polyphenols, Concentrated dispersions, Physico-chemical properties

Effects of Aronia polyphenols on the physico-chemical properties of whey, soy, and pea protein isolate dispersions

Mackenzie M. Hansen[a,b*], Richard W. Hartel[b], Yrjö H. Roos[a]

[a] Food Technology, School of Food and Nutritional Sciences, University College Cork, Ireland

[b] Department of Food Science, College of Agricultural and Life Sciences, University of Wisconsin-Madison

Published as: Hansen, M.M., Hartel, R.W. & Roos, Y.H. Effects of Aronia polyphenols on the physico-chemical properties of whey, soy, and pea protein isolate dispersions. *Food Production, Processing and Nutrition* 3, 29 (2021), 10.1186/s43014-021-00074-w

Abstract

Bioactive compounds including polyphenols (PP) have been observed to naturally form non-covalent complexation interactions with proteins under mild pH and temperature conditions, affecting protein structures and functionality. Previously, addition of Aronia berry PP to liquid dispersions containing whey protein isolate (WPI) and sucrose was found to alter characteristics including viscosity, surface tension, and particle sizes, with changes being attributed to protein-PP interactions. In this study we aimed to investigate whether Aronia PP would interact with soy and pea protein isolates (SPI and PPI, respectively) to a similar extent as with WPI in liquid protein-sucrose-PP mixtures. We hypothesized that formulations containing PPI (comprised of larger proteins) and hydrolyzed SPI (containing more carboxyl groups) may exhibit increased viscosities and decreased aggregate sizes due to enhanced protein-PP interactions. Concentrated liquid dispersions of varied ratios of protein to sucrose contents, containing different protein isolates (WPI, SPI, and PPI), and varied Aronia PP concentrations were formulated, and physical properties were evaluated to elucidate the effects of PP addition. PP addition altered physical characteristics differently depending on the protein isolate used, with changes attributed to protein-PP interactions. SPI and PPI appeared to have higher propensities for PP interactions and exhibited more extensive shifts in physical properties than WPI formulations. These findings may be useful for practical applications such as formulating products containing fruit and proteins to obtain desirable sensory attributes.

4.1 Introduction

As consumers' interest towards bioactives-containing health foods grows, so does the demand for novel products with high protein contents and fruit components. Bioactives can be defined as natural compounds that may affect human health (González, 2020). Globular bovine whey proteins, especially whey protein isolate (WPI) with its wide range of functionality, continue to be favored for developing products with high nutritional value (Kulmyrzaev et al., 2000; Cao and Xiong, 2017; Hansen et al., 2021b). However, consumers are also demonstrating increased interest in shifting their diets away from animal-sourced proteins for health, social, and environmental reasons, placing higher demand on plant-based nutritional options (Aschemann-Witzel and Peschel, 2019). Soybeans are a rich alternative source of high-quality but inexpensive globular proteins, and soy protein isolates (SPI) are increasingly popular for product development (Li, 2005). Also globular in nature, pea protein isolates (PPI) provide another alternative in formulated food products. As constituent protein sources are changed, the functional properties of the resulting food products will also be altered due to variations in the composition and physicochemical properties of the different protein sources.

Fruits are a rich source of polyphenols (PP), bioactive compounds with strong antioxidant and anti-inflammatory activities linked to a host of positive health outcomes (Mink et al., 2007; Li et al., 2017). Good sources of PP like fresh produce often have short shelf lives, and PP are known to be chemically unstable in storage and highly susceptible to degradation (Zhao et al., 2019; Cao et al., 2021). A propensity for complexation exists between PP and proteins, with weak, non-covalent van der Waal's interactions, hydrogen bonding, and hydrophobic interactions commonly occurring in foods with neutral and acidic pH (Schneider, 2016). Complexation of PP with proteins has been reported to significantly change protein structures at

room temperature (Rawel et al., 2005), and may potentially aid in the protection and delivery of bioactives (Cao and Xiong, 2017; Ma and Zhao, 2019; Quan et al., 2019). Additionally, plant-based protein sources including SPI and PPI tend to retain low levels of lipids that can oxidize over time, and complexation with PP may help mitigate negative effects due to their antioxidant activity.

Water hydration capacity (WHC) is a measurement of a protein powder's absorption and retention of water and is indicative of its functionality as an ingredient (Quinn and Paton, 1979). WHC is influenced by the surface properties of proteins interacting with water, the charges on protein molecules, functional groups exposed, molecular flexibility, molecular weight, and amino acid composition, and values may vary depending on how it is measured (Kneifel et al., 1991; Zayas, 1997). Proteins interact with water via hydrogen bonds with polar, hydroxyl, and carboxyl groups, electrostatic interactions with charged amino acid side chains, and hydrophobic interactions via nonpolar, hydrophobic groups exposed at the surface (Morr, 1990). Proteins interact non-covalently with polyphenols at many of the same sites (Kanakis et al., 2011; Bohin et al., 2012; Le Bourvellec and Renard, 2012; Chung et al., 2015; Oancea et al., 2017). WHC is used to describe protein isolate interactions with water, but it may also serve as an indicator for the likelihood of protein-PP interactions.

While the consequences of non-covalent protein-PP interactions are not as extensively reported as those of covalent interactions (Cao and Xiong, 2017; Xue et al., 2020), liquid formulations containing WPI, sucrose, and Aronia berry extract (a rich source of PP) were found to exhibit measurable changes in physicochemical properties, attributed to non-covalent complexation interactions formed between PP and proteins (Hansen et al., 2021b). The aim of this study is to investigate whether Aronia PP interact with plant-based SPI and PPI to a similar

extent as with WPI in liquid protein-sucrose-PP mixtures, as demonstrated in our previous work. Given that WPI is known to have low WHC (Kneifel et al., 1991; Resch and Daubert, 2002) and was still found to interact with Aronia PP, we expect that protein sources with different structures, such as SPI & PPI, would have different WHC and propensities for interactions with Aronia PP. Varying extents of protein-PP interactions would likely result in measurable changes in physicochemical properties of the dispersions. We hypothesize that PPI formulations comprised of proteins with larger molecular masses (average molecular mass of WPI ~ 17 kDa, PPI ~ 260 kDa) may exhibit enhanced viscosities, and aggregate sizes may be reduced with enhanced PP interactions (Lam et al., 2018; Ma and Zhao, 2019). It would be expected that the hydrolyzed SPI, though typically imparting reduced viscosity due to smaller protein fractions (< 35 kDa), would interact with PP more extensively due to the presence of more carboxyl groups for potential hydrogen bonding and electrostatic interactions, allowing for increased water holding, enhanced viscosities, and reduced particle sizes (Li et al., 2021). In earlier work, we presented a continuous process to form dry beads from concentrated dispersions of WPI and sucrose, with the goal of utilizing these structures for bioactives encapsulation in subsequent experiments (Hansen et al., 2020). In later studies, we developed a modified process for dry bead formation from concentrated dispersions, thought to provide better retention of protein structures during processing as well as bioactives (Aronia PP) upon storage (Hansen et al., 2021c). Preparation methods for the concentrated feed dispersions remain virtually unchanged, and this work investigates the interactions occurring in dispersions and the changes in physical behaviors of the feeds that would be prepared for subsequent dry bead formation. This work would build on the findings from previous experiments, providing insight into the non-covalent interactions between plant-based proteins and polyphenols and their effects on the physico-chemical

properties of dispersions. This information may be used practically for further applications such as stabilization and delivery of actives, as well as inform the formulation and processing steps in the development of foods containing mixtures of proteins and fruit such as sports drinks, nutritional bars, smoothies, and yogurt, as well as puddings and frozen desserts in order to obtain desirable sensory properties.

4.2 Materials and Methods

4.2.1 Materials

WPI (IsoChill 9000), was supplied by Agropur, Inc. (Luxemburg, WI, USA) containing 4.6% water, 91.6% protein (dry basis), 0.7% fat, and 3.1% ash. SPI (ProFam® 781, hydrolyzed), was supplied by Archer Daniels Midland Co. (Decatur, IL, USA) containing 3.7% water, 94.7% protein (dry basis), 0.4% fat, and 1.2% ash. PPI (VITESSENCE™ Pulse 1803), was supplied by Ingredion™ (Westchester, IL, USA) containing 8% water, 80% protein (dry basis), 7.8% fat, and 4.2% ash. Sucrose (pure cane, extra fine, granulated sugar) was supplied by Domino Foods, Inc. (Yonkers, NY, USA). Standardized Aronia berry (Chokeberry) powder, containing a minimum of 15% anthocyanins, 10% proanthocyanidins, and 55.6% total PP, was supplied by Artemis International (Fort Wayne, IN, USA) and stored in the dark at -18°C. A similar extract examined in other studies was found to have high quantities of cyanidin-3-galactoside and cyanidin-3-glucoside anthocyanins, as well as high levels of chlorogenic acid (Xie et al., 2016, 2017; Hansen et al., 2021a). Technical data sheets for the extract reported < 5% water content, 2.13% protein, 1.3% fiber, 0.85% sugars, 0.29% fat, and a reconstituted pH of 3-4. Deionized (D.I.) water was used throughout all experiments.

4.2.2 Protein isolate powders characterization:

4.2.2.1 Water hydration capacity

WPI, SPI, and PPI powders were evaluated for their respective WHC by modifying the two-step method presented by Quinn and Paton (1979). The first step, used to obtain an approximate WHC for each protein isolate, was performed in triplicate. The test involved the gradual wetting of 5 g of protein powder with unmeasured amounts of deionized (D.I.) water in 50 mL centrifuge tubes, mixing vigorously with a spatula until the samples were thoroughly wetted and mixtures had paste-like consistencies. Tubes were placed in a Sorvall ® RC 26 Plus centrifuge (Sorvall Products, L.P., Newtown, CT, USA) and spun at 5100 rpm (~2000 x g) for 10 min at 20-25˚C. The small quantities of supernatant formed were decanted and tubes were weighed to determine the masses of water absorbed by the powders. Triplicate data were averaged and crude WHC values obtained were used to determine water addition levels for step 2. A minimum of 5 tubes containing 5 g of protein powder were prepared as described for step 1, but with a range of known water contents in 1 g increments, both above and below the approximate WHC. After centrifugation under the same conditions, tubes were evaluated to determine the water addition level at which a supernatant was formed, giving more exact WHC values within 1 g.

4.2.3 Dispersion preparation

Dispersions were prepared as described in previous work (Hansen et al., 2021b), where dry protein-sucrose blends were dispersed in D.I. water, then aliquots of Aronia extract solution were added to form the final mixtures at room temperature. pH was measured with a FiveEasy Plus pH/mV meter with InLab® Viscous Pro-ISM probe (Mettler Toledo, Hampton,

Schwerzenbach, Switzerland) after calibrating the electrode at pH four and seven at room temperature, < 25˚C.

Twenty-seven formulations of varied compositions were prepared in triplicate for subsequent, randomized triplicate analysis in a 3x3x4 factorial design (**Table 4.1**); the 9 remaining WPI-based formulations were prepared and analyzed previously, and the data were used for comparison (Hansen et al., 2021b). Protein to sucrose ratios and total solids contents of dispersions were selected based on findings from previous work (Hansen et al., 2020, 2021b). We aimed to compare dispersions without the active (0%) to formulations with three different concentrations of PP, selecting concentrations to build upon the findings from previous studies (Hansen et al., 2021b). Dispersions defoamed at room temperature for a minimum of one hour before analyses.

Table 4.1.

Protein:sucrose	Protein isolate	[PP]	pH	Density	Diameter (calculated)	Diameter (frozen)
-	-	% w/w	-	kg/m^3	mm	mm
0.75	*WPI*	*0*	*6.03*	*1019 ± 10*	*4.59 ± 0.02*	*4.45 ± 0.09*
1	*WPI*	*0*	*6.08*	*1019 ± 6*	*4.60 ± 0.02*	*4.58 ± 0.10*
1.25	*WPI*	*0*	*6.01*	*1014 ± 15*	*4.54 ± 0.03*	*4.48 ± 0.05*
0.75	*WPI*	*0.5*	*5.73*	*1015 ± 11*	*4.67 ± 0.03*	*4.63 ± 0.03*
1	*WPI*	*0.5*	*5.94*	*994 ± 25*	*4.67 ± 0.04*	*4.63 ± 0.09*
1.25	*WPI*	*0.5*	*5.95*	*993 ± 28*	*4.65 ± 0.06*	*4.55 ± 0.14*
0.75	*WPI*	*1*	*5.57*	*994 ± 15*	*4.65 ± 0.08**	*4.39 ± 0.08**
1	*WPI*	*1*	*5.72*	*1021 ± 10*	*4.70 ± 0.03*	*4.50 ± 0.12*
1.25	*WPI*	*1*	*5.84*	*1020 ± 8*	*4.67 ± 0.05*	*4.65 ± 0.02*
0.75	WPI	1.5	5.29	1026 ± 30	4.67 ± 0.06	4.57 ± 0.15
1	WPI	1.5	5.36	1012 ± 7	4.69 ± 0.01*	4.47 ± 0.09*
1.25	WPI	1.5	5.41	1006 ± 12	4.64 ± 0.07*	4.53 ± 0.12*
0.75	SPI	0	6.56	1041 ± 13	4.52 ± 0.02*	4.45 ± 0.07*
1	SPI	0	6.52	1051 ± 9	4.41 ± 0.05*	4.50 ± 0.09*
1.25	SPI	0	6.55	1037 ± 14	4.50 ± 0.02	4.52 ± 0.14
0.75	SPI	0.5	6.30	1021 ± 13	4.51 ± 0.07	4.49 ± 0.07
1	SPI	0.5	6.32	1032 ± 11	4.47 ± 0.04*	4.39 ± 0.09*
1.25	SPI	0.5	6.35	1021 ± 11	4.50 ± 0.03	4.51 ± 0.12
0.75	SPI	1	6.03	1022 ± 11	4.54 ± 0.03	4.57 ± 0.11
1	SPI	1	6.09	1016 ± 14	4.53 ± 0.03*	4.41 ± 0.13*
1.25	SPI	1	6.21	1021 ± 21	4.49 ± 0.06	4.50 ± 0.14
0.75	SPI	1.5	5.84	844 ± 164	4.86 ± 0.34*	4.54 ± 0.08*
1	SPI	1.5	5.98	956 ± 92	4.63 ± 0.14	4.55 ± 0.13
1.25	SPI	1.5	5.98	788 ± 94	4.79 ± 0.23*	4.39 ± 0.18*
0.75	PPI	0	6.85	1043 ± 20	4.39 ± 0.10	4.31 ± 0.07
1	PPI	0	6.75	1042 ± 21	4.21 ± 0.03*	4.53 ± 0.15*
1.25	PPI	0	6.96	976 ± 24	4.29 ± 0.07*	4.58 ± 0.17*
0.75	PPI	0.5	6.67	1037 ± 15	4.51 ± 0.10*	4.75 ± 0.15*
1	PPI	0.5	6.46	1039 ± 15	4.31 ± 0.05*	4.57 ± 0.19*
1.25	PPI	0.5	6.58	1019 ± 32	4.20 ± 0.09*	4.67 ± 0.14*
0.75	PPI	1	6.15	1021 ± 27	4.67 ± 0.05*	4.81 ± 0.16*
1	PPI	1	6.22	1025 ± 35	4.60 ± 0.08	4.68 ± 0.22
1.25	PPI	1	6.42	1020 ± 15	4.46 ± 0.05*	4.71 ± 0.26*
0.75	PPI	1.5	5.82	1027 ± 20	4.65 ± 0.04	4.64 ± 0.21
1	PPI	1.5	6.03	1029 ± 18	4.62 ± 0.04*	4.92 ± 0.23*
1.25	PPI	1.5	6.26	1028 ± 15	4.54 ± 0.02	4.72 ± 0.27

*indicates significant differences between calculated and measured diameters
values in italics were from previous work (Hansen et al., 2021a; averaged data reported, n = 6, 3 for frozen diameters)

Density and estimated drop diameters measured and calculated from flow tests data and measured diameters (mm) of frozen drops (averaged data reported, n = 9) formed from feed dispersions with varied protein:sucrose, protein isolates, polyphenols (PP) concentrations, and pH.

4.2.4 Feed characterization:

4.2.4.1 Flow testing

Flow properties of dispersions including the time required to deposit 10 mL of dispersion, the number of drops deposited per 1 min, the mass of 10 mL of dispersion, and individual drop masses were measured at room temperature, as detailed in previous work (Hansen et al., 2020, 2021b), while pumping dispersions at a constant rate through a benchtop peristaltic pump (120 S/DV, Watson Marlow, Falmouth, England; silicon tubing 85 cm length, 2 mm bore, 1 mm wall, BÜCHI Labortechnik AG, Flawil, Switzerland). Those measurements provided the data necessary to calculate mass and volume flow rates, dispersion densities, drop surface tensions, drop diameters, and drop volumes (Hansen et al., 2020, 2021b).

4.2.4.2 Viscosity

Utilizing methods reported in previous work (Hansen et al., 2021b), where 1% strain was determined to be within the LVR of dispersions measured, a DHR-2 rheometer (TA Instruments, DE, USA) was used to measure the rheological properties of dispersions at 25˚C in triplicate with small-strain oscillatory measurements; complex viscosity values were recorded.

4.2.4.3 Particle size distribution

Using the methods explained in Hansen et al. (2021b), particle size distributions of dispersions were measured with a Malvern Mastersizer 2000 (Malvern Instruments Ltd., Worcestershire, U.K.) in triplicate, by injecting drops of dispersions at room temperature into a Hydro 2000S liquid sampler with D.I. water as the dispersant until dilutions reached obscurations between 11 and 15% (WPI refractive index 1.545, D.I. water refractive index 1.33, absorbance 0.001).

4.2.4.4 Optical light microscopy

Protein particles and protein-PP complexes in diluted dispersions at room temperature were observed with a Nikon Eclipse FN1 optical microscope (Nikon Instruments Inc., Melville, NY, USA) and a Nikon Digital Sight DS-U3 camera control unit attached (ver. 1), as reported in previous work (Hansen et al., 2021b).

4.2.4.5 Centrifuge separation

Slightly modifying sample preparation methods from previous studies (Hansen et al., 2021b), 1.25 g aliquots of 5-times diluted dispersions were pipetted into tubes (1.5mL graduated tubes with flat caps, Fisherbrand ®, Fisher Scientific, Hampton, NH, USA) and centrifuged at 12,000 rpm (~13,523 x g) and 20˚C for 20 min in a microcentrifuge (Centrifuge 5424 R with FA-45-24-11 rotor, Eppendorf, Hamburg, Germany). Tubes were observed after centrifugation.

4.2.5 Frozen drop preparation

Beads were frozen solid as described in previous work (Hansen et al., 2021b), by dropping dispersions into liquid nitrogen (LN_2) (100% purity; Airgas, Madison, WI, USA). Drops were allowed to solidify for ~5 min prior to removal from the LN_2 and immediate diameter measurements.

4.2.5.1 Frozen drop diameters

As in previous work, digital Vernier calipers (0-150 mm; Stainless Hard) were used to measure the diameters of frozen beads (Hansen et al., 2021b). Measurements were performed in triplicate for each formulation replicate (n=9).

4.2.6 Statistical analysis

Experiments were performed three times and analyzed in triplicate (n=9); mean values and standard deviations were calculated from the data collected. To compare mean values, analysis of variance (3-way ANOVA; Tukey's HSD test) and independent measures t-tests (equal variance not assumed) were performed using JMP® Pro version 15.0.0 (SAS Institute Inc., Cary, NC, USA). The level of significance was determined at $p < 0.05$.

4.3 Results and Discussion

4.3.1 Protein isolate powders characterization:

4.3.1.1 Water hydration capacity

WHC is indicative of a protein powder's functionality as an ingredient. WHC values for WPI, SPI (hydrolyzed), and PPI powders are reported in **Table 4.2**. As reported in previous studies, WPI solubilized well in D.I. water and after centrifugation a single, viscous phase remained, giving a WHC value of 0 grams of water absorbed per gram of WPI (Kneifel et al., 1991; Resch and Daubert, 2002). Five grams of SPI absorbed between 6.5 and 7.5 grams of water (~1.4 g/g), and five grams of PPI absorbed between 14.1 and 15.1 grams of water (~2.9 g/g), in agreement with the ranges of capacities reported by Owusu-Ansah and McCurdy (1991) and Zayas (1997). Fleming et al. (1974) reported higher water absorption values for commercial SPI powders, ranging from 4.15-7.75 g water absorbed per g SPI; it is possible that the commercial powders studied underwent greater extents of hydrolysis than ours, resulting in higher quantities of carboxyl groups present for interactions with water. Sosulski and McCurdy (1987) reported water holding capacity values of 2.65 and 2.52 grams of water per gram of SPI and PPI at 21˚C, respectively. Swanson (1990) reported that at neutral pH, SPI retained 4-5 times its initial weight of water, and 2.7-2.8 times its weight for PPI. Fuhrmeister and Meuser (2003)

reported WHC values of 4.6 g water per g commercial SPI, and 4 g water per g commercial PPI. It is likely that the isolates used in this study have different properties from those used in other work, thus resulting in differing WHC data.

Table 4.2.

Protein isolate	**Water hydration capacity**
-	(g water absorbed per g powder)
Whey	0
Soy (hydrolysate)	1.4
Pea	2.9

Water hydration capacity of WPI, SPI (hydrolyzed), and PPI powders, reported as grams of water absorbed per gram of protein isolate powder.

As there is substantial overlap between the locations where proteins can interact with water and interact non-covalently with PP (Morr, 1990; Kanakis et al., 2011; Bohin et al., 2012; Le Bourvellec and Renard, 2012; Chung et al., 2015; Oancea et al., 2017), WHC, typically used to describe interactions with water, might also be able to describe the potential for protein-PP interactions. Given that WPI had the lowest WHC of the proteins studied, it is possible that WPI would have the least interactions with PP. SPI and PPI, with higher WHC values imparted by their differing structures with more sites available for interactions, may interact more extensively with the Aronia PP and yield greater measurable changes in physicochemical properties than WPI formulations.

4.3.2 Feed characterization:

4.3.2.1 pH

As reported in earlier work (Hansen et al., 2021b), pH of the dispersions was observed to decrease slightly with increasing PP concentration (**Table 4.1**). Variations in pH may influence the structure of proteins in solution, determining which side groups are exposed and how many bindings sites may be available for intermolecular interactions and binding (Rawel et al., 2005), as well as affect functional properties of dispersions including viscosity and particle size (Spencer et al., 1988; Saluja and Kalonia, 2005; Cao and Xiong, 2017; Hong et al., 2018). As the pH of dispersions approaches the protein isoelectric point (pI), proteins are more likely to undergo intermolecular interactions and aggregate, which can result in increased viscosity (Song, 2009; Coupland, 2014).

Use of 1.5% Aronia PP in WPI dispersions induced pH to near the pI values reported in the literature for constituent β-lactoglobulin (pI ~ 5.2-5.3; the major protein fraction in WPI), though values for α-lactalbumin (~ 4.2-4.8) were not reached (**Table 4.1**) (Kilara and Harwalkar, 1996; Demetriades and McClements, 1998; Jean et al., 2006). pH of SPI dispersions was found to decrease with increasing PP concentration and approach the range of pI values reported for β-conglycinin, the minor 7S protein fraction in SPI (pI ~ 5.2-6.4; **Table 4.1**). The pI of the major 11S protein fraction, glycinin (pI ~ 4.8), was not nearly reached (Petruccelli and Añón, 1995; Li, 2005). pH values of PPI dispersions were also reduced with increased PP concentration (**Table 4.1**), but did not approach the pI values reported in the literature for constituent vicilin (pI ~ 5.5) or legumin (pI ~ 4.8) protein fractions (Owusu-Ansah and McCurdy, 1991; Lam et al., 2018).

Assuming a range of pI for WPI, SPI, and PPI, it is possible that the reduced pH values could play a minor role affecting the physical properties of these dispersions.

4.3.2.2 Interfacial tension

An individual drop will form when the gravitational forces acting on it overcome the surface tension forces around the circumference of the tubing tip, confirming surface tension as a major determinant of the sizes of drops produced (Hansen et al., 2021b). The ANOVA reported that changing the ratio of protein to sucrose had a significant effect ($p < 0.05$) on calculated surface tensions of dispersions. Tukey's HSD tests clarified further, indicating that as protein:sucrose ratios increased, surface tensions significantly decreased ($p < 0.05$), and all three ratios had significantly different surface tension values (**Figure 4.1A**). Sucrose is not thought to appreciably affect surface tension, as sugars are not particularly surface-active; proteins are known surfactants and may adsorb to liquid-gas interfaces and decrease surface tensions (Kitabatake and Doi, 1988). In previous studies, changing the ratio of WPI to sucrose in dispersions did not meaningfully impact surface tension (**Figure 4.1A** samples marked*****; Hansen et al., 2021b); this observation was confirmed by additional data for WPI dispersions containing 1.5% PP. Similarly, altering SPI:sucrose ratios in dispersions did not notably affect surface tension. Surface tensions of PPI dispersions decreased with increasing PPI concentrations, regardless of PP concentration (**Figure 4.1A**).

Changing the type of protein isolate in formulations between WPI, SPI, and PPI also had a significant effect ($p < 0.05$) on surface tension, according to the ANOVA. Corresponding Tukey's HSD tests indicated that WPI dispersions had the highest surface tensions, while PPI formulations had the lowest, and all three protein isolates were significantly different from each

other. In ranking the surfactant abilities to reduce surface tensions of dispersions, WPI would be lowest and PPI highest; these mirror the findings for WHC, which may indicate the differing extent to which the isolates interact with water.

According to the ANOVA, changing the PP concentrations in dispersions had a significant effect on surface tension ($p < 0.05$). Tukey's HSD tests provided more detail, specifying that increasing PP concentrations resulted in significantly increased surface tensions ($p < 0.05$), and the values for all four PP concentrations were significantly different from each other (**Figure 4.1B**). This trend was observed most clearly in dispersions formulated with PPI, while many conditions, including WPI formulations and some SPI dispersions, showed no meaningful trends. These findings build on those from earlier studies, where increasing PP concentrations in WPI-sucrose dispersions resulted in increased surface tensions under few conditions, but many conditions showed no meaningful trends (**Figure 4.1B** samples marked***** with unfilled markers; Hansen et al., 2021b). As in previous work, variations in trends observed may be attributed to air entrapped in dispersions giving altered surface tension calculations. With optimal PP and protein types and environmental conditions, protein-PP complexation interactions may be enhanced with increased PP, forming complexes that can grow into larger aggregates (Spencer et al., 1988; Charlton et al., 2002; Rawel et al., 2005; Ozdal et al., 2013). As discussed in previous studies (Hansen et al., 2021b), the increased incidence of large protein-PP aggregates in dispersions would likely generate more intermolecular interactions, and liquids containing higher quantities of strong, attractive intermolecular forces are known to have higher surface tensions (He et al., 2011; Tro et al., 2014); this may explain the rising surface tensions observed with increasing PP. It is also possible that, as PP increased, the surfactant abilities of proteins in dispersions to lower surface tension were reduced as a result of enhanced protein-PP

interactions occurring and occupying sites available for other interactions. This may also explain the increased surface tensions with increasing PP.

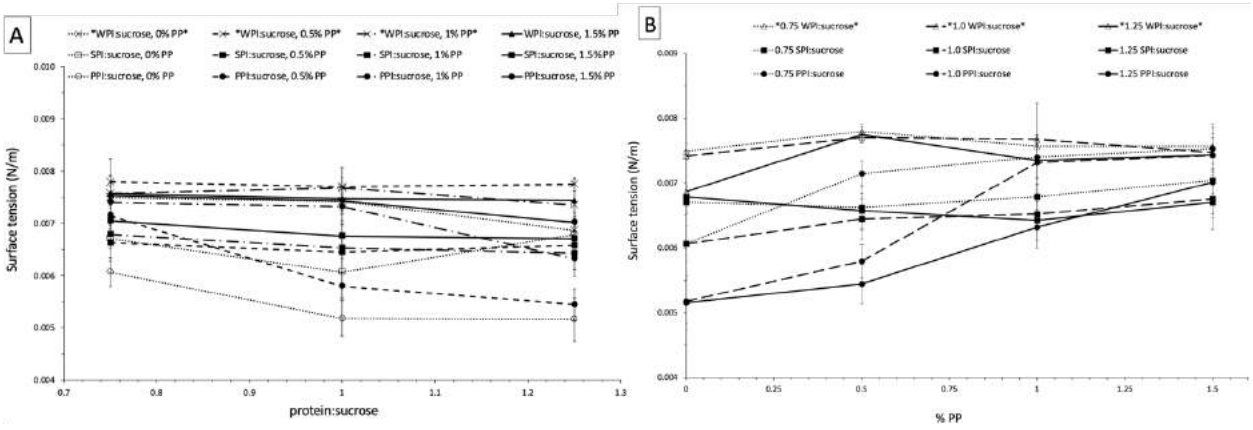


Figure 4.1. Effect of protein:sucrose ratio [**A**] and PP content (%) [**B**] on the calculated surface tension (N/m) of dispersions at 25˚C; (averaged data plotted, n = 9). Legend entries marked * contain data reported in previous work (Hansen et al., 2021a; averaged data plotted, n = 6). Lines are for guiding purposes only.

Previous studies have indicated that drop diameters and surface tensions are directly related; as surface tensions decrease, so do the diameters of the resulting drops (Chan et al., 2009). The best fit line applied upon plotting the calculated diameters of drops against the calculated surface tensions of dispersions showed a positive slope (**Figure 4.2**), indicative of a direct correlation ($R^2 = 0.72$), as described by Lee and Chan (2013) and observed in previous work (Hansen et al., 2021b). As discussed in earlier work, the few data points scattered from the correlation may be caused by inaccurate drop diameter and surface tension calculations based on density measurements that can vary with the inclusion of air bubbles in the protein-containing dispersions, as well as the inherent variation within food ingredients (Hansen et al., 2021b). Corresponding density data indicates relatively consistent amounts of entrapped air in

dispersions, with few formulations showing enhanced air holding abilities and thus lower measured densities, which may affect the scatter (**Table 4.1**).

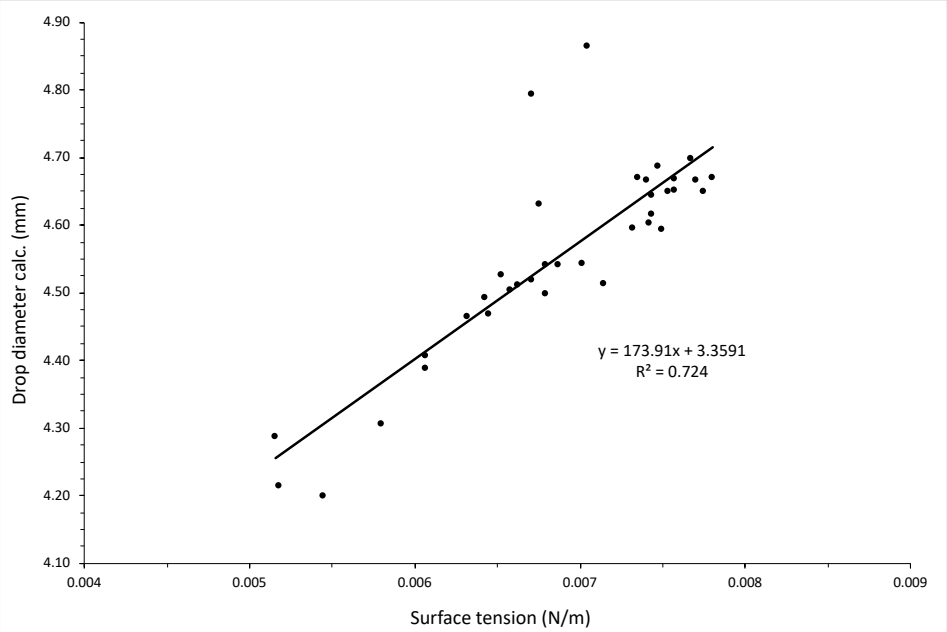


Figure 4.2. The relationship between the average surface tensions (N/m) of feed dispersions containing protein:sucrose ratios of 0.75, 1.0, and 1.25, PP contents of 0, 0.5, 1, and 1.5%, and protein isolates including WPI, SPI, and PPI at 25˚C and average calculated diameters (mm) of drops.

As reported in earlier studies, more specific methods of surface tension measurement could potentially provide more accuracy than the drop mass method employed (Worley, 1992). However, these methods would not be compatible with the dispersions in focus due to their viscosities, stickiness, turbidity, entrapped air, and dark colors when Aronia is present (Hansen et al., 2021a).

4.3.2.3 Viscosity

Viscosity is related to the fluid flow properties of dispersions and can strongly influence processing and manufacturing operations (Johnson et al., 1975; Hartel et al., 2018; Hansen et al.,

2021b). According to the ANOVA, the ratio of protein to sucrose had a significant ($p < 0.05$) effect on viscosity, where increases in ratios resulted in increased viscosities. Tukey's HSD tests clarified that all ratios had significantly different viscosities from one another. These ANOVA results are only visually demonstrated in **Figure 4.3A** for PPI formulations containing 0 and 0.5% PP and SPI dispersions with 1.5% PP; those few formulations most strongly influenced the ANOVA results, despite the majority of formulations showing no major changes in viscosity with increasing protein:sucrose ratios. Earlier work also reported significant increases in dispersion viscosities with increasing WPI:sucrose ratios, but only when dispersions total solids contents were greater than 35% (Hansen et al., 2021b). These results are generally in agreement with those from previous experiments, where dispersions containing 25% total solids did not show major shifts in viscosity with changing WPI:sucrose ratios, as the effect of changing protein:sucrose ratios was thought to be relatively weak compared to the effect of % total solids. The increases in dispersion viscosities observed with increasing PPI:sucrose ratios and low PP concentrations may be due to the large molecular mass proteins at higher concentrations having increased opportunities for overlapping, intermolecular protein-protein interactions, and network formation (Song, 2009; Coupland, 2014); lower PPI:sucrose ratios may have a diluting effect on the protein-protein networks and thus behave more similarly to other, less viscous WPI and SPI dispersions.

Changing the protein isolate in formulations between WPI, SPI, and PPI had a significant effect ($p < 0.05$) on viscosities of dispersions, according to the ANOVA. Tukey's HSD tests provided further detail, reporting that WPI dispersions had the lowest average viscosities, while PPI dispersions had the highest, and the average viscosities of dispersions containing each protein isolate were significantly different from each other. These findings generally agree with

those reported by Krstonošić et al. (2020), where aqueous solutions of whey protein concentrate at varied concentrations had lower viscosities than pea and soy protein isolate solutions. In comparing the different protein isolates abilities to reduce surface tensions of dispersions, WPI was found to have the lowest efficacy and PPI the highest, mirroring the findings for the WHC of the isolates. Similarly, WPI had the lowest impact on viscosities of dispersions, indicative of adequate electrostatic repulsion between proteins, while PPI had the highest impact on viscosity, likely due to its large average molecular mass and the increased likelihood of protein-protein interactions. Additionally, PPI dispersions may have differing viscous properties due to the varied extents of hydration undergone by each protein isolate; PPI appears to have undergone a lesser extent of protein hydration prior to testing, as indicated by the presence of large insoluble PPI particles in dispersions.

According to the ANOVA, increasing PP in dispersions was found to have a significant effect ($p < 0.05$) on viscosity, where viscosities generally decreased with increasing PP until increasing at 1.5% PP. Corresponding Tukey's HSD tests indicated that dispersions with differing PP had significantly different viscosities from one another. The decreasing viscosity relationship with increasing PP reported by the ANOVA is strongly determined by a small minority of the formulations studied; this trend is only observed for 1.25 PPI:sucrose dispersions with 0 and 0.5% PP, though 1.0 PPI:sucrose dispersions at the same PP concentrations have slightly higher viscosities than the majority of formulations studied. When PP concentration is greater than 0.5%, viscosities of PPI dispersions resemble those of the other formulations (**Figure 4.3B**). The relatively high viscosities measured for PPI dispersions with low PP concentrations (< 1% PP) may be due to the presence of large unhydrated protein particles remaining in dispersions during measurements. As PP increase in the system, there may be more

opportunities for protein-PP complexation interactions resulting in aggregates that are smaller than the unhydrated particles and thus reducing system viscosity.

Increased viscosities at 1.5% PP are only demonstrated in **Figure 4.3B** for 1.0 and 1.25 SPI:sucrose dispersions, while the majority of formulations showed no meaningful variation in viscosity with increasing PP. The 1.0 and 1.25 SPI:sucrose dispersions, while a minority of the formulations studied, strongly influenced the ANOVA results reported as their viscosities were significantly higher than the other formulations studied. The hydrolyzed SPI was designed to disperse more readily in water with minimal aggregation. Hydrolyzed protein structures have more potential sites available for PP complexation interactions as well, but it appears that a concentration threshold must be met for the SPI in order to start forming an interaction network at high PP concentrations. High PP concentrations likely gave rise to increased intermolecular interactions in the system upon the formation of protein-PP complexes, resulting in increased viscosities and behavioral complexity of the dispersions. Significant increases in viscosity were not observed to occur in formulations with the same SPI:sucrose ratios at lower PP concentrations, indicating that the extreme increase at 1.5% PP is likely due to a strong network forming with protein-PP complexation at high protein and PP concentrations. Results reported are generally in agreement with those from earlier experiments, where increasing PP resulted in slight shifts in viscosity for dispersions containing 25% total solids (Hansen et al., 2021b).

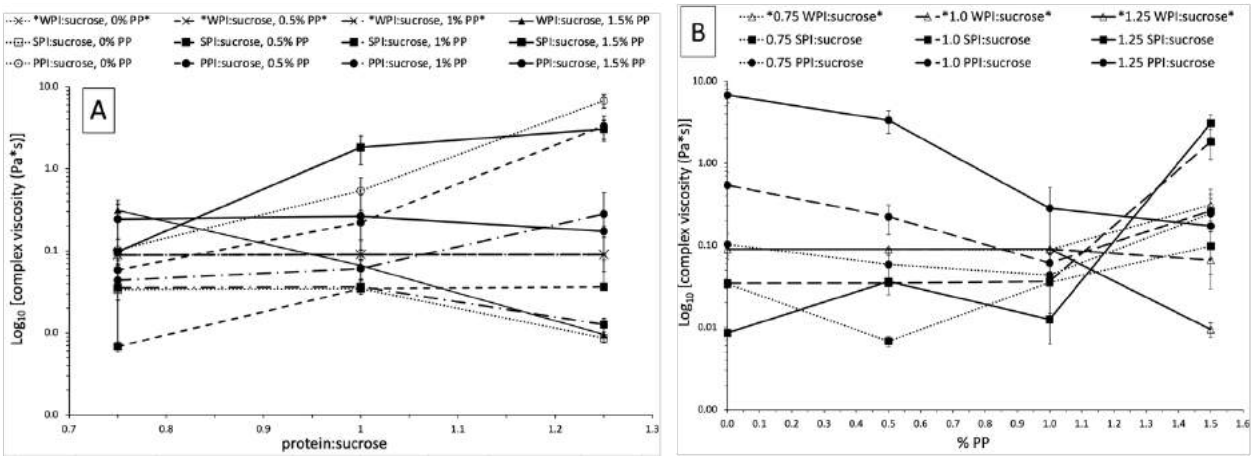


Figure 4.3. Effect of protein:sucrose ratio [**A**] and PP content (%) [**B**] on the average complex viscosity (Pa*s) of dispersions at 25˚C; (averaged data plotted, n = 9). Legend entries marked * contain data points reported in previous work (Hansen et al., 2021a; averaged data plotted, n = 6). Lines are for guiding purposes only.

4.3.2.4 Particle size distribution

Particle size analysis is useful for evaluating protein-PP interactions in dispersions, as the introduction of PP changes protein structures, conformation, and electrostatic repulsion, thus affecting the extent of aggregation and resulting particle size distributions of dispersions (Bandyopadhyay et al., 2012; Le Bourvellec and Renard, 2012; Coupland, 2014; Schneider, 2016; Hong et al., 2018; Hansen et al., 2021b). According to the ANOVA, protein:sucrose ratio had a significant effect ($p < 0.05$) on the average particle size (volume-weighted mean, $d_{4,3}$) of dispersions. Tukey's HSD tests clarified that increasing protein:sucrose ratios from 0.75 to 1.0 resulted in significantly increased average particle sizes ($p < 0.05$), but the slight increase observed from 1.0 to 1.25 protein:sucrose was not significant ($p > 0.05$). Despite the ANOVA reporting some apparently significant changes in particle size with changing protein:sucrose ratios, plotting the data in **Figure 4.4A** indicated that the shifts were small. These observations are generally in agreement with results from earlier experiments, where WPI:sucrose ratio did not strongly impact the average particle sizes of dispersions (Hansen et al., 2021b).

Changing the protein isolate in formulations between WPI, SPI, and PPI had a significant effect ($p < 0.05$) on the average particle sizes of dispersions, according to the ANOVA. Tukey's HSD tests provided further detail, reporting that WPI dispersions had the smallest average particle sizes, PPI dispersions had the largest, and the average particle sizes of dispersions containing each protein isolate were significantly different from each other. The differences between the average particle sizes of SPI and WPI dispersions are best demonstrated in **Figure 4.4B**, where SPI formulations containing higher PP concentrations (> 0.5%) are shown to have slightly larger average particle sizes. These findings mirror the trends observed for WHC and viscosity measurements, with WPI having the lowest values and PPI having the highest, likely influenced by differences in the average molecular masses of the isolates and the potential for protein-protein interactions.

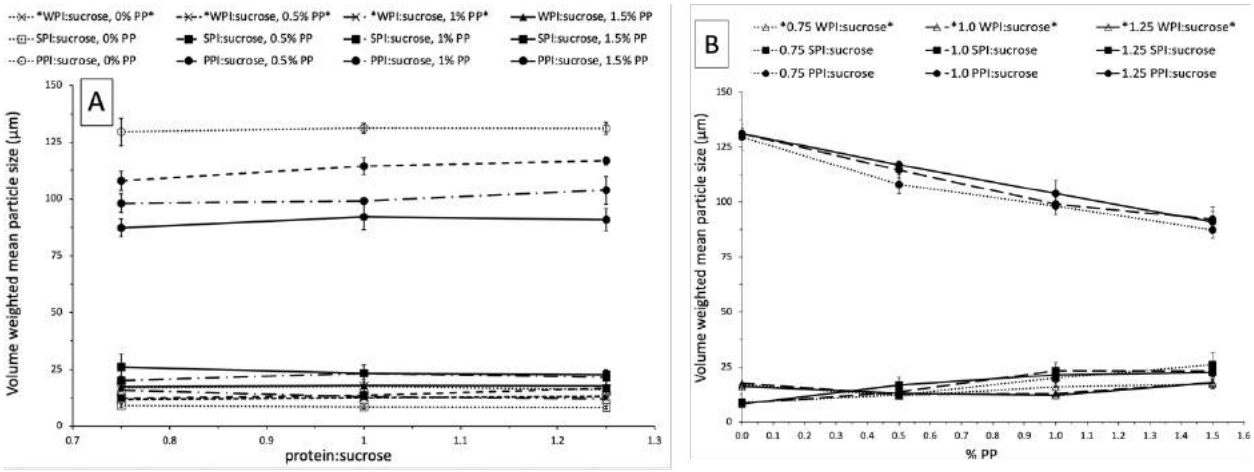


Figure 4.4. Effect of protein:sucrose ratio [**A**] and PP content (%) [**B**] on the average particle size (µm) of dispersions at 25˚C; (averaged data plotted, n = 9). Legend entries marked * contain data points reported in previous work (Hansen et al., 2021b; averaged data plotted, n = 6). Lines are for guiding purposes only.

While earlier work reported normal distributions for WPI dispersions (Hansen et al., 2021b), the particle size distributions for SPI and PPI dispersions were observed to have different shapes with tails and shoulders to the left and right of the main peaks, as demonstrated in **Figure 4.5**. These differences in distribution shapes may be indicative of the presence of unhydrated particles and protein-PP conjugates of different sizes in dispersions.

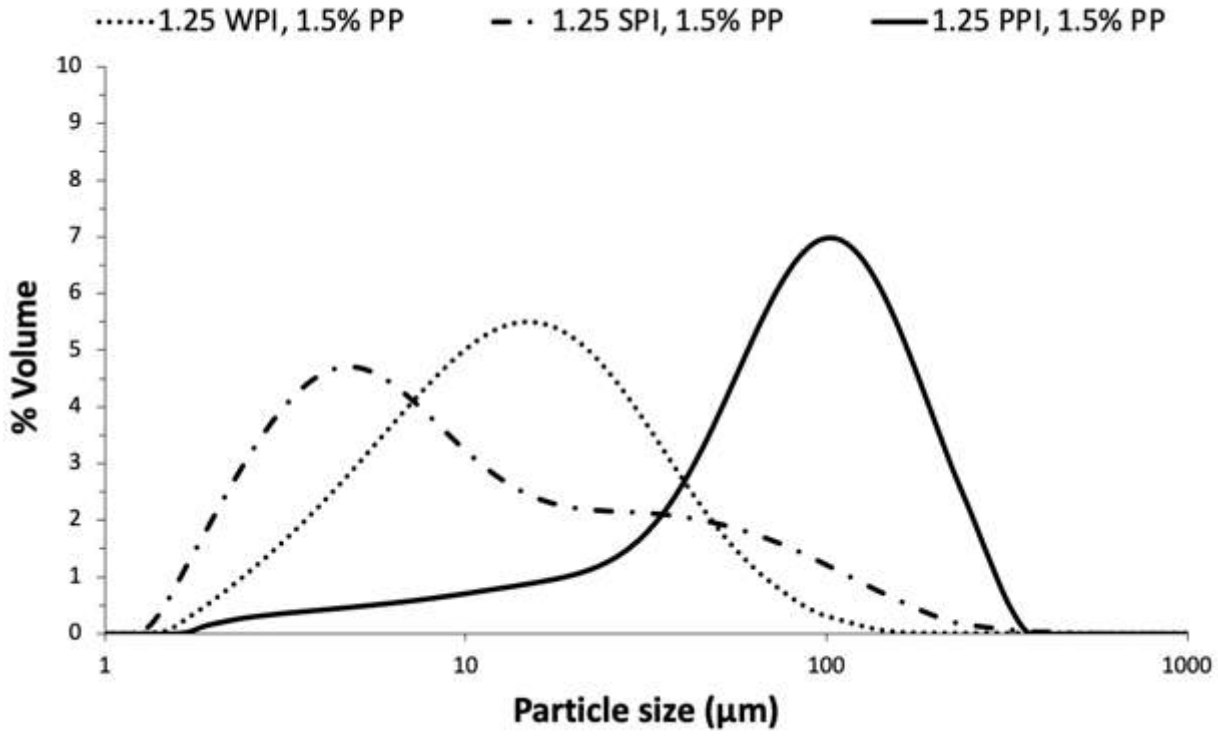


Figure 4.5. Particle size distributions of dispersions with 1.25 protein:sucrose ratios and 1.5% PP contents comprised of WPI, SPI, and PPI at 25˚C; (averaged data plotted, n = 9).

According to the ANOVA, average particle sizes of dispersions were significantly affected by PP concentration ($p < 0.05$); Tukey's HSD tests expanded on this, reporting that particle sizes decreased significantly with the addition of 0.5 and 1% PP to dispersions, with no further change upon 1.5% PP addition ($p > 0.05$). While in agreement with the findings from

previous work with 25% total solids WPI dispersions (Hansen et al., 2021b), these results appear to be strongly influenced by the data for PPI formulations specifically. Though the results reported by the ANOVA may be observed for PPI dispersions in **Figure 4.4B**, trends observed for WPI and SPI formulations were different; SPI dispersions showed slightly increasing particle sizes with increasing PP, while WPI dispersions generally showed no meaningful trends or changes, indicative of less extensive protein-PP interactions. Apparently, PPI underwent the least extent of hydration prior to testing, resulting in the presence of many large aggregates in dispersions upon measurement and observation. Formation of protein-PP aggregates in PPI dispersions, which were smaller than the unhydrated PPI particles, likely caused the average particle sizes of dispersions to go down with increasing PP. Additionally, further hydration may have occurred over time, reducing the sizes of larger unhydrated particles in dispersions.

The slight increasing trends observed for particle sizes in SPI dispersions with increasing PP may be due to the same factors that affected viscosity. The hydrolyzed SPI used in this study had smaller average molecular mass proteins than regular SPI; hence, it dispersed easily with minimal protein aggregation, explaining the small particle sizes observed when PP were absent. The hydrolyzed protein structures have more potential sites available for protein-PP interactions than non-hydrolyzed SPI, which may explain the steady increase in particle sizes detected as PP increased in dispersions. While an opposite trend was observed for changes in particle size by Xue et al. (2020) when studying complexation between SPI and cyanidin-3-galactoside, this may be due to the use of different SPI sources. Thus, increased particle sizes measured in SPI dispersions may be attributed to enhanced protein-PP interactions in the system.

4.3.2.5 Optical light microscopy

As with earlier work, particle size data generated by Mastersizer light scattering were supported by microscopy (Hansen et al., 2021b). Although inherent differences exist between the methods making direct comparison of results difficult (Schneider, 2016), microscope images depicted Mastersizer data visually, including the variations observed in particle size distributions between dispersions containing WPI, SPI, and PPI (**Figure 4.5; Figure 4.6A-C**). Mastersizer data reporting increased average particle sizes with increasing PP in SPI dispersions were reinforced with optical light microscopy (**Figure 4.7A-D**), as were the reduced average particle sizes observed for PPI dispersions with increased PP (**Figure 4.8A-D**).

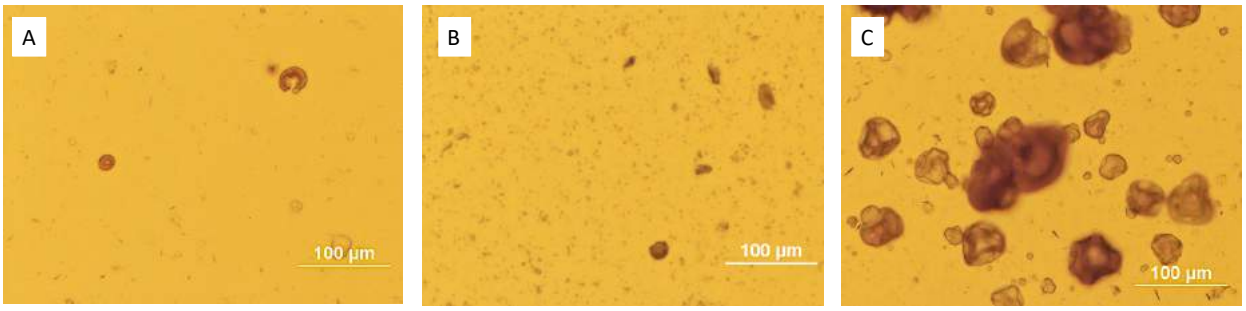


Figure 4.6. Optical light microscope images at 200x magnification depicting the microstructures of diluted feed dispersions with a 1.25 protein:sucrose ratio and 1.5% PP formulated with WPI (**A**), SPI (**B**), and PPI (**C**).

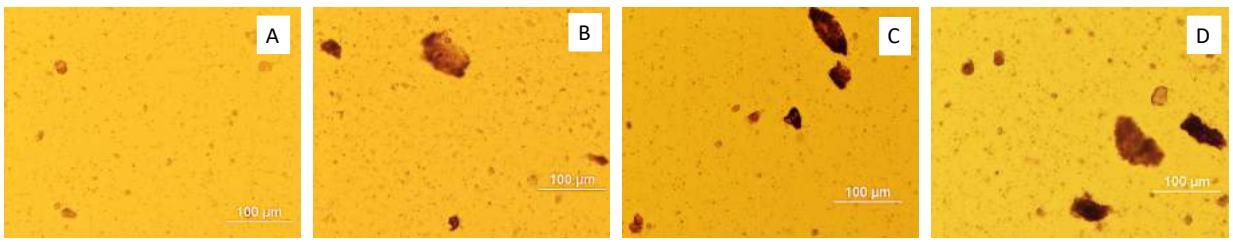


Figure 4.7. Optical light microscope images at 200x magnification depicting the microstructures of diluted feed dispersions with 1.0 SPI:sucrose with 0% (**A**), 0.5% (**B**), 1% (**C**), and 1.5% PP addition (**D**).

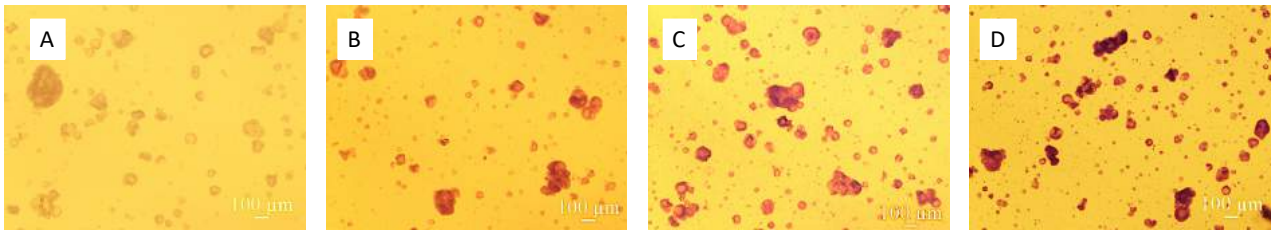


Figure 4.8. Optical light microscope images at 40x magnification depicting the microstructures of diluted feed dispersions with 1.0 PPI:sucrose with 0% (**A**), 0.5% (**B**), 1% (**C**), and 1.5% PP addition (**D**).

4.3.2.6 Centrifuge separation

Centrifugation resulted in the easy precipitation of pellets out of diluted dispersions, as observed with earlier experiments involving WPI (Hansen et al., 2021b). Centrifuged samples without Aronia PP formed clear supernatants and off-white to tan-colored pellets, while those containing PP formed dark purple pellets (**Figure 4.10)**, indicative of protein-PP complexation, as formation of a colored precipitate is a crude method to confirm protein-PP complexation (Van Teeling et al., 1971). Similar to observations from earlier experiments (Hansen et al., 2021b), diluted PP-containing dispersions formed dark purple, transparent supernatant fractions after centrifugation.

Precipitated pellets appeared to be smallest for diluted 1.25 protein-sucrose dispersions with 1.5% PP containing WPI, and largest for PPI (**Figure 4.9**). Comparing observations from previous experiments (Hansen et al., 2021b), WPI-containing dispersions appeared to form the smallest pellets upon centrifugation (regardless of PP concentration), while SPI dispersions formed slightly larger pellets and PPI formed the largest. Differences in the relative precipitate sizes of the protein isolates may be attributed to the differences in size, where proteins with

larger average molecular masses (such as SPI and PPI) may be more susceptible to precipitating out of solution upon centrifugation than smaller molecular mass proteins like WPI.

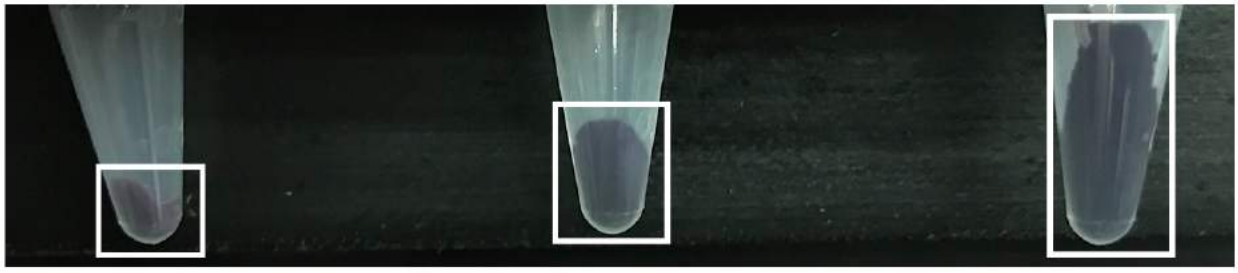


Figure 4.9. Image depicting the precipitated fractions (highlighted in boxes) of centrifuged 5x-diluted dispersions with 1.25 protein:sucrose and 1.5% PP with WPI (Left), SPI (Center), and PPI (Right).

Pellet sizes generally appeared to increase slightly with increasing PP in diluted SPI and PPI dispersions (**Figure 4.10**), akin to observations made in previous work for WPI dispersions with increasing PP (Hansen et al., 2021b). Negligible precipitate was formed upon centrifugation of a diluted 1% Aronia extract solution in previous experiments, indicating that the apparent increases in pellet sizes with increasing PP may be a result of the formation of larger, aggregated complexes precipitating out of solution (Hansen et al., 2021b).

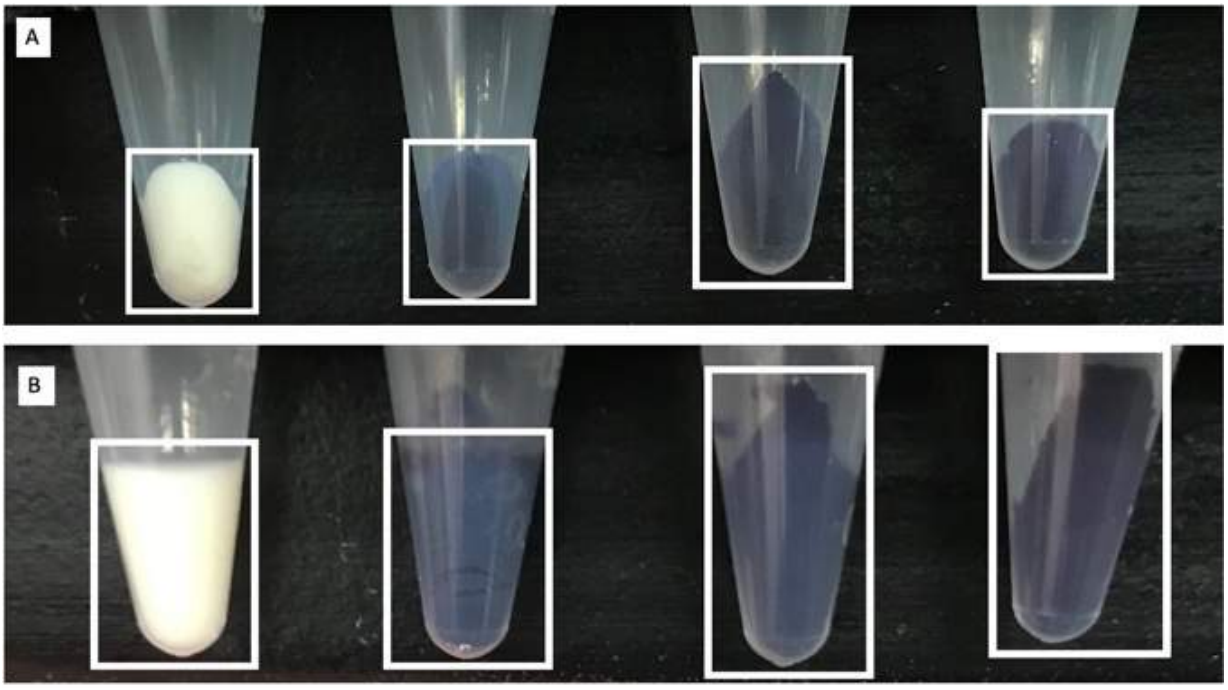


Figure 4.10. Images depicting the precipitated fractions (highlighted in boxes) of centrifuged 5x-diluted dispersions with 1.25 SPI:sucrose (**A**) and 5:4 PPI:sucrose (**B**) and 0% (Left), 0.5% (Center, left), 1% (Center, right), and 1.5% PP addition (Right).

4.3.3 Frozen drop characterization:

4.3.3.1 Comparison of diameters

Dispersions were frozen into drops and diameters were measured to observe the effects of changing protein:sucrose ratios, protein isolate types, and PP concentrations on the sizes of drops formed. According to the ANOVA and corresponding Tukey's HSD tests, changing the protein:sucrose ratios in dispersions did not have a significant impact ($p > 0.05$) on frozen drop diameters (**Figure 4.11A**).

Changing the protein isolate in dispersions between WPI, SPI, and PPI had a slight but statistically significant effect ($p < 0.05$) on the diameters of frozen drops formed, according to

the ANOVA. Corresponding Tukey's HSD tests specified that PPI beads had significantly larger diameters than the other isolates ($p < 0.05$), while the smaller diameters of SPI and WPI beads were not significantly different from each other. These findings are depicted in **Figure 4.11B**, where the average frozen diameters of all formulations containing each respective protein isolate are reported. Although surface tension and drop diameters are reported to be directly correlated, our results for measured drop diameters are at odds with this; dispersions with the lowest surface tensions (in this case, PPI formulations) would be expected to have the smallest drop diameters but were actually found to have the largest diameters of the formulations studied. The viscous PPI dispersions (and few SPI formulations) were observed to drip irregularly from the tubing tip into nonuniform shapes indicative of more complex fluid behaviors, in contrast to the spherical drops formed by WPI, contributing to the higher variation observed in diameters for beads produced with those isolates.

PP concentration was found to have a significant ($p < 0.05$) impact on frozen drop diameters, according to the ANOVA. In line with previous findings (Hansen et al., 2021a), Tukey's HSD tests reported a significant increase in diameters ($p < 0.05$) when PP was increased from 0 to 0.5%, but the minor increases in diameters observed as PP increased from 0.5 to 1 and 1.5% were not statistically significant. Drop diameters generally increased with Aronia addition, although some scatter was observed; the increasing trend is most clearly demonstrated for dispersions comprised of PPI:sucrose as PP increased from 0 to 0.5% in **Figure 4.11C**. These findings are in agreement with the surface tension data, as both surface tension and frozen drop diameters increase with PP addition, in agreement with reports indicating their direct correlation.

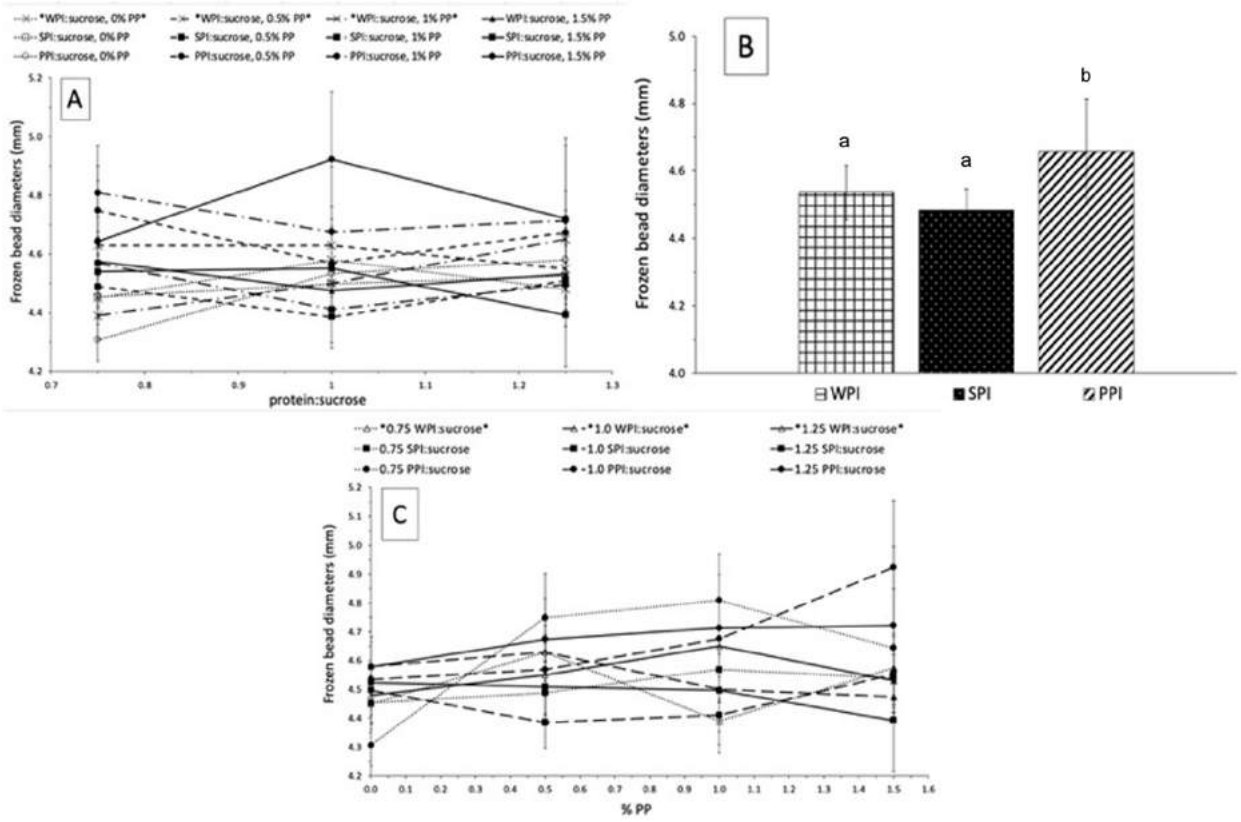


Figure 4.11. Effect of protein:sucrose ratio [**A**], protein isolate type [**B**], and PP content (%) [**C**] on the on the diameters (mm) of frozen drops formed from dispersions; (averaged data plotted, n = 9). Legend entries marked * contain data points reported in previous work (Hansen et al., 2021b; averaged data plotted, n = 3). Lines are for guiding purposes only [**A, B**]. Values connected by the same letter are not significantly different ($p > 0.05$).

Estimated values calculated from flow testing data were compared with the measured diameters of frozen drops (**Table 4.1**). While the prediction of drop diameters by calculations was generally successful in previous work focused on WPI dispersions (Hansen et al., 2020, 2021b), the success rates (no significant differences between calculated and measured values; $p < 0.05$) here were notably lower. No significant differences were found between the estimated diameters calculated from flow data and the actual measured diameters 75% of the time for WPI dispersions. SPI dispersions had a success rate of 50%, and PPI dispersions only 33%. It is possible that the estimated calculations became less accurate in predicting drop diameters

because variability increased for the measured drop diameters of SPI and particularly PPI dispersions, when more irregularly shaped, less spherical drops were observed to form.

4.4 Conclusions

To expand on the findings from previous experiments, where liquid dispersions containing WPI, sucrose, and Aronia extract were found to exhibit measurable changes in physicochemical properties attributed to naturally occurring, non-covalent complexation interactions between PP and proteins, this work aimed to investigate whether Aronia PP would interact with plant-based SPI and PPI to a similar extent. The occurrence of non-covalent protein-PP interactions was found to have different effects in SPI and PPI dispersions, nevertheless indicative of more extensive protein-PP interactions than observed in WPI formulations. Increased viscosities and particle sizes were observed for SPI dispersions with increasing PP, while PPI formulations were observed to have reduced viscosities and particle sizes and increased surface tensions. These findings build from previous work to contribute to the body of research describing the physical effects of non-covalent interactions between non-dairy proteins and PP under mild pH and temperature conditions. Additionally, our results provide empirical insight for applications utilizing concentrated protein-PP mixtures for the development of protective delivery vehicles such as the dry, high protein beads formed by the processes presented in other experiments (Hansen et al., 2020, 2021b). Findings from this study may also inform the formulation of functional foods containing proteins and PP sources like fruit, such as sports beverages, nutritional bars, smoothies, and yogurts, as well as everyday products including pudding and frozen desserts, where specific sensory attributes may be at risk if formulations contain levels of PP and proteins that would be prone to more extensive complexation interactions in mixtures.

Funding

Funding for this study was provided by the Lauritzson Foundation via the Lauritzson Research Scholarship, through the College of Science, Engineering and Food Science (SEFS) at University College Cork.

Chapter 5

Bioactives and extract effects on the physico-chemical properties of concentrated whey protein isolate dispersions

Mackenzie M. Hansen[a,b*], Richard W. Hartel[b], Yrjö H. Roos[a]

[a] Food Technology, School of Food and Nutritional Sciences, University College Cork, Ireland

[b] Department of Food Science, College of Agricultural and Life Sciences, University of Wisconsin-Madison

Abstract

Non-covalent complexation interactions are known to occur between bioactive compounds and proteins. While formulating with these components can have positive outcomes such as stabilization of colors and actives, it can also result in changes to the structures and physical properties of proteins, affecting product functionality and sensory attributes. Previous experiments reported measurable changes in the physico-chemical properties of whey protein isolate (WPI) dispersions upon formulation with Aronia berry extract, ascribing changes to protein-polyphenol (PP) interactions in the systems. Pure gallotannin, beet extract, and cranberry extract, providing a diverse variety of structures and sizes, were selected for further experimentation and comparison with the effects of Aronia extract. Concentrated dispersions with varying WPI:sucrose ratios, formulated with several bioactives contents from multiple different sources were analyzed to identify the effects of different bioactives on physico-chemical properties of dispersions. Dispersions formulated with cranberry extract demonstrated the largest increases in surface tensions, viscosities, and particle sizes, while those formulated with beet extract were the least affected by the presence of bioactives, suggesting that different bioactives and extracts had varying propensities for complexation interactions with WPI, despite their relatively low levels of addition (0, 0.5, and 1%).

5.1 Introduction

Consumer interest is often a catalyst for the development of new and improved products in the food industry. Increased demand for health-supporting and functional products has driven the development of high protein foods with bioactives and other nutrients from fruits and vegetables due to the perceived benefits of consuming naturally-derived, bioactive compounds that are thought to positively affect human health (Kapsak et al., 2011; Banovic et al., 2018; Calderón-Oliver and Ponce-Alquicira, 2018; González, 2020; Hansen et al., 2021a, b). In addition to the demand for healthy foods, consumers have pushed developers to replace synthetic colorants in foods with naturally derived color compounds (Sigurdson et al., 2017). Fruits and vegetables are an attractive source of natural pigments that may also provide health benefits when formulated into food products (Calderón-Oliver and Ponce-Alquicira, 2018; Akbar Hussain et al., 2018; de Mejia et al., 2020), though natural color compounds, like polyphenols (PP) and betalains, are known to have low chemical stability in foods during storage (Miguel, 2018; de Mejia et al., 2020; Hansen et al., 2021a, 2021b).

Polyphenols are a family of compounds ubiquitous in fruits and vegetables reported to have strong antioxidant properties, are most commonly found as glycosides with sugar units on the polyphenol structures, and can be divided into monomeric and polymeric PP categories (Tsao, 2010; Hansen et al., 2021a, b). Monomeric PP, such as phenolic acids and flavonoids, are relatively small compounds; anthocyanins are a common flavonoid varying in color from orange to purple, and are the primary bioactive pigment compounds found in Aronia berries (Dabas, 2016; Xie et al., 2016, 2017). Polymeric PP are larger compounds with greater molecular masses and can be categorized as condensed or hydrolysable tannins. Condensed tannins are more abundant in the human diet and include proanthocyanidins, the main bioactive pigment

compounds lending the red-purple color to cranberries and other fruits and vegetables (Oliveira et al., 2013). Hydrolysable tannins such as gallotannin, while less common in the human diet, can be found in almonds and mango peel (Girard and Awika, 2020). Betalains, while relatively small and water-soluble, are nitrogenous and not chemically or structurally related to anthocyanins. They can be divided into betaxanthins and betacyanins, including betanin, the main bioactive compound imparting the deep red-violet color in beets (Miguel, 2018; de Mejia et al., 2020).

Polyphenols and betalains have been reported to possess innate abilities to complex with proteins in neutral and acidic pH formulations primarily via weak, non-covalent hydrophobic interactions and hydrogen bonds to varying extents, depending on the compound (Gad and El-Salam, 2010; Schneider, 2016; Girard and Awika, 2020; Zhao et al., 2020; Hansen et al., 2021a, 2021b). When considering polymeric PP, structural characteristics including higher degrees of polymerization, larger molecular sizes, more conformational flexibility, and larger numbers of hydroxyl groups and hydrophobic regions available may be indicative of greater volumes and strength of protein-PP interactions (Hagerman, 1989; Harbertson et al., 2014; Ropiak et al., 2017; Girard and Awika, 2020). Girard et al. (2019) reported that the affinity of condensed tannins for gluten protein interactions was greater than that of hydrolysable tannins likely due to the enhanced conformational flexibility of condensed tannins. Although the interaction affinity between anthocyanins and proteins may be more limited due to the relatively small size of the flavonoids compared to polymerized PP, in previous experiments measurable changes in the physical properties of protein dispersions with anthocyanin-rich Aronia berry extract addition were observed, indicative of some extent of protein-PP interaction (Hansen et al., 2021a, b, c). Despite the relatively small molecular structures compared to polymerized PP, betalains are

larger than anthocyanins and have been reported to have some affinity for protein interactions, likely due to the presence of hydroxyl groups and hydrophobic regions available (Martínez et al., 2019; Zhao et al., 2020). Complexation interactions between proteins and bioactive compounds including PP and betalains are known to affect protein structures and hydrodynamic volumes in dispersions (Rawel et al., 2005; Martínez et al., 2019; Sęczyk et al., 2019; Zhao et al., 2020), as well as physico-chemical, functional and nutritional properties of the products (Girard et al., 2016; Hansen et al., 2021a, b; Li et al., 2021; Sharma et al., 2021). Additionally, complexation interactions may be useful for bioactives protection and delivery as well as color retention (Cao and Xiong, 2017; Ma and Zhao, 2019; Quan et al., 2019; Zhao et al., 2020; Baba et al., 2021).

The objective of this study is to investigate the extent of interactions between whey protein isolate (WPI) and bioactive compounds from various sources, indicated by measurable changes in the physical properties of concentrated, liquid feed dispersions with varied formulations, including flow properties, viscosity, particle size distribution, pH, centrifuge separation, and microstructure imaging. Bioactives sources including pure gallotannin and Aronia berry, beet, and cranberry extracts were selected for their health-promoting properties and variety of predominant compounds with diverse molecular structures and sizes for comparison. Extracts known to have predominantly larger-sized bioactive compounds with higher flexibility and degrees of polymerization and more hydroxyl groups and hydrophobic regions (such as cranberry extract or gallotannin), would be expected to interact with proteins more extensively than extracts delivering smaller-sized bioactive compounds with fewer potential sites for interactions (such as Aronia and beet extracts) in the same concentration in dispersions (de Mejia et al., 2020; Girard and Awika, 2020). More extensive protein-bioactive interactions may result in greater changes in the physical properties of dispersions measured such as viscosity, particle

size distribution, flow properties, etc., compared to formulations containing actives with lower propensities for interactions with proteins. This work furthers previous experimental findings, providing additional information regarding the effects of different bioactive compound addition to the physico-chemical properties of concentrated whey protein dispersions, and the potential for non-covalent protein-bioactive interactions. We presented multiple processes for producing dry, stable beads intended for the encapsulation of bioactives from concentrated WPI-sucrose dispersions in earlier experiments (Hansen et al., 2020, 2021c). This study focuses on alterations of the physico-chemical properties of the dispersions intended for bead formation as different bioactives are added to mixtures and subsequent interactions occur between matrix components. These findings might inform developers' decisions regarding the addition of even small amounts of natural extracts as colorants or sources of bioactives to protein-containing food matrices, as sensory properties could be jeopardized with changes in the physical properties of products.

5.2 Materials and Methods

5.2.1 Materials

IsoChill 9000 WPI was provided by Agropur, Inc. (Luxemburg, Wisconsin, USA), comprised of approximately 91.6% protein (dry basis), 4.6% water, 0.7% fat, and 3.1% ash. Extra fine, granulated, pure can sucrose was obtained from Domino Foods, Inc. (Yonkers, New York, USA). Pure gallotannin in crystalline solid form (≥ 98% purity) was purchased from Cayman Chemical Company (Ann Arbor, Michigan, USA). Standardized Aronia berry (chokeberry) powder comprised of 55.6% total PP and a minimum of 15% anthocyanins, and Standardized cranberry powder with a minimum of 15% proanthocyanidins were provided by Artemis International (Fort Wayne, Indiana, USA). Red beet extract containing 30.2% betanins and approximately 50% total betalains was provided by FutureCeuticals, Inc. (Momence,

Illinois, USA). Gallotannin and all extracts were stored in light-blocking, airtight packaging in the dark at -18˚C. Deionized (D.I.) water was used in all dispersion preparation.

5.2.2 Dispersion preparation

Similar to the dispersion preparation methods described in previous work (Hansen et al., 2021a, b, c), dry WPI or WPI-sucrose blends were first mixed into D.I. water, and aliquots of 50% gallotannin or extract solutions (gallotannin and extract powders mixed into D.I. water to obtain a 50% solids content in solution) were subsequently added (when appropriate) and mixed to form completed dispersions. As the different bioactives sources had varying bioactives contents, different quantities of extract solutions were required to reach the desired bioactives concentrations in final dispersions; in cases where more extract solution was required, the total quantities of WPI or WPI-sucrose blends added to mixtures were reduced (ratios remained the same) to maintain a constant % total solids in feeds. A FiveEasy Plus pH/mV meter with InLab ® Viscous Pro-ISM probe (Mettler Toledo, Hampton, Schwerzenbach, Switzerland) was calibrated at pH four and seven prior to pH measurements for dispersions.

Dispersions with eighteen different formulations were prepared three times each for randomized triplicate analysis in a factorial design with four sources of bioactives, three bioactives contents, and two WPI-sucrose ratios (**Table 5.1**). Total solids content (35%), extract/bioactive contents, and WPI-sucrose ratios (1:0 and 1:1) used were determined based on results from previous experiments (Hansen et al., 2020, 2021a, b, c). Dispersions formulated with 1:0 WPI:sucrose had virtually double the WPI concentrations and subsequent protein concentrations (ranging from 27-34% protein) compared to those formulated with 1:1 WPI:sucrose (ranging from 14-17% protein), given that all dispersions maintained 35% total

solids contents. Samples were analyzed after a minimum of one hour for defoaming at room temperature.

Table 5.1

WPI-sucrose ratio	Bioactives source	[bioactives]	pH	Density	Diameter (calculated)	Diameter (frozen)
-	-	%	-		mm	mm
1:0	n/a	0	6.33	1062 ± 9	4.51 ± 0.02	4.48 ± 0.11
1:1	n/a	0	6.22	1057 ± 11	4.54 ± 0.02*	4.36 ± 0.13*
1:0	Pure gallotannin	0.5	6.20	1055 ± 15	4.58 ± 0.08	4.52 ± 0.13
1:1	Pure gallotannin	0.5	6.15	1055 ± 6	4.65 ± 0.02*	4.45 ± 0.13*
1:0	Pure gallotannin	1	6.19	1062 ± 13	4.55 ± 0.10	4.47 ± 0.14
1:1	Pure gallotannin	1	6.00	1061 ± 13	4.67 ± 0.04*	4.53 ± 0.05*
1:0	Aronia extract	0.5	6.19	1030 ± 17	4.59 ± 0.04*	4.50 ± 0.14
1:1	Aronia extract	0.5	6.14	1052 ± 3	4.59 ± 0.01*	4.51 ± 0.06*
1:0	Aronia extract	1	6.05	1042 ± 17	4.60 ± 0.02*	4.43 ± 0.08*
1:1	Aronia extract	1	5.81	1033 ± 15	4.64 ± 0.02*	4.45 ± 0.07*
1:0	Beet extract	0.5	6.17	1023 ± 9	4.59 ± 0.03	4.52 ± 0.11
1:1	Beet extract	0.5	6.02	1038 ± 10	4.56 ± 0.03*	4.46 ± 0.07*
1:0	Beet extract	1	6.11	1019 ± 14	4.58 ± 0.04	4.53 ± 0.10
1:1	Beet extract	1	5.87	1038 ± 11	4.57 ± 0.02*	4.32 ± 0.09*
1:0	Cranberry extract	0.5	5.95	1044 ± 26	4.67 ± 0.06*	4.56 ± 0.10*
1:1	Cranberry extract	0.5	5.51	837 ± 179	4.96 ± 0.37*	4.42 ± 0.16*
1:0	Cranberry extract	1	5.49	n/a	n/a	n/a
1:1	Cranberry extract	1	4.96	580 ± 17	5.63 ± 0.07*	5.91 ± 0.19*

Density and estimated drop diameters from flow tests data and measured diameters (mm) of frozen drops formed from feed dispersions with varied WPI:sucrose, bioactives sources and concentrations, and pH.

5.2.3 Feed characterization:

5.2.3.1 Flow testing

As dispersions were pumped at a constant speed through a benchtop peristaltic pump (120 S/DV, Watson Marlow, Falmouth, England; silicon tubing 85 cm length, 2 mm bore, 1 mm

wall, BÜCHI Labortechnik AG, Flawil, Switzerland), the time needed to deposit 10 mL of dispersion, the mass of 10 mL of dispersion, individual drop masses, and the number of drops deposited per 1 min were measured in triplicate, as presented in previous experiments (Hansen et al., 2021a, b, c). Subsequently, feed densities, mass and volume flow rates, and drop surface tensions, diameters, and volumes were calculated from the flow data collected (Hansen et al., 2020, 2021a, b, c).

5.2.3.2 Particle size distribution

Particle size distributions were measured in triplicate with methods detailed in earlier studies (Hansen et al., 2021a, b, c) via Malvern Mastersizer 2000 (Malvern Instruments Ltd., Worcestershire, U.K.), adding dispersions dropwise into a Hydro 2000S liquid sampler.

5.2.3.4 Optical light microscopy

Diluted dispersions were observed as detailed in previous experiments (Hansen et al., 2021a, b, c), at 40 and 200x magnification, via Nikon Eclipse FN1 optical microscope (Nikon Instruments Inc., Melville, NY, USA) with Nikon Digital Sight DS-U3 camera control unit (ver. 1).

5.2.3.5 Viscosity

Small-strain oscillatory measurement methods detailed in previous experiments (Hansen et al., 2021a, b, c) were modified for triplicate complex viscosity measurements via DHR-2 rheometer (TA Instruments, Delaware, USA). Dispersions were oscillated under 0.2% strain at 1 Hz frequency once strain sweeps confirmed that 0.2% strain was within their linear viscoelastic region (LVR; not shown).

5.2.3.6 Centrifuge separation

As detailed in previous work (Hansen et al., 2021a, b, c), small portions (1.25 g) of seven times diluted dispersions and 1% solutions made from each source of bioactives were added to 1.5mL tubes (graduated with flat caps, Fisherbrand ®, Fisher Scientific, Hampton, New Hampshire, USA), centrifuged at 12,000 rpm (~13,523 x g) and 20˚C for 20 min (Centrifuge 5424 R with FA-45-24-11 rotor, Eppendorf, Hamburg, Germany), and subsequently observed.

5.2.4 Frozen drop preparation

As detailed in earlier studies (Hansen et al., 2021a, b, c), dispersions were deposited dropwise into pans filled with liquid nitrogen (LN_2) (100% purity; Airgas, Madison, Wisconsin, USA), held for ~5 min to harden, and diameters were measured immediately upon removal.

5.2.4.1 Frozen drop diameters

Digital Vernier calipers (0-150 mm; Stainless Hard) were used to measure the diameters of frozen beads as described in earlier experiments (n=9) (Hansen et al., 2021a, b).

5.2.5 Statistical analysis

Data from triplicate experiments, analyzed in triplicate (n=9), were used to calculate mean and standard deviation values. Mean values were compared by analysis of variance (2 and 3-way ANOVA; Tukey's HSD test) and independent measures t-tests (equal variance not assumed) performed with JMP ® Pro version 15.0.0 (SAS Institute Inc., Cary, North Carolina, USA) when appropriate, with the level of significance determined at $p < 0.05$.

5.3 Results and Discussion

5.3.1 Feed characterization:

5.3.1.1 pH

As solution pH affects protein structures, exposed groups available for intermolecular interactions, and consequent functionality, pH measurement was a critical analytical tool for comparing the effects of bioactives and extracts on the physico-chemical properties of dispersions with different formulations, as discussed in previous work (Hansen et al., 2021a, b, c). Dispersions containing higher protein contents (1:0 WPI:sucrose ratios) had slightly higher pH values than those with equal parts protein and sucrose (1:1 WPI:sucrose ratios) (**Table 5.1**), likely due to enhanced pH buffering effects in the system from the additional protein present (Hansen et al., 2021c). In agreement with the results from previous studies (Hansen et al., 2021a, b, c), pH was reduced when dispersions were formulated with increasing bioactives or extract contents. If pH is reduced so much that values reach the isoelectric point (pI) of proteins (major WPI protein fraction- β-lactoglobulin, pI ~ 5.2-5.3, minor WPI protein fraction-α-lactalbumin, pI ~ 4.2-4.8), protein-protein repulsion interactions are minimized, resulting in aggregation and precipitation that may impact physical properties of dispersions including particle size distribution and viscosity (Kilara and Harwalkar, 1996; Demetriades and McClements, 1998; Song, 2009; Coupland, 2014; Hansen et al., 2021a, b, c). In the case of pure gallotannin, Aronia berry extract, and beet extract, pH reductions with increasing bioactives concentrations were unlikely to elicit notable changes in the physical properties of dispersions, as pH values did not approach the pI of WPI proteins. Dispersions formulated with cranberry extract showed the most extensive pH reductions, although only one formulation approached the pI of WPI proteins (1:1 WPI:sucrose, 1% cranberry PP), with pH reaching the pI of β-lactoglobulin and being further

reduced. In this case, it is likely that the reduced protein content in the dispersions did not buffer pH as effectively as higher protein concentrations and may be responsible for some of the aggregation and precipitation observed for dispersions with that formulation, affecting particle size distributions and viscosities measured.

5.3.1.2 Surface tension and droplet size

The surface tension forces of a dispersion acting around the circumference of the outlet tubing must be exceeded by the force of gravity pulling on an emerging drop for it to detach, identifying the effect of surface tension on drop size (Hansen et al., 2021a, b, c), with some studies reporting direct relationships between surface tension and drop diameters (Chan et al., 2009; Lee and Chan, 2013). Of the eighteen different dispersion formulations studied, all but one were able to pump under the experimental conditions; dispersions with 1:0 WPI:sucrose and 1% cranberry extract PP were too viscous to pump and form individual droplets, likely due to extensive interactions occurring in the dispersions at pH values near protein pI. As such, flow data could not be obtained for those samples, and multiple separate statistical analyses were required to assess the data collected due to the loss in degrees of freedom from missing data preventing analysis of all data together. Additionally, because all dispersion formulations shared common '0% bioactives' data points, separate statistical analyses were required to qualify trends observed within formulations with the same bioactives source.

Figure 5.1A depicts the effects of bioactives content (%) on the surface tensions of dispersions, though effects of WPI:sucrose ratios may also be observed. Data plotted with solid connecting lines (1:1 WPI:sucrose) are often slightly higher than those plotted with dotted connecting lines (1:0 WPI:sucrose), indicating that dispersions containing less WPI and thus less total protein had slightly higher surface tensions than those with more protein. This was observed

for samples prepared with pure gallotannin, Aronia extract, and cranberry extract (0.5% PP), and the two-way ANOVAs and Student's t-tests used to analyze data confirmed that formulations with 1:0 WPI:sucrose ratios had significantly lower ($p < 0.05$) surface tensions than those with 1:1 WPI:sucrose. Dispersions formulated with beet extract did not have significant changes in surface tension with different WPI:sucrose ratios ($p > 0.05$), which can also be observed in **Fig. 5.1A** for data with triangle markers. While these results generally make sense, as increasing the protein content in dispersions would likely have greater surface tension-reducing effects (Kitabatake and Doi, 1988), the differences between the mean values for different WPI:sucrose ratios were very slight, indicative of little-to-no meaningful, overall effects on surface tension. Results reported are generally in agreement with the findings from previous experiments, and it is possible that the changes in WPI concentrations of dispersions with 35% total solids were not strong enough to drive notable changes in surface tension (Hansen et al., 2021a, b, c).

While some data plotted in **Figure 5.1A** show very slightly increasing surface tensions with increasing bioactives concentrations, an increasing trend is most clearly observed for dispersions formulated with 1:1 WPI:sucrose and cranberry extract (circle markers connected by solid lines). The surface tensions of feeds prepared with gallotannin had significantly ($p < 0.05$) higher surface tensions than feeds without bioactives (0%). Similarly, surface tensions also increased significantly ($p < 0.05$) with increasing Aronia PP concentrations in dispersions. Surface tensions of dispersions also increased significantly ($p < 0.05$) with increasing cranberry PP concentrations, seen clearly in **Fig. 5.1A** for data with circle markers. Dispersions containing 1% bioactives were reported to have significantly higher surface tensions ($p < 0.05$) than those with 0.5% bioactives, although in this case, the ANOVA was strongly influenced by the data for dispersions with 1:1 WPI:sucrose and cranberry extract, as that is the most clear example in **Fig.**

5.1A of a significant increase in surface tension with increasing bioactives concentrations. Interestingly, no significant changes in surface tensions of dispersions were observed with changing beet extract bioactives concentrations ($p > 0.05$), demonstrating the negligible effects of beet extract on the surface tension of dispersions. These findings are also in good agreement with those from earlier work, where dispersions containing WPI experienced increasing surface tensions with increasing Aronia PP concentrations under some conditions, with others exhibiting no meaningful trends (Hansen et al., 2021a, b, c).

Figure 5.1B displays the average surface tension values of all dispersions containing each respective bioactives source for comparison; cranberry extract was found to impact the surface tensions of dispersions most strongly, giving the highest average surface tension compared to other bioactives sources. The one-way ANOVA used to compare dispersions with 1:0 WPI:sucrose and 0.5% bioactives confirmed that bioactives source had a significant ($p < 0.05$) effect on surface tension. Tukey's HSD tests specified, showing that dispersions formulated with cranberry extract had significantly higher surface tensions than those formulated with Aronia and beet extracts ($p < 0.05$), but not pure gallotannin ($p > 0.05$). Surface tensions of dispersions with gallotannin were also not significantly different from those with Aronia and beet extracts ($p > 0.05$). Comparing dispersions with 1:1 WPI:sucrose and 0.5 and 1% bioactives reported that the surface tensions of dispersions with pure gallotannin and Aronia, beet, and cranberry extracts were all significantly different from one another ($p < 0.05$). Dispersions formulated with cranberry extract had the highest surface tensions, followed by pure gallotannin, Aronia extract, and then beet extract, mirroring the data in **Fig. 5.1B**.

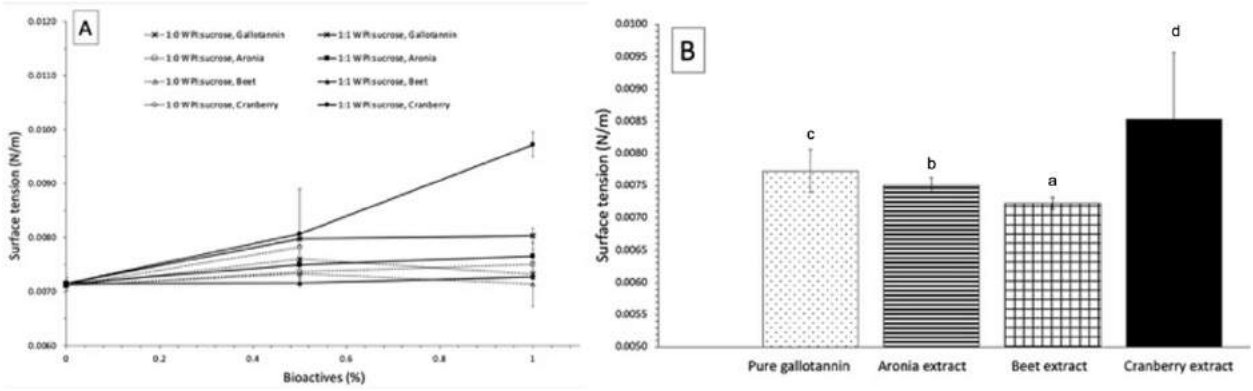


Figure 5.1. Effect of bioactives content (%) [**A**] on the surface tensions (N/m) of dispersions at 25˚C (n=9); the effect of bioactives source [**B**] on the average surface tensions of all dispersions formulated with pure gallotannin, Aronia berry, beet, and cranberry extracts, respectively, at 25˚C; (n = 12 for gallotannin, Aronia, and beet dispersions, n = 9 for cranberry dispersions). Lines are for guiding purposes only [**A**]. Values connected by the same letter are not significantly different ($p > 0.05$).

Figure 5.2 depicts the results of plotting calculated drop diameters against calculated surface tension values derived from flow tests data, and the best fit line applied indicates a strong, direct correlation ($R^2 = 0.89$). The one point with notably higher surface tension and a larger diameter represents the 1:1 WPI:sucrose, 1% cranberry extract PP dispersions, which retained more air than the other formulations after mixing due to its high viscosity stabilizing the foam, thus giving a lower density dispersion to pump and requiring larger drops to form before detaching (**Table 5.1**).

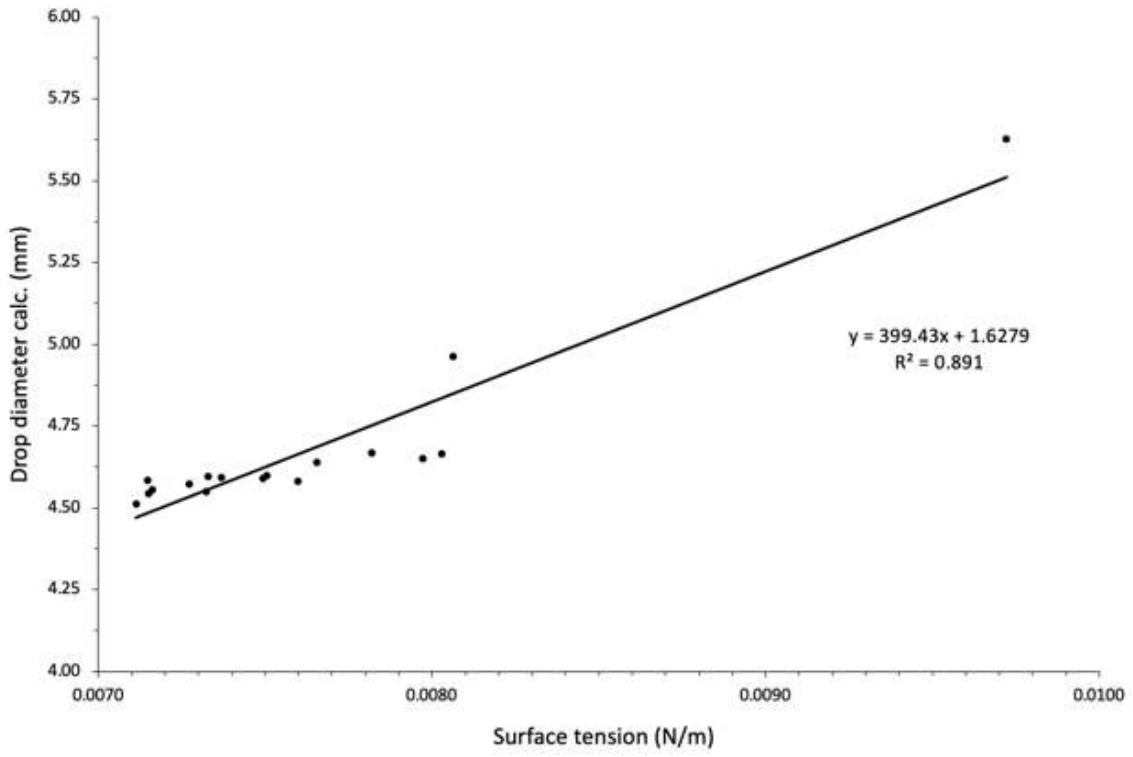


Figure 5.2. The relationship between the surface tensions (N/m) of feed dispersions containing WPI:sucrose ratios of 1:0 and 1:1, bioactives contents of 0, 0.5, and 1%, and bioactives sources including pure gallotannin and Aronia berry, beet, and cranberry extracts at 25˚C, and calculated diameters (mm) of drops.

5.3.1.3 Particle size distribution

Measuring the particle size distributions of dispersions with varying compositions is another way to evaluate the effects of formulation on the physico-chemical properties of dispersions, as compositional changes may induce conformational changes in proteins (Hansen et al., 2021a, b, c). Complex-forming interactions between matrix components (such as proteins and bioactives) may result, forming aggregates of varied sizes depending on the environmental conditions (Schneider, 2016; Hong et al., 2018b). While data trends were difficult to distinguish in **Figure 5.3A**, statistical analyses indicated that 1:0 WPI:sucrose dispersions had significantly larger ($p < 0.05$) volume-weighted mean ($d_{4,3}$) particle sizes than 1:1 WPI:sucrose dispersions

when Aronia, beet, and cranberry extracts were present. Overall differences in mean values were never more than a few microns, indicating that the changes were very slight. Interestingly, comparison of dispersions formulated with pure gallotannin found that 1:0 WPI:sucrose dispersions had significantly ($p < 0.05$) smaller average particle sizes than dispersions formulated with 1:1 WPI:sucrose ratios. These findings may potentially indicate excesses of protein in the systems for complexation, though optimization was not the focus of this experiment. As a whole, these results are in good agreement with the findings of previous experiments, where the changes in average particle sizes with changing protein:sugar ratios were either insignificant or very small, indicating that carbohydrates were unlikely to affect protein or protein-PP interactions and simply dissolved into solutions (Hansen et al., 2021a, b, c).

Most formulations in **Figure 5.3A** show no notable changes in particle size with changing bioactives concentrations. A minority of the formulations- dispersions containing cranberry extract (circle markers) and dispersions comprised of 1:1 WPI:sucrose with pure gallotannin (x markers connected by solid lines)- show increasing particle size trends to differing extents. The two-way ANOVAs and Tukey's HSD tests used to analyze dispersions with pure gallotannin and cranberry extract reported that the average particle sizes of dispersions steadily and significantly ($p < 0.05$) increased with increasing bioactives concentrations at each level of addition. In dispersions with Aronia extract, the only significant increase ($p < 0.05$) occurred between 0.5 and 1% PP concentrations, and the changes in mean sizes were notably smaller (only a few microns). Dispersions containing beet extract underwent no significant changes in particle size with changing bioactives concentrations ($p > 0.05$), in accordance with the results of Martínez et al. (2019), indicating no changes in aggregate sizes upon complexation of betalains with proteins. The three-way ANOVA used to compare all dispersions containing bioactives

indicated that particle size increased with increasing bioactives concentrations, despite most formulations (often those containing Aronia and beet extracts) not exhibiting the same extent of change. The increases in particle size data observed for the few formulations containing cranberry extract and 1:1 WPI:sucrose with pure gallotannin in **Fig. 5.3A** strongly influenced the ANOVA report to the point where it was not representative of the majority of dispersions examined. These results are in overall agreement with those from earlier works, where changes in average particle sizes of WPI dispersions with changing Aronia PP concentrations were typically slight (only a few microns difference), even when identified as 'significant' by ANOVA analyses (Hansen et al., 2021a, b, c). Results also align with the observations made when Giloy juice to was added to goat milk, resulting in slightly larger particle sizes in beverages (Sharma et al., 2021).

In **Figure 5.3B**, the average particle size values of all dispersions containing each respective bioactives source may be compared. The three-way ANOVA used to compare dispersions formulated with bioactives reported that bioactives sources had a significant ($p < 0.05$) effect on average particle sizes. Tukey's HSD tests clarified, indicating that dispersions formulated with beet extract had the smallest average particle sizes, followed by Aronia extract, then pure gallotannin, and dispersions with cranberry extract were found to have the largest average particle sizes by far compared to the others (**Fig. 5.3B**). Particle sizes of dispersions with Aronia and beet extracts were not found to be significantly different from one another ($p > 0.05$) but were found to be significantly different ($p < 0.05$) from both pure gallotannin and cranberry extract, which were both significantly different from one another ($p < 0.05$). These observations support our hypothesis, that larger polyphenolic compounds (like those in the cranberry extract) would result in greater responses in the functional properties of dispersions.

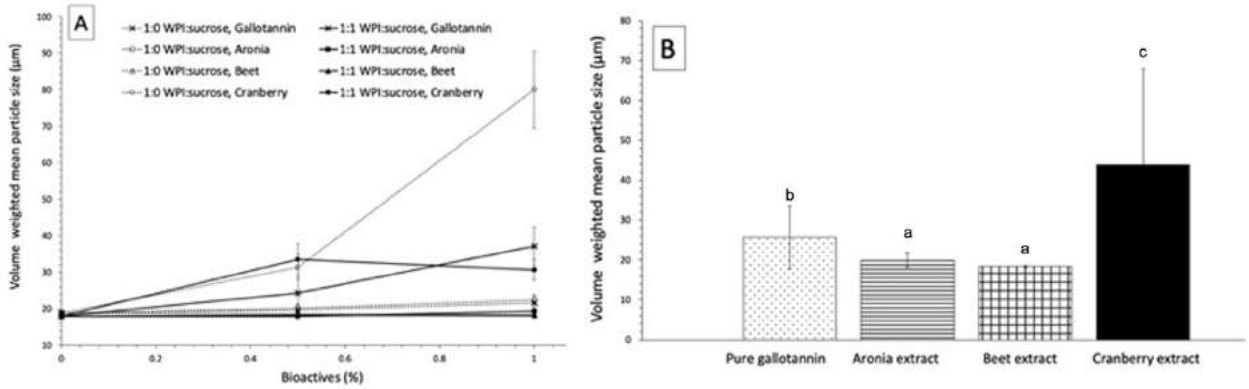


Figure 5.3. Effect of bioactives content (%) [**A**] on the average particle sizes (µm) of dispersions at 25˚C; the effect of bioactives source [**B**] on the average particle sizes (µm) of all dispersions comprised of pure gallotannin, Aronia berry, beet, and cranberry extracts, respectively, at 25˚C; (n = 9). Lines are for guiding purposes only [**A**]. Values connected by the same letter are not significantly different ($p > 0.05$).

WPI dispersions have resulted in normal particle size distributions when measured in previous experiments (Hansen et al., 2021a, b, c), with peaks representing unhydrated protein particles remaining in dispersions. Dispersions formulated with pure gallotannin and Aronia extract also exhibited relatively normal distributions (**Figure 5.4**), but with small tails at larger sizes. The major peaks likely continue to represent the unhydrated protein particles remaining in solution but present in slightly smaller volumes; the small tails formed likely include larger sized complexes formed between proteins and bioactives. Dispersions containing beet extract showed virtually no change in particle size distribution compared to WPI dispersions without bioactives, indicating that very little complexation interactions occurred in the system (**Fig. 5.4**). Dispersions containing cranberry extract, however, demonstrated very different particle size distributions compared to the other extracts. The distribution was very broad with a peak at larger sizes and a significant, broad shoulder to the left of the peak (likely representative of insoluble protein particles remaining). Dispersions formulated with cranberry extract exhibited the largest increases in surface tensions and particle sizes of all formulations, demonstrating the

extent of strong protein-PP complexation interactions occurring in the system and resulting in large aggregate formation.

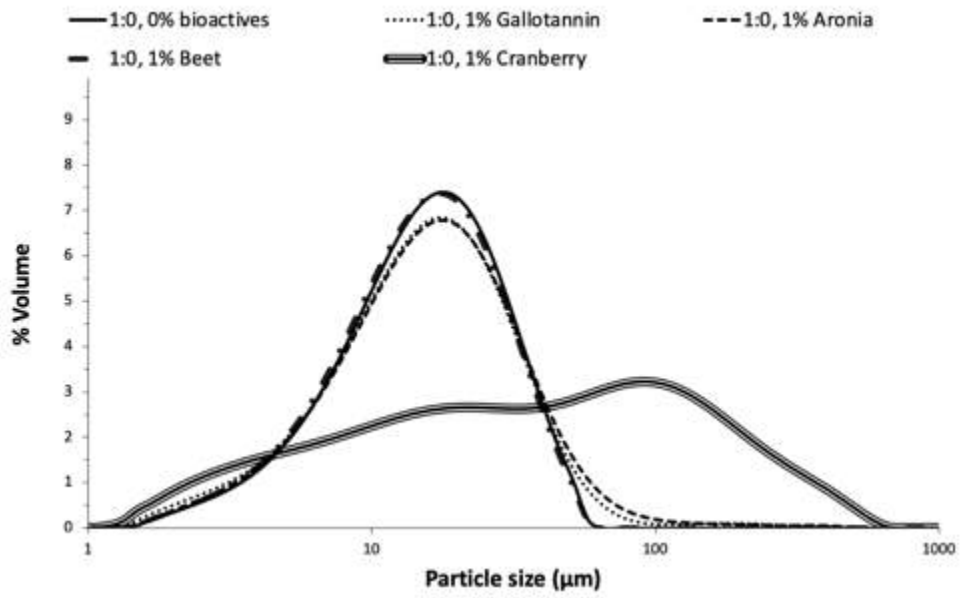


Figure 5.4. Particle size distributions of feed dispersions comprised of 1:0 WPI:sucrose ratios with 0% bioactives and 1% bioactives from pure gallotannin, Aronia berry, beet, and cranberry extracts at 25˚C; (n = 9).

Imaging the diluted dispersions with an optical microscope supported the trends observed with Mastersizer particle size measurements, as in previous work (Hansen et al., 2021a, b, c). The significant increases in particle sizes for dispersions formulated with cranberry extract are confirmed in **Figure 5.5**, and **Figure 5.6** supports the Mastersizer data indicating that the largest changes in particle size occurred in formulations containing cranberry extract.

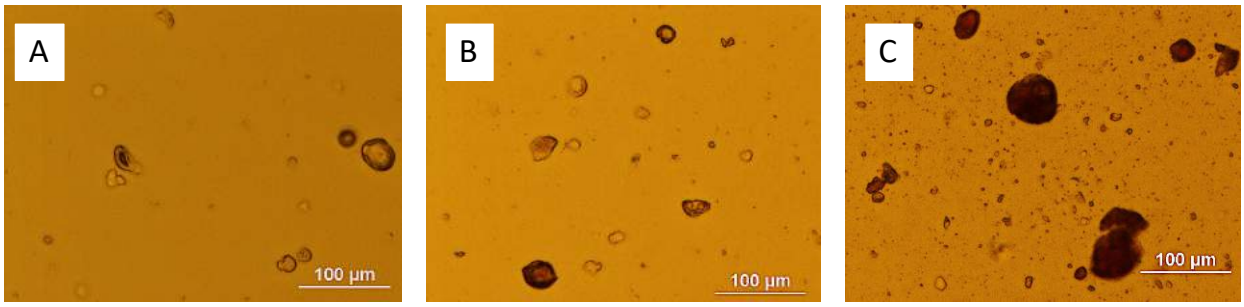


Figure 5.5. Optical light microscope images at 200x magnification depicting the microstructures of diluted feed dispersions with 1:0 WPI:sucrose with 0% bioactives (**A**), 0.5% bioactives (**B**), and 1% bioactives from cranberry extract (**C**).

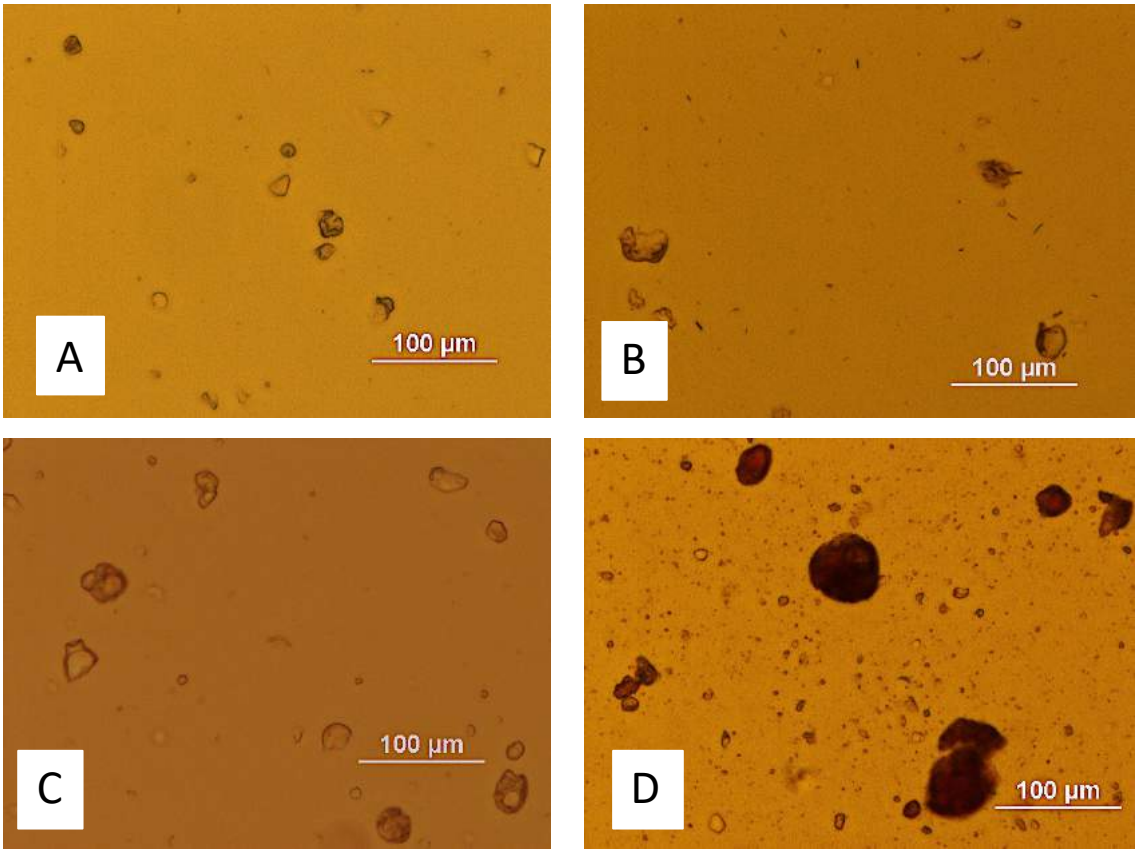


Figure 5.6. Optical light microscope images at 200x magnification depicting the microstructures of diluted feed dispersions with 1:0 WPI:sucrose with 1% bioactives from pure gallotannin (**A**), Aronia berry extract (**B**), beet extract (**C**), and cranberry extract (**D**).

5.3.1.4 Viscosity

Small changes in composition can influence the types and volumes of intermolecular interactions that may occur in a system, potentially altering the viscosity of a dispersion and other functional properties as well (Hansen et al., 2021a, b, c). In **Figure 5.7A**, viscosity data for dispersions formulated with pure gallotannin and Aronia and beet extracts connected with dotted lines (1:0 WPI:sucrose) were notably higher compared to those connected with solid lines (1:1 WPI:sucrose), indicating that feeds with higher WPI concentrations generally had higher viscosities. Dispersions deviated from this trend slightly when cranberry PP were present, showing that dispersions with 1:1 WPI:sucrose had higher viscosities, but only slightly at 1% PP. The two-way ANOVAs and student's t-tests used to analyze dispersions prepared with pure gallotannin, Aronia extract, and beet extract reported that 1:0 WPI:sucrose dispersions had significantly ($p < 0.05$) higher viscosities than those formulated with 1:1 WPI:sucrose, as seen in **Fig. 5.7A**. The two-way ANOVA and student's t-test used to compare feeds with cranberry extract reported that dispersions with 1:1 WPI:sucrose had significantly higher ($p < 0.05$) viscosities than those with 1:0 WPI:sucrose, as did the 3-way ANOVA and Student's t-test comparing all dispersions containing bioactives. In this case, the ANOVA report was strongly driven by the data for dispersions containing cranberry extract. When cranberry extract was added to dispersions, viscosities increased notably compared to other formulations, but most extremely in the case of 1:1 WPI:sucrose dispersions. It is possible that the extreme jump in viscosities of 1:1 WPI:sucrose dispersions with the addition of cranberry could be attributed in part to the reduced pH of feeds to the point of pI precipitation of aggregates that would increase viscosity in the system, as protein-PP interactions are more abundant near pI, and less protein is present for pH buffering in the systems. Another possibility is that a synergistic relationship may

occur between WPI and cranberry PP at those specific levels of use, thus enhancing complexation interactions present. These findings generally make sense, as previous work has reported that higher protein contents in dispersions resulted in higher viscosities under some conditions (Hansen et al., 2020), though no meaningful trends were observed in many cases (Hansen et al., 2021a, b, c), likely due to an overall weak effect or total solids contents that were too low for detectable shifts.

The only statistically significant ($p < 0.05$) increases in viscosities of dispersions containing gallotannin, Aronia, and cranberry extracts occurred when bioactives concentrations increased from 0.5 to 1%. Interestingly, the complex viscosities of feeds formulated with beet extract were reported to decrease significantly between each level of increasing bioactives concentrations ($p < 0.05$). Changes in viscosities were only clearly observed for dispersions containing cranberry, while changes in feeds with pure gallotannin, Aronia, and beet extracts appeared too slight to be impactful (**Fig. 5.7A)**. Overall, these findings are similar to those reported in previous studies, where increasing Aronia PP contents in dispersions resulted in slight increases in viscosities under some conditions (Hansen et al., 2021a, b, c), but not all conditions resulted in meaningful trends; similarly, results reported by Sharma et al. (2021) indicated that the addition of Giloy juice (a natural source of polyphenols) to goats milk beverages resulted in increased system viscosities, confirming protein-polyphenol interactions with microscopy.

In **Figure 5.7B**, the average complex viscosity values of dispersions containing each respective bioactives source at 0.5 and 1% are plotted for comparison at 1:0 and 1:1 WPI:sucrose ratios. Dispersions containing cranberry extract underwent the largest changes in viscosity and had notably higher viscosities compared to dispersions containing the other bioactives sources,

which appeared to have similar average viscosities. The three-way ANOVA and corresponding Tukey's HSD test used to analyze dispersions containing bioactives reported that the only bioactives source to significantly increase ($p < 0.05$) the viscosities of dispersions was cranberry extract, while the viscosities of feeds with pure gallotannin, Aronia extract, and beet extract were not significantly different from one another ($p > 0.05$), as seen in **Fig. 5.7B**. These findings generally agree with the findings of Girard et al. (2019), where it was found that the viscosities of pastry flour batters containing proteins were relatively unchanged with the addition of monomeric polyphenols (catechins), increased slightly when hydrolyzed tannins (tannic acids) were added, and significantly increased with the addition of condensed tannins (proanthocyanidins). Dispersions formulated with cranberry extract were prepared with slightly less total WPI and sucrose solids due to the need for higher levels of extract addition to reach desired bioactives concentrations and maintain a constant % total solids. Findings from previous experiments indicated that changes in WPI concentrations in dispersions with similar total solids contents were slight, insinuating that the viscosities of dispersions containing cranberry extract (and thus less WPI solids) may exhibit only minor, if not undetectable, reductions (Hansen et al., 2020). In contrast, dispersions formulated with cranberry extract experienced large increases in the viscosities of their continuous phases likely due to enhanced protein-PP complexation interactions in the system forming larger aggregates when protein pI was approached. Additional complex carbohydrates and oligosaccharides (~60% of the cranberry extract studied) present in the systems at higher cranberry PP concentrations may be a minor contributor to the increased viscosities observed as well (Coleman and Ferreira, 2020). It is likely that the viscosity became so high that the air naturally incorporated into dispersions by the mixing process was stabilized by the continuous phase and large aggregates present, rather than defoaming over time like other

dispersions, thus forming something resembling a stabilized foam with significantly lower densities than other dispersions (**Table 5.1**), which would have significantly different viscous properties.

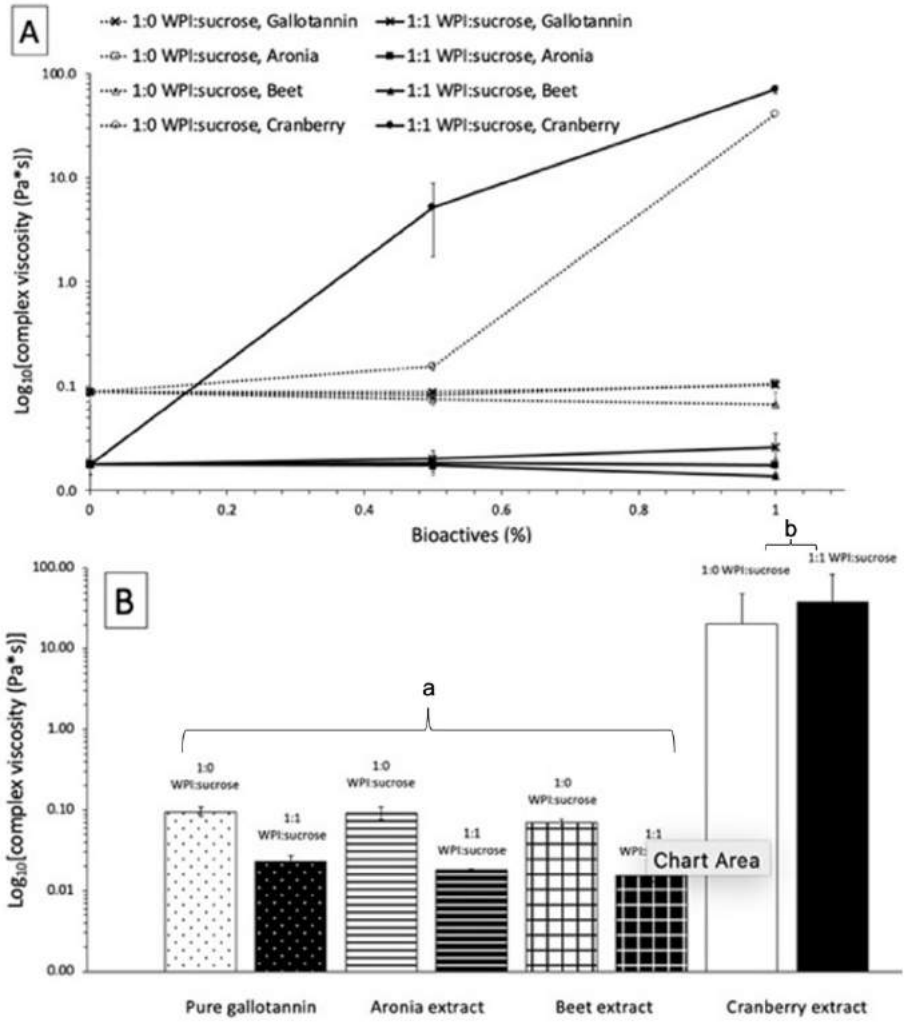


Figure 5.7. Effect of bioactives content (%) [**A**] on the complex viscosities (Pa*s) of dispersions at 25˚C; the effect of bioactives source [**B**] on the averaged complex viscosities of dispersions comprised of 1:0 and 1:1 WPI:sucrose with pure gallotannin, Aronia berry, beet, and cranberry extracts at 0.5 and 1% at 25˚C; (n = 9). Lines are for guiding purposes only [**A**]. Values connected by the same letter are not significantly different ($p > 0.05$).

5.3.1.5 Centrifuge separation

Evaluating dispersions for the formation of colored precipitates and monitoring the relative size of pellets formed after centrifugation can be used as a crude method of identifying the presence of protein-bioactive complexation interactions and aggregate formation (Van Teeling et al., 1971; Hansen et al., 2021a, b, c). Without bioactives present in dispersions, precipitates were white in color and very small, and supernatant was off-white and transparent,

as observed in earlier work (Hansen et al., 2021a, b, c); dispersions with pure gallotannin had similar appearances but slightly larger pellets (**Figure 5.8A**). Dispersions containing Aronia extract also had the same appearances as described in previous work (Hansen et al., 2021a, b, c), with deep purple-colored pellets and clear, purple supernatants. Dispersions with cranberry extract had similar appearances, but with slightly larger pellets (**Figure 5.8**); those containing beet extract had pink pellets and deep red, transparent supernatants. Although not pictured, 1:0 WPI:sucrose dispersions generally had larger pellets than 1:1 WPI:sucrose dispersions, likely due to the larger quantity of protein present available for precipitation.

The sizes of pellets formed from centrifuged dispersions generally increased with increasing bioactives concentrations from all sources (**Figure 5.8**). These findings are in agreement with those from earlier studies using Aronia extract (Hansen et al., 2021a, b, c), but to validate that the growing pellet sizes could be attributed to greater quantities of protein-bioactives complexes in dispersions, 1% bioactives solutions were prepared and centrifuged to determine the amount of precipitate formed at that level of addition (images not shown). No precipitate formed after centrifuging a 1% gallotannin dispersion, indicative of complete dissolution in D.I. water, and very small, nearly negligible precipitates formed after centrifuging 1% bioactives solutions with Aronia and beet extracts. Slightly larger pellets formed from centrifuging 1% cranberry extract PP solutions, though this was expected since more extract was required in the solution to reach the desired 1% bioactives concentrations. This assessment yielded similar findings to previous work (Hansen et al., 2021b), where the minimal precipitation observed after centrifugation of 1% extract solutions supported claims that the slightly increasing pellet sizes with increasing bioactives concentrations was attributed to increased complex formation. Of the precipitates formed by dispersions of varying composition, those containing

gallotannin were typically smallest, likely because the smallest quantity of extract was required to reach the desired bioactives concentrations. Pellets formed from dispersions formulated with beet extract were also small, which may suggest minimal WPI-bioactives complexation interactions in the system, as indicated by the other analyses in this study. Dispersions made with Aronia extract had slightly larger pellets, and the largest precipitates were formed from dispersions containing cranberry extract, further indicating more extensive protein-PP interactions in the system (**Figures 5.8, 5.9**).

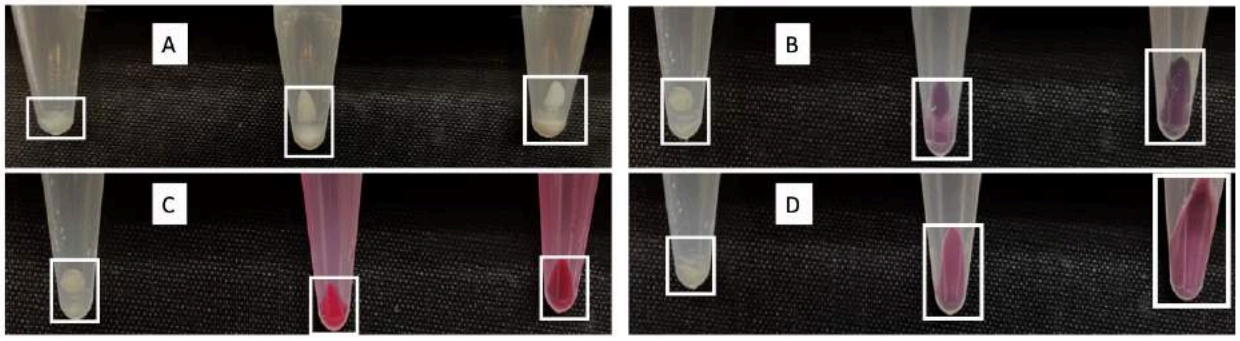


Figure 5.8. Image depicting the precipitated fractions (highlighted in boxes) of 7 times diluted, centrifuged dispersions with 1:0 WPI:sucrose and 0% (Left), 0.5% (Center), and 1% bioactives (Right) from pure gallotannin [A], Aronia berry extract [B], beet extract [C], and cranberry extract [D].

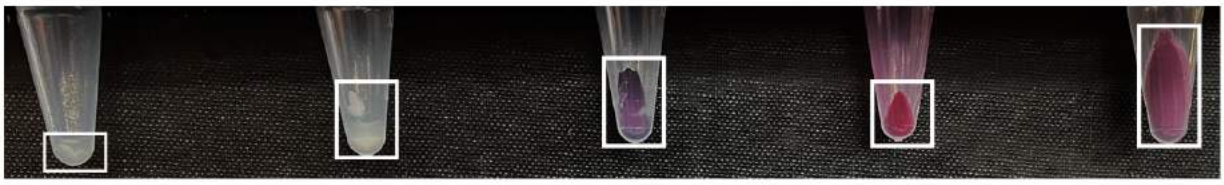


Figure 5.9. Image depicting the precipitated fractions (highlighted in boxes) of 7 times diluted, centrifuged dispersions with 1:0 WPI:sucrose and 0% bioactives (Left) and 1% bioactives from pure gallotannin (Center, Left), Aronia berry extract (Center), beet extract (Center, Right), and cranberry extract (Left).

5.3.2 Frozen drop characterization:

5.3.2.1 Comparison of diameters

Similar to the findings from earlier work (Hansen et al., 2021c), ten of the seventeen dispersion formulations that were able to undergo flow testing were found to produce frozen beads that had significantly ($p < 0.05$) smaller measured diameters than predicted with calculations (**Table 5.1**); this was most likely due to the inadequacy of the correction factor used in calculations of drop diameters to consider the amount of liquid lost upon entering the LN_2 bath when small volumes of feeds detach from the main drop upon impact. Only one dispersion formulation produced drops with diameters that were significantly ($p < 0.05$) larger than calculated estimates (1:1 WPI:sucrose, 1% cranberry extract PP). This phenomenon can be attributed to the notably lower density compared to most of the other dispersions due to the entrapped air that could not defoam due to the highly viscous continuous phase of the matrix (**Table 5.1**), thus requiring the drop to grow larger before gravity caused it to detach from the tubing tip. These results give an overall 'success rate' of 35% for calculations accurately predicting drop diameters, occurring for six of the seventeen dispersion formulations pumped. The one- and two-way ANOVAs and associated Student's t- and Tukey's HSD tests used to compare dispersions reported little-to-no meaningful effects from WPI:sucrose ratios, bioactives concentrations, or bioactives sources on the diameters of drops formed by dispersions. The only exception to these findings was from the Tukey's HSD test used to separately evaluate the effects of bioactives concentrations on drop diameters for dispersions containing 1:1 WPI:sucrose and cranberry extract, where the increase in drop diameters between 0.5 and 1% cranberry extract PP was considered significant. As already noted, this specific case can likely be attributed to enhanced viscosities and air-holding in the dispersions.

5.4 Conclusions

In these experiments, we aimed to continue our investigation into the effects of bioactives on the physical properties of dispersions containing different WPI:sucrose ratios. Mixing with Aronia berry extract elicited measurable alterations in the viscosities, surface tensions, and particle sizes of dispersions in earlier studies, with changes being attributed to non-covalent protein-PP complexation interactions (Hansen et al., 2021a, b). To build from these findings, we identified a variety of bioactives sources that possessed diverse structures and sizes for comparison with Aronia extract, including pure gallotannin, beet extract, and cranberry extract. We hypothesized that bioactives/extracts with larger molecular sizes and more hydroxyl groups and hydrophobic regions would be likely to interact more extensively with WPI, which may result in greater measurable changes in physico-chemical properties of dispersions. We observed the largest shifts in the surface tensions, viscosities, and particle size distributions for dispersions formulated with cranberry extract, with the predominant bioactive compound present being proanthocyanidins, condensed tannins that are known to have a high propensity for protein-PP complexation interactions. Dispersions formulated with beet extract, with the predominant bioactive compound present being betanins, exhibited the least extent of changes in physical properties. This work expands on earlier reports, providing more information on the physical effects of adding different bioactive compounds to concentrated WPI dispersions, and continuing the investigation into the potential for non-covalent protein-bioactive interactions in these feed systems that are ultimately intended for dry bead formation as potential bioactives delivery vehicles (Hansen et al., 2020, 2021c). These findings may inform the formulation and processing stages in the development of functional and nutritional products with high protein contents and natural extracts used as colorants or sources of bioactives, as significant changes in the physical

properties due to the addition of relatively low levels of some types of bioactives may compromise desired sensory attributes.

Funding

Funding for this study was provided by the Lauritzson Foundation via the Lauritzson Research Scholarship, through the College of Science, Engineering and Food Science (SEFS) at University College Cork.

Chapter 6



Journal of Food Engineering 317 (2022) 110847

Contents lists available at ScienceDirect

Journal of Food Engineering

journal homepage: www.elsevier.com/locate/jfoodeng

Formation of dry beads for bioactives encapsulation by freeze granulation

Mackenzie M. Hansen [a,b,*], Richard W. Hartel [b], Yrjö H. Roos [a]

[a] Food Technology, School of Food and Nutritional Sciences, University College Cork, Ireland
[b] Department of Food Science, College of Agricultural and Life Sciences, University of Wisconsin-Madison, USA

ARTICLE INFO

Keywords:
Freeze granulation
Beads
Whey protein
Sugars
Encapsulation

ABSTRACT

Solid beads formed by whey protein isolate (WPI) and various sugars/polyols with a wide range of glass transition temperatures showed potential as structures for encapsulation of Aronia berry bioactives. Whey protein isolate (WPI), Aronia extract, and carbohydrates (maltitol, sucrose, or trehalose) were mixed into water to form concentrated liquid feed dispersions with varied pH. Microstructures were imaged and physical properties including complex viscosities, surface tensions, particle size distributions, and centrifuge separation were measured to investigate the effects of carbohydrate type, WPI:sugar ratio, and Aronia polyphenols (PP) concentration on liquid properties. Feed dispersions were used to produce dry beads with an adapted freeze granulation method, where individual drops were pumped into liquid nitrogen for flash freezing and harvested for subsequent freeze-drying to remove water. Dry bead diameters, water contents, and water activities were measured prior to measuring hardness and glass transition temperatures. While formulating with different sugars did not meaningfully impact liquid feed characteristics that impact processing, compositional differences were found to influence characteristics of the final dried beads more notably.

Formation of dry beads for bioactives encapsulation by freeze granulation

Mackenzie M. Hansen[a,b*], Richard W. Hartel[b], Yrjö H. Roos[a]

[a] Food Technology, School of Food and Nutritional Sciences, University College Cork, Ireland

[b] Department of Food Science, College of Agricultural and Life Sciences, University of Wisconsin-Madison

Published as: Hansen, M. M., Hartel, R.W., and Roos, Y. H. (2022). Formation of dry beads for bioactives encapsulation by freeze granulation. *Journal of Food Engineering*, *317*, 110847.

Abstract

Solid beads formed by whey protein isolate (WPI) and various sugars/polyols with a wide range of glass transition temperatures showed potential as structures for encapsulation of Aronia berry bioactives. Whey protein isolate (WPI), Aronia extract, and carbohydrates (maltitol, sucrose, or trehalose) were mixed into water to form concentrated liquid feed dispersions with varied pH. Microstructures were imaged and physical properties including complex viscosities, surface tensions, particle size distributions, and centrifuge separation were measured to investigate the effects of carbohydrate type, WPI:sugar ratio, and Aronia polyphenols (PP) concentration on liquid properties. Feed dispersions were used to produce dry beads with an adapted freeze granulation method, where individual drops were pumped into liquid nitrogen for flash freezing and harvested for subsequent freeze-drying to remove water. Dry bead diameters, water contents, and water activities were measured prior to measuring hardness and glass transition temperatures. While formulating with different carbohydrates did not meaningfully impact liquid feed characteristics that impact processing, compositional differences were found to influence characteristics of the final dried beads more notably.

6.1 Introduction

Proteins and sugars are popular macromolecules often used in combination when developing food products. Both components possess desirable functional properties and impart nutritional value onto formulated products. Their respective functional properties may be utilized to form structures that encapsulate and protect sensitive natural bioactives for delivery, such as polyphenols (PP) derived from fruits and vegetables, addressing the increased consumer demand for health foods (Hansen et al., 2021a, b; Schneider, 2016). Correspondingly, consumer attitudes towards sugar have shifted as their role in dental health and chronic disease has come into question, creating demand for 'better for you' food products formulated with lower calorie sweeteners or even sugar-free formulations. Polyols such as sorbitol, xylitol, and maltitol are alternatives used by industry to replace sugars, providing benefits including a lack of insulin response, caloric reduction, and non-cariogenic properties (Hartel et al., 2018; Rice et al., 2020).

Formulating with different sugars/polyols can result in products with a wide variety of characteristics such as texture, appearance, and flavor retention, depending on differences in carbohydrate properties such as their glass transition temperatures (T_g) under selected conditions. Glass transition (T_g) occurs when the molecular mobility within an amorphous material is slowed so significantly that the matter changes from a more flexible, rubbery state to a hard, glassy state. In general, stability of glasses is enhanced greatly when T_g is higher than ambient temperature (Hartel et al., 2018; Kawai & Suzuki, 2007; Roos & Drusch, 2015; White & Cakebread, 1966), where diffusion-based modes of deterioration may be slowed, and degradation mechanisms may be better controlled (Ergun et al., 2010; Roos, 2020). Stability of glassy products is related to T_g, which is determined by formulation components as well as water content (Ergun et al., 2010). Products formulated with components with higher T_g would be expected to have greater storage

stability under ambient conditions than products formulated with lower T_g components, potentially serving as better protectants for bioactives during storage (Roos, 2010).

In earlier experiments, we developed a continuous process that formed dry, stable beads from concentrated mixed dispersions of whey protein isolate (WPI) and sucrose (Hansen et al., 2020). The structure forming method presented initially involved the exposure of feed dispersions to moderate heat conditions (100˚C) for a short time by dispensing feeds dropwise into a heated oil bath to promote solid structure formation via gelation. We adapted the original drop formation process to no longer require heating, protein gelation, or oven drying to form dry, stable beads. Instead, we utilized the same method for pumping concentrated liquid dispersions dropwise into a bath of liquid nitrogen (LN_2) to instantly solidify beads that were subsequently transferred to a freeze- dryer to remove water. This method resembles the freeze granulation technology employed in clay/ceramic materials and pharmaceuticals, where droplets of liquid suspensions are sprayed into LN_2 and then freeze-dried (Bhatta et al., 2020; La Lumia et al., 2019; Ouadaker et al., 2020; Shanmugam, 2015).

Protein-sugar mixtures can be used for encapsulation, and the properties of structures formed can be manipulated with compositional alterations. The potential for freeze granulation processes to produce protein-sugar structures that may be used for encapsulation, however, has not yet been investigated. Therefore, the aim of this experiment was to explore the effects of sugar/polyol type (with a wide range of known T_g) and WPI-sugar ratios on the physical properties of liquid dispersions and resulting dry beads formed by a modified freeze granulation process, both with and without Aronia extract. We hypothesize that replacement of sucrose with other glass formers (maltitol and trehalose) is unlikely to give rise to significant changes in the physical properties of liquid dispersions that affect processing and pumping such as viscosity,

flow behavior, or particle size distributions, as the sugars are all similar in molecular size and sugars are not particularly surface-active molecules (Hartel et al., 2018). Properties of the dry beads formed by the modified drop formation method presented, such as T_g onset and hardness, would be expected to change with the use of different sugars, as related to their respective T_g and water contents (Roos & Drusch, 2015). It would be expected that beads formulated with sugars/polyols with higher T_g in higher quantities would have higher bead T_g and corresponding hardness values than those formulated with lower T_g carbohydrates, demonstrating their greater physical stability and potential protective abilities imparted on the Aronia PP by the molecular freezing and glass formation by sugars (Sosa et al., 2011).

This work builds on previous experiments characterizing the physicochemical effects of Aronia extract in liquid dispersions (Hansen et al., 2021a) and the consequences of varying protein sources on protein-PP interactions (Hansen et al., 2021b), expanding the investigation to characterize the effects on the physical properties of dry beads formed from the liquid mixtures. We examined the effects of sugar/polyol type and WPI-sugar ratio on the physical properties of beads formed, which may indicate the potential of the matrices to protect PP during storage. To our knowledge, the method of freeze granulation employed has not yet been attempted in food matrix applications which makes this a novel study. We present a successful adaptation of this technology, utilized in other materials science and pharmaceutical applications, applied to food materials to form structures.

6.2 Materials and Methods

6.2.1 Materials

WPI (IsoChill 9000), was supplied by Agropur, Inc. (Luxemburg, Wisconsin, USA) with approximately 4.6% water, 91.6% protein (dry basis), 0.7% fat, and 3.1% ash. Sucrose (pure

cane, extra fine, granulated sugar) was supplied by Domino Foods, Inc. (Yonkers, New York, USA). Maltitol (Maltisweet ® CM9820 Crystalline Maltitol 263051) was supplied by Ingredion (Westchester, IL, USA). Trehalose (Treha TM) was supplied by Hayashibara Co., LTD. (NAGASE Group, Okayama, Japan). Standardized Aronia berry (Chokeberry) Powder, with a minimum level of 15% anthocyanins, was supplied by Artemis International (Fort Wayne, Indiana, USA) and stored at -18°C in the absence of light. Deionized (D.I.) water was used in all formulations.

6.2.2 Dispersion preparation

Dispersion preparation was performed as described in previous studies (Hansen et al., 2021a, b). Dry blends of WPI and sugars/polyols were mixed into D.I. water, followed by the addition of Aronia extract solution (when appropriate) to constitute final mixtures. pH was measured with a FiveEasy Plus pH/mV meter with InLab® Viscous Pro-ISM probe (Mettler Toledo, Hampton, Schwerzenbach, Switzerland) after electrode calibration.

Triplicates of twenty-four formulations with different compositions were prepared for triplicate analysis in a 4x3x2 factorial design, with experiments conducted randomly (**Table 6.1**). Ratios of WPI to sugar, Aronia extract/ PP concentrations, and % total solids were selected based on findings from our previous work (Hansen et al., 2020, 2021a, b). After preparation, dispersions were left to defoam at room temperature for one hour minimum prior to analyses.

Table 6.1.

WPI:sugar	Sugar	[PP]	pH	Water activity	Water content	Diameter (calculated)	Diameter (dry)	Tg (midpoint)
-	-	%	-	-	%	mm	mm	˚C
0	Maltitol	0	5.80	n/a	n/a	5.01 ± 0.02	n/a	n/a
0.75	Maltitol	0	5.91	0.037 ± 0.017	1.13 ± 0.17	4.62 ± 0.06	4.13 ± 0.06*	41 ± 3
1	Maltitol	0	5.93	0.036 ± 0.008	1.26 ± 0.22	4.62 ± 0.05	4.17 ± 0.11*	44 ± 3
1.25	Maltitol	0	5.88	0.027 ± 0.001	0.93 ± 0.29	4.62 ± 0.03	4.10 ± 0.08*	46 ± 4
0	Maltitol	1	3.48	n/a	n/a	4.96 ± 0.04	n/a	n/a
0.75	Maltitol	1	5.40	0.036 ± 0.010	1.02 ± 0.17	4.69 ± 0.02	4.20 ± 0.09*	42 ± 2
1	Maltitol	1	5.35	0.029 ± 0.004	1.50 ± 0.20	4.61 ± 0.06	4.22 ± 0.08*	50 ± 4
1.25	Maltitol	1	5.55	0.027 ± 0.001	1.38 ± 0.25	4.68 ± 0.04	4.19 ± 0.12*	50 ± 4
0	Sucrose	0	6.02	0.135 ± 0.015	2.68 ± 0.41	5.02 ± 0.03	4.36 ± 0.13*	48 ± 2
0.75	Sucrose	0	5.88	0.027 ± 0.001	1.17 ± 0.25	4.64 ± 0.04	4.11 ± 0.07*	57 ± 4
1	Sucrose	0	5.87	0.027 ± 0.001	1.01 ± 0.12	4.62 ± 0.05	4.11 ± 0.09*	62 ± 3
1.25	Sucrose	0	5.85	0.027 ± 0.001	0.98 ± 0.34	4.63 ± 0.05	4.09 ± 0.09*	61 ± 2
0	Sucrose	1	3.54	0.146 ± 0.037	1.37 ± 0.42	4.97 ± 0.05	4.39 ± 0.06*	47 ± 2
0.75	Sucrose	1	5.43	0.027 ± 0.001	1.27 ± 0.30	4.68 ± 0.04	4.14 ± 0.16*	60 ± 2
1	Sucrose	1	5.44	0.029 ± 0.003	0.99 ± 0.24	4.69 ± 0.03	4.16 ± 0.14*	58 ± 2
1.25	Sucrose	1	5.45	0.030 ± 0.004	1.16 ± 0.27	4.65 ± 0.05	4.16 ± 0.10*	61 ± 2
0	Trehalose	0	6.50	0.046 ± 0.009	2.47 ± 0.60	5.01 ± 0.03	4.33 ± 0.17*	78 ± 2
0.75	Trehalose	0	5.85	0.027 ± 0.001	0.80 ± 0.20	4.61 ± 0.05	4.13 ± 0.07*	125 ± 8
1	Trehalose	0	5.85	0.027 ± 0.001	0.50 ± 0.15	4.60 ± 0.04	4.13 ± 0.07*	127 ± 3
1.25	Trehalose	0	5.89	0.027 ± 0.001	1.12 ± 0.30	4.61 ± 0.03	4.06 ± 0.15*	133 ± 4
0	Trehalose	1	3.37	0.030 ± 0.004	1.03 ± 0.37	4.95 ± 0.04	4.25 ± 0.06*	79 ± 7
0.75	Trehalose	1	5.48	0.028 ± 0.001	0.82 ± 0.28	4.67 ± 0.04	4.15 ± 0.10*	125 ± 2
1	Trehalose	1	5.53	0.029 ± 0.003	0.99 ± 0.45	4.66 ± 0.03	4.18± 0.12*	131 ± 4
1.25	Trehalose	1	5.36	0.028 ± 0.001	0.73 ± 0.27	4.62 ± 0.07	4.13 ± 0.10*	126 ± 5

* indicates significant differences between calculated and measured diameter values

Formulations, pH, and estimated drop diameters (mm) calculated from flow tests data for liquid dispersions with varied WPI:sugar ratios, sugar types, and polyphenols concentrations, as well as water activity (a_w), water content (%), T_g midpoint, and measured diameters of dried drops formed from dispersions.

6.2.3 Feed characterization:

6.2.3.1 Flow testing

Flow testing was performed in triplicate as described in previous studies (Hansen et al., 2020, 2021a, b), by pumping dispersions through a benchtop peristaltic pump (120 S/DV, Watson Marlow, Falmouth, England; silicon tubing 85 cm length, 2 mm bore, 1 mm wall, BÜCHI Labortechnik AG, Flawil, Switzerland) at a constant speed of 13 RPM. Measurements

obtained included individual drop masses, the number of drops deposited per 1 min, the time required to deposit 10 mL of dispersions, and the mass of 10 mL of dispersions; these data were used to calculate drop diameters, volumes, and surface tensions, as well as densities of dispersions and mass and volume flow rates (Hansen et al., 2020, 2021a, b).

6.2.3.2 Viscosity

Methods described in previous studies (Hansen et al., 2021a, b) were adapted to measure the complex viscosities of dispersions in triplicate with a DHR-2 rheometer (TA Instruments, Delaware, USA) using small-strain oscillatory measurements. Samples were oscillated under 4% strain and 1Hz frequency; strain sweeps determined that 4% strain was within their linear viscoelastic region (LVR; not shown).

6.2.3.3 Particle size distribution

A Malvern Mastersizer 2000 (Malvern Instruments Ltd., Worcestershire, U.K.) with Hydro 2000S liquid sampler was utilized for triplicate particle size distribution measurements of dispersions, as described in previous work (Hansen et al., 2021a, b). Dispersions formulated without WPI were unable to reach the desired obscuration range (11-15%), as the program was designed with WPI particles in mind. As such, those transparent dispersions were unable to be measured as the sugars dissolved in the water and did not yield detectable particles. Dispersions formulated without WPI but with Aronia extract showed particle size distributions that were different from feeds containing protein, despite the program design intended for WPI particle detection; as such, volume-weighted mean ($d_{4,3}$) values were not taken from these distributions for comparison as the program was not designed for particle detection of Aronia extracts.

6.2.3.4 Optical Light Microscopy

A Nikon Eclipse FN1 optical microscope (Nikon Instruments Inc., Melville, NY, USA) with a Nikon Digital Sight DS-U3 camera control unit attached (ver. 1) was used to observe diluted dispersions at 40x and 200x magnification, as described in previous studies (Hansen et al., 2021a, b).

6.2.3.5 Centrifuge separation

Similar to the centrifugation methods described in previous experiments (Hansen et al., 2021a, b), 1.25 g of selected undiluted and 10-times diluted dispersions were pipetted into tubes (1.5mL graduated tubes with flat caps, Fisherbrand ®, Fisher Scientific, Hampton, New Hampshire, USA), spun at 13,523 x g and 20˚C for 20 min in a microcentrifuge (Centrifuge 5424 R with FA-45-24-11 rotor, Eppendorf, Hamburg, Germany), and observed after centrifugation.

6.2.4 Solid drop preparation- freeze granulation process adaptation

As the first step in solid bead formation, feeds were dropped into liquid nitrogen (100% purity; Airgas, Madison, WI, USA) and frozen, as explained in earlier experiments (Hansen et al., 2021a, b). Drops were left to harden in the LN_2 for ~5 min, and pans were transferred to a VirTis SP Scientific Genesis 25 EL Pilot freeze-dryer with Wizard 2.0 control (SP Industries, Warminster, PA, USA), onto shelves pre-cooled to -40˚C with a condenser temperature below -80˚C. A vacuum was applied and beads were held at the -40˚C shelf temperature for 4 h, then the shelf temperature was increased to -10˚C and beads were left to dry for 17 h with chamber pressures < 0.007 mbar. The adapted freeze granulation process for bead formation is depicted in **Figure 6.1**. Beads were removed from trays after drying and placed into moisture-proof pouches for storage prior to analyses (black matte double-sided, zip-lock, lined with aluminum foil, 8.4 x

13 cm, QQ Studio, New York, NY, USA). **Figure 6.2** provides a visual representation of the cross-sectional structure of freeze-dried beads comprised of glassy carbohydrates, glassy and insoluble/unhydrated protein particles, and protein-PP complexed aggregates.

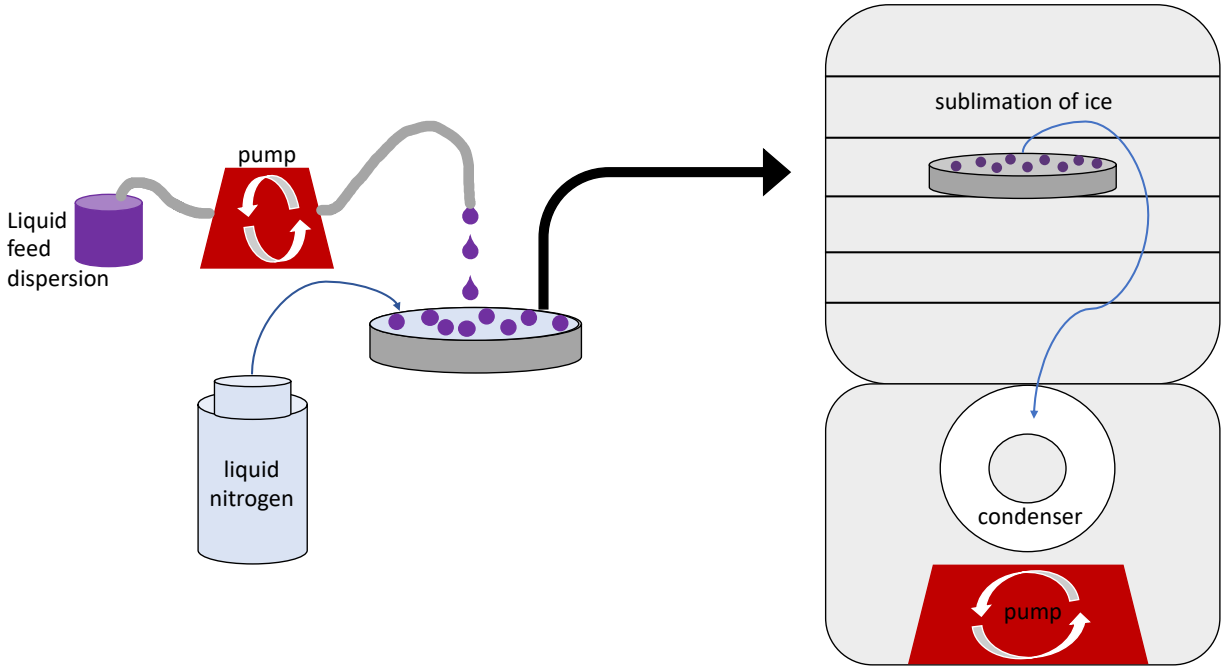


Figure 6.1. Modified freeze granulation process adapted to produce dry beads from concentrated liquid feed dispersions with varied WPI:sugar ratios, sugar types, polyphenols concentrations, and pH.

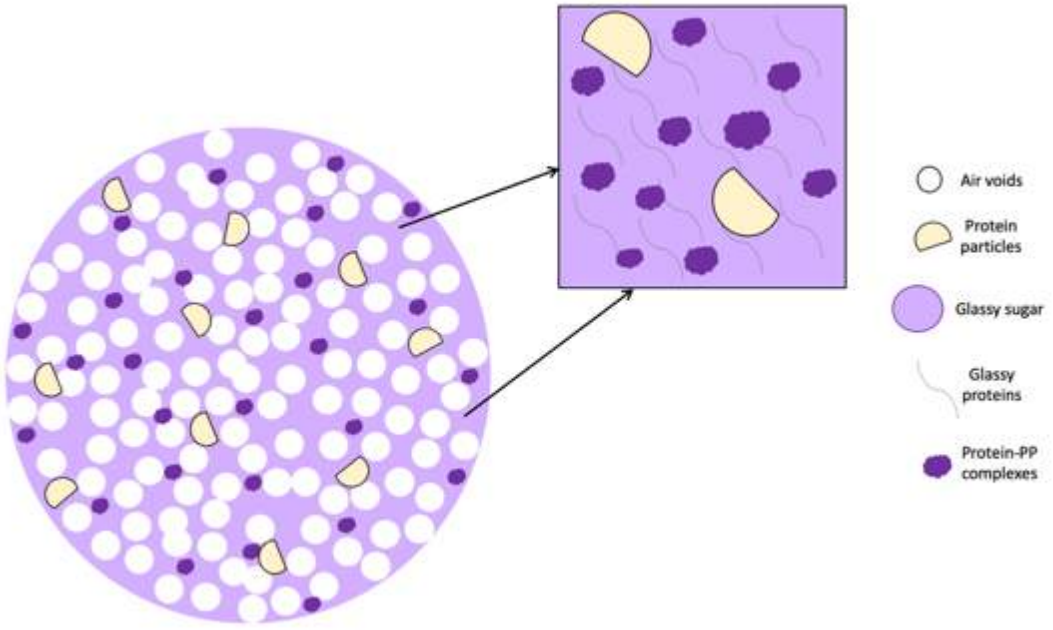


Figure 6.2. Schematic drawing of the cross-sectional structure of dry beads containing WPI, sugars, and Aronia extract after freeze drying; Inset: the proposed structure of the continuous glassy phase (not to scale).

6.2.5 Dried bead characterization

6.2.5.1 Dried bead diameters

Diameters of freeze-dried beads were measured 3 times per formulation replicate (n=9) with digital Vernier calipers (0-150 mm; Stainless Hard) on the day they were removed from the freeze-dryer (Day '0'), as described in previous studies (Hansen et al., 2021a, b).

6.2.5.2 Water activity (a_w)

a_w of beads was measured on the day they were removed from the freeze-dryer (Day '0') with a water activity meter (Aqua Lab model Series 3, version 5, Decagon Devices, Inc., Pullman, WA, USA) at ~22°C after meter calibration with D.I. water. Approximately 0.5 g of

sample was placed in plastic sample cups (Meter disposable sample containers and lids) for measurement.

6.2.5.3 Water content

Water content of beads was measured gravimetrically on the day they were removed from the freeze-dryer (Day '0'), modifying methods used by Fitzpatrick et al. (2004) and Shuck et al. (2005). Approximately 0.5 g of beads (triplicate measurements per replicate, n=9) were placed into pre-weighed aluminum pans, and masses were recorded before oven drying at 105°C for 5 h (Lindberg/ Blue M mechanical oven, model MO1490A-1, 120 V, 50/60 HZ, temperature range 40-260˚C, Asheville, NC, USA). Aluminum pans and lids were pre-dried at 105˚C prior to filling with beads. Masses were recorded again after drying, once the pans cooled to room temperature while covered to prevent water uptake; differences in masses due to water loss were determined, as well as the total solids remaining in dry beads.

6.2.5.4 Thermal analysis - differential scanning calorimetry (DSC)

The glass transition (T_g) onset temperatures of freeze-dried beads were determined using a DSC 8500 with an Intracooler 2 Cooling Accessory (Perkin Elmer, Waltham, MA, USA), between 1 and 3 days after removal from the freeze-dryer (replicates of the same formulation were always tested on the same day after freeze-drying). Beads were pressed into condensed tablet form, fractured for transfer into pre-weighed aluminum DSC pans (50 µL, PerkinElmer Health Sciences Inc., Shelton, CT, USA), and hermetically sealed. An empty pan was used as a reference. Calibration of the DSC was performed with Indium.

To observe T_g of dried beads, samples were scanned according to the sugar used in formulation: beads comprised of maltitol were cooled from 20°C to 0°C with a -10°C/min

cooling rate, then heated from 0˚C to 70°C with a heating rate of 10°C/min; those made from sucrose were cooled identically, but heated from 0˚C to 90˚C; beads made with trehalose were scanned from 40˚C to 160˚C. These methods were then repeated- the first scan to eliminate any T_g overshoot information caused by enthalpy relaxation of sugars during aging, and the second scan to gather T_g data (Hartel et al., 2011). Onset and midpoint temperatures (half C_p extrapolated) of glass transition events were calculated by the Pyris 11.0 software from the heat flow curve of the final heating step.

6.2.5.5 Hardness

Sample preparation – Beads were individually placed onto double-sided tape adhered to the platform, fixed aligned with the center of the platen. All replicates were analyzed in triplicate (9 hardness values per formulation) and average values were reported.

Texture analysis - Beads were tested for hardness with TA.XTplus Texture Analyser (Texture Technologies Corp., Scarsdale, New York, USA), between 1 and 3 days after removal from the freeze-dryer (replicates of the same formulation were always tested on the same day after freeze-drying). A 25 mm cylindrical, resin platen was utilized to compress beads 1 mm once contact was made with the individual bead exceeding a trigger force of 2g, at a speed of 1mm/s. Peak positive compression force was measured and recorded in the Exponent software (Stable Micro Systems, Version 6,1,16,0) for reporting sample hardness.

6.2.6 Statistical analysis

Triplicate experiments were analyzed in triplicate (n=9), and data collected were used to calculate mean values and standard deviations. Analysis of variance (2 and 3-way ANOVA; Tukey's HSD test) and independent measures t-tests (equal variance not assumed) were

performed when appropriate to compare mean values using JMP® Pro version 15.0.0 (SAS Institute Inc., Cary, North Carolina, USA). The level of significance was determined at $p < 0.05$.

6.3 Results and Discussion

6.3.1 Feed characterization:

6.3.1.1 pH

As pH can impact intermolecular interactions between proteins in dispersions and measurements of their associated physical properties, monitoring pH values in dispersions with varying compositions is important (Hansen et al., 2021a, b). All formulations with the same WPI:sugar compositions containing Aronia extract had significantly ($p < 0.05$) lower pH than those without. Similar to observations from earlier experiments, pH of dispersions containing WPI decreased slightly with PP (**Table 6.1**), but were unlikely to cause significant changes to the properties of dispersions, since pH did not closely approach the known isoelectric points (pI) reported for constituent β-lactoglobulin (pH ~5.2-5.3) and α-lactalbumin (pH ~4.2-4.8) protein fractions in WPI (Hansen et al., 2021a, b). Dispersions containing only sugars lacked the benefit of pH buffering in the systems that occurs when proteins are present, thus experiencing greater reductions in pH when PP were added.

6.3.1.2 Surface tension

The surface tension of a liquid strongly influences the size of drops formed once the surface tension forces acting around the circumference of the outlet are exceeded by the gravitational forces acting on the drop (Hansen et al., 2021a, b). According to the ANOVA, the ratio of WPI to sugar had a significant effect ($p < 0.05$) on the surface tension of dispersions.

Tukey's HSD tests provided clarity, reporting that dispersions without WPI ('0' ratios) had significantly ($p < 0.05$) higher surface tensions than those containing WPI, but once WPI was present, surface tension remained effectively unchanged upon increasing the WPI to sugar ratio, regardless of other formulation components (**Figure 6.3a**). Surface tensions of feeds with 1.0 WPI:sugar ratios were not significantly different ($p > 0.05$) from the 0.75 or 1.25 ratios, similar to findings reported in previous work (Hansen et al., 2021a). Sugars and other sweeteners are not thought to affect surface tension notably, as they are typically not very surface-active molecules. The differences in whey proteins, known to behave as surfactants, were not sufficient to impact surface tension in these systems as WPI:sugar ratios shifted, indicating that the slight shifts in composition at 25% total solids were not strong enough for detection.

The presence of Aronia PP in dispersions at 1% concentration was not found to have a significant ($p > 0.05$) effect on surface tension compared to feeds formulated without PP, according to the ANOVA and Student's t-tests applied. In formulations containing WPI, no differences in surface tension were observed between samples with 0% and 1% PP, generally in agreement with findings from previous experiments where increasing PP contents in feeds containing protein resulted in increased surface tensions under some conditions, but many showed no meaningful trends (Hansen et al., 2021a, b). In feeds without WPI, surface tension decreased notably with 1% PP compared to those without PP, as demonstrated in **Figure 6.3a** for the '0' WPI:sugar ratio. The Aronia extract utilized in this experiment was primarily comprised of small molecular mass polyphenolic compounds; technical data sheets provided by the manufacturer specified that the extract contained maximum fiber and protein contents of 1.3 and 2.3%, respectively. The reduced surface tensions of sugar solutions with PP may be a result of slight surfactant behavior of the minor biopolymer components in the extract, acting in a similar

manner to WPI in dispersions, but to a lesser extent due to lesser concentrations (Chan et al., 2009; B. B. Lee & Chan, 2013).

Formulations containing sucrose, maltitol, or trehalose did not have a significant effect ($p > 0.05$) on surface tensions of feed dispersions, according to the ANOVA and corresponding Tukey's HSD tests. These findings are depicted in **Figure 6.3b**, where the average surface tensions of all formulations containing each respective sugar may be compared. This finding supports our hypothesis, that no major changes would be expected to result from sugars in formulations, as all three sugars/polyols were of corresponding molecular size (Hartel et al., 2018).

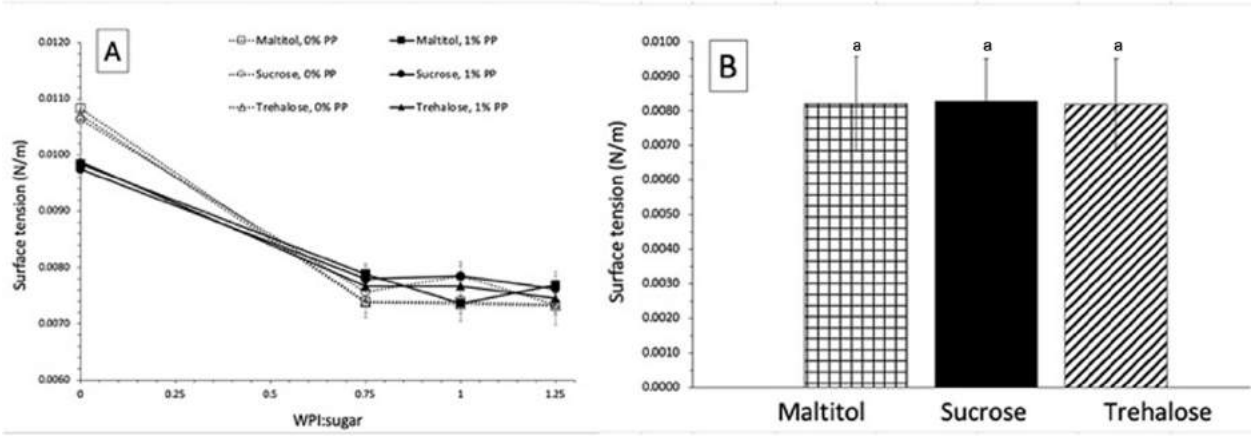


Figure 6.3. Effect of WPI:sugar ratio [**A**] on the surface tensions (N/m) of dispersions at 25˚C; the effect of sugar type [**B**] on the average surface tensions of all dispersions comprised of maltitol, sucrose, and trehalose, respectively, at 25˚C; (n = 9). Open markers with dotted lines- 0% PP, filled markers with solid lines- 1% PP [**A**]; lines are for guiding purposes only [**A**]. Values connected by the same letter are not significantly different ($p > 0.05$).

As previous studies reported that drop diameters and surface tensions were directly related (Chan et al., 2009; B. B. Lee & Chan, 2013), calculated surface tensions were plotted against calculated diameters of drops formed by the same dispersions, and a best fit line was applied (**Figure 6.4**). In agreement with previous reports (Hansen et al., 2021a, b), the plots

indicated a positive, strong, direct correlation ($R^2 = 0.98$). The few points in the plot with high surface tensions/drop diameters represent the sweetener solutions formulated with 0 and 1% PP that had very high surface tension values relative to feed formulations containing WPI, which reduced surface tensions.

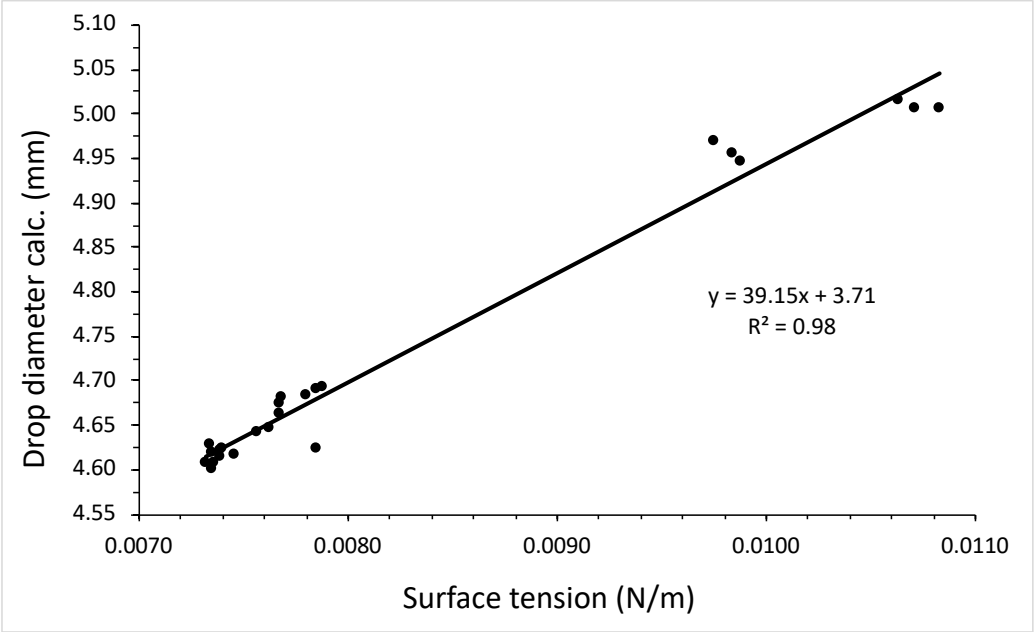


Figure 6.4. The relationship between the surface tensions (N/m) of feed dispersions containing WPI:sugar ratios of 0, 0.75, 1.0, and 1.25, sugars/polyols including maltitol, sucrose, and trehalose, and polyphenols contents of 0 and 1%, at 25˚C and calculated diameters (mm) of drops.

6.3.1.3 Viscosity

Minor changes in the composition of dispersions can result in shifts in viscosity, which is a critical factor in determining conditions for processing (Hansen et al., 2021a, b). According to the ANOVA, changing the ratio of WPI to sugar had a significant ($p < 0.05$) effect on viscosity; as the WPI:sugar ratio increased (thus increasing total protein content in dispersions), viscosity was observed to increase as well. Tukey's HSD tests clarified the report, indicating that the only

significant difference ($p < 0.05$) was between feeds formulated without WPI ("0" WPI:sugar ratios) and those containing WPI. Feeds formulated without WPI had significantly lower ($p < 0.05$) viscosities than those formulated with WPI, and once WPI was present, slight increasing trends were generally observed as WPI:sugar ratio increased, though differences were not significant ($p > 0.05$), and some variation was observed (**Figure 6.5a**). Given the common 25% total solids contents in feeds, alterations to compositions were too slight to have strong effects on system viscosities. In previous work, the ANOVA indicated that complex viscosity significantly increased ($p < 0.05$) with increasing ratios of WPI to sucrose (and thus total protein content) in feed dispersions (Hansen et al., 2021a). The effect of increasing the WPI:sucrose ratio was thought to be relatively weak compared to that of % total solids, as lower (25 and 35) % total solids formulations did not clearly demonstrate the trends reported by the ANOVA as consistently as the 45% total solids feeds.

The presence of Aronia PP in feeds at 1% was found to have a significant effect ($p < 0.05$) on viscosity, compared to feeds formulated without PP, according to the ANOVA and Student's t-tests applied. Feed dispersions containing 1% PP had significantly higher ($p < 0.05$) viscosities than those with 0% PP, correlating with the reduced pH values in systems containing PP. Reducing pH closer to pI would result in greater intermolecular interactions in the system as repulsions are reduced between proteins and protein-PP complexation is more likely to occur. Enhanced system intermolecular interactions would result in increased viscosities and behavioral complexities of the fluids. With the exception of a few minor variations, **Figure 6.5a** displays that feeds containing 1% PP (solid lines and filled markers) tended to have higher viscosities than those with 0% PP (dotted lines and unfilled markers). These results build upon those from our previous work suggesting a weak effect of PP on viscosity, providing further evidence that

increasing PP content in feeds results in increased viscosities, even as % total solids in the system remains constant (Hansen et al., 2021a).

Changing the sugar/polyol in formulations between sucrose, maltitol, and trehalose did not have a significant effect ($p > 0.05$) on viscosities of feed dispersions, according to the ANOVA and Tukey's HSD test reports. These findings are depicted in **Figure 6.5b**, where the average viscosities of all formulations containing each respective sugar may be compared. This finding builds on the surface tension results in support of our hypothesis, that no major changes would be expected to occur with changes in sugars in formulations, as all three sugars/polyols are of similar molecular sizes and thus would be expected to have similar effects on solution or syrup viscosities (Hartel et al., 2018).

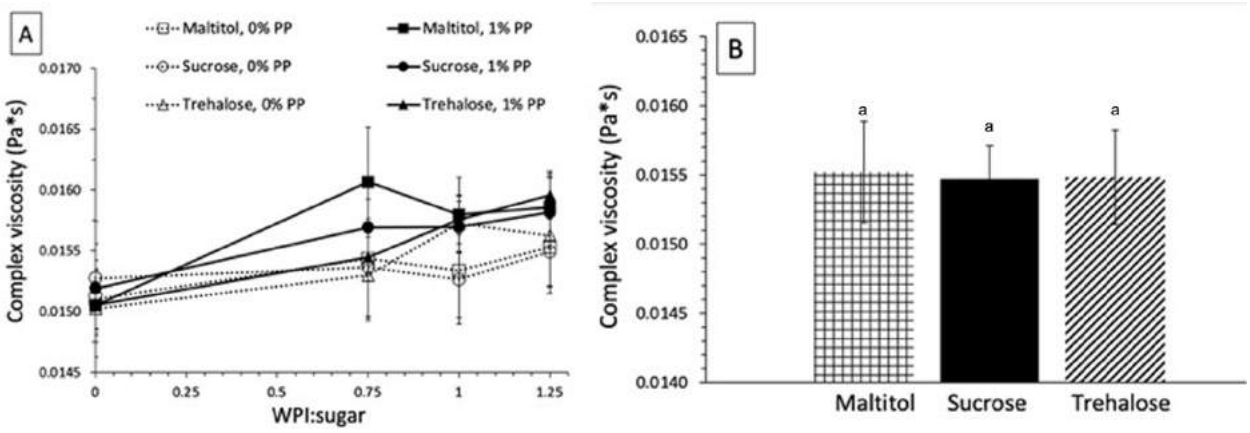


Figure 6.5. Effect of WPI:sugar ratio [**A**] on the complex viscosities (Pa*s) of dispersions at 25˚C; the effect of sugar type [**B**] on the average complex viscosities of all dispersions comprised of maltitol, sucrose, and trehalose, respectively, at 25˚C; (n = 9). Open markers with dotted lines- 0% PP, filled markers with solid lines- 1% PP [**A**]; lines are for guiding purposes only [**A**]. Values connected by the same letter are not significantly different ($p > 0.05$).

6.3.1.4 Particle size

Particle size measurement is a useful tool for examining the physical effects of altered compositions and other conditions within dispersions, which are known to affect the interactions between proteins and other components (Hansen et al., 2021a, b). Feeds containing WPI had normal distributions and PP addition affected distributions by shifting their peaks towards smaller particle sizes, as seen in **Figure 6.6** for dispersions with sucrose (all sugars/polyols followed the same trend). Schneider (2016) also reported relatively normal particle size distributions for weakly acidic dispersions of juices with lower phenolics concentrations mixed with WPI to form complexes, reporting similar average particle size values as well.

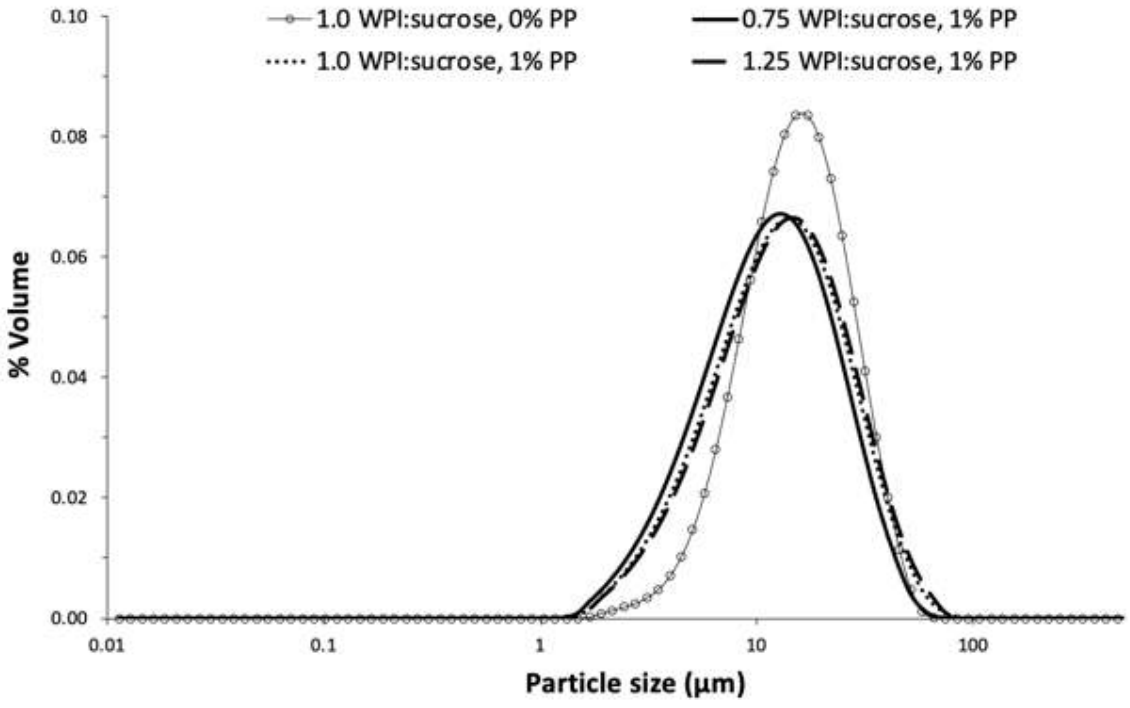


Figure 6.6. Particle size distributions of feed dispersions comprised of 1.0 WPI:sucrose ratios with 0% and 1% PP, and 0.75 and 1.25 WPI:sucrose ratios with 1% PP at 25˚C; (n = 9).

Altered ratios of WPI to sugar in dispersions did not significantly ($p > 0.05$) affect particle size distributions, according to the ANOVA (**Figure 6.7a**). No significant differences in average particle size were observed between dispersions prepared at the three different WPI-sugar ratios ($p > 0.05$) according to the Tukey's HSD tests, with all formulations displaying approximately normal distributions. These results support and build upon findings from earlier work, indicating that varying levels of sugars in the systems did not influence aggregate sizes, potentially due to their easy dissolution into water (Hansen et al., 2021a).

The presence of Aronia PP in feeds at 1% was found to have a significant effect ($p < 0.05$) on the average particle sizes of dispersions, according to the ANOVA and Student's t-tests applied to the data. Feed dispersions containing 1% PP had significantly smaller ($p < 0.05$) average particle sizes than those with 0% PP, with average values of 14.84 and 16.31μm, respectively. This is also demonstrated in **Figure 6.7a**, which shows all formulations containing 1% PP (solid lines and filled markers) have lower average particle sizes than feeds formulated with 0% PP (dotted lines and unfilled markers), regardless of sugar/polyol type and WPI-sugar ratios. These results are in agreement with findings from previous studies, where particle sizes were found to decrease upon PP addition (Hansen et al., 2021c; Siebert et al., 1996; Thongkaew et al., 2014; Xue et al., 2020).

The ANOVA and Tukey's HSD tests reported that average particle size values for maltitol and sucrose formulations were slightly but significantly different from one another ($p < 0.05$), but neither value was significantly different from that for trehalose formulations. The average particle sizes of all formulations comprised of each respective sugar/polyol are plotted in **Figure 6.7b**, where differences determined to be significant in the statistical analysis appear to

be negligible once error bars are applied to the data for comparison. In theory, variations in dispersion particle size distributions could impact viscosity, but because the differences detected were so small, they did not impact dispersion viscosities (**Fig. 6.5b**).

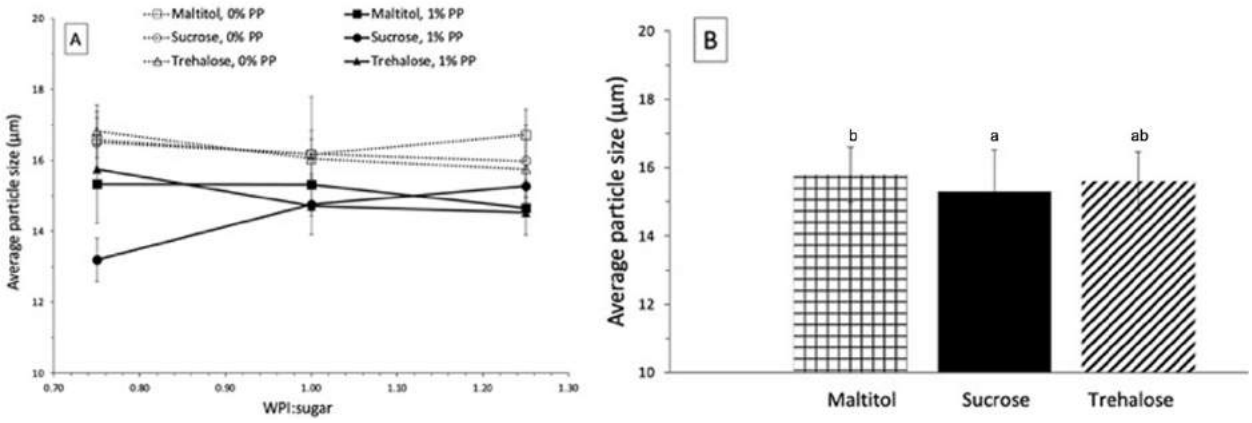


Figure 6.7. Effect of WPI:sugar ratio [**A**] on the average particle sizes (µm) of dispersions at 25˚C; effect of sugar type [**B**] on the average particle sizes (µm) of all dispersions comprised of maltitol, sucrose, and trehalose, respectively, averaged together at 25˚C; (n = 9). Open markers with dotted lines- 0% PP, filled markers with solid lines- 1% PP [**A**]; lines are for guiding purposes only [**A**]. Values connected by the same letter are not significantly different ($p > 0.05$).

In line with previous experiments (Hansen et al., 2021a, b), microscopy generally supported laser diffraction particle size data. Microscopy visually confirmed the lack of changes in particle size observed with altered sugar types in dispersions (data not shown), as well as the reduced particle sizes observed with 1% PP in dispersions (**Figure 6.8**). The insoluble protein particles remaining in dispersions without PP were larger than the protein-PP complexes formed in dispersions containing Aronia, thus resulting in reduced average particle sizes, similar to the findings for pea protein isolate dispersions with and without PP in earlier work (Hansen et al., 2021a).

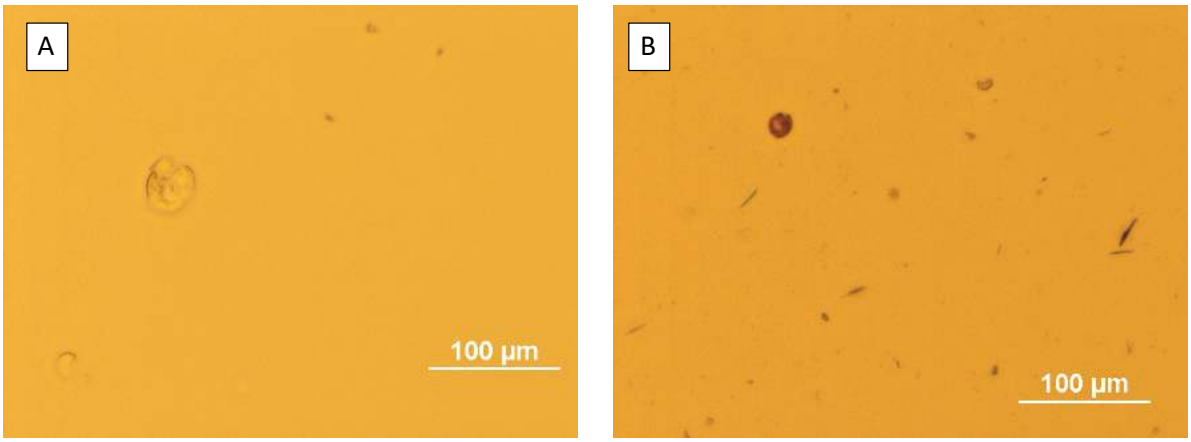


Figure 6.8. Optical light microscope images at 200x magnification depicting the microstructures of diluted feed dispersions with 1.0 WPI:sucrose with 0% PP (**A**) and 1% PP (**B**).

6.3.1.5 Centrifuge separation

Precipitate pellets formed after dispersions containing WPI were centrifuged, mirroring observations from earlier experiments involving other protein-sucrose dispersions (Hansen et al., 2021a, b). Pure sugar solutions did not form pellets upon centrifugation, indicating their complete dissolution in water. As described in previous studies, the pellets formed by WPI-containing dispersions with Aronia were dark purple (**Figure 6.9)**, and the formation of a colored precipitate indicated protein-PP complexation (Hansen et al., 2021a, b; Van Teeling et al., 1971).

No differences in appearance were observed for centrifuged dispersions and their dilutions formulated with different sugars, regardless of WPI or PP presence (images not shown). Precipitated pellets were slightly larger in size for dispersions containing 1% PP, compared to those with 0% PP (**Figure 6.9**). While **Figure 6.9** demonstrates this observation for samples formulated with sucrose, the same trend was observed for both maltitol and trehalose (images not shown). Similar observations were made in earlier experiments, where little-to-no precipitate

formed after centrifuging a diluted 1% Aronia extract solution, suggesting that the observed increases in pellet size with increasing PP concentrations were due to enhanced aggregation and larger complexes precipitating out (Hansen et al., 2021a, b).

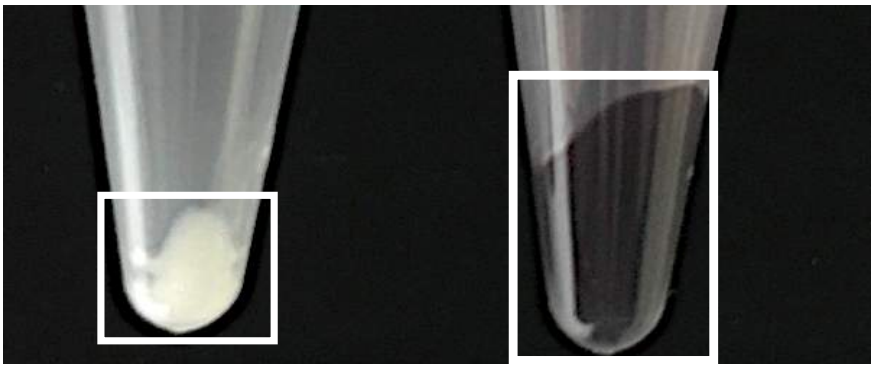


Figure 6.9. Image depicting the precipitated fractions (highlighted in boxes) of centrifuged dispersions with 1.0 WPI:sucrose with 0% PP (Left) and 1% PP (Right)

6.3.2 Dried bead characterization:

6.3.2.1 Comparison of drop diameters

Measured diameters of drops formed from liquid dispersions were found to be significantly smaller ($p < 0.05$) than the estimated diameter values calculated from flow testing data for all formulations (**Table 6.1**), similar to the findings of Chan et al. (2009) when calcium-alginate drops formed by dripping methods were smaller than predicted with Tate's law calculations. These differences likely arose from the breaking of dispersion drops upon contact with the LN_2 surface, with resulting hardened drops having smaller sizes than estimated. While the correction factor used in calculating the estimated drop diameters describes the phenomenon of not all liquid detaching from the tubing tip, it does not account for the amount of liquid lost when drops break into smaller droplets, rendering the calculation method less accurate in estimating drop size in this case compared to previous experiments.

6.3.2.2 Water activity (a_w)

Water activities of fresh beads were measured after freeze-drying, and all but two formulations were found to have $a_w < 0.05$; sucrose beads without WPI were found to have higher a_w values (< 0.15) (**Table 6.1**). Compared to the a_w values obtained in previous work (Hansen et al., 2020) for beads formed by gelation in heated oil and subsequent oven drying, the freeze granulation method presented in this study can more effectively form dry, solid beads with lower a_w values than the original drop formation method, which may result in beads with enhanced microbial stability. Other products formed with milk proteins have been reported to have a_w values similar to the beads in this study: Spray dried skim milk powders with 1.5% and 3% water contents are reported to have typical a_w values of ~0.02 and 0.1, respectively (Walstra, 1999). Variations in a_w of beads may be due to slight changes in environmental temperature during measurements or measurement variability.

6.3.2.3 Water content

After freeze-drying, fresh beads were oven dried to determine water content, as water content is known to affect physical properties of dried materials including texture and T_g (Roos, 1993). All dispersions formed dry beads with < 3% water (**Table 6.1**), except for maltitol dispersions formulated without WPI, which were unable to form dry beads upon freeze-drying and instead appeared moist and were sticky to the touch. Often considered the 'critical formulation temperature' for determining profiles for freeze-drying processes, T_g' is the temperature at which glass transition occurs for the maximally freeze-concentrated solute (Roos & Drusch, 2015; Roos & Karel, 1991); T_g' varies with product composition, but it is recommended that shelf temperatures are adjusted so that product temperatures remain below T_g' for efficient drying (Kadoya et al., 2010). It is possible that the first step of the freeze-drying

process, with shelf temperatures set to -40˚C, was not sufficient to maintain the glassy state of ice in maltitol beads, as the product temperature may have approached or exceeded T_g' when the LN_2 evaporated (Meister & Gieseler, 2008). T_g' onset and midpoint values for frozen maltitol solutions have been reported as -47˚C and -42˚C, respectively (Roos & Drusch, 2015), and were likely lower than the actual product temperatures during drying. If T_g' was approached or exceeded, beads would be prone to physical collapse, increased molecular mobility, and decreased viscosity as some of the ice present melted rather than sublimed as melting onset temperature (T_m') was approached, resulting in the sticky, moist products observed (Hartel et al., 2018; Kadoya et al., 2010).

Dispersions comprised of sucrose and trehalose, as well as maltitol beads containing WPI, were able to form dry beads upon freeze-drying because T_g' was sufficiently high to avoid cross-over with product temperatures during drying. T_g' onset and midpoint values for frozen sucrose solutions are reported as -46˚C and -41˚C, respectively, and those for trehalose are reported as -40˚C and -35˚C, respectively (Roos & Drusch, 2015). It has also been reported that frozen sugar solutions mixed with proteins gave higher T_g' values compared to pure sugars, suggesting miscibility of the components on a molecular level in the dry products and allowing synergistic stabilization, potentially explaining why maltitol dispersions were able to be dried into glassy beads when WPI was present (Kadoya et al., 2010). Dry beads formed with both sucrose and trehalose were found to have higher water contents in the absence of WPI compared to beads formed with WPI, as pure sugars have enhanced susceptibility for undergoing some extent of physical collapse, which is known to result in higher residual water content (Kadoya et al., 2010). Additionally, macromolecules- including proteins- are known to be useful drying aids in various food preservation techniques, further explaining the reduced water contents when

beads were formulated with WPI (Bazaria & Kumar, 2016). The mechanisms of drying, while not the focus of this study, could be further investigated by FTIR analysis.

6.3.2.4 Thermal analysis – glass transition temperature (T_g)

Glass transition measurements are used as an indicator for the stability of glassy matrices and the resulting protection of components encapsulated within, rendering T_g significant in understanding product stability (Hartel et al., 2011; Levine & Slade, 1992; Roos & Drusch, 2015). The term T_g refers to the temperature range over which a glassy material softens; both onset and midpoint temperatures of the transition range are commonly referred to as T_g, though Roos and Drusch (2015) recommend that T_g is taken from the calorimetric onset temperature of the change in heat capacity. According to the ANOVA used to compare the T_g onset temperatures for beads containing WPI, WPI:sugar ratio had a significant effect on T_g ($p < 0.05$); Tukey's HSD tests expanded on this and clarified that the only significant increases in T_g onset temperatures were observed between the 0.75 and 1.0 WPI:sugar ratios. This finding can be observed in **Fig. 6.10a**, when the T_g onset temperature values of beads increase between the 0.75 and 1.0 WPI:sugar/polyol ratios for nearly all formulations. The ANOVA used to compare the T_g onset values for beads without maltitol also reported that WPI:sugar ratio significantly impacted T_g, with significant increases ($p < 0.05$) observed between the 0 and 0.75 WPI:sugar ratios. These findings can be clearly visualized in **Fig. 6.10a** for beads made with sucrose and trehalose. The ANOVA used to compare T_g of beads prepared with maltitol reported significant differences when WPI:polyol changed from 0.75 to 1.0 ratios ($p < 0.05$). These results generally agree with the literature; while considered 'problematic' and difficult to detect consistently due to very small changes in heat capacity and wide temperature ranges for transitions (Adhikari et al., 2009; Pikal et al., 2007, 2008; Zhou & Labuza, 2007), the T_g of macromolecular proteins is known to

be high, and increasing the concentrations of protein in the mixtures may raise T_g slightly as the average molecular mass of the system is increased (Sarciaux & Hageman, 1997; Tzannis & Prestrelski, 1999; Maidannyk & Roos, 2017).

Protein isolates and other biopolymers are comprised of several fractions with differing complex structures and thermal properties, including T_g. Compositional diversity in complex systems and mixtures often results in weak, wide glass transition events for protein isolates where midpoints may be difficult to detect and T_g zones are more commonly reported (Bengoechea et al., 2007). Thermal properties are influenced by molecular mass and configuration, structural purity, compactness, the incidence of intermolecular interactions and aggregation, and the extent of hydration water and plasticization by solvents (Ahmed et al., 2008; Bengoechea et al., 2007; Jansson et al., 2011; Maidannyk & Roos, 2017; Modi et al., 2012; Roos & Drusch, 2015; Roos & Potes, 2015). Between the onset temperatures presented in **Figure 6.10** and midpoint temperatures in **Table 6.1**, we report data that describes the width of T_g events observed in our beads. Large proteins such as WPI and smaller molecular mass compounds like sugars are frequently reported to be immiscible, and phase segregation/ separation is common, with proteins rarely affecting T_g in a strong manner (Roos & Drusch, 2015; Roos & Potes, 2015; Shrestha et al., 2007). Under specific mixing conditions, small extents of weak interactions between components have been observed to occur, as indicated by slight changes in DSC T_g measurements (Modi et al., 2012). Further investigation of component miscibility in our systems would require different experimental designs and protocols.

Addition of PP had only a small effect on the T_g onset values of beads. However, the ANOVA for beads containing WPI reported that PP significantly ($p < 0.05$) impacted T_g, with Tukey's HSD tests clarifying that the presence of Aronia extract resulted in beads with higher T_g

onset temperatures than those without PP. This trend was only clearly observed for beads produced with maltitol, indicating that those points strongly influenced the ANOVA report (**Fig. 6.10a**). The ANOVA for beads without maltitol did not report a significant difference ($p > 0.05$) in T_g upon the addition of PP to the bead matrices, as indicated by the lack of trends observed for beads made with sucrose and trehalose. The relatively small amounts of PP/ Aronia present appeared to occasionally induce minor changes in the T_g of beads.

The T_g of confectionery products are heavily influenced by the type of sugar used and its water content (Hartel et al., 2018). Upon averaging the data obtained for beads formulated from each respective sugar, the onset T_g of beads formulated with trehalose was found to be the highest, while those comprised of maltitol were found to have the lowest T_g (**Fig. 6.10b**). The ANOVAs used to compare the T_g onset temperatures of beads containing WPI as well as the T_g of beads without maltitol indicated that sugar type has a significant ($p < 0.05$) effect on T_g, with Tukey's HSD tests reporting the same trend as observed in **Figure 6.10b** (trehalose highest, maltitol lowest) and all three sugars being significantly different from each other. These results are similar to what would be expected based on the T_g values reported in the literature for each sugar/polyol: Dry T_g for maltitol is reported to be ~ 39˚C (Hartel et al., 2018), sucrose ~ 60-70˚C (Hartel et al., 2018; Roe & Labuza, 2005), and a range of temperatures are reported in the literature for trehalose between ~ 75 and 120˚C, likely influenced by the presence of unmeasured or unreported water (Cardona et al., 1997; Roe & Labuza, 2005).

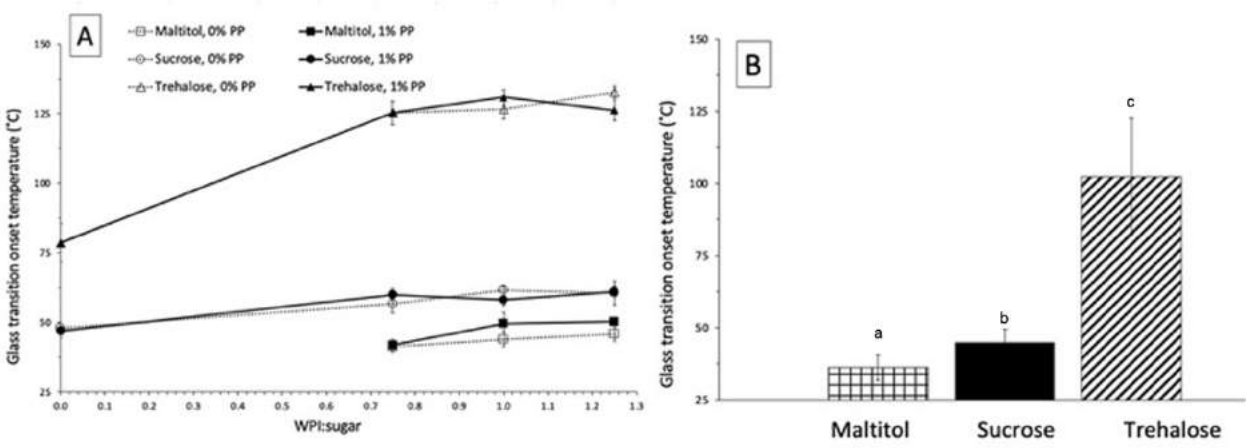


Figure 6.10. Effect of WPI:sugar ratio [**A**] on the glass transition onset temperatures (˚C) of beads; the effect of sugar type [**B**] on the average glass transition onset temperatures (˚C) of all dried beads comprised of maltitol, sucrose, and trehalose, respectively, at 25˚C; (n = 9). Values connected by the same letter are not significantly different ($p > 0.05$).

Water content is reported to have a strong effect on the T_g of sugars: 2-3% water can decrease the T_g of dry sucrose from ~ 62-70 to ~ 42-50˚C (Hartel et al., 2018), and trehalose T_g dropped to ~ 65˚C with 4% water (Iglesias et al., 1997). Like sugar glasses, freeze-dried proteins easily sorb water and show greatly reduced T_g values with increasing water contents, leading to reduced product stability (Lu et al., 2007; Pikal et al., 2007; P. Zhou & Labuza, 2007). In the case of elastin proteins, T_g was found to decrease from temperatures exceeding 200˚C when dry, to below 20˚C when water content was greater than 20% (Kakivaya & Hoeve, 1975; Roos & Drusch, 2015). Kadoya et al. (2010) observed enhanced T_g values for dried sugar solutions (water content < 2%) when BSA protein was present, compared to those of the pure sugars (maltitol ~40.6˚C, with BSA ~56˚C; sucrose ~62˚C, with BSA ~68˚C; trehalose >80˚C, with BSA >90˚C), and suggested that the increased T_g values may be indicative of molecular-level miscibility of the components. Wilson et al. (2019) reported T_g values for mixtures of β-lactoglobulin with sucrose and trehalose (1:9 protein:sugar), with T_g of β-lactoglobulin-sucrose with a water content of 0.7% to be ~71.8˚C, and β-lactoglobulin-trehalose with 0.3% water

having T_g ~106.5˚C. The values obtained in this experiment are in agreement with the results reported in the literature, taking into account the effects of residual water in the freeze-dried beads. Confirming microscopic homogeneity of glassy structures would require different experiments designed to study component interactions.

6.3.2.5 Hardness

Hardness of a glassy product may also be used as an indicator of its stability and whether water uptake has affected its physical state or sensory properties. When the hardness values of freeze-dried beads were measured, it was found that beads containing WPI were less hard than those formulated without WPI. According to the ANOVA used to compare the hardness of beads containing WPI, WPI:sugar ratio had a significant effect on hardness ($p < 0.05$); Tukey's HSD tests specified that increased WPI to sugar ratios resulted in decreased hardness, though the difference was only significant between the 1.0 and 1.25 ratios. The ANOVA used to compare beads formed without maltitol also indicated that the WPI:sugar ratio had a significant effect ($p < 0.05$), with Tukey's HSD tests clarifying that the only difference in hardness was observed between the 0 and 0.75 WPI:sugar ratios, which can be clearly visualized in **Fig. 6.11a** for beads formulated with sucrose and trehalose. The ANOVA used to compare beads containing maltitol was in agreement that WPI:sugar ratio significantly affected hardness, but Tukey's HSD tests did not show meaningful trends. As alluded to in previous work (Hansen et al., 2020), we postulate that protein particles and protein-PP complexes are embedded throughout the continuous glassy matrices formed by the sugars, breaking up and weakening the glasses compared to beads with uninterrupted glassy structures. The effect of protein on reducing the hardness of beads was strong, and as such, it may not be as useful to compare hardness of beads with WPI to those without.

The presence of PP was not found to drastically affect the hardness of beads. The ANOVA used to compare the hardness of beads containing WPI reported that PP presence did not significantly affect the hardness of beads ($p > 0.05$); the ANOVA used to compare the hardness of beads containing maltitol was in agreement. The ANOVA used to compare the hardness of beads formed without maltitol indicated that PP presence significantly influenced hardness ($p < 0.05$), where beads prepared with sucrose and trehalose without PP were significantly harder than those containing PP (**Figure 6.11a**). Aronia extract may have introduced impurities into the glassy matrix, weakening it in the same way that protein and protein-PP complexes are thought to.

We hypothesized that beads comprised of sugars/polyols with higher known T_g values may be harder and more brittle than those formulated with lower T_g sugars, as that rule generally applies to many confectionery products (Hartel et al., 2018). According to the ANOVA used to compare the hardness of beads containing WPI, the sugar type used to formulate beads significantly influenced hardness ($p < 0.05$); Tukey's HSD tests indicated that beads prepared with maltitol were the hardest, and those made from trehalose were softest, in contrast to expectations based on T_g. While the effect of sugar type on hardness was found to be statistically significant, closer examination of the data plotted in **Fig. 6.11a** for beads containing WPI show considerable overlap between sugar types, indicating that the effects were small. The ANOVA used to compare the hardness of beads prepared without maltitol reported that sugar type did not significantly affect hardness ($p > 0.05$); beads made of trehalose had slightly but not significantly higher hardness values than those made of sucrose. These findings can also be observed in **Fig. 6.11a**, where trehalose beads without WPI were the only point where hardness was clearly higher than the corresponding beads formulated with sucrose, and even in that case, was not

significantly different. These findings are summarized visually in **Fig. 6.11b**, where the hardness values of all beads formulated with each respective sugar type are averaged for comparison of sugar/polyol effects, showing maltitol beads were, on average, the least hard, and trehalose the hardest. Trehalose and sucrose formulations had higher variation, since hardness was strongly influenced by the presence of WPI in formulations, as discussed previously. These findings were interesting, as greater differences in hardness were expected when sugar type was changed, though WPI influenced the hardness of beads more strongly than sugar type. Beads formulated with lower T_g sugars may have had slightly more fluid properties and molecular mobility at room temperature and were more susceptible to ambient water, which could result in a sticky outer surface forming on the beads, resulting in enhanced hardness and tackiness, as opposed to the more crisp, brittle texture of more dry glasses.

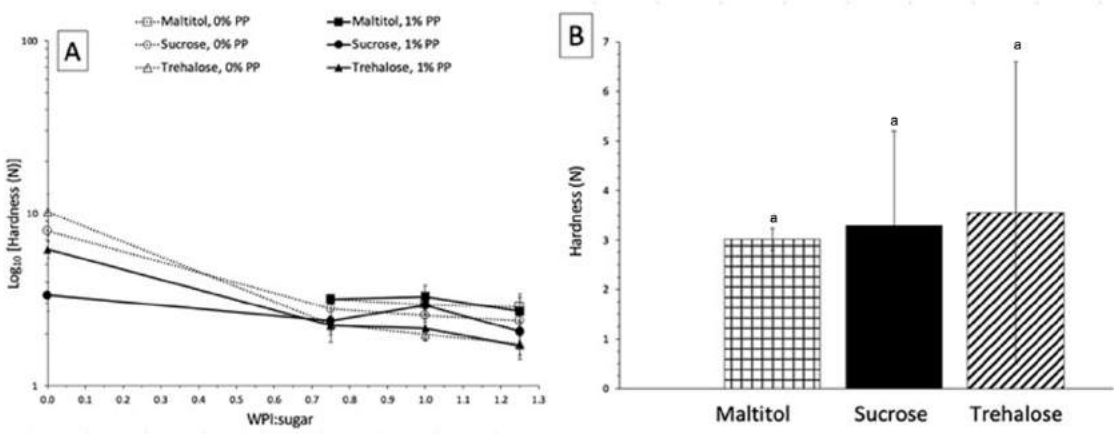


Figure 6.11. Effect of WPI:sugar ratio [**A**] on the hardness (N) of dried beads at 25˚C; the effect of sugar type [**B**] on the average hardness values of all dried beads comprised of maltitol, sucrose, and trehalose, respectively, at 25˚C; (n = 9). Open markers with dotted lines- 0% PP,

filled markers with solid lines- 1% PP [**A**]; lines are for guiding purposes only [**A**]. Values connected by the same letter are not significantly different ($p > 0.05$).

6.3.3 Effects of dispersion properties on dry beads

No strong correlations were found upon investigating the relationships that may exist between properties of feed dispersions and those of the final beads formed (data not shown). No correlation was found between the viscosities of feed dispersions and the glass transition onset temperatures, diameters, or hardness of beads formed. Surface tensions of dispersions were not correlated with the hardness of beads formed either. Water contents of dried beads did not have a strong relationship with T_g or hardness. Diameters of dried beads were not related to their hardness. pH values of dispersions did not correlate with the diameters of beads formed or their hardness. Particle sizes of dispersions did not correlate with the hardness, T_g, or diameters of dried beads formed.

6.4 Conclusion

In a variety of pharmaceutical, food, and biomedical applications, freeze-dried protein-sugar mixtures in the glassy state have been shown to 1) have increased T_g compared to that of the sugar alone, 2) prevent sugar crystallization in storage, and 3) diminish decomposition of the proteins in the mixture from their native structures during freeze-drying and subsequent storage by immersion in the glassy matrices and increasing denaturation temperature (Corradini et al., 2013; Imamura et al., 2001; Jena et al., 2017; Liao et al., 2005; Lu et al., 2007; Nilsson & Larsson, 2007; Pikal et al., 2007, 2008; Sarciaux & Hageman, 1997; Souillac, Middaugh, et al.,

2002). It is for these reasons that we believe that the adapted freeze granulation process presented produces structures with the potential to act as good stabilizers and subsequent delivery vehicles for bioactive ingredients such as polyphenols. Substitution of glass formers with lower T_g by others with higher T_g resulted in the formation of beads with increased T_g, indicative of better physical stabilities. Compositional modifications such as these may improve the protective abilities of bead structures as their physical stabilities are known to enhance storage stability. Further investigations of bioactives delivery, as well as retention and shelf life studies, are critical to determine the efficacy of these structures as encapsulation matrices as well as optimization for applications.

Funding

The Lauritzson Foundation provided funding for this research via the Lauritzson Research Scholarship, through the College of Science, Engineering and Food Science (SEFS) at University College Cork.

Chapter 7

General discussion

Mackenzie M. Hansen

7.1 Overview of key themes explored

Several themes were explored within this thesis, the first being the development and presentation of two continuous processes for forming concentrated protein-sugar or -polyol feed dispersions into solid, stable bead structures with potential for bioactives encapsulation (Chapters 2 and 6). Both processes presented involved two major steps: First, structure formation via dispersions undergoing temperature changes; next, water removal. Particle size, viscosity, and surface tension properties are altered by formulation changes in a system and influence the drop formation abilities of dispersions. As such, the effects of formulation including total solids (Chapters 2 and 3), protein:sugar ratios (Chapters 3, 4, 5, 6), bioactives contents (Chapters 3, 4, 5, 6), and protein (Chapter 4), carbohydrate (Chapter 6), and bioactives sources (Chapter 5) on the physico-chemical properties of feed dispersions were investigated, as well as their effects on the physical properties of solid beads formed (Chapters 2 and 6). The focus of studies was primarily on the physical properties of matrices and processing conditions.

7.1.1 Bead formation methods

In Chapter 2 we aimed to investigate whether dispersions of varying compositions could be formed into dry, solid beads under a variety of processing conditions (time, temperature). We present a full process design for simple, continuous solidification of concentrated liquid dispersions for developing structures with the potential for water- and oil-soluble bioactives encapsulation. Feeds containing 40% w/w whey protein isolate (WPI) with 10% sucrose demonstrated the best individual structure formation abilities, producing beads with consistent sizes and shapes that were retained in the oil bath as well as upon oven drying. Optimized feeds formed dry beads with the best shape retention and avoided excessive oil uptake when pumped dropwise into a moderately heated (100˚C) oil bath with gentle stirring over a two-minute

hardening period as proteins underwent gelation. Beads formed by this method demonstrated bulk oil inclusion and emulsification into small drops dispersed throughout the structures. They were subsequently dried via vacuum oven to remove water from bead structures and drive sucrose glass formation for enhanced protein stabilization in the dry state. Beads formed from aqueous blends of hydrophilic sugars and amphiphilic proteins were solid and stable, making them structures of interest for further studies formulating with water-soluble bioactives for potential entrapment. Next steps involved the incorporation of Aronia berry extract, rich in hydrophilic anthocyanin polyphenols, into blends and investigation of the physical properties of dispersions and dry materials formed.

7.1.2 Modified bead formation methods

The bead formation method presented in Chapter 2 required the exposure of dispersions to moderate heat conditions for a short time in order to promote solidification of beads. Chapter 6 presents a modified process, where gel formation does not occur for solidification. The adapted method is similar to the freeze granulation process utilized in pharmaceutical and ceramic materials applications (Bhatta et al., 2020; La Lumia et al., 2019; Ouadaker et al., 2020; Shanmugam, 2015): Dispersions were pumped dropwise into liquid nitrogen baths for instant solidification and glass formation, then transferred to a freeze-dryer for water removal (**Figure 7**). Altering compositional elements in formulations modulated the physical properties and states of beads formed, providing greater physical stability and potential for bioactives stabilization.

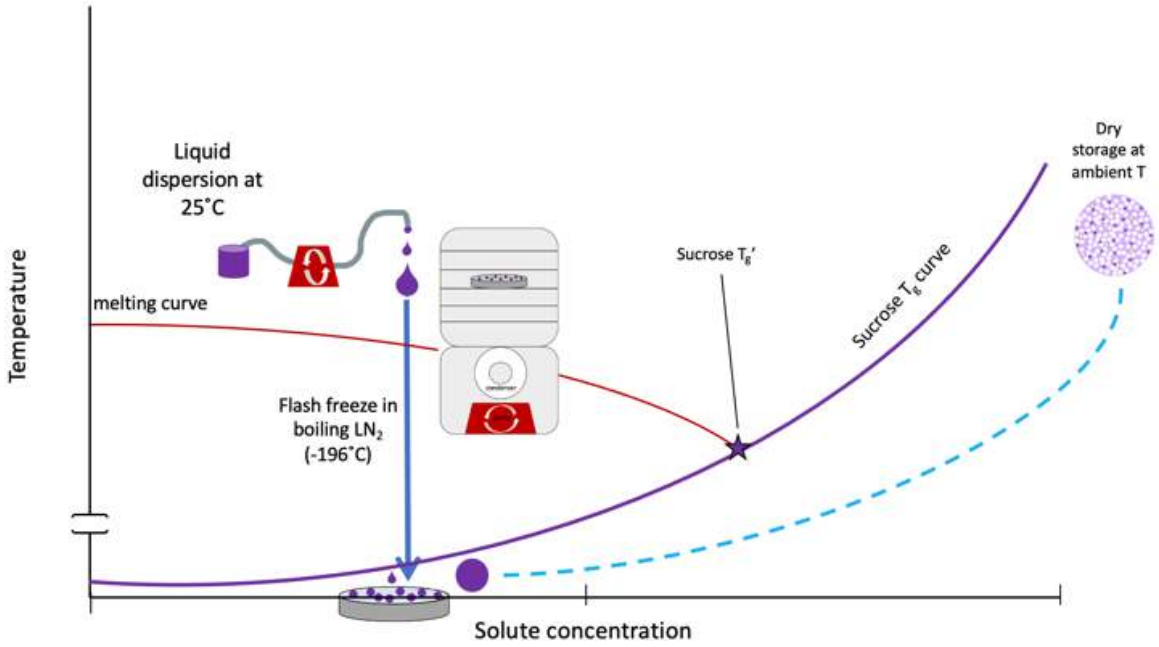


Figure 7. Schematic state diagram of sucrose overlaid with the modified bead formation method presented in Chapter 6.

7.1.3 Effects of formulation on the physico-chemical properties of feed dispersions

7.1.3.1 Total solids

The effects of total solids contents in dispersions were examined in Chapters 2 and 3. In Chapter 2, dispersions were found to have slightly increasing viscosities and surface tensions with increasing WPI concentrations until significantly increasing above 30% WPI w/w, in agreement with the findings of other researchers (Alizadehfard and Wiley, 1995; Patocka et al., 2006). Additionally, we reported that dispersions with equal WPI contents had increasing viscosities with increasing sucrose contents (w/w), attributed to increased total solids contents, while surface tensions did not undergo notable changes. Experimental findings from Chapter 3 are generally in agreement: dispersions generally showed minimal changes in viscosities when increasing from 25 to 35% TS but increased significantly at 45% TS. Correspondingly, Chapter 3

results indicated that, for some formulations, dispersions containing 25% total solids (TS) had significantly higher surface tensions than dispersions with 35 and 45% TS. In addition, dispersions without Aronia extract polyphenols (PP) did not differ in average particle size when % TS increased. When PP were present, however, average particle sizes of dispersions increased with increasing % TS. These findings suggested the formation of protein-PP complexation interactions resulting in larger aggregated particles, since Aronia extract did not decrease system pH conditions sufficiently to reach the isoelectric point of proteins for enhanced protein aggregation.

7.1.3.2 Protein:sugar ratios

The effects of protein:sugar ratios in dispersions were examined in Chapters 3, 4, 5, and 6. In Chapter 3, alteration of WPI:sucrose ratios in feeds did not meaningfully impact surface tension values calculated from flow data. Although it would be expected that increased protein contents may provide more surface activity in the system, differences in WPI contents did not appear to be sufficient to affect calculated values. In dispersions containing WPI and soy protein isolate (SPI) studied in Chapter 4, increasing protein:sucrose ratios did not significantly affect surface tension. Surface tensions of dispersions formulated with pea protein isolate (PPI) significantly decreased with increasing protein:sucrose ratios. Chapter 5 reported little-to-no variation in surface tension as a result of differences in WPI:sucrose ratios, though values were generally slightly larger in dispersions with 1:1 WPI:sucrose ratios compared to those with 1:0 WPI:sucrose at the same % TS, with higher surface tensions attributed to the reduced protein contents in the system and thus reduced surface active properties (Kitabatake and Doi, 1988). Dispersions formulated with 0:1 WPI:sugar ratios in Chapter 6 had significantly higher surface

tensions than dispersions containing WPI at any WPI:sugar ratio, as the lack of proteins resulted in the lack of surface activity.

The overall effect of WPI:sucrose ratios on viscosity was found to be weak compared to the effect of % TS in Chapter 3; only formulations with 45% TS showed increased viscosities when WPI:sucrose ratios increased. Only a few formulations studied in Chapter 4 showed significant increases in viscosities when protein:sugar ratios were increased; most dispersions did not experience effects in viscosities with various protein:sugar ratios. Chapter 5 results reported that the viscosities of dispersions containing 1:0 WPI:sucrose were significantly higher than those containing 1:1 WPI:sucrose at the same % TS, due to increased total protein concentrations more strongly enhancing viscosities. In Chapter 6 the viscosities of feeds with WPI present at any WPI:sugar ratio were significantly higher than the viscosities of 0:1 WPI:sugar solutions due to the concentration of biopolymers present.

Results from Chapter 3 reported that altered WPI:sucrose ratios had no significant effects on particle sizes in dispersions, suggesting that varied quantities of sucrose in the systems did not affect the occurrence of protein aggregation interactions. In agreement with the findings reported in Chapter 3, results from Chapter 4 indicated that variations in particle sizes due to formulation differences were relatively small as protein:sucrose ratios in dispersions changed. Chapter 5 results indicated only very slight differences between the particle sizes of dispersions with 1:1 WPI:sucrose and 1:0 WPI:sucrose. Particle sizes of dispersions were not significantly affected by WPI:sugar ratios in Chapter 6 as well.

7.1.3.3 Protein sources

Chapter 4 investigated the effects of protein sources with different compositions and total protein contents on the physico-chemical properties of dispersions, comparing formulations with

WPI, SPI, or PPI. WPI had the lowest water hydration capacity of the isolates and the smallest pellets formed upon centrifugation, indicative of its superior solubility. PPI had the highest water hydration capacity and formed the largest pellets upon centrifugation, suggesting lower solubility. Protein isolate type was found to have a significant effect on the surface tension of dispersions, with WPI dispersions having the highest surface tensions and PPI dispersions the lowest. Protein type also had a significant effect on viscosity, potentially influenced by differing purities of isolates; WPI dispersions had the lowest average viscosities, and PPI the highest, in agreement with the findings from other studies (Krstonošić et al., 2020). Average particle sizes of dispersions were also significantly different. PPI dispersions had the largest average particle sizes, while WPI dispersions had the smallest, confirmed by observations via optical microscopy. Differences in the physico-chemical properties of dispersions formulated with different protein isolates were primarily attributed to their structural differences and available sites for interactions with water, PP, and other proteins, though solubility would strongly affect functional properties as well.

7.1.3.4 Carbohydrates

One objective of Chapter 6 was to explore effects of differences of sucrose, maltitol, and trehalose formulations on the physico-chemical properties of feed dispersions for subsequent bead formation, though no major differences were expected given the corresponding molecular masses of these carbohydrates (Hartel et al., 2018). Surface tensions and viscosities of dispersions were not significantly affected by carbohydrates used in formulations. Unsurprisingly, the differences in average particle sizes of dispersions containing each respective carbohydrate were negligible, in agreement with our hypothesis.

7.1.3.5 Bioactives concentrations

The effects of bioactives concentrations on the physical properties of dispersions were investigated in Chapters 3, 4, 5, and 6. Plant extracts containing bioactives slightly decreased the pH of protein-sugar dispersions in all experiments, due to the low pH of extracts containing phenolic acids. Chapter 3 reported little-to-no variation in the surface tensions of most WPI:sucrose dispersions with increasing Aronia extract PP, though few formulations experienced increased surface tensions with increased PP concentrations. Protein-sucrose dispersions formulated with WPI and SPI did not experience significant changes in surface tensions with increasing Aronia PP concentrations in Chapter 4, but the surface tensions of PPI dispersions increased significantly with increasing PP concentrations. Chapter 5 reported generally increasing trends in the surface tensions of WPI:sucrose dispersions with increasing bioactives concentrations from pure gallotannin and Aronia and cranberry extracts, but no significant shifts in surface tension when dispersions had varying beet extract bioactives concentrations. In Chapter 6, the presence of 1% Aronia PP in dispersions containing WPI had no significant effect on surface tensions, though when WPI was absent, the presence of 1% PP decreased the surface tensions of sugar and polyol solutions likely due to the slight surface activity from minor constituents in the extract.

The viscosities of WPI:sucrose dispersions with 45% TS in Chapter 3 were found to significantly increase with increasing PP concentrations, though the majority of formulations did not significantly change with altered PP concentrations indicating the weak effect of PP concentration on viscosity. Chapter 4 also reported that most formulations studied showed negligible differences in viscosities with changing Aronia PP concentrations. Dispersions formulated with PPI generally had decreasing viscosities with increasing PP concentrations, as

insoluble PPI particles and aggregates were generally larger than protein-PP complexes and enhanced the viscosities of dispersions with low/no PP. SPI-sucrose dispersions with higher SPI contents had increased viscosities at high PP concentrations resulting from the enhanced capacities of hydrolyzed protein structures for PP complexation. Viscosities of WPI:sucrose dispersions in Chapter 5 increased significantly when cranberry PP concentrations increased, but shifts caused by altered gallotannin and Aronia and beet extract bioactives concentrations were negligible. In Chapter 6, WPI:sucrose feeds with 1% Aronia PP had significantly higher viscosities than those without PP, due to the formation of protein-PP interactions and complexed aggregates enhancing viscosities.

Particle sizes of WPI:sucrose dispersions were found to be weakly affected by PP concentrations in Chapter 3, with particle sizes decreasing upon PP addition to dispersions, in agreement with the findings of other researchers and attributed to the formation of protein-PP complexes preventing protein-protein interactions and aggregation (Siebert et al., 1996; Thongkaew et al., 2014; Xue et al., 2020). Chapter 4 reported little-to-no differences in the particle sizes of WPI dispersions, slightly increased particle sizes in SPI dispersions, and generally decreasing particle sizes in PPI dispersions as PP concentrations increased due to the formation of protein-PP complexation interactions driving the formation of aggregates. Particle sizes of WPI:sucrose dispersions generally did not change with increasing bioactives concentrations in Chapter 5, though few formulations had slightly increased sizes with increasing cranberry and gallotannin PP concentrations. In Chapter 6, particle sizes of WPI:sucrose dispersions decreased with 1% PP, compared to those without PP.

7.1.3.6 Bioactives sources

Chapter 5 studied the effects of bioactives sources on the physico-chemical properties of WPI:sucrose dispersions intended for subsequent bead formation. The effects of pure gallotannin (polymeric, hydrolysable tannin PP) and extracts from Aronia (rich in monomeric anthocyanin PP), cranberry (rich in polymeric, condensed proanthocyanidin tannin PP), and beet (rich in small betacyanin compounds) were compared due to the diverse molecular sizes and structures of predominant compounds. All bioactives sources slightly reduced the pH of dispersions, although gallotannin had the smallest effect. Feeds formulated with cranberry extract had significantly higher surface tensions than those with Aronia and beet extracts, due to cranberry proanthocyanidins having higher degrees of polymerization and more groups available for interactions. Surface tensions of dispersions with gallotannin were not significantly different from those with cranberry, Aronia, or beet extracts. Bioactives sources were found to significantly affect the average particle sizes of dispersions: beet extract dispersions had the smallest sizes, followed by Aronia extract, then gallotannin was significantly larger, and cranberry extract were significantly larger yet, suggesting cranberry PP had the largest propensity for protein interactions. The average viscosities of dispersions prepared with cranberry extract were also significantly higher than those formulated with other bioactives sources. Larger bioactives structures with more side groups available for interactions with proteins tended to have greater impacts on the physical properties of dispersions as complexation interactions were enhanced, in agreement with results from other researchers (Girard et al., 2019).

7.1.4 Effects of formulation on the physical properties of dry beads

Chapters 2 and 6 studied the effects of composition on the physical properties of dried beads formed by feed dispersions as well as those of the dispersions. Chapter 2 reported that dispersions with 40% WPI w/w and 40% WPI with 10% sucrose produced uniform, spherical beads with similar porosities. Vacuum oven drying to remove water from bead structures resulted in the shrinkage of larger drops formed with only WPI, but shrinkage was prevented when formulating with sucrose due to the formation of sugar glass for structure stabilization. The formation of the sucrose glass in 40% WPI, 10% sucrose beads resulted in reduced hardness compared to dry 40% WPI beads, with brittle glassy regions breaking up the dried, dense protein gel network and enhancing structural fragility.

Chapter 6 reported that beads formed with freeze granulation had corresponding water contents, but lower water activity (a_w) values than those produced in Chapter 2. Beads formed without WPI had higher water contents and a_w than those with WPI, indicative of protein behavior as a drying aid (Kadoya et al., 2010). Different WPI:sugar ratios generally did not strongly impact the glass transition (T_g) temperatures of dried beads, though some formulations with higher protein contents had slightly greater T_g values, due to the higher T_g values of proteins as a result of their large molecular masses (Sarciaux and Hageman, 1997; Tzannis and Prestrelski, 1999). The presence of 1% Aronia PP resulted in slightly increased (< 2˚C) T_g onset temperatures in beads, indicating that small amounts of bioactives in formulations did not strongly impact the T_g of beads, suggesting preservation of their physical stability. Beads formed with trehalose had the highest T_g onset temperatures, while those made with maltitol had the lowest T_g. Beads formulated without WPI were harder than beads containing WPI, which may have been a result of the breaking up of the hard, continuous glassy phase with protein particles

and complexed protein-PP aggregates dispersed throughout. Changing WPI:sugar ratios showed no meaningful trends for many formulations, though sometimes increased ratios resulted in the slight softening of bead structures. Similarly, the presence of 1% Aronia PP did not strongly affect the hardness of dry beads when WPI was present, though the hardness of beads with sucrose and trehalose without PP tended to be slightly higher than those of beads containing 1% PP. When comparing the average hardness values of all beads comprised of each respective sugar or polyol, maltitol beads were least hard and trehalose beads were hardest. Hardness of beads was more strongly influenced by the presence of WPI in formulations than sugar or polyol type.

7.2 Applications of outcomes

The process designs presented in this thesis demonstrate potential for developing high protein foods with hydrophilic and hydrophobic phases that could act as carriers for entrapped flavors, colors, emulsion droplets, and bioactives. These processes provide novel alternatives to traditional drying or extrusion methods. Careful selection of wall materials based on their physico-chemical properties can result in formulated structures with enhanced physical stabilities, suggesting enhanced protection of entrapped sensitive compounds.

This work also provides information on the physico-chemical properties of highly concentrated dispersions, which can be practically applied for the formulation of high protein products. It documents the effects of mixing protein wall materials from various sources with a variety of bioactive compounds intended for encapsulation on the physical properties of liquid dispersions. Measurable changes in the physical properties of dispersions reported in these investigations contribute data to the more limited body of research describing the physico-chemical effects of naturally occurring non-covalent complexation interactions between proteins

and bioactives in mixtures under neutral and acidic pH conditions and ambient temperatures, especially regarding changes in viscosity.

These data may be useful for further applications such as the formulation of functional nutritional foods with high protein and bioactive compounds, while also maintaining desirable textural attributes and color retention during formulation, processing, and storage. The development of products including (but not limited to) nutritional bars, sports beverages, smoothies, yogurts, and frozen desserts may benefit from the information provided in this thesis. The development of foods with unique textures and functional attributes may be driven by selective formulation of mixtures with proteins and bioactives to enhance interactions and aggregate formation.

7.3 Recommendations for future research

With the understanding of the physical properties of dispersions and the physical states of resulting dried beads reported in this thesis, it would be prudent to design future studies to evaluate bead structures as encapsulating matrices. Shelf life stability and retention studies for entrapped bioactive compounds could be utilized to determine the protectant abilities of bead matrices as well as their efficacy as encapsulants to optimize formulations for enhanced protection. Different processing factors such as the number of processing steps, oxygen exposure, and heat duration are known to affect the bioactives content and antioxidant capacity retention in food products (Hager et al., 2008). Chemical reactions during processing and storage can also result in the formation of process derived products that alter the phenolic profiles and bioactivity in products (Debelo et al., 2020; Howard et al., 2012). While larger molecular mass PP have been reported to have limited absorption, their conversion to smaller compounds in the large intestine by gut microbes results in enhanced absorption and health benefits (Howard et al.,

2012). Performing extractions and subsequent quantification experiments after each step in the bead formation processes would yield data indicating the effects of processing on the retention of the actives in formulations, suggesting their potential bioavailability. In-vitro simulated digestion/ dissolution experiments would be useful to examine the delivery and release of bioactive compounds upon ingestion and may also highlight the effects of processing and protein-bioactives complexation interactions on the bioaccessibility and bioactivity of encapsulated compounds (Cilla et al., 2018).

References

Adhikari, B., Howes, T., Bhandari, B. R., & Langrish, T. A. G. (2009). Effect of addition of proteins on the production of amorphous sucrose powder through spray drying. *J. Food Eng*, *94*(2), 144–153. https://doi.org/10.1016/j.jfoodeng.2009.01.029

Afifi, H. S., Abu Shelaibi, A. A., Laleye, L. C., & Ismail, I. A. (2009). Measurement of thermal characteristics of spray-dried milk and juice blend. *Int J Food Sci Nutr*, *60*(sup7), 89–98. https://doi.org/10.1080/09637480802595526

Ahmed, J., Ramaswamy, H. S., & Raghavan, V. G. S. (2008). Dynamic viscoelastic, calorimetric and dielectric characteristics of wheat protein isolates. *Journal of Cereal Science*, *47*(3), 417–428. https://doi.org/10.1016/j.jcs.2007.05.013

Akbar Hussain, E., Sadiq, Z., & Zia-Ul-Haq, M. (2018). *Betalains: Biomolecular Aspects*. Springer International Publishing. https://doi.org/10.1007/978-3-319-95624-4

Alawode, A. O. (2014). *Quantification of protein fractions in aqueous phases of whey and emulsions* [Masters Food Science]. Swedish University of Agricultural Sciences.

Alizadehfard, M. R., & Wiley, D. E. (1995). Viscosity of whey protein solutions. *Iranian Journal of Polymer Science and Technology*, *4*(2), 126–133.

Allison, S. D., Chang, B., Randolph, T. W., & Carpenter, J. F. (1999). Hydrogen bonding between sugar and protein Is responsible for inhibition of dehydration-induced protein unfolding. *Arch. Biochem. Biophys.*, *365*(2), 289–298. https://doi.org/10.1006/abbi.1999.1175

Al-Marhoobi, I. M., & Kasapis, S. (2005). Further evidence of the changing nature of biopolymer networks in the presence of sugar. *Carbohydrate Research*, *340*(4), 771–774. https://doi.org/10.1016/j.carres.2004.12.018

Aschemann-Witzel, J., & Peschel, A. O. (2019). Consumer perception of plant-based proteins: The value of source transparency for alternative protein ingredients. *Food Hydrocolloids*, *96*, 20–28. https://doi.org/10.1016/j.foodhyd.2019.05.006

Augustin, M. A., & Oliver, C. M. (2014). Use of Milk Proteins for Encapsulation of Food Ingredients. In *Microencapsulation in the Food Industry* (pp. 211–226). Elsevier. https://doi.org/10.1016/B978-0-12-404568-2.00019-4

Auty, M. A. E., Twomey, M., Guinee, T. P., & Mulvihill, D. M. (2001). Development and application of confocal scanning laser microscopy methods for studying the distribution of fat and protein in selected dairy products. *Journal of Dairy Research*, *68*(03). https://doi.org/10.1017/S0022029901004873

Baba, W. N., McClements, D. J., & Maqsood, S. (2021). Whey protein–polyphenol conjugates and complexes: Production, characterization, and applications. *Food Chemistry*, *365*, 130455. https://doi.org/10.1016/j.foodchem.2021.130455

Baier, S., & McClements, D. J. (2001). Impact of preferential interactions on thermal stability and gelation of bovine serum albumin in aqueous sucrose solutions. *J Agr Food Chem*, *49*(5), 2600–2608. https://doi.org/10.1021/jf001096j

Bąkowska, A., Kucharska, A. Z., & Oszmiański, J. (2003). The effects of heating, UV irradiation, and storage on stability of the anthocyanin–polyphenol copigment complex. *Food Chem*, *81*(3), 349–355. https://doi.org/10.1016/S0308-8146(02)00429-6

Bakowska-Barczak, A. M., & Kolodziejczyk, P. P. (2011). Black currant polyphenols: Their storage stability and microencapsulation. *Ind Crop Prod*, *34*(2), 1301–1309. https://doi.org/10.1016/j.indcrop.2010.10.002

Bandyopadhyay, P., Ghosh, A. K., & Ghosh, C. (2012). Recent developments on polyphenol–protein interactions: Effects on tea and coffee taste, antioxidant properties and the digestive system. *Food & Function*, *3*(6), 592. https://doi.org/10.1039/c2fo00006g

Banovic, M., Arvola, A., Pennanen, K., Duta, D. E., Brückner-Gühmann, M., Lähteenmäki, L., & Grunert, K. G. (2018). Foods with increased protein content: A qualitative study on European consumer preferences and perceptions. *Appetite*, *125*, 233–243. https://doi.org/10.1016/j.appet.2018.01.034

Barthelmes, G., Pratsinis, S. E., & Buggisch, H. (2003). Particle size distributions and viscosity of suspensions undergoing shear-induced coagulation and fragmentation. *Chemical Engineering Science*, *58*(13), 2893–2902. https://doi.org/10.1016/S0009-2509(03)00133-7

Bayraktar, M. K., Harbourne, N. B., & Fagan, C. C. (2019). Impact of heat treatment and acid gelation on polyphenol enriched milk samples. *LWT*, *113*, 108282. https://doi.org/10.1016/j.lwt.2019.108282

Bazaria, B., & Kumar, P. (2016). Effect of whey protein concentrate as drying aid and drying parameters on physicochemical and functional properties of spray dried beetroot juice concentrate. *Food Bioscience*, *14*, 21–27. https://doi.org/10.1016/j.fbio.2015.11.002

Bengoechea, C., Arrachid, A., Guerrero, A., Hill, S. E., & Mitchell, J. R. (2007). Relationship between the glass transition temperature and the melt flow behavior for gluten, casein and soya. *Journal of Cereal Science*, *45*(3), 275–284. https://doi.org/10.1016/j.jcs.2006.08.011

Bermudez-Soto, M., Larrosa, M., Garciacantalejo, J., Espin, J., Tomasbarberan, F., & Garciaconesa, M. (2007). Up-regulation of tumor suppressor carcinoembryonic antigen-related cell adhesion molecule 1 in human colon cancer Caco-2 cells following repetitive exposure to dietary levels of a polyphenol-rich chokeberry juice. *J Nutr Biochem*, *18*(4), 259–271. https://doi.org/10.1016/j.jnutbio.2006.05.003

Bhatta, S., Stevanovic Janezic, T., & Ratti, C. (2020). Freeze-Drying of Plant-Based Foods. *Foods*, *9*(1), 87. https://doi.org/10.3390/foods9010087

Biesalski, H.-K., Dragsted, L. O., Elmadfa, I., Grossklaus, R., Müller, M., Schrenk, D., Walter, P., & Weber, P. (2009). Bioactive compounds: Definition and assessment of activity. *Nutrition*, *25*(11–12), 1202–1205. https://doi.org/10.1016/j.nut.2009.04.023

Bilbao-Sainz, C., Sinrod, A. J. G., Chiou, B., & McHugh, T. (2019). Functionality of strawberry powder on frozen dairy desserts. *J Texture Stud*, *50*(6), 556–563. https://doi.org/10.1111/jtxs.12464

Bilbao-Sainz, C., Thai, S., Sinrod, A. J. G., Chiou, B., & McHugh, T. (2019). Functionality of freeze-dried berry powder on frozen dairy desserts. *J Food Process Preserv*, *43*(9). https://doi.org/10.1111/jfpp.14076

Bleiel, S. B., Kent, R. M., & Brodkorb, A. (2017). Encapsulation Efficiency and Capacity of Bioactive Delivery Systems. In Y. H. Roos & Y. D. Livney (Eds.), *Engineering Foods for Bioactives Stability and Delivery* (pp. 171–197). Springer Science+ Business Media.

Bohin, M. C., Vincken, J.-P., van der Hijden, H. T. W. M., & Gruppen, H. (2012). Efficacy of food proteins as carriers for flavonoids. *J Agr Food Chem*, *60*(16), 4136–4143. https://doi.org/10.1021/jf205292r

Buitimea-Cantúa, N. E., Gutiérrez-Uribe, J. A., & Serna-Saldívar, S. O. (2018). Phenolic–Protein Interactions: Effects on Food Properties and Health Benefits. *Journal of Medicinal Food*, *21*(2), 188–198.

Burey, P., Bhandari, B. R., Howes, T., & Gidley, M. J. (2008). Hydrocolloid gel particles: Formation, characterization, and application. *Crit Rev Food Sci Nutr*, *48*(5), 361–377. https://doi.org/10.1080/10408390701347801

Cai, Y. Z., & Corke, H. (2000). Production and properties of spray-dried amaranthus betacyanin pigments. *J Food Sci*, *65*(7), 1248–1252. https://doi.org/10.1111/j.1365-2621.2000.tb10273.x

Calderón-Oliver, M., & Ponce-Alquicira, E. (2018). Fruits: A Source of Polyphenols and Health Benefits. In A. M. Grumezescu & A. M. Holban (Eds.), *Natural and Artificial Flavoring Agents and Dyes* (Vol. 7, pp. 189–228). Academic Press.

Cao, H., Saroglu, O., Karadag, A., Diaconeasa, Z., Zoccatelli, G., Conte-Junior, C. A., Gonzalez-Aguilar, G. A., Ou, J., Bai, W., Zamarioli, C. M., Freitas, L. A. P., Shpigelman, A., Campelo, P. H., Capanoglu, E., Hii, C. L., Jafari, S. M., Qi, Y., Liao, P., Wang, M., … Xiao, J. (2021). Available technologies on improving the stability of polyphenols in food processing. *Food Frontiers*, fft2.65. https://doi.org/10.1002/fft2.65

Cao, Y., & Xiong, Y. L. (2017). Interaction of Whey Proteins with Phenolic Derivatives Under Neutral and Acidic pH Conditions: Protein-phenolic interaction…. *Journal of Food Science*, *82*(2), 409–419. https://doi.org/10.1111/1750-3841.13607

Cardona, S., Schebor, C., Buera, M. P., Karel, M., & Chirife, J. (1997). Thermal Stability of Invertase in Reduced-Moisture Amorphous Matrices in Relation to Glassy State and Trehalose Crystallization. *Journal of Food Science*, *62*(1), 105–112. https://doi.org/10.1111/j.1365-2621.1997.tb04378.x

Cassidy, A., Mukamal, K. J., Liu, L., Franz, M., Eliassen, A. H., & Rimm, E. B. (2013). High anthocyanin intake Is associated with a reduced risk of myocardial infarction in young and middle-aged women. *Circulation*, *127*(2), 188–196. https://doi.org/10.1161/CIRCULATIONAHA.112.122408

Castañeda-Ovando, A., Pacheco-Hernández, Ma. de L., Páez-Hernández, Ma. E., Rodríguez, J. A., & Galán-Vidal, C. A. (2009). Chemical studies of anthocyanins: A review. *Food Chem*, *113*(4), 859–871. https://doi.org/10.1016/j.foodchem.2008.09.001

Chan, E.-S., Lee, B.-B., Ravindra, P., & Poncelet, D. (2009). Prediction models for shape and size of ca-alginate macrobeads produced through extrusion–dripping method. *J Colloid Interface Sci*, *338*(1), 63–72. https://doi.org/10.1016/j.jcis.2009.05.027

Chang, L. (Lucy), & Pikal, M. J. (2009). Mechanisms of protein stabilization in the solid state. *J Pharm Sci*, *98*(9), 2886–2908. https://doi.org/10.1002/jps.21825

Chang, L. (Lucy), Shepherd, D., Sun, J., Ouellette, D., Grant, K. L., Tang, X. (Charlie), & Pikal, M. J. (2005). Mechanism of protein stabilization by sugars during freeze-drying and storage: Native structure preservation, specific interaction, and/or immobilization in a glassy matrix? *J Pharm Sci*, *94*(7), 1427–1444. https://doi.org/10.1002/jps.20364

Charlton, A. J., Baxter, N. J., Khan, M. L., Moir, A. J. G., Haslam, E., Davies, A. P., & Williamson, M. P. (2002). Polyphenol/peptide binding and precipitation. *J Agr Food Chem*, *50*(6), 1593–1601. https://doi.org/10.1021/jf010897z

Chen, L., Remondetto, G. E., & Subirade, M. (2006). Food protein-based materials as nutraceutical delivery systems. *Trends in Food Science & Technology*, *17*(5), 272–283. https://doi.org/10.1016/j.tifs.2005.12.011

Chung, C., Rojanasasithara, T., Mutilangi, W., & McClements, D. J. (2015). Enhanced stability of anthocyanin-based color in model beverage systems through whey protein isolate complexation. *Food Res Int*, *76*, 761–768. https://doi.org/10.1016/j.foodres.2015.07.003

Cilla, A., Bosch, L., Barberá, R., & Alegría, A. (2018). Effect of processing on the bioaccessibility of bioactive compounds – A review focusing on carotenoids, minerals, ascorbic acid, tocopherols and polyphenols. *Journal of Food Composition and Analysis*, *68*, 3–15. https://doi.org/10.1016/j.jfca.2017.01.009

Coleman, C. M., & Ferreira, D. (2020). Oligosaccharides and Complex Carbohydrates: A New Paradigm for Cranberry Bioactivity. *Molecules*, *25*(4), 881. https://doi.org/10.3390/molecules25040881

Corradini, D., Strekalova, E. G., Stanley, H. E., & Gallo, P. (2013). Microscopic mechanism of protein cryopreservation in an aqueous solution with trehalose. *Sci Rep*, *3*(1). https://doi.org/10.1038/srep01218

Correia, R., Grace, M. H., Esposito, D., & Lila, M. A. (2017). Wild blueberry polyphenol-protein food ingredients produced by three drying methods: Comparative physico-chemical properties, phytochemical content, and stability during storage. *Food Chem*, *235*, 76–85. https://doi.org/10.1016/j.foodchem.2017.05.042

Coupland, J. N. (2014). *An Introduction to the Physical Chemistry of Food* (illustrated ed.). Springer Science+ Business Media.

Ćujić, N., Kardum, N., Šavikin, K., Zdunić, G., Janković, T., & Menković, N. (2018). Potential of chokeberry (Aronia melanocarpa L.) as a therapeutic food. In *Therapeutic Foods* (Vol. 8, pp. 209–237). Academic Press- Elsevier Inc.

Dabas, D. (2016). Polyphenols as Colorants. *Adv Food Technol Nutr Sci Open J*, *SE*(2), S1–S6. https://doi.org/10.17140/AFTNSOJ-SE-2-101

de Mejia, E. G., Zhang, Q., Penta, K., Eroglu, A., & Lila, M. A. (2020). The Colors of Health: Chemistry, Bioactivity, and Market Demand for Colorful Foods and Natural Food Sources of Colorants. *Annual Review of Food Science and Technology*, *11*(1), 145–182. https://doi.org/10.1146/annurev-food-032519-051729

Debelo, H., Li, M., & Ferruzzi, M. G. (2020). Processing influences on food polyphenol profiles and biological activity. *Current Opinion in Food Science*, *32*, 90–102. https://doi.org/10.1016/j.cofs.2020.03.001

Demetriades, K., & McClements, D. J. (1998). Influence of pH and Heating on Physicochemical Properties of Whey Protein-Stabilized Emulsions Containing a Nonionic Surfactant. *Journal of Agricultural and Food Chemistry*, *46*(10), 3936–3942. https://doi.org/10.1021/jf980463c

Desai, K. G. H., & Jin Park, H. (2005). Recent Developments in Microencapsulation of Food Ingredients. *Drying Technology*, *23*(7), 1361–1394. https://doi.org/10.1081/DRT-200063478

Dissanayake, M., Ramchandran, L., & Vasiljevic, T. (2013). Influence of pH and protein concentration on rheological properties of whey protein dispersions. *International Food Research Journal*, *20*(5), 2167.

Du, J., Ge, Z.-Z., Xu, Z., Zou, B., Zhang, Y., & Li, C.-M. (2014). Comparison of the efficiency of five different drying carriers on the spray drying of persimmon pulp powders. *Dry Technol*, *32*(10), 1157–1166. https://doi.org/10.1080/07373937.2014.886259

Ergun, R., Lietha, R., & Hartel, R. W. (2010). Moisture and shelf life in sugar confections. *Crit Rev Food Sci Nutr*, *50*(2), 162–192. https://doi.org/10.1080/10408390802248833

Ersus, S., & Yurdagel, U. (2007). Microencapsulation of anthocyanin pigments of black carrot (Daucus carota L.) by spray drier. *J. Food Eng*, *80*(3), 805–812. https://doi.org/10.1016/j.jfoodeng.2006.07.009

Fang, Z., & Bhandari, B. (2010). Encapsulation of polyphenols – a review. *Trends in Food Science & Technology*, *21*(10), 510–523. https://doi.org/10.1016/j.tifs.2010.08.003

Fang, Z., & Bhandari, B. (2011). Effect of spray drying and storage on the stability of bayberry polyphenols. *Food Chemistry*, *129*(3), 1139–1147. https://doi.org/10.1016/j.foodchem.2011.05.093

Fang, Z., & Bhandari, B. (2012). Comparing the efficiency of protein and maltodextrin on spray drying of bayberry juice. *Food Res Int*, *48*(2), 478–483. https://doi.org/10.1016/j.foodres.2012.05.025

Fang, Z., & Bhandari, B. (2017). Spray Drying of Bioactives. In Y. H. Roos & Y. D. Livney (Eds.), *Engineering Foods for Bioactives Stability and Delivery* (pp. 261–284). Springer.

Fennema, O. R. (2017). *Fennema's Food Chemistry* (S. Damodaran & K. L. Parkin, Eds.; 5th ed.). CRC Press Taylor & Francis Group.

Fitzpatrick, J. J., Iqbal, T., Delaney, C., Twomey, T., & Keogh, M. K. (2004). Effect of powder properties and storage conditions on the flowability of milk powders with different fat contents. *Journal of Food Engineering*, *64*(4), 435–444. https://doi.org/10.1016/j.jfoodeng.2003.11.011

Fitzsimons, S. M., Mulvihill, D. M., & Morris, E. R. (2007). Denaturation and aggregation processes in thermal gelation of whey proteins resolved by differential scanning calorimetry. *Food Hydrocolloids*, *21*(4), 638–644. https://doi.org/10.1016/j.foodhyd.2006.07.007

Fleming, S. E., Sosulski, F. W., Kilara, A., & Humbert, E. S. (1974). Viscosity and water absorption characteristics of slurries of sunflower and soybean flours, concentrates and isolates. *J Food Sci*, *39*(1), 188–192. https://doi.org/10.1111/j.1365-2621.1974.tb01019.x

Foegeding, E. A., Plundrich, N., Schneider, M., Campbell, C., & Lila, M. A. (2017). Protein-polyphenol particles for delivering structural and health functionality. *Food Hydrocoll.*, *72*, 163–173. https://doi.org/10.1016/j.foodhyd.2017.05.024

Francis, F. J., & Markakis, P. C. (1989). Food colorants: Anthocyanins. *Crit Rev Food Sci Nutr*, *28*(4), 273–314. https://doi.org/10.1080/10408398909527503

Friedman, M., & Jürgens, H. S. (2000). Effect of pH on the stability of plant phenolic compounds. *J Agr Food Chem*, *48*(6), 2101–2110. https://doi.org/10.1021/jf990489j

Fuhrmann, P. L., Sala, G., Stieger, M., & Scholten, E. (2019). Clustering of oil droplets in o/w emulsions: Controlling cluster size and interaction strength. *Food Res Int*, *122*, 537–547. https://doi.org/10.1016/j.foodres.2019.04.027

Fuhrmeister, H., & Meuser, F. (2003). Impact of processing on functional properties of protein products from wrinkled peas. *Journal of Food Engineering*, *56*(2–3), 119–129. https://doi.org/10.1016/S0260-8774(02)00241-8

Gad, A. S., & El-Salam, M. H. A. (2010). The antioxidant properties of skim milk supplemented with rosemary and green tea extracts in response to pasteurisation, homogenisation and the addition of salts. *International Journal of Dairy Technology*, *63*(3), 349–355. https://doi.org/10.1111/j.1471-0307.2010.00585.x

Gerrard, J. A. (2002). Protein–protein crosslinking in food: Methods, consequences, applications. *Trends Food Sci Technol*, *13*(12), 391–399.

Girard, A. L., & Awika, J. M. (2020). Effects of edible plant polyphenols on gluten protein functionality and potential applications of polyphenol–gluten interactions. *Comprehensive Reviews in Food Science and Food Safety*, *19*(4), 2164–2199. https://doi.org/10.1111/1541-4337.12572

Girard, A. L., Bean, S. R., Tilley, M., Adrianos, S. L., & Awika, J. M. (2018). Interaction mechanisms of condensed tannins (proanthocyanidins) with wheat gluten proteins. *Food Chem*, *245*, 1154–1162. https://doi.org/10.1016/j.foodchem.2017.11.054

Girard, A. L., Castell-Perez, M. E., Bean, S. R., Adrianos, S. L., & Awika, J. M. (2016). Effect of Condensed Tannin Profile on Wheat Flour Dough Rheology. *Journal of Agricultural and Food Chemistry*, *64*(39), 7348–7356. https://doi.org/10.1021/acs.jafc.6b02601

Girard, A. L., Teferra, T., & Awika, J. M. (2019). Effects of condensed vs hydrolysable tannins on gluten film strength and stability. *Food Hydrocolloids*, *89*, 36–43. https://doi.org/10.1016/j.foodhyd.2018.10.018

González, S. (2020). Dietary Bioactive Compounds and Human Health and Disease. *Nutrients*, *12*(2), 348. https://doi.org/10.3390/nu12020348

Hager, T. J., Howard, L. R., & Prior, R. L. (2008). Processing and Storage Effects on Monomeric Anthocyanins, Percent Polymeric Color, and Antioxidant Capacity of Processed Blackberry Products. *J Agr Food Chem*, *56*(3), 689–695. https://doi.org/10.1021/jf071994g

Hagerman, A. E. (1989). Chemistry of Tannin-Protein Complexation. In R. W. Hemingway, J. J. Karchesy, & S. J. Branham (Eds.), *Chemistry and Significance of Condensed Tannins* (pp. 323–333). Springer Boston, MA.

Hagerman, A. E., & Butler, L. G. (1978). Protein precipitation method for the quantitative determination of tannins. *J Agr Food Chem*, *26*(4), 809–812. https://doi.org/10.1021/jf60218a027

Hagerman, A. E., & Butler, L. G. (1981). The Specificity of Proanthocyanidin-Protein Interactions. *J Biol. Chem.*, *256*(9), 4494–4497.

Han, J., Chang, Y., Britten, M., St-Gelais, D., Champagne, C. P., Fustier, P., & Lacroix, M. (2019). Interactions of phenolic compounds with milk proteins. *European Food Research and Technology*, *245*(9), 1881–1888. https://doi.org/10.1007/s00217-019-03293-1

Hansen, M. M., Hartel, R. W., & Roos, Y. H. (2021a). *Effects of Aronia polyphenols on the physico-chemical properties of whey, soy, and pea protein isolate dispersions* [In Press, in Food Production, Processing and Nutrition].

Hansen, M. M., Hartel, R. W., & Roos, Y. H. (2021b). *Formation of dry beads for bioactives encapsulation by freeze granulation* [Manuscript submitted to Journal of Food Engineering].

Hansen, M. M., Hartel, R. W., & Roos, Y. H. (2021c). Encapsulant-bioactives interactions impact on physico-chemical properties of concentrated dispersions. *Journal of Food Engineering*, *302*, 110586. https://doi.org/10.1016/j.jfoodeng.2021.110586

Hansen, M. M., Hartel, R. W., & Roos, Y. H. (2021d). Formation of dry beads for bioactives encapsulation by freeze granulation. *Journal of Food Engineering*, 110847. https://doi.org/10.1016/j.jfoodeng.2021.110847

Hansen, M. M., Maidannyk, V. A., & Roos, Y. H. (2020). Thermal gelation and hardening of whey protein beads for subsequent dehydration and encapsulation using vitrifying sugars. *Journal of Food Engineering*, *279*, 109966. https://doi.org/10.1016/j.jfoodeng.2020.109966

Harbertson, J. F., Kilmister, R. L., Kelm, M. A., & Downey, M. O. (2014). Impact of condensed tannin size as individual and mixed polymers on bovine serum albumin precipitation. *Food Chemistry*, *160*, 16–21. https://doi.org/10.1016/j.foodchem.2014.03.026

Harbourne, N., Jacquier, J. C., & O'Riordan, D. (2011). Effects of addition of phenolic compounds on the acid gelation of milk. *Int Dairy J*, *21*(3), 185–191. https://doi.org/10.1016/j.idairyj.2010.10.003

Hartel, R. W., Ergun, R., & Vogel, S. (2011). Phase/State Transitions of Confectionery Sweeteners: Thermodynamic and Kinetic Aspects. *Comprehensive Reviews in Food Science and Food Safety*, *10*(1), 17–32. https://doi.org/10.1111/j.1541-4337.2010.00136.x

Hartel, R. W., von Elbe, J. H., & Hofberger, R. (2018). *Confectionery Science and Technology*. Springer International Publishing. https://doi.org/10.1007/978-3-319-61742-8

He, F., Woods, C. E., Litowski, J. R., Roschen, L. A., Gadgil, H. S., Razinkov, V. I., & Kerwin, B. A. (2011). Effect of sugar molecules on the viscosity of high concentration monoclonal antibody solutions. *Pharm Res*, *28*(7), 1552–1560. https://doi.org/10.1007/s11095-011-0388-7

Heljo, V. P., Jouppila, K., Hatanpää, T., & Juppo, A. M. (2011). The use of disaccharides in inhibiting enzymatic activity loss and secondary structure changes in freeze-dried β-galactosidase during storage. *Pharm Res*, *28*(3), 540–552. https://doi.org/10.1007/s11095-010-0300-x

Hermansson, A.-M. (1975). Functional properties of proteins for foods-flow properties. *J Texture Stud*, *5*(4), 425–439.

Hong, T., Iwashita, K., & Shiraki, K. (2018a). Viscosity Control of Protein Solution by Small Solutes: A Review. *Current Protein & Peptide Science*, *19*(8), 746–758. https://doi.org/10.2174/1389203719666171213114919

Hong, T., Iwashita, K., & Shiraki, K. (2018b). Viscosity control of protein solution by small solutes: A review. *Curr Protein Pept Sc*, *19*(8), 746–758. https://doi.org/10.2174/1389203719666171213114919

Howard, L. R., Prior, R. L., Liyanage, R., & Lay, J. O. (2012). Processing and Storage Effect on Berry Polyphenols: Challenges and Implications for Bioactive Properties. *Journal of Agricultural and Food Chemistry*, *60*(27), 6678–6693. https://doi.org/10.1021/jf2046575

Iglesias, H. A., Chirife, J., & Buera, M. P. (1997). Adsorption isotherm of amorphous trehalose. *J Sci Food Agric*, *75*, 183–186.

Imamura, K., Fukushima, A., Sakaura, K., Sugita, T., Sakiyama, T., & Nakanishi, K. (2002). Water sorption and glass transition behaviors of freeze-dried sucrose–dextran mixtures. *J Pharm Sci*, *91*(10), 2175–2181. https://doi.org/10.1002/jps.10218

Imamura, K., Iwai, M., Ogawa, T., Sakiyama, T., & Nakanishi, K. (2001). Evaluation of hydration states of protein in freeze-dried amorphous sugar matrix. *J Pharm Sci*, *90*(12), 1955–1963. https://doi.org/10.1002/jps.1146

Imamura, K., Ogawa, T., Sakiyama, T., & Nakanishi, K. (2003). Effects of types of sugar on the stabilization of protein in the dried state. *J Pharm Sci*, *92*(2), 266–274. https://doi.org/10.1002/jps.10305

Imamura, K., Suzuki, T., Kirii, S., Tatsumichi, T., & Okazaki, M. (1998). Influence of protein on phase transition of amorphous sugar. *J Chem Eng JPN*, *31*(3), 325–329.

Imamura, K., Yokoyama, T., Fukushima, A., Kinuhata, M., & Nakanishi, K. (2010). Water sorption, glass transition, and protein-stabilizing behavior of an amorphous sucrose matrix combined with various materials. *J Pharm Sci*, *99*(11), 4669–4677. https://doi.org/10.1002/jps.22162

Islesias, H. A., & Chirife, J. (1978). Delayed crystallization of amorphous sucrose in humidified freeze dried model systems. *Int J Food Sci Tech*, *13*(2), 137–144. https://doi.org/10.1111/j.1365-2621.1978.tb00787.x

Jansson, H., Bergman, R., & Swenson, J. (2011). Role of Solvent for the Dynamics and the Glass Transition of Proteins. *The Journal of Physical Chemistry B*, *115*(14), 4099–4109. https://doi.org/10.1021/jp1089867

Jean, K., Renan, M., Famelart, M.-H., & Guyomarc'h, F. (2006). Structure and surface properties of the serum heat-induced protein aggregates isolated from heated skim milk. *International Dairy Journal*, *16*(4), 303–315. https://doi.org/10.1016/j.idairyj.2005.04.001

Jena, S., Horn, J., Suryanarayanan, R., Friess, W., & Aksan, A. (2017). Effects of excipient interactions on the state of the freeze-concentrate and protein stability. *Pharm Res*, *34*(2), 462–478. https://doi.org/10.1007/s11095-016-2078-y

Jiang, J., Zhang, Z., Zhao, J., & Liu, Y. (2018). The effect of non-covalent interaction of chlorogenic acid with whey protein and casein on physicochemical and radical-scavenging activity of in vitro protein digests. *Food Chemistry*, *268*, 334–341. https://doi.org/10.1016/j.foodchem.2018.06.015

Johnson, J. F., Martin, J. R., & Porter, R. S. (1975). Determination of Viscosity of Food Systems. In *Theory, Determination and Control of Physical Properties of Food Materials* (Vol. 1, pp. 25–38). Springer.

Joye, I. J., & McClements, D. J. (2014). Biopolymer-based nanoparticles and microparticles: Fabrication, characterization, and application. *Curr. Opin. Colloid Interface Sci*, *19*(5), 417–427. https://doi.org/10.1016/j.cocis.2014.07.002

Kadoya, S., Fujii, K., Izutsu, K., Yonemochi, E., Terada, K., Yomota, C., & Kawanishi, T. (2010). Freeze-drying of proteins with glass-forming oligosaccharide-derived sugar alcohols. *Int. J. Pharm*, *389*(1–2), 107–113. https://doi.org/10.1016/j.ijpharm.2010.01.027

Kakivaya, S. R., & Hoeve, C. A. (1975). The glass point of elastin. *Proceedings of the National Academy of Sciences*, *72*(9), 3505–3507. https://doi.org/10.1073/pnas.72.9.3505

Kamerzell, T. J., Esfandiary, R., Joshi, S. B., Middaugh, C. R., & Volkin, D. B. (2011). Protein–excipient interactions: Mechanisms and biophysical characterization applied to protein formulation development. *Adv. Drug Deliv. Rev.*, *63*(13), 1118–1159. https://doi.org/10.1016/j.addr.2011.07.006

Kanakis, C. D., Hasni, I., Bourassa, P., Tarantilis, P. A., Polissiou, M. G., & Tajmir-Riahi, H.-A. (2011). Milk β-lactoglobulin complexes with tea polyphenols. *Food Chem*, *127*(3), 1046–1055. https://doi.org/10.1016/j.foodchem.2011.01.079

Kapsak, W. R., Rahavi, E. B., Childs, N. M., & White, C. (2011). Functional Foods: Consumer Attitudes, Perceptions, and Behaviors in a Growing Market. *Journal of the American Dietetic Association*, *111*(6), 804–810. https://doi.org/10.1016/j.jada.2011.04.003

Kawai, K., & Suzuki, T. (2007). Stabilizing effect of four types of disaccharide on the enzymatic activity of freeze-dried lactate dehydrogenase: Step by step evaluation from freezing to storage. *Pharm Res*, *24*(10), 1883–1890. https://doi.org/10.1007/s11095-007-9312-6

Khoo, H. E., Azlan, A., Tang, S. T., & Lim, S. M. (2017). Anthocyanidins and anthocyanins: Colored pigments as food, pharmaceutical ingredients, and the potential health benefits. *Food Nutr. Res.*, *61*(1), 1361779. https://doi.org/10.1080/16546628.2017.1361779

Kilara, A., & Harwalkar, V. R. (1996). Denaturation. In *Food proteins: Properties and characterization*. Wiley-VCH.

Kitabatake, N., & Doi, E. (1988). Surface Tension and Foamability of Protein and Surfactant Solutions. *Journal of Food Science*, *53*(5), 1542–1569. https://doi.org/10.1111/j.1365-2621.1988.tb09319.x

Kneifel, W., Paquin, P., Abert, T., & Richard, J.-P. (1991). Water-holding capacity of proteins with special regard to milk proteins and methodological aspects—A review. *J Dairy Sci*, *74*(7), 2027–2041. https://doi.org/10.3168/jds.S0022-0302(91)78373-2

Kornev, K. G., & Neimark, A. V. (2001). Spontaneous Penetration of Liquids into Capillaries and Porous Membranes Revisited. *Journal of Colloid and Interface Science*, *235*(1), 101–113. https://doi.org/10.1006/jcis.2000.7347

Krstonošić, V. S., Kalić, M. D., Dapčević-Hadnađev, T. R., Lončarević, I. S., & Hadnađev, M. S. (2020). Physico-chemical characterization of protein stabilized oil-in-water emulsions. *Colloids and Surfaces A: Physicochemical and Engineering Aspects*, *602*, 125045. https://doi.org/10.1016/j.colsurfa.2020.125045

Kulling, S., & Rawel, H. (2008). Chokeberry (Aronia melanocarpa)– A review on the characteristic components and potential health effects. *Planta Medica*, *74*(13), 1625–1634. https://doi.org/10.1055/s-0028-1088306

Kulmyrzaev, A., Bryant, C., & McClements, D. J. (2000). Influence of sucrose on the thermal denaturation, gelation, and emulsion stabilization of whey proteins. *J Agr Food Chem*, *48*(5), 1593–1597. https://doi.org/10.1021/jf9911949

La Lumia, F., Ramond, L., Pagnoux, C., & Bernard-Granger, G. (2019). Fabrication of homogenous pellets by freeze granulation of optimized TiO2-Y2O3 suspensions. *Journal of the European Ceramic Society*, *39*(6), 2168–2178. https://doi.org/10.1016/j.jeurceramsoc.2019.01.036

Laine, P., Kylli, P., Heinonen, M., & Jouppila, K. (2008). Storage stability of microencapsulated cloudberry (Rubus chamaemorus) phenolics. *J Agr Food Chem*, *56*(23), 11251–11261. https://doi.org/10.1021/jf801868h

Lakkis, J. M. (2016). *Encapsulation and Controlled Release Technologies in Food Systems* (2nd ed.). John Wiley & Sons.

Lam, A. C. Y., Can Karaca, A., Tyler, R. T., & Nickerson, M. T. (2018). Pea protein isolates: Structure, extraction, and functionality. *Food Reviews International*, *34*(2), 126–147. https://doi.org/10.1080/87559129.2016.1242135

Le Bourvellec, C., & Renard, C. M. G. C. (2012). Interactions between Polyphenols and Macromolecules: Quantification Methods and Mechanisms. *Critical Reviews in Food Science and Nutrition*, *52*(3), 213–248. https://doi.org/10.1080/10408398.2010.499808

Lee, B. B., & Chan, E. S. (2013). Size and shape of calcium alginate beads produced by extrusion dripping. *Chem Eng Technol*, *36*(10), 1627–1642. https://doi.org/10.1002/ceat.201300230

Lee, J. C., & Timasheff, S. N. (1981). The stabilization of proteins by sucrose. *J Biol. Chem.*, *256*(14), 7193–7201.

Levine, H., & Slade, L. (1992). Glass transitions in foods. In H. Schwartzberg & R. W. Hartel (Eds.), *Physical chemistry of foods* (pp. 83–221). Marcel Dekker, Inc.

Li, C., Dai, T., Chen, J., Li, X., Li, T., Liu, C., & McClements, D. J. (2021). Protein-polyphenol functional ingredients: The foaming properties of lactoferrin are enhanced by forming complexes with procyanidin. *Food Chemistry*, *339*, 128145. https://doi.org/10.1016/j.foodchem.2020.128145

Li, D., Wang, P., Luo, Y., Zhao, M., & Chen, F. (2017). Health benefits of anthocyanins and molecular mechanisms: Update from recent decade. *Crit Rev Food Sci Nutr*, *57*(8), 1729–1741. https://doi.org/10.1080/10408398.2015.1030064

Li, T. S. (2005). *Functional and Structural Properties of Molecular Soy Protein Fractions* [Doctor of Philosophy]. National University of Singapore.

Li, Y., He, D., Li, B., Lund, M. N., Xing, Y., Wang, Y., Li, F., Cao, X., Liu, Y., Chen, X., Yu, J., Zhu, J., Zhang, M., Wang, Q., Zhang, Y., Li, B., Wang, J., Xing, X., & Li, L. (2021). Engineering polyphenols with biological functions via polyphenol-protein interactions as additives for functional foods. *Trends in Food Science & Technology*, *110*, 470–482. https://doi.org/10.1016/j.tifs.2021.02.009

Liao, X., Krishnamurthy, R., & Suryanarayanan, R. (2005). Influence of the active pharmaceutical ingredient concentration on the physical state of mannitol—Implications in freeze-drying. *Pharm Res*, *22*(11), 1978–1985. https://doi.org/10.1007/s11095-005-7625-x

Livney, Y. D. (2010). Milk proteins as vehicles for bioactives. *Current Opinion in Colloid & Interface Science*, *15*(1–2), 73–83. https://doi.org/10.1016/j.cocis.2009.11.002

López-Díez, E. C., & Bone, S. (2000). An investigation of the water-binding properties of protein + sugar systems. *Phys. Med. Biol.*, *45*(12), 3577–3588. https://doi.org/10.1088/0031-9155/45/12/305

Lu, J., Wang, X.-J., Liu, Y.-X., & Ching, C.-B. (2007). Thermal and FTIR investigation of freeze-dried protein-excipient mixtures. *J. Therm. Anal. Calorim.*, *89*(3), 913–919. https://doi.org/10.1007/s10973-006-7598-y

Ma, C.-M., & Zhao, X.-H. (2019). Depicting the Non-Covalent Interaction of Whey Proteins with Galangin or Genistein Using the Multi-Spectroscopic Techniques and Molecular Docking. *Foods*, *8*(9), 360. https://doi.org/10.3390/foods8090360

Maher, P. G., Auty, M. A. E., Roos, Y. H., Zychowski, L. M., & Fenelon, M. A. (2015). Microstructure and lactose crystallization properties in spray dried nanoemulsions. *Food Structure*, *3*, 1–11. https://doi.org/10.1016/j.foostr.2014.10.001

Maidannyk, V. A., & Roos, Y. H. (2017). Water sorption, glass transition and "strength" of lactose – Whey protein systems. *Food Hydrocolloids*, *70*, 76–87. https://doi.org/10.1016/j.foodhyd.2017.03.025

Malik, M., Zhao, C., Schoene, N., Guisti, M. M., Moyer, M. P., & Magnuson, B. A. (2003). Anthocyanin-rich extract from Aronia meloncarpa E. induces a cell cycle block in colon cancer but not normal colonic cells. *Nutr. Cancer*, *46*(2), 186–196. https://doi.org/10.1207/S15327914NC4602_12

Martínez, J. H., Velázquez, F., Burrieza, H. P., Martínez, K. D., Paula Domínguez Rubio, A., dos Santos Ferreira, C., del Pilar Buera, M., & Pérez, O. E. (2019). Betanin loaded nanocarriers based on quinoa seed 11S globulin. Impact on the protein structure and antioxidant activity. *Food Hydrocolloids*, *87*, 880–890. https://doi.org/10.1016/j.foodhyd.2018.09.016

Matalanis, A., Jones, O. G., & McClements, D. J. (2011). Structured biopolymer-based delivery systems for encapsulation, protection, and release of lipophilic compounds. *Food Hydrocoll.*, *25*(8), 1865–1880. https://doi.org/10.1016/j.foodhyd.2011.04.014

Mazza, G., & Brouillard, R. (1987). Recent developments in the stabilization of anthocyanins in food products. *Food Chem*, *25*(3), 207–225. https://doi.org/10.1016/0308-8146(87)90147-6

Mazza, G., & Brouillard, R. (1990). The mechanism of co-pigmentation of anthocyanins in aqueous solutions. *Phytochemistry*, *29*(4), 1097–1102. https://doi.org/10.1016/0031-9422(90)85411-8

McClements, D. J. (2001). Estimation of steric exclusion and differential interaction contributions to protein transfer free energies in aqueous cosolvent solutions. *Food Hydrocoll.*, *15*(4–6), 355–363. https://doi.org/10.1016/S0268-005X(01)00045-5

McClements, D. J. (2002). Modulation of globular protein functionality by weakly interacting cosolvents. *Crit Rev Food Sci Nutr*, *42*(5), 417–471. https://doi.org/10.1080/20024091054210

McClements, D. J. (2017). Recent progress in hydrogel delivery systems for improving nutraceutical bioavailability. *Food Hydrocoll.*, *68*, 238–245. https://doi.org/10.1016/j.foodhyd.2016.05.037

McClements, D. J., Decker, E. A., Park, Y., & Weiss, J. (2009). Structural design principles for delivery of bioactive components in nutraceuticals and functional foods. *Crit Rev Food Sci Nutr*, *49*(6), 577–606. https://doi.org/10.1080/10408390902841529

Meister, E., & Gieseler, H. (2008). A significant comparison between collapse and glass transition temperatures. *European Pharmaceutical Review*, *5*.

Meister, E., & Gieseler, H. (2009). Freeze-dry microscopy of protein/sugar mixtures: Drying behavior, interpretation of collapse temperatures and a comparison to corresponding glass transition data. *J Pharm Sci*, *98*(9), 3072–3087. https://doi.org/10.1002/jps.21586

Mensink, M. A., Frijlink, H. W., van der Voort Maarschalk, K., & Hinrichs, W. L. J. (2017). How sugars protect proteins in the solid state and during drying (review): Mechanisms of stabilization in relation to stress conditions. *Eur. J. Pharm. Biopharm.*, *114*, 288–295. https://doi.org/10.1016/j.ejpb.2017.01.024

Miguel, M. (2018). Betalains in Some Species of the Amaranthaceae Family: A Review. *Antioxidants*, *7*(4), 53. https://doi.org/10.3390/antiox7040053

Mink, P. J., Scrafford, C. G., Barraj, L. M., Harnack, L., Hong, C.-P., Nettleton, J. A., & Jacobs, D. R. (2007). Flavonoid intake and cardiovascular disease mortality: A prospective study in postmenopausal women. *Am. J. Clin. Nutr*, *85*(3), 895–909. https://doi.org/10.1093/ajcn/85.3.895

Modi, S., Koelling, K., & Vodovotz, Y. (2012). Miscibility of poly(3-hydroxybutyrate-co-3-hydroxyvalerate) with high molecular weight poly(lactic acid) blends determined by thermal analysis. *Journal of Applied Polymer Science*, *124*(4), 3074–3081. https://doi.org/10.1002/app.35343

Morr, C. V. (1990). Current status of soy protein functionality in food systems. *Journal of the American Oil Chemists' Society*, *67*(5), 265–271. https://doi.org/10.1007/BF02539674

Moser, P., Gallo, T. C. B., Zuanon, L. A. C., Pereira, G. E., & Nicoletti, V. R. (2018). Water sorption and stickiness of spray-dried grape juice and anthocyanins stability. *J Food Process Preserv*, *42*(12), e13830. https://doi.org/10.1111/jfpp.13830

Moser, P., Souza, R. T. D., & Nicoletti Telis, V. R. (2017). Spray drying of grape juice from hybrid cv. BRS violeta: Microencapsulation of anthocyanins using protein/maltodextrin blends as drying aids. *J Food Process Preserv*, *41*(1), e12852. https://doi.org/10.1111/jfpp.12852

Moskovitz, J., Yim, M. B., & Chock, P. B. (2002). Free radicals and disease. *Arch. Biochem. Biophys.*, *397*(2), 354–359. https://doi.org/10.1006/abbi.2001.2692

Nicolai, T. (2016). Formation and functionality of self-assembled whey protein microgels. *Colloids and Surfaces B: Biointerfaces*, *137*, 32–38. https://doi.org/10.1016/j.colsurfb.2015.05.055

Nicolai, T., Britten, M., & Schmitt, C. (2011). β-lactoglobulin and WPI aggregates: Formation, structure and applications. *Food Hydrocoll.*, *25*(8), 1945–1962. https://doi.org/10.1016/j.foodhyd.2011.02.006

Nicolai, T., & Durand, D. (2013). Controlled food protein aggregation for new functionality. *Curr. Opin. Colloid Interface Sci*, *18*(4), 249–256. https://doi.org/10.1016/j.cocis.2013.03.001

Nilsson, E., & Larsson, A. (2007). Stability of chicken IgY antibodies freeze-dried in the presence of lactose, sucrose and threalose. *J. Poult. Sci.*, *44*, 58–62.

Oancea, A.-M., Aprodu, I., Râpeanu, G., Bahrim, G., & Stanciuc, N. (2017). The Binding mechanism of anthocyanins from sour cherries (*Prunus cerasus* L) skins to bovine β-lactoglobulin: A fluorescence and *in silico* -based approach. *International Journal of Food Properties*, *20*(sup3), S3096–S3111. https://doi.org/10.1080/10942912.2017.1343347

Obón, J. M., Castellar, M. R., Alacid, M., & Fernández-López, J. A. (2009). Production of a red–purple food colorant from Opuntia stricta fruits by spray drying and its application in food model systems. *J. Food Eng*, *90*(4), 471–479. https://doi.org/10.1016/j.jfoodeng.2008.07.013

Ohtake, S., Kita, Y., & Arakawa, T. (2011). Interactions of formulation excipients with proteins in solution and in the dried state. *Adv. Drug Deliv. Rev.*, *63*(13), 1053–1073. https://doi.org/10.1016/j.addr.2011.06.011

Ojha, H., Mishra, K., Hassan, M. I., & Chaudhury, N. K. (2012). Spectroscopic and isothermal titration calorimetry studies of binding interaction of ferulic acid with bovine serum albumin. *Thermochimica Acta*, *548*, 56–64. https://doi.org/10.1016/j.tca.2012.08.016

Oliveira, J., Mateus, N., & de Freitas, V. (2013). Flavanols: Catechins and Proanthocyanidins. In K. G. Ramawat & J.-M. Mérillon (Eds.), *Natural Products* (pp. 1753–1801). Springer Berlin Heidelberg. https://doi.org/10.1007/978-3-642-22144-6_58

Ouadaker, M., Jiang, X., Bowen, P., Bienia, M., Pagnoux, C., & Aimable, A. (2020). Porous granules by freeze granulation of Pickering emulsions stabilized with halloysite particles. *Colloids and Surfaces A: Physicochemical and Engineering Aspects*, *585*, 124156. https://doi.org/10.1016/j.colsurfa.2019.124156

Owusu-Ansah, Y. J., & McCurdy, S. M. (1991). Pea proteins: A review of chemistry, technology of production, and utilization. *Food Rev. Int.*, *7*(1), 103–134. https://doi.org/10.1080/87559129109540903

Ozdal, T., Capanoglu, E., & Altay, F. (2013). A review on protein–phenolic interactions and associated changes. *Food Res Int*, *51*(2), 954–970. https://doi.org/10.1016/j.foodres.2013.02.009

Pang, S. F., Yusoff, M. M., & Gimbun, J. (2014). Assessment of phenolic compounds stability and retention during spray drying of Orthosiphon stamineus extracts. *Food Hydrocoll.*, *37*(Supplement C), 159–165. https://doi.org/10.1016/j.foodhyd.2013.10.022

Patocka, G., Cervenkova, R., Narine, S., & Jelen, P. (2006). Rheological behaviour of dairy products as affected by soluble whey protein isolate. *Int Dairy J*, *16*(5), 399–405. https://doi.org/10.1016/j.idairyj.2005.05.010

Petruccelli, S., & Añón, M. C. (1995). Soy Protein Isolate Components and Their Interactions. *Journal of Agricultural and Food Chemistry*, *43*(7), 1762–1767. https://doi.org/10.1021/jf00055a004

Pikal, M. J., Rigsbee, D. R., & Roy, M. L. (2007). Solid state chemistry of proteins: I. Glass transition behavior in freeze dried disaccharide formulations of human growth hormone (HGH). *J Pharm Sci*, *96*(10), 2765–2776. https://doi.org/10.1002/jps.20960

Pikal, M. J., Rigsbee, D., Roy, M. L., Galreath, D., Kovach, K. J., Wang, B. (Stuart), Carpenter, J. F., & Cicerone, M. T. (2008). Solid state chemistry of proteins: II. The correlation of storage stability of freeze-dried human growth hormone (hGH) with structure and dynamics in the glassy solid. *J Pharm Sci*, *97*(12), 5106–5121. https://doi.org/10.1002/jps.21374

Povey, J. F., Perez-Moral, N., Noel, T. R., Parker, R., Howard, M. J., & Smales, C. M. (2009). Investigating variables and mechanisms that influence protein integrity in low water content amorphous carbohydrate matrices. *Biotechnol. Prog.*, *25*(5), 1217–1227. https://doi.org/10.1002/btpr.207

Pradipasena, P., & Rha, C. (1977). PSEUDOPLASTIC AND RHEOPECTIC PROPERTIES OF A GLOBULAR PROTEIN (β-LACTOGLOBULIN) SOLUTION1. *Journal of Texture Studies*, *8*(3), 311–325. https://doi.org/10.1111/j.1745-4603.1977.tb01184.x

Prigent, S. V. E., Voragen, A. G. J., van Koningsveld, G. A., Baron, A., Renard, C. M. G. C., & Gruppen, H. (2009). Interactions between globular proteins and procyanidins of different degrees of polymerization. *Journal of Dairy Science*, *92*(12), 5843–5853. https://doi.org/10.3168/jds.2009-2261

Purwanti, N., van der Goot, A. J., Boom, R., & Vereijken, J. (2010). New directions towards structure formation and stability of protein-rich foods from globular proteins. *Trends Food Sci Technol*, *21*(2), 85–94. https://doi.org/10.1016/j.tifs.2009.10.009

Quan, T. H., Benjakul, S., Sae-leaw, T., Balange, A. K., & Maqsood, S. (2019). Protein–polyphenol conjugates: Antioxidant property, functionalities and their applications. *Trends Food Sci Technol*, *91*, 507–517. https://doi.org/10.1016/j.tifs.2019.07.049

Quinn, J. R., & Paton, D. (1979). A practical measurement of water hydration capacity of protein materials. *Cereal Chem*, *56*(1), 38–40.

Rawel, H. M., Meidtner, K., & Kroll, J. (2005). Binding of selected phenolic compounds to proteins. *J Agr Food Chem*, *53*(10), 4228–4235. https://doi.org/10.1021/jf0480290

Rein, M. (2005). *Copigmentation reactions and color stability of berry anthocyanins* [PhD Dissertation]. University of Helsinki, Department of Applied Chemistry and Microbiology.

Resch, J. J., & Daubert, C. R. (2002). Rheological and physicochemical properties of derivatized whey protein concentrate powders. *Int. J. Food Prop.*, *5*(2), 419–434. https://doi.org/10.1081/JFP-120005795

Rice, T., Zannini, E., Arendt, E. K., & Coffey, A. (2020). A review of polyols – biotechnological production, food applications, regulation, labeling and healt. *Crit Rev Food Sci Nutr*, *60*(12), 2034–2051.

Robert, P., Gorena, T., Romero, N., Sepulveda, E., Chavez, J., & Saenz, C. (2010). Encapsulation of polyphenols and anthocyanins from pomegranate (Punica granatum) by spray drying: Encapsulation of polyphenols and anthocyanins. *Int J Food Sci Tech*, *45*(7), 1386–1394. https://doi.org/10.1111/j.1365-2621.2010.02270.x

Rodriguez-Saona, L. E., Giusti, M. M., & Wrolstad, R. E. (1999). Color and pigment stability of red radish and red-fleshed potato anthocyanins in juice model systems. *J Food Sci*, *64*(3), 451–456. https://doi.org/10.1111/j.1365-2621.1999.tb15061.x

Roe, K. D., & Labuza, T. P. (2005). Glass transition and crystallization of amorphous trehalose-sucrose mixtures. *Int. J. Food Prop.*, *8*(3), 559–574. https://doi.org/10.1080/10942910500269824

Roopchand, D. E., Kuhn, P., Krueger, C. G., Moskal, K., Lila, M. A., & Raskin, I. (2013). Concord grape pomace polyphenols complexed to soy protein isolate are stable and hypoglycemic in diabetic mice. *J Agr Food Chem*, *61*(47), 11428–11433. https://doi.org/10.1021/jf403238e

Roos, Y., & Drusch, S. (2015). *Phase transitions in foods* (Second Edition). Academic Press.

Roos, Y. H. (1987). Effect of moisture on the thermal behavior of strawberries studied using differential scanning calorimetry. *J Food Sci*, *52*(1), 146–149. https://doi.org/10.1111/j.1365-2621.1987.tb13992.x

Roos, Y. H. (1993). WATER ACTIVITY and PHYSICAL STATE EFFECTS ON AMORPHOUS FOOD STABILITY. *Journal of Food Processing and Preservation*, *16*(6), 433–447. https://doi.org/10.1111/j.1745-4549.1993.tb00221.x

Roos, Y. H. (2010). Glass Transition Temperature and Its Relevance in Food Processing. *Annu. Rev. Food Sci. Technol.*, 469–496.

Roos, Y. H. (2020). Water Activity and Glass Transition. In *Water Activity in Foods: Fundamentals and Applications* (2nd ed., pp. 29–45). John Wiley & Sons, Incorporated.

Roos, Y. H., & Potes, N. (2015). Quantification of protein hydration, glass transitions, and structural relaxations of aqueous protein and carbohydrate-protein systems. *J Phys Chem B*, *119*(23), 7077–7086.

Roos, Y., & Karel, M. (1991a). Amorphous state and delayed ice formation in sucrose solutions. *Int J Food Sci Tech*, *26*(6), 553–566. https://doi.org/10.1111/j.1365-2621.1991.tb02001.x

Roos, Y., & Karel, M. (1991b). Phase transitions of amorphous sucrose and frozen sucrose solutions. *J Food Sci*, *56*(1), 266–267. https://doi.org/10.1111/j.1365-2621.1991.tb08029.x

Roos, Y., & Karel, M. (1991c). Plasticizing effect of water on thermal behavior and crystallization of amorphous food models. *J Food Sci*, *56*(1), 38–43. https://doi.org/10.1111/j.1365-2621.1991.tb07970.x

Ropiak, H. M., Lachmann, P., Ramsay, A., Green, R. J., & Mueller-Harvey, I. (2017). Identification of Structural Features of Condensed Tannins That Affect Protein Aggregation. *PLOS ONE*, *12*(1), e0170768. https://doi.org/10.1371/journal.pone.0170768

Ruffin, E., Schmit, T., Lafitte, G., Dollat, J.-M., & Chambin, O. (2014). The impact of whey protein preheating on the properties of emulsion gel bead. *Food Chemistry*, *151*, 324–332. https://doi.org/10.1016/j.foodchem.2013.11.071

Saluja, A., & Kalonia, D. S. (2005). Application of Ultrasonic Shear Rheometer to Characterize Rheological Properties of High Protein Concentration Solutions at Microliter Volume. *Journal of Pharmaceutical Sciences*, *94*(6), 1161–1168. https://doi.org/10.1002/jps.20342

Sarciaux, J.-M. E., & Hageman, M. J. (1997). Effects of bovine somatotropin (rbSt) concentration at different moisture levels on the physical stability of sucrose in freeze-dried rbSt/sucrose mixtures. *J Pharm Sci*, *86*(3), 365–371. https://doi.org/10.1021/js960217k

Sawyer, L. (2003). β-Lactoglobulin. In P. F. Fox & P. L. H. McSweeney (Eds.), *Advanced Dairy Chemistry: Vol. 1: Proteins* (3rd ed., pp. 319–386). Springer.

Schmidt, R. H., Packard, V. S., & Morris, H. A. (1984). Effect of processing on whey protein functionality. *J Dairy Sci*, *67*(11), 2723–2733.

Schneider, M. E. (2016). *Formation of Whey Protein-Polyphenol Aggregates and Incorporation into Various Food Structures* [PhD Food Science]. North Carolina State University.

Schuck, P., Blanchard, E., Dolivet, A., Méjean, S., Onillon, E., & Jeantet, R. (2005). Water activity and glass transition in dairy ingredients. *Le Lait*, *85*(4–5), 295–304. https://doi.org/10.1051/lait:2005020

Sęczyk, Ł., Świeca, M., Kapusta, I., & Gawlik-Dziki, U. (2019). Protein–Phenolic Interactions as a Factor Affecting the Physicochemical Properties of White Bean Proteins. *Molecules*, *24*(3), 408. https://doi.org/10.3390/molecules24030408

Semenova, M. G., Antipova, A. S., & Belyakova, L. E. (2002). Food protein interactions in sugar solutions. *Curr. Opin. Colloid Interface Sci*, *7*(5–6), 438–444.

Semenova, M. G., & Dickinson, E. (2010). *Biopolymers in Food Colloids: Thermodynamics and Molecular Interactions*. CRC Press.

Shanmugam, S. (2015). Granulation techniques and technologies: Recent progresses. *BioImpacts*, *5*(1), 55–63.

Sharma, H., Singh, A. K., Deshwal, G. K., Rao, P. S., & Kumar, M. D. (2021). Functional Tinospora cordifolia (giloy) based pasteurized goat milk beverage: Impact of milk protein-polyphenol interaction on bioactive compounds, anti-oxidant activity and microstructure. *Food Bioscience*, *42*, 101101. https://doi.org/10.1016/j.fbio.2021.101101

Shrestha, A., Howes, T., Adhikari, B., Wood, B., & Bhandari, B. (2007). Effect of protein concentration on the surface composition, water sorption and glass transition temperature of spray-dried skim milk powders. *Food Chemistry*, *104*(4), 1436–1444. https://doi.org/10.1016/j.foodchem.2007.02.015

Siebert, K. J., Troukhanova, N. V., & Lynn, P. Y. (1996). Nature of Polyphenol−Protein Interactions. *Journal of Agricultural and Food Chemistry*, *44*(1), 80–85. https://doi.org/10.1021/jf9502459

Sigurdson, G. T., Tang, P., & Giusti, M. M. (2017). Natural Colorants: Food Colorants from Natural Sources. *Annual Review of Food Science and Technology*, *8*(1), 261–280. https://doi.org/10.1146/annurev-food-030216-025923

Simeonov, S. B., Botushanov, N. P., Karahanian, E. B., Pavlova, M. B., Husianitis, H. K., & Troev, D. M. (2002). Effects of Aronia melanocarpa juice as part of the dietary regimen in patients with diabetes mellitus. *Folia Med (Plovdiv)*, *44*(3).

Singh, R. P., & Heldman, D. (2013). *Introduction to Food Engineering* (5th Edition). Academic Press.

Soltanizadeh, N., Mirmoghtadaie, L., Nejati, F., Najafabadi, L. I., Heshmati, M. K., & Jafari, M. (2014). Solid-state protein-carbohydrate interactions and their application in the food industry. *Comp. Rev. Food Sci. Food Saf.*, *13*(5), 860–870. https://doi.org/10.1111/1541-4337.12089

Song, J. (2009). Insight into “insoluble proteins” with pure water. *FEBS Letters*, *583*(6), 953–959. https://doi.org/10.1016/j.febslet.2009.02.022

Sosa, N., Zamora, M. C., Chirife, J., & Schebor, C. (2011). Spray-drying encapsulation of citral in sucrose or trehalose matrices: Physicochemical and sensory characteristics: Spray-drying of citral in sugar matrices. *International Journal of Food Science & Technology*, *46*(10), 2096–2102. https://doi.org/10.1111/j.1365-2621.2011.02721.x

Sosulski, F. W., & McCurdy, Ar. (1987). Functionality of flours, protein fractions and isolates from field peas and faba bean. *J Food Sci*, *52*(4), 1010–1014. https://doi.org/10.1111/j.1365-2621.1987.tb14263.x

Souillac, P. O., Costantino, H. R., Middaugh, C. R., & Rytting, J. H. (2002). Investigation of protein/carbohydrate interactions in the dried state. 1. Calorimetric studies. *J Pharm Sci*, *91*(1), 206–216. https://doi.org/10.1002/jps.10023

Souillac, P. O., Middaugh, C. R., & Rytting, J. H. (2002). Investigation of protein/carbohydrate interactions in the dried state. 2. Diffuse reflectance FTIR studies. *Int. J. Pharm*, *235*(1–2), 207–218. https://doi.org/10.1016/S0378-5173(01)00987-5

Spencer, C. M., Cai, Y., Martin, R., Gaffney, S. H., Goulding, P. N., Magnolato, D., Lilley, T. H., & Haslam, E. (1988). Polyphenol complexation—Some thoughts and observations. *Phytochemistry*, *27*(8), 2397–2409. https://doi.org/10.1016/0031-9422(88)87004-3

Sui, X., Sun, H., Qi, B., Zhang, M., Li, Y., & Jiang, L. (2018). Functional and conformational changes to soy proteins accompanying anthocyanins: Focus on covalent and non-covalent interactions. *Food Chem*, *245*, 871–878. https://doi.org/10.1016/j.foodchem.2017.11.090

Swanson, B. G. (1990). Pea and lentil protein extraction and functionality. *J. Am. Oil Chem. Soc.*, *67*(5), 276–280. https://doi.org/10.1007/BF02539676

Taheri, R., Connolly, B. A., Brand, M. H., & Bolling, B. W. (2013). Underutilized Chokeberry (Aronia melanocarpa, Aronia arbutifolia, Aronia prunifolia) Accessions Are Rich Sources of Anthocyanins, Flavonoids, Hydroxycinnamic Acids, and Proanthocyanidins. *Journal of Agricultural and Food Chemistry*, *61*(36), 8581–8588. https://doi.org/10.1021/jf402449q

te Booy, M. P. W. M., de Ruiter, R. A., & de Meere, A. L. J. (1992). Evaluation of the physical stability of freeze-dried sucrose-containing formulations by differential scanning calorimetry. *Pharm Res*, *9*(1), 109–114.

Thongkaew, C., Gibis, M., Hinrichs, J., & Weiss, J. (2014). Polyphenol interactions with whey protein isolate and whey protein isolate–pectin coacervates. *Food Hydrocoll.*, *41*, 103–112. https://doi.org/10.1016/j.foodhyd.2014.02.006

To, E. C., & Flink, J. M. (1978a). 'Collapse', a structural transition in freeze dried carbohydrates: II. Effect of solute composition. *Int J Food Sci Tech*, *13*(6), 567–581. https://doi.org/10.1111/j.1365-2621.1978.tb00837.x

To, E. C., & Flink, J. M. (1978b). 'Collapse', a structural transition in freeze dried carbohydrates: III. Prerequisite of recrystallization. *Int J Food Sci Tech*, *13*(6), 583–594. https://doi.org/10.1111/j.1365-2621.1978.tb00838.x

Tonon, R. V., Brabet, C., & Hubinger, M. D. (2010). Anthocyanin stability and antioxidant activity of spray-dried açai (Euterpe oleracea Mart.) juice produced with different carrier agents. *Food Res Int*, *43*(3), 907–914. https://doi.org/10.1016/j.foodres.2009.12.013

Trappe, V., Prasad, V., Cipelletti, L., Segre, P. N., & Weitz, D. A. (2001). Jamming phase diagram for attractive particles. *Nature*, *411*(6839), 772–775. https://doi.org/10.1038/35081021

Tro, N. J., Fridgen, T. D., & Shaw, L. (2014). *Chemistry: A Molecular Approach*. Pearson Canada.

Tsao, R. (2010). Chemistry and Biochemistry of Dietary Polyphenols. *Nutrients*, *2*(12), 1231–1246. https://doi.org/10.3390/nu2121231

Tzannis, S. T., & Prestrelski, S. J. (1999). Moisture effects on protein-excipient interactions in spray-dried powders. Nature of destabilizing effects of sucrose. *J Pharm Sci*, *88*(3), 360–370. https://doi.org/10.1021/js9800127

Uekusa, Y., Takeshita, Y., Ishii, T., & Nakayama, T. (2008). Partition coefficients of polyphenols for phosphatidylcholine investigated by HPLC with an immobilized artificial membrane column. *Biosci. Biotech. Bioch.*, *72*(12), 3289–3292. https://doi.org/10.1271/bbb.80435

Valcheva-Kuzmanova, S., Kuzmanov, K., Mihova, V., Krasnaliev, I., Borisova, P., & Belcheva, A. (2007). Antihyperlipidemic effect of Aronia melanocarpa fruit juice in rats fed a high-cholesterol diet. *Plant Foods Hum. Nutr.*, *62*(1), 19–24. https://doi.org/10.1007/s11130-006-0036-2

Valcheva-Kuzmanova, S., Kuzmanov, K., Tancheva, S., & Belcheva, A. (2007). Hypoglycemic effects of Aronia melanocarpa fruit juice in streptozotocin-induced diabetic rats. *Methods Find. Exp. Clin. Pharmacol.*, *29*(2), 101. https://doi.org/10.1358/mf.2007.29.2.1075349

Valcheva-Kuzmanova, S., Kuzmanov, K., Tsanova-Savova, S., Mihova, V., Krasnaliev, I., Borisova, P., & Belcheva, A. (2007). Lipid-lowering effects of Aronia Melanocarpa fruit juice in rats fed cholesterol-containing diets. *J. Food Biochem.*, *31*(5), 589–602. https://doi.org/10.1111/j.1745-4514.2007.00132.x

Van Teeling, C. G., Cansfield, P. E., & Gallop, R. A. (1971). An anthocyanin complex isolated from the syrup of canned blueberries. *Journal of Food Science*, *36*, 1061–1063. https://doi.org/10.1111/j.1365-2621.1971.tb03346.x

Verheul, M., & Roefs, S. (1998). Structure of whey protein gels, studied by permeability, scanning electron microscopy and rheology. *Food Hydrocoll.*, *12*(1), 17–24.

Viljanen, K., Kylli, P., Hubbermann, E.-M., Schwarz, K., & Heinonen, M. (2005). Anthocyanin Antioxidant Activity and Partition Behavior in Whey Protein Emulsion. *Journal of Agricultural and Food Chemistry*, *53*(6), 2022–2027. https://doi.org/10.1021/jf047975d

Volf, I., Ignat, I., Neamtu, M., & Popa, V. (2014). Thermal stability, antioxidant activity, and photo-oxidation of natural polyphenols. *Chem. Pap.*, *68*(1). https://doi.org/10.2478/s11696-013-0417-6

von Staszewski, M., Jagus, R. J., & Pilosof, A. M. R. (2011). Influence of green tea polyphenols on the colloidal stability and gelation of WPC. *Food Hydrocoll.*, *25*(5), 1077–1084. https://doi.org/10.1016/j.foodhyd.2010.10.004

Walstra, P. (Ed.). (1999). *Dairy Technology: Principles of Milk Properties and Processes*. CRC Press.

Wang, B., Tchessalov, S., Cicerone, M. T., Warne, N. W., & Pikal, M. J. (2009). Impact of sucrose level on storage stability of proteins in freeze-dried solids: II. Correlation of aggregation rate with protein structure and molecular mobility. *J Pharm Sci*, *98*(9), 3145–3166. https://doi.org/10.1002/jps.21622

Wang, B., Tchessalov, S., Warne, N. W., & Pikal, M. J. (2009). Impact of sucrose level on storage stability of proteins in freeze-dried solids: I. Correlation of protein–sugar interaction with native structure preservation. *Journal of Pharmaceutical Sciences*, *98*(9), 3131–3144. https://doi.org/10.1002/jps.21621

Wang, R., & Hartel, R. W. (2020). Effects of moisture content and saccharide distribution on the stickiness of syrups. *Journal of Food Engineering*, *284*, 110067. https://doi.org/10.1016/j.jfoodeng.2020.110067

Warren, M. M., & Hartel, R. W. (2014). Structural, Compositional, and Sensorial Properties of United States Commercial Ice Cream Products: United States commercial ice cream products …. *Journal of Food Science*, *79*(10), E2005–E2013. https://doi.org/10.1111/1750-3841.12592

White, G. W., & Cakebread, S. H. (1966). The glassy state in certain sugar-containing food products *. *Int J Food Sci Tech*, *1*(1), 73–82. https://doi.org/10.1111/j.1365-2621.1966.tb01031.x

Williams, M. L., Landel, R. F., & Ferry, J. D. (1955). The temperature dependence of relaxation mechanisms in amorphous polymers and other glass-forming liquids. *J. Am. Chem. Soc.*, *77*(14), 3701–3707. https://doi.org/10.1021/ja01619a008

Wilson, N. E., Topp, E. M., & Zhou, Q. T. (2019). Effects of drying method and excipient on structure and stability of protein solids using solid-state hydrogen/deuterium exchange mass spectrometry (ssHDX-MS). *Int. J. Pharm*, *567*, 118470. https://doi.org/10.1016/j.ijpharm.2019.118470

Worley, J. D. (1992). Capillary radius and surface tensions. Using calculations based on Tate's law. *Journal of Chemical Education*, *69*(8), 678.

Xie, L., Lee, S. G., Vance, T. M., Wang, Y., Kim, B., Lee, J.-Y., Chun, O. K., & Bolling, B. W. (2016). Bioavailability of anthocyanins and colonic polyphenol metabolites following consumption of aronia berry extract. *Food Chemistry*, *211*, 860–868. https://doi.org/10.1016/j.foodchem.2016.05.122

Xie, L., Vance, T., Kim, B., Lee, S. G., Caceres, C., Wang, Y., Hubert, P. A., Lee, J.-Y., Chun, O. K., & Bolling, B. W. (2017). Aronia berry polyphenol consumption reduces plasma total and low-density lipoprotein cholesterol in former smokers without lowering biomarkers of inflammation and oxidative stress: A randomized controlled trial. *Nutrition Research*, *37*, 67–77. https://doi.org/10.1016/j.nutres.2016.12.007

Xue, F., Li, C., & Adhikari, B. (2020). Physicochemical properties of soy protein isolates-cyanidin-3-galactoside conjugates produced using free radicals induced by ultrasound. *Ultrasonics Sonochemistry*, *64*, 104990. https://doi.org/10.1016/j.ultsonch.2020.104990

Yildirim-Elikoglu, S., & Erdem, Y. K. (2018). Interactions between milk proteins and polyphenols: Binding mechanisms, related changes, and the future trends in the dairy industry. *Food Rev. Int.*, *34*(7), 665–697.

Yoshioka, S., Forney, K. M., Aso, Y., & Pikal, M. J. (2011). Effect of sugars on the molecular motion of freeze-dried protein formulations reflected by NMR relaxation times. *Pharm Res*, *28*(12), 3237–3247. https://doi.org/10.1007/s11095-011-0512-8

Yousuf, B., Gul, K., Wani, A. A., & Singh, P. (2016). Health benefits of anthocyanins and their encapsulation for potential use in food systems: A review. *Crit Rev Food Sci Nutr*, *56*(13), 2223–2230. https://doi.org/10.1080/10408398.2013.805316

Yu, H., & Li, Y. (2012). State diagrams of freeze dried colostral whey powders: Effects of additives on the stability of colostral whey powders. *J. Food Eng*, *110*(1), 117–126. https://doi.org/10.1016/j.jfoodeng.2011.12.001

Zayas, J. F. (1997). *Functionality of Proteins in Food*. Springer Berlin Heidelberg. https://doi.org/10.1007/978-3-642-59116-7

Zhang, Y., Chen, S., Qi, B., Sui, X., & Jiang, L. (2018). Complexation of thermally-denatured soybean protein isolate with anthocyanins and its effect on the protein structure and in vitro digestibility. *Food Res Int*, *106*, 619–625. https://doi.org/10.1016/j.foodres.2018.01.040

Zhang, Z., Zhang, R., & McClements, D. J. (2016). Encapsulation of β-carotene in alginate-based hydrogel beads: Impact on physicochemical stability and bioaccessibility. *Food Hydrocoll.*, *61*, 1–10. https://doi.org/10.1016/j.foodhyd.2016.04.036

Zhang, Z., Zhang, R., Zou, L., Chen, L., Ahmed, Y., Al Bishri, W., Balamash, K., & McClements, D. J. (2016). Encapsulation of curcumin in polysaccharide-based hydrogel beads: Impact of bead type on lipid digestion and curcumin bioaccessibility. *Food Hydrocoll.*, *58*, 160–170. https://doi.org/10.1016/j.foodhyd.2016.02.036

Zhao, C., Giusti, M. M., Malik, M., Moyer, M. P., & Magnuson, B. A. (2004). Effects of commercial anthocyanin-rich extracts on colonic cancer and nontumorigenic colonic cell growth. *J Agr Food Chem*, *52*(20), 6122–6128. https://doi.org/10.1021/jf049517a

Zhao, C., Liu, Y., Lai, S., Cao, H., Guan, Y., San Cheang, W., Liu, B., Zhao, K., Miao, S., Riviere, C., Capanoglu, E., & Xiao, J. (2019). Effects of domestic cooking process on the chemical and biological properties of dietary phytochemicals. *Trends in Food Science & Technology*, *85*, 55–66. https://doi.org/10.1016/j.tifs.2019.01.004

Zhao, H.-S., Ma, Z., & Jing, P. (2020). Interaction of soy protein isolate fibrils with betalain from red beetroots: Morphology, spectroscopic characteristics and thermal stability. *Food Research International*, *135*, 109289. https://doi.org/10.1016/j.foodres.2020.109289

Zhou, P., & Labuza, T. P. (2007). Effect of water content on glass transition and protein aggregation of whey protein powders during short-term storage. *Food Biophys.*, *2*(2–3), 108–116. https://doi.org/10.1007/s11483-007-9037-4

Zhou, S.-D., Lin, Y.-F., Xu, X., Meng, L., & Dong, M.-S. (2020). Effect of non-covalent and covalent complexation of (−)-epigallocatechin gallate with soybean protein isolate on protein structure and in vitro digestion characteristics. *Food Chemistry*, *309*, 125718. https://doi.org/10.1016/j.foodchem.2019.125718

Zhou, Y., & Roos, Y. H. (2012). Stability and Plasticizing and Crystallization Effects of Vitamins in Amorphous Sugar Systems. *Journal of Agricultural and Food Chemistry*, *60*(4), 1075–1083. https://doi.org/10.1021/jf204168f

Zielińska-Przyjemska, M., Dobrowolska-Zachwieja, A., Grajek, W., & Olejnik, A. (2007). Effects of Aronia melanocarpa polyphenols on oxidative metabolism and apoptosis of neutrophils from obese and non-obese individuals. *Acta Sci. Pol. Technol. Aliment.*, *6*(3), 75–87.

Zuidam, N. J., & Nedovic, V. (Eds.). (2010). *Encapsulation Technologies for Active Food Ingredients and Food Processing*. Springer New York. https://doi.org/10.1007/978-1-4419-1008-0

Appendix 1: Additional Figures for Chapter 2

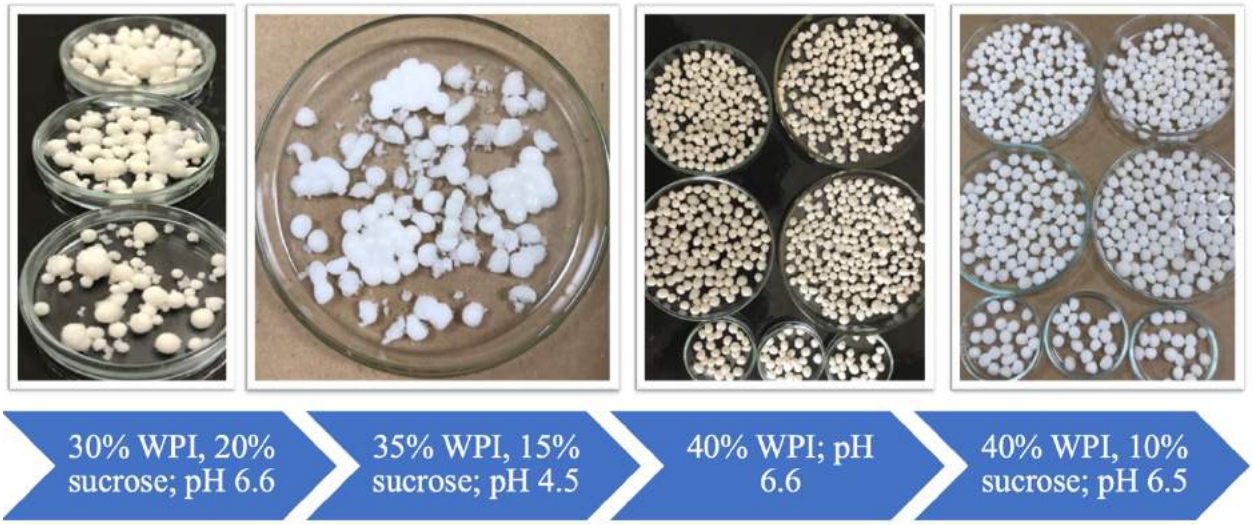


Figure A2.1. Images of solid products formed by dispersions containing WPI or WPI and sucrose.

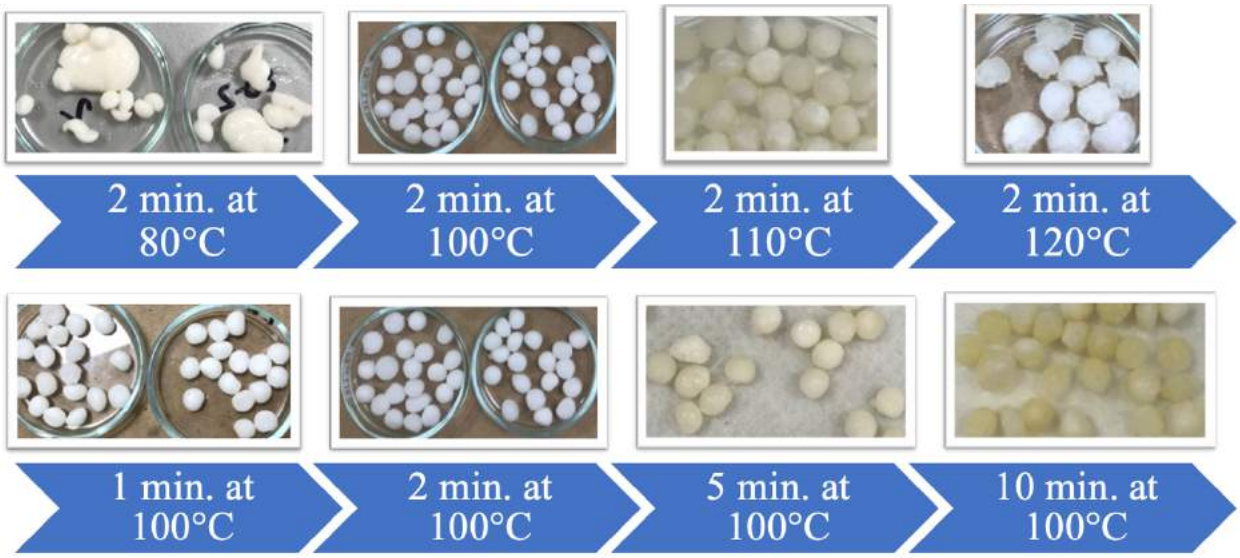


Figure A2.2. Images of solid beads formed by dispersions formulated with 40% WPI and 10% sucrose w/w under varied heat conditions.

Appendix 2

Published manuscripts

Journal of Food Engineering 279 (2020) 109966

Contents lists available at ScienceDirect

Journal of Food Engineering

journal homepage: http://www.elsevier.com/locate/jfoodeng

Thermal gelation and hardening of whey protein beads for subsequent dehydration and encapsulation using vitrifying sugars

Mackenzie M. Hansen [a], Valentyn A. Maidannyk [b], Yrjö H. Roos [a,*]

[a] Food Technology, School of Food and Nutritional Sciences, University College Cork, Ireland
[b] Teagasc, Food Research Centre, Moorepark, Fermoy, Co. Cork, P61 C996, Ireland

ARTICLE INFO

Keywords:
Concentrated
Protein
Viscosity
Drops
Beads

ABSTRACT

Solid beads were developed using whey protein isolate (WPI) and sugars for controlled hardening and vitrification of wall materials. A concentrated mixture of WPI and sucrose in water, intended for use as gelling and glass-forming ingredients, respectively, was used to form liquid feeds with varying pH, viscosities, surface tensions, solids contents and compositions. Using a peristaltic pump, feeds flowed continuously through silicon tubing and formed droplets. Rapid solidification occurred when droplets were submerged in heated, stirred oil; beads were harvested for vacuum oven drying. Dispersions were characterized by viscosity and flow testing. Dried beads were characterized for porosity, hardness, diameters, and water activity, and microstructures were analyzed with microscopy. Drop-forming dispersions comprised of 40% WPI with 10% sucrose by mass possessed structure forming and shape retention qualities. Feed composition influenced characteristics of the final product more strongly than processing conditions including heating times and temperatures.

1. Introduction

Bovine whey proteins are a popular choice when aiming to develop new textures, structures, functions, and products in food (Kulmyrzaev et al., 2000). Whey proteins are often utilized for their nutritional contribution as well as wide range of functional properties including foaming, emulsifying, and gelation. Thermal treatment of whey proteins in solution may result in the formation of a gel network, driving the formation of desired food structures. The first step in gel formation from globular proteins is denaturation. Applying heat causes protein conformations to shift and structures unravel, exposing formerly internally oriented hydrophobic groups. In β-lactoglobulin, a free thiol group from Cys_{121} is exposed, promoting its availability to adopt new intramolecular and intermolecular linkages (Sawyer, 2003; Nicolai et al., 2011). At high protein concentrations, intermolecular protein-protein interactions between denatured molecules will lead to aggregation, the second step in gel formation (Fennema, 2017). Segments of different protein molecules interacting via hydrophobic interactions, electrostatic interactions, hydrogen bond formation, and disulfide bond formation leads to formation of aggregates. The final step is the formation of the gel network by successive addition of intermolecular bonds (particularly hydrogen-bonds and hydrophobic interactions) between subunits to make up the 3D structure (Kamerzell et al., 2011).

When sugar was included in protein solutions, Lee and Timasheff (1981) reported an unfavorable change in free energy, resulting in sugar molecules being preferentially excluded from the region immediately surrounding proteins. Exclusion occurred due to the higher cohesive force of the sucrose-water system and effect of sucrose to increase surface tension of water (Lee and Timasheff, 1981), as well as a combination of excluded volume effects (sugar molecules are larger than water molecules) and differential interaction effects including protein-dependent interactions comprising of the sum of numerous types of interactions at varied locations on protein surfaces, and protein-independent interactions involving cosolvent molecules at interfaces, depending on cosolvent molecular properties (Baier and McClements, 2001; McClements, 2001, 2002; Semenova et al., 2002). Preferential hydration of proteins results in differences in the composition of the solvent surrounding proteins and that of the bulk solution, thus forming a concentration gradient and applied osmotic stress to protein molecules, where proteins have tendencies to alter their conformations and fold to limit exposure to sugars; some studies suggest that sucrose may be near to fully excluded from protein domains (Lee and Timasheff, 1981; McClements, 2002).

In the liquid state, proteins are both protected against unfolding and

* Corresponding author. Room 348, School of Food & Nutritional Sciences University College Cork, Cork, Ireland.
E-mail address: yrjo.roos@ucc.ie (Y.H. Roos).

https://doi.org/10.1016/j.jfoodeng.2020.109966
Received 16 August 2019; Received in revised form 4 February 2020; Accepted 6 February 2020
Available online 10 February 2020
0260-8774/© 2020 Elsevier Ltd. All rights reserved.

encouraged to form aggregates after denaturation due to the presence of sucrose in the system. There are two major hypotheses to explain sugars' impact on proteins in the solid state resulting from dehydration: the glass dynamics/vitrification theory and the water replacement theory (Allison et al., 1999; Chang and Pikal, 2009; Mensink et al., 2017). Both theories require sugar to be in the same amorphous phase as protein in order to impart their effects (Wang et al., 2009), and emphasize the significance of reducing proteins' molecular mobility (Ohtake et al., 2011). It can be presumed, then, that glass formation occurs in the preferentially excluded sucrose fraction of protein-sucrose dispersions.

Most previous studies have been performed under low concentration conditions; our interest is in highly concentrated systems. Schmidt et al. (1984) found that more aggregated, opaque gels would be expected to form at higher protein concentrations and under more severe heating (above 90 °C). Additionally, it has been reported that preferential exclusion of sugars increases at higher protein concentrations when sugars and proteins have been combined (He et al., 2011). Regarding relatively dilute protein-solvent-cosolvent systems, McClements (2002) conceded that in practice, it was not possible to completely determine all molecular characteristics of a system due to a large number of differing chemical groups and interactions occurring simultaneously, the highly dynamic nature of the system itself, and limitations of analytical techniques. The challenge to understand the entire body of molecular characteristics of a highly concentrated protein-water-sucrose dispersion is likely even more improbable.

The design and formation of desired food ingredient-based structures, such as biopolymer hydrogels beads from proteins, can be accomplished when the material and functional properties of the components are understood. The injection method of drop formation involves filling syringes or tubing with solution, which is then extruded/injected into a different solution that promotes gelation at selected conditions (Burey et al., 2008; Matalanis et al., 2011; McClements, 2017). The solution drop detachment mechanism is inter-influenced by the physical properties of solution, tip diameter, and solution flow rates (Lee and Chan, 2013), which aid in determining the physiochemical and structural properties of drops such as size, shape, porosity, and hardness (Joye and McClements, 2014; Zhang et al., 2016a, 2016b).

The hypothesis for this study was that a continuous process forming concentrated, liquid feeds into dry, stable particles could be developed. A blend of ice powder and whey protein isolate powder were used for rapid protein hydration during microwave thawing. Rehydrated WPI provided gelation properties of whey proteins to harden beads from a continuous liquid feed with subsequent glass formation of sucrose intended for encapsulation and protection of functional feed components. Our objective was to investigate effects of feed composition and pH on viscosity, surface tension, and bead formation as well as to analyze physicochemical properties of dehydrated beads. Results of this study provide insight into physical behaviors of high solids-concentrated protein dispersions.

2. Materials and methods

2.1. Materials

Whey Protein Isolate, WPI (Isolac®), used in the present study was supplied by Carbery Food Ingredients (Ballineen, Cork, Ireland). Sunflower oil (Musgrave Excellence™, Musgrave Wholesale Partners, Dublin, Ireland) was purchased from local suppliers. Sucrose (≥99.5 GC) of analytical grade was purchased from Sigma-Aldrich, Co. (St. Louis, MO, USA). Citric acid was purchased from KB Scientific Ltd. (Cork, Ireland). Ice was utilized as the source of water in experiments.

2.2. Dispersion preparation

A dry blend of sucrose and WPI powder was prepared and stored in a −40 °C chest freezer. To prepare liquid feeds, ice at −20 °C was weighed and blended in a Duronic BL 1200 stainless steel kitchen blender (4 blades, 1200 W, Duronic, United Kingdom) into a powder with 'ice crush' mode inside a walk-in freezer at −20 °C, to prevent melting. The blend of dry ingredients with the powdered ice was mixed together for 15 s prior to thawing in a microwave oven (White manual microwave oven, frequency 2450 MHz, power output 650–700 W, Argos, Ireland) first for 5 min on low settings (120 W, 17% microwave output). The dispersions were mixed by hand to break up any clumps and then heated an additional 1–9 min with the same settings, depending on solids content. Once all ice was melted, dispersions were mixed with a Tefal Infinityforce Ultimate hand blender (ActivFlow Technology with 4 blades, 1000 W, Tefal, Ireland) on 'turbo' mode at a speed setting of '15' for 60 s to break up any larger agglomerates prior to analysis. The pH was measured with the SevenEasy™ probe by Mettler Toledo (Scientific Laboratory Supplies, Nottingham, UK) and adjusted to desired levels with aqueous, 2M citric acid.

2.3. Feed characterization

2.3.1. Viscosity

Viscosity of liquid feed was measured with a Haake RotoVisco 1 (Thermo Scientific, MA, USA). Samples (~13 g) were weighed into a DG43 cup, and a Z41 standard rotor was employed. The water bath surrounding the sample cup was temperature-controlled and held at 20 °C. Samples were sheared in a ramp from 0 to 100 s^{-1} over 3 min, held at 100 s^{-1} for 3 min, then ramped back down to 0 s^{-1} within 3 min. A total of 100 measurements were taken over each 3-min period. Haake RheoWin Job Manager software was used to view and analyze data.

2.3.2. Flow testing

Flow properties of liquid feed at room temperature were measured by pumping through a benchtop, manual control, variable speed, peristaltic pump (120 S/DV; Watson Marlow, Falmouth, England) with silicon tubing of 85 cm length, 2 mm bore, and 1 mm wall thickness (BÜCHI Labortechnik AG, Flawil, Switzerland) at a pump speed of 10 rpm. The time required to deposit 10 mL of liquid feed was measured. Additionally, the number of drops deposited per 1 min was recorded. Mass of 10 mL of liquid feed was taken, as well as the average mass of a drop (triplicate measurement). These measured and recorded values allowed for mass flow rates, volume flow rates, liquid feed densities, drop surface tensions, drop diameters, and drop volumes to be calculated.

Density of liquid feed (kg/m^3) was calculated by (1):

$$\frac{mass\ (g)\ of\ 10\ mL\ liquid}{10\ mL\ of\ liquid} \quad (1)$$

Average drop volume (mL) was calculated by (2):

$$\frac{10\ mL\ liquid}{time\ (s)\ to\ deposit\ 10\ mL\ of\ liquid} * \frac{60s\ per\ min}{\#\ drops\ per\ min} \quad (2)$$

Mass flow rate (kg/s) was calculated by (3):

$$\frac{mass\ (g)\ of\ 10\ mL\ liquid}{time\ (s)\ to\ deposit\ 10\ mL\ of\ liquid} \quad (3)$$

Volume flow rate (m^3/s) was calculated by (4):

$$\frac{mass\ flow\ rate\ \left(\frac{kg}{s}\right)}{liquid\ density\ \left(\frac{kg}{m^3}\right)} \quad (4)$$

Drop surface tension was calculated with Tate's Law (Worley, 1992) (5):

$$\frac{\left(Average\ drop\ mass\ (g)*acceleration\ due\ to\ gravity\left[9.8\ \frac{m}{s^2}\right]\right)}{2\pi*\left(external\ diameter\ of\ tubing\ tip[mm]*correction\ factor\left[\frac{drop\ radius}{(drop\ volume)^{\frac{1}{3}}}\right]\right)}$$

The correction factor in this calculation is in place because the total drop formed at the tip of the outlet tubing does not release, and residual liquid is left on the end of the tube.

Drop diameter was calculated by (6):

$$\left[\frac{(3*average\ drop\ volume[mL])}{4*\pi}\right]^{\frac{1}{3}}*2$$

This equation is built off the assumption that drops form a perfectly spherical shape, and thus is derived from the equation for the volume of a sphere:

$$V=\frac{4}{3}\pi r^3$$

and the fact that $diameter = 2*radius$

2.4. Drop preparation

Liquid feeds at room temperature were pumped through a peristaltic pump (120 S/DV; Watson Marlow, Falmouth, England) with silicon tubing of 85 cm length, 2 mm bore, and 1 mm wall thickness (BÜCHI Labortechnik AG, Flawil, Switzerland). Pump speed settings of 150–200 RPM were used to fill the tube, then pump speed was set to 10 RPM, forming drops of liquid feed. The outlet tubing was placed between a clamp on a retort stand. For bead formation, a 500 mL glass beaker with a magnetic stir bar was set on a Stuart hotplate and magnetic mixer (Cole-Parmer, Staffordshire, UK), filled with 450 mL of heated sunflower oil. The retort stand was arranged so that the end of the outlet tubing was situated above the surface of the hot oil. Liquid feed was pumped through the tubing and dispensed dropwise into the hot oil, being gently stirred with low magnetic agitation by the magnetic stir bar. Drops were allowed to harden in the oil and harvested to dry on absorbent paper before being transferred to Anumbra® glass petri dishes (80 × 15 mm, Scientific Glass Laboratories Ltd., Staffs, UK) for drying. To determine the optimal heating time and temperature conditions to produce beads, drops of the same composition were formed under a range of temperatures and times: at 100 °C for 1, 2, 5, and 10 min, and for 2 min at 80, 100, 110, and 120 °C.

Glass dishes with beads were placed into a WTB Binder vacuum oven (Binder GmbH, Tuttingen, Germany) at 70 °C for 3 h. After drying a_w and diameters were measured prior to packaging in heat-sealed, 12/40 Camplex® Metallized Polyester Laminate packaging (Solventless adhesive laminate of: 12 μm printable polyester film, Camplus® metallized on one side, 40 μm polyethylene film; Camvac Limited, UK). Packages were weighed and placed into an incubator (Cooling Incubator, KBP 6151, Series 6000, Termaks, Bergen, Norway) set at 25 °C until testing. Packages were reweighed when removed from the incubator for testing, prior to opening (data not reported.)

A range of formulations of varied solids concentrations and compositions, pH, and viscosities were developed and assessed for their ability to form spherical, solid drops that retained their shape and did not stick to one another (see Table 1). Liquid feed dispersions of 35% WPI with 10% sucrose at pH 3.5 and 35% WPI with 15% sucrose at pH 4.0 were not pumpable and thus flow testing was not performed.

2.5. Bead characterization

2.5.1. Water activity, a_w

Bead a_w was measured with a water activity meter (4 TE, AquaLab, Decagon Devices, Inc., WA, USA) at 20 °C before and after drying.

Table 1
Feed formulations with WPI and sucrose concentrations (%) as well as pH.

[WPI]	[Sucrose]	pH
%		–
10	0	6.6
15	10	6.6
20	0	6.6
20	20	6.6
25	10	6.6
30	0	6.6
30	10	6.6
30	20	6.6
35	10	3.5, 4.0, 4.1, 4.2, 4.5, 5.0, 6.7
35	15	4.0, 4.5, 5.0, 6.6
35	20	4.5, 5.4, 6.6
40	0	6.6
40	5	6.6
40	10	4.5, 6.5

Approximately 0.5 g of sample was placed in glass Steriplan dishes (6 mm internal height x 35 mm internal diameter) used as sample cups.

2.5.2. Water content

Fresh bead water content was measured gravimetrically by placing approximately 0.5 g of beads into pre-weighed, glass dishes and recording the mass before placing into a vacuum oven for drying at 70 °C for 24 h. Masses were recorded again after drying to obtain the difference in mass due to water loss as well as the sum of total solids plus oil remaining in dry beads.

2.5.3. Drop diameters

Diameters of beads were measured 5 times per sample before and after drying with digital Vernier calipers (0–150 mm; Mitutoyo, Japan), and an average value was reported. Accuracy was not a concern as products measured were not particularly viscoelastic or soft, but had semi-solid structures and held their shape (Lee and Chan, 2013). To compare with calculated values for bead diameters, 3 of the 5 measurements were used.

2.5.4. Hardness

Sample preparation - Beads were removed from storage at 25 °C and weighed. Drops were placed in a single layer, covering the bottom area (1520 mm^2) of a transparent, polypropylene sample cup with a yellow screw cap (70 mL, 55 × 44 mm, Starstedt, Australia), samples weights were recorded, and lids were placed on the samples until testing. All samples were prepared for texture analysis in triplicate.

Texture analysis - Beads were tested for hardness with TA-XT2i Texture Analyser (Stable Micro Systems, Surrey, UK). A 35 mm platen was utilized to compress drops 3 mm once contact was made with samples. Compression force was measured, and Texture Expert Exceed software was employed to analyze data.

2.5.5. Density

A Micromeritics AccuPyc II 1340 Gas Pycnometer (Micromeritics Instrument Corporation, GA, USA) was utilized to measure average apparent volume and true density of beads by using Helium gas to 4.5 standard (99.995% purity; Irish Oxygen Company Ltd, Cork, Ireland) as the displacement medium, pumped at a steady rate of 145–172 kPa. A sample cup with 10 cm^3 capacity was partially filled, and each sample was measured 10 times during a single test. AccuPyc II 1340 for Windows software was utilized to run tests and view data reports. A Micromeritics GeoPyc™ 1360 (Micromeritics Instrument Corporation, GA, USA) envelope density analyser was utilized to measure the average envelope density and volume of samples by combining Micromeritics DryFlo™ displacement material and sample (filling roughly ¼ of the chamber) in a 38.1 mm I.D. chamber and measuring 7 times during a single test. The volumes given from the two tests were utilized to

calculate sample porosities. All density testing was completed in duplicate.

$$\text{Porosity was calculated by: } \frac{Total\ volume - Volume\ of\ solids}{Total\ volume} * 100$$
$$or\ \frac{GeoPyc\ volume - AccuPyc\ volume}{GeoPyc\ volume}$$

2.5.6. Optical light microscopy

Microscopy observation of dried beads was done using an Olympus BX51 (Olympus Corporation, Tokyo, Japan) light microscope with 20× dry objective lens with polarized light. Digital images (TIFF, 8-bit) were taken and captured using Jenoptik C14 Imagic camera. Beads were crushed to produce fragments of smaller sizes that could be imaged.

2.5.7. Confocal laser scanning microscopy

Leica TCS SP5 confocal laser scanning microscope (CLSM; Leica Microsystems CMS GmbH, Wetzlar, Germany) was used for dried beads visualization. Fragments of broken beads were placed onto a glass slide and labeled using a mixture of Fast Green and Nile Red (Auty et al., 2001; Maher et al., 2015). The dye mixture containing Fast Green (aq. 0.01 g/0.1 L) and Nile Red were dissolved in polyethylene glycol 400 g/mol (0.1 g/0.1 L) mixed in a ratio 1:40 of Fast Green to Nile Red, which allowed diffusion of the dye molecules into the particles whilst not influencing the particle morphology and preventing solubilization (Maher et al., 2015). Dual excitation at 488 nm/633 nm was used. The confocal images of drop fragments were taken using 20× oil immersion objective with numerical aperture 0.7 z. Stacks were obtained in order to generate a three-dimensional structure of the particle and to identify surface lipid staining (Maher et al., 2015). Red and Green pseudo-colored pictures (8-bit), 512 × 512 pixels in size, were acquired using a zoom factor of 1–3.

2.5.8. Scanning electron microscopy

Fragments from broken dried beads were attached to double-sided adhesive carbon tabs mounted on scanning electron microscope stubs, and then coated with chromium (K550×, Emitech, Ashford, UK). Scanning electron microscopy images were collected using a Zeiss Supra 40P field emission SEM (Carl Zeiss SMT Ltd., Cambridge, UK) at 2.00 kV. Representative micrographs were taken at 200 × , 500 × , 1000 × , 5000 × , and 10000 × magnification.

2.6. Statistical analysis

All analyses were carried out in triplicate with the exception of envelope and true densities, done in duplicate. The obtained data were analyzed by calculating mean values and standard deviations. Additionally, *t*-test and analysis of variance (ANOVA; Tukey's HSD test) were performed using R i386 version 3.5.1 (R Foundation for Statistical Computing, Vienna, Austria) on mean values for different samples. The level of significance was determined at $p < 0.05$.

3. Results and discussion

3.1. Feed characterization

3.1.1. Viscosity

Feed viscosity plays a significant role in drop formation, requiring sufficiently high viscosities to form and retain spherical shapes upon hardening, as competing forces exist between the viscous, surface tension forces of the droplet that must exceed the impact, drag forces from the bath attempting to disrupt shape (Chan et al., 2009). Increasing the concentration of biopolymers in the dispersion is known to increase feed viscosity exponentially (Chan et al., 2009; Matalanis et al., 2011; Lee and Chan, 2013). Highly concentrated WPI dispersions exhibited pseudoplastic flow behavior (data not shown), also observed by Pradipasena and Rha (1977) for β-lactoglobulin above 5% w/w. The apparent viscosity of liquid feeds sheared at 100 s^{-1} increases non-linearly with WPI concentration, with an extreme, significant jump occurring above 30% WPI w/w (Fig. 1, A), potentially highlighting a critical packing point where particle volume fractions and interactions become sufficiently high to arrest feed dynamics. Above this critical concentration, feed dispersions undergo a transition from fluid-like to more solid-like behavior due to the crowding or jamming of particles' and aggregates' mobility, resulting in the formation of a stress-bearing, interconnected network (Trappe et al., 2001; Coupland, 2014). Our results are in agreement with those reported by Alizadehfard and Wiley (1995) and Patocka et al. (2006), who found that WPI dispersions sheared at a fixed rate of 6.45 s^{-1} showed marginally increasing viscosity up to 30% WPI concentration followed by sharp increases. He et al. (2011) reported similar findings, with increases being minimal at lower protein concentrations and the slope of viscosity change significantly increasing at higher protein concentrations when two types of monoclonal antibody proteins were studied. Small shifts in solution conditions, including altered concentration of solutes, can result in the partial unfolding of protein molecules and the exposure of hydrophobic groups. This increases the tendency of protein particles to cluster and form aggregates, as exposed hydrophobic groups are attracted, ultimately increasing the viscosity of the aqueous phase (Song, 2009). Matalanis et al. (2011) explained that increased concentrations of biopolymers increase viscosity until the packing of molecules becomes so tight that a critical packing parameter is reached, above which systems behave more like solids. When protein molecules exceed a critical concentration in a sol, increased entangling and overlap results in increased system viscosity (Coupland, 2014). Crowding results in increased viscosities due to steric repulsion between molecules causing jamming of protein particle movement and ultimately adopting solid-like behavior (Hong et al., 2018). We observed the solid-like behavior of dispersions as feeds that were unable to flow through tubing to form drops.

Sugars increase biopolymer dispersion viscosities (McClements, 2002; Semenova et al., 2002). He et al. (2011) demonstrated that seven different sugars significantly increased viscosity of highly-concentrated protein dispersions. Disaccharides showed stronger effects than monosaccharides when dispersions contained equal amounts of monosaccharide units. Our study showed that feeds of equal protein concentrations exhibited increasing viscosities with increased sucrose concentrations, potentially due to the increase in total system solids as well (Fig. 1, B).

Proteins are particles that may exhibit more hydrophilic or hydrophobic behavior, depending on which constituent groups are exposed to the bulk solvent. Globular proteins in their native, folded state are often fairly soluble in water due to their 3D structures having mainly hydrophilic surface groups exposed to water in solution, while the majority of hydrophobic residues are buried within the internal core of the molecule and shielded from interacting with water (Coupland, 2014). The hydrophilic residues exposed to the bulk solvent may contribute to hydrogen bond formation with water molecules. At pH values away from the protein isoelectric point (pI), charged protein molecules repel one another strongly and hydrophobic groups are not exposed. These conditions are unfavorable for the formation of intermolecular interactions and allow protein molecules to exist as separated, suspended particles in water with low solution viscosities (Song, 2009; Coupland, 2014). At pH values near the protein pI, net charges on protein molecules are neutralized and electrostatic interactions are weak. Under these conditions, protein molecules have a stronger tendency to aggregate due to attractive electrostatic forces, reducing solubility. Therefore, altering pH conditions may change the viscosity of biopolymer dispersions, as the volume of electrostatic repulsions and attractive forces between molecules in solution can change with pH (Hong et al., 2018).

Effects of pH of feeds on viscosity are shown in Fig. 1, C. Dispersions comprised of 35% WPI with 10% sucrose showed high viscosities below and up to pH 4, followed by a rapid decrease in viscosity between pH 4

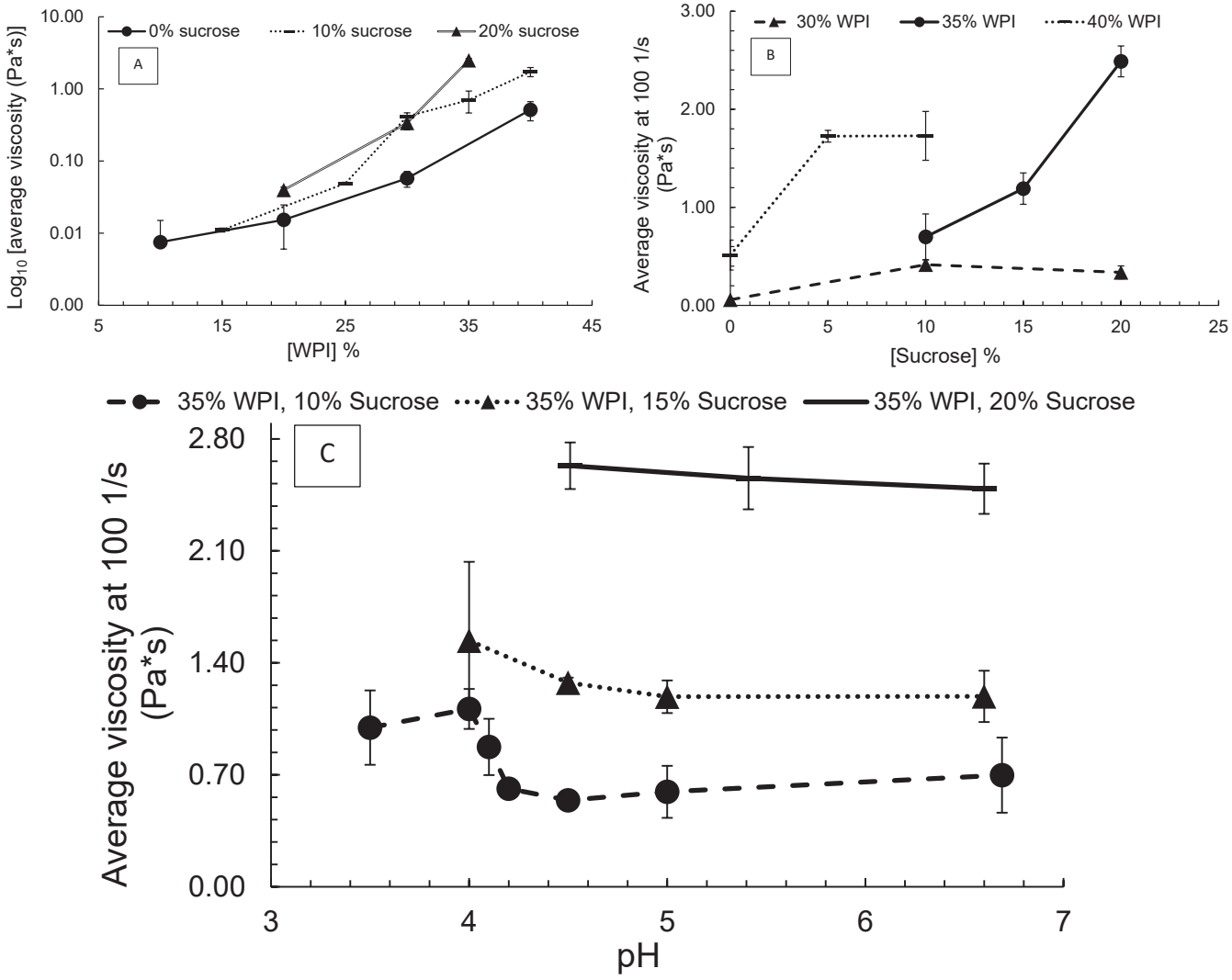


Fig. 1. **A.** Effect of protein concentration (%) in feeds containing 0, 10, and 20% sucrose on the apparent viscosity at 100 s^{-1}; n = 3. Lines are for guiding purposes only. **B.** Effect of sucrose concentration (%) in feeds containing 30, 35, and 40% WPI on apparent viscosity at 100 s^{-1}; n = 3. Lines are for guiding purposes only. **C.** Effect of pH in feeds containing 35% WPI with 10%, 15%, and 20% sucrose on apparent viscosity at 100 s^{-1}; n = 3. Lines are for guiding purposes only.

and 4.5, and finally an increasing viscosity with increasing pH above 4.5. Higher pH ranging over 4 to 6.8 showed no significant differences ($p > 0.05$). Our findings were in line with those of Hermansson (1975), who found that increased pH slightly increased viscosities of aqueous whey protein concentrates above the isoelectric point range (pH 4–5). Dissanayake et al. (2013) also reported that whey protein dispersions at pH 4 had higher initial viscosities than at pH 5 and 6. Hong et al. (2018) reported that bovine serum albumin (BSA) has a pI of 5.1 and a U-shaped curve for viscosity as a function of pH. BSA solutions with acidic and basic pH were more viscous than BSA solutions at the pI, indicating that monopole-monopole electrostatic repulsions were the dominant factor in solution viscosity and were most reduced at neutral pH.

3.1.2. Flow

The surface tension of feed dispersions strongly determines the mass and size of detached drops, as drops only detach once the gravitational forces pulling down exceed the surface tension forces acting around the circumference of the dripping tip; diameters of drops formed tend to decrease with the surface tension of feeds (Lee and Chan, 2013). Previous studies indicated that surface tension decreased as viscosity and biopolymer concentrations were increased (Chan et al., 2009; Lee and Chan, 2013). Our findings demonstrated that surface tension increased marginally with WPI concentration until there was a significant increase ($p < 0.05$) above 30% w/w WPI (Fig. 2, A). Sucrose concentrations did not appear to affect surface tension to the same extent observed with WPI (Fig. 2, B). Proteins are generally more surface-active molecules than sugars, as they contain both hydrophilic and hydrophobic groups and amino acid residues, and can participate in self-assembly as factors such as charges, temperature, or pH are adjusted (Nicolai, 2016). Adjusting the pH of formulations containing 35% WPI with 10 and 15% sucrose showed very similar effects on surface tension as on viscosity, indicating that pH adjustment was not effective for improving drop formation and retention of spherical shapes (data not shown).

While the overall effect of sucrose and protein concentration on surface tension was unexpected (Chan et al., 2009; Lee and Chan, 2013), drop diameters and surface tension had high correlation. Higher solids concentrations result in increased intermolecular interactions and may increase the viscosity of fluid systems, resulting in complex fluid behaviors (He et al., 2011; Tro et al., 2014). Additionally, there may have been variations in protein hydration levels in different feed dispersions. A corresponding effect applies to surface tension; liquids containing molecules with stronger and larger numbers of attractive intermolecular forces tend to have higher surface tension values (Tro et al., 2014). WPI dispersions were highly concentrated and as such, it may be inferred that feeds had high levels of intermolecular interactions and thus displayed highly viscous behavior and high surface tensions as well.

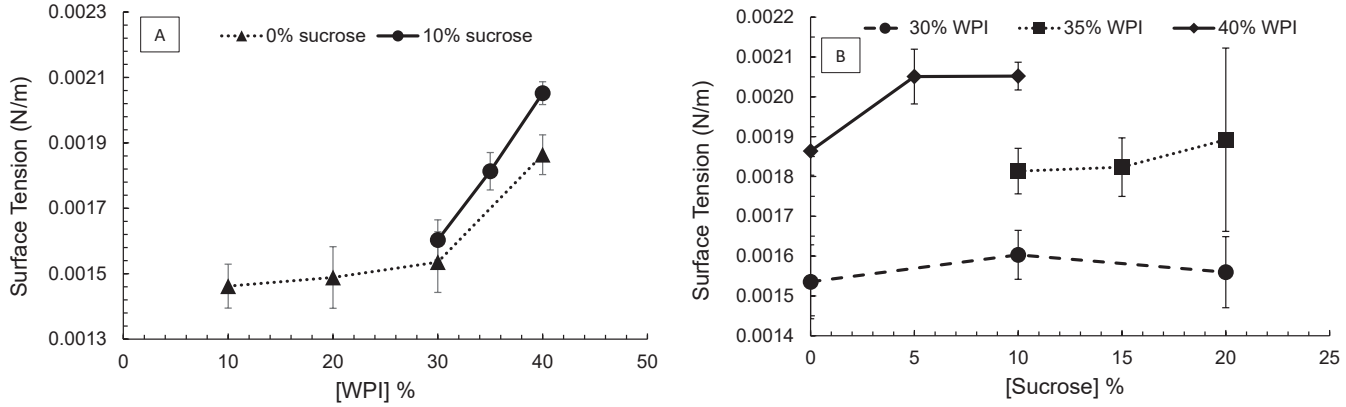


Fig. 2. A. Effect of WPI concentration (%) in feeds containing 0 and 10% sucrose on calculated surface tension in N/m; n = 3. Lines are for guiding purposes only. **B.** Effect of sucrose concentration (%) in feeds containing 30, 35, and 40% WPI on calculated surface tension; n = 3. Lines are for guiding purposes only.

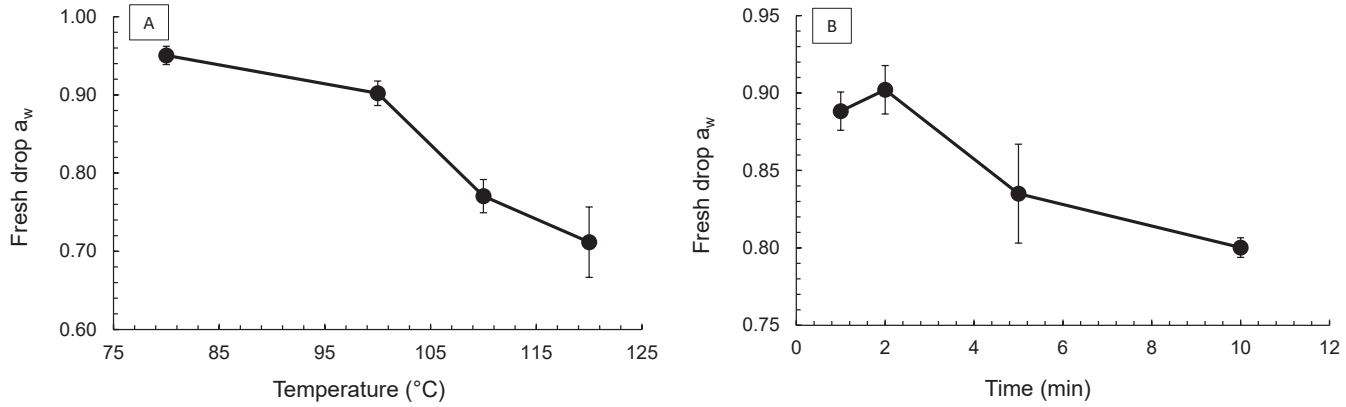


Fig. 3. A. Effect of oil temperature (°C) on dehydration shown by a_w of fresh drops comprised of 40% WPI with 10% sucrose for 2 min; n = 3. Lines are for guiding purposes only. **B.** Effect of heating time (min) at 100 °C on dehydration shown by a_w of fresh drops comprised of 40% WPI with 10% sucrose; n = 3. Lines are for guiding purposes only.

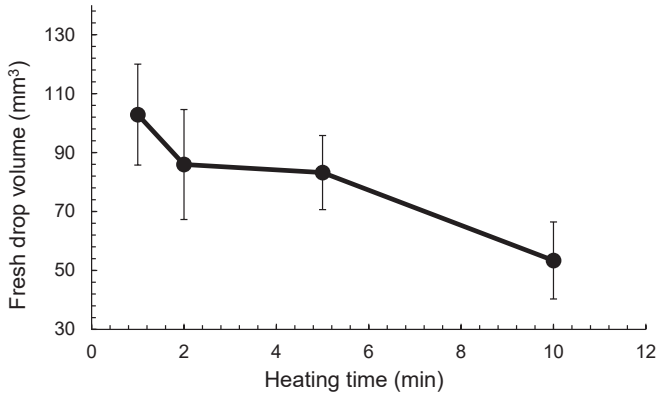


Fig. 4. Effect of dehydration shown by heating time (min) at 100 °C on the volume (mm^3) of drops comprised of 40% WPI with 10% sucrose; n = 3. Lines are for guiding purposes only.

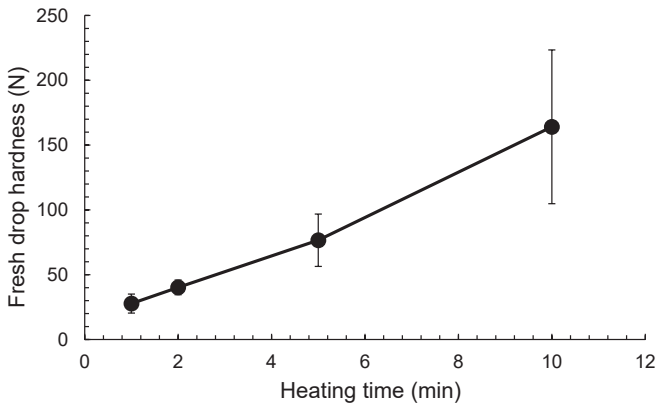


Fig. 5. Effect of dehydration shown by heating time (min) at 100 °C on the hardness (N) of drops comprised of 40% WPI with 10% sucrose; n = 3.

Another example of increasing viscosities and corresponding increases in surface tension is in water as temperature decreases (Tro et al., 2014).

3.2. Bead characterization

3.2.1. Drop formation and composition

Formulations in Table 1 include 4 formulations that showed potential for solid beads formation (30% WPI with 20% sucrose, 35% WPI with 15% sucrose at pH 4.5, 40% WPI, and 40% WPI with 10% sucrose). Compositional and water activity data collected from the liquid feeds, fresh beads, and dry beads are provided in Tables 2–4. Feed dispersions that formed solid beads were comprised of similar total system solids (40–50%) but exhibited a wide range of apparent viscosities (Table 5), indicating that viscosity may not be the strongest parameter determining drop forming abilities in this process. Interestingly, all 4 dispersions fell within a narrow range of surface tension values from

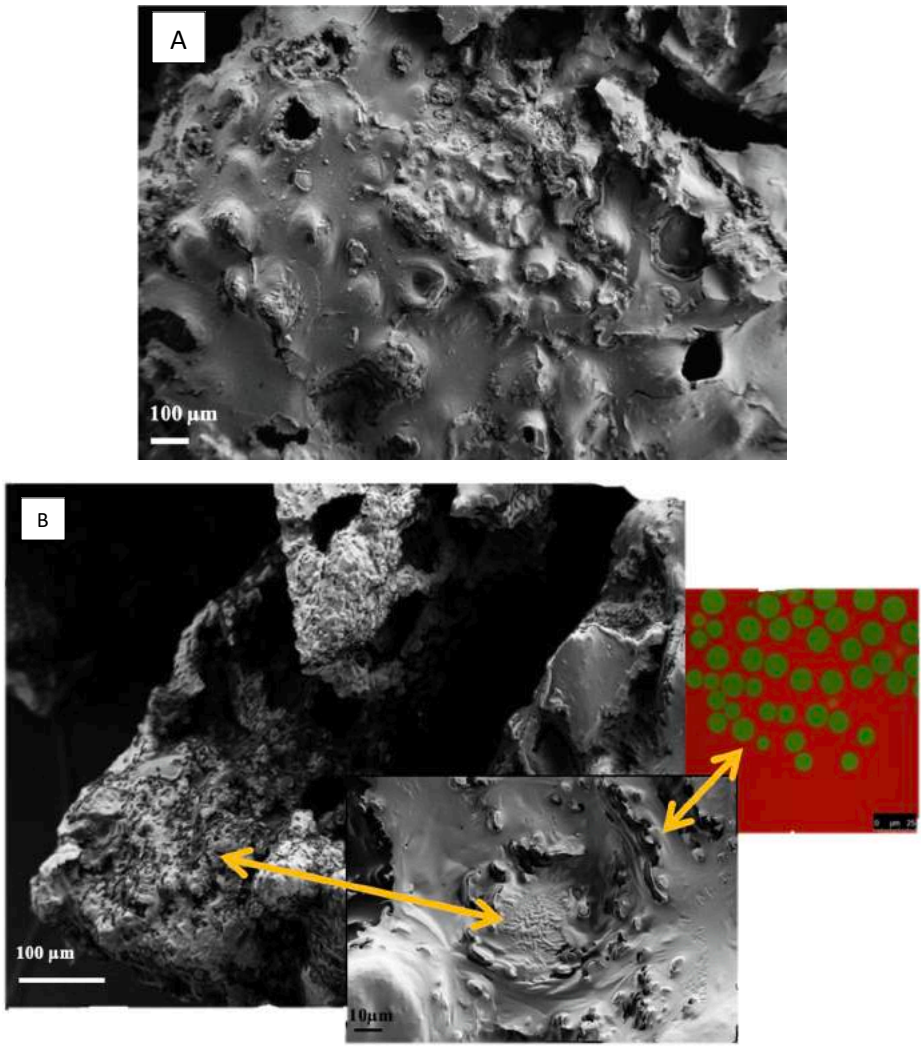


Fig. 6. A. Scanning electron micrograph image at 500× magnification, depicting the microstructure of a dried, 40% WPI bead. **B.** Left: Scanning electron micrograph image at 1000× magnification, depicting the microstructure of a dried, 40% WPI bead. Center: Scanning electron micrograph image at 5000× magnification, depicting the microstructure of a dried, 40% WPI bead. Right: Confocal laser scanning micrograph image depicting the microstructure of a dried, 40% WPI bead, with oil droplets dispersed throughout image. The left arrow points towards the appearance of the protein network in the left and center images, and the right arrow highlights the oil droplets protruding throughout the structure in the center and right images. (For interpretation of the references to colour in this figure legend, the reader is referred to the Web version of this article.).

Table 2
Composition of liquid feeds chosen for bead formation.

Liquid Feed Formulation	Water %	Total solids %	Protein (WPI) %	Sucrose %
30% WPI with 20% sucrose	50	50	30	20
35% WPI with 15% sucrose, pH 4.5	50	50	35	15
40% WPI	60	40	40	n/a
40% WPI with 10% sucrose	50	50	40	10

0.0016 to 0.0021 N/m, indicating that surface tension was a more significant factor in determining feeds' ability to form solid beads with our process. Two formulations (40% WPI and 40% WPI with 10% sucrose) produced uniform, spherical beads chosen for further characterization.

Studies by Kulmyrzaev et al. (2000) and Fitzsimons et al. (2007) showed differential scanning calorimetry (DSC) heating of native WPI gave a broad, endothermic transition between 60 and 90 °C with 2 peaks, the more significant around 70–71 °C corresponding to β-lactoglobulin denaturation, and the minor peak shoulder at around 60 °C representing α-lactalbumin (Ruffin et al., 2014). Knowledge of these temperatures for thermal denaturation allowed the presumption that when liquid drops enter the oil at 100 °C they solidify as the whey proteins aggregate and form a gel network. Additionally, drops of the hydrophilic feeds are likely driven to assume compact, spherical conformations within the oil bath to reduce the surface area in contact with the hydrophobic oil. Simultaneous, rapid vaporization of water expands

Table 3
Water activity (a_w) of intermediate, fresh beads prior to drying.

Fresh Bead Formulation	a_w
30% WPI with 20% sucrose	0.91 ± 0.01
35% WPI with 15% sucrose, pH 4.5	0.91 ± 0.01
40% WPI	0.95 ± 0.01
40% WPI with 10% sucrose	0.90 ± 0.02

Table 4
Composition and a_w of final, dried beads.

Dry Bead Formulation	a_w	Water %	[Solids + Oil] %
30% WPI with 20% sucrose	0.22 ± 0.05	2 ± 1	98 ± 1
35% WPI with 15% sucrose, pH 4.5	0.19 ± 0.03	1 ± 1	99 ± 1
40% WPI	0.20 ± 0.01	3 ± 1	97 ± 1
40% WPI with 10% sucrose	0.14 ± 0.02	1 ± 1	99 ± 1

Table 5
Total feed solids, viscosity, and surface tension data for feed dispersions that formed beads; n = 3.

Feed	Total Solids (%)	Viscosity (Pa-s)	Surface tension (N/m)
40% WPI	40	0.51 ± 0.15	0.00186 ± 0.00006
40% WPI, 10% sucrose	50	1.73 ± 0.25	0.00205 ± 0.00003
30% WPI, 20% sucrose	50	0.34 ± 0.07	0.00156 ± 0.00009
35% WPI, 15% sucrose- pH 4.5	50	1.28 ± 0.03	0.00189 ± 0.00025

the protein gel, followed by diffusion and dehydration. Heating and evaporation of the water in liquid drops results in droplet expansion, occurring concomitantly with dehydration and gel formation. Expansion can occur due elasticity of the gel network structure, while removal of water from the structure results in pore formation (as seen in Fig. 7, A & B; 8, A & D) and decreased drop densities. Hardening decreases shrinkage and the final volume is dependent on the extent of viscous flow during dehydration. Further dehydration in the vacuum oven transforms the sucrose to form a glass with fragile sucrose membranes on the dry protein. Such conclusion was based on the glass formation properties of sugars in mixes with proteins when glass transition of sucrose occurs above normal ambient temperature at $a_w < 0.2$ (Roos and Drusch, 2016).

Fig. 6, A depicts the appearance of a 40% WPI, dried product with dispersed oil droplets and the dehydrated protein network spanning the structure. Fig. 6, B, left shows the structure with the mixture of protein network and oil droplets. Fig. 6, B, center shows a more magnified view of the mixed protein and oil droplet structures, indicated by the arrows. The left arrow points towards the appearance of the protein network, and the right arrow highlights the oil droplets protruding throughout the structure. Fig. 6, B, right (confocal) shows a number of the tiny oil droplets found in the structure and confirms their identity, as their sizes are of the same magnitude as those in the SEM images. Thermal gelation of whey proteins involves the self-aggregation of protein molecules into the 3D network which entraps water by capillary forces (Chen et al., 2006); as water diffuses out of the structures in this process, it is possible that the same capillary forces responsible for water entrapment may drive oil uptake into the structure of the bead during gelation and hardening (oil droplets dispersion in the structure may be seen in Figs. 7, B; 8, B & D; and 9). The forces driving this oil uptake appear to be strong enough to force the bulk liquid into tiny droplets that fit throughout the structure and could potentially be enhanced by the gentle magnetic stirring of the oil bath (Kornev and Neimark, 2001). Further investigation would be required to determine the mechanism of such oil droplet formation.

3.2.2. *Water activity, a_w*

The process of drying fresh beads at 70 °C for 3 h in the vacuum oven resulted in the reduction of a_w (from ~0.9 (Table 3) to ~0.2 (Table 4), resulting in increased microbial stability. In the comparison of thermal treatments of drops, it was found that increased oil temperatures and heating times resulted in reduced a_w values of fresh beads (Fig. 3, A & B). Results show a decreasing trend in a_w as oil temperature is increased, with a significant reduction ($p < 0.05$) in a_w occurring between 100 and 110 °C (from 0.90 to 0.77 a_w, respectively). A similar, decreasing trend in a_w is observed with increased heating times, with a significant reduction ($p < 0.05$) in a_w occurring between 2 and 5 min of heating (from 0.90 to 0.84 a_w, respectively). Apparently heating time and oil temperature determine the extent of drying, as shown by reduced water contents and water activities.

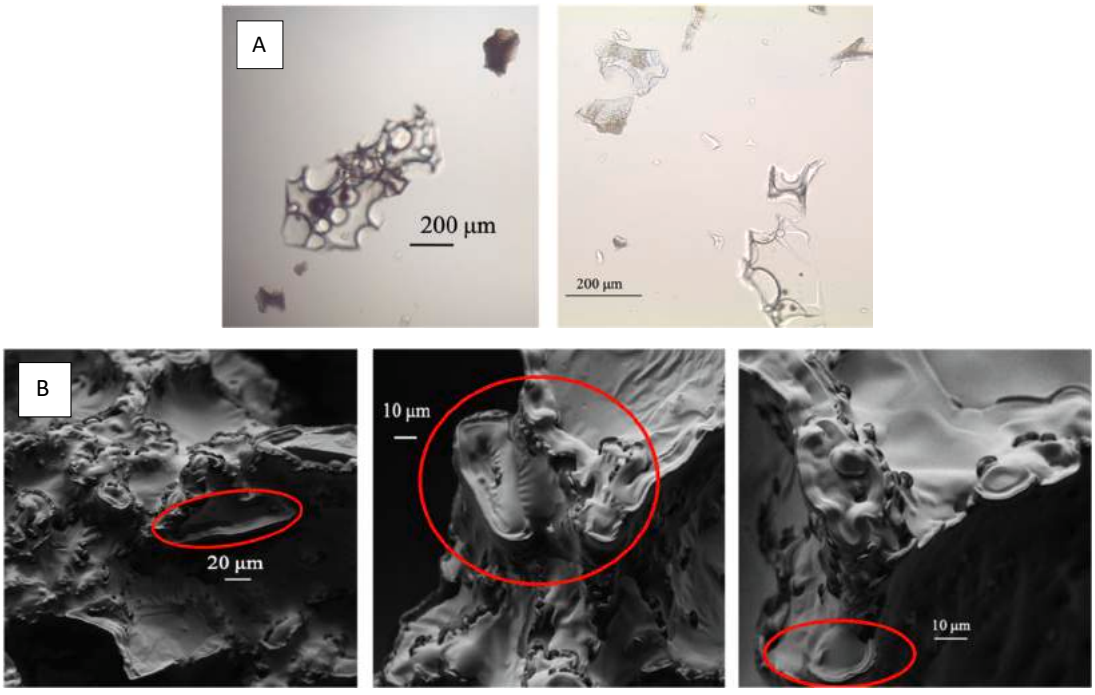


Fig. 7. A. Left: Optical light microscope image at 4× magnification, depicting the microstructure of a dried, 40% WPI with 10% sucrose bead. Right: Optical light microscope image at 10× magnification, depicting the microstructure of a dried, 40% WPI with 10% sucrose bead. **B.** Left: Scanning electron micrograph image at 500× magnification, depicting the microstructure of a dried, 40% WPI with 10% sucrose bead. Center: Scanning electron micrograph image at 1000× magnification, depicting the microstructure of a dried, 40% WPI with 10% sucrose bead. Right: Scanning electron micrograph image at 2000× magnification, depicting the microstructure of a dried, 40% WPI with 10% sucrose bead. .

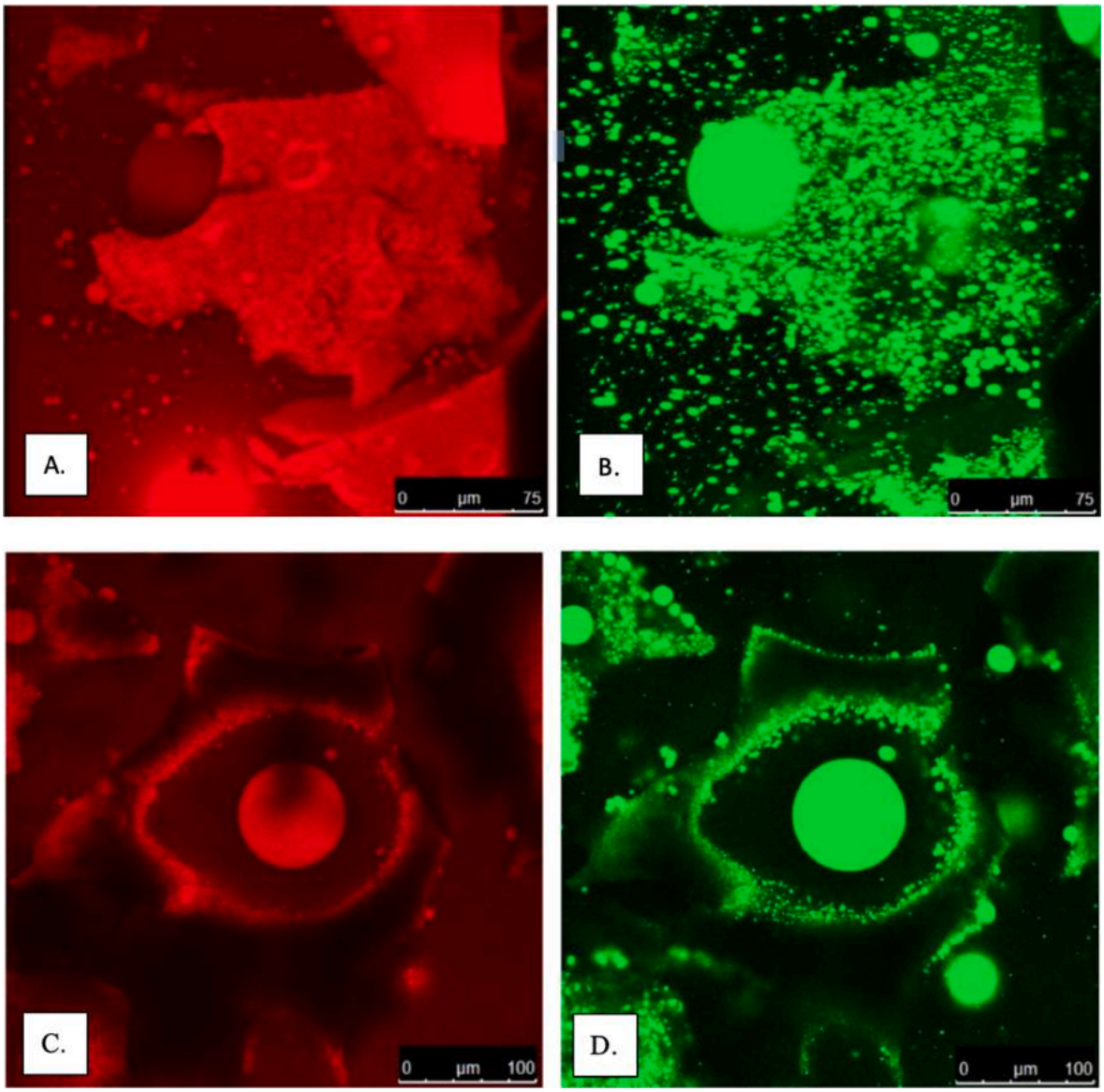


Fig. 8. A–D. Confocal laser scanning micrograph images depicting the microstructure of a dried, 40% WPI with 10% sucrose bead, with oil droplets dispersed throughout image. A and C: Highlight protein in bright red and other components as darker colors. B and D: Highlight fat in bright green and other components as darker colors. (For interpretation of the references to colour in this figure legend, the reader is referred to the Web version of this article.).

3.2.3. Drop diameter

Diameters were measured for beads made from 40% WPI, 40% WPI with 10% sucrose, and 30% WPI with 20% sucrose. Beads obtained from 35% WPI with 15% sucrose at pH 4.5 were not spherical in shape (data not reported). Our results indicated that upon drying, significant shrinkage (as obtained from bead diameters; $p < 0.05$) occurred in the beads made from 40% WPI (from 5.06 fresh to 4.50 mm dried), while beads containing sucrose did not experience shrinkage. This was likely due to the formation of sucrose glass upon drying, preventing further shrinking by stabilizing the protein network structure.

Chan et al. (2009) reported that drops formed from calcium-alginate by dripping sometimes have smaller size than predicted, possibly due to shrinkage experienced in gelling solutions. Our beads produced with 40% WPI had larger fresh diameters than predicted with Equation 6, with the 40% WPI products having significantly larger ($p < 0.05$) diameters than predicted (5.06 and 4.79 mm, respectively). While all beads were observed to show expansion behaviors of the gel networks within the heated oil, it would appear that beads without sucrose underwent more extensive expansion. Feeds containing 40% WPI with 10% sucrose had significantly higher ($p < 0.05$) viscosity compared to those with 40% WPI (1.73 and 0.51 Pa*s, respectively) (Fig. 1, B); as a result of its higher viscosity, 40% WPI with 10% sucrose beads may have undergone expansion to a lesser extent upon heating. Additionally, feeds with 40% WPI and 10% sucrose contained less water than 40% WPI feeds and thus underwent less drying. Corresponding results would be expected for the beads comprised of 30% WPI with 20% sucrose, but the data showed a significant reduction ($p < 0.05$) in drop diameters compared to predicted values (only 2.19 mm fresh compared to predicted 4.39 mm; data not reported). That may be due to the reduced protein content causing weakness in the typically strong forces of self-assembly imparted by high (40% w/w) concentrations of protein within the feed drops, which were overcome by the drag forces upon impact with the oil as well as the magnetic stir bar, thus causing the observed breaking of drop structures within the oil bath. The diameters of 40% WPI with 10% sucrose drops were only slightly larger than predicted and not statistically significant, indicating that calculations used to predict drop diameters were accurate.

Drop diameters were also measured to compare thermal treatments

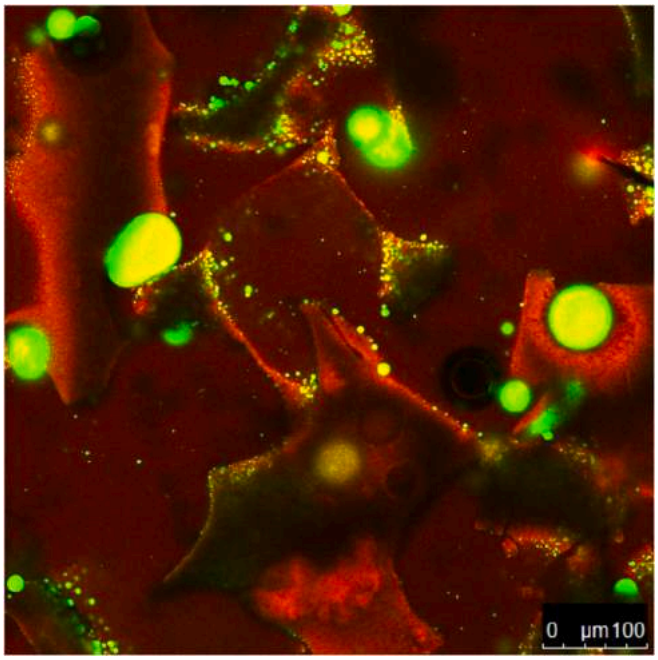


Fig. 9. Confocal laser scanning micrograph image depicting the microstructure of a dried, 40% WPI with 10% sucrose bead, with oil droplets dispersed throughout image; highlighting proteins in bright red, fat in bright green, and other components (mainly sucrose) as darker colors. The darker colored sucrose is thought to form the translucent, glassy fragments shown throughout the image (For interpretation of the references to colour in this figure legend, the reader is referred to the Web version of this article.).

of beads and used to calculate bead volumes (Fig. 4). Results show a relationship between decreasing bead volumes and increasing heating times, with a significant reduction ($p < 0.05$) in bead volume occurring between 5 and 10 min of heating (from 83 to 53 mm^3). Decreasing volumes of beads with increasing heating times could be a result of more extensive dehydration occurring within the drops, as confirmed by a_w data, causing further shrinking as more water was lost and structure hardening occurred. Products formed at increasing temperatures were more irregular in morphology and structures were broken, therefore diameters could not be measured.

3.2.4. Hardness

The hardness of dried beads formed by 40% WPI and 40% WPI with 10% sucrose were compared. Hardness was shown to be less with 10% w/w sucrose (from 232 to 155 N), likely due to the formation of a sucrose glass upon drying; Fig. 7, B shows that the gel structure is largely not visible in dried beads, and it is assumed that much of the gel network may have the smooth, amorphous sucrose glass form around it. When injection methods have been employed to extrude biopolymer solutions containing multiple components, it is possible to form particles with heterogeneous, dispersion-type internal structures where one component may be dispersed within the other (Matalanis et al., 2011). This describes what our data suggests is happening within bead structures, as it appears that the protein phase is independent and forms a gel that is surrounded by the protective, smooth, glassy matrix after dehydration. The presence of glass may cause the product to be more fragile by breaking up regions of dense protein-protein interactions with brittle glass, potentially weakening the otherwise dense protein gel network that would form if no sucrose were present. Figs. 7, A; 8, A-C, and 9 all depict the glass that forms upon drying, and the clouded appearance of some pieces may be due to the dried, aggregated protein network dispersed throughout or located at the glassy interface. A study by Al-Marhoobi and Kasapis (2005) of concentrated dispersions of gelatin with sugar as a co-solvent indicated that sugars were preferentially excluded from the protein region, with TEM analysis confirming the presence of separate sugar- and protein-rich phases in the product rather than homogeneous mixtures. They reported that the presence of sugars promoted protein association in their system, giving high network strength retention.

In the comparison of thermal treatments of beads, it was found that the hardness of fresh beads increased linearly with heating time (Fig. 5). The irregular morphologies and broken nature of beads formed with varied oil temperatures prevented the samples from being measured for hardness, as uniform beads were critical for accuracy of comparisons. Overall, large variations in hardness were recorded, potentially due to the nature of the products as well as the test involving multiple beads per single measurement. Testing of multiple products at once was determined important in describing the products overall, with inherent variability better accounted for.

3.2.5. Densities and porosity

The total volume and true densities of dried beads formed by 40% WPI and 40% WPI with 10% sucrose were measured and used to calculate average total volume and average solids volume in order to calculate porosity. Porosity was not significantly ($p > 0.05$) different for beads prepared from feeds containing 40% WPI and 40% WPI with 10% sucrose. Water dehydrates out of structures containing only WPI and leaves pores in the structure, as can be seen in Figs. 7, A; and 8, A, C, & D with rounded cavities throughout the fragments. Structures containing sucrose experience some dehydration and loss of water, but likely remain more fluid and may experience slightly more collapse as the protein network may be diluted by sugars present. These concentrated sucrose solutions form a glassy structure when oven dried, slightly reducing total unoccupied space in the structure as sucrose molecules are sterically larger than water. This is visualized in Fig. 7, B, where smooth, fractured edges highlighted in the images tend to have relatively rounded edges, indicating that sucrose glass formed within the pores left behind from water drying from the product.

In the comparison of thermal treatments of beads composed of 40% WPI with 10% sucrose, it was found that there was no significant variation in porosity of beads with increased heating (Table 6). This may indicate that feed composition may more strongly determine drop porosity than processing conditions.

3.2.6. Microscopy

Combinations of optical light-, confocal laser scanning-, and scanning electron microscope images of fractured beads aided in demonstrating the porous, oil-embedded, aggregated protein network structures produced by feeds containing 40% WPI and indicated the presence of a glassy structure in samples containing sucrose.

Fig. 8, A-D are confocal images for 40% WPI with 10% sucrose, and aid in discerning the 'layers' of the structure of the fractured material. Image 'A' highlights proteins in bright red, while other components have darker color. The broken, glassy, translucent structure appears in the image, either embedded with red protein particles or populated with proteins at the glassy surface, and having a round cavity carved into its side, indicative of a broken porous structure. Image 'B' highlights oil in bright green, with other components having a darker color. It is apparent that the glassy structure is covered with oil droplets, as oil is known to be dispersed throughout the 3D structure based on videos comprised of 'stacked' confocal images taken at different depths. Images 'C' and 'D' also aid in demonstrating the porous structure of the beads as well as the presence of a glassy matrix, protein network, and oil droplets in the structure. Image 'C' highlights proteins in bright red and other components with darker hues. A glassy, fractured piece of the structure is at the center of the image in the shape of a cavity, indicative of the presence of a pore in the 3D structure, and an oil droplet (confirmed by image 'D,' highlighting oil in bright green) directly at its center. The dark areas of the glassy structures may be sucrose, while the bright red parts lining the pore shows the presence of the protein network. Image

Table 6
Total volumes (cm^3) and true densities (g/cm^3) of dried drops comprised of 40% WPI with 10% sucrose (40/10) obtained at various heating times (min) at 100 °C; values were used to calculate average total volumes and average solids volumes (cm^3), respectively, in order to calculate porosity (%).

Sample	Heating time at 100 °C (min)	Total volume (cm^3)		Calculated average total volume (cm^3)	True density (g/cm^3)		Calculated average solids volume (cm^3)	Calculated Porosity (%)
		Rep 1	Rep 2		Rep 1	Rep 2		
40/10	1	3.90 ± 0.01	5.16 ± 0.02	4.53	1.11 ± 0.01	1.10 ± 0.01	2.61	42 ± 3[a]
40/10	2	3.86 ± 0.01	3.75 ± 0.01	3.80	1.07 ± 0.01	1.08 ± 0.01	2.27	41 ± 2[a]
40/10	5	4.09 ± 0.01	2.30 ± 0.02	3.19	0.99 ± 0.01	1.07 ± 0.01	2.09	34 ± 4[a]
40/10	10	2.65 ± 0.01	3.88 ± 0.01	3.26	1.07 ± 0.01	1.09 ± 0.01	2.02	38 ± 1[a]

Superscript letters in the same column indicate statistically significant ($p < 0.05$) difference.

'D' shows a dispersion of small oil droplets along the glassy pore. The dark background of the glassy portion indicates the presence of sucrose.

Fig. 9 is a confocal image of the 40% WPI with 10% sucrose beads and a good example of the protein- and oil-highlighted images being layered to give an idea of overall structure composition. Fat appears as bright green, proteins are bright red, and other components (mainly sucrose in this case) are darker. Translucent, glassy fragments are present in the image, with protein scattered throughout, as well as oil droplets dispersed throughout the structure.

4. Conclusions

We report a full process design for simple solidification of liquid dispersions (in an oil bath at 100 °C for 2 min) and a structure-forming formulation (40% WPI with 10% sucrose) used further to vitrify; apparent bulk oil inclusion and its emulsification into small drops throughout the structure is demonstrated. This study presents a potential process to make foods with entrapped flavors or actives, including emulsion droplets. The process may be a novel alternative to drying or extrusion that is simple, economic, and effective.

Future work is necessary to expand our understanding of the physical properties of feed dispersions including thermal properties and physical states of final beads, to adapt the process to form beads containing active ingredients, and to determine the protectant abilities of wall components and the location of active ingredients in the matrix. A major challenge when aiming to encapsulate bioactive ingredients is the retention of the active throughout the process in order to obtain final materials in which the actives are still accessible. Similar to spray drying, the process presented forms beads capable of containing bioactives that are not expected to suffer exposure to high temperatures; evaporation of water from the structures keeps beads at low temperatures, and the oil temperature is primarily a measure of energy input.

Author contribution statement

Mackenzie M. Hansen: Conceptualization, Methodology, Validation, Formal analysis, Investigation, Resources, Writing - original draft, Writing - review & editing, Visualization, Project administration, Funding acquisition. **Valentyn A. Maidannyk:** Investigation, Resources, Writing - original draft. **Yrjö H. Roos:** Conceptualization, Resources, Writing - review & editing, Visualization, Supervision, Funding acquisition.

Declaration of competing interest

The authors hereby declare no conflict of interest.

Acknowledgements

This research was supported by funding provided by the Lauritzson Foundation in the form of the Lauritzson Research Scholarship, through the College of Science, Engineering and Food Science (SEFS) at University College Cork. The authors would like to thank the anonymous reviewers and Journal Editor for thorough reading of the manuscript and helpful comments for revision.

References

Alizadehfard, M.R., Wiley, D.E., 1995. Viscosity of whey protein solutions. Iran. J. Polym. Sci. Technol. 4 (2), 126–133.
Allison, S.D., Chang, B., Randolph, T.W., Carpenter, J.F., 1999. Hydrogen bonding between sugar and protein is responsible for inhibition of dehydration-induced protein unfolding. Arch. Biochem. Biophys. 365 (2), 289–298. https://doi.org/10.1006/abbi.1999.1175.
Al-Marhoobi, I.M., Kasapis, S., 2005. Further evidence of the changing nature of biopolymer networks in the presence of sugar. Carbohydr. Res. 340 (4), 771–774. https://doi.org/10.1016/j.carres.2004.12.018.
Auty, M.A.E., Twomey, M., Guinee, T.P., Mulvihill, D.M., 2001. Development and application of confocal scanning laser microscopy methods for studying the distribution of fat and protein in selected dairy products. J. Dairy Res. 68 (03) https://doi.org/10.1017/S0022029901004873.
Baier, S., McClements, D.J., 2001. Impact of preferential interactions on thermal stability and gelation of bovine serum albumin in aqueous sucrose solutions. J. Agric. Food Chem. 49 (5), 2600–2608. https://doi.org/10.1021/jf001096j.
Burey, P., Bhandari, B.R., Howes, T., Gidley, M.J., 2008. Hydrocolloid gel particles: formation, characterization, and application. Crit. Rev. Food Sci. Nutr. 48 (5), 361–377. https://doi.org/10.1080/10408390701347801.
Chan, E.-S., Lee, B.-B., Ravindra, P., Poncelet, D., 2009. Prediction models for shape and size of ca-alginate macrobeads produced through extrusion–dripping method. J. Colloid Interface Sci. 338 (1), 63–72. https://doi.org/10.1016/j.jcis.2009.05.027.
Chang, L., Pikal, M.J., 2009. Mechanisms of protein stabilization in the solid state. J. Pharmaceut. Sci. 98 (9), 2886–2908. https://doi.org/10.1002/jps.21825.
Chen, L., Remondetto, G.E., Subirade, M., 2006. Food protein-based materials as nutraceutical delivery systems. Trends Food Sci. Technol. 17 (5), 272–283. https://doi.org/10.1016/j.tifs.2005.12.011.
Coupland, J.N., 2014. *An Introduction To the Physical Chemistry of Food* (Illustrated). Springer.
Dissanayake, M., Ramchandran, L., Vasiljevic, T., 2013. Influence of pH and protein concentration on rheological properties of whey protein dispersions. Int. Food Res. J. 20 (5), 2167.
Fennema, O.R., 2017. In: Damodaran, S., Parkin, K.L. (Eds.), Fennema's Food Chemistry, fifth ed. CRC Press Taylor & Francis Group.
Fitzsimons, S.M., Mulvihill, D.M., Morris, E.R., 2007. Denaturation and aggregation processes in thermal gelation of whey proteins resolved by differential scanning calorimetry. Food Hydrocolloids 21 (4), 638–644. https://doi.org/10.1016/j.foodhyd.2006.07.007.
He, F., Woods, C.E., Litowski, J.R., Roschen, L.A., Gadgil, H.S., Razinkov, V.I., Kerwin, B. A., 2011. Effect of sugar molecules on the viscosity of high concentration monoclonal antibody solutions. Pharmaceut. Res. 28 (7), 1552–1560. https://doi.org/10.1007/s11095-011-0388-7.
Hermansson, A.-M., 1975. Functional properties of proteins for foods-flow properties. J. Texture Stud. 5 (4), 425–439.
Hong, T., Iwashita, K., Shiraki, K., 2018. Viscosity control of protein solution by small solutes: a review. Curr. Protein Pept. Sci. 19 (8), 746–758. https://doi.org/10.2174/1389203719666171213114919.
Joye, I.J., McClements, D.J., 2014. Biopolymer-based nanoparticles and microparticles: fabrication, characterization, and application. Curr. Opin. Colloid Interface Sci. 19 (5), 417–427. https://doi.org/10.1016/j.cocis.2014.07.002.
Kamerzell, T.J., Esfandiary, R., Joshi, S.B., Middaugh, C.R., Volkin, D.B., 2011. Protein–excipient interactions: mechanisms and biophysical characterization applied to protein formulation development. Adv. Drug Deliv. Rev. 63 (13), 1118–1159. https://doi.org/10.1016/j.addr.2011.07.006.
Kornev, K.G., Neimark, A.V., 2001. Spontaneous penetration of liquids into capillaries and porous membranes revisited. J. Colloid Interface Sci. 235 (1), 101–113. https://doi.org/10.1006/jcis.2000.7347.
Kulmyrzaev, A., Bryant, C., McClements, D.J., 2000. Influence of sucrose on the thermal denaturation, gelation, and emulsion stabilization of whey proteins. J. Agric. Food Chem. 48 (5), 1593–1597. https://doi.org/10.1021/jf9911949.
Lee, B.B., Chan, E.S., 2013. Size and shape of calcium alginate beads produced by extrusion dripping. Chem. Eng. Technol. 36 (10), 1627–1642. https://doi.org/10.1002/ceat.201300230.

Lee, J.C., Timasheff, S.N., 1981. The stabilization of proteins by sucrose. J. Biol. Chem. 256 (14), 7193–7201.
Maher, P.G., Auty, M.A.E., Roos, Y.H., Zychowski, L.M., Fenelon, M.A., 2015. Microstructure and lactose crystallization properties in spray dried nanoemulsions. Food Struct. 3, 1–11. https://doi.org/10.1016/j.foostr.2014.10.001.
Matalanis, A., Jones, O.G., McClements, D.J., 2011. Structured biopolymer-based delivery systems for encapsulation, protection, and release of lipophilic compounds. Food Hydrocolloids 25 (8), 1865–1880. https://doi.org/10.1016/j.foodhyd.2011.04.014.
McClements, D.J., 2001. Estimation of steric exclusion and differential interaction contributions to protein transfer free energies in aqueous cosolvent solutions. Food Hydrocolloids 15 (4–6), 355–363. https://doi.org/10.1016/S0268-005X(01)00045-5.
McClements, D.J., 2002. Modulation of globular protein functionality by weakly interacting cosolvents. Crit. Rev. Food Sci. Nutr. 42 (5), 417–471. https://doi.org/10.1080/20024091054210.
McClements, D.J., 2017. Recent progress in hydrogel delivery systems for improving nutraceutical bioavailability. Food Hydrocolloids 68, 238–245. https://doi.org/10.1016/j.foodhyd.2016.05.037.
Mensink, M.A., Frijlink, H.W., van der Voort Maarschalk, K., Hinrichs, W.L.J., 2017. How sugars protect proteins in the solid state and during drying (review): mechanisms of stabilization in relation to stress conditions. Eur. J. Pharm. Biopharm. 114, 288–295. https://doi.org/10.1016/j.ejpb.2017.01.024.
Nicolai, T., 2016. Formation and functionality of self-assembled whey protein microgels. Colloids Surf. B Biointerfaces 137, 32–38. https://doi.org/10.1016/j.colsurfb.2015.05.055.
Nicolai, T., Britten, M., Schmitt, C., 2011. β-Lactoglobulin and WPI aggregates: formation, structure and applications. Food Hydrocolloids 25 (8), 1945–1962. https://doi.org/10.1016/j.foodhyd.2011.02.006.
Ohtake, S., Kita, Y., Arakawa, T., 2011. Interactions of formulation excipients with proteins in solution and in the dried state. Adv. Drug Deliv. Rev. 63 (13), 1053–1073. https://doi.org/10.1016/j.addr.2011.06.011.
Patocka, G., Cervenkova, R., Narine, S., Jelen, P., 2006. Rheological behaviour of dairy products as affected by soluble whey protein isolate. Int. Dairy J. 16 (5), 399–405. https://doi.org/10.1016/j.idairyj.2005.05.010.
Pradipasena, P., Rha, C., 1977. Pseudoplastic and RHEOPECTIC properties OF a globular protein (β-LACTOGLOBULIN) SOLUTION1. J. Texture Stud. 8 (3), 311–325. https://doi.org/10.1111/j.1745-4603.1977.tb01184.x.
Roos, Y., Drusch, S., 2016. Phase Transitions in Foods, 2nd. Academic Press.
Ruffin, E., Schmit, T., Lafitte, G., Dollat, J.-M., Chambin, O., 2014. The impact of whey protein preheating on the properties of emulsion gel bead. Food Chem. 151, 324–332. https://doi.org/10.1016/j.foodchem.2013.11.071.
Sawyer, L., 2003. β-Lactoglobulin. In: Fox, P.F., McSweeney, P.L.H. (Eds.), Advanced Dairy Chemistry, third ed., vol 1. Springer, pp. 319–386. Proteins.
Schmidt, R.H., Packard, V.S., Morris, H.A., 1984. Effect of processing on whey protein functionality. J. Dairy Sci. 67 (11), 2723–2733.
Semenova, M.G., Antipova, A.S., Belyakova, L.E., 2002. Food protein interactions in sugar solutions. Curr. Opin. Colloid Interface Sci. 7 (5–6), 438–444.
Song, J., 2009. Insight into "insoluble proteins" with pure water. FEBS Lett. 583 (6), 953–959.
Trappe, V., Prasad, V., Cipelletti, L., Segre, P.N., Weitz, D.A., 2001. Jamming phase diagram for attractive particles. Nature 411 (6839), 772–775. https://doi.org/10.1038/35081021.
Tro, N.J., Fridgen, T.D., Shaw, L., 2014. Chemistry: A Molecular Approach. Pearson Canada.
Wang, B., Tchessalov, S., Warne, N.W., Pikal, M.J., 2009. Impact of sucrose level on storage stability of proteins in freeze-dried solids: I. correlation of protein–sugar interaction with native structure preservation. J. Pharmaceut. Sci. 98 (9), 3131–3144. https://doi.org/10.1002/jps.21621.
Worley, J.D., 1992. Capillary radius and surface tensions. Using calculations based on Tate's law. J. Chem. Educ. 69 (8), 678.
Zhang, Z., Zhang, R., McClements, D.J., 2016a. Encapsulation of β-carotene in alginate-based hydrogel beads: impact on physicochemical stability and bioaccessibility. Food Hydrocolloids 61, 1–10. https://doi.org/10.1016/j.foodhyd.2016.04.036.
Zhang, Z., Zhang, R., Zou, L., Chen, L., Ahmed, Y., Al Bishri, W., Balamash, K., McClements, D.J., 2016b. Encapsulation of curcumin in polysaccharide-based hydrogel beads: impact of bead type on lipid digestion and curcumin bioaccessibility. Food Hydrocolloids 58, 160–170. https://doi.org/10.1016/j.foodhyd.2016.02.036.

Journal of Food Engineering 302 (2021) 110586

Contents lists available at ScienceDirect

Journal of Food Engineering

journal homepage: http://www.elsevier.com/locate/jfoodeng

Encapsulant-bioactives interactions impact on physico-chemical properties of concentrated dispersions

Mackenzie M. Hansen [a,b,*], Richard W. Hartel [b], Yrjö H. Roos [a]

[a] Food Technology, School of Food and Nutritional Sciences, University College Cork, Ireland
[b] Department of Food Science, College of Agricultural and Life Sciences, University of Wisconsin, Madison, USA

ARTICLE INFO

Keywords:
Bioactive
Whey protein
Polyphenols
Concentrated dispersions
Physico-chemical properties

ABSTRACT

Occasionally, bioactive ingredients desired for encapsulation (such as polyphenols) naturally interact with the structure-forming food components intended for their protection and delivery. Non-covalent protein-polyphenol conjugation interactions have been reported to occur naturally under mild pH and temperature conditions, causing changes to protein structures and consequent functionality. Highly concentrated liquid dispersions of varied solids contents, ratios of whey protein isolate (WPI) to sucrose contents, and Aronia berry polyphenols contents were formulated and analyzed to determine potential effects of protein-polyphenol conjugation in the system on the physical properties of dispersions. Dispersions were characterized by rheological measurements, flow testing, particle size analysis, centrifuge separation, and drop sizes produced, and microstructures were visualized with optical light microscopy. Addition of polyphenols was found to alter dispersions physical characteristics including increased viscosity and surface tension and reduced particle size of dispersions, with changes being attributed to conjugation interactions between proteins and polyphenols.

1. Introduction

When aiming to develop novel food products with high nutritional value, satisfactory processing properties, and unique structures and functional properties, Bovine whey proteins continue to be a popular choice (Kulmyrzaev et al., 2000). Whey protein isolate (WPI) is often selected in particular for development due to its solubility, wide range of functionality, and broad food applications (Cao and Xiong, 2017). Foods with enhanced protein contents and fruit components are in high demand due to increased consumer interest in health foods containing bioactives. Bioactives are natural compounds found in foods that may affect human health, and polyphenols from fruits are one type of bioactive compound known to have many benefits (Biesalski et al., 2009; Schneider, 2016; Fang and Bhandari, 2017).

Polyphenols (PPO) are a group of compounds found naturally in plants, including tea, coffee, fruits, and vegetables regularly consumed in the human diet. The compounds strong antioxidant and anti-inflammatory activities have been shown to aid in preventing the development of diseases and disorders including colon cancer (Malik et al., 2003; Zhao et al., 2004; Bermudez-Soto et al., 2007), cardiovascular disease (Mink et al., 2007), neurodegenerative diseases encountered upon aging (Moskovitz et al., 2002; Li et al., 2017), diabetes (Simeonov et al., 2002), and obesity (Zielińska-Przyjemska et al., 2007; Li et al., 2017). Polyphenols antioxidant and anti-inflammatory properties are associated with mitigation of heart attack risk (Cassidy et al., 2013) and atherosclerosis (Yousuf et al., 2016; Khoo et al., 2017; Li et al., 2017), as well as promoting healthy serum cholesterol levels (Valcheva-Kuzmanova et al., 2007a, b, c). These findings have driven developers to formulate food products with polyphenols in an attempt to impart additional nutritional benefits (Cao and Xiong, 2017; Ćujić et al., 2018).

Polyphenols are known to be chemically unstable in storage and highly susceptible to degradation (Mazza and Brouillard, 1987; Francis and Markakis, 1989; Volf et al., 2014). Stability can be affected by polyphenolic molecular structure, concentration, environmental conditions including solvent, water activity, pH, temperature, light, oxygen, ionic strength, the presence of other compounds including ascorbic acid, metals, sugars and their degradation products, enzymes, and reactions including copigmentation, self-association, and condensation (Mazza and Brouillard, 1990; Rodriguez-Saona et al., 1999; Friedman and Jürgens, 2000; Bąkowska et al., 2003; Castañeda-Ovando et al., 2009). Fresh polyphenol sources tend to have short shelf lives, and much care

* Corresponding author. Office A11, Babcock Hall, 1605 Linden Drive, Madison, WI, 53706, USA.
E-mail address: 116220787@umail.ucc.ie (M.M. Hansen).

https://doi.org/10.1016/j.jfoodeng.2021.110586
Received 2 January 2021; Received in revised form 11 February 2021; Accepted 7 March 2021
Available online 11 March 2021
0260-8774/© 2021 The Author(s). Published by Elsevier Ltd. This is an open access article under the CC BY license (http://creativecommons.org/licenses/by/4.0/).

must be taken to maintain polyphenols through formulation and processing of food products with longer shelf lives. Recently, complexation of polyphenols with other molecules has been utilized as a method of active stabilization, with milk protein-polyphenol conjugates being widely popular to study for potential bioactive delivery and health benefits (Chung et al., 2015; Cao and Xiong, 2017; Quan et al., 2019).

Decades of research focused on the addition of phenolic compounds to protein-containing food matrices have reported a common finding: a natural affinity exists between polyphenols and proteins to complex and form conjugates (Hagerman and Butler, 1978; Foegeding et al., 2017). Polyphenols (relatively small molecules, ~180–700 Da) are able to bind to sites on proteins (comparatively large molecules; average MW of WPI ~17,000 Da (Ma and Zhao, 2019)) forming small, soluble complexes of varied nature at low concentrations. While Spencer et al. (1988) postulated that protein-polyphenol complexation was likely pH-dependent, Schneider (2016) found that large conjugate particles formed from mixtures of proteins and juices containing polyphenols were not formed in corresponding 'imitation juices' with identical pH but without polyphenols, confirming that changes to physicochemical properties of dispersions were not simply due to a pH effect. Conjugation interactions between polyphenols and proteins in food systems are mainly divided into non-covalent and covalent interactions. The extent and type of interactions are dependent on pH, protein and polyphenol types present, concentration ratios, and reaction times (Schneider, 2016; Quan et al., 2019). Non-covalent interactions are common in processed foods, occur under neutral and acidic environmental pH conditions, and consist mainly of weak binding interactions including van der Waal's forces, hydrogen bonding, and hydrophobic interactions (Kanakis et al., 2011; Bohin et al., 2012; Le Bourvellec and Renard, 2012; Chung et al., 2015; Schneider, 2016; Oancea et al., 2017). Non-covalent complexes formed between proteins and polyphenols, driven mainly by hydrophobic interactions, have been reported to significantly change the structures of the proteins at room temperature (Rawel et al., 2005; Cao and Xiong, 2017; Ma and Zhao, 2019; Quan et al., 2019).

In previous work, we presented a continuous process for forming concentrated, liquid dispersions comprised of WPI and sucrose into dry, stable beads with high protein contents that could serve to encapsulate active ingredients (Hansen et al., 2020). We identified the "next step" to be completed in subsequent experiments was the addition of an active ingredient to the protein-sucrose matrix. Aronia berries are reported to be a rich source of dietary polyphenols including anthocyanins, flavonoids, chlorogenic acid, proanthocyanidins, and hydroxycinnamic acids (Taheri et al., 2013; Xie et al., 2016, 2017). Thus, Aronia is of interest for formulation. Though acknowledged to occur, the functional effects of non-covalent interactions under neutral and acidic pH conditions at mild temperatures have not been investigated as thoroughly as their covalent counterparts, despite developers opting for gentle processing conditions to better protect actives in nutritional products (Cao and Xiong, 2017; Ma and Zhao, 2019; Xue et al., 2020).

The aim of this study is to investigate and characterize the physical, functional, and practical processing consequences of non-covalent conjugation interactions on the physical properties of liquid feed dispersions. We hypothesize that the addition of polyphenols (via Aronia extract) will give rise to changes in the physical properties of feeds including viscosity, flow behavior, and particle size distribution due to protein-polyphenol complexation, compared to properties of dispersions without Aronia. This work would contribute to the limited body of research describing non-covalent interactions between proteins and polyphenols under mild conditions, characterizing their effects on the physical properties of mixtures. In addition, we hope to provide practical knowledge for further applications such as encapsulation, protection, and delivery with concentrated protein-polyphenol mixtures.

2. Materials and methods

2.1. Materials

Whey Protein Isolate, WPI (IsoChill 9000), was supplied by Agropur, Inc. (Luxemburg, Wisconsin, USA). Sucrose (pure cane, extra fine, granulated sugar) was supplied by Domino Foods, Inc. (Yonkers, New York, USA). Standardized Aronia berry (Chokeberry) Powder, containing a minimum level of 15% anthocyanins and 55.6% total polyphenols, was supplied by Artemis International (Fort Wayne, Indiana, USA) and stored in a freezer at −18 °C in the absence of light. Deionized (D.I.) water was utilized in all experiments.

2.2. Dispersion preparation

A dry blend of sucrose and WPI powder was prepared at room temperature. To prepare liquid feeds, D.I. water was weighed and the WPI-sucrose blend was mixed into the water with a Fisher Scientific PowerGen 125 Homogenizer (125 W, 115 V, 50/60 Hz; maximum volume 100 mL; speed 8000–30,000 RPM; Hampton, New Hampshire, USA) at a speed setting of '6' for ~45 s. The WPI-sucrose solution was subsequently combined with an aliquot of 50% Aronia extract solution (Aronia powder containing 55.6% total polyphenols mixed into D.I. water) to obtain desired WPI, sucrose, polyphenols (PPO), and water proportions (~30 s additional mixing). More extract solution was required to reach the desired polyphenol content of mixtures due to the presence of other compounds besides PPO in the Aronia extract. pH was measured with an Accumet Basic AB15 meter (Fisher Scientific, Hampton, New Hampshire, USA) after calibrating the electrode at pH four and seven.

Duplicates of twenty-seven formulations of varied solids contents and compositions were prepared for subsequent triplicate analysis in a 3

Table 1
Estimated drop diameters calculated from flow tests data and measured diameters (mm) of frozen drops formed from feed dispersions with varied WPI: sucrose, total solids contents, polyphenols concentrations, and pH.

WPI: sucrose	Total Solids	[PPO]	pH	Diameter (calculated)	Diameter (frozen)
–	%		–	mm	mm
0.75	25	0	6.03	4.59 ± 0.02	4.45 ± 0.09
1	25	0	6.08	4.60 ± 0.02	4.58 ± 0.10
1.25	25	0	6.01	4.54 ± 0.03	4.48 ± 0.05
0.75	25	0.5	5.73	4.67 ± 0.03	4.63 ± 0.03
1	25	0.5	5.94	4.67 ± 0.04	4.63 ± 0.09
1.25	25	0.5	5.95	4.65 ± 0.06	4.55 ± 0.14
0.75	25	1	5.57	4.65 ± 0.08[a]	4.39 ± 0.08[a]
1	25	1	5.72	4.70 ± 0.03	4.50 ± 0.12
1.25	25	1	5.84	4.67 ± 0.05	4.65 ± 0.02
0.75	35	0	6.00	4.37 ± 0.14	4.22 ± 0.10
1	35	0	6.19	4.55 ± 0.05	4.50 ± 0.03
1.25	35	0	6.09	4.57 ± 0.03[a]	4.41 ± 0.03[a]
0.75	35	0.5	5.79	4.55 ± 0.02	4.51 ± 0.03
1	35	0.5	5.98	4.51 ± 0.10	4.35 ± 0.06
1.25	35	0.5	5.92	4.52 ± 0.03	4.44 ± 0.08
0.75	35	1	5.79	4.63 ± 0.04[a]	4.46 ± 0.04[a]
1	35	1	5.81	4.63 ± 0.03	4.52 ± 0.11
1.25	35	1	5.82	4.63 ± 0.03	4.59 ± 0.07
0.75	45	0	6.16	4.51 ± 0.03[a]	4.24 ± 0.10[a]
1	45	0	6.10	4.50 ± 0.02	4.37 ± 0.11
1.25	45	0	6.06	4.50 ± 0.02	4.39 ± 0.16
0.75	45	0.5	5.89	4.53 ± 0.04	4.41 ± 0.10
1	45	0.5	5.82	4.23 ± 0.02	4.31 ± 0.09
1.25	45	0.5	6.03	4.55 ± 0.06	4.49 ± 0.05
0.75	45	1	5.78	4.51 ± 0.05	4.35 ± 0.12
1	45	1	5.88	4.57 ± 0.06	4.45 ± 0.12
1.25	45	1	5.79	4.52 ± 0.05	4.48 ± 0.06

[a] indicates significant differences between calculated and measured diameters.

× 3 × 3 factorial design, with experiments conducted in a random order (Table 1). Ratios of WPI to sucrose and total solids contents were selected based on findings from our previous work (Hansen et al., 2020); all formulations were prepared within a range of total solids (%) projected to pump successfully under the selected conditions. Levels of Aronia extract/PPO were selected to compare formulations without the active (0%) to formulations with 2 different levels of addition. Studies have indicated that complexation may occur at PPO addition levels from 0.1% to 1%, rendering the selection of 0.5 and 1% PPO reasonable (Harbourne et al., 2011; von Staszewski et al., 2011; Thongkaew et al., 2014; Bayraktar et al., 2019). All dispersions were left to defoam for at least 1 h before analysis.

2.3. Feed characterization

2.3.1. Flow testing

Flow properties of feed dispersions at room temperature were measured as reported in our previous work (Hansen et al., 2020). Briefly, dispersions were pumped through a benchtop, manual control, variable speed, peristaltic pump (120 S/DV; Watson Marlow, Falmouth, England) with silicon tubing 85 cm length, 2 mm bore, and 1 mm wall thickness (BÜCHI Labortechnik AG, Flawil, Switzerland) at a constant speed (13 RPM). The time required to deposit 10 mL of feed, the number of drops deposited per 1 min, mass of 10 mL of feed, and average masses of individual drops were measured in triplicate and recorded, allowing for mass flow rates, volume flow rates, feed densities, drop surface tensions, drop diameters, and drop volumes to be calculated.

Density of liquid feed (kg/m^3) was calculated by:

$$\frac{mass\ (g)\ of\ 10\ mL\ feed}{10\ mL} \tag{1}$$

Average drop volume (mL) was calculated by:

$$\frac{10\ mL\ feed}{time\ (s)\ to\ deposit\ 10\ mL} * \frac{60s\ per\ min}{\#\ drops\ per\ min} \tag{2}$$

Mass flow rate (kg/s) was calculated by:

$$\frac{mass\ (g)\ of\ 10\ mL\ feed}{time\ (s)\ to\ deposit\ 10\ mL} \tag{3}$$

Volume flow rate (m^3/s) was calculated by:

$$\frac{mass\ flow\ rate\ \left(\frac{kg}{s}\right)}{feed\ density\ \left(\frac{kg}{m^3}\right)} \tag{4}$$

Drop surface tension was calculated with Tate's Law (Worley, 1992):

$$\frac{\left(Average\ drop\ mass\ (g) * acceleration\ due\ to\ gravity\ \left[9.8\frac{m}{s^2}\right]\right)}{2\pi * \left(external\ diameter\ of\ tubing\ tip\ [mm] * correction\ factor\ \left[\frac{drop\ radius}{(drop\ volume)^{\frac{1}{3}}}\right]\right)} \tag{5}$$

The correction factor in this calculation is in place because the total drop formed at the tip of the outlet tubing does not release, and residual liquid is left on the end of the tube.

Drop diameter was calculated by

$$\left[\frac{(3 * average\ drop\ volume\ [mL])}{4 * \pi}\right]^{\frac{1}{3}} * 2 \tag{6}$$

This equation is built off the assumption that drops form a perfectly spherical shape, and thus is derived from the equation for the volume of a sphere:

$$V = \frac{4}{3}\pi r^3 \tag{7}$$

2.3.2. Rheology

A DHR-2 rheometer (TA Instruments, Delaware, USA) was used to measure the rheological properties of feed dispersions in triplicate, modifying the methods used by Harbourne et al. (2011) and Wang and Hartel (2020). Small-strain oscillatory measurements were conducted with a concentric cylinder attachment set, with a bob (28 mm diameter, 42 mm length) and cup (30 mm diameter). Dispersions (20 mL samples) were poured into the cup and the bob was inserted into the sample until it reached the geometry gap (5917.1 μm). After the system was conditioned at 25 °C for 60s, the samples were oscillated within their linear viscoelastic region (LVR; not shown) for 180s under 1% strain and 1 Hz frequency. *G*', *G*", complex viscosity, and other parameters were recorded.

To confirm that the strain selected for oscillatory measurements (1%) was within the LVR, a strain sweep test from 0.1 to 10% at a frequency of 1 Hz was performed along with oscillatory measurements for each formulation.

2.3.3. Particle size distribution

Particle size distribution of feed dispersions was measured in triplicate using a Malvern Mastersizer 2000 (Malvern Instruments Ltd., Worcestershire, U.K.) with Hydro 2000S liquid sampler. The laser light diffraction and light scattering techniques described by Warren and Hartel (2014) were modified to measure the sizes of insoluble WPI particles and potential WPI-polyphenol conjugates in the dispersions. Dispersions were injected dropwise into the liquid sampling unit to obtain distributions. D.I. water was used as the dispersant, with a refractive index of 1.33. The WPI refractive index was set at 1.545 with absorbance set at 0.001. Measurements were taken at obscurations between 11% and 15% as described by Alawode (2014).

2.3.4. Optical light microscopy

The sizes of WPI particles and potential WPI-polyphenol conjugates in dispersions were observed by optical light microscopy. The preparation method described by Warren and Hartel (2014) was utilized; 2 drops of feed dispersion were diluted with ~2 mL of D.I. water. Samples were lightly mixed to obtain a homogeneous mixture with the water. One drop of diluted sample was placed on a glass slide and covered with a cover slip. Samples were imaged at 40x and 200x magnification via Nikon Eclipse FN1 optical microscope (Nikon Instruments Inc., Melville, NY, USA) with a Nikon Digital Sight DS-U3 camera control unit attached (ver. 1). Sample observation, photo capturing, and error-bars placement were performed in NIS-Elements D Imaging Software (ver. 4).

2.3.5. Centrifuge separation

Aliquots (1.25 g) of not diluted and 10 times diluted feed dispersions containing 45% total solids, as well as 1% Aronia polyphenols solution, were pipetted into microcentrifuge tubes in duplicate (1.5 mL graduated tubes with flat caps, Fisherbrand ®, Fisher Scientific, Hampton, New Hampshire, USA) to observe separation after centrifugation at 12,000 rpm (~13,523×*g*) and 20 °C for 20 min in a microcentrifuge (Centrifuge 5424 R with FA-45-24-11 rotor, Eppendorf, Hamburg, Germany). Sample tubes were visually assessed and photographed to identify the location of the colored polyphenolic compounds after centrifugation, as a colored precipitate after separation could confirm the formation of protein-polyphenol conjugates. Supernatant was carefully removed from one of the sample tubes and placed in an empty tube so that supernatant and precipitate could be observed separately as well.

2.4. Frozen drop preparation

For solid bead formation, an aluminum pan was filled with liquid nitrogen (LN_2) (100% purity; Airgas, Madison, WI, USA) and placed on a Styrofoam layer to insulate between the pan and the worktop. A retort stand was arranged so that the end of the outlet tubing was situated above the surface of the LN_2. Liquid feed was pumped through the

tubing and dispensed dropwise into the LN_2, with irregular, gentle hand-stirring via metal spatula to discourage drop coalescence prior to solidification. Drops were left to freeze/harden in the LN_2 for ~5 min before removal and immediate triplicate diameter measurements.

2.4.1. Frozen drop diameters

Diameters of frozen beads were measured 3 times per formulation after hardening in LN_2 with digital Vernier calipers (0–150 mm; Stainless Hard), and an average value was reported. Accuracy was not a concern as beads were measured immediately upon removal from LN_2 to prevent any shrinkage due to melting, maintaining solid structures and shapes for measurements (Lee and Chan, 2013). Measured bead diameters were compared with calculated estimate values.

2.5. Statistical analysis

Repeated experiments were analyzed in triplicate. The obtained data were analyzed by calculating mean values and standard deviations. Analysis of variance (3-way ANOVA; Tukey's HSD test) and independent measures t-tests (equal variance not assumed) were performed to compare mean values when appropriate using JMP® Pro version 15.0.0 (SAS Institute Inc., Cary, North Carolina, USA). The level of significance was determined at $p < 0.05$.

3. Results and discussion

3.1. Feed characterization

3.1.1. pH

Dispersions pH was observed to decrease slightly with increasing PPO addition (Table 1). pH effects have potential to influence intermolecular interactions and functional properties including viscosity and particle size (Spencer et al., 1988; Saluja and Kalonia, 2005; Cao and Xiong, 2017; Hong et al., 2018). When solution pH is away from the protein isoelectric point (pI) intermolecular interactions are unfavorable, allowing proteins to remain suspended with a relatively low viscosity; when pH approaches pI proteins are more likely to aggregate (Song, 2009; Coupland, 2014). pH may also influence which protein side groups are exposed in the system and thus determine the number of binding sites available for protein-polyphenol interactions to occur, which may affect the size of conjugates formed (Rawel et al., 2005). Assuming an average pI for WPI between pH 4.2 and 5.3, it is unlikely that the slight downward shift in pH resulting from the addition of small proportions of Aronia extract was cause for measurable changes to dispersions physical properties or protein functionality, as pH was still substantially higher than the pI values reported in the literature for constituent β-lactoglobulin (pI ~ 5.2–5.3) and α-lactalbumin (~4.2–4.8) (Kilara and Harwalkar, 1996; Demetriades and McClements, 1998; Jean et al., 2006). Work by Schneider (2016) also verified that particle size

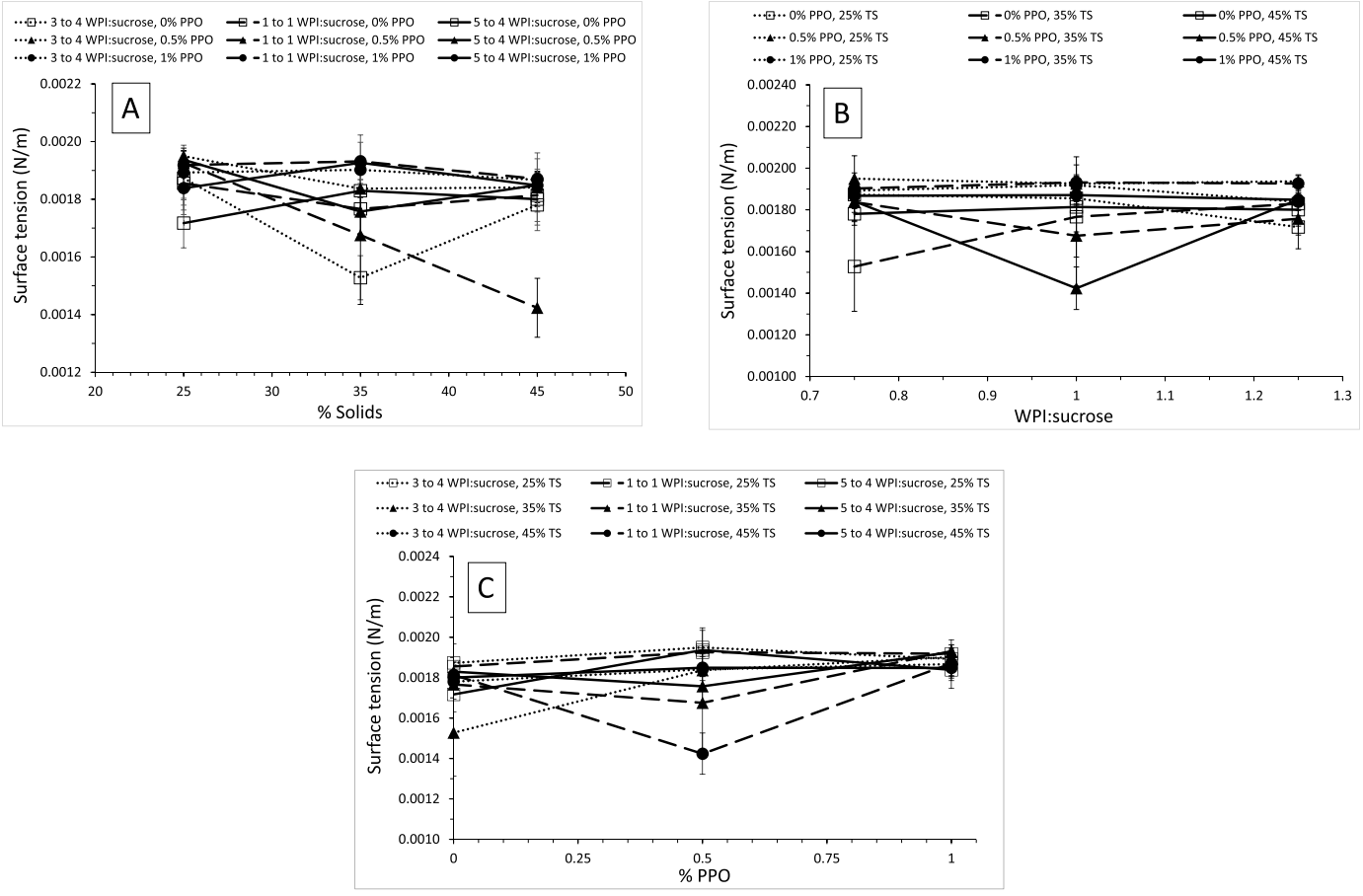


Fig. 1. Effect of total solids content (%) [**A**], WPI:sucrose ratio [**B**], and PPO content (%) [**C**] on the calculated surface tension (N/m) of dispersions at 25 °C; (n = 6). Lines are for guiding purposes only.

changes in protein-juice dispersions were not due to changes in pH alone.

3.1.2. Interfacial tension

Individual drops will form out of feeds when the gravitational forces acting on the drop overcome the surface tension forces acting around the circumference of the tip of tubing, rendering surface tension properties critical in determination of drop sizes produced. Feeds containing 1% PPO had slightly higher surface tensions than corresponding feed formulations with lower PPO, though generally no large changes in surface tension were observed with increasing % TS (Fig. 1a). According to the ANOVA, % TS significantly impacted the surface tension of feeds. Tukey's HSD tests further clarified that feeds with lower solids contents (25% TS) had significantly higher ($p < 0.05$) surface tension values than those with higher solids concentrations (35 and 45% TS); this finding is best demonstrated by feeds containing 0.5% PPO in Fig. 1a. Previous studies have found that increased biopolymer concentrations and viscosities in dispersions have resulted in decreased surface tensions as well (Chan et al., 2009; Lee and Chan, 2013).

Changing the ratio of WPI to sucrose in feeds was not found to meaningfully impact the surface tension of feeds studied (Fig. 1b) according to the ANOVA, though feeds containing 1% PPO had slightly higher surface tensions than corresponding formulations with lower levels of PPO. WPI to sucrose ratios of 5:4 and 1:1 were found to be significantly different from one another ($p < 0.05$) when Tukey's HSD tests were applied, but neither ratio was significantly different from the 3:4 WPI to sucrose ratio. Sucrose alone is not thought to affect surface tension notably, as sugars are not particularly surface-active molecules. The differences in whey proteins, which are known to behave as surfactants, were not sufficient to affect surface tension in these systems.

According to the ANOVA, changing the PPO concentration in feeds had a significant overall effect on surface tension ($p < 0.05$). Tukey's HSD tests expanded on this, indicating that increasing PPO content from 0 or 0.5%–1% resulted in significantly increased surface tension values ($p < 0.05$). This trend was only observed under a few conditions, while many conditions showed no meaningful trends (Fig. 1c); the variations in trends may be attributed to air entrapped in feeds giving altered surface tension calculations. Feeds comprised of 25% TS were observed to have the highest surface tensions of the formulations. Complexation of polyphenols and proteins is known to form conjugates that can grow to the point of forming larger aggregates, if environmental conditions, polyphenol and protein concentrations, ratios, and types are optimal (Schneider, 2016; Quan et al., 2019). As polyphenol concentrations increase (in this case, > 0.5%), so does complexation until sufficient coating promotes protein cross-linking via polyphenols serving as cooperative bridges, ultimately leading to precipitation of larger aggregates formed from smaller conjugates when the 'critical coating level' is exceeded (Spencer et al., 1988; Charlton et al., 2002; Rawel et al., 2005; Ozdal et al., 2013). The increased presence of larger protein-polyphenol complexes and aggregates in dispersions would likely result in increased total intermolecular interactions in the system; liquids containing larger numbers of strong attractive intermolecular forces often have higher surface tensions (He et al., 2011; Tro et al., 2014), which may explain increased surface tensions observed with increasing PPO for some formulations.

It has been reported that drop diameters and surface tension are directly related; as surface tension decreases, so does the diameter of the resulting drop, indicating that the pendant drop is sufficiently dense or packed with solids to detach at lower volumes and its surface tension was more easily overcome by gravitational forces. Upon plotting the calculated diameters of drops against the calculated surface tension of feed formulations the best fit line applied to our data showed a positive slope value (Fig. 2) illustrating a positive, direct correlation, as described by Lee and Chan (2013). The scatter in the correlation is likely due to drop diameter and surface tension calculations built from calculated drop volumes and densities measured, which may change with inclusion of unavoidable air in the dispersions, as well as the inherent variation within food ingredients.

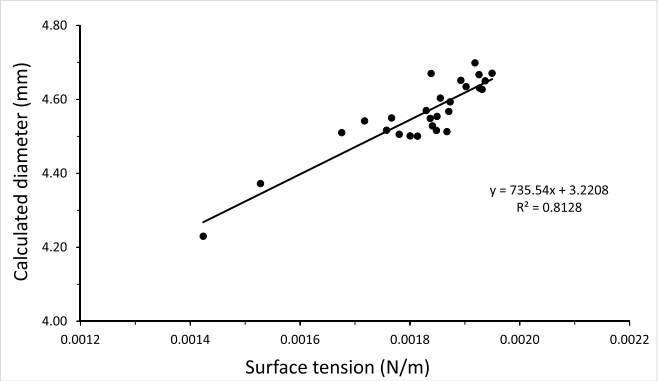


Fig. 2. The relationship between the surface tensions (N/m) of feed dispersions containing WPI:sucrose ratios of 0.75, 1.0, and 1.25, polyphenols contents of 0, 0.5, and 1%, and total solids contents of 25, 35, and 45% at 25 °C and calculated diameters (mm) of drops.

Worley (1992) found that Tate's law could be used to determine unknown surface tensions within reasonable accuracy despite the simplicity of the drop weight method used. Other more traditional, commonly used methods including Wilhelmy plates, du Nuoy rings, capillary rise, maximum bubble pressure, and pendant drop measurements may provide more accuracy, but were not as compatible with the feed dispersions of interest due to their viscosity, stickiness, turbidity, remaining air bubbles present, and dark coloration when Aronia is present. All of these characteristics would make it harder to measure surface tension with conventional methods.

3.1.3. Viscosity

Viscosity is another important physical property of dispersions related to fluid flow properties, and often informs processing and manufacturing operations for a given product (Johnson et al., 1975; Hartel et al., 2018). Even slight alterations to composition and other dispersion conditions can cause increased crowding and entangling of particles, as well as promote conformational changes to protein structures that may enhance aggregation depending on side groups exposed, both of which increase viscosity (Song, 2009; Coupland, 2014). In addition to averaged complex viscosity data obtained from oscillatory time sweeps, information about the internal friction of feed materials was also obtained by measuring the viscous/loss modulus- G'', the storage modulus describing elasticity- G', and their ratio-tan δ (data not shown). G' was always greater than G'' (tan δ was always < 1) for all formulations, indicating that feed dispersions demonstrated more elastic behaviors than viscous. Feeds comprised of 25% TS, 35% TS, and 45% TS had tan δ values < 0.1, <0.2, and <0.9 on average, respectively.

In previous work with dispersions containing only WPI and sucrose, we observed that viscosity increased with WPI concentration, in agreement with the findings from numerous earlier studies reporting direct, positive relationships between biopolymer concentrations and viscosity (Alizadehfard and Wiley, 1995; Patocka et al., 2006; Chan et al., 2009; He et al., 2011; Matalanis et al., 2011; Lee and Chan, 2013; Coupland, 2014; Hong et al., 2018). Specifically, we observed minimally increasing viscosities with increasing concentrations at lower levels until a significant increase was observed at what was thought to be a 'critical packing point' concentration, where particle volume fractions and interactions became so abundant and crowded that viscosity was significantly increased due to steric repulsion between molecules causing jamming and arrested feed dynamics (Hansen et al., 2020). This experiment yields complementary findings: although the ANOVA reported that % TS significantly ($p < 0.05$) impacted viscosity, when % TS increased from 25 to 35%, no appreciable change in viscosity was observed with

Tukey's HSD tests for any feed formulations, indicating no significant differences between the conditions. Further increase to 45% TS resulted in significantly increased viscosities for all formulations ($p < 0.05$), with feeds comprised of 5:4 and 1:1 WPI:sucrose ratios generally having higher viscosities at 45% TS than those with 3:4 WPI:sucrose ratios (Fig. 3a). It is likely that the threshold for 'critical packing concentration' was reached between 35 and 45% TS, as increased solids contents led to increased intermolecular interactions in the system, resulting in the significant increase in viscosity (Tro et al., 2014). Correspondingly, the ANOVA indicated that as the ratio of WPI to sucrose (and as a result, total protein content) increased in feed dispersions, complex viscosity was also found to significantly increase ($p < 0.05$). The increasing trend described by the ANOVA is only clearly demonstrated by feeds containing 45% TS in Fig. 3b, which may be a result of the strong effect of 45% solids content on viscosity. The effect of increasing the WPI:sucrose ratio may be relatively weak compared to that of % TS, and thus may not demonstrate strong, clear trends consistently unless more extreme (in this case, 45% TS) conditions are present. These results build upon those from our previous work, providing further evidence that specifically increasing WPI content results in increased viscosity, even as % total solids in the system remains constant. Fig. 3b also shows that among all feeds containing 45% TS, those containing 1% PPO had consistently higher viscosities than corresponding feeds with lower PPO.

According to the ANOVA, with all other parameters (% TS and WPI:sucrose ratios) being held constant, viscosity was significantly ($p < 0.05$) influenced by PPO content; Tukey's HSD tests expanded on this, reporting significantly increased ($p < 0.05$) viscosities with increasing addition of Aronia PPO to feed dispersions. This increasing trend described by the ANOVA is only clearly demonstrated by feeds containing 45% TS in Fig. 3c, which may also be attributed to the strong effect of 45% TS on viscosity discussed earlier. Additionally, feeds containing 45% TS were observed to have higher viscosities at higher WPI:sucrose ratios in Fig. 3c. The effect of increased PPO may be weak relative to that of % TS (similar to the WPI:sucrose effect), and thus may not demonstrate strong trends consistently unless more extreme conditions (high % TS) are also present that may make slight shifts more noticeable. It is known that polyphenols and proteins complex under weak acidic pH conditions and form non-covalent conjugates where polyphenols may act as bridges to polymerize protein molecules. The extent and type of interactions formed depend on factors including system pH, protein and polyphenol types, concentration ratios, etc., but when concentrations of both components are optimal, proteins have been shown to form relatively large network structures non-covalently (Siebert et al., 1996; Schneider, 2016; Zhou et al., 2020). Protein-polyphenol interactions have been found to induce significant changes to protein structures, which can consequently alter their functional and nutritional properties (Schneider, 2016; Ma and Zhao, 2019; Xue et al., 2020; Zhou et al., 2020). The addition of polyphenols to WPI-sucrose feeds increases intermolecular interactions within the fluid system with the formation of protein-polyphenol complexes and may result in increases in viscosity and behavioral complexity.

3.1.4. Power requirements for pumping

Viscosity, density, and flow rate data collected for dispersions were used to determinate representative values for use in calculations of the estimated power requirements for the benchtop peristaltic pump to pump feed dispersions at a constant rate of 13 RPM. Power requirements for the pump (Φ; Watts) were calculated by multiplying an average mass

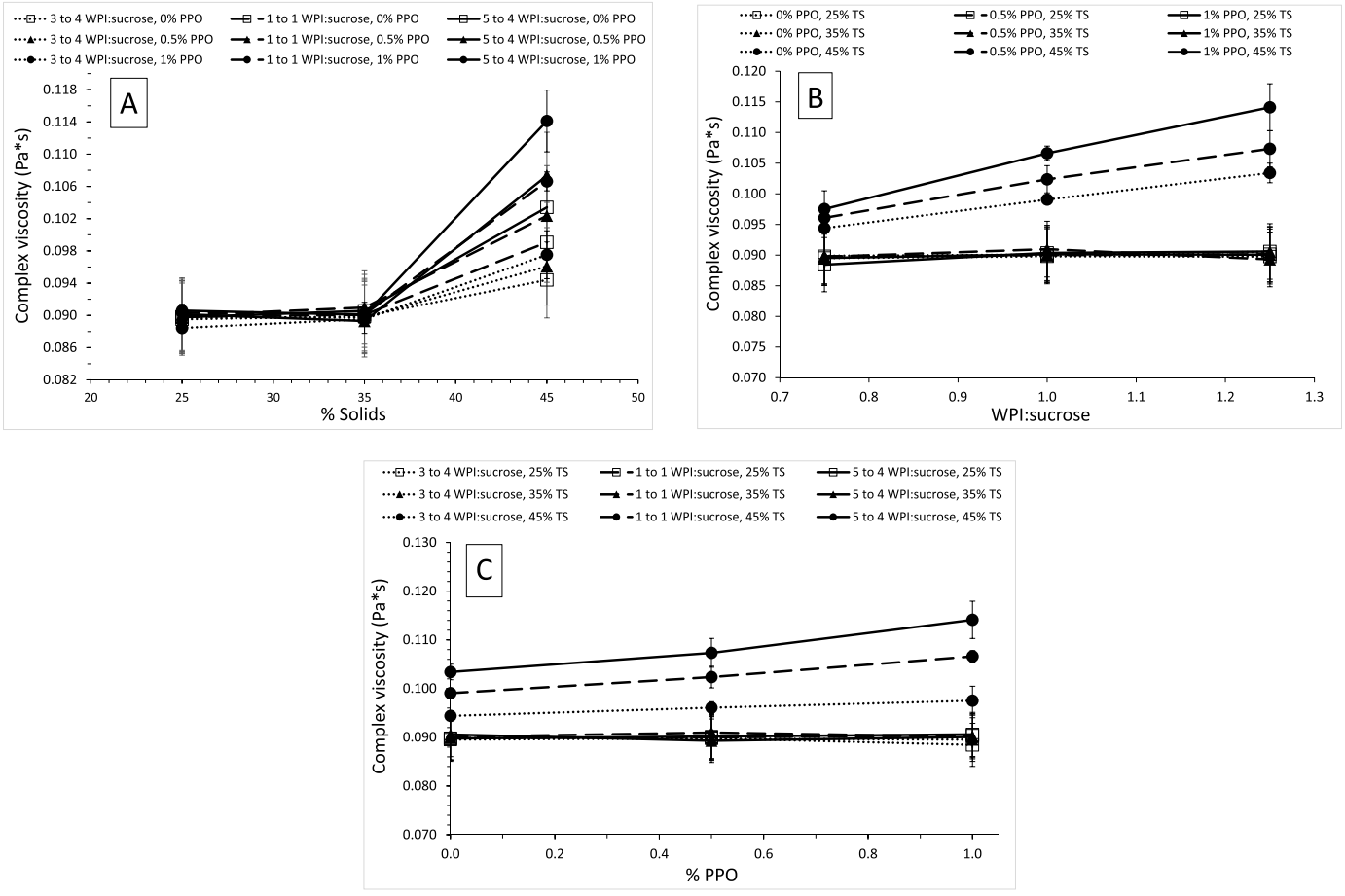


Fig. 3. Effect of total solids content (%) [**A**], WPI:sucrose ratio [**B**], and PPO content (%) [**C**] on the complex viscosity (Pa*s) of dispersions at 25 °C; (n = 6). Lines are for guiding purposes only.

flow rate representative of feeds studied ($\dot{m} = 5 \times 10^{-5}$ kg/s) by the work done per unit mass by the pump on the feeds (E_p; J/kg). E_p was calculated from derivations of Bernoulli's equation, based on assumptions including constant density of feeds (Singh and Heldman, 2013). No major changes in pressure, elevation, or feed velocities were thought to occur with the process studied, so E_p was calculated based on the energy losses due to friction (both major and minor). Expansions and contractions were accounted for as minor frictional losses resulting from the rotary peristaltic pumping action. With known dimensions for the tubing and containers used for uptake and depositing feeds, and representative values selected for feed density ($\rho = 1000$ kg/m^3), mean velocity ($\bar{u} = 0.016$ m/s), mass flow rate ($\dot{m}$), and feed viscosity ($\mu = 0.09$ Pa*s) based on experimental data, E_p was calculated to be approximately 23,050 J/kg, and $\Phi = 1.15$ Watts.

3.1.5. Particle size distribution

Numerous studies have reported structural changes to proteins imparted by interactions with polyphenols, since protein-polyphenol complexation can alter dispersion conditions that influence protein conformation and electrostatic repulsion in solution (Rawel et al., 2005; Song, 2009; Bandyopadhyay et al., 2012; Coupland, 2014; Cao and Xiong, 2017; Girard et al., 2018; Ma and Zhao, 2019; Quan et al., 2019). These changes have the potential to amplify the formation of protein-protein aggregates as well as the growth of protein-polyphenol conjugates (Hong et al., 2018). It may be expected, then, that dispersion particle sizes may undergo measurable changes due to these interaction effects as well. Particle size analysis could be considered a useful tool in assessing protein-polyphenol interactions, as particle size may influence numerous functional properties (Le Bourvellec and Renard, 2012; Schneider, 2016).

According to the ANOVA, % TS had a significant ($p < 0.05$) effect on the average particle size (volume-weighted mean, $d_{4,3}$) of dispersions. Tukey's HSD tests clarified that increasing % TS resulted in significantly increased average particle sizes ($p < 0.05$) in feeds. This increasing trend was most clearly demonstrated by feeds containing 0.5 and 1% PPO in Fig. 4a; feeds with 0% PPO showed virtually no change in particle size with increasing % TS. Increases in average particle sizes with increasing % TS in feeds containing PPO are indicative of conjugation interactions between proteins and PPO aiding in the formation of larger particles, as more proteins are present for interactions with other proteins as well as PPO. Similarly, the largest particles detected in the dispersions also shifted towards larger sizes with increasing total solids, with all feeds displaying approximately normal distributions. Increased solids concentrations, and thus more total protein in feeds, resulted in more extensive and larger aggregate formation due to more frequent overlapping and entangling interactions (Coupland, 2014).

According to the ANOVA report, altered ratios of WPI to sucrose in dispersions did not significantly ($p > 0.05$) affect particle size distributions (data not shown). No significant differences in particle size were observed between dispersions prepared at three different WPI-sucrose ratios ($p > 0.05$), as indicated by the Tukey's HSD tests, with all feeds displaying approximately normal distributions. This suggests that varying levels of sucrose in the highly concentrated systems do not strongly affect the occurrence of protein-protein interactions in solution that result in aggregate formation. This may be due in part to the hygroscopic nature of the sugar and its strong affinity for water and easy dissolution into the bulk solvent at room temperature at the concentrations used. In this case, more protein present in feeds did not result in increased aggregate sizes as was observed when total system solids increased.

According to the ANOVA, average particle sizes of dispersions were significantly affected by PPO content ($p < 0.05$); Tukey's HSD tests expanded on this, reporting that feeds formulated with 0% PPO had significantly larger average particle sizes ($p < 0.05$) than those formulated with 0.5 and 1% PPO. Although these effects were attributed to PPO addition, they were dependent on feed % TS as well. Feeds containing 25% TS most clearly demonstrated the decreasing trend described by the ANOVA (Fig. 4b) and generally had the smallest particle sizes compared to feeds with higher % TS; those containing 35% TS showed only slight reductions in particle size with increasing PPO. Interestingly, feeds containing 45% TS showed increased particle sizes with increasing PPO, which may be attributed to the strong effect of % TS interfering with the visibility of comparatively weaker PPO effects on average particle sizes of dispersions. Siebert et al. (1996) also detected small particle sizes with light scattering techniques, and attributed the smaller particle sizes observed at higher polyphenol concentrations to the saturation of possible binding sites on proteins with polyphenols, causing repulsive interactions to dominate the system and prevent formation of larger aggregates. Thongkaew et al. (2014) observed reduced particle sizes even at low levels of polyphenol addition to dispersions with WPI and WPI-pectin complexes. Similar trends were observed by Xue et al. (2020) when studying complexation between soy protein isolate (SPI) and cyanidin-3-galactoside; conjugation was found to break down aggregates and lead to reduced particle sizes by disrupting SPI hydrogen bonds, increasing electrostatic repulsion, and decreasing hydrophobic interactions between protein molecules, thus reducing protein-protein interactions.

3.1.6. Optical light microscopy

Particle size distributions and average particle size measurements of feed dispersions generated by Mastersizer light scattering were supported by optical light microscopy. Microscope images illustrate the

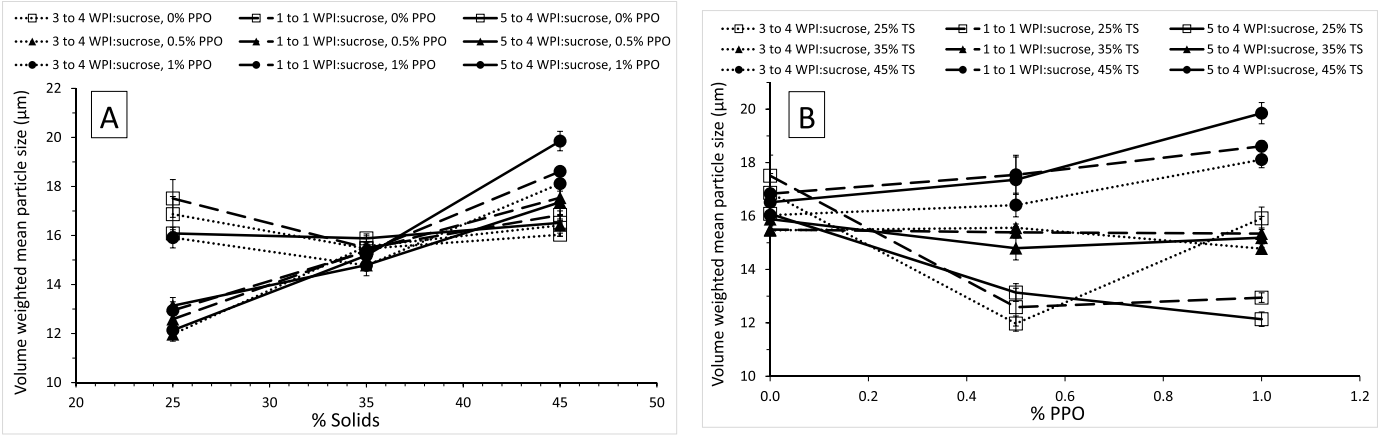


Fig. 4. Effect of total solids content (%) [**A**] and PPO content (%) [**B**] on the average particle size (µm) of dispersions at 25 °C; (n = 6). Lines are for guiding purposes only.

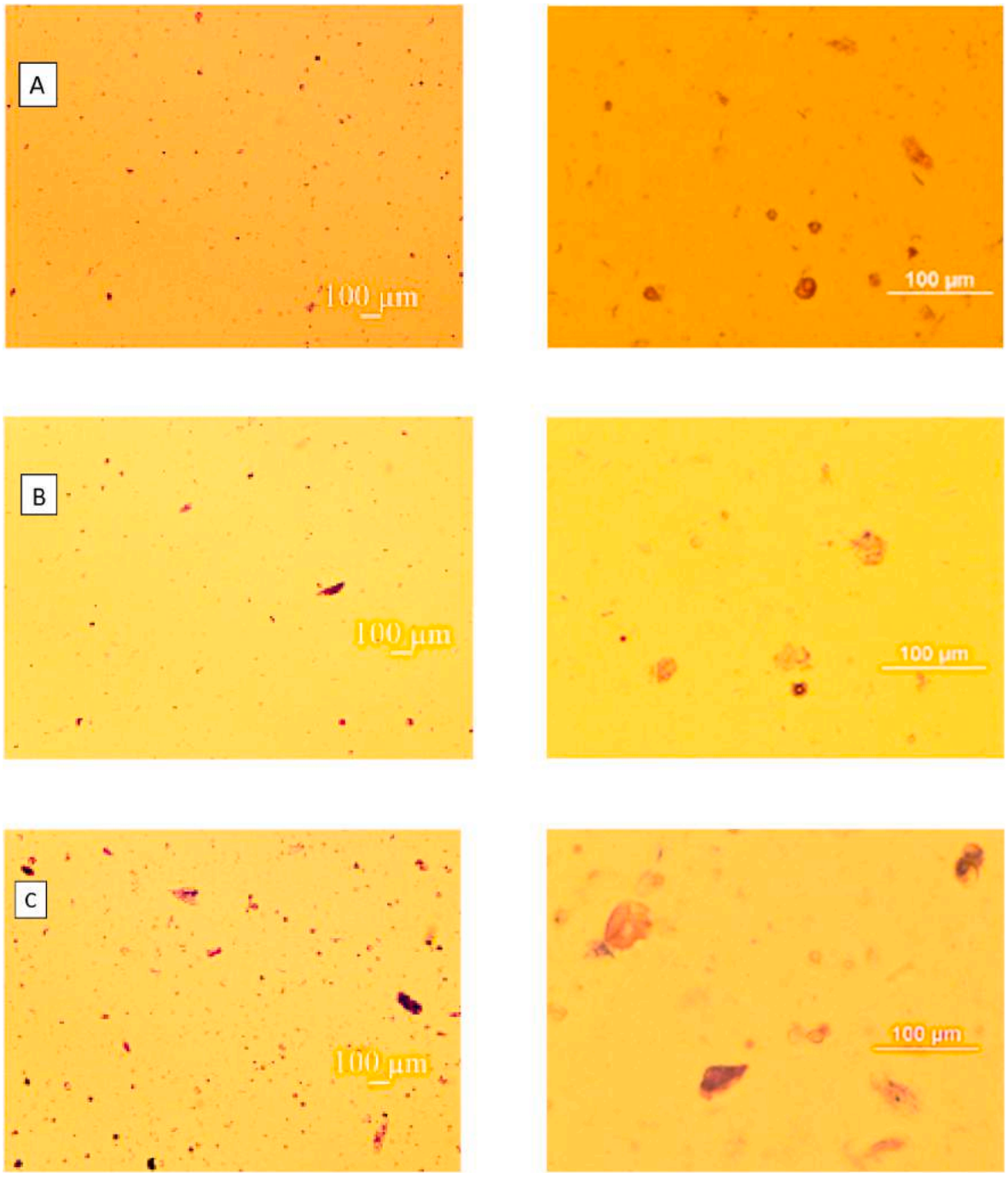


Fig. 5. Optical light microscope images at 40x (left) and 200x magnification (right), depicting the microstructures of diluted feed dispersions with a 5:4 WPI:sucrose ratio and 1% PPO at 25% (**A**), 35% (**B**), and 45% total solids contents (**C**).

findings from Mastersizer data visually, depicting the increases in average and largest aggregate sizes in the dispersions as total solids content increased in the system, promoting more extensive aggregation (Fig. 5a, b, c). Microscopy also mirrored the Mastersizer findings indicating that increasing the ratio of WPI to sucrose in dispersions resulted in no changes in average particle size (images not shown). Mastersizer data reporting reduced particle size with the addition of polyphenols to dispersions were reinforced with optical light microscopy as well (images not shown). Microscope images were useful for visual demonstration of the increased incidence of small particles in feeds formulated with Aronia extract (Fig. 6a, b, c), also shown in Mastersizer particle size distributions (not shown). Comparing particle size distributions and frequencies at which certain sizes occur between laser light scattering techniques and microscope imaging may be difficult due to inherent differences between methods (Schneider, 2016); nevertheless, optical microscopy generally confirmed the Mastersizer results.

3.1.7. Centrifuge separation

Centrifuge treatments resulted in the formation of precipitated pellets from feed dispersions and their dilutions, indicating that the 'gels' were weak in nature and underwent separation relatively easily. Dispersions were visually assessed to identify the location of the colored polyphenolic compounds after centrifugation, as sedimentation of a colored precipitate has been used as a crude method to confirm the

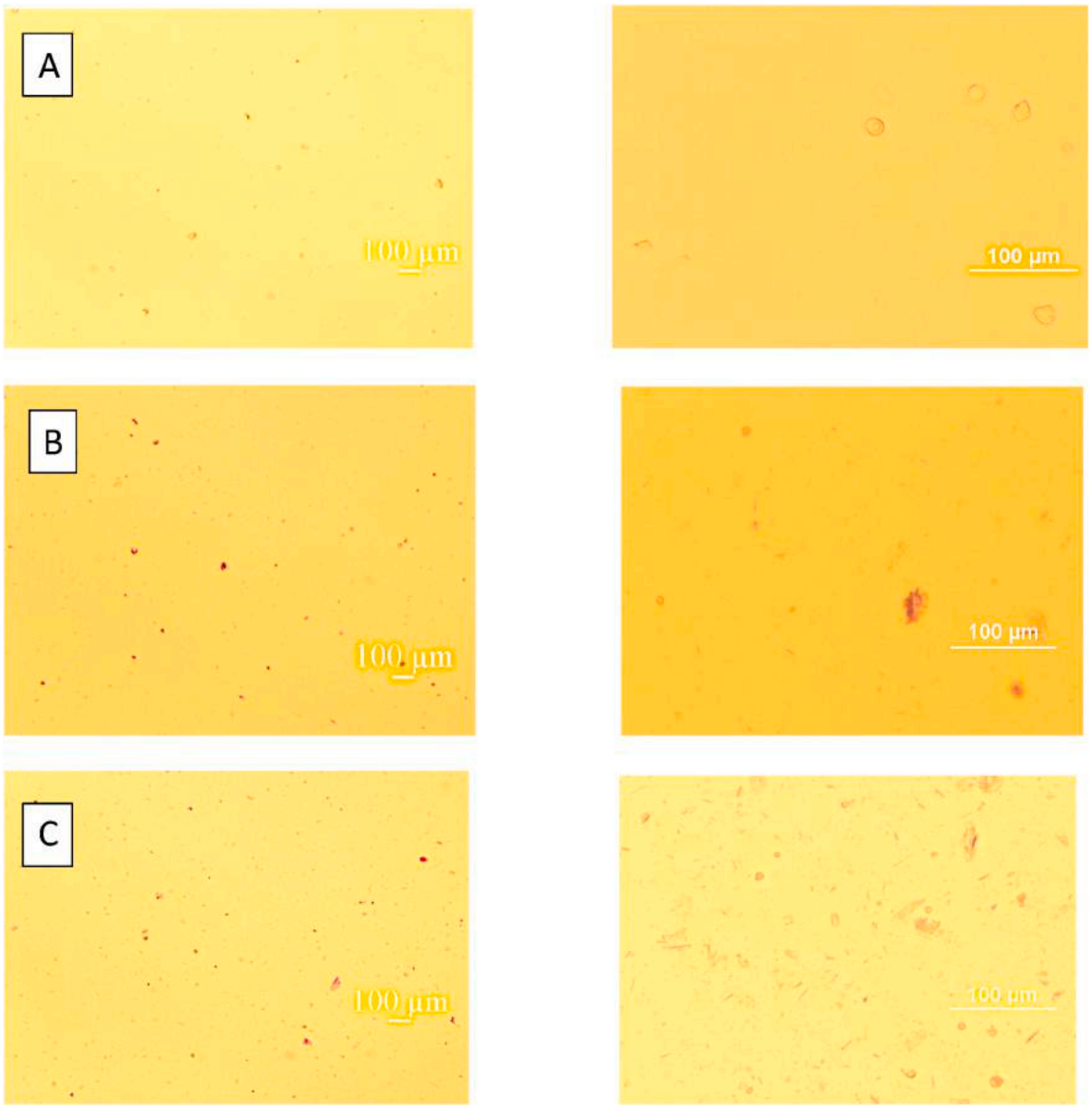


Fig. 6. Optical light microscope images at 40x (left) and 200x magnification (right), depicting the microstructures of diluted feed dispersions with a 1:1 WPI:sucrose ratio at 25% TS with 0% PPO (**A**), 0.5% PPO (**B**), and 1% PPO addition (**C**).

formation of protein-polyphenol conjugates (Van Teeling et al., 1971). An Aronia berry powder similar to the extract used in this study was found to be most abundant in cyanidin-3-galactoside, cyanidin-3-glucoside, and chlorogenic acid polyphenols (Xie et al., 2016, 2017), with cyanidin-3-galactoside and cyanidin-3-glucoside both being anthocyanins. The powder used in this study was standardized to contain a minimum of 15% anthocyanins and 10% proanthocyanidins. Both compounds are known to contribute pigmentation to Aronia and make up the majority of polyphenolic compounds in the extract (a minimum 25g of the 40g total PPO in 100g of extract). Dispersions formulated without polyphenols had white-colored pellets after centrifugation; inclusion of Aronia PPO resulted in dark purple pellet formation (Fig. 7). Thus, formation of colored precipitates was an indicator for protein-polyphenol complexation. After being diluted 10x,

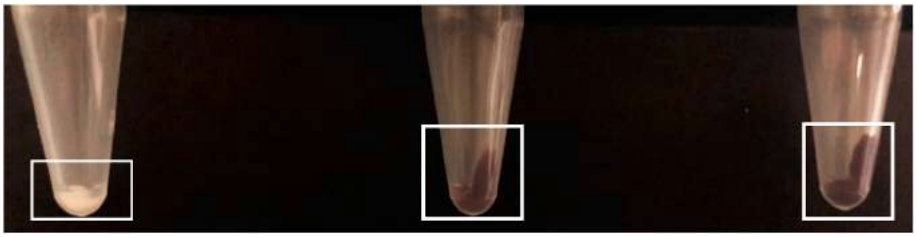


Fig. 7. Image depicting the precipitated fractions (highlighted in boxes) of centrifuged 10x-diluted dispersions with 5:4 WPI:sucrose ratios and 45% total solids contents with 0% PPO (Left), 0.5% PPO (Center), and 1% PPO (Right).

PPO-containing dispersions had dark purple precipitated pellets and transparent supernatant fractions that maintained slight purple-pink coloration. The pigmentation may be due in part to the saturation of potential conjugation sites (as influenced by factors including system pH, temperature, protein and polyphenol types involved, and relative concentration ratios), resulting in uncomplexed polyphenols remaining in solution and imparting pigmentation (Schneider, 2016; Quan et al., 2019). Alternatively, supernatant pigmentation may be due to the presence of smaller sized protein-polyphenol conjugates that remain dispersed in solution as they had not become heavy or insoluble enough to precipitate out (Spencer et al., 1988; Charlton et al., 2002; Rawel et al., 2005; Ozdal et al., 2013).

No changes in appearance were observed for the relative amount of precipitate formed as the ratio of WPI to sucrose was increased. Precipitated pellet size appeared to increase slightly upon addition of polyphenols to feed dispersions and their dilutions, as compared to those containing 0% polyphenols (Fig. 7). Dilution of a 1% Aronia polyphenol solution by a factor of 10x and the extremely small precipitate formed upon centrifugation (image not shown) helped to confirm that the apparent increase in precipitate formed with addition of PPO cannot be attributed only to an increase in Aronia extract carbohydrates, fiber, and protein solids, but likely a result of the formation of larger, aggregated conjugates that fell out of solution.

3.2. Frozen drop characterization

3.2.1. Comparison of diameters

The surface tension of feed dispersions strongly determines the size of drops formed, as detachment of pendant drops only occurs when gravitational forces pulling down exceed the surface tension forces acting around the circumference of the tubing tip. Surface tension has been reported to decrease with increased viscosity and biopolymer concentrations, and drop diameters tend to decrease with decreasing surface tension of feeds (Chan et al., 2009; Lee and Chan, 2013).

Diameters of frozen drops were measured to observe the effects of composition on drop sizes. According to the ANOVA, drop diameters were significantly ($p < 0.05$) affected by % TS; diameters were generally found to decrease with increasing % TS in dispersions (Fig. 8a). Tukey's HSD tests reported significant decreases in diameters when % TS increased from 25 to 35% ($p < 0.05$), but the decrease in size between 35 and 45% TS was not found to be statistically significant. The reduction in diameters of drops formed by feeds containing higher total solids contents may be a result of increasing density, ultimately resulting in pendant drops becoming heavier and overcoming reduced surface tension forces more quickly and thus detaching at smaller volumes. Any variations observed in the generally decreasing trends may be attributed to larger drops forming in order to release from the tubing tip due to entrapped air reducing feed density.

According to the ANOVA, diameters were significantly ($p < 0.05$) impacted by the WPI to sucrose ratio in feeds; diameters were generally observed to increase with increasing ratios of WPI to sucrose in dispersions, best visualized by feeds containing 1% PPO in Fig. 8b. Tukey's HSD tests clarified, reporting a significant ($p < 0.05$) increase in diameters with increased WPI to sucrose ratios from 3:4 to 1:1, though the change in size between 1:1 and 5:4 WPI:sucrose ratios was not found to be statistically significant. These trends are best demonstrated in feeds containing 0 and 1% PPO, as feeds containing 0.5% PPO showed more variation from the trends described by the ANOVA (Fig. 8b). Despite the

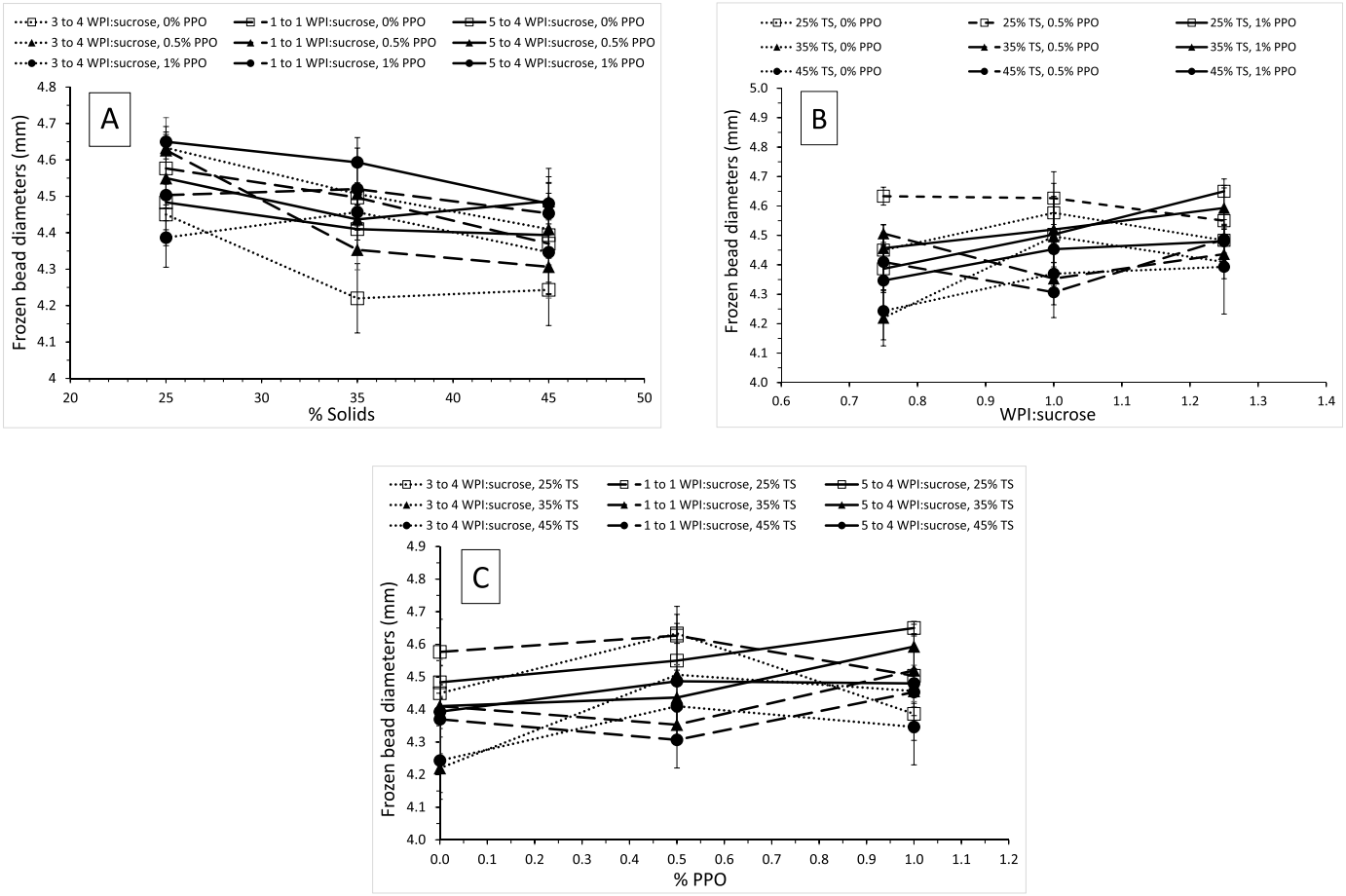


Fig. 8. Effect of total solids content (%) **[A]**, WPI:sucrose ratio **[B]**, and PPO content (%) **[C]** on the on the diameters (mm) of frozen drops formed from dispersions; (n = 6). Lines are for guiding purposes only.

larger molecular mass of proteins and space occupied, dispersions containing more protein have higher foaming ability and may entrap more air that cannot be removed entirely from feeds as they are left to defoam prior to analysis. In this case, it is possible that pendant drops comprised of more WPI had to grow to larger sizes and heavier in order to overcome surface tension forces and detach, as feed density was lower than would be expected due to air bubbles being entrapped during dispersion preparation. Variation with 0.5% PPO feeds may be due to minor inhibition of protein-protein interactions with the presence of protein-PPO interactions.

The ANOVA indicated that PPO content had a significant ($p < 0.05$) impact on drop diameters; Tukey's HSD tests reported significant increases in diameters ($p < 0.05$) when PPO content increased from 0 to 0.5%. The minor increase in diameters from 0.5% to 1% PPO was not found to be statistically significant. With the addition of Aronia PPO to feeds, drop diameters were generally observed to increase, although with significant scatter; this trend is most clearly demonstrated for feeds comprised of 5:4 WPI:sucrose in Fig. 8c. The increasing trend described by the statistical analysis and observed in Fig. 8c may be influenced by the effects of the high WPI:sucrose ratio enhancing diameters as well. Additionally, feeds containing 25% TS generally had larger average drop diameters than those containing 35–45% TS. Although comprised mainly of small molecular weight polyphenolic compounds, the Aronia extract also contributed small quantities of fiber and protein (1.3 and 2.3% of extract composition, respectively) to dispersions. These additional compounds may have enabled dispersions to entrap more air bubbles upon preparation of feeds, resulting in increased drop diameters as drops needed to grow larger and heavier to detach.

Diameters of frozen drops were compared with calculated estimate values from data produced by flow testing of dispersions (Equation (6); Table 1). No significant differences ($p < 0.05$) were found between the estimated diameters calculated from flow data and the actual measured diameters for 23 of the 27 feed dispersions studied. One possible reason that the calculations did not always accurately predict diameters could be that the calculated values were built from measured density data. Density measurements may not always be perfectly representative of feeds, as they cannot account for the air that is inevitably part of the viscous dispersions and is unable to be fully removed by allowing feeds to settle before testing, depending on composition of feeds and their ability to entrap air bubbles. Thus, inaccurate density measurements may carry through the calculations to give less accurate drop diameter estimates as a result of the air present. Nevertheless, estimated drop size calculations accurately estimated drop diameters the majority of the time, indicating that the method was generally successful, similar to findings from earlier experiments (Hansen et al., 2020).

4. Conclusions

In an effort to expand on previous work in which a continuous process for forming concentrated, liquid dispersions of WPI-sucrose combinations into structures with potential to encapsulate active ingredients was presented, this work aimed to study the effects of formulation with Aronia extract polyphenols as the active ingredient. Naturally occurring, non-covalent WPI-polyphenol interactions were found to have functional, physical, and practical processing consequences including increased viscosities and surface tensions and reduced particle sizes of feeds, though the effect of total solids content appeared to most strongly influence dispersion properties. These findings contribute to the body of research describing the physical effects of non-covalent interactions between proteins and polyphenols under mild pH and temperature conditions, as well as provide practical knowledge for further applications such as encapsulation, protection, and delivery with concentrated protein-polyphenol mixtures.

Authors contribution statement

Mackenzie M. Hansen: Conceptualization, Methodology, Validation, Formal analysis, Investigation, Resources, Writing- Original Draft, Writing- Review & Editing, Visualization, Project administration, Funding acquisition. Richard W. Hartel: Conceptualization, Resources, Writing- Review & Editing, Visualization, Supervision. Yrjö H. Roos: Conceptualization, Resources, Writing- Review & Editing, Visualization, Supervision, Funding acquisition.

Declaration of competing interest

The authors hereby declare no conflict of interest.

Acknowledgements

This research was supported by funding provided by the Lauritzson Foundation in the form of the Lauritzson Research Scholarship, through the College of Science, Engineering and Food Science (SEFS) at University College Cork. The authors would like to thank the anonymous reviewers and Journal Editor for thorough reading of the manuscript and helpful comments for revision.

References

Alawode, A.O., 2014. Quantification of Protein Fractions in Aqueous Phases of Whey and Emulsions. Masters Food Science. Swedish University of Agricultural Sciences.
Alizadehfard, M.R., Wiley, D.E., 1995. Viscosity of whey protein solutions. Iran. J. Polym. Sci. Technol. 4 (2), 126–133.
Bąkowska, A., Kucharska, A.Z., Oszmiański, J., 2003. The effects of heating, UV irradiation, and storage on stability of the anthocyanin–polyphenol copigment complex. Food Chem. 81 (3), 349–355. https://doi.org/10.1016/S0308-8146(02)00429-6.
Bandyopadhyay, P., Ghosh, A.K., Ghosh, C., 2012. Recent developments on polyphenol–protein interactions: effects on tea and coffee taste, antioxidant properties and the digestive system. Food & Function 3 (6), 592. https://doi.org/10.1039/c2fo00006g.
Bayraktar, M.K., Harbourne, N.B., Fagan, C.C., 2019. Impact of heat treatment and acid gelation on polyphenol enriched milk samples. Lebensm. Wiss. Technol. 113, 108282. https://doi.org/10.1016/j.lwt.2019.108282.
Bermudez-Soto, M., Larrosa, M., Garciacantalejo, J., Espin, J., Tomasbarberan, F., Garciaconesa, M., 2007. Up-regulation of tumor suppressor carcinoembryonic antigen-related cell adhesion molecule 1 in human colon cancer Caco-2 cells following repetitive exposure to dietary levels of a polyphenol-rich chokeberry juice. J. Nutr. Biochem. 18 (4), 259–271. https://doi.org/10.1016/j.jnutbio.2006.05.003.
Biesalski, H.-K., Dragsted, L.O., Elmadfa, I., Grossklaus, R., Müller, M., Schrenk, D., Walter, P., Weber, P., 2009. Bioactive compounds: definition and assessment of activity. Nutrition 25 (11–12), 1202–1205. https://doi.org/10.1016/j.nut.2009.04.023.
Bohin, M.C., Vincken, J.-P., van der Hijden, H.T.W.M., Gruppen, H., 2012. Efficacy of food proteins as carriers for flavonoids. J. Agric. Food Chem. 60 (16), 4136–4143. https://doi.org/10.1021/jf205292r.
Cao, Y., Xiong, Y.L., 2017. Interaction of whey proteins with phenolic derivatives under neutral and acidic pH conditions: protein-phenolic interaction. J. Food Sci. 82 (2), 409–419. https://doi.org/10.1111/1750-3841.13607.
Cassidy, A., Mukamal, K.J., Liu, L., Franz, M., Eliassen, A.H., Rimm, E.B., 2013. High anthocyanin intake Is associated with a reduced risk of myocardial infarction in young and middle-aged women. Circulation 127 (2), 188–196. https://doi.org/10.1161/CIRCULATIONAHA.112.122408.
Castañeda-Ovando, A., Pacheco-Hernández, Ma, de L., Páez-Hernández, Ma, E., Rodríguez, J.A., Galán-Vidal, C.A., 2009. Chemical studies of anthocyanins: a review. Food Chem. 113 (4), 859–871. https://doi.org/10.1016/j.foodchem.2008.09.001.
Chan, E.-S., Lee, B.-B., Ravindra, P., Poncelet, D., 2009. Prediction models for shape and size of ca-alginate macrobeads produced through extrusion–dripping method. J. Colloid Interface Sci. 338 (1), 63–72. https://doi.org/10.1016/j.jcis.2009.05.027.
Charlton, A.J., Baxter, N.J., Khan, M.L., Moir, A.J.G., Haslam, E., Davies, A.P., Williamson, M.P., 2002. Polyphenol/peptide binding and precipitation. J. Agric. Food Chem. 50 (6), 1593–1601. https://doi.org/10.1021/jf010897z.
Chung, C., Rojanasasithara, T., Mutilangi, W., McClements, D.J., 2015. Enhanced stability of anthocyanin-based color in model beverage systems through whey protein isolate complexation. Food Res. Int. 76, 761–768. https://doi.org/10.1016/j.foodres.2015.07.003.
Coupland, J.N., 2014. An Introduction to the Physical Chemistry of Food, illustrated ed. Springer.
Ćujić, N., Kardum, N., Šavikin, K., Zdunić, G., Janković, T., Menković, N., 2018. Potential of chokeberry (Aronia melanocarpa L.) as a therapeutic food. In: Therapeutic Foods, vol. 8. Academic Press- Elsevier Inc, pp. 209–237.

Demetriades, K., McClements, D.J., 1998. Influence of pH and heating on physicochemical properties of whey protein-stabilized emulsions containing a nonionic surfactant. J. Agric. Food Chem. 46 (10), 3936–3942. https://doi.org/10.1021/jf980463c.
Fang, Z., Bhandari, B., 2017. Spray drying of bioactives. In: Roos, Y.H., Livney, Y.D. (Eds.), Engineering Foods for Bioactives Stability and Delivery. Springer, pp. 261–284.
Foegeding, E.A., Plundrich, N., Schneider, M., Campbell, C., Lila, M.A., 2017. Protein-polyphenol particles for delivering structural and health functionality. Food Hydrocolloids 72, 163–173. https://doi.org/10.1016/j.foodhyd.2017.05.024.
Francis, F.J., Markakis, P.C., 1989. Food colorants: anthocyanins. Crit. Rev. Food Sci. Nutr. 28 (4), 273–314. https://doi.org/10.1080/10408398909527503.
Friedman, M., Jürgens, H.S., 2000. Effect of pH on the stability of plant phenolic compounds. J. Agric. Food Chem. 48 (6), 2101–2110. https://doi.org/10.1021/jf990489j.
Girard, A.L., Bean, S.R., Tilley, M., Adrianos, S.L., Awika, J.M., 2018. Interaction mechanisms of condensed tannins (proanthocyanidins) with wheat gluten proteins. Food Chem. 245, 1154–1162. https://doi.org/10.1016/j.foodchem.2017.11.054.
Hagerman, A.E., Butler, L.G., 1978. Protein precipitation method for the quantitative determination of tannins. J. Agric. Food Chem. 26 (4), 809–812. https://doi.org/10.1021/jf60218a027.
Hansen, M.M., Maidannyk, V.A., Roos, Y.H., 2020. Thermal gelation and hardening of whey protein beads for subsequent dehydration and encapsulation using vitrifying sugars. J. Food Eng. 279, 109966. https://doi.org/10.1016/j.jfoodeng.2020.109966.
Harbourne, N., Jacquier, J.C., O'Riordan, D., 2011. Effects of addition of phenolic compounds on the acid gelation of milk. Int. Dairy J. 21 (3), 185–191. https://doi.org/10.1016/j.idairyj.2010.10.003.
Hartel, R.W., von Elbe, J.H., Hofberger, R., 2018. Confectionery Science and Technology. Springer International Publishing. https://doi.org/10.1007/978-3-319-61742-8.
He, F., Woods, C.E., Litowski, J.R., Roschen, L.A., Gadgil, H.S., Razinkov, V.I., Kerwin, B. A., 2011. Effect of sugar molecules on the viscosity of high concentration monoclonal antibody solutions. Pharm. Res. (N. Y.) 28 (7), 1552–1560. https://doi.org/10.1007/s11095-011-0388-7.
Hong, T., Iwashita, K., Shiraki, K., 2018. Viscosity control of protein solution by small solutes: a review. Curr. Protein Pept. Sci. 19 (8), 746–758. https://doi.org/10.2174/1389203719666171213114919.
Jean, K., Renan, M., Famelart, M.-H., Guyomarc'h, F., 2006. Structure and surface properties of the serum heat-induced protein aggregates isolated from heated skim milk. Int. Dairy J. 16 (4), 303–315. https://doi.org/10.1016/j.idairyj.2005.04.001.
Johnson, J.F., Martin, J.R., Porter, R.S., 1975. Determination of VIscosity of food systems. In: Theory, Determination and Control of Physical Properties of Food Materials, vol. 1. Springer, pp. 25–38.
Kanakis, C.D., Hasni, I., Bourassa, P., Tarantilis, P.A., Polissiou, M.G., Tajmir-Riahi, H.-A., 2011. Milk β-lactoglobulin complexes with tea polyphenols. Food Chem. 127 (3), 1046–1055. https://doi.org/10.1016/j.foodchem.2011.01.079.
Khoo, H.E., Azlan, A., Tang, S.T., Lim, S.M., 2017. Anthocyanidins and anthocyanins: colored pigments as food, pharmaceutical ingredients, and the potential health benefits. Food Nutr. Res. 61 (1), 1361779. https://doi.org/10.1080/16546628.2017.1361779.
Kilara, A., Harwalkar, V.R., 1996. Denaturation. In: Food Proteins: Properties and Characterization. Wiley-VCH.
Kulmyrzaev, A., Bryant, C., McClements, D.J., 2000. Influence of sucrose on the thermal denaturation, gelation, and emulsion stabilization of whey proteins. J. Agric. Food Chem. 48 (5), 1593–1597. https://doi.org/10.1021/jf9911949.
Le Bourvellec, C., Renard, C.M.G.C., 2012. Interactions between polyphenols and macromolecules: quantification methods and mechanisms. Crit. Rev. Food Sci. Nutr. 52 (3), 213–248. https://doi.org/10.1080/10408398.2010.499808.
Lee, B.B., Chan, E.S., 2013. Size and shape of calcium alginate beads produced by extrusion dripping. Chem. Eng. Technol. 36 (10), 1627–1642. https://doi.org/10.1002/ceat.201300230.
Li, D., Wang, P., Luo, Y., Zhao, M., Chen, F., 2017. Health benefits of anthocyanins and molecular mechanisms: update from recent decade. Crit. Rev. Food Sci. Nutr. 57 (8), 1729–1741. https://doi.org/10.1080/10408398.2015.1030064.
Ma, C.-M., Zhao, X.-H., 2019. Depicting the non-covalent interaction of whey proteins with galangin or genistein using the multi-spectroscopic techniques and molecular docking. Foods 8 (9), 360. https://doi.org/10.3390/foods8090360.
Malik, M., Zhao, C., Schoene, N., Guisti, M.M., Moyer, M.P., Magnuson, B.A., 2003. Anthocyanin-rich extract from Aronia meloncarpa E. induces a cell cycle block in colon cancer but not normal colonic cells. Nutr. Canc. 46 (2), 186–196. https://doi.org/10.1207/S15327914NC4602_12.
Matalanis, A., Jones, O.G., McClements, D.J., 2011. Structured biopolymer-based delivery systems for encapsulation, protection, and release of lipophilic compounds. Food Hydrocolloids 25 (8), 1865–1880. https://doi.org/10.1016/j.foodhyd.2011.04.014.
Mazza, G., Brouillard, R., 1987. Recent developments in the stabilization of anthocyanins in food products. Food Chem. 25 (3), 207–225. https://doi.org/10.1016/0308-8146(87)90147-6.
Mazza, G., Brouillard, R., 1990. The mechanism of co-pigmentation of anthocyanins in aqueous solutions. Phytochemistry 29 (4), 1097–1102. https://doi.org/10.1016/0031-9422(90)85411-8.
Mink, P.J., Scrafford, C.G., Barraj, L.M., Harnack, L., Hong, C.-P., Nettleton, J.A., Jacobs, D.R., 2007. Flavonoid intake and cardiovascular disease mortality: a prospective study in postmenopausal women. Am. J. Clin. Nutr. 85 (3), 895–909. https://doi.org/10.1093/ajcn/85.3.895.
Moskovitz, J., Yim, M.B., Chock, P.B., 2002. Free radicals and disease. Arch. Biochem. Biophys. 397 (2), 354–359. https://doi.org/10.1006/abbi.2001.2692.
Oancea, A.-M., Aprodu, I., Râpeanu, G., Bahrim, G., Stanciuc, N., 2017. The Binding mechanism of anthocyanins from sour cherries (*Prunus cerasus* L) skins to bovine β-lactoglobulin: a fluorescence and *in silico* -based approach. Int. J. Food Prop. 20 (Suppl. 3), S3096–S3111. https://doi.org/10.1080/10942912.2017.1343347.
Ozdal, T., Capanoglu, E., Altay, F., 2013. A review on protein–phenolic interactions and associated changes. Food Res. Int. 51 (2), 954–970. https://doi.org/10.1016/j.foodres.2013.02.009.
Patocka, G., Cervenkova, R., Narine, S., Jelen, P., 2006. Rheological behaviour of dairy products as affected by soluble whey protein isolate. Int. Dairy J. 16 (5), 399–405. https://doi.org/10.1016/j.idairyj.2005.05.010.
Quan, T.H., Benjakul, S., Sae-leaw, T., Balange, A.K., Maqsood, S., 2019. Protein–polyphenol conjugates: antioxidant property, functionalities and their applications. Trends Food Sci. Technol. 91, 507–517. https://doi.org/10.1016/j.tifs.2019.07.049.
Rawel, H.M., Meidtner, K., Kroll, J., 2005. Binding of selected phenolic compounds to proteins. J. Agric. Food Chem. 53 (10), 4228–4235. https://doi.org/10.1021/jf0480290.
Rodriguez-Saona, L.E., Giusti, M.M., Wrolstad, R.E., 1999. Color and pigment stability of red radish and red-fleshed potato anthocyanins in juice model systems. J. Food Sci. 64 (3), 451–456. https://doi.org/10.1111/j.1365-2621.1999.tb15061.x.
Saluja, A., Kalonia, D.S., 2005. Application of ultrasonic shear rheometer to characterize rheological properties of high protein concentration solutions at microliter volume. J. Pharmaceut. Sci. 94 (6), 1161–1168. https://doi.org/10.1002/jps.20342.
Schneider, M.E., 2016. *Formation of Whey Protein-Polyphenol Aggregates and Incorporation into Various Food Structures* [PhD Food Science]. North Carolina State University.
Siebert, K.J., Troukhanova, N.V., Lynn, P.Y., 1996. Nature of Polyphenol−Protein interactions. J. Agric. Food Chem. 44 (1), 80–85. https://doi.org/10.1021/jf9502459.
Simeonov, S.B., Botushanov, N.P., Karahanian, E.B., Pavlova, M.B., Husianitis, H.K., Troev, D.M., 2002. Effects of Aronia melanocarpa juice as part of the dietary regimen in patients with diabetes mellitus. Folia Med. (Plovdiv) 44 (3).
Singh, R.P., Heldman, D., 2013. Introduction to Food Engineering, fifth ed. Academic Press.
Song, J., 2009. Insight into "insoluble proteins" with pure water. FEBS (Fed. Eur. Biochem. Soc.) Lett. 583 (6), 953–959. https://doi.org/10.1016/j.febslet.2009.02.022.
Spencer, C.M., Cai, Y., Martin, R., Gaffney, S.H., Goulding, P.N., Magnolato, D., Lilley, T. H., Haslam, E., 1988. Polyphenol complexation—some thoughts and observations. Phytochemistry 27 (8), 2397–2409. https://doi.org/10.1016/0031-9422(88)87004-3.
Taheri, R., Connolly, B.A., Brand, M.H., Bolling, B.W., 2013. Underutilized chokeberry (aronia melanocarpa, aronia arbutifolia, aronia prunifolia) accessions are rich sources of anthocyanins, flavonoids, hydroxycinnamic acids, and proanthocyanidins. J. Agric. Food Chem. 61 (36), 8581–8588. https://doi.org/10.1021/jf402449q.
Thongkaew, C., Gibis, M., Hinrichs, J., Weiss, J., 2014. Polyphenol interactions with whey protein isolate and whey protein isolate–pectin coacervates. Food Hydrocolloids 41, 103–112. https://doi.org/10.1016/j.foodhyd.2014.02.006.
Tro, N.J., Fridgen, T.D., Shaw, L., 2014. Chemistry: A Molecular Approach. Pearson Canada.
Valcheva-Kuzmanova, S., Kuzmanov, K., Mihova, V., Krasnaliev, I., Borisova, P., Belcheva, A., 2007a. Antihyperlipidemic effect of Aronia melanocarpa fruit juice in rats fed a high-cholesterol diet. Plant Foods Hum. Nutr. 62 (1), 19–24. https://doi.org/10.1007/s11130-006-0036-2.
Valcheva-Kuzmanova, S., Kuzmanov, K., Tancheva, S., Belcheva, A., 2007b. Hypoglycemic effects of Aronia melanocarpa fruit juice in streptozotocin-induced diabetic rats. Methods Find. Exp. Clin. Pharmacol. 29 (2), 101. https://doi.org/10.1358/mf.2007.29.2.1075349.
Valcheva-Kuzmanova, S., Kuzmanov, K., Tsanova-Savova, S., Mihova, V., Krasnaliev, I., Borisova, P., Belcheva, A., 2007c. Lipid-lowering effects of Aronia Melanocarpa fruit juice in rats fed cholesterol-containing diets. J. Food Biochem. 31 (5), 589–602. https://doi.org/10.1111/j.1745-4514.2007.00132.x.
Van Teeling, C.G., Cansfield, P.E., Gallop, R.A., 1971. An anthocyanin complex isolated from the syrup of canned blueberries. J. Food Sci. 36, 1061–1063. https://doi.org/10.1111/j.1365-2621.1971.tb03346.x.
Volf, I., Ignat, I., Neamtu, M., Popa, V., 2014. Thermal stability, antioxidant activity, and photo-oxidation of natural polyphenols. Chem. Pap. 68 (1) https://doi.org/10.2478/s11696-013-0417-6.
von Staszewski, M., Jagus, R.J., Pilosof, A.M.R., 2011. Influence of green tea polyphenols on the colloidal stability and gelation of WPC. Food Hydrocolloids 25 (5), 1077–1084. https://doi.org/10.1016/j.foodhyd.2010.10.004.
Wang, R., Hartel, R.W., 2020. Effects of moisture content and saccharide distribution on the stickiness of syrups. J. Food Eng. 284, 110067. https://doi.org/10.1016/j.jfoodeng.2020.110067.
Warren, M.M., Hartel, R.W., 2014. Structural, compositional, and sensorial properties of United States commercial ice cream products: United States commercial ice cream products. J. Food Sci. 79 (10), E2005–E2013. https://doi.org/10.1111/1750-3841.12592.
Worley, J.D., 1992. Capillary radius and surface tensions. Using calculations based on Tate's law. J. Chem. Educ. 69 (8), 678.
Xie, L., Lee, S.G., Vance, T.M., Wang, Y., Kim, B., Lee, J.-Y., Chun, O.K., Bolling, B.W., 2016. Bioavailability of anthocyanins and colonic polyphenol metabolites following consumption of aronia berry extract. Food Chem. 211, 860–868. https://doi.org/10.1016/j.foodchem.2016.05.122.
Xie, L., Vance, T., Kim, B., Lee, S.G., Caceres, C., Wang, Y., Hubert, P.A., Lee, J.-Y., Chun, O.K., Bolling, B.W., 2017. Aronia berry polyphenol consumption reduces plasma total and low-density lipoprotein cholesterol in former smokers without

lowering biomarkers of inflammation and oxidative stress: a randomized controlled trial. Nutr. Res. 37, 67–77. https://doi.org/10.1016/j.nutres.2016.12.007.

Xue, F., Li, C., Adhikari, B., 2020. Physicochemical properties of soy protein isolates-cyanidin-3-galactoside conjugates produced using free radicals induced by ultrasound. Ultrason. Sonochem. 64, 104990. https://doi.org/10.1016/j.ultsonch.2020.104990.

Yousuf, B., Gul, K., Wani, A.A., Singh, P., 2016. Health benefits of anthocyanins and their encapsulation for potential use in food systems: a review. Crit. Rev. Food Sci. Nutr. 56 (13), 2223–2230. https://doi.org/10.1080/10408398.2013.805316.

Zhao, C., Giusti, M.M., Malik, M., Moyer, M.P., Magnuson, B.A., 2004. Effects of commercial anthocyanin-rich extracts on colonic cancer and nontumorigenic colonic cell growth. J. Agric. Food Chem. 52 (20), 6122–6128. https://doi.org/10.1021/jf049517a.

Zhou, S.-D., Lin, Y.-F., Xu, X., Meng, L., Dong, M.-S., 2020. Effect of non-covalent and covalent complexation of (−)-epigallocatechin gallate with soybean protein isolate on protein structure and in vitro digestion characteristics. Food Chem. 309, 125718. https://doi.org/10.1016/j.foodchem.2019.125718.

Zielińska-Przyjemska, M., Dobrowolska-Zachwieja, A., Grajek, W., Olejnik, A., 2007. Effects of Aronia melanocarpa polyphenols on oxidative metabolism and apoptosis of neutrophils from obese and non-obese individuals. Acta Sci. Pol. Technol. Aliment. 6 (3), 75–87.

Food Production, Processing and Nutrition

RESEARCH Open Access

Effects of Aronia polyphenols on the physico-chemical properties of whey, soy, and pea protein isolate dispersions

Mackenzie M. Hansen[1,2*], Richard W. Hartel[2] and Yrjö H. Roos[1]

Abstract

Bioactive compounds including polyphenols (PP) have been observed to naturally form non-covalent complexation interactions with proteins under mild pH and temperature conditions, affecting protein structures and functionality. Previously, addition of Aronia berry PP to liquid dispersions containing whey protein isolate (WPI) and sucrose was found to alter characteristics including viscosity, surface tension, and particle sizes, with changes being attributed to protein-PP interactions. In this study we aimed to investigate whether Aronia PP would interact with soy and pea protein isolates (SPI and PPI, respectively) to a similar extent as with WPI in liquid protein-sucrose-PP mixtures. We hypothesized that formulations containing PPI (comprised of larger proteins) and hydrolyzed SPI (containing more carboxyl groups) may exhibit increased viscosities and decreased aggregate sizes due to enhanced protein-PP interactions. Concentrated liquid dispersions of varied ratios of protein to sucrose contents, containing different protein isolates (WPI, SPI, and PPI), and varied Aronia PP concentrations were formulated, and physical properties were evaluated to elucidate the effects of PP addition. PP addition altered physical characteristics differently depending on the protein isolate used, with changes attributed to protein-PP interactions. SPI and PPI appeared to have higher propensities for PP interactions and exhibited more extensive shifts in physical properties than WPI formulations. These findings may be useful for practical applications such as formulating products containing fruit and proteins to obtain desirable sensory attributes.

Keywords: Whey protein, Soy protein, Pea protein, Polyphenols, Concentrated dispersions, Physico-chemical properties

Introduction

As consumers' interest towards bioactives-containing health foods grows, so does the demand for novel products with high protein contents and fruit components. Bioactives can be defined as natural compounds that may affect human health (González 2020). Globular bovine whey proteins, especially whey protein isolate (WPI) with its wide range of functionality, continue to be favored for developing products with high nutritional value (Kulmyrzaev et al. 2000; Cao & Xiong 2017; Hansen et al. 2021a). However, consumers are also demonstrating increased interest in shifting their diets away from animal-sourced proteins for health, social, and environmental reasons, placing higher demand on plant-based nutritional options (Aschemann-Witzel & Peschel 2019). Soybeans are a rich alternative source of high-quality but inexpensive globular proteins, and soy protein isolates (SPI) are increasingly popular for product development (Li 2005). Also globular in nature, pea protein isolates (PPI) provide another alternative in formulated food products. As constituent protein sources are changed, the functional properties of the resulting food products will also be altered due to variations in the

* Correspondence: 116220787@umail.ucc.ie
[1]Food Technology, School of Food and Nutritional Sciences, University College Cork, Cork, Ireland
[2]Department of Food Science, College of Agricultural and Life Sciences, University of Wisconsin, Office A11, Babcock Hall, 1605 Linden Drive, Madison, WI 53706, USA

© The Author(s). 2021 **Open Access** This article is licensed under a Creative Commons Attribution 4.0 International License, which permits use, sharing, adaptation, distribution and reproduction in any medium or format, as long as you give appropriate credit to the original author(s) and the source, provide a link to the Creative Commons licence, and indicate if changes were made. The images or other third party material in this article are included in the article's Creative Commons licence, unless indicated otherwise in a credit line to the material. If material is not included in the article's Creative Commons licence and your intended use is not permitted by statutory regulation or exceeds the permitted use, you will need to obtain permission directly from the copyright holder. To view a copy of this licence, visit http://creativecommons.org/licenses/by/4.0/.

composition and physicochemical properties of the different protein sources.

Fruits are a rich source of polyphenols (PP), bioactive compounds with strong antioxidant and anti-inflammatory activities linked to a host of positive health outcomes (Mink et al. 2007; Li et al. 2017). Good sources of PP like fresh produce often have short shelf lives, and PP are known to be chemically unstable in storage and highly susceptible to degradation (Zhao et al. 2019; Cao et al. 2021). A propensity for complexation exists between PP and proteins, with weak, non-covalent van der Waal's interactions, hydrogen bonding, and hydrophobic interactions commonly occurring in foods with neutral and acidic pH (Schneider, 2016). Complexation of PP with proteins has been reported to significantly change protein structures at room temperature (Rawel et al. 2005), and may potentially aid in the protection and delivery of bioactives (Cao & Xiong 2017; Ma & Zhao 2019; Quan et al. 2019). Additionally, plant-based protein sources including SPI and PPI tend to retain low levels of lipids that can oxidize over time, and complexation with PP may help mitigate negative effects due to their antioxidant activity.

Water hydration capacity (WHC) is a measurement of a protein powder's absorption and retention of water and is indicative of its functionality as an ingredient (Quinn & Paton 1979). WHC is influenced by the surface properties of proteins interacting with water, the charges on protein molecules, functional groups exposed, molecular flexibility, molecular masst, and amino acid composition, and values may vary depending on how it is measured (Kneifel et al. 1991; Zayas, 1997). Proteins interact with water via hydrogen bonds with polar, hydroxyl, and carboxyl groups, electrostatic interactions with charged amino acid side chains, and hydrophobic interactions via nonpolar, hydrophobic groups exposed at the surface (Morr 1990). Proteins interact non-covalently with polyphenols at many of the same sites (Kanakis et al. 2011; Bohin et al. 2012; Le Bourvellec & Renard 2012; Chung et al. 2015; Oancea et al., 2017). WHC is used to describe protein isolate interactions with water, but it may also serve as an indicator for the likelihood of protein-PP interactions.

While the consequences of non-covalent protein-PP interactions are not as extensively reported as those of covalent interactions (Cao & Xiong 2017; Xue et al. 2020), liquid formulations containing WPI, sucrose, and Aronia berry extract (a rich source of PP) were found to exhibit measurable changes in physicochemical properties, attributed to non-covalent complexation interactions formed between PP and proteins (Hansen et al. 2021a). The aim of this study is to investigate whether Aronia PP interact with plant-based SPI and PPI to a similar extent as with WPI in liquid protein-sucrose-PP mixtures, as demonstrated in our previous work. Given that WPI is known to have low WHC (Kneifel et al. 1991; Resch & Daubert, 2002) and was still found to interact with Aronia PP, we expect that protein sources with different structures, such as SPI & PPI, would have different WHC and propensities for interactions with Aronia PP. Varying extents of protein-PP interactions would likely result in measurable changes in physicochemical properties of the dispersions. We hypothesize that PPI formulations comprised of proteins with larger molecular masses (average for WPI ~ 17 kDa, PPI ~ 260 kDa) may exhibit enhanced viscosities, and aggregate sizes may be reduced with enhanced PP interactions (Lam et al. 2018; Ma & Zhao 2019). It would be expected that the hydrolyzed SPI, though typically imparting reduced viscosity due to smaller protein fractions (< 35 kDa), would interact with PP more extensively due to the presence of more carboxyl groups for potential hydrogen bonding and electrostatic interactions, allowing for increased water holding, enhanced viscosities, and reduced particle sizes (Li et al. 2021). In earlier work, we presented a continuous process to form dry beads from concentrated dispersions of WPI and sucrose, with the goal of utilizing these structures for bioactives encapsulation in subsequent experiments (Hansen et al. 2020). In later studies, we developed a modified process for dry bead formation from concentrated dispersions containing Aronia PP (Hansen et al. 2021b). Preparation methods for the concentrated feed dispersions remain virtually unchanged, and this work investigates the interactions occurring in dispersions and the changes in physical behaviors of the feeds that would be prepared for subsequent dry bead formation. This work would build on the findings from previous experiments, providing insight into the non-covalent interactions between plant-based proteins and polyphenols and their effects on the physico-chemical properties of dispersions. This information may be used practically for further applications such as stabilization and delivery of actives, as well as inform the formulation and processing steps in the development of foods containing mixtures of proteins and fruit such as sports drinks, nutritional bars, smoothies, and yogurt, as well as puddings and frozen desserts in order to obtain desirable sensory properties.

Materials and methods

Materials

WPI (IsoChill 9000), was supplied by Agropur, Inc. (Luxemburg, WI, USA) containing 4.6% water, 91.6% protein (dry basis), 0.7% fat, and 3.1% ash. SPI (ProFam® 781, hydrolyzed), was supplied by Archer Daniels Midland Co. (Decatur, IL, USA) containing 3.7% water, 94.7% protein (dry basis), 0.4% fat, and 1.2%

ash. PPI (VITESSENCE™ Pulse 1803), was supplied by Ingredion™ (Westchester, IL, USA) containing 8% water, 80% protein (dry basis), 7.8% fat, and 4.2% ash. Sucrose (pure cane, extra fine, granulated sugar) was supplied by Domino Foods, Inc. (Yonkers, NY, USA). Standardized Aronia berry (Chokeberry) powder, containing a minimum of 15% anthocyanins, 10% proanthocyanidins, and 55.6% total PP, was supplied by Artemis International (Fort Wayne, IN, USA) and stored in the dark at − 18 °C. A similar extract examined in other studies was found to have high quantities of cyanidin-3-galactoside and cyanidin-3-glucoside anthocyanins, as well as high levels of chlorogenic acid (Xie et al., 2016, 2017; Hansen et al., 2021a). Technical data sheets for the extract reported < 5% water content, 2.13% protein, 1.3% fiber, 0.85% sugars, 0.29% fat, and a reconstituted pH of 3–4. Deionized (D.I.) water was used throughout all experiments.

Protein isolate powders characterization

Water hydration capacity

WPI, SPI, and PPI powders were evaluated for their respective WHC by modifying the two-step method presented by Quinn and Paton (1979). The first step, used to obtain an approximate WHC for each protein isolate, was performed in triplicate. The test involved the gradual wetting of 5 g of protein powder with unmeasured amounts of deionized (D.I.) water in 50 mL centrifuge tubes, mixing vigorously with a spatula until the samples were thoroughly wetted and mixtures had paste-like consistencies. Tubes were placed in a Sorvall® RC 26 Plus centrifuge (Sorvall Products, L.P., Newtown, CT, USA) and spun at 5100 rpm (~ 2000 x g) for 10 min at 20–25 °C. The small quantities of supernatant formed were decanted and tubes were weighed to determine the masses of water absorbed by the powders. Triplicate data were averaged and crude WHC values obtained were used to determine water addition levels for step 2. A minimum of 5 tubes containing 5 g of protein powder were prepared as described for step 1, but with a range of known water contents in 1 g increments, both above and below the approximate WHC. After centrifugation under the same conditions, tubes were evaluated to determine the water addition level at which a supernatant was formed, giving more exact WHC values within 1 g.

Dispersion preparation

Dispersions were prepared as described in previous work (Hansen et al. 2021a), where dry protein-sucrose blends were dispersed in D.I. water, then aliquots of Aronia extract solution were added to form the final mixtures at room temperature. pH was measured with a FiveEasy Plus pH/mV meter with InLab® Viscous Pro-ISM probe (Mettler Toledo, Hampton, Schwerzenbach, Switzerland) after calibrating the electrode at pH four and seven at room temperature, < 25 °C.

Twenty-seven formulations of varied compositions were prepared in triplicate for subsequent, randomized triplicate analysis in a 3x3x4 factorial design (Table 1); the 9 remaining WPI-based formulations were prepared and analyzed previously, and the data were used for comparison (Hansen et al. 2021a). Protein to sucrose ratios and total solids contents of dispersions were selected based on findings from previous work (Hansen et al. 2020, 2021a). We aimed to compare dispersions without the active (0%) to formulations with three different concentrations of PP, selecting concentrations to build upon the findings from previous studies (Hansen et al. 2021a). Dispersions defoamed at room temperature for a minimum of 1 h before analyses.

Feed characterization

Flow testing

Flow properties of dispersions including the time required to deposit 10 mL of dispersion, the number of drops deposited per 1 min, the mass of 10 mL of dispersion, and individual drop masses were measured at room temperature, as detailed in previous work (Hansen et al. 2020, 2021b), while pumping dispersions at a constant rate through a benchtop peristaltic pump (120 S/DV, Watson Marlow, Falmouth, England; silicon tubing 85 cm length, 2 mm bore, 1 mm wall, BÜCHI Labortechnik AG, Flawil, Switzerland). Those measurements provided the data necessary to calculate mass and volume flow rates, dispersion densities, drop surface tensions, drop diameters, and drop volumes (Hansen et al. 2020, 2021a).

Viscosity

Utilizing methods reported in previous work (Hansen et al. 2021a), where 1% strain was determined to be within the LVR of dispersions measured, a DHR-2 rheometer (TA Instruments, DE, USA) was used to measure the rheological properties of dispersions at 25 °C in triplicate with small-strain oscillatory measurements; complex viscosity values were recorded.

Particle size distribution

Using the methods explained in Hansen et al. (2021a), particle size distributions of dispersions were measured with a Malvern Mastersizer 2000 (Malvern Instruments Ltd., Worcestershire, U.K.) in triplicate, by injecting drops of dispersions at room temperature into a Hydro 2000S liquid sampler with D.I. water as the dispersant until dilutions reached obscurations between 11 and 15% (WPI refractive index 1.545, D.I. water refractive index 1.33, absorbance 0.001).

Table 1 Formulations

Protein:sucrose	Protein isolate	[PP]	pH	Density	Diameter (calculated)	Diameter (frozen)
–	–	% w/w	–	kg/m^3	mm	mm
0.75	*WPI*	*0*	*6.03*	*1019 ± 10*	*4.59 ± 0.02*	*4.45 ± 0.09*
1	*WPI*	*0*	*6.08*	*1019 ± 6*	*4.60 ± 0.02*	*4.58 ± 0.10*
1.25	*WPI*	*0*	*6.01*	*1014 ± 15*	*4.54 ± 0.03*	*4.48 ± 0.05*
0.75	*WPI*	*0.5*	*5.73*	*1015 ± 11*	*4.67 ± 0.03*	*4.63 ± 0.03*
1	*WPI*	*0.5*	*5.94*	*994 ± 25*	*4.67 ± 0.04*	*4.63 ± 0.09*
1.25	*WPI*	*0.5*	*5.95*	*993 ± 28*	*4.65 ± 0.06*	*4.55 ± 0.14*
0.75	*WPI*	*1*	*5.57*	*994 ± 15*	*4.65 ± 0.08**	*4.39 ± 0.08*[a]
1	*WPI*	*1*	*5.72*	*1021 ± 10*	*4.70 ± 0.03*	*4.50 ± 0.12*
1.25	*WPI*	*1*	*5.84*	*1020 ± 8*	*4.67 ± 0.05*	*4.65 ± 0.02*
0.75	WPI	1.5	5.29	1026 ± 30	4.67 ± 0.06	4.57 ± 0.15
1	WPI	1.5	5.36	1012 ± 7	4.69 ± 0.01[a]	4.47 ± 0.09[a]
1.25	WPI	1.5	5.41	1006 ± 12	4.64 ± 0.07[a]	4.53 ± 0.12[a]
0.75	SPI	0	6.56	1041 ± 13	4.52 ± 0.02[a]	4.45 ± 0.07[a]
1	SPI	0	6.52	1051 ± 9	4.41 ± 0.05[a]	4.50 ± 0.09[a]
1.25	SPI	0	6.55	1037 ± 14	4.50 ± 0.02	4.52 ± 0.14
0.75	SPI	0.5	6.30	1021 ± 13	4.51 ± 0.07	4.49 ± 0.07
1	SPI	0.5	6.32	1032 ± 11	4.47 ± 0.04[a]	4.39 ± 0.09[a]
1.25	SPI	0.5	6.35	1021 ± 11	4.50 ± 0.03	4.51 ± 0.12
0.75	SPI	1	6.03	1022 ± 11	4.54 ± 0.03	4.57 ± 0.11
1	SPI	1	6.09	1016 ± 14	4.53 ± 0.03[a]	4.41 ± 0.13[a]
1.25	SPI	1	6.21	1021 ± 21	4.49 ± 0.06	4.50 ± 0.14
0.75	SPI	1.5	5.84	844 ± 164	4.86 ± 0.34[a]	4.54 ± 0.08[a]
1	SPI	1.5	5.98	956 ± 92	4.63 ± 0.14	4.55 ± 0.13
1.25	SPI	1.5	5.98	788 ± 94	4.79 ± 0.23[a]	4.39 ± 0.18[a]
0.75	PPI	0	6.85	1043 ± 20	4.39 ± 0.10	4.31 ± 0.07
1	PPI	0	6.75	1042 ± 21	4.21 ± 0.03[a]	4.53 ± 0.15[a]
1.25	PPI	0	6.96	976 ± 24	4.29 ± 0.07[a]	4.58 ± 0.17[a]
0.75	PPI	0.5	6.67	1037 ± 15	4.51 ± 0.10[a]	4.75 ± 0.15[a]
1	PPI	0.5	6.46	1039 ± 15	4.31 ± 0.05[a]	4.57 ± 0.19[a]
1.25	PPI	0.5	6.58	1019 ± 32	4.20 ± 0.09[a]	4.67 ± 0.14[a]
0.75	PPI	1	6.15	1021 ± 27	4.67 ± 0.05[a]	4.81 ± 0.16[a]
1	PPI	1	6.22	1025 ± 35	4.60 ± 0.08	4.68 ± 0.22
1.25	PPI	1	6.42	1020 ± 15	4.46 ± 0.05[a]	4.71 ± 0.26[a]
0.75	PPI	1.5	5.82	1027 ± 20	4.65 ± 0.04	4.64 ± 0.21
1	PPI	1.5	6.03	1029 ± 18	4.62 ± 0.04[a]	4.92 ± 0.23[a]
1.25	PPI	1.5	6.26	1028 ± 15	4.54 ± 0.02	4.72 ± 0.27

*values with superscript letters showed significant differences between calculated and measured diameters
values in italics were from previous work (Hansen et al., 2021a; averaged data reported, $n = 6$, 3 for frozen diameters)
Density and estimated drop diameters measured and calculated from flow tests data and measured diameters (mm) of frozen drops (averaged data reported, $n = 9$) formed from feed dispersions with varied protein:sucrose, protein isolates, polyphenols (PP) concentrations, and pH

Optical light microscopy

Protein particles and protein-PP complexes in diluted dispersions at room temperature were observed with a Nikon Eclipse FN1 optical microscope (Nikon Instruments Inc., Melville, NY, USA) and a Nikon Digital Sight DS-U3 camera control unit attached (ver. 1), as reported in previous work (Hansen et al. 2021a).

Centrifuge separation

Slightly modifying sample preparation methods from previous studies (Hansen et al. 2021a), 1.25 g aliquots of 5-times diluted dispersions were pipetted into tubes (1.5 mL graduated tubes with flat caps, Fisherbrand®, Fisher Scientific, Hampton, NH, USA) and centrifuged at 12,000 rpm (~ 13,523 x g) and 20 °C for 20 min in a microcentrifuge (Centrifuge 5424 R with FA-45-24-11 rotor, Eppendorf, Hamburg, Germany). Tubes were observed after centrifugation.

Frozen drop preparation

Beads were frozen solid as described in previous work (Hansen et al. 2021a), by dropping dispersions into liquid nitrogen (LN_2) (100% purity; Airgas, Madison, WI, USA). Drops were allowed to solidify for ~ 5 min prior to removal from the LN_2 and immediate diameter measurements.

Frozen drop diameters

As in previous work, digital Vernier calipers (0–150 mm; Stainless Hard) were used to measure the diameters of frozen beads (Hansen et al. 2021a). Measurements were performed in triplicate for each formulation replicate ($n = 9$).

Statistical analysis

Experiments were performed three times and analyzed in triplicate (n = 9); mean values and standard deviations were calculated from the data collected. To compare mean values, analysis of variance (3-way ANOVA; Tukey's HSD test) and independent measures t-tests (equal variance not assumed) were performed using JMP® Pro version 15.0.0 (SAS Institute Inc., Cary, NC, USA). The level of significance was determined at $p < 0.05$.

Results and discussion

Protein isolate powders characterization

Water hydration capacity

WHC is indicative of a protein powder's functionality as an ingredient. WHC values for WPI, SPI (hydrolyzed), and PPI powders are reported in Table 2. As reported in previous studies, WPI solubilized well in D.I. water and after centrifugation a single, viscous phase remained, giving a WHC value of 0 g of water absorbed per gram of WPI (Kneifel et al. 1991; Resch & Daubert 2002). Five grams of SPI absorbed between 6.5 and 7.5 g of water (~ 1.4 g/g), and five grams of PPI absorbed between 14.1 and 15.1 g of water (~ 2.9 g/g), in agreement with the ranges of capacities reported by Owusu-Ansah and McCurdy (1991) and Zayas (1997). Fleming et al. (1974) reported higher water absorption values for commercial SPI powders, ranging from 4.15–7.75 g water absorbed per g SPI; it is possible that the commercial powders studied underwent greater extents of hydrolysis than ours, resulting in higher quantities of carboxyl groups present for interactions with water. Sosulski and McCurdy (1987) reported water holding capacity values of 2.65 and 2.52 g of water per gram of SPI and PPI at 21 °C, respectively. Swanson (1990) reported that at neutral pH, SPI retained 4–5 times its initial weight of water, and 2.7–2.8 times its weight for PPI. Fuhrmeister and Meuser (2003) reported WHC values of 4.6 g water per g commercial SPI, and 4 g water per g commercial PPI. It is likely that the isolates used in this study have different properties from those used in other work, thus resulting in differing WHC data.

Table 2 Water hydration capacity

Protein isolate	Water hydration capacity
–	(g water absorbed per g powder)
Whey	0
Soy (hydrolysate)	1.4
Pea	2.9

Water hydration capacity of WPI, SPI (hydrolyzed), and PPI powders, reported as grams of water absorbed per gram of protein isolate powder

As there is substantial overlap between the locations where proteins can interact with water and interact non-covalently with PP (Morr 1990; Kanakis et al. 2011; Bohin et al. 2012; Le Bourvellec & Renard 2012; Chung et al. 2015; Oancea et al. 2017), WHC, typically used to describe interactions with water, might also be able to describe the potential for protein-PP interactions. Given that WPI had the lowest WHC of the proteins studied, it is possible that WPI would have the least interactions with PP. SPI and PPI, with higher WHC values imparted by their differing structures with more sites available for interactions, may interact more extensively with the Aronia PP and yield greater measurable changes in physicochemical properties than WPI formulations.

Feed characterization

pH

As reported in earlier work (Hansen et al. 2021a), pH of the dispersions was observed to decrease slightly with increasing PP concentration (Table 1). Variations in pH may influence the structure of proteins in solution, determining which side groups are exposed and how many bindings sites may be available for intermolecular interactions and binding (Rawel et al. 2005), as well as affect functional properties of dispersions including viscosity and particle size (Spencer et al. 1988; Saluja & Kalonia 2005; Cao & Xiong 2017; Hong et al. 2018). As the pH of dispersions approaches the protein isoelectric point (pI), proteins are more likely to undergo intermolecular

interactions and aggregate, which can result in increased viscosity (Song 2009; Coupland 2014).

Use of 1.5% Aronia PP in WPI dispersions induced pH to near the pI values reported in the literature for constituent β-lactoglobulin (pI ~ 5.2–5.3; the major protein fraction in WPI), though values for α-lactalbumin (~ 4.2–4.8) were not reached (Table 1) (Kilara & Harwalkar 1996; Demetriades & McClements 1998; Jean et al. 2006). pH of SPI dispersions was found to decrease with increasing PP concentration and approach the range of pI values reported for β-conglycinin, the minor 7S protein fraction in SPI (pI ~ 5.2–6.4; Table 1). The pI of the major 11S protein fraction, glycinin (pI ~ 4.8), was not nearly reached (Petruccelli & Añón 1995; Li 2005). pH values of PPI dispersions were also reduced with increased PP concentration (Table 1), but did not approach the pI values reported in the literature for constituent vicilin (pI ~ 5.5) or legumin (pI ~ 4.8) protein fractions (Owusu-Ansah & McCurdy 1991; Lam et al. 2018). Assuming a range of pI for WPI, SPI, and PPI, it is possible that the reduced pH values could play a minor role affecting the physical properties of these dispersions.

Interfacial tension

An individual drop will form when the gravitational forces acting on it overcome the surface tension forces around the circumference of the tubing tip, confirming surface tension as a major determinant of the sizes of drops produced (Hansen et al. 2021a). The ANOVA reported that changing the ratio of protein to sucrose had a significant effect ($p < 0.05$) on calculated surface tensions of dispersions. Tukey's HSD tests clarified further, indicating that as protein:sucrose ratios increased, surface tensions significantly decreased ($p < 0.05$), and all three ratios had significantly different surface tension values (Fig. 1a). Sucrose is not thought to appreciably affect surface tension, as sugars are not particularly surface-active; proteins are known surfactants and may adsorb to liquid-gas interfaces and decrease surface tensions (Kitabatake & Doi 1988). In previous studies, changing the ratio of WPI to sucrose in dispersions did not meaningfully impact surface tension (Fig. 1a samples marked*; Hansen et al. 2021a); this observation was confirmed by additional data for WPI dispersions containing 1.5% PP. Similarly, altering SPI:sucrose ratios in dispersions did not notably affect surface tension. Surface tensions of PPI dispersions decreased with increasing PPI concentrations, regardless of PP concentration (Fig. 1a).

Changing the type of protein isolate in formulations between WPI, SPI, and PPI also had a significant effect ($p < 0.05$) on surface tension, according to the ANOVA. Corresponding Tukey's HSD tests indicated that WPI dispersions had the highest surface tensions, while PPI formulations had the lowest, and all three protein isolates were significantly different from each other. In ranking the surfactant abilities to reduce surface tensions of dispersions, WPI would be lowest and PPI highest; these mirror the findings for WHC, which may indicate the differing extent to which the isolates interact with water.

According to the ANOVA, changing the PP concentrations in dispersions had a significant effect on surface tension ($p < 0.05$). Tukey's HSD tests provided more detail, specifying that increasing PP concentrations resulted in significantly increased surface tensions ($p < 0.05$), and the values for all four PP concentrations were significantly different from each other (Fig. 1b). This trend was observed most clearly in dispersions formulated with

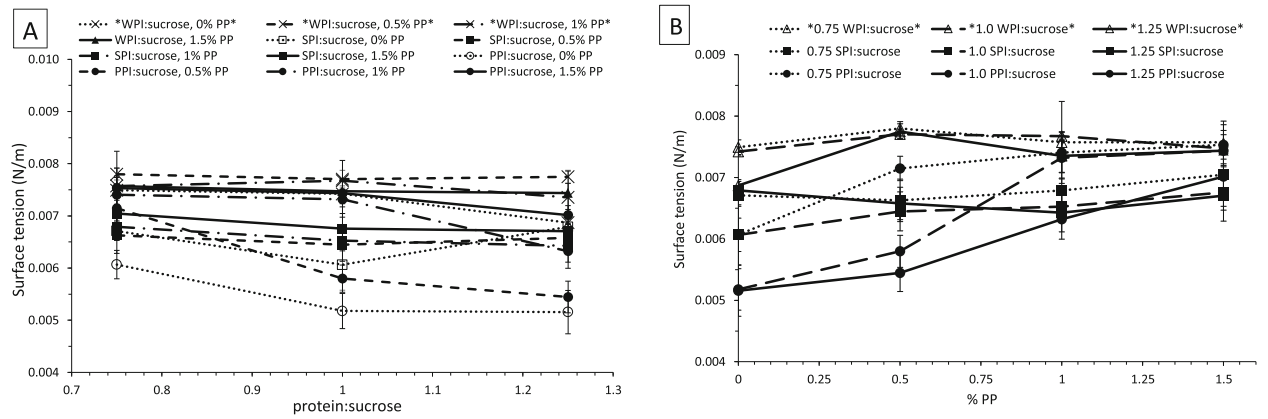


Fig. 1 Effect of protein:sucrose ratio (**A**) and PP content (%) (**B**) on the calculated surface tension (N/m) of dispersions at 25 °C; (averaged data plotted, $n = 9$). Legend entries marked * contain data reported in previous work (Hansen et al., 2021a; averaged data plotted, $n = 6$). Lines are for guiding purposes only

PPI, while many conditions, including WPI formulations and some SPI dispersions, showed no meaningful trends. These findings build on those from earlier studies, where increasing PP concentrations in WPI-sucrose dispersions resulted in increased surface tensions under few conditions, but many conditions showed no meaningful trends (Fig. 1b samples marked* with unfilled markers; Hansen et al. 2021a). As in previous work, variations in trends observed may be attributed to air entrapped in dispersions giving altered surface tension calculations. With optimal PP and protein types and environmental conditions, protein-PP complexation interactions may be enhanced with increased PP, forming complexes that can grow into larger aggregates (Spencer et al. 1988; Charlton et al. 2002; Rawel et al. 2005; Ozdal et al. 2013). As discussed in previous studies (Hansen et al. 2021a), the increased incidence of large protein-PP aggregates in dispersions would likely generate more intermolecular interactions, and liquids containing higher quantities of strong, attractive intermolecular forces are known to have higher surface tensions (He et al. 2011; Tro et al. 2014); this may explain the rising surface tensions observed with increasing PP. It is also possible that, as PP increased, the surfactant abilities of proteins in dispersions to lower surface tension were reduced as a result of enhanced protein-PP interactions occurring and occupying sites available for other interactions. This may also explain the increased surface tensions with increasing PP.

Previous studies have indicated that drop diameters and surface tensions are directly related; as surface tensions decrease, so do the diameters of the resulting drops (Chan et al. 2009). The best fit line applied upon plotting the calculated diameters of drops against the calculated surface tensions of dispersions showed a positive slope (Fig. 2), indicative of a direct correlation ($R^2 = 0.72$), as described by Lee and Chan (2013) and observed in previous work (Hansen et al., 2021a). As discussed in earlier work, the few data points scattered from the correlation may be caused by inaccurate drop diameter and surface tension calculations based on density measurements that can vary with the inclusion of air bubbles in the protein-containing dispersions, as well as the inherent variation within food ingredients (Hansen et al. 2021a). Corresponding density data indicates relatively consistent amounts of entrapped air in dispersions, with few formulations showing enhanced air holding abilities and thus lower measured densities, which may affect the scatter (Table 1).

As reported in earlier studies, more specific methods of surface tension measurement could potentially provide more accuracy than the drop mass method employed (Worley 1992). However, these methods would not be compatible with the dispersions in focus due to their viscosities, stickiness, turbidity, entrapped air, and dark colors when Aronia is present (Hansen et al. 2021a).

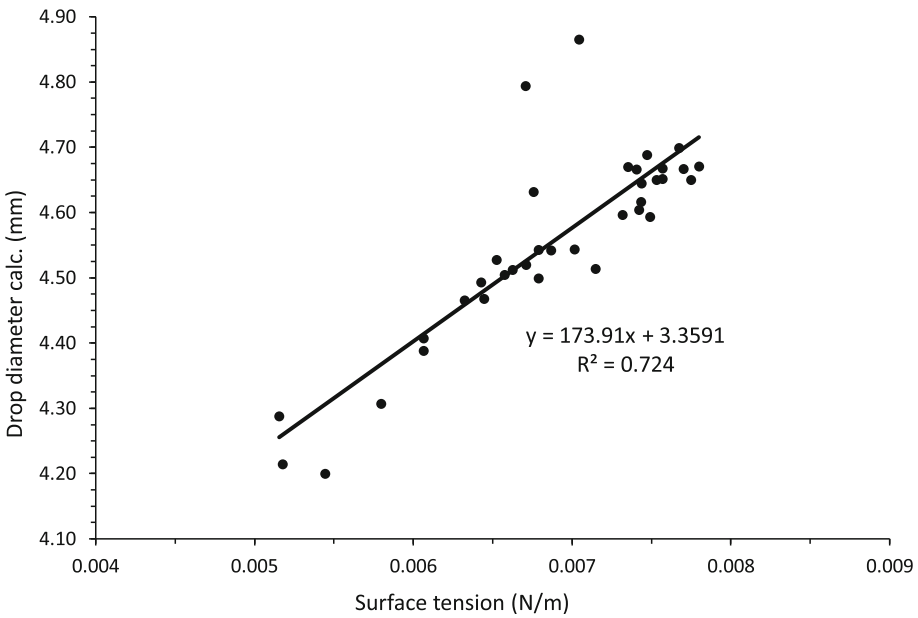


Fig. 2 The relationship between the average surface tensions (N/m) of feed dispersions containing protein:sucrose ratios of 0.75, 1.0, and 1.25, PP contents of 0, 0.5, 1, and 1.5%, and protein isolates including WPI, SPI, and PPI at 25 °C and average calculated diameters (mm) of drops

Viscosity

Viscosity is related to the fluid flow properties of dispersions and can strongly influence processing and manufacturing operations (Johnson et al. 1975; Hartel et al. 2018; Hansen et al. 2021a). According to the ANOVA, the ratio of protein to sucrose had a significant ($p < 0.05$) effect on viscosity, where increases in ratios resulted in increased viscosities. Tukey's HSD tests clarified that all ratios had significantly different viscosities from one another. These ANOVA results are only visually demonstrated in Fig. 3a for PPI formulations containing 0 and 0.5% PP and SPI dispersions with 1.5% PP; those few formulations most strongly influenced the ANOVA results, despite the majority of formulations showing no major changes in viscosity with increasing protein:sucrose ratios. Earlier work also reported significant increases in dispersion viscosities with increasing WPI:sucrose ratios, but only when dispersions total solids contents were greater than 35% (Hansen et al. 2021a). These results are generally in agreement with those from previous experiments, where dispersions containing 25% total solids did not show major shifts in viscosity with changing WPI:sucrose ratios, as the effect of changing protein:sucrose ratios was thought to be relatively weak compared to the effect of % total solids. The increases in dispersion viscosities observed with increasing PPI:sucrose ratios and low PP concentrations may be due to the large molecular mass proteins at higher concentrations having increased opportunities for overlapping, intermolecular protein-protein interactions, and network formation (Song 2009; Coupland 2014); lower PPI:sucrose ratios may have a diluting effect on the protein-protein networks and thus behave more similarly to other, less viscous WPI and SPI dispersions.

Changing the protein isolate in formulations between WPI, SPI, and PPI had a significant effect ($p < 0.05$) on viscosities of dispersions, according to the ANOVA. Tukey's HSD tests provided further detail, reporting that WPI dispersions had the lowest average viscosities, while PPI dispersions had the highest, and the average viscosities of dispersions containing each protein isolate were significantly different from each other. These findings generally agree with those reported by Krstonošić et al. (2020), where aqueous solutions of whey protein concentrate at varied concentrations had lower viscosities than pea and soy protein isolate solutions. In comparing the different protein isolates abilities to reduce surface tensions of dispersions, WPI was found to have the lowest efficacy and PPI the highest, mirroring the findings for the WHC of the isolates. Similarly, WPI had the lowest impact on viscosities of dispersions, indicative of adequate electrostatic repulsion between proteins, while PPI had the highest impact on viscosity, likely due to its large average molecular mass and the increased likelihood of protein-protein interactions. Additionally, PPI dispersions may have differing viscous properties due to the varied extents of hydration undergone by each protein isolate; PPI appears to have undergone a lesser extent of protein hydration prior to testing, as indicated by the presence of large insoluble PPI particles in dispersions.

According to the ANOVA, increasing PP in dispersions was found to have a significant effect ($p < 0.05$) on viscosity, where viscosities generally decreased with increasing PP until increasing at 1.5% PP. Corresponding Tukey's HSD tests indicated that dispersions with differing PP had significantly different viscosities from one another. The decreasing viscosity relationship with

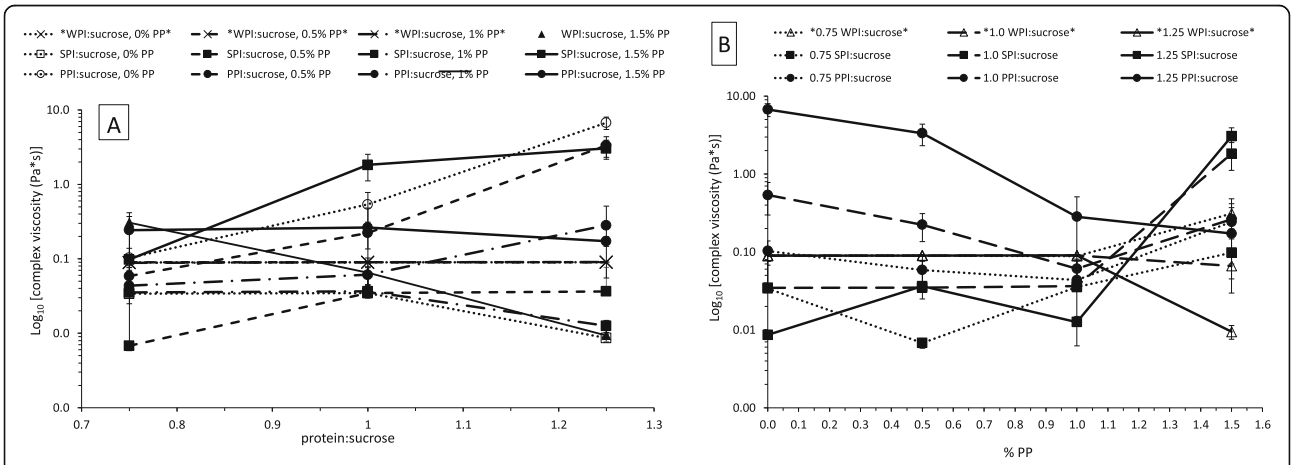


Fig. 3 Effect of protein:sucrose ratio (**A**) and PP content (%) (**B**) on the complex viscosity (Pa*s) of dispersions at 25 °C; (averaged data plotted, n = 9). Legend entries marked * contain data points reported in previous work (Hansen et al., 2021a; averaged data plotted, n = 6). Lines are for guiding purposes only

increasing PP reported by the ANOVA is strongly determined by a small minority of the formulations studied; this trend is only observed for 1.25 PPI:sucrose dispersions with 0 and 0.5% PP, though 1.0 PPI:sucrose dispersions at the same PP concentrations have slightly higher viscosities than the majority of formulations studied. When PP concentration is greater than 0.5%, viscosities of PPI dispersions resemble those of the other formulations (Fig. 3b). The relatively high viscosities measured for PPI dispersions with low PP concentrations (< 1% PP) may be due to the presence of large insoluble protein particles remaining in dispersions during measurements. As PP increase in the system, there may be more opportunities for protein-PP complexation interactions resulting in aggregates that are smaller than the unhydrated particles and thus reducing system viscosity.

Increased viscosities at 1.5% PP are only demonstrated in Fig. 3b for 1.0 and 1.25 SPI:sucrose dispersions, while the majority of formulations showed no meaningful variation in viscosity with increasing PP. The 1.0 and 1.25 SPI:sucrose dispersions, while a minority of the formulations studied, strongly influenced the ANOVA results reported as their viscosities were significantly higher than the other formulations studied. The hydrolyzed SPI was designed to disperse more readily in water with minimal aggregation. Hydrolyzed protein structures have more potential sites available for PP complexation interactions as well, but it appears that a concentration threshold must be met for the SPI in order to start forming an interaction network at high PP concentrations. High PP concentrations likely gave rise to increased intermolecular interactions in the system upon the formation of protein-PP complexes, resulting in increased viscosities and behavioral complexity of the dispersions. Significant increases in viscosity were not observed to occur in formulations with the same SPI:sucrose ratios at lower PP concentrations, indicating that the extreme increase at 1.5% PP is likely due to a strong network forming with protein-PP complexation at high protein and PP concentrations. Results reported are generally in agreement with those from earlier experiments, where increasing PP resulted in slight shifts in viscosity for dispersions containing 25% total solids (Hansen et al. 2021a).

Particle size distribution

Particle size analysis is useful for evaluating protein-PP interactions in dispersions, as the introduction of PP changes protein structures, conformation, and electrostatic repulsion, thus affecting the extent of aggregation and resulting particle size distributions of dispersions (Bandyopadhyay et al. 2012; Le Bourvellec & Renard, 2012; Coupland 2014; Schneider 2016; Hong et al. 2018; Hansen et al. 2021a). According to the ANOVA, protein:sucrose ratio had a significant effect ($p < 0.05$) on the average particle size (volume-weighted mean, $d_{4,3}$) of dispersions. Tukey's HSD tests clarified that increasing protein:sucrose ratios from 0.75 to 1.0 resulted in significantly increased average particle sizes ($p < 0.05$), but the slight increase observed from 1.0 to 1.25 protein:sucrose was not significant ($p > 0.05$). Despite the ANOVA reporting some apparently significant changes in particle size with changing protein:sucrose ratios, plotting the data in Fig. 4a indicated that the shifts were small. These observations are generally in agreement with results from earlier experiments, where WPI:sucrose ratio did not strongly impact the average particle sizes of dispersions (Hansen et al. 2021a).

Changing the protein isolate in formulations between WPI, SPI, and PPI had a significant effect ($p < 0.05$) on the average particle sizes of dispersions, according to the ANOVA. Tukey's HSD tests provided further detail, reporting that WPI dispersions had the smallest average particle sizes, PPI dispersions had the largest, and the average particle sizes of dispersions containing each protein isolate were significantly different from each other. The differences between the average particle sizes of SPI and WPI dispersions are best demonstrated in Fig. 4b, where SPI formulations containing higher PP concentrations (> 0.5%) are shown to have slightly larger average particle sizes. These findings mirror the trends observed for WHC and viscosity measurements, with WPI having the lowest values and PPI having the highest, likely influenced by differences in the average MW of the isolates and the potential for protein-protein interactions.

While earlier work reported normal distributions for WPI dispersions (Hansen et al. 2021a), the particle size distributions for SPI and PPI dispersions were observed to have different shapes with tails and shoulders to the left and right of the main peaks, as demonstrated in Fig. 5. These differences in distribution shapes may be indicative of the presence of unhydrated particles and protein-PP conjugates of different sizes in dispersions.

According to the ANOVA, average particle sizes of dispersions were significantly affected by PP concentration ($p < 0.05$); Tukey's HSD tests expanded on this, reporting that particle sizes decreased significantly with the addition of 0.5 and 1% PP to dispersions, with no further change upon 1.5% PP addition ($p > 0.05$). While in agreement with the findings from previous work with 25% total solids WPI dispersions (Hansen et al. 2021a), these results appear to be strongly influenced by the data for PPI formulations specifically. Though the results reported by the ANOVA may be observed for PPI dispersions in Fig. 4b, trends observed for WPI and SPI formulations were different; SPI dispersions showed

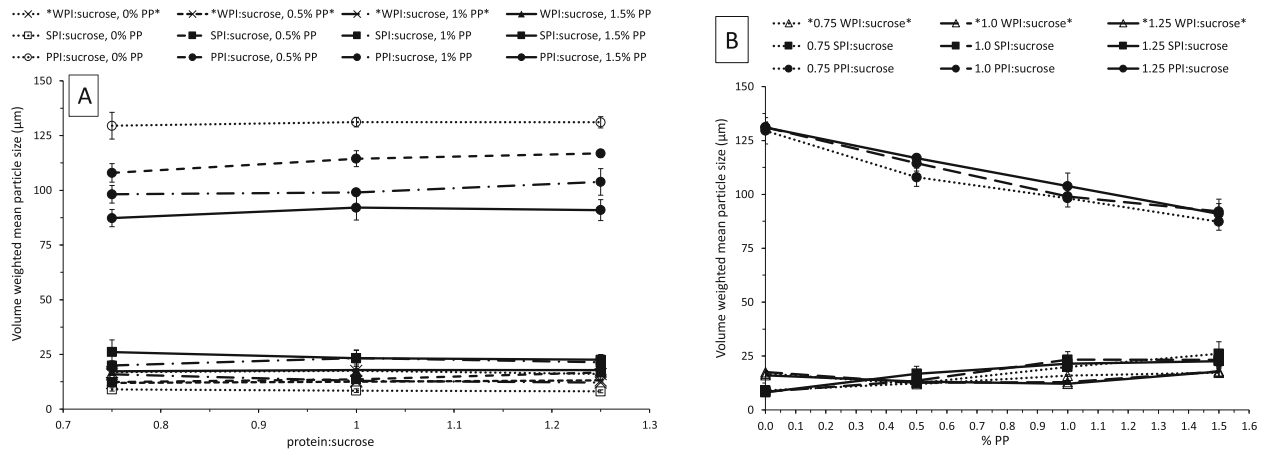


Fig. 4 Effect of protein:sucrose ratio (**A**) and PP content (%) (**B**) on the average particle size (µm) of dispersions at 25 °C; (averaged data plotted, $n = 9$). Legend entries marked * contain data points reported in previous work (Hansen et al., 2021a; averaged data plotted, n = 6). Lines are for guiding purposes only

slightly increasing particle sizes with increasing PP, while WPI dispersions generally showed no meaningful trends or changes, indicative of less extensive protein-PP interactions. Apparently, PPI underwent the least extent of hydration prior to testing, resulting in the presence of many large aggregates in dispersions upon measurement and observation. Formation of protein-PP aggregates in PPI dispersions, which were smaller than the unhydrated PPI particles, likely caused the average particle sizes of dispersions to go down with increasing PP. Additionally, further hydration may have occurred over time, reducing the sizes of larger unhydrated particles in dispersions.

The slight increasing trends observed for particle sizes in SPI dispersions with increasing PP may be due to the same factors that affected viscosity. The hydrolyzed SPI used in this study had smaller average MW proteins than regular SPI; hence, it dispersed easily with minimal protein aggregation, explaining the small particle sizes observed when PP were absent. The hydrolyzed protein structures have more potential sites available for protein-PP interactions than non-hydrolyzed SPI, which may explain the steady increase in particle sizes detected as PP increased in dispersions. While an opposite trend was observed for changes in particle size by Xue et al.

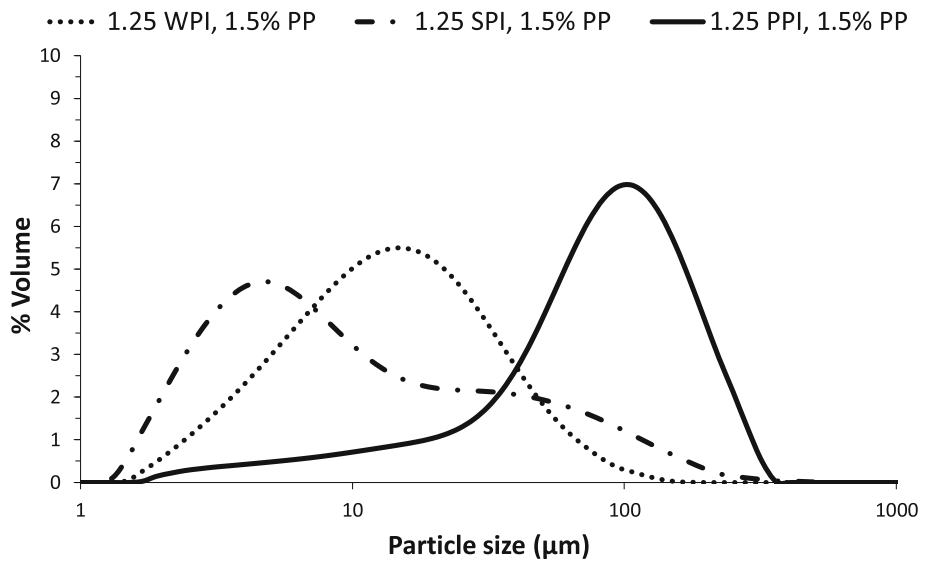


Fig. 5 Particle size distributions of dispersions with 1.25 protein:sucrose ratios and 1.5% PP contents comprised of WPI, SPI, and PPI at 25 °C; (averaged data plotted, n = 9)

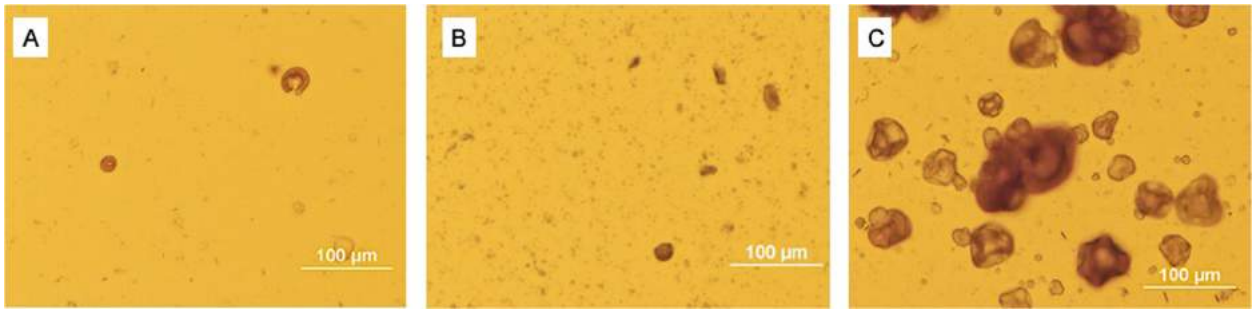


Fig. 6 Optical light microscope images at 200x magnification depicting the microstructures of diluted feed dispersions with a 1.25 protein:sucrose ratio and 1.5% PP formulated with WPI (**A**), SPI (**B**), and PPI (**C**)

(2020) when studying complexation between SPI and cyanidin-3-galactoside, this may be due to the use of different SPI sources. Thus, increased particle sizes measured in SPI dispersions may be attributed to enhanced protein-PP interactions in the system.

Optical light microscopy

As with earlier work, particle size data generated by Mastersizer light scattering were supported by microscopy (Hansen et al. 2021a). Although inherent differences exist between the methods making direct comparison of results difficult (Schneider 2016), microscope images depicted Mastersizer data visually, including the variations observed in particle size distributions between dispersions containing WPI, SPI, and PPI (Fig. 5**;** Fig. 6). Mastersizer data reporting increased average particle sizes with increasing PP in SPI dispersions were reinforced with optical light microscopy (Fig. 7), as were the reduced average particle sizes observed for PPI dispersions with increased PP (Fig. 8).

Centrifuge separation

Centrifugation resulted in the easy precipitation of pellets out of diluted dispersions, as observed with earlier experiments involving WPI (Hansen et al. 2021a). Centrifuged samples without Aronia PP formed clear supernatants and off-white to tan-colored pellets, while those containing PP formed dark purple pellets (Fig. 10**)**, indicative of protein-PP complexation, as formation of a colored precipitate is a crude method to confirm protein-PP complexation (Van Teeling et al. 1971). Similar to observations from earlier experiments (Hansen et al. 2021a), diluted PP-containing dispersions formed dark purple, transparent supernatant fractions after centrifugation.

Precipitated pellets appeared to be smallest for diluted 1.25 protein-sucrose dispersions with 1.5% PP containing WPI, and largest for PPI (Fig. 9). Comparing observations from previous experiments (Hansen et al. 2021a), WPI-containing dispersions appeared to form the smallest pellets upon centrifugation (regardless of PP concentration), while SPI dispersions formed slightly larger pellets and PPI formed the largest. Differences in the relative precipitate sizes of the protein isolates may be attributed to the differences in size, where proteins with larger average MW (such as SPI & PPI) may be more susceptible to precipitating out of solution upon centrifugation than smaller MW proteins like WPI.

Pellet sizes generally appeared to increase slightly with increasing PP in diluted SPI and PPI dispersions (Fig. 10), akin to observations made in previous work for WPI dispersions with increasing PP (Hansen et al. 2021a). Negligible precipitate was formed upon centrifugation of a diluted 1% Aronia extract solution in

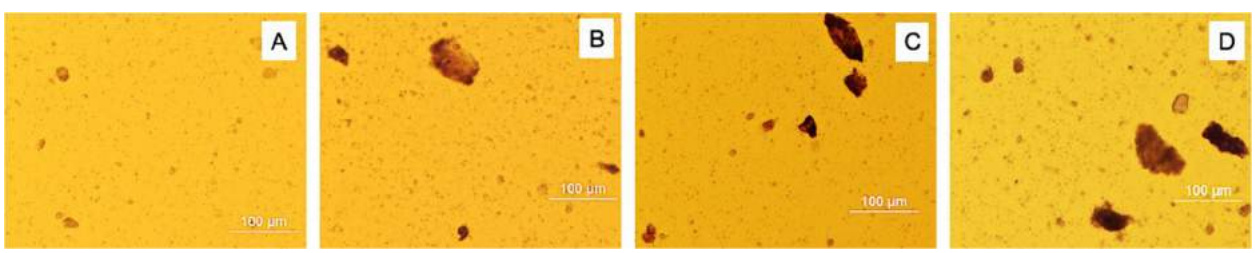


Fig. 7 Optical light microscope images at 200x magnification depicting the microstructures of diluted feed dispersions with 1.0 SPI:sucrose with 0% (**A**), 0.5% (**B**), 1% (**C**), and 1.5% PP addition (**D**)

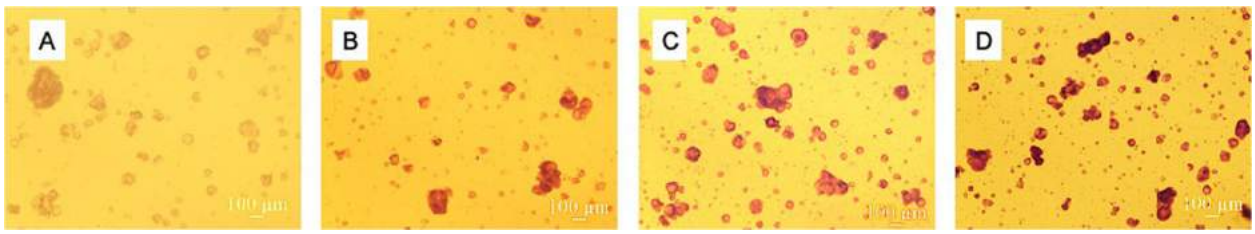


Fig. 8 Optical light microscope images at 40x magnification depicting the microstructures of diluted feed dispersions with 1.0 PPI:sucrose with 0% (**A**), 0.5% (**B**), 1% (**C**), and 1.5% PP addition (**D**)

previous experiments, indicating that the apparent increases in pellet sizes with increasing PP may be a result of the formation of larger, aggregated conjugates precipitating out of solution (Hansen et al. 2021a).

Frozen drop characterization

Comparison of diameters

Dispersions were frozen into drops and diameters were measured to observe the effects of changing protein: sucrose ratios, protein isolate types, and PP concentrations on the sizes of drops formed. According to the ANOVA and corresponding Tukey's HSD tests, changing the protein:sucrose ratios in dispersions did not have a significant impact ($p > 0.05$) on frozen drop diameters (Fig. 11a).

Changing the protein isolate in dispersions between WPI, SPI, and PPI had a slight but statistically significant effect ($p < 0.05$) on the diameters of frozen drops formed, according to the ANOVA. Corresponding Tukey's HSD tests specified that PPI beads had significantly larger diameters than the other isolates ($p < 0.05$), while the smaller diameters of SPI and WPI beads were not significantly different from each other. These findings are depicted in Fig. 11b, where the average frozen diameters of all formulations containing each respective protein isolate are reported. Although surface tension and drop diameters are reported to be directly correlated, our results for measured drop diameters are at odds with this; dispersions with the lowest surface tensions (in this case, PPI formulations) would be expected to have the smallest drop diameters but were actually found to have the largest diameters of the formulations studied. The viscous PPI dispersions (and few SPI formulations) were observed to drip irregularly from the tubing tip into nonuniform shapes indicative of more complex fluid behaviors, in contrast to the spherical drops formed by WPI, contributing to the higher variation observed in diameters for beads produced with those isolates.

PP concentration was found to have a significant ($p < 0.05$) impact on frozen drop diameters, according to the ANOVA. In line with previous findings (Hansen et al. 2021a), Tukey's HSD tests reported a significant increase in diameters ($p < 0.05$) when PP was increased from 0 to 0.5%, but the minor increases in diameters observed as PP increased from 0.5 to 1 and 1.5% were not statistically significant. Drop diameters generally increased with Aronia addition, although some scatter was observed; the increasing trend is most clearly demonstrated for dispersions comprised of PPI:sucrose as PP increased from 0 to 0.5% in Fig. 11c. These findings are in agreement with the surface tension data, as both surface tension and frozen drop diameters increase with PP addition, in agreement with reports indicating their direct correlation.

Estimated values calculated from flow testing data were compared with the measured diameters of frozen drops (Table 1). While the prediction of drop diameters by calculations was generally successful in previous work focused on WPI dispersions (Hansen et al. 2020, 2021a), the success rates (no significant differences between calculated and measured values; $p < 0.05$) here were notably

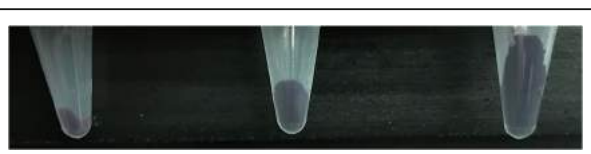


Fig. 9 Image depicting the precipitated fractions (highlighted in boxes) of centrifuged 5x-diluted dispersions with 1.25 protein:sucrose and 1.5% PP with WPI (Left), SPI (Center), and PPI (Right)

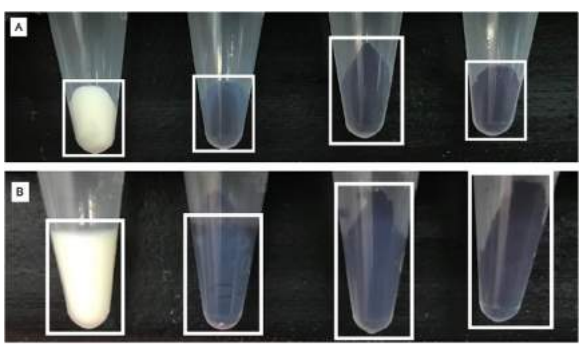


Fig. 10 Images depicting the precipitated fractions (highlighted in boxes) of centrifuged 5x-diluted dispersions with 1.25 SPI:sucrose (**A**) and 5:4 PPI:sucrose (**B**) and 0% (Left), 0.5% (Center, left), 1% (Center, right), and 1.5% PP addition (Right)

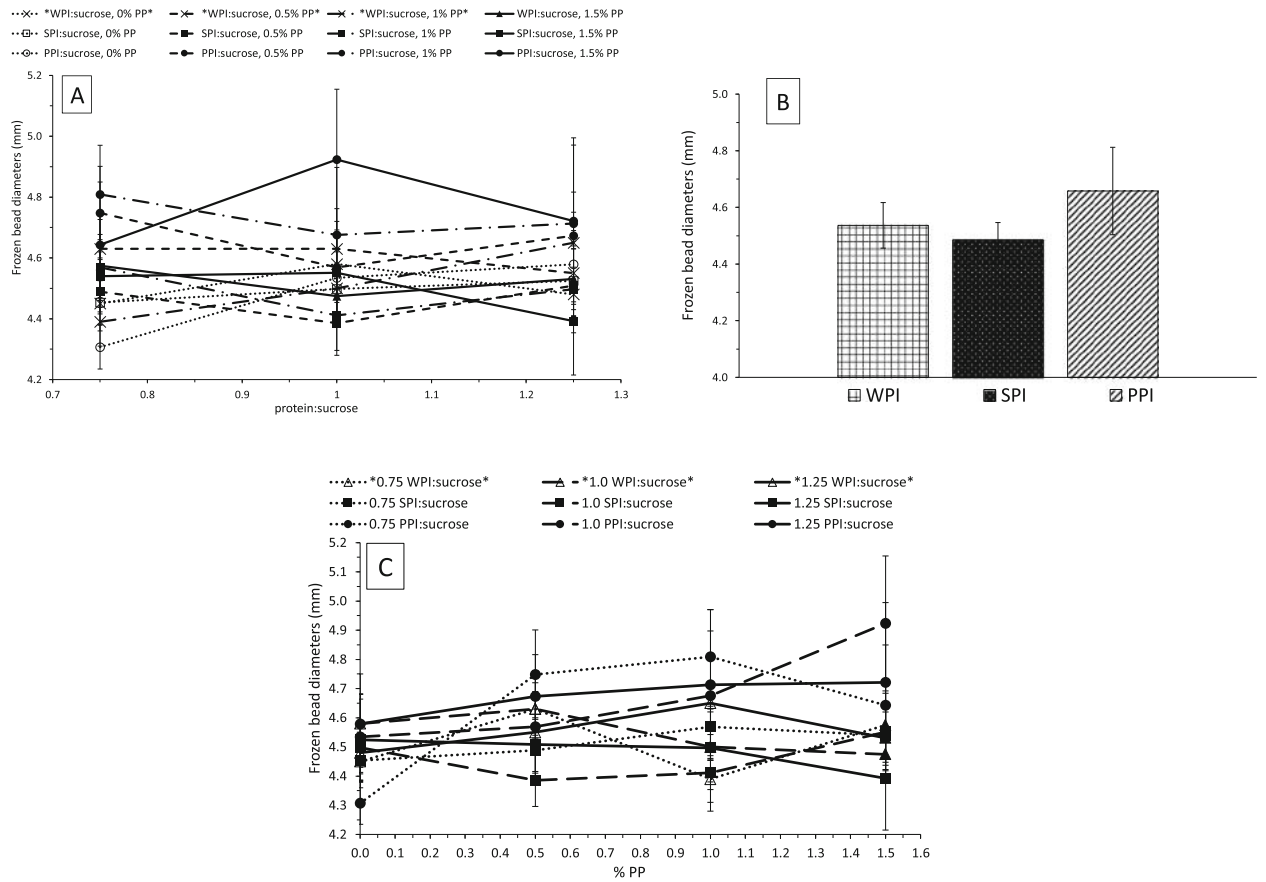


Fig. 11 Effect of protein:sucrose ratio (**A**), protein isolate type (**B**), and PP content (%) (**C**) on the on the diameters (mm) of frozen drops formed from dispersions; (averaged data plotted, n = 9). Legend entries marked * contain data points reported in previous work (Hansen et al., 2021a; averaged data plotted, *n* = 3). Lines are for guiding purposes only [**A, B**]

lower. No significant differences were found between the estimated diameters calculated from flow data and the actual measured diameters 75% of the time for WPI dispersions. SPI dispersions had a success rate of 50%, and PPI dispersions only 33%. It is possible that the estimated calculations became less accurate in predicting drop diameters because variability increased for the measured drop diameters of SPI and particularly PPI dispersions, when more irregularly shaped, less spherical drops were observed to form.

Conclusions

To expand on the findings from previous experiments, where liquid dispersions containing WPI, sucrose, and Aronia extract were found to exhibit measurable changes in physicochemical properties attributed to naturally occurring, non-covalent complexation interactions between PP and proteins, this work aimed to investigate whether Aronia PP would interact with plant-based SPI and PPI to a similar extent. The occurrence of non-covalent protein-PP interactions was found to have different effects in SPI and PPI dispersions, nevertheless indicative of more extensive protein-PP interactions than observed in WPI formulations. Increased viscosities and particle sizes were observed for SPI dispersions with increasing PP, while PPI formulations were observed to have reduced viscosities and particle sizes and increased surface tensions. These findings build from previous work to contribute to the body of research describing the physical effects of non-covalent interactions between non-dairy proteins and PP under mild pH and temperature conditions. Additionally, our results provide empirical insight for applications utilizing concentrated protein-PP mixtures for the development of protective delivery vehicles such as the dry, high protein beads formed by the processes presented in other experiments (Hansen et al. 2020, 2021b). Findings from this study may also inform the formulation of functional foods containing proteins and PP sources like fruit, such as sports beverages, nutritional bars, smoothies, and yogurts, as well as everyday products including pudding and frozen desserts, where specific sensory attributes may be at risk if formulations contain levels of PP and proteins that would be prone to more extensive complexation interactions in mixtures.

Acknowledgements
The authors would like to thank the reviewers and Journal Editor for thoughtful reading of the manuscript and constructive comments.

Authors' contributions
Mackenzie M. Hansen: Conceptualization, Methodology, Validation, Formal analysis, Investigation, Resources, Writing- Original Draft, Writing- Review & Editing, Visualization, Project administration, Funding acquisition. Richard W. Hartel: Conceptualization, Resources, Writing- Review & Editing, Visualization, Supervision. Yrjö H. Roos: Conceptualization, Resources, Writing- Review & Editing, Visualization, Supervision, Funding acquisition. The author(s) read and approved the final manuscript.

Funding
Funding for this study was provided by the Lauritzson Foundation via the Lauritzson Research Scholarship, through the College of Science, Engineering and Food Science (SEFS) at University College Cork.

Availability of data and materials
The datasets used and/or analyzed during the current study are available from the corresponding author on reasonable request.

Declarations

Ethics approval and consent to participate
Not applicable.

Consent for publication
Not applicable.

Competing interests
The authors hereby declare no conflict of interest.

Received: 5 August 2021 Accepted: 7 September 2021
Published online: 01 November 2021

References

Aschemann-Witzel, J., & Peschel, A. O. (2019). Consumer perception of plant-based proteins: The value of source transparency for alternative protein ingredients. Food Hydrocolloids, 96, 20–28. https://doi.org/https://doi.org/10.1016/j.foodhyd.2019.05.006

Bandyopadhyay, P., Ghosh, A. K., & Ghosh, C. (2012). Recent developments on polyphenol–protein interactions: Effects on tea and coffee taste, antioxidant properties and the digestive system. Food & Function, 3(6), 592. https://doi.org/https://doi.org/10.1039/c2fo00006g, 605

Bohin, M. C., Vincken, J.-P., van der Hijden, H. T. W. M., & Gruppen, H. (2012). Efficacy of food proteins as carriers for flavonoids. J Agr Food Chem, 60(16), 4136–4143. https://doi.org/https://doi.org/10.1021/jf205292r

Cao, H., Saroglu, O., Karadag, A., Diaconeasa, Z., Zoccatelli, G., Conte-Junior, C. A., Gonzalez-Aguilar, G. A., Ou, J., Bai, W., Zamarioli, C. M., Freitas, L. A. P., Shpigelman, A., Campelo, P. H., Capanoglu, E., Hii, C. L., Jafari, S. M., Qi, Y., Liao, P., Wang, M., Zou L., Bourke P., Simal-Gandara J. Xiao, J. (2021). Available technologies on improving the stability of polyphenols in food processing. Food Frontiers, fft2.65. https://doi.org/https://doi.org/10.1002/fft2.65, 2, 2, 109, 139

Cao, Y., & Xiong, Y. L. (2017). Interaction of Whey Proteins with Phenolic Derivatives Under Neutral and Acidic pH Conditions: Protein-phenolic interaction. *Journal of Food Science*, 82(2), 409–419. https://doi.org/https://doi.org/10.1111/1750-3841.13607

Chan, E.-S., Lee, B.-B., Ravindra, P., & Poncelet, D. (2009). Prediction models for shape and size of ca-alginate macrobeads produced through extrusion–dripping method. Journal of Colloid and Interface Science, 338(1), 63–72. https://doi.org/https://doi.org/10.1016/j.jcis.2009.05.027

Charlton, A. J., Baxter, N. J., Khan, M. L., Moir, A. J. G., Haslam, E., Davies, A. P., & Williamson, M. P. (2002). Polyphenol/peptide binding and precipitation. J Agr Food Chem, 50(6), 1593–1601. https://doi.org/https://doi.org/10.1021/jf010897z

Chung, C., Rojanasasithara, T., Mutilangi, W., & McClements, D. J. (2015). Enhanced stability of anthocyanin-based color in model beverage systems through whey protein isolate complexation. Food Research International, 76, 761–768. https://doi.org/https://doi.org/10.1016/j.foodres.2015.07.003, Pt 3

Coupland, J. N. (2014). *An introduction to the physical chemistry of food*, (illustrated ed.,). Springer Science + Business Media. New York, NY. https://doi.org/10.1007/978-1-4939-0761-8 .

Demetriades, K., & McClements, D. J. (1998). Influence of pH and heating on physicochemical properties of whey protein-stabilized emulsions containing a nonionic surfactant. Journal of Agricultural and Food Chemistry, 46(10), 3936–3942. https://doi.org/https://doi.org/10.1021/jf980463c

Fleming, S. E., Sosulski, F. W., Kilara, A., & Humbert, E. S. (1974). Viscosity and water absorption characteristics of slurries of sunflower and soybean flours, concentrates and isolates. Journal of Food Science, 39(1), 188–192. https://doi.org/https://doi.org/10.1111/j.1365-2621.1974.tb01019.x

Fuhrmeister, H., & Meuser, F. (2003). Impact of processing on functional properties of protein products from wrinkled peas. Journal of Food Engineering, 56(2–3), 119–129. https://doi.org/https://doi.org/10.1016/S0260-8774(02)00241-8

González, S. (2020). Dietary bioactive compounds and human health and disease. Nutrients, 12(2), 348. https://doi.org/https://doi.org/10.3390/nu12020348

Hansen, M. M., Hartel, R. W., & Roos, Y. H. (2021a). Encapsulant-bioactives interactions impact on physico-chemical properties of concentrated dispersions. Journal of Food Engineering, 302, 110586. https://doi.org/https://doi.org/10.1016/j.jfoodeng.2021.110586

Hansen, M. M., Hartel, R. W., & Roos, Y. H. (2021b). Formation of dry beads for bioactives encapsulation by freeze granulation [manuscript submitted to journal of food engineering].

Hansen, M. M., Maidannyk, V. A., & Roos, Y. H. (2020). Thermal gelation and hardening of whey protein beads for subsequent dehydration and encapsulation using vitrifying sugars. Journal of Food Engineering, 279, 109966. https://doi.org/https://doi.org/10.1016/j.jfoodeng.2020.109966

Hartel, R. W., von Elbe, J. H., & Hofberger, R. (2018). Confectionery science and technology. Springer International Publishing. https://doi.org/https://doi.org/10.1007/978-3-319-61742-8

He, F., Woods, C. E., Litowski, J. R., Roschen, L. A., Gadgil, H. S., Razinkov, V. I., & Kerwin, B. A. (2011). Effect of sugar molecules on the viscosity of high concentration monoclonal antibody solutions. Pharmaceutical Research, 28(7), 1552–1560. https://doi.org/https://doi.org/10.1007/s11095-011-0388-7

Hong, T., Iwashita, K., & Shiraki, K. (2018). Viscosity control of protein solution by small solutes: A review. Curr Protein Pept Sc, 19(8), 746–758. https://doi.org/https://doi.org/10.2174/1389203719666171213114919

Jean, K., Renan, M., Famelart, M.-H., & Guyomarc'h, F. (2006). Structure and surface properties of the serum heat-induced protein aggregates isolated from heated skim milk. International Dairy Journal, 16(4), 303–315. https://doi.org/https://doi.org/10.1016/j.idairyj.2005.04.001

Johnson, J. F., Martin, J. R., & Porter, R. S. (1975). Determination of Viscosity of food systems. In *Theory, determination and control of physical properties of food materials*, (vol. 1, pp. 25–38). Dordrecht, Springer.

Kanakis, C. D., Hasni, I., Bourassa, P., Tarantilis, P. A., Polissiou, M. G., & Tajmir-Riahi, H.-A. (2011). Milk β-lactoglobulin complexes with tea polyphenols. Food Chemistry, 127(3), 1046–1055. https://doi.org/https://doi.org/10.1016/j.foodchem.2011.01.079

Kilara, A., & Harwalkar, V. R. (1996). Denaturation. In *Food proteins: Properties and characterization*. Weinheim, Wiley-VCH.

Kitabatake, N., & Doi, E. (1988). Surface tension and Foamability of protein and surfactant solutions. Journal of Food Science, 53(5), 1542–1569. https://doi.org/https://doi.org/10.1111/j.1365-2621.1988.tb09319.x

Kneifel, W., Paquin, P., Abert, T., & Richard, J.-P. (1991). Water-holding capacity of proteins with special regard to milk proteins and methodological aspects—A review. Journal of Dairy Science, 74(7), 2027–2041. https://doi.org/https://doi.org/10.3168/jds.S0022-0302(91)78373-2

Krstonošić, V. S., Kalić, M. D., Dapčević-Hadnađev, T. R., Lončarević, I. S., & Hadnađev, M. S. (2020). Physico-chemical characterization of protein stabilized oil-in-water emulsions. Colloids and Surfaces A: Physicochemical and Engineering Aspects, 602, 125045. https://doi.org/https://doi.org/10.1016/j.colsurfa.2020.125045

Kulmyrzaev, A., Bryant, C., & McClements, D. J. (2000). Influence of sucrose on the thermal denaturation, gelation, and emulsion stabilization of whey proteins. J Agr Food Chem, 48(5), 1593–1597. https://doi.org/https://doi.org/10.1021/jf9911949

Lam, A. C. Y., Can Karaca, A., Tyler, R. T., & Nickerson, M. T. (2018). Pea protein isolates: Structure, extraction, and functionality. Food Reviews International, 34(2), 126–147. https://doi.org/https://doi.org/10.1080/87559129.2016.1242135

Le Bourvellec, C., & Renard, C. M. G. C. (2012). Interactions between polyphenols and macromolecules: Quantification methods and mechanisms. Critical

Reviews in Food Science and Nutrition, 52(3), 213–248. https://doi.org/https://doi.org/10.1080/10408398.2010.499808
Lee, B. B., & Chan, E. S. (2013). Size and shape of calcium alginate beads produced by extrusion dripping. Chemical Engineering and Technology, 36(10), 1627–1642. https://doi.org/https://doi.org/10.1002/ceat.201300230
Li, D., Wang, P., Luo, Y., Zhao, M., & Chen, F. (2017). Health benefits of anthocyanins and molecular mechanisms: Update from recent decade. Critical Reviews in Food Science and Nutrition, 57(8), 1729–1741. https://doi.org/https://doi.org/10.1080/10408398.2015.1030064
Li, T. S. (2005). *Functional and structural properties of molecular soy protein fractions [doctor of philosophy]*. Singapore, National University of Singapore.
Li, Y., He, D., Li, B., Lund, M. N., Xing, Y., Wang, Y., Li, F., Cao, X., Liu, Y., Chen, X., Yu, J., Zhu, J., Zhang, M., Wang, Q., Zhang, Y., Li, B., Wang, J., Xing, X., & Li, L. (2021). Engineering polyphenols with biological functions via polyphenol-protein interactions as additives for functional foods. Trends in Food Science & Technology, 110, 470–482. https://doi.org/https://doi.org/10.1016/j.tifs.2021.02.009
Ma, C.-M., & Zhao, X.-H. (2019). Depicting the non-covalent interaction of whey proteins with Galangin or Genistein using the multi-spectroscopic techniques and molecular docking. Foods, 8(9), 360. https://doi.org/https://doi.org/10.3390/foods8090360
Mink, P. J., Scrafford, C. G., Barraj, L. M., Harnack, L., Hong, C.-P., Nettleton, J. A., & Jacobs, D. R. (2007). Flavonoid intake and cardiovascular disease mortality: A prospective study in postmenopausal women. The American Journal of Clinical Nutrition, 85(3), 895–909. https://doi.org/https://doi.org/10.1093/ajcn/85.3.895
Morr, C. V. (1990). Current status of soy protein functionality in food systems. Journal of the American Oil Chemists' Society, 67(5), 265–271. https://doi.org/https://doi.org/10.1007/BF02539674
Oancea, A.-M., Aprodu, I., Râpeanu, G., Bahrim, G., & Stanciuc, N. (2017). The binding mechanism of anthocyanins from sour cherries (*Prunus cerasus* L) skins to bovine β-lactoglobulin: A fluorescence and *in silico* -based approach. International Journal of Food Properties, 20(sup3), S3096–S3111. https://doi.org/https://doi.org/10.1080/10942912.2017.1343347
Owusu-Ansah, Y. J., & McCurdy, S. M. (1991). Pea proteins: A review of chemistry, technology of production, and utilization. Food Review International, 7(1), 103–134. https://doi.org/https://doi.org/10.1080/87559129109540903
Ozdal, T., Capanoglu, E., & Altay, F. (2013). A review on protein–phenolic interactions and associated changes. Food Research International, 51(2), 954–970. https://doi.org/https://doi.org/10.1016/j.foodres.2013.02.009
Petruccelli, S., & Añón, M. C. (1995). Soy protein isolate components and their interactions. Journal of Agricultural and Food Chemistry, 43(7), 1762–1767. https://doi.org/https://doi.org/10.1021/jf00055a004
Quan, T. H., Benjakul, S., Sae-leaw, T., Balange, A. K., & Maqsood, S. (2019). Protein–polyphenol conjugates: Antioxidant property, functionalities and their applications. Trends in Food Science and Technology, 91, 507–517. https://doi.org/https://doi.org/10.1016/j.tifs.2019.07.049
Quinn, J. R., & Paton, D. (1979). A practical measurement of water hydration capacity of protein materials. *Cereal Chemistry*, *56*(1), 38–40.
Rawel, H. M., Meidtner, K., & Kroll, J. (2005). Binding of selected phenolic compounds to proteins. J Agr Food Chem, 53(10), 4228–4235. https://doi.org/https://doi.org/10.1021/jf0480290
Resch, J. J., & Daubert, C. R. (2002). Rheological and physicochemical properties of derivatized whey protein concentrate powders. International Journal of Food Properties, 5(2), 419–434. https://doi.org/https://doi.org/10.1081/JFP-120005795
Saluja, A., & Kalonia, D. S. (2005). Application of ultrasonic shear Rheometer to characterize rheological properties of high protein concentration solutions at microliter volume. Journal of Pharmaceutical Sciences, 94(6), 1161–1168. https://doi.org/https://doi.org/10.1002/jps.20342
Schneider, M. E. (2016). *Formation of whey protein-polyphenol aggregates and incorporation into various food structures [PhD food science]*. Raleigh, NC, North Carolina State University.
Song, J. (2009). Insight into "insoluble proteins" with pure water. FEBS Letters, 583(6), 953–959. https://doi.org/https://doi.org/10.1016/j.febslet.2009.02.022
Sosulski, F. W., & McCurdy, Ar. (1987). Functionality of flours, protein fractions and isolates from field peas and faba bean. eJournal of Food Science, 52(4), 1010–1014. https://doi.org/https://doi.org/10.1111/j.1365-2621.1987.tb14263.x
Spencer, C. M., Cai, Y., Martin, R., Gaffney, S. H., Goulding, P. N., Magnolato, D., Lilley, T. H., & Haslam, E. (1988). Polyphenol complexation—Some thoughts and observations. Phytochemistry, 27(8), 2397–2409. https://doi.org/https://doi.org/10.1016/0031-9422(88)87004-3
Swanson, B. G. (1990). Pea and lentil protein extraction and functionality. Journal of the American Oil Chemists' Society, 67(5), 276–280. https://doi.org/https://doi.org/10.1007/BF02539676
Tro, N. J., Fridgen, T. D., & Shaw, L. (2014). *Chemistry: A molecular approach*. Toronto, Pearson Canada.
Van Teeling, C. G., Cansfield, P. E., & Gallop, R. A. (1971). An anthocyanin complex isolated from the syrup of canned blueberries. Journal of Food Science, 36, 1061–1063. https://doi.org/https://doi.org/10.1111/j.1365-2621.1971.tb03346.x, 7
Worley, J. D. (1992). Capillary radius and surface tensions. Using calculations based on Tate's law. *Journal of Chemical Education*, *69*(8), 678.
Xie, L., Lee, S. G., Vance, T. M., Wang, Y., Kim, B., Lee, J.-Y., Chun, O. K., & Bolling, B. W. (2016). Bioavailability of anthocyanins and colonic polyphenol metabolites following consumption of aronia berry extract. Food Chemistry, 211, 860–868. https://doi.org/https://doi.org/10.1016/j.foodchem.2016.05.122
Xie, L., Vance, T., Kim, B., Lee, S. G., Caceres, C., Wang, Y., Hubert, P. A., Lee, J.-Y., Chun, O. K., & Bolling, B. W. (2017). Aronia berry polyphenol consumption reduces plasma total and low-density lipoprotein cholesterol in former smokers without lowering biomarkers of inflammation and oxidative stress: A randomized controlled trial. Nutrition Research, 37, 67–77. https://doi.org/https://doi.org/10.1016/j.nutres.2016.12.007
Xue, F., Li, C., & Adhikari, B. (2020). Physicochemical properties of soy protein isolates-cyanidin-3-galactoside conjugates produced using free radicals induced by ultrasound. Ultrasonics Sonochemistry, 64, 104990. https://doi.org/https://doi.org/10.1016/j.ultsonch.2020.104990
Zayas, J. F. (1997). Functionality of proteins in food. Springer Berlin Heidelberg, Springer-Verlag. https://doi.org/10.1007/978-3-642-59116-7
Zhao, C., Liu, Y., Lai, S., Cao, H., Guan, Y., San Cheang, W., Liu, B., Zhao, K., Miao, S., Riviere, C., Capanoglu, E., & Xiao, J. (2019). Effects of domestic cooking process on the chemical and biological properties of dietary phytochemicals. Trends in Food Science & Technology, 85, 55–66. https://doi.org/https://doi.org/10.1016/j.tifs.2019.01.004

Publisher's Note

Springer Nature remains neutral with regard to jurisdictional claims in published maps and institutional affiliations.

Ready to submit your research? Choose BMC and benefit from:

- fast, convenient online submission
- thorough peer review by experienced researchers in your field
- rapid publication on acceptance
- support for research data, including large and complex data types
- gold Open Access which fosters wider collaboration and increased citations
- maximum visibility for your research: over 100M website views per year

At BMC, research is always in progress.

Learn more biomedcentral.com/submissions

BMC

Journal of Food Engineering 317 (2022) 110847

Contents lists available at ScienceDirect

Journal of Food Engineering

journal homepage: www.elsevier.com/locate/jfoodeng

Formation of dry beads for bioactives encapsulation by freeze granulation

Mackenzie M. Hansen [a,b,*], Richard W. Hartel [b], Yrjö H. Roos [a]

[a] Food Technology, School of Food and Nutritional Sciences, University College Cork, Ireland
[b] Department of Food Science, College of Agricultural and Life Sciences, University of Wisconsin-Madison, USA

ARTICLE INFO

Keywords:
Freeze granulation
Beads
Whey protein
Sugars
Encapsulation

ABSTRACT

Solid beads formed by whey protein isolate (WPI) and various sugars/polyols with a wide range of glass transition temperatures showed potential as structures for encapsulation of Aronia berry bioactives. Whey protein isolate (WPI), Aronia extract, and carbohydrates (maltitol, sucrose, or trehalose) were mixed into water to form concentrated liquid feed dispersions with varied pH. Microstructures were imaged and physical properties including complex viscosities, surface tensions, particle size distributions, and centrifuge separation were measured to investigate the effects of carbohydrate type, WPI:sugar ratio, and Aronia polyphenols (PP) concentration on liquid properties. Feed dispersions were used to produce dry beads with an adapted freeze granulation method, where individual drops were pumped into liquid nitrogen for flash freezing and harvested for subsequent freeze-drying to remove water. Dry bead diameters, water contents, and water activities were measured prior to measuring hardness and glass transition temperatures. While formulating with different sugars did not meaningfully impact liquid feed characteristics that impact processing, compositional differences were found to influence characteristics of the final dried beads more notably.

1. Introduction

Proteins and sugars are popular macromolecules often used in combination when developing food products. Both components possess desirable functional properties and impart nutritional value onto formulated products. Their respective functional properties may be utilized to form structures that encapsulate and protect sensitive natural bioactives for delivery, such as polyphenols (PP) derived from fruits and vegetables, addressing the increased consumer demand for health foods (Hansen et al., 2021a, b; Schneider, 2016). Correspondingly, consumer attitudes towards sugar have shifted as their role in dental health and chronic disease has come into question, creating demand for 'better for you' food products formulated with lower calorie sweeteners or even sugar-free formulations. Polyols such as sorbitol, xylitol, and maltitol are alternatives used by industry to replace sugars, providing benefits including a lack of insulin response, caloric reduction, and non-cariogenic properties (Hartel et al., 2018; Rice et al., 2020).

Formulating with different sugars/polyols can result in products with a wide variety of characteristics such as texture, appearance, and flavor retention, depending on differences in carbohydrate properties such as their glass transition temperatures (T_g) under selected conditions. Glass transition (T_g) occurs when the molecular mobility within an amorphous material is slowed so significantly that the matter changes from a more flexible, rubbery state to a hard, glassy state. In general, stability of glasses is enhanced greatly when T_g is higher than ambient temperature (Hartel et al., 2018; Kawai and Suzuki, 2007; Roos and Drusch, 2015; White and Cakebread, 1966), where diffusion-based modes of deterioration may be slowed, and degradation mechanisms may be better controlled (Ergun et al., 2010; Roos, 2020). Stability of glassy products is related to T_g, which is determined by formulation components as well as water content (Ergun et al., 2010). Products formulated with components with higher T_g would be expected to have greater storage stability under ambient conditions than products formulated with lower T_g components, potentially serving as better protectants for bioactives during storage (Roos, 2010).

In earlier experiments, we developed a continuous process that formed dry, stable beads from concentrated mixed dispersions of whey protein isolate (WPI) and sucrose (Hansen et al., 2020). The structure forming method presented initially involved the exposure of feed dispersions to moderate heat conditions (100 °C) for a short time by dispensing feeds dropwise into a heated oil bath to promote solid structure formation via gelation. We adapted the original drop formation process to no longer require heating, protein gelation, or oven drying to form dry, stable beads. Instead, we utilized the same method

* Corresponding author. Hartel Laboratory A11, Babcock Hall, 1605 Linden Drive, Madison, WI, 53706, USA.
E-mail address: 116220787@umail.ucc.ie (M.M. Hansen).

https://doi.org/10.1016/j.jfoodeng.2021.110847
Received 11 August 2021; Received in revised form 6 October 2021; Accepted 16 October 2021
Available online 20 October 2021
0260-8774/© 2021 Published by Elsevier Ltd.

for pumping concentrated liquid dispersions dropwise into a bath of liquid nitrogen (LN_2) to instantly solidify beads that were subsequently transferred to a freeze-dryer to remove water. This method resembles the freeze granulation technology employed in clay/ceramic materials and pharmaceuticals, where droplets of liquid suspensions are sprayed into LN_2 and then freeze-dried (Bhatta et al., 2020; La Lumia et al., 2019; Ouadaker et al., 2020; Shanmugam, 2015).

Protein-sugar mixtures can be used for encapsulation, and the properties of structures formed can be manipulated with compositional alterations. The potential for freeze granulation processes to produce protein-sugar structures that may be used for encapsulation, however, has not yet been investigated. Therefore, the aim of this experiment was to explore the effects of sugar/polyol type (with a wide range of known T_g) and WPI-sugar ratios on the physical properties of liquid dispersions and resulting dry beads formed by a modified freeze granulation process, both with and without Aronia extract. We hypothesize that replacement of sucrose with other glass formers (maltitol and trehalose) is unlikely to give rise to significant changes in the physical properties of liquid dispersions that affect processing and pumping such as viscosity, flow behavior, or particle size distributions, as the sugars are all similar in molecular size and sugars are not particularly surface-active molecules (Hartel et al., 2018). Properties of the dry beads formed by the modified drop formation method presented, such as T_g onset and hardness, would be expected to change with the use of different sugars, as related to their respective T_g and water contents (Roos and Drusch, 2015). It would be expected that beads formulated with sugars/polyols with higher T_g in higher quantities would have higher bead T_g and corresponding hardness values than those formulated with lower T_g carbohydrates, demonstrating their greater physical stability and potential protective abilities imparted on the Aronia PP by the molecular freezing and glass formation by sugars (Sosa et al., 2011).

This work builds on previous experiments characterizing the physicochemical effects of Aronia extract in liquid dispersions (Hansen et al., 2021a) and the consequences of varying protein sources on protein-PP interactions (Hansen et al., 2021b), expanding the investigation to characterize the effects on the physical properties of dry beads formed from the liquid mixtures. We examined the effects of sugar/polyol type and WPI-sugar ratio on the physical properties of beads formed, which may indicate the potential of the matrices to protect PP during storage. To our knowledge, the method of freeze granulation employed has not yet been attempted in food matrix applications which makes this a novel study. We present a successful adaptation of this technology, utilized in other materials science and pharmaceutical applications, applied to food materials to form structures.

2. Materials and methods

2.1. Materials

WPI (IsoChill 9000), was supplied by Agropur, Inc. (Luxemburg, Wisconsin, USA) with approximately 4.6% water, 91.6% protein (dry basis), 0.7% fat, and 3.1% ash. Sucrose (pure cane, extra fine, granulated sugar) was supplied by Domino Foods, Inc. (Yonkers, New York, USA). Maltitol (Maltisweet ® CM9820 Crystalline Maltitol 263,051) was supplied by Ingredion (Westchester, IL, USA). Trehalose (Treha TM) was supplied by Hayashibara Co., LTD. (NAGASE Group, Okayama, Japan). Standardized Aronia berry (Chokeberry) Powder, with a minimum level of 15% anthocyanins, was supplied by Artemis International (Fort Wayne, Indiana, USA) and stored at −18 °C in the absence of light. Deionized (D.I.) water was used in all formulations.

2.2. Dispersion preparation

Dispersion preparation was performed as described in previous studies (Hansen et al., 2021a, b). Dry blends of WPI and sugars/polyols were mixed into D.I. water, followed by the addition of Aronia extract solution (when appropriate) to constitute final mixtures. pH was measured with a FiveEasy Plus pH/mV meter with InLab® Viscous Pro-ISM probe (Mettler Toledo, Hampton, Schwerzenbach, Switzerland) after electrode calibration.

Triplicates of twenty-four formulations with different compositions were prepared for triplicate analysis in a 4 × 3 × 2 factorial design, with experiments conducted randomly (Table 1). Ratios of WPI to sugar, Aronia extract/PP concentrations, and % total solids were selected based on findings from our previous work (Hansen et al., 2020, 2021a, b). After preparation, dispersions were left to defoam at room temperature for 1 h minimum prior to analyses.

2.3. Feed characterization

2.3.1. Flow testing

Flow testing was performed in triplicate as described in previous studies (Hansen et al., 2020, 2021a, b), by pumping dispersions through a benchtop peristaltic pump (120 S/DV, Watson Marlow, Falmouth, England; silicon tubing 85 cm length, 2 mm bore, 1 mm wall, BÜCHI Labortechnik AG, Flawil, Switzerland) at a constant speed of 13 RPM. Measurements obtained included individual drop masses, the number of drops deposited per 1 min, the time required to deposit 10 mL of dispersions, and the mass of 10 mL of dispersions; these data were used to calculate drop diameters, volumes, and surface tensions, as well as densities of dispersions and mass and volume flow rates (Hansen et al., 2020, 2021a, b).

2.3.2. Viscosity

Methods described in previous studies (Hansen et al., 2021a, b) were adapted to measure the complex viscosities of dispersions in triplicate with a DHR-2 rheometer (TA Instruments, Delaware, USA) using small-strain oscillatory measurements. Samples were oscillated under 4% strain and 1Hz frequency; strain sweeps determined that 4% strain was within their linear viscoelastic region (LVR; not shown).

2.3.3. Particle size distribution

A Malvern Mastersizer 2000 (Malvern Instruments Ltd., Worcestershire, U.K.) with Hydro 2000S liquid sampler was utilized for triplicate particle size distribution measurements of dispersions, as described in previous work (Hansen et al., 2021a, b). Dispersions formulated without WPI were unable to reach the desired obscuration range (11–15%), as the program was designed with WPI particles in mind. As such, those transparent dispersions were unable to be measured as the sugars dissolved in the water and did not yield detectable particles. Dispersions formulated without WPI but with Aronia extract showed particle size distributions that were different from feeds containing protein, despite the program design intended for WPI particle detection; as such, volume-weighted mean ($d_{4,3}$) values were not taken from these distributions for comparison as the program was not designed for particle detection of Aronia extracts.

2.3.4. Optical light microscopy

A Nikon Eclipse FN1 optical microscope (Nikon Instruments Inc., Melville, NY, USA) with a Nikon Digital Sight DS-U3 camera control unit attached (ver. 1) was used to observe diluted dispersions at 40× and 200× magnification, as described in previous studies (Hansen et al., 2021a, b).

2.3.5. Centrifuge separation

Similar to the centrifugation methods described in previous experiments (Hansen et al., 2021a, b), 1.25 g of selected undiluted and 10-times diluted dispersions were pipetted into tubes (1.5 mL graduated tubes with flat caps, Fisherbrand ®, Fisher Scientific, Hampton, New Hampshire, USA), spun at 13,523×*g* and 20 °C for 20 min in a microcentrifuge (Centrifuge 5424 R with FA-45-24-11 rotor, Eppendorf, Hamburg, Germany), and observed after centrifugation.

Table 1
Formulations, pH, and estimated drop diameters (mm) calculated from flow tests data for liquid dispersions with varied WPI:sugar ratios, sugar types, and polyphenols concentrations, as well as water activity (a_w), water content (%), T_g midpoint, and measured diameters of dried drops formed from dispersions.

WPI:sugar	Sugar	[PP]	pH	Water activity	Water content	Diameter (calculated)	Diameter (dry)	T_g (midpoint)
–	–	%	–	–	%	mm	mm	°C
0	Maltitol	0	5.80	n/a	n/a	5.01 ± 0.02	n/a	n/a
0.75	Maltitol	0	5.91	0.037 ± 0.017	1.13 ± 0.17	4.62 ± 0.06	4.13 ± 0.06[a]	41 ± 3
1	Maltitol	0	5.93	0.036 ± 0.008	1.26 ± 0.22	4.62 ± 0.05	4.17 ± 0.11[a]	44 ± 3
1.25	Maltitol	0	5.88	0.027 ± 0.001	0.93 ± 0.29	4.62 ± 0.03	4.10 ± 0.08[a]	46 ± 4
0	Maltitol	1	3.48	n/a	n/a	4.96 ± 0.04	n/a	n/a
0.75	Maltitol	1	5.40	0.036 ± 0.010	1.02 ± 0.17	4.69 ± 0.02	4.20 ± 0.09[a]	42 ± 2
1	Maltitol	1	5.35	0.029 ± 0.004	1.50 ± 0.20	4.61 ± 0.06	4.22 ± 0.08[a]	50 ± 4
1.25	Maltitol	1	5.55	0.027 ± 0.001	1.38 ± 0.25	4.68 ± 0.04	4.19 ± 0.12[a]	50 ± 4
0	Sucrose	0	6.02	0.135 ± 0.015	2.68 ± 0.41	5.02 ± 0.03	4.36 ± 0.13[a]	48 ± 2
0.75	Sucrose	0	5.88	0.027 ± 0.001	1.17 ± 0.25	4.64 ± 0.04	4.11 ± 0.07[a]	57 ± 4
1	Sucrose	0	5.87	0.027 ± 0.001	1.01 ± 0.12	4.62 ± 0.05	4.11 ± 0.09[a]	62 ± 3
1.25	Sucrose	0	5.85	0.027 ± 0.001	0.98 ± 0.34	4.63 ± 0.05	4.09 ± 0.09[a]	61 ± 2
0	Sucrose	1	3.54	0.146 ± 0.037	1.37 ± 0.42	4.97 ± 0.05	4.39 ± 0.06[a]	47 ± 2
0.75	Sucrose	1	5.43	0.027 ± 0.001	1.27 ± 0.30	4.68 ± 0.04	4.14 ± 0.16[a]	60 ± 2
1	Sucrose	1	5.44	0.029 ± 0.003	0.99 ± 0.24	4.69 ± 0.03	4.16 ± 0.14[a]	58 ± 2
1.25	Sucrose	1	5.45	0.030 ± 0.004	1.16 ± 0.27	4.65 ± 0.05	4.16 ± 0.10[a]	61 ± 2
0	Trehalose	0	6.50	0.046 ± 0.009	2.47 ± 0.60	5.01 ± 0.03	4.33 ± 0.17[a]	78 ± 2
0.75	Trehalose	0	5.85	0.027 ± 0.001	0.80 ± 0.20	4.61 ± 0.05	4.13 ± 0.07[a]	125 ± 8
1	Trehalose	0	5.85	0.027 ± 0.001	0.50 ± 0.15	4.60 ± 0.04	4.13 ± 0.07[a]	127 ± 3
1.25	Trehalose	0	5.89	0.027 ± 0.001	1.12 ± 0.30	4.61 ± 0.03	4.06 ± 0.15[a]	133 ± 4
0	Trehalose	1	3.37	0.030 ± 0.004	1.03 ± 0.37	4.95 ± 0.04	4.25 ± 0.06[a]	79 ± 7
0.75	Trehalose	1	5.48	0.028 ± 0.001	0.82 ± 0.28	4.67 ± 0.04	4.15 ± 0.10[a]	125 ± 2
1	Trehalose	1	5.53	0.029 ± 0.003	0.99 ± 0.45	4.66 ± 0.03	4.18 ± 0.12[a]	131 ± 4
1.25	Trehalose	1	5.36	0.028 ± 0.001	0.73 ± 0.27	4.62 ± 0.07	4.13 ± 0.10[a]	126 ± 5

[a] Indicates significant differences between calculated and measured diameter values.

2.4. Solid drop preparation-freeze granulation process adaptation

As the first step in solid bead formation, feeds were dropped into liquid nitrogen (100% purity; Airgas, Madison, WI, USA) and frozen, as explained in earlier experiments (Hansen et al., 2021a, b). Drops were left to harden in the LN_2 for ~5 min, and pans were transferred to a VirTis SP Scientific Genesis 25 EL Pilot freeze-dryer with Wizard 2.0 control (SP Industries, Warminster, PA, USA), onto shelves pre-cooled to −40 °C with a condenser temperature below −80 °C. A vacuum was applied and beads were held at the −40 °C shelf temperature for 4 h, then the shelf temperature was increased to −10 °C and beads were left to dry for 17 h with chamber pressures <0.007 mbar. The adapted freeze granulation process for bead formation is depicted in Fig. 1. Beads were removed from trays after drying and placed into moisture-proof pouches for storage prior to analyses (black matte double-sided, zip-lock, lined with aluminum foil, 8.4 × 13 cm, QQ Studio, New York, NY, USA). Fig. 2 provides a visual representation of the cross-sectional structure of freeze-dried beads comprised of glassy sweeteners, glassy and unhydrated protein particles, and protein-PP complexed aggregates.

2.5. Dried bead characterization

2.5.1. Dried bead diameters

Diameters of freeze-dried beads were measured 3 times per formulation replicate (n = 9) with digital Vernier calipers (0–150 mm; Stainless Hard) on the day they were removed from the freeze-dryer (Day '0'), as described in previous studies (Hansen et al., 2021a, b).

2.5.2. Water activity (a_w)

a_w of beads was measured on the day they were removed from the

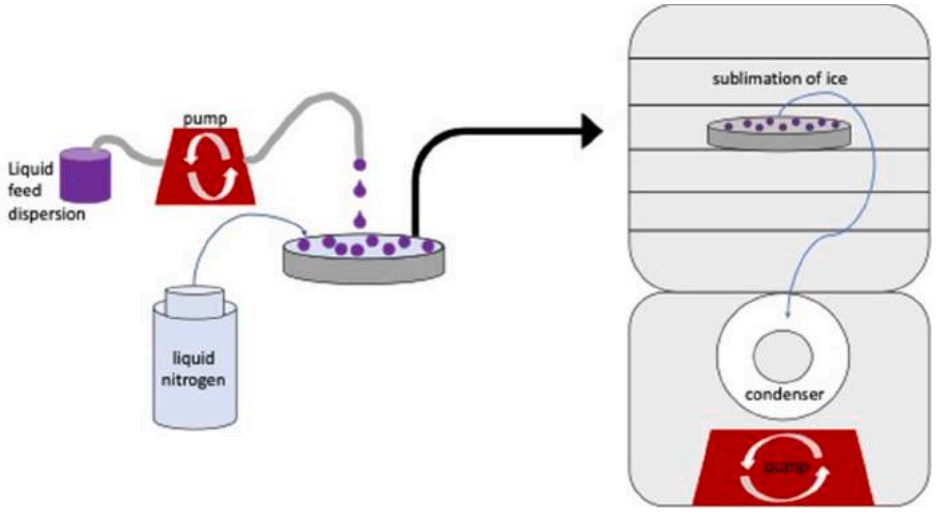


Fig. 1. Modified freeze granulation process adapted to produce dry beads from concentrated liquid feed dispersions with varied WPI:sugar ratios, sugar types, polyphenols concentrations, and pH. *COLOR REQUIRED*. (For interpretation of the references to color in this figure legend, the reader is referred to the Web version of this article.)

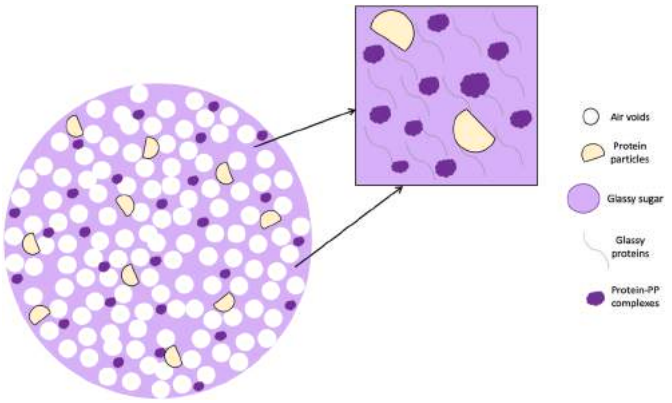


Fig. 2. Schematic drawing of the cross-sectional structure of dry beads containing WPI, sugars, and Aronia extract after freeze drying; Inset: the proposed structure of the continuous glassy phase (not to scale). *COLOR REQUIRED*. (For interpretation of the references to color in this figure legend, the reader is referred to the Web version of this article.)

freeze-dryer (Day '0') with a water activity meter (Aqua Lab model Series 3, version 5, Decagon Devices, Inc., Pullman, WA, USA) at ~22 °C after meter calibration with D.I. water. Approximately 0.5 g of sample was placed in plastic sample cups (Meter disposable sample containers and lids) for measurement.

2.5.3. Water content

Water content of beads was measured gravimetrically on the day they were removed from the freeze-dryer (Day '0'), modifying methods used by Fitzpatrick et al. (2004) and Schuck et al. (2005). Approximately 0.5 g of beads (triplicate measurements per replicate, n = 9) were placed into pre-weighed aluminum pans, and masses were recorded before oven drying at 105 °C for 5 h (Lindberg/Blue M mechanical oven, model MO1490A-1, 120 V, 50/60 HZ, temperature range 40–260 °C, Asheville, NC, USA). Aluminum pans and lids were pre-dried at 105 °C prior to filling with beads. Masses were recorded again after drying, once the pans cooled to room temperature while covered to prevent water uptake; differences in masses due to water loss were determined, as well as the total solids remaining in dry beads.

2.5.4. Thermal analysis - differential scanning calorimetry (DSC)

The glass transition (T_g) onset temperatures of freeze-dried beads were determined using a DSC 8500 with an Intracooler 2 Cooling Accessory (PerkinElmer, Waltham, MA, USA), between 1 and 3 days after removal from the freeze-dryer (replicates of the same formulation were always tested on the same day after freeze-drying). Beads were pressed into condensed tablet form, fractured for transfer of into pre-weighed aluminum DSC pans (50 μL, PerkinElmer Health Sciences Inc., Shelton, CT, USA), and hermetically sealed. An empty pan was used as a reference. Calibration of the DSC was performed with Indium.

To observe T_g of dried beads, samples were scanned according to the sugar used in formulation: beads comprised of maltitol were cooled from 20 °C to 0 °C with a −10 °C/min cooling rate, then heated from 0 °C to 70 °C with a heating rate of 10 °C/min; those made from sucrose were cooled identically, but heated from 0 °C to 90 °C; beads made with trehalose were scanned from 40 °C to 160 °C. These methods were then repeated-the first scan to eliminate any T_g overshoot information caused by enthalpy relaxation of sugars during aging, and the second scan to gather T_g data (Hartel et al., 2011). Onset and midpoint temperatures (half C_p extrapolated) of glass transition events were calculated by the Pyris 11.0 software from the heat flow curve of the final heating step.

2.5.5. Hardness

Sample preparation – Beads were individually placed onto double-sided tape adhered to the platform, fixed aligned with the center of the platen. All replicates were analyzed in triplicate (9 hardness values per formulation) and average values were reported.

Texture analysis - Beads were tested for hardness with TA.XTplus Texture Analyser (Texture Technologies Corp., Scarsdale, New York, USA), between 1 and 3 days after removal from the freeze-dryer (replicates of the same formulation were always tested on the same day after freeze-drying). A 25 mm cylindrical, resin platen was utilized to compress beads 1 mm once contact was made with the individual bead exceeding a trigger force of 2g, at a speed of 1 mm/s. Peak positive compression force was measured and recorded in the Exponent software (Stable Micro Systems, Version 6,1,16,0) for reporting sample hardness.

2.6. Statistical analysis

Triplicate experiments were analyzed in triplicate (n = 9), and data collected were used to calculate mean values and standard deviations. Analysis of variance (2 and 3-way ANOVA; Tukey's HSD test) and independent measures t-tests (equal variance not assumed) were performed when appropriate to compare mean values using JMP® Pro version 15.0.0 (SAS Institute Inc., Cary, North Carolina, USA). The level of significance was determined at $p < 0.05$.

3. Results and discussion

3.1. Feed characterization

3.1.1. pH

As pH can impact intermolecular interactions between proteins in dispersions and measurements of their associated physical properties, monitoring pH values in dispersions with varying compositions is important (Hansen et al., 2021a, b). All formulations with the same WPI: sugar compositions containing Aronia extract had significantly ($p < 0.05$) lower pH than those without. Similar to observations from earlier experiments, pH of dispersions containing WPI decreased slightly with PP (Table 1), but were unlikely to cause significant changes to the properties of dispersions, since pH did not closely approach the known isoelectric points (pI) reported for constituent β-lactoglobulin (pH ~5.2–5.3) and α-lactalbumin (pH ~4.2–4.8) protein fractions in WPI (Hansen et al., 2021a, b). Dispersions containing only sugars lacked the benefit of pH buffering in the systems that occurs when proteins are present, thus experiencing greater reductions in pH when PP were added.

3.1.2. Surface tension

The surface tension of a liquid strongly influences the size of drops formed once the surface tension forces acting around the circumference of the outlet are exceeded by the gravitational forces acting on the drop (Hansen et al., 2021a, b). According to the ANOVA, the ratio of WPI to sugar had a significant effect ($p < 0.05$) on the surface tension of dispersions. Tukey's HSD tests provided clarity, reporting that dispersions without WPI ('0' ratios) had significantly ($p < 0.05$) higher surface tensions than those containing WPI, but once WPI was present, surface tension remained effectively unchanged upon increasing the WPI to sugar ratio, regardless of other formulation components (Fig. 3a). Surface tensions of feeds with 1.0 WPI:sugar ratios were not significantly different ($p > 0.05$) from the 0.75 or 1.25 ratios, similar to findings reported in previous work (Hansen et al., 2021a). Sugars and other sweeteners are not thought to affect surface tension notably, as they are typically not very surface-active molecules. The differences in whey proteins, known to behave as surfactants, were not sufficient to impact surface tension in these systems as WPI:sugar ratios shifted, indicating that the slight shifts in composition at 25% total solids were not strong enough for detection.

The presence of Aronia PP in dispersions at 1% concentration was not found to have a significant ($p > 0.05$) effect on surface tension compared to feeds formulated without PP, according to the ANOVA and

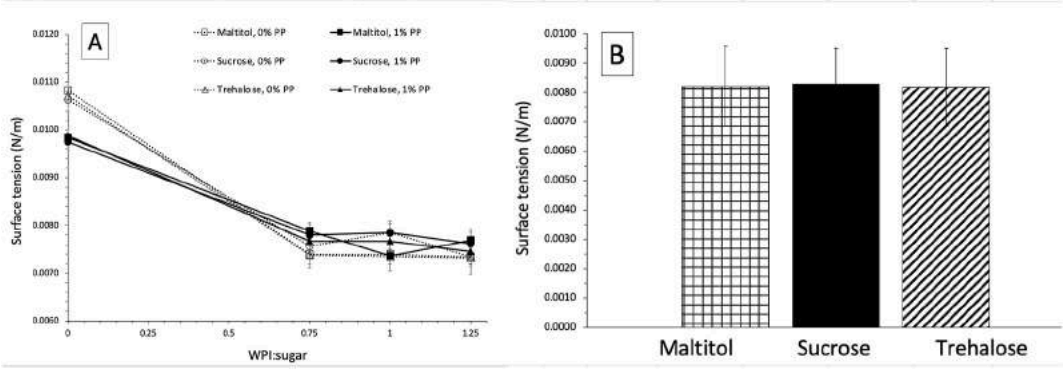


Fig. 3. Effect of WPI:sugar ratio [**A**] on the surface tensions (N/m) of dispersions at 25 °C; the effect of sugar type [**B**] on the average surface tensions of all dispersions comprised of maltitol, sucrose, and trehalose, respectively, at 25 °C; (n = 9). Open markers with dotted lines- 0% PP, filled markers with solid lines- 1% PP [**A**]; lines are for guiding purposes only [**A**].

Student's t-tests applied. In formulations containing WPI, no differences in surface tension were observed between samples with 0% and 1% PP, generally in agreement with findings from previous experiments where increasing PP contents in feeds containing protein resulted in increased surface tensions under some conditions, but many showed no meaningful trends (Hansen et al., 2021a, b). In feeds without WPI, surface tension decreased notably with 1% PP compared to those without PP, as demonstrated in Fig. 3a for the '0' WPI:sugar ratio. The Aronia extract utilized in this experiment was primarily comprised of small molecular mass polyphenolic compounds; technical data sheets provided by the manufacturer specified that the extract contained maximum fiber and protein contents of 1.3 and 2.3%, respectively. The reduced surface tensions of sugar solutions with PP may be a result of slight surfactant behavior of the minor biopolymer components in the extract, acting in a similar manner to WPI in dispersions, but to a lesser extent due to lesser concentrations (Chan et al., 2009; Lee and Chan, 2013).

Formulations containing sucrose, maltitol, or trehalose did not have a significant effect ($p > 0.05$) on surface tensions of feed dispersions, according to the ANOVA and corresponding Tukey's HSD tests. These findings are depicted in Fig. 3b, where the average surface tensions of all formulations containing each respective sugar may be compared. This finding supports our hypothesis, that no major changes would be expected to result from sugars in formulations, as all three sugars/polyols were of corresponding molecular size (Hartel et al., 2018).

As previous studies reported that drop diameters and surface tensions were directly related (Chan et al., 2009; Lee and Chan, 2013), calculated surface tensions were plotted against calculated diameters of drops formed by the same dispersions, and a best fit line was applied (Fig. 4). In agreement with previous reports (Hansen et al., 2021a, b), the plots indicated a positive, strong, direct correlation ($R^2 = 0.98$). The few points in the plot with high surface tensions/drop diameters represent the sweetener solutions formulated with 0 and 1% PP that had very high surface tension values relative to feed formulations containing WPI, which reduced surface tensions.

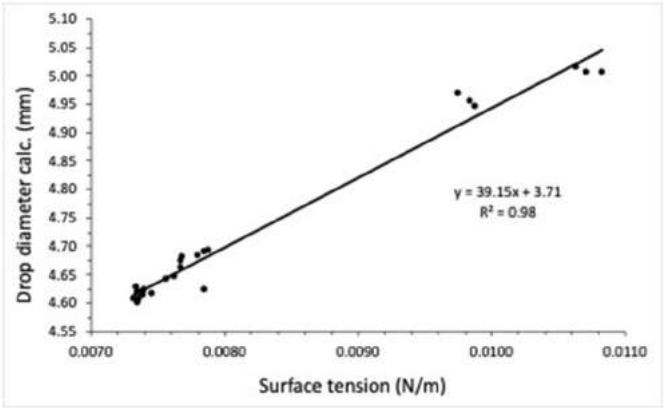


Fig. 4. The relationship between the surface tensions (N/m) of feed dispersions containing WPI:sugar ratios of 0, 0.75, 1.0, and 1.25, sugars including maltitol, sucrose, and trehalose, and polyphenols contents of 0 and 1%, at 25 °C and calculated diameters (mm) of drops.

3.1.3. Viscosity

Minor changes in the composition of dispersions can result in shifts in viscosity, which is a critical factor in determining conditions for processing (Hansen et al., 2021a, b). According to the ANOVA, changing the ratio of WPI to sugar had a significant ($p < 0.05$) effect on viscosity; as the WPI:sugar ratio increased (thus increasing total protein content in dispersions), viscosity was observed to increase as well. Tukey's HSD tests clarified the report, indicating that the only significant difference ($p < 0.05$) was between feeds formulated without WPI ("0" WPI:sugar ratios) and those containing WPI. Feeds formulated without WPI had significantly lower ($p < 0.05$) viscosities than those formulated with WPI, and once WPI was present, slight increasing trends were generally observed as WPI:sucrose ratio increased, though differences were not significant ($p > 0.05$), and some variation was observed (Fig. 5a). Given the common 25% total solids contents in feeds, alterations to compositions were too slight to have strong effects on system viscosities. In previous work, the ANOVA indicated that complex viscosity significantly increased ($p < 0.05$) with increasing ratios of WPI to sucrose (and thus total protein content) in feed dispersions (Hansen et al., 2021a). The effect of increasing the WPI:sucrose ratio was thought to be relatively weak compared to that of % total solids, as lower (25 and 35) % total solids formulations did not clearly demonstrate the trends reported by the ANOVA as consistently as the 45% total solids feeds.

The presence of Aronia PP in feeds at 1% was found to have a significant effect ($p < 0.05$) on viscosity, compared to feeds formulated without PP, according to the ANOVA and Student's t-tests applied. Feed dispersions containing 1% PP had significantly higher ($p < 0.05$) viscosities than those with 0% PP, correlating with the reduced pH values in systems containing PP. Reducing pH closer to pI would result in greater intermolecular interactions in the system as repulsions are reduced between proteins and protein-PP complexation is more likely to occur. Enhanced system intermolecular interactions would result in increased viscosities and behavioral complexities of the fluids. With the exception of a few minor variations, Fig. 5a displays that feeds containing 1% PP (solid lines and filled markers) tended to have higher viscosities than those with 0% PP (dotted lines and unfilled markers). These results build upon those from our previous work suggesting a weak effect of PP on viscosity, providing further evidence that increasing PP content in feeds results in increased viscosities, even as %

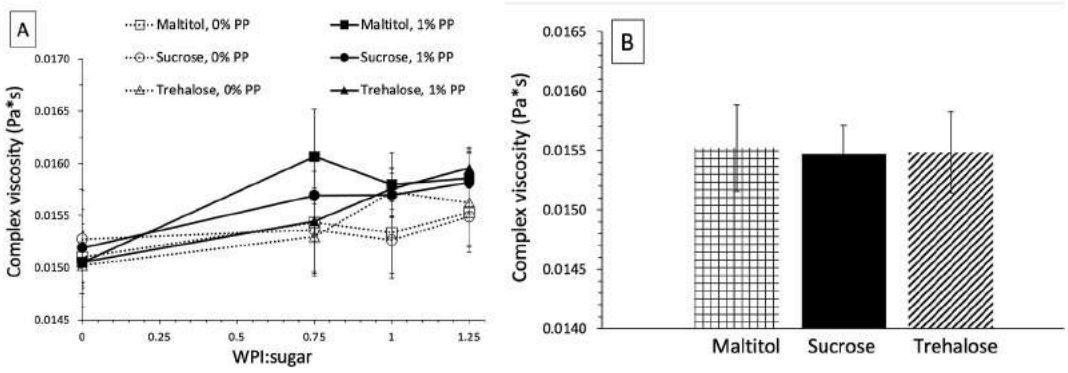


Fig. 5. Effect of WPI:sugar ratio [**A**] on the complex viscosities (Pa*s) of dispersions at 25 °C; the effect of sugar type [**B**] on the average complex viscosities of all dispersions comprised of maltitol, sucrose, and trehalose, respectively, at 25 °C; (n = 9). Open markers with dotted lines- 0% PP, filled markers with solid lines- 1% PP [**A**]; lines are for guiding purposes only [**A**].

total solids in the system remains constant (Hansen et al., 2021a).

Changing the sugar/polyol in formulations between sucrose, maltitol, and trehalose did not have a significant effect ($p > 0.05$) on viscosities of feed dispersions, according to the ANOVA and Tukey's HSD test reports. These findings are depicted in Fig. 5b, where the average viscosities of all formulations containing each respective sugar may be compared. This finding builds on the surface tension results in support of our hypothesis, that no major changes would be expected to occur with changes in sugars in formulations, as all three sugars/polyols are of similar molecular sizes and thus would be expected to have similar effects on solution or syrup viscosities (Hartel et al., 2018).

3.1.4. Particle size

Particle size measurement is a useful tool for examining the physical effects of altered compositions and other conditions within dispersions, which are known to affect the interactions between proteins and other components (Hansen et al., 2021a, b). Feeds containing WPI had normal distributions and PP addition affected distributions by shifting their peaks towards smaller particle sizes, as seen in Fig. 6 for dispersions with sucrose (all sugars/polyols followed the same trend). Schneider (2016) also reported relatively normal particle size distributions for weakly acidic dispersions of juices with lower phenolics concentrations mixed with WPI to form complexes, reporting similar average particle size values as well.

Altered ratios of WPI to sugar in dispersions did not significantly ($p > 0.05$) affect particle size distributions, according to the ANOVA (Fig. 7a). No significant differences in average particle size were observed between dispersions prepared at the three different WPI-sugar ratios ($p > 0.05$) according to the Tukey's HSD tests, with all formulations displaying approximately normal distributions. These results support and build upon findings from earlier work, indicating that varying levels of sugars in the systems did not influence aggregate sizes, potentially due to their easy dissolution into water (Hansen et al., 2021a).

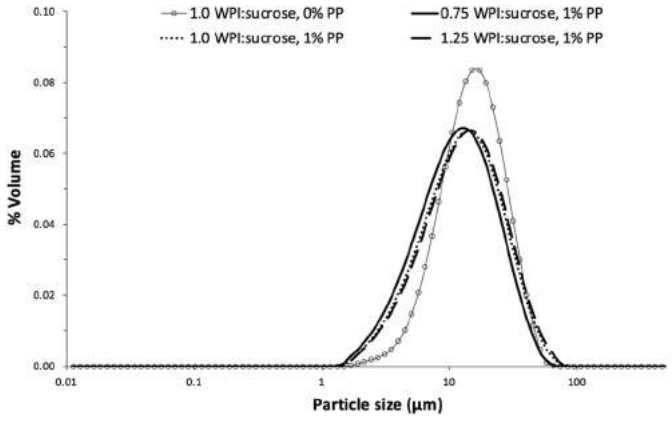


Fig. 6. Particle size distributions of feed dispersions comprised of 1.0 WPI: sucrose ratios with 0% and 1% PP, and 0.75 and 1.25 WPI:sucrose ratios with 1% PP at 25 °C; (n = 9).

The presence of Aronia PP in feeds at 1% was found to have a significant effect ($p < 0.05$) on the average particle sizes of dispersions, according to the ANOVA and Student's t-tests applied to the data. Feed dispersions containing 1% PP had significantly smaller ($p < 0.05$) average particle sizes than those with 0% PP, with average values of 14.84 and 16.31 μm, respectively. This is also demonstrated in Fig. 7a, which shows all formulations containing 1% PP (solid lines and filled markers) have lower average particle sizes than feeds formulated with 0% PP (dotted lines and unfilled markers), regardless of sugar/polyol type and WPI-sugar ratios. These results are in agreement with findings from previous studies, where particle sizes were found to decrease upon PP addition (Hansen et al., 2021b; Siebert et al., 1996; Thongkaew et al., 2014; Xue et al., 2020).

The ANOVA and Tukey's HSD tests reported that average particle size values for maltitol and sucrose formulations were slightly but significantly different from one another ($p < 0.05$), but neither value was significantly different from that for trehalose formulations. The average particle sizes of all formulations comprised of each respective sugar/polyol are plotted in Fig. 7b, where differences determined to be significant in the statistical analysis appear to be negligible once error bars are applied to the data for comparison. In theory, variations in dispersion particle size distributions could impact viscosity, but because the differences detected were so small, they did not impact dispersion viscosities (Fig. 5b).

In line with previous experiments (Hansen et al., 2021a, b), microscopy generally supported laser diffraction particle size data. Microscopy visually confirmed the lack of changes in particle size observed with altered sugar types in dispersions (data not shown), as well as the reduced particle sizes observed with 1% PP in dispersions (Fig. 8). The insoluble protein particles remaining in dispersions without PP were larger than the protein-PP complexes formed in dispersions containing Aronia, thus resulting in reduced average particle sizes, similar to the findings for pea protein isolate dispersions with and without PP in earlier work (Hansen et al., 2021b).

3.1.5. Centrifuge separation

Precipitate pellets formed after dispersions containing WPI were centrifuged, mirroring observations from earlier experiments involving other protein-sucrose dispersions (Hansen et al., 2021a, b). Pure sugar solutions did not form pellets upon centrifugation, indicating their complete dissolution in water. As described in previous studies, the pellets formed by WPI-containing dispersions with Aronia were dark

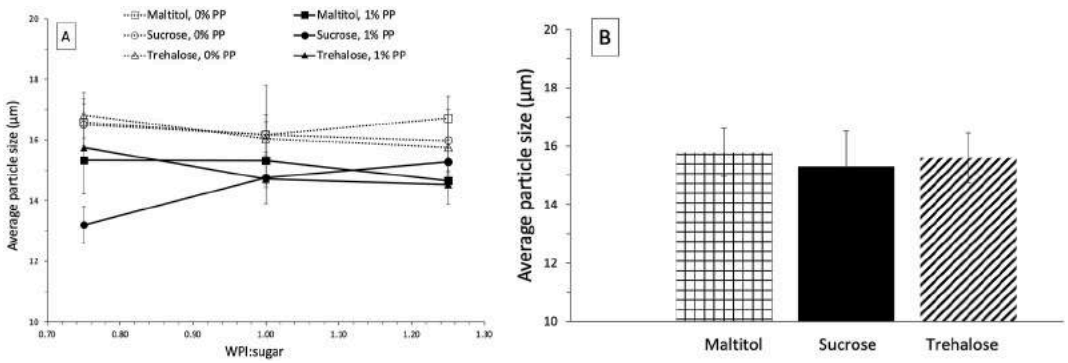


Fig. 7. Effect of WPI:sugar ratio [**A**] on the average particle sizes (µm) of dispersions at 25 °C; effect of sugar type [**B**] on the average particle sizes (µm) of all dispersions comprised of maltitol, sucrose, and trehalose, respectively, averaged together at 25 °C; (n = 9). Open markers with dotted lines- 0% PP, filled markers with solid lines- 1% PP [**A**]; lines are for guiding purposes only [**A**].

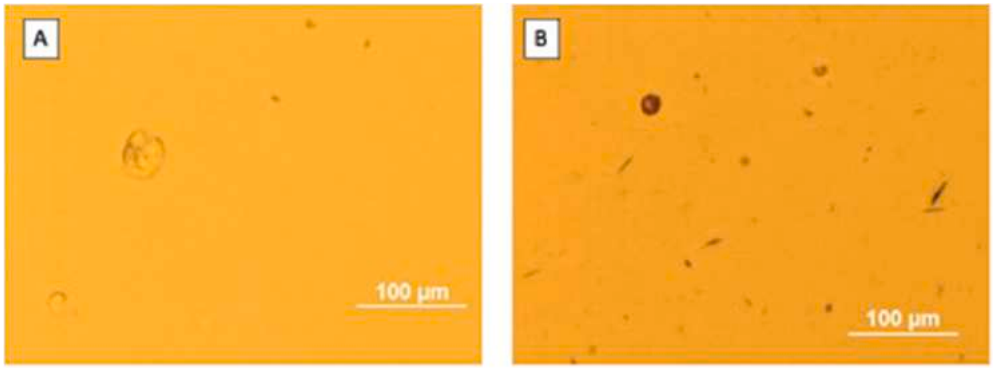


Fig. 8. Optical light microscope images at 200× magnification depicting the microstructures of diluted feed dispersions with 1.0 WPI:sucrose with 0% PP (**A**) and 1% PP addition (**B**). *COLOR REQUIRED*. (For interpretation of the references to color in this figure legend, the reader is referred to the Web version of this article.)

purple (Fig. 9), and the formation of a colored precipitate indicated protein-PP complexation (Hansen et al., 2021a, b; Van Teeling et al., 1971).

No differences in appearance were observed for centrifuged dispersions and their dilutions formulated with different sugars, regardless of WPI or PP presence (images not shown). Precipitated pellets were slightly larger in size for dispersions containing 1% PP, compared to those with 0% PP (Fig. 9). While Fig. 9 demonstrates this observation for samples formulated with sucrose, the same trend was observed for both maltitol and trehalose (images not shown). Similar observations were made in earlier experiments, where little-to-no precipitate formed after centrifuging a diluted 1% Aronia extract solution, suggesting that the observed increases in pellet size with increasing PP concentrations were due to enhanced aggregation and larger complexes precipitating out (Hansen et al., 2021a, b).

3.2. Dried bead characterization

3.2.1. Comparison of drop diameters

Measured diameters of drops formed from liquid dispersions were found to be significantly smaller ($p < 0.05$) than the estimated diameter values calculated from flow testing data for all formulations (Table 1), similar to the findings of Chan et al. (2009) when calcium-alginate drops formed by dripping methods were smaller than predicted with Tate's

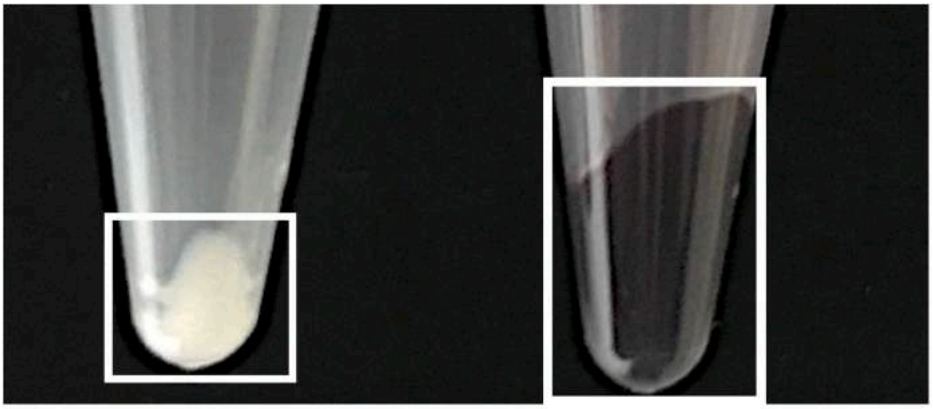


Fig. 9. Image depicting the precipitated fractions (highlighted in boxes) of centrifuged dispersions with 1.0 WPI:sucrose with 0% PP (Left) and 1% PP addition (Right). *COLOR REQUIRED*.

law calculations. These differences likely arose from the breaking of dispersion drops upon contact with the LN_2 surface, with resulting hardened drops having smaller sizes than estimated. While the correction factor used in calculating the estimated drop diameters describes the phenomenon of not all liquid detaching from the tubing tip, it does not account for the amount of liquid lost when drops break into smaller droplets, rendering the calculation method less accurate in estimating drop size in this case compared to previous experiments.

3.2.2. Water activity (a_w)

Water activities of fresh beads were measured after freeze-drying, and all but two formulations were found to have $a_w < 0.05$; sucrose beads without WPI were found to have higher a_w values (<0.15) (Table 1). Compared to the a_w values obtained in previous work (Hansen et al., 2020) for beads formed by gelation in heated oil and subsequent oven drying, the freeze granulation method presented in this study can more effectively form dry, solid beads with lower a_w values than the original drop formation method, which may result in beads with enhanced microbial stability. Other products formed with milk proteins have been reported to have a_w values similar to the beads in this study: Spray dried skim milk powders with 1.5% and 3% water contents are reported to have typical a_w values of ~0.02 and 0.1, respectively (Walstra, 1999). Variations in a_w of beads may be due to slight changes in environmental temperature during measurements or measurement variability.

3.2.3. Water content

After freeze-drying, fresh beads were oven dried to determine water content, as water content is known to affect physical properties of dried materials including texture and T_g (Roos, 1993). All dispersions formed dry beads with <3% water (Table 1), except for maltitol dispersions formulated without WPI, which were unable to form dry beads upon freeze-drying and instead appeared moist and were sticky to the touch. Often considered the 'critical formulation temperature' for determining profiles for freeze-drying processes, T_g' is the temperature at which glass transition occurs for the maximally freeze-concentrated solute (Roos and Drusch, 2015; Roos and Karel, 1991); T_g' varies with product composition, but it is recommended that shelf temperatures are adjusted so that product temperatures remain below T_g' for efficient drying (Kadoya et al., 2010). It is possible that the first step of the freeze-drying process, with shelf temperatures set to −40 °C, was not sufficient to maintain the glassy state of ice in maltitol beads, as the product temperature may have approached or exceeded T_g' when the LN_2 evaporated (Meister and Gieseler, 2008). T_g' onset and midpoint values for frozen maltitol solutions have been reported as −47 °C and −42 °C, respectively (Roos and Drusch, 2015), and were likely lower than the actual product temperatures during drying. If T_g' was approached or exceeded, beads would be prone to physical collapse, increased molecular mobility, and decreased viscosity as some of the ice present melted rather than sublimed as melting onset temperature (T_m') was approached, resulting in the sticky, moist products observed (Hartel et al., 2018; Kadoya et al., 2010).

Dispersions comprised of sucrose and trehalose, as well as maltitol beads containing WPI, were able to form dry beads upon freeze-drying because T_g' was sufficiently high to avoid cross-over with product temperatures during drying. T_g' onset and midpoint values for frozen sucrose solutions are reported as −46 °C and −41 °C, respectively, and those for trehalose are reported as −40 °C and −35 °C, respectively (Roos and Drusch, 2015). It has also been reported that frozen sugar solutions mixed with proteins gave higher T_g' values compared to pure sugars, suggesting miscibility of the components on a molecular level in the dry products and allowing synergistic stabilization, potentially explaining why maltitol dispersions were able to be dried into glassy beads when WPI was present (Kadoya et al., 2010). Dry beads formed with both sucrose and trehalose were found to have higher water contents in the absence of WPI compared to beads formed with WPI, as pure sugars have enhanced susceptibility for undergoing some extent of physical collapse, which is known to result in higher residual water content (Kadoya et al., 2010). Additionally, macromolecules-including proteins-are known to be useful drying aids in various food preservation techniques, further explaining the reduced water contents when beads were formulated with WPI (Bazaria & Kumar, 2016). The mechanisms of drying, while not the focus of this study, could be further investigated by FTIR analysis.

3.2.4. Thermal analysis – glass transition temperature (T_g)

Glass transition measurements are used as an indicator for the stability of glassy matrices and the resulting protection of components encapsulated within, rendering T_g significant in understanding product stability (Hartel et al., 2011; Levine and Slade, 1992; Roos and Drusch, 2015). The term T_g refers to the temperature range over which a glassy material softens; both onset and midpoint temperatures of the transition range are commonly referred to as T_g, though Roos and Drusch (2015) recommend that T_g is taken from the calorimetric onset temperature of the change in heat capacity. According to the ANOVA used to compare the T_g onset temperatures for beads containing WPI, WPI:sugar ratio had a significant effect on T_g ($p < 0.05$); Tukey's HSD tests expanded on this and clarified that the only significant increases in T_g onset temperatures were observed between the 0.75 and 1.0 WPI:sugar ratios. This finding can be observed in Fig. 10a, when the T_g onset temperature values of beads increase between the 0.75 and 1.0 WPI:sugar/polyol ratios for nearly all formulations. The ANOVA used to compare the T_g onset values for beads without maltitol also reported that WPI:sugar ratio significantly impacted T_g, with significant increases ($p < 0.05$) observed between the 0 and 0.75 WPI:sugar ratios. These findings can be clearly visualized in Fig. 10a for beads made with sucrose and trehalose. The ANOVA used to compare T_g of beads prepared with maltitol reported significant differences when WPI:polyol changed from 0.75 to 1.0 ratios ($p < 0.05$). These results generally agree with the literature; while considered 'problematic' and difficult to detect consistently due to very small changes in heat capacity (Adhikari et al., 2009; Pikal et al., 2007, 2008; Zhou and Labuza, 2007), the T_g of high molecular mass proteins is known to be high, and increasing the concentrations of protein in the mixtures may raise T_g slightly (Sarciaux and Hageman, 1997; Tzannis and Prestrelski, 1999).

Addition of PP had only a small effect on the T_g onset values of beads. However, the ANOVA for beads containing WPI reported that PP significantly ($p < 0.05$) impacted T_g, with Tukey's HSD tests clarifying that the presence of Aronia extract resulted in beads with higher T_g onset temperatures than those without PP. This trend was only clearly observed for beads produced with maltitol, indicating that those points strongly influenced the ANOVA report (Fig. 10a). The ANOVA for beads without maltitol did not report a significant difference ($p > 0.05$) in T_g upon the addition of PP to the bead matrices, as indicated by the lack of trends observed for beads made with sucrose and trehalose. The relatively small amounts of PP/Aronia present appeared to occasionally induce minor changes in the T_g of beads.

The T_g of confectionery products are heavily influenced by the type of sugar used and its water content (Hartel et al., 2018). Upon averaging the data obtained for beads formulated from each respective sugar, the onset T_g of beads formulated with trehalose was found to be the highest, while those comprised of maltitol were found to have the lowest T_g (Fig. 10b). The ANOVAs used to compare the T_g onset temperatures of beads containing WPI as well as the T_g of beads without maltitol indicated that sugar type has a significant ($p < 0.05$) effect on T_g, with Tukey's HSD tests reporting the same trend as observed in Fig. 10b (trehalose highest, maltitol lowest) and all three sugars being significantly different from each other. These results are similar to what would be expected based on the T_g values reported in the literature for each sugar/polyol: Dry T_g for maltitol is reported to be ~39 °C (Hartel et al., 2018), sucrose ~ 60–70 °C (Hartel et al., 2018; Roe and Labuza, 2005), and a range of temperatures are reported in the literature for trehalose

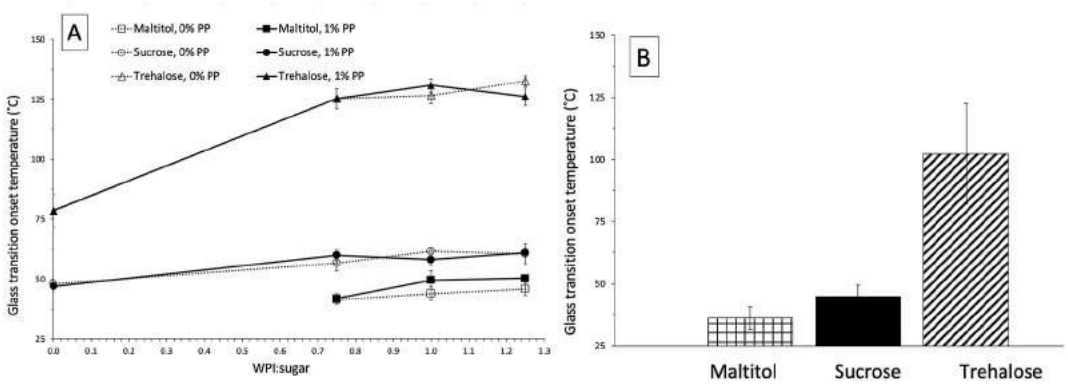


Fig. 10. Effect of WPI:sugar ratio [**A**] on the glass transition onset temperatures (°C) of beads; the effect of sugar type [**B**] on the average glass transition onset temperatures (°C) of all dried beads comprised of maltitol, sucrose, and trehalose, respectively, at 25 °C; (n = 9).

between ~ 75 and 120 °C, likely influenced by the presence of unmeasured or unreported water (Cardona et al., 1997; Roe and Labuza, 2005).

Water content is reported to have a strong effect on the T_g of sugars: 2–3% water can decrease the T_g of dry sucrose from ~62 to 70 to ~42–50 °C (Hartel et al., 2018), and trehalose T_g dropped to ~ 65 °C with 4% water (Iglesias et al., 1997). Like sugar glasses, freeze-dried proteins easily sorb water and show greatly reduced T_g values with increasing water contents, leading to reduced product stability (Lu et al., 2007; Pikal et al., 2007; Zhou and Labuza, 2007). In the case of elastin proteins, T_g was found to decrease from temperatures exceeding 200 °C when dry, to below 20 °C when water content was greater than 20% (Kakivaya and Hoeve, 1975; Roos and Drusch, 2015). Kadoya et al. (2010) observed enhanced T_g values for dried sugar solutions (water content <2%) when BSA protein was present, compared to those of the pure sugars (maltitol ~40.6 °C, with BSA ~56 °C; sucrose ~62 °C, with BSA ~68 °C; trehalose >80 °C, with BSA >90 °C), and suggested that the increased T_g values may be indicative of molecular-level miscibility of the components. Wilson et al. (2019) reported T_g values for mixtures of β-lactoglobulin with sucrose and trehalose (1:9 protein:sweetener), with T_g of β-lactoglobulin-sucrose with a water content of 0.7% to be ~71.8 °C, and β-lactoglobulin-trehalose with 0.3% water having T_g ~106.5 °C. The values obtained in this experiment are in agreement with the results reported in the literature, taking into account the effects of residual water in the freeze-dried beads. Confirming microscopic homogeneity of glassy structures would require different experiments designed to study component interactions.

3.2.5. Hardness

Hardness of a glassy product may also be used as an indicator of its stability and whether water uptake has affected its physical state or sensory properties. When the hardness values of freeze-dried beads were measured, it was found that beads containing WPI were less hard than those formulated without WPI. According to the ANOVA used to compare the hardness of beads containing WPI, WPI:sugar ratio had a significant effect on hardness ($p < 0.05$); Tukey's HSD tests specified that increased WPI to sugar ratios resulted in decreased hardness, though the difference was only significant between the 1.0 and 1.25 ratios. The ANOVA used to compare beads formed without maltitol also indicated that the WPI:sugar ratio had a significant effect ($p < 0.05$), with Tukey's HSD tests clarifying that the only difference in hardness was observed between the 0 and 0.75 WPI:sugar ratios, which can be clearly visualized in Fig. 11a for beads formulated with sucrose and trehalose. The ANOVA used to compare beads containing maltitol was in agreement that WPI:sugar ratio significantly affected hardness, but Tukey's HSD tests did not show meaningful trends. As alluded to in previous work (Hansen et al., 2020), we postulate that protein particles and protein-PP complexes are embedded throughout the continuous glassy matrices formed by the sugars, breaking up and weakening the glasses compared to beads with uninterrupted glassy structures. The effect of protein on reducing the hardness of beads was strong, and as such, it may not be as useful to compare hardness of beads with WPI to those without.

The presence of PP was not found to drastically affect the hardness of beads. The ANOVA used to compare the hardness of beads containing WPI reported that PP presence did not significantly affect the hardness

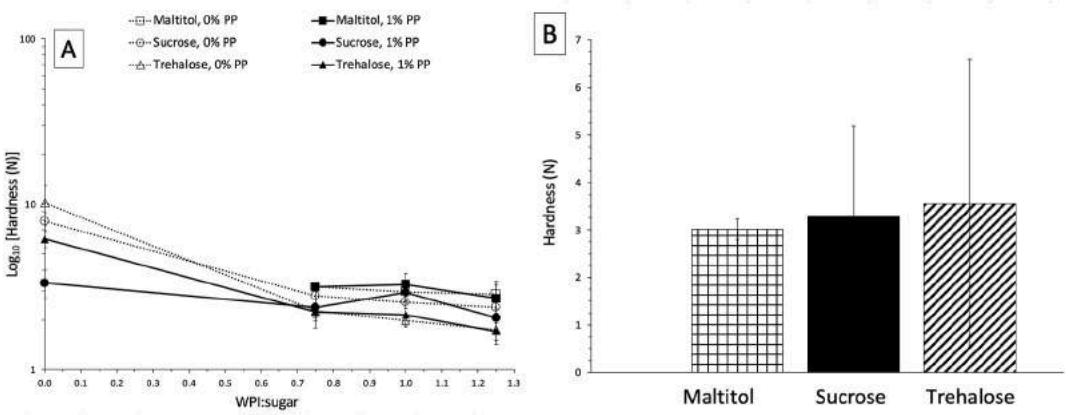


Fig. 11. Effect of WPI:sugar ratio [**A**] on the hardness (N) of dried beads at 25 °C; the effect of sugar type [**B**] on the average hardness values of all dried beads comprised of maltitol, sucrose, and trehalose, respectively, at 25 °C; (n = 9). Open markers with dotted lines- 0% PP, filled markers with solid lines- 1% PP [**A**]; lines are for guiding purposes only [**A**].

of beads ($p > 0.05$); the ANOVA used to compare the hardness of beads containing maltitol was in agreement. The ANOVA used to compare the hardness of beads formed without maltitol indicated that PP presence significantly influenced hardness ($p < 0.05$), where beads prepared with sucrose and trehalose without PP were significantly harder than those containing PP (Fig. 11a). Aronia extract may have introduced impurities into the glassy matrix, weakening it in the same way that protein and protein-PP complexes are thought to.

We hypothesized that beads comprised of sugars/polyols with higher known T_g values may be harder and more brittle than those formulated with lower T_g sugars, as that rule generally applies to many confectionery products (Hartel et al., 2018). According to the ANOVA used to compare the hardness of beads containing WPI, the sugar type used to formulate beads significantly influenced hardness ($p < 0.05$); Tukey's HSD tests indicated that beads prepared with maltitol were the hardest, and those made from trehalose were softest, in contrast to expectations based on T_g. While the effect of sugar type on hardness was found to be statistically significant, closer examination of the data plotted in Fig. 11a for beads containing WPI show considerable overlap between sugar types, indicating that the effects were small. The ANOVA used to compare the hardness of beads prepared without maltitol reported that sugar type did not significantly affect hardness ($p > 0.05$); beads made of trehalose had slightly but not significantly higher hardness values than those made of sucrose. These findings can also be observed in Fig. 11a, where trehalose beads without WPI were the only point where hardness was clearly higher than the corresponding beads formulated with sucrose, and even in that case, was not significantly different. These findings are summarized visually in Fig. 11b, where the hardness values of all beads formulated with each respective sugar type are averaged for comparison of sugar/polyol effects, showing maltitol beads were, on average, the least hard, and trehalose the hardest. Trehalose and sucrose formulations had higher variation, since hardness was strongly influenced by the presence of WPI in formulations, as discussed previously. These findings were interesting, as greater differences in hardness were expected when sugar type was changed, though WPI influenced the hardness of beads more strongly than sugar type. Beads formulated with lower T_g sugars may have had slightly more fluid properties and molecular mobility at room temperature and were more susceptible to ambient water, which could result in a sticky outer surface forming on the beads, resulting in enhanced hardness and tackiness, as opposed to the more crisp, brittle texture of more dry glasses.

3.3. Effects of dispersion properties on dry beads

No strong correlations were found upon investigating the relationships that may exist between properties of feed dispersions and those of the final beads formed (data not shown). No correlation was found between the viscosities of feed dispersions and the glass transition onset temperatures, diameters, or hardness of beads formed. Surface tensions of dispersions were not correlated with the hardness of beads formed either. Water contents of dried beads did not have a strong relationship with T_g or hardness. Diameters of dried beads were not related to their hardness. pH values of dispersions did not correlate with the diameters of beads formed or their hardness. Particle sizes of dispersions did not correlate with the hardness, T_g, or diameters of dried beads formed.

4. Conclusion

In a variety of pharmaceutical, food, and biomedical applications, freeze-dried protein-sugar mixtures in the glassy state have been shown to 1) have increased T_g compared to that of the sugar alone, 2) prevent sugar crystallization in storage, and 3) diminish decomposition of the proteins in the mixture from their native structures during freeze-drying and subsequent storage by immersion in the glassy matrices and increasing denaturation temperature (Corradini et al., 2013; Imamura et al., 2001; Jena et al., 2017; Liao et al., 2005; Lu et al., 2007; Nilsson and Larsson, 2007; Pikal et al., 2007, 2008; Sarciaux and Hageman, 1997; Souillac et al., 2002). It is for these reasons that we believe that the adapted freeze granulation process presented produces structures with the potential to act as good stabilizers and subsequent delivery vehicles for bioactive ingredients such as polyphenols. Substitution of glass formers with lower T_g by others with higher T_g resulted in the formation of beads with increased T_g, indicative of better physical stabilities. Compositional modifications such as these may improve the protective abilities of bead structures as their physical stabilities are known to enhance storage stability. Further investigations of bioactives delivery, as well as retention and shelf life studies, are critical to determine the efficacy of these structures as encapsulation matrices as well as optimization for applications.

Funding

The Lauritzson Foundation provided funding for this research via the Lauritzson Research Scholarship, through the College of Science, Engineering and Food Science (SEFS) at University College Cork.

Authors contributions

Mackenzie M. Hansen: Conceptualization, Methodology, Validation, Formal analysis, Investigation, Resources, Writing – original draft, Writing – review & editing, Visualization, Project administration, Funding acquisition. **Richard W. Hartel:** Conceptualization, Resources, Writing – review & editing, Visualization, Supervision. **Yrjö H. Roos:** Conceptualization, Resources, Writing – review & editing, Visualization, Supervision, Funding acquisition.

Declaration of competing interest

The authors hereby declare no conflict of interest.

Acknowledgements

The authors would like to thank the reviewers and Journal Editor for careful reading of the manuscript and thoughtful feedback.

References

Adhikari, B., Howes, T., Bhandari, B.R., Langrish, T.A.G., 2009. Effect of addition of proteins on the production of amorphous sucrose powder through spray drying. J. Food Eng. 94 (2), 144–153. https://doi.org/10.1016/j.jfoodeng.2009.01.029.

Bazaria, B., Kumar, P., 2016. Effect of whey protein concentrate as drying aid and drying parameters on physicochemical and functional properties of spray dried beetroot juice concentrate. Food Biosci. 14, 21–27. https://doi.org/10.1016/j.fbio.2015.11.002.

Bhatta, S., Stevanovic Janezic, T., Ratti, C., 2020. Freeze-drying of plant-based foods. Foods 9 (1), 87. https://doi.org/10.3390/foods9010087.

Cardona, S., Schebor, C., Buera, M.P., Karel, M., Chirife, J., 1997. Thermal stability of invertase in reduced-moisture amorphous matrices in relation to glassy state and trehalose crystallization. J. Food Sci. 62 (1), 105–112. https://doi.org/10.1111/j.1365-2621.1997.tb04378.x.

Chan, E.-S., Lee, B.-B., Ravindra, P., Poncelet, D., 2009. Prediction models for shape and size of ca-alginate macrobeads produced through extrusion–dripping method. J. Colloid Interface Sci. 338 (1), 63–72. https://doi.org/10.1016/j.jcis.2009.05.027.

Corradini, D., Strekalova, E.G., Stanley, H.E., Gallo, P., 2013. Microscopic mechanism of protein cryopreservation in an aqueous solution with trehalose. Sci. Rep. 3 (1) https://doi.org/10.1038/srep01218.

Ergun, R., Lietha, R., Hartel, R.W., 2010. Moisture and shelf life in sugar confections. Crit. Rev. Food Sci. Nutr. 50 (2), 162–192. https://doi.org/10.1080/10408390802248833.

Fitzpatrick, J.J., Iqbal, T., Delaney, C., Twomey, T., Keogh, M.K., 2004. Effect of powder properties and storage conditions on the flowability of milk powders with different fat contents. J. Food Eng. 64 (4), 435–444. https://doi.org/10.1016/j.jfoodeng.2003.11.011.

Hansen, M.M., Hartel, R.W., Roos, Y.H., 2021a. Effects of Aronia Polyphenols on the Physico-Chemical Properties of Whey, Soy, and Pea Protein Isolate Dispersions (in press), in Food Production, Processing and Nutrition.

Hansen, M.M., Hartel, R.W., Roos, Y.H., 2021b. Encapsulant-bioactives interactions impact on physico-chemical properties of concentrated dispersions. J. Food Eng. 302, 110586. https://doi.org/10.1016/j.jfoodeng.2021.110586.

Hansen, M.M., Maidannyk, V.A., Roos, Y.H., 2020. Thermal gelation and hardening of whey protein beads for subsequent dehydration and encapsulation using vitrifying sugars. J. Food Eng. 279, 109966. https://doi.org/10.1016/j.jfoodeng.2020.109966.
Hartel, R.W., Ergun, R., Vogel, S., 2011. Phase/state transitions of confectionery sweeteners: thermodynamic and kinetic aspects. Compr. Rev. Food Sci. Food Saf. 10 (1), 17–32. https://doi.org/10.1111/j.1541-4337.2010.00136.x.
Hartel, R.W., von Elbe, J.H., Hofberger, R., 2018. Confectionery Science and Technology. Springer International Publishing. https://doi.org/10.1007/978-3-319-61742-8.
Iglesias, H.A., Chirife, J., Buera, M.P., 1997. Adsorption isotherm of amorphous trehalose. J. Sci. Food Agric. 75, 183–186.
Imamura, K., Iwai, M., Ogawa, T., Sakiyama, T., Nakanishi, K., 2001. Evaluation of hydration states of protein in freeze-dried amorphous sugar matrix. J. Pharmacol. Sci. 90 (12), 1955–1963. https://doi.org/10.1002/jps.1146.
Jena, S., Horn, J., Suryanarayanan, R., Friess, W., Aksan, A., 2017. Effects of excipient interactions on the state of the freeze-concentrate and protein stability. Pharm. Res. (N. Y.) 34 (2), 462–478. https://doi.org/10.1007/s11095-016-2078-y.
Kadoya, S., Fujii, K., Izutsu, K., Yonemochi, E., Terada, K., Yomota, C., Kawanishi, T., 2010. Freeze-drying of proteins with glass-forming oligosaccharide-derived sugar alcohols. Int. J. Pharm. 389 (1–2), 107–113. https://doi.org/10.1016/j.ijpharm.2010.01.027.
Kakivaya, S.R., Hoeve, C.A., 1975. The glass point of elastin. Proc. Natl. Acad. Sci. Unit. States Am. 72 (9), 3505–3507. https://doi.org/10.1073/pnas.72.9.3505.
Kawai, K., Suzuki, T., 2007. Stabilizing effect of four types of disaccharide on the enzymatic activity of freeze-dried lactate dehydrogenase: step by step evaluation from freezing to storage. Pharm. Res. (N. Y.) 24 (10), 1883–1890. https://doi.org/10.1007/s11095-007-9312-6.
La Lumia, F., Ramond, L., Pagnoux, C., Bernard-Granger, G., 2019. Fabrication of homogenous pellets by freeze granulation of optimized TiO2-Y2O3 suspensions. J. Eur. Ceram. Soc. 39 (6), 2168–2178. https://doi.org/10.1016/j.jeurceramsoc.2019.01.036.
Lee, B.B., Chan, E.S., 2013. Size and shape of calcium alginate beads produced by extrusion dripping. Chem. Eng. Technol. 36 (10), 1627–1642. https://doi.org/10.1002/ceat.201300230.
Levine, H., Slade, L., 1992. Glass transitions in foods. In: Schwartzberg, H., Hartel, R.W. (Eds.), Physical Chemistry of Foods. Marcel Dekker, Inc, pp. 83–221.
Liao, X., Krishnamurthy, R., Suryanarayanan, R., 2005. Influence of the active pharmaceutical ingredient concentration on the physical state of mannitol—implications in freeze-drying. Pharm. Res. (N. Y.) 22 (11), 1978–1985. https://doi.org/10.1007/s11095-005-7625-x.
Lu, J., Wang, X.-J., Liu, Y.-X., Ching, C.-B., 2007. Thermal and FTIR investigation of freeze-dried protein-excipient mixtures. J. Therm. Anal. Calorim. 89 (3), 913–919. https://doi.org/10.1007/s10973-006-7598-y.
Meister, E., Gieseler, H., 2008. A significant comparison between collapse and glass transition temperatures. Eur. Pharm. Rev. 5.
Nilsson, E., Larsson, A., 2007. Stability of chicken IgY antibodies freeze-dried in the presence of lactose, sucrose and threalose. J. Poult. Sci. 44, 58–62.
Ouadaker, M., Jiang, X., Bowen, P., Bienia, M., Pagnoux, C., Aimable, A., 2020. Porous granules by freeze granulation of Pickering emulsions stabilized with halloysite particles. Colloid. Surface. Physicochem. Eng. Aspect. 585, 124156. https://doi.org/10.1016/j.colsurfa.2019.124156.
Pikal, M.J., Rigsbee, D.R., Roy, M.L., 2007. Solid state chemistry of proteins: I. Glass transition behavior in freeze dried disaccharide formulations of human growth hormone (HGH). J. Pharmacol. Sci. 96 (10), 2765–2776. https://doi.org/10.1002/jps.20960.
Pikal, M.J., Rigsbee, D., Roy, M.L., Galreath, D., Kovach, K.J., Wang, B., Stuart), Carpenter, J.F., Cicerone, M.T., 2008. Solid state chemistry of proteins: II. The correlation of storage stability of freeze-dried human growth hormone (hGH) with structure and dynamics in the glassy solid. J. Pharmacol. Sci. 97 (12), 5106–5121. https://doi.org/10.1002/jps.21374.
Rice, T., Zannini, E., Arendt, E.K., Coffey, A., 2020. A review of polyols – biotechnological production, food applications, regulation, labeling and healt. Crit. Rev. Food Sci. Nutr. 60 (12), 2034–2051.
Roe, K.D., Labuza, T.P., 2005. Glass transition and crystallization of amorphous trehalose-sucrose mixtures. Int. J. Food Prop. 8 (3), 559–574. https://doi.org/10.1080/10942910500269824.
Roos, Y., Drusch, S., 2015. Phase Transitions in Foods, second ed. Academic Press.
Roos, Y.H., 1993. WATER ACTIVITY and PHYSICAL STATE EFFECTS ON AMORPHOUS FOOD STABILITY. J. Food Process. Preserv. 16 (6), 433–447. https://doi.org/10.1111/j.1745-4549.1993.tb00221.x.
Roos, Y.H., 2010. Glass transition temperature and its relevance in food processing. Annu. Rev. Food Sci. Technol. 469–496.
Roos, Y.H., 2020. Water activity and glass transition. In: Water Activity in Foods: Fundamentals and Applications, second ed. John Wiley & Sons, Incorporated, pp. 29–45.
Roos, Y., Karel, M., 1991. Amorphous state and delayed ice formation in sucrose solutions. Int. J. Food Sci. Technol. 26 (6), 553–566. https://doi.org/10.1111/j.1365-2621.1991.tb02001.x.
Sarciaux, J.-M.E., Hageman, M.J., 1997. Effects of bovine somatotropin (rbSt) concentration at different moisture levels on the physical stability of sucrose in freeze-dried rbSt/sucrose mixtures. J. Pharmacol. Sci. 86 (3), 365–371. https://doi.org/10.1021/js960217k.
Schneider, M.E., 2016. Formation of Whey Protein-Polyphenol Aggregates and Incorporation into Various Food Structures. PhD Food Science. North Carolina State University.
Schuck, P., Blanchard, E., Dolivet, A., Méjean, S., Onillon, E., Jeantet, R., 2005. Water activity and glass transition in dairy ingredients. Lait 85 (4–5), 295–304. https://doi.org/10.1051/lait:2005020.
Shanmugam, S., 2015. Granulation techniques and technologies: recent progresses. Bioimpacts 5 (1), 55–63.
Siebert, K.J., Troukhanova, N.V., Lynn, P.Y., 1996. Nature of Polyphenol−Protein interactions. J. Agric. Food Chem. 44 (1), 80–85. https://doi.org/10.1021/jf9502459.
Sosa, N., Zamora, M.C., Chirife, J., Schebor, C., 2011. Spray-drying encapsulation of citral in sucrose or trehalose matrices: physicochemical and sensory characteristics: spray-drying of citral in sugar matrices. Int. J. Food Sci. Technol. 46 (10), 2096–2102. https://doi.org/10.1111/j.1365-2621.2011.02721.x.
Souillac, P.O., Middaugh, C.R., Rytting, J.H., 2002. Investigation of protein/carbohydrate interactions in the dried state. 2. Diffuse reflectance FTIR studies. Int. J. Pharm. 235 (1–2), 207–218. https://doi.org/10.1016/S0378-5173(01)00987-5.
Thongkaew, C., Gibis, M., Hinrichs, J., Weiss, J., 2014. Polyphenol interactions with whey protein isolate and whey protein isolate–pectin coacervates. Food Hydrocolloids 41, 103–112. https://doi.org/10.1016/j.foodhyd.2014.02.006.
Tzannis, S.T., Prestrelski, S.J., 1999. Moisture effects on protein-excipient interactions in spray-dried powders. Nature of destabilizing effects of sucrose. J. Pharmacol. Sci. 88 (3), 360–370. https://doi.org/10.1021/js9800127.
Van Teeling, C.G., Cansfield, P.E., Gallop, R.A., 1971. An anthocyanin complex isolated from the syrup of canned blueberries. J. Food Sci. 36, 1061–1063. https://doi.org/10.1111/j.1365-2621.1971.tb03346.x.
Walstra, P. (Ed.), 1999. Dairy Technology: Principles of Milk Properties and Processes. CRC Press.
White, G.W., Cakebread, S.H., 1966. The glassy state in certain sugar-containing food products. Int. J. Food Sci. Technol. 1 (1), 73–82. https://doi.org/10.1111/j.1365-2621.1966.tb01031.x.
Wilson, N.E., Topp, E.M., Zhou, Q.T., 2019. Effects of drying method and excipient on structure and stability of protein solids using solid-state hydrogen/deuterium exchange mass spectrometry (ssHDX-MS). Int. J. Pharm. 567, 118470. https://doi.org/10.1016/j.ijpharm.2019.118470.
Xue, F., Li, C., Adhikari, B., 2020. Physicochemical properties of soy protein isolates-cyanidin-3-galactoside conjugates produced using free radicals induced by ultrasound. Ultrason. Sonochem. 64, 104990. https://doi.org/10.1016/j.ultsonch.2020.104990.
Zhou, P., Labuza, T.P., 2007. Effect of water content on glass transition and protein aggregation of whey protein powders during short-term storage. Food Biophys. 2 (2–3), 108–116. https://doi.org/10.1007/s11483-007-9037-4.